The Response of Mediterranean River Basins to Pleistocene Glaciation

A thesis submitted to the University of Manchester
for the degree of Doctor of Philosophy in the Faculty of Humanities

2012

Kathryn Adamson

School of Environment and Development

CONTENTS

SECTION ONE – BACKGROUND

Word Count: 54,560

LIST OF FIGURES

CHAPTER 7

CHAPTER 8

CHAPTER 9

LIST OF TABLES

LIST OF PLATES

ABSTRACT

The response of Mediterranean river basins to Pleistocene glaciation

Fluvial morphosedimentary records surrounding the Orjen massif, western Montenegro, have been studied to investigate the response of Mediterranean river systems to Pleistocene glaciation. A range of depositional contexts, across 12 sites, have been analysed, including: terraced alluvial valley fills, poljes and alluvial fans. These sites include both ice marginal contexts and more distal locations. It can be argued that these settings are broadly representative of the depositional environments found within glaciated upland catchments across the Mediterranean, and especially those in limestone landscapes. The timing of fluvial activity has been constrained using detailed stratigraphical analysis, 35 U-series dates, calcite micromorphology, and soil profile analysis. The fluvial record is fragmentary but is in good agreement with the Pleistocene glacial history of the Orjen massif, developed by Hughes *et al*. (2010). Two main phases of Pleistocene fluvial sedimentation have been identified in the morphosedimentary record. The most extensive phase of fluvial aggradation is correlated to MIS 12 (Kotorska-Sušica Member) and is characterised by the infilling of large depocentres beyond the maximum MIS 12 ice margins. These deposits dominate the fluvial record. The next recorded phase of fluvial deposition is correlated to MIS 6 (Krivošije Member) and contains only limited evidence of fluvial activity. No morphosedimentary evidence for fluvial deposition in MIS 5d-2 has yet been observed in the study area. An analysis of published studies shows that the Pleistocene glacial and fluvial archives are highly fragmentary across the Mediterranean basin.

The limestone karst terrain of Mount Orjen has exerted an important influence on sediment delivery and the meltwater pathways draining the Orjen ice cap over successive glacial cycles. Evidence suggests that, since MIS 12, sediment supply to the fluvial system has declined in accord with the decreasing magnitude of glaciation and subterranean karst flows have become increasingly dominant over surface flows. As ice volume and extent decreased in the cold stages following MIS 12, the Pleistocene glacial and surface fluvial systems became progressively decoupled. Two types of surface meltwater routes operated during MIS 12: Type 1 – steep sided limestone bedrock gorges; and Type 2 - alluvial channels draining directly from the ice margin. These contrasting pathways are associated with distinctive sedimentological signatures both at the macro-scale and within the fine (<63 μm) matrix fraction This study provides one of the first attempts to directly correlate Pleistocene glacial and fluvial records – and to consider the process interactions – in a range of depositional contexts at the landscape scale.

Kathryn Adamson
The University of Manchester
17th August 2012

DECLARATION AND COPYRIGHT STATEMENT

Declaration

No portion of the work referred to in the thesis has been submitted in support of an application for another degree or qualification of this or any other university or other institute of learning.

Copyright Statement

The author of this thesis (including any appendices and/or schedules to this thesis) owns certain copyright or related rights in it (the "Copyright") and s/he has given The University of Manchester certain rights to use such Copyright, including for administrative purposes.

Copies of this thesis, either in full or in extracts and whether in hard or electronic copy, may be made **only** in accordance with the Copyright, Designs and Patents Act 1988 (as amended) and regulations issued under it or, where appropriate, in accordance with licensing agreements which the University has from time to time. This page must form part of any such copies made.

The ownership of certain Copyright, patents, designs, trade marks and other intellectual property (the "Intellectual Property") and any reproductions of copyright works in the thesis, for example graphs and tables ("Reproductions"), which may be described in this thesis, may not be owned by the author and may be owned by third parties. Such Intellectual Property and Reproductions cannot and must not be made available for use without the prior written permission of the owner(s) of the relevant Intellectual Property and/or Reproductions.

Further information on the conditions under which disclosure, publication and commercialisation of this thesis, the Copyright and any Intellectual Property and/or Reproductions described in it may take place is available in the University IP Policy (see http://www.campus.manchester.ac.uk/medialibrary/policies/intellectual-property.pdf), in any relevant Thesis restriction declarations deposited in the University Library, The University Library's regulations (see http://www.manchester.ac.uk/library/aboutus/regulations) and in The University's policy on presentation of Theses.

ACKNOWLEDGEMENTS

CHAPTER ONE

Introduction

Synopsis

Pleistocene glaciation had a profound impact on landscape processes in many parts of the world (Boulton and Eyles, 1979; Benn and Evans, 1998). River systems draining glaciated catchments would have responded to changes in glacial mass balance and associated modifications to sediment supply and meltwater runoff regime. Records of these changes may be preserved within a range of alluvial depositional contexts extending from the glaciated headwaters to the coastal zone. Quaternary river sediments and landforms can therefore provide a valuable link between upland, lowland and offshore records. In some settings they could present a more complete archive of Pleistocene glaciation than the glacial records themselves (Woodward *et al.*, 2008). Our understanding of Pleistocene glacial-fluvial interactions is currently limited and provides a major research impetus for the investigation of long-term landscape dynamics. In the Mediterranean the excellent preservation of datable glacial and fluvial landforms makes it an unrivalled location to explore glacial and fluvial landsystem dynamics (Evans, 2003) over several glacial cycles. This chapter outlines the nature of Quaternary climate change at the global and Mediterranean scale. This provides context for the aims and objectives of current investigations in the glaciated catchments of the Orjen massif, Montenegro.

1.1 Quaternary climate change and stratigraphic subdivisions

The Quaternary is the most recent geological period, spanning the last 2.58 Ma, and is divided into two epochs: the Pleistocene (2.58 Ma – c. 11.7 ka) and the Holocene (c. 11.7 ka – present) (Lowe *et al*., 2007). The term 'Quaternary' was first introduced in the sixteenth century by Italian engineer Giovanni Arduino who identified four orders of geological time (Primary, Secondary, Tertiary and Quaternary) (Schneer, 1969). The term was later applied by Desnoyers (1829) and Reboul (1833) whilst the term 'Pleistocene' was coined by Scottish geologist, Charles Lyell in 1839 (Elias, 2007). The Quaternary Period is characterised by episodic glacial activity during a series of cold stages that saw the expansion of mountain glaciers and the build up of major continental ice sheets in the mid-latitudes. These glacial phases were interspersed with warmer interglacial periods (Elias, 2007) where temperatures often exceeded those of the

present day. The Quaternary is a particularly distinctive time period due to the high amplitude and high frequency of these climatic oscillations (Walker and Lowe, 2007). The causes of these large-scale and long-term climatic changes are now largely attributed to astronomical forcing factors. The Astronomical Theory, developed by James Croll and elaborated by Milutin Milankovitch, proposes that the Earth's climate responds to periodic changes in three of the Earth's orbital parameters. The shape of the Earth's orbit (eccentricity) fluctuates over a period of 100,000 years; the tilt of the Earth's axis relative to the orbital plane (obliquity of the ecliptic) varies over 41,000 years; and the direction of tilt (precession) undergoes a 23,000 year cycle (Berger and Loutre, 2007). One of the earliest attempts to subdivide the Quaternary period into distinct glacial-interglacial cycles was undertaken by Penck and Brückner (1909) on the basis of glacial and fluvial stratigraphical sequences in the European Alps. They identified four glacial phases: Günz, Mindel, Riss, and Würm (Bowen, 1978; Fig. 1.1). This was a highly novel study into the interactions of Quaternary glacial and fluvial landsystems at a time when radiometric dating methods were unavailable. During the twentieth century, their Alpine model was one of the most widely used methods of correlation between Pleistocene deposits throughout Europe and between continents (Elias, 2007).

The fragmentary nature of terrestrial geological records means that evidence of Pleistocene glaciation often varies significantly between locations. This is a major limitation for the use of early models, such as Penck and Brückner's Alpine framework, for wider scale correlations. More recent investigation of deep ocean sediment and polar ice sheet records has revolutionised our understanding of global-scale Quaternary climate change. These records suggest that over 50 glacial stages and associated interglacials have occurred since the onset of the Quaternary, with at least ten glacial-interglacial cycles during the last 800,000 years (Shackleton and Opdyke, 1973; Hays *et al.,* 1976; Imbrie *et al.*, 1984; Shackleton, *et al.*, 1990). Unlike many terrestrial records, ocean sediments have accumulated almost continuously throughout the Quaternary. Analysis of stable oxygen isotope (^{16}O and ^{18}O) ratios from foraminifera tests within these deep ocean sediments provides a detailed record of global ice volume. Ice core records from the polar ice sheets also accumulate quasi-continuously and preserve a high resolution record of high latitude Quaternary environmental change. These records have led to a more detailed stratigraphical subdivision of Quaternary time, based on marine isotope stages (MIS) (Fig. 1.1) and have allowed the correlation of Quaternary palaeoenvironmental records from both terrestrial and offshore settings (Walker and Lowe, 2007). Quaternary climatic fluctuations have had significant impacts on geomorphological processes such as changes in glacial mass balance, sea levels, and river regimes. As well as

deep ocean sediments and polar ice sheet records, evidence of these global changes are also preserved in a variety of terrestrial archives including glacial, fluvial and lacustrine settings. Today, over a century since the development of the classical Alpine model of Penck and Brückner, it is possible to revisit these ideas of glacial and fluvial system interactions using modern dating and analytical techniques within the context of the high-resolution marine and ice core records.

1.2 Quaternary environmental change in the Mediterranean

The Mediterranean region is a major archive of Quaternary environmental change. Located at the interface between several tectonic and climatic systems, the Mediterranean is a highly distinctive physical environment (Woodward, 2009). This location has made it particularly sensitive to Quaternary environmental perturbations. The Mediterranean climate is typified by mild, wet winters and warm, dry summers (type Cs under the Köppen classification) (Harding *et al*., 2009). Within several high mountain regions, such as the Dinaric Alps, the Pyrenees, and the Pindus Mountains, annual precipitation levels as high as 3,000 mm/yr have been fundamental to the development of Pleistocene mountain glaciers and ice caps. A number of these valley glaciers persist to the present day in the Pyrenees, the Dinaric Alps and the Apennines (Harding *et al*., 2009; Hughes *et al*., 2006a; Hughes and Woodward, 2009; Grunewald and Sheithauer, 2010). During the Quaternary the Mediterranean environment has been considerably influenced by Northern Hemisphere ice sheets (Rohling *et al*., 2009) through changes in ocean and atmospheric circulation, meltwater routes and vegetation dynamics, for example. Over the last few decades, research has shown that major orbitally-forced Quaternary climatic oscillations, as well as millennial and centennial scale climatic excursions (von Graftenstein *et al*., 1999; Sierro *et al*., 2005; Fletcher and Sánchez Goñi, 2008), are frequently well-preserved within the Mediterranean geological record (Rohling *et al*., 2009; Allen *et al*., 2000; Fletcher *et al.,* 2010).

Due to its location beyond the margins of the Eurasian Ice Sheet, many parts of the Mediterranean formed important refugia for flora and fauna during the major cold phases of the Quaternary. The geological setting of the Mediterranean, with its long history of uplifting mountain regions, as well as subsiding basins, has created thick sequences of undisturbed sediments (Tzedakis, 2009). These often contain detailed records of Quaternary environmental change. Sites across the Mediterranean, from a range of depositional contexts, provide

detailed and often continuous palaeoenvironmental records that allow more fragmentary archives to be correlated with global marine and ice core records. A selection of these is shown in Figure 1.2.
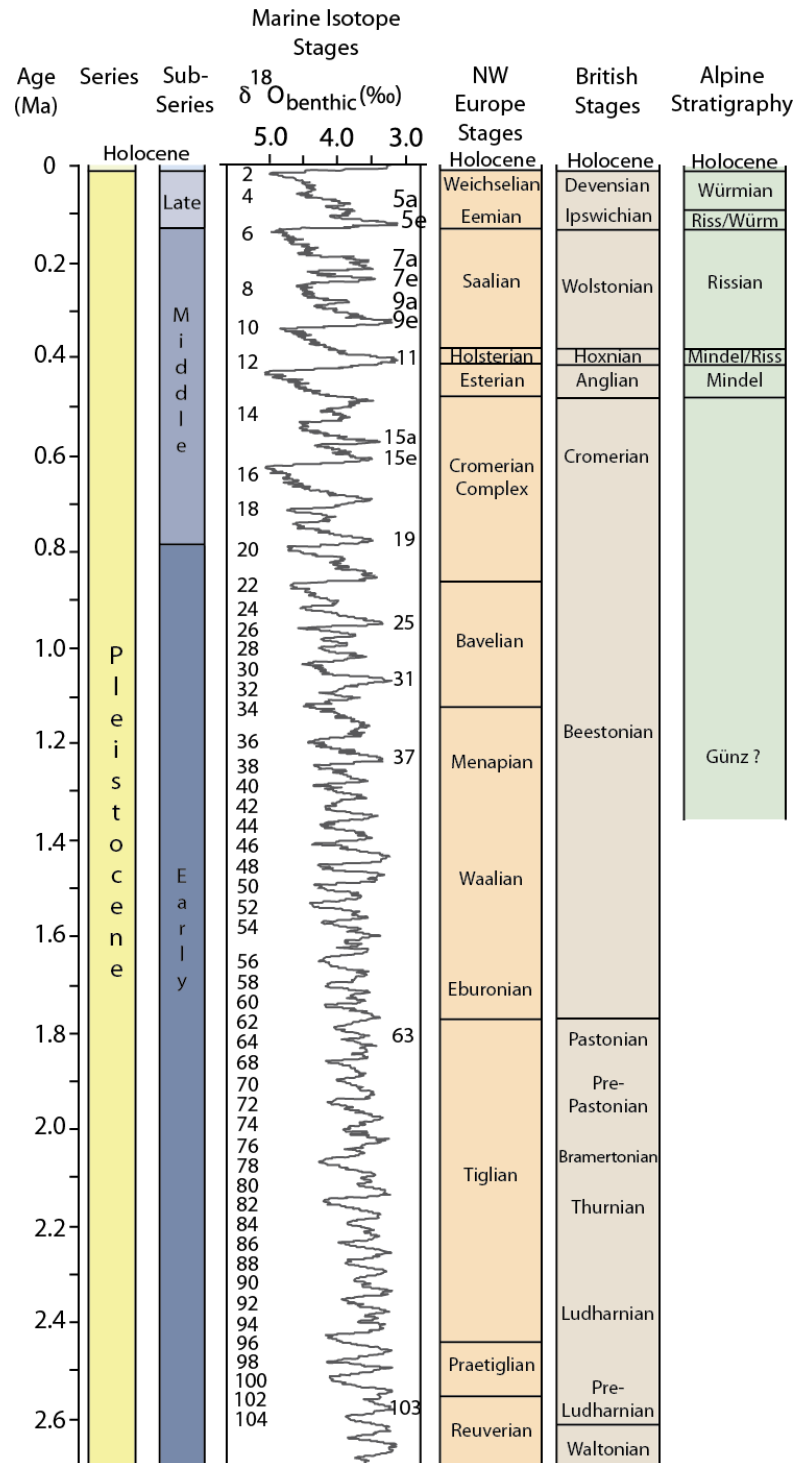
Figure 1.1 – The Quaternary stratigraphical sequence and marine benthic ^{18}O isotope record. Marine isotope stages (MIS) and the stratigraphical subdivisions of Northwest Europe, Britain and the Alpine glacial scheme of Penck and Brückner (1909) are indicated. Adapted from the

global chronostratigraphical framework of the Subcommission on Quaternary Stratigraphy (Gibbard and Cohen, 2008; Cohen and Gibbard, 2010).

The wider application of radiometric dating techniques, notably: radiocarbon (^{14}C), uranium-series (U-series), luminescence and cosmogenic nuclide methods, alongside morphosedimentary analysis, has been a key advance in Quaternary research over the last several decades (Walker and Lowe, 2007). This has enabled more robust comparisons both between Mediterranean sites and with the wider marine and ice core chronostratigraphies (Macklin *et al*., 2002; Hughes and Woodward, 2008).

Legend

● Selected Mediterranean palaeoenvironmental records

N   0   500   1,000 km

1 - The Alboran Sea - marine cores
2 - The Adriatic Sea - marine cores
3 - Crvena Stijena - rockshelter
4 - Lago Grande di Monticchio - lacustrine sequence
5 - Tenaghi Philippon - lacustrine sequence
6 - Ioannina - lacustrine sequence
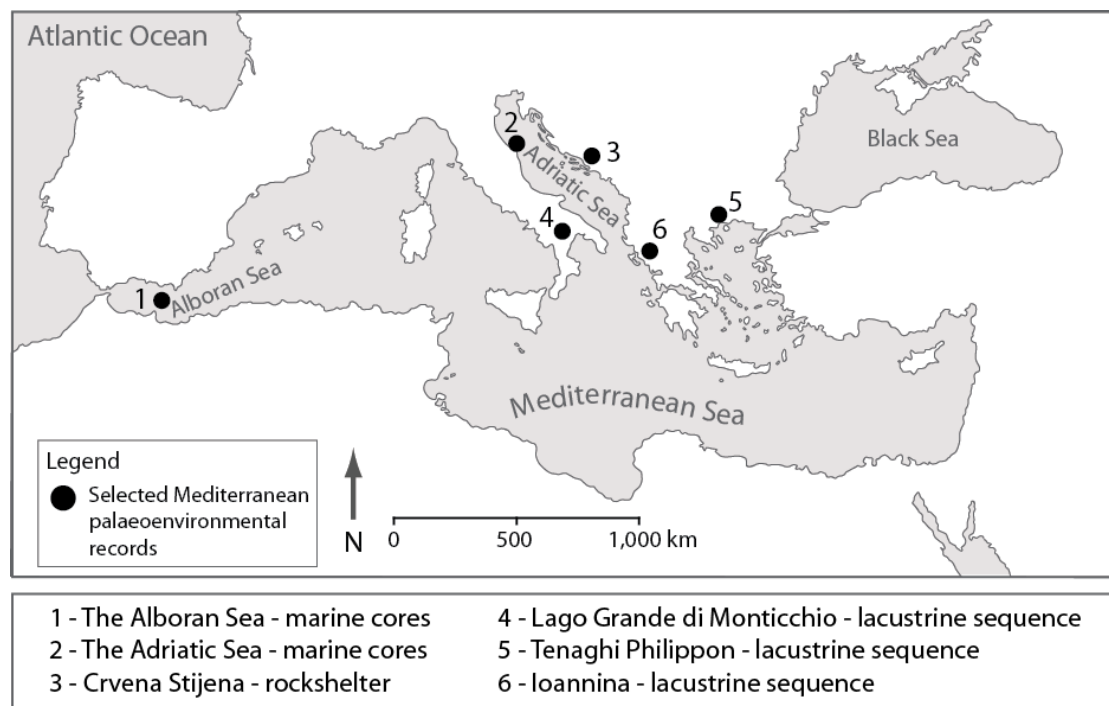
Figure 1.2 – A selection of key palaeoenvironmental records from depositional settings across the Mediterranean. These demonstrate the variety of archives across this region.

In the terrestrial record, one of the earliest investigations into the glacial history of the Mediterranean was undertaken by Bruno Messerli (1967). This remains one of the most comprehensive, though undated, syntheses of Mediterranean glaciation to date. Our understanding of the timing of glacial activity in the Mediterranean is now much better understood (Chapter 2), with evidence of Pleistocene glaciation during several glacial cycles since MIS 14. These glacial records are, however, inherently discontinuous and provide records only of cold climate conditions (Hughes 2006c; Lewis *et al*., 2009; Hughes *et al*., 2010; 2011b).

Mediterranean fluvial records also provide valuable archives of Quaternary environmental change. Since the early review of Quaternary fluvial sequences by Vita-Finzi (1969), a series of

well-dated alluvial records from both glaciated and unglaciated catchments across the Mediterranean has enhanced our understanding of Pleistocene landscape dynamics over multiple glacial-interglacial cycles (Macklin *et al.*, 2002; Macklin and Woodward, 2009; Chapter 2). Within glaciated basins these can contribute considerable detail to the glacial archives upstream (e.g. Woodward *et al.*, 2008; Lewis *et al.*, 2009).

On land, some of the most detailed archives of environmental change in the Mediterranean are derived from lacustrine sequences. A series of continuous palaeoecological records from sites such as Ioannina (Tzedakis, 1994) and Tenaghi Philippon (Wijmstra, 1969; Tzedakis, 1994; 1997; Tzedakis *et al.*, 2003; 2006) in Greece, and Lago Grande di Monticchio in southern Italy (Watts *et al.,* 1996; Allen *et al.*, 1999; Zolitschka *et al.*, 1996; Wulf *et al.*, 2004) (Fig. 1.2) present important records of environmental change extending as far back as 1.35 Ma (Allen *et al.*, 1999). These sites allow important correlations of the Mediterranean terrestrial record with global marine and ice core isotopic stratigraphies.

The Mediterranean Sea is also highly sensitive to Quaternary environmental change (Cacho *et al.*, 2002; Rohling *et al.*, 2009). Palaeoceanographic reconstructions reveal distinct precessional and obliquity signals, reflecting the strong influence of orbital parameters on the Mediterranean region (Lourens *et al.*, 1992; Lourens and Hilgen, 1997). The western Mediterranean is particularly sensitive to large scale and rapid climatic oscillations. Marine sedimentary records from the Alboran Sea display a close connectivity with the climatic variability recorded within the Greenland ice cores and deep ocean sediment records in the North Atlantic (Cacho *et al.*, 1999a; b; 2000; 2002; Nebout *et al.*, 1999; Fletcher and Sánchez Goñi, 2008; Sánchez Goñi *et al.*, 2008; Fletcher *et al.*, 2010; von Graftenstein, 1999). The eastern Mediterranean contains a series of sapropel horizons (organically-enriched accumulations) within the deep ocean sedimentary record (Rohling and Thunell, 1999). These reflect major changes in Mediterranean oceanographic conditions and have been used to highlight the impacts of orbitally-forced fluctuations in the African monsoon system upon the Mediterranean Sea (Rossignol-Strick, 1985; Cheddadi and Rossignol-Strick, 1995; Revel *et al.*, 2010). Tephra horizons within Quaternary sedimentary sequences of the central and eastern Mediterranean provide important time synchronous marker horizons. These tephra deposits are preserved within a range of environments such as marine sediments from the Adriatic Sea (Lowe *et al.*, 2007) as well as terrestrial lacustrine records from Lago Grande di Monticchio in Italy (Wulf *et al.*, 2004) and cave and rockshelter sediments at Crvena Stijena in Montenegro

(Morley and Woodward, 2011) allowing marine and terrestrial archives to be more securely correlated (Lowe *et al.*, 2007).

1.3 Mediterranean fluvial systems and Quaternary glaciation

Fluvial systems draining glaciated catchments are highly responsive to modifications in sediment supply and meltwater runoff regime (Clark, 1987). Recent work in the Mediterranean has shown that there were significant variations in both the extent of glaciation between Pleistocene cold stages (Kotarba *et al.*, 2001; Girauldi, 2003; Hughes *et al.*, 2006a) and the timing of maximum ice advance (Hughes and Woodward, 2008). This would have had considerable impacts on the meltwater and sediment characteristics within river basins downstream.

The classic synthesis of Mediterranean river basins by Vita-Finzi (1969) has been succeeded by several decades of investigation into the fluvial history of the Mediterranean. The dominant factors influencing river activity here include: tectonics, local lithology, and climatic change (including its impacts on glaciation and sea level) (Macklin and Woodward, 2009). In the mountainous regions of the Mediterranean, Quaternary glacial activity is considered one of the most important influences on river behaviour. Our understanding of the impacts of Quaternary glaciation on river systems downstream is, however, poorly understood and few studies have attempted to directly correlate Mediterranean glacial and fluvial records (see Sancho *et al.*, 2003; Bavec *et al.*, 2004; Lewis *et al.*, 2009; Woodward *et al.*, 2008). The Mediterranean provides a unique opportunity to explore these long-term landsystem interactions. The tectonic regime of many parts of the Mediterranean means that Quaternary fluvial records are commonly well preserved in the form of uplifted river terraces, or as sediment accumulations within subsiding basins. These may therefore provide a valuable, yet currently under-investigated record of Pleistocene glacial activity (Macklin and Woodward, 2009).

1.4 Research aims: the study region of Orjen, Montenegro

This study focuses on the Orjen massif in western Montenegro. During the Pleistocene, this part of the Balkans contained some of the largest ice masses of the Mediterranean basin (Hughes *et al.*, 2010; 2011b). Montenegro receives some of the highest precipitation totals in Europe. The mountains of Orjen are the wettest part of Montenegro, receiving an average of

4,962 mm/yr (Chapter 3). During the Pleistocene, these high precipitation inputs sustained the development of ice caps and valley glaciers at elevations below 2,000 m a.s.l. (Hughes *et al*., 2010). Fluvial sediments and landforms are well preserved in most of the valleys that drain from Mount Orjen. These are situated within a classic mountain limestone karst environment and contain a range of alluvial depositional settings that are representative of upland glacierized basins in many parts of the Mediterranean. The close proximity of glacially moulded uplands, downstream alluvial environments and the coastal zone means that in the region surrounding Orjen it is possible to develop an integrated reconstruction of landsystem dynamics both on and offshore. The research has four overarching aims:

- To establish the nature and timing of fluvial response to Pleistocene glaciation in Montenegro, and explore its wider significance for glaciated catchments across the Mediterranean and elsewhere.
- To examine the stratigraphy and sedimentology of the fluvial record in a range of depositional contexts.
- To examine post-depositional pedogenic and surface processes and establish the palaeoenvironmental significance of secondary carbonates formed within alluvial deposits.
- To test current hypotheses of fluvial geomorphological and sedimentological response to Pleistocene glacial activity.

The thesis is divided into three sections:

Section 1 discusses the background to the research, and incorporates: Chapter 2 – Literature Review – Pleistocene Glaciation and River Behaviour: Global and Mediterranean Perspectives; Chapter 3 – Study Area; and Chapter 4 – Field and Laboratory Methods.

Section 2 presents the results of field and laboratory analysis within four chapters: Chapter 5 – Field Evidence: Geomorphology and Sedimentology; Chapter 6 – Laboratory Evidence: Particle Size Analysis and Carbonate Content; Chapter 7 – Secondary Carbonates: Field Macromorphology and Thin Section Micromorphology; and Chapter 8 – Geochronology: U-series and Harden Index.

Section 3 develops the overall findings and implications of the research within Chapter 9 – Discussion and Implications; and Chapter 10 – Conclusions and Further Research.

Pleistocene Glaciation and River Behaviour: Global and Mediterranean Perspectives

Synopsis

Our understanding of Pleistocene Mediterranean glacial activity and landscape processes has been greatly advanced over the last few decades. This is due to the increased application of radiometric dating methods, such as uranium series (U-series), cosmogenic nuclide and luminescence techniques, to morphosedimentary sequences within glaciated basins. Used in conjunction with stratigraphical and sedimentological data these methods have allowed glacial landforms to be more effectively correlated to fluvial archives downstream. Unfortunately, however, the majority of well-dated fluvial archives are derived from unglaciated catchments (Woodward *et al.*, 2008) (e.g. Fuller *et al*., 1998; Macklin *et al*., 2002; Demir *et al*., 2004; Santisteban and Schulte, 2007; Bridgland and Westaway, 2008; Schulte *et al.,* 2008) and few studies have developed an integrated analysis of glacial and fluvial systems at the river basin scale over multiple glacial-interglacial cycles.

This review explores the impacts of Pleistocene Mediterranean glaciation on fluvial systems downstream. It focuses specifically on the timing and nature of glacial activity and its impacts on fluvial morphosedimentary dynamics. Section 2.1 discusses the dominant current hypotheses of long-term landscape processes within glaciated basins. These ideas are tested in Section 2.2 using Pleistocene morphosedimentary and geochronological evidence from selected catchments across the globe. These hypotheses are explored in more detail in Sections 2.3 and 2.4 which develop a Mediterranean-wide synthesis of Pleistocene glaciation and fluvial activity using over 200 published ages. This provides context for current investigations in the glaciated catchments surrounding Mount Orjen, western Montenegro.

2.1   Pleistocene glacial and fluvial interactions: concepts in Quaternary geomorphology

Some of the earliest work on Quaternary fluvial records was undertaken in the European Alps by Penck and Brückner (1909) who proposed a fundamental model of cold stage alluviation and warm period incision (Chapter 1). This pattern is evident in the geomorphological records of many river systems, from glaciated and unglaciated basins, across the world (e.g. Bridgland, 1994; Rittenour *et al.*, 2007; Lewis *et al.*, 2009). These archives highlight the role of Quaternary

climatic change in driving fluvial landscape processes (Knox, 1985). In many mountain regions, Quaternary glacial activity has also significantly influenced landscape dynamics. As will be discussed, the impacts of glaciation on river systems downstream can often lead to highly contrasting morphosedimentary signatures between glaciated and unglaciated catchments.

2.1.1 Unglaciated basins

Within unglaciated basins the dominant controls on river regime are: tectonic activity and associated uplift; and climatically-induced changes in vegetation, hydrological regime and sediment flux (e.g. Macklin *et al*., 2002; Maddy *et al*., 2008). River systems respond to these autogenic and allogenic forcing factors over multiple spatial and temporal scales. In many cases they can be conditioned by large-scale Quaternary climatic changes but also reflect intrinsic, basin-scale processes (Gibbard and Lewin, 2009). In the Mediterranean, since the classic work of Claudio Vita-Finzi (1969), many studies have highlighted the dominant influence of Quaternary climate change on river system characteristics. Macklin *et al*. (2002) have reviewed the geochronological and morphosedimentary records of 11 Mediterranean catchments; in Spain, Libya and Greece. Alluviation phases broadly correspond to Pleistocene cold stages during the last 200,000 years. At least 13 major alluviation episodes have been identified since MIS 6. The observed synchrony of these episodes across basins with highly contrasting tectonic regimes suggests that regional climatic change is the dominant driver of fluvial dynamics in these systems over timescales of 10^3 to 10^4 years (Macklin *et al*., 2002). Catchment-specific variations in the amplitude, frequency and duration of these aggradation/incision phases (Macklin *et al*., 2002), however, highlight the local-scale conditioning of fluvial process response to allogenic forcing (Gibbard and Lewin, 2009).

Elsewhere in the Mediterranean, several studies demonstrate the interactions between external climatic drivers and internal tectonic forcing and their impacts on river activity. Aggradation and incision cycles in the Aguas and Feos valleys of southeast Spain reflect landscape processes driven by Quaternary climatic oscillations, set within a more localised framework of tectonic control (Harvey and Wells, 1987; Maher *et al*., 2007). In contrast, the Ebro basin, northeast Spain, presents only minor tectonic influence on Quaternary landscape processes. Here, Fuller *et al*. (1998) developed a detailed infrared stimulated luminescence (IRSL) chronology of the Rio Guadalope. Four major geomorphological phases are identified at: 183-130 ka (aggradation during MIS 6); 130-122 ka (incision during MIS 5e); 122-121 ka (aggradation at the MIS 5e/d transition); and 111 ka (aggradation during MIS 5d). Each major

phase of aggradation occurred during cool or cooling conditions, whilst incisional phases corresponded to interstadials/interglacials. Climate-controlled variations in runoff and sediment supply are considered the dominant drivers of Pleistocene river behaviour in the Guadalope basin, whilst tectonic activity plays only a minor role in fluvial system development (Fuller *et al.*, 1998).

In Turkey, where tectonic activity exerts a major control on landscape dynamics (Demir *et al.*, 2004) Maddy *et al.* (2008) suggest that a Quaternary climatic signal is still clearly discernible within the fluvial record. Alluvial fan and floodplain deposits within the Gediz river basin present a cyclic alluviation-incision pattern through the Quaternary. Sediment transport and depositional phases are associated with warm-cold transitional periods, characterised by increased discharge and sediment supply. During cold-warm transitions, increasing vegetation cover is thought to have inhibited sediment supply, whilst sustained runoff would have led to fan entrenchment. In this system, Quaternary climatic fluctuations are considered the dominant control on sediment supply and delivery within an uplift-driven basin (Maddy *et al.*, 2008). This highlights the interaction between external climatic forcing and more local catchment processes in the development of Quaternary fluvial landscapes (Gibbard and Lewin, 2009).

2.1.2   Glaciated basins

Fluvial processes within glaciated catchments can vary significantly from ice-free basins. The advance and retreat of Quaternary ice margins influenced the hydrological regime and sediment dynamics of many river systems (Østrem, 1975; Rittenour *et al.*, 2007) producing highly distinctive sediment transportation and depositional characteristics (Fisk, 1951; Avouac *et al.*, 1993; Baker, 1994; Hamilton, 2001; Nádor *et al.*, 2003; Doğan, 2010; Salcher and Wagreich, 2010). In some instances these systems are still adjusting to the glacially-driven landscape alterations of Pleistocene cold stages. Glaciers are highly erosive geomorphological agents and glaciated catchments frequently have much higher sediment yields than unglaciated regions (Dühnforth *et al.*, 2008). Dühnforth *et al.* (2008) explored the influence of Pleistocene glaciation on long-term sediment evacuation in the eastern Sierra Nevada, California. Empirical and conceptually-modelled data from two neighbouring basins indicate a strong positive relationship between the percentage glaciated area of each valley and the depth of fan head incision. Catchments with 'significant glacial activity' (i.e. ≥50% glaciated) present up to 40 m of fan incision, whilst fan sediments in unglaciated basins were incised to

only 5 m. The thickness of deposits was also estimated to be 20-50% greater within glaciated catchments than in unglaciated basins, and also displayed a more variable spatial sediment distribution. This is associated with the greater sediment production and storage capacity of glaciated basins, which provides long-term sources of glacigenic sediments (Dühnforth *et al.*, 2008).

Within glaciated catchments, the classic dichotomy of cold-stage aggradation and warm-period incision (Penck and Brückner 1909; Rittenour *et al.*, 2007; Dühnforth *et al.*, 2008; Lewis *et al.*, 2009) has been increasingly challenged by several studies highlighting the geomorphological significance of climatic *transitional* periods (Bridgland, 1994; Macklin *et al.*, 2002; Vandenberghe, 1995; 2008). Under this model, full glacial and interglacial conditions may have been characterised by relative geomorphological quiescence with the development of extensive permafrost/frozen ground or vegetation cover, respectively. Evidence of fluvial instability has been demonstrated during warm-cold (i.e. during glacier build-up) and cold-warm (deglacial) transitions. Marren (2005) presents an idealised model of glacial meltwater discharge (Fig. 2.1) in response to changes in glacial mass balance over a full glacial cycle. Maximum discharge is suggested to occur shortly after the glacial maximum, with the onset of mass wastage during deglaciation. In this model, meltwater discharge returns to a baseline minimum during interglacial stages.
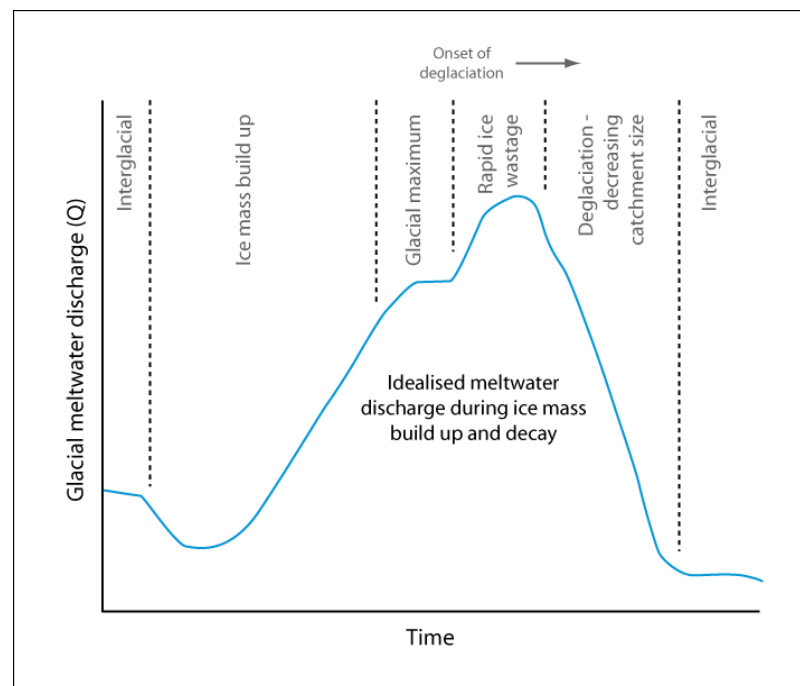
Figure 2.1 – Idealised model of glacial meltwater discharge over a full glacial cycle. Based on a synthesis of observations from existing meltwater studies. Adapted from Marren (2005).

This leads us to consider how the sediment flux of glaciated catchments might map onto this meltwater curve, particularly with regard to any leads or lags of meltwater-sediment interactions. Glacial mass balance oscillations during individual glacial cycles, or during stadials and interstadials, may also produce more complex meltwater and sediment dynamics than such simplified models might suggest. Sediments prepared by glacial action during a given period may not be readily transported until conditions become more favourable, for example, through increased discharge during a subsequent climatic regime (Østrem, 1975). Sediment transfer within glaciated catchments can therefore be perturbed by storage and redistribution at a variety of timescales. Alluvial sequences may not necessarily reflect the meltwater patterns of an individual glacial cycle and could instead record a palimpsest of fluvial responses to headwater glacial activity.

In this regard, the paraglacial sedimentation hypothesis, first defined by Church and Ryder (1972) as a non-glacial process directly conditioned by glaciation, provides a useful model of long-term morphosedimentary response to glacial activity (see discussions in: Church and Ryder, 1972; Church and Slaymaker, 1989; Ballantyne, 2002; Meigs *et al.,* 2006). The term refers to the prolonged redistribution of glacially-derived sediment following glacial advance (Church and Ryder, 1972; Fig. 2.2) whilst the landscape reverts back to primary denudation (Ballantyne, 2002). Consequently, within glaciated basins, landforms and sediments constituting the paraglacial landsystem (Evans, 2003) are considered the storage component of an interrupted 'sediment cascade' (Ballantyne, 2002). Internal sediment storage can form a significant source of readily erodible material, which is important for sustaining the long-term evacuation of sediment over multiple timescales (Dühnforth *et al.*, 2008). Glacial activity generates sediment storage space through a variety of mechanisms such as: the overdeepening of hollows; the development of talus deposits; and the oversteepening of slopes. These glacially-moulded landscape components form effective sediment traps that can be exploited through fluvial activity, mass wasting and further glacial erosion during later climatic phases. Unglaciated catchments have a comparatively limited capacity to develop this sediment accommodation space. Instead, sediment within unglaciated basins is deemed to be transported quasi-continuously and fluctuations between net deposition and incision are less apparent than in glaciated settings (Dühnforth *et al.*, 2008) (Fig. 2.3).

The degree of glaciation not only influences the spatial distribution of sediment storage within a catchment (Dühnforth *et al.*, 2008), but also the patterns of sediment evacuation over time. As ice margins advance and retreat, different zones of the paraglacial sediment assemblage

become eroded, overrun by ice, exposed and reworked at different times. This can cause temporal shifts in the locations of sediment sources and the depocentres downstream. In comparison to unglaciated basins, this may lead to higher amplitude oscillations in river discharge, sediment aggradation, and incision, as the landscape is moulded by successive glacial cycles (Marren, 2005; Dühnforth *et al.*, 2008).
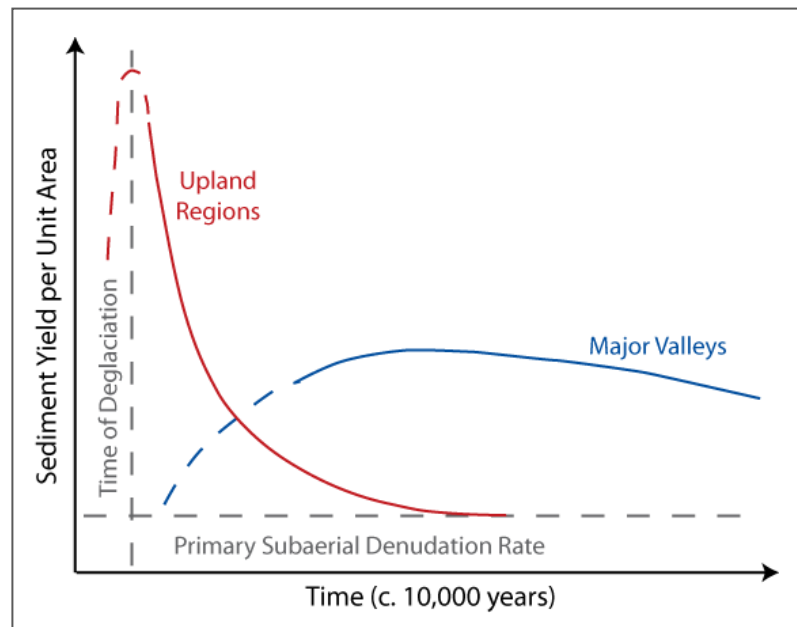
Figure 2.2 – Schematic representation of paraglacial sediment yield within glaciated basins over time. Adapted from Church and Slaymaker (1989).

One major conceptual limitation of the paraglacial theory is the assumption that between glacial phases the landscape resumes a state of 'background stability'. Defining the characteristics of such landscape equilibrium is problematic. Successive glacial phases might not occur with sufficient time interval to allow the landscape to attain a state of primary denudation. The abundance of sediment accommodation space within glaciated basins means that paraglacial sediment entrainment may be rejuvenated long after the initial phase of paraglacial debris transport and deposition (Ballantyne, 2002). Fluvial sedimentation within glaciated basins does not always exclusively reflect contemporaneous land surface erosion, and may also comprise sediments delivered to the system during previous climatic cycles and remobilised once boundary conditions have changed (Schumm, 1978). This is highlighted in the glacial and fluvial records of Pleistocene glaciation in the Trevinca Mountains in Galicia northwest Spain (Alberti *et al.*, 2011). Sediments deposited at the confluence of two glaciers have been dated using optically stimulated luminescence (OSL) methods to 27 ± 2 ka, 31 ± 3 ka, and 33 ± 3 ka (MIS 4-3). Morphosedimentary evidence indicates that ice marginal

fluctuations and landscape instability have led to the reworking of existing deposits, and only small remnants of the original sedimentary sequence are preserved. This forms a palimpsest of deposits, each of different age and transportation-deposition history.
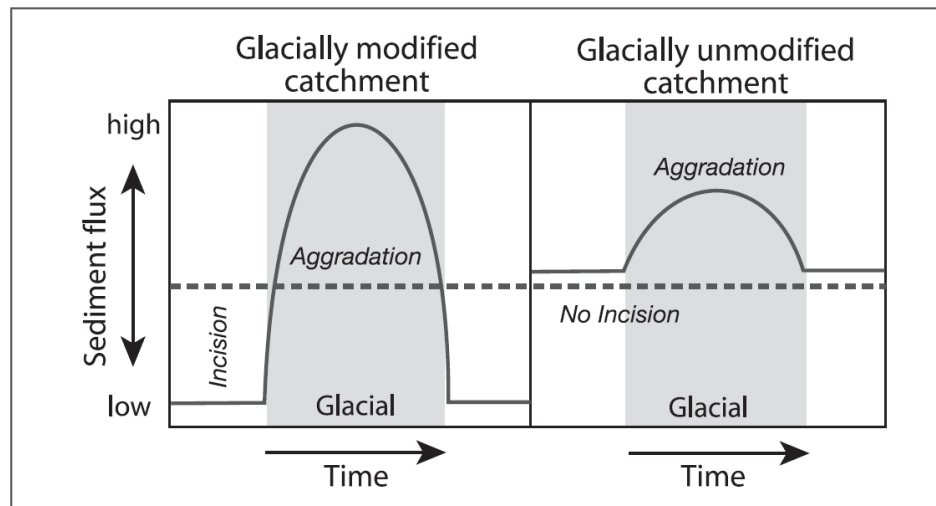
Figure 2.3 – Conceptual model of the relative sediment flux over time within glaciated and unglaciated catchments. From Dühnforth *et al*. (2008).

Studies have demonstrated that landscape relaxation time following deglaciation is in the order of $10^1 - 10^4$ years (Church and Slaymaker, 1989; Ballantyne, 2002). This is likely to vary between different components of the paraglacial landform assemblage, potentially prolonging the paraglacial period and forming different morphosedimentary records within neighbouring valleys. This is discussed in a recent study of the landform associations surrounding the North Patagonian Icefield and associated outlet glaciers (Glasser *et al*., 2010). Individual geomorphological settings surrounding a central ice mass have responded very differently to glacial activity and have produced contrasting morphosedimentary expressions within both glacial and glaciofluvial settings. Evidence from the Rocky Mountains and the European Alps also suggests that within a single mountain range, glaciers may reach different maximum extents at different times (Gillespie and Molnar, 1995). This can produce 'asymmetrical' and 'asynchronous' Pleistocene sedimentary records within contrasting depositional settings, and has not yet been studied in detail. Within individual basins, fluctuations in the position of the ice margin over a single glacial phase can lead to adjustments in fluvial style downstream. During ice advance, a given location in front of the ice margin can be transformed from an ice-distal to ice-marginal depositional environment. This has important implications for the development and preservation of the Quaternary fluvial sedimentary record (Miall, 1996; Bini and Zuccoli, 2004; Cordier *et al*., 2006).

2.2   Fluvial response to Pleistocene glaciation: a global perspective

The conceptual models of Pleistocene glacial and fluvial interactions can be tested against empirical morphosedimentary archives of Pleistocene glacial activity. Several of the most securely-dated records from four glaciated catchments, in four continents (Table 2.1), are used to explore current hypotheses of the timing and nature of fluvial response to headwater glaciation. This provides a broad representation of Pleistocene glacial-fluvial interactions to which the Mediterranean record can be compared (Section 2.4). Case studies focus on fluvial systems draining valley glaciers or outlet glaciers from larger ice caps, which allow representative comparisons to be drawn with Mediterranean Pleistocene systems.

Author	Location	Latitude, Longitude	Mountain Range	Max. Elevation (m a.s.l.)	Dominant Lithology	Valley	Max. Ice Extent	Dating Method	MIS
Schildgen *et al.* (2002)	Colorado, N.America	39.9668 N, 105.4776 E	Colorado Front Range	-	Granite	Boulder Canyon	-	^{26}Al, ^{10}Be, ^{14}C	1, 2-3 and 5-6
Hein *et al.* (2009)	Argentina, Patagonia	-47.2500 N, -71.0000 E	Andes	-	Granite	Lago Pueyrredón Valley	-	^{26}Al, ^{10}Be,	2-3, 3, 5 and 8
Xu and Zhou (2009)	Southeast Tibetan Plateau	29.1266 N, 100.2175 E	Shaluli Mountains	> 5,000	Cretaceous Granite, Triassic Slate	Kuzhaori and Daocheng Valleys	3,600 km²	ESR	2, 3, 6, 12/14 and 16
Rother *et al.* (2010)	New Zealand	-42.5883 N, 172.5738 E	Southern Alps	2,300	-	Hope Valley	40 m	IRSL	3-5, 6 and >6?

Table 2.1 - Geochronological records from Pleistocene glacial and fluvial deposits in selected glaciated catchments across the world. Dashed lines indicate unavailable data. These records are used to create a representation of Pleistocene glacial-fluvial interactions and test current hypotheses of the timing and nature of glacial activity and fluvial system response.

2.2.1   North America: The Rocky Mountains

A wealth of empirical studies has been undertaken in the glaciated catchments of North America (see Desloges, 1990; Knox, 1996; Philips *et al.*, 1997; Hamilton, 2001; Brardinoni and Hassan, 2006; Hanson *et al.*, 2006; Laabs *et* al., 2007; Rittenour *et al.*, 2007; Hartman and Clague, 2008). Glacial and fluvial morphosedimentary records have been dated using a variety of geochronological techniques and indicate that individual basins often present highly contrasting Quaternary glacial histories. River terraces in Middle Boulder Creek of the Colorado Front Range, Rocky Mountains, record episodic aggradation and incision phases in response to Quaternary glacial fluctuations (Schildgen *et al.*, 2002). Three major depositional phases have been identified (Fig. 2.4) and have been dated using ^{26}Al and ^{10}Be exposure

techniques to 164-108 ka (MIS 6), c. 32-10 ka (MIS 3-2) and <10 ka (Holocene). No sediments pre-dating MIS 6 have been identified.
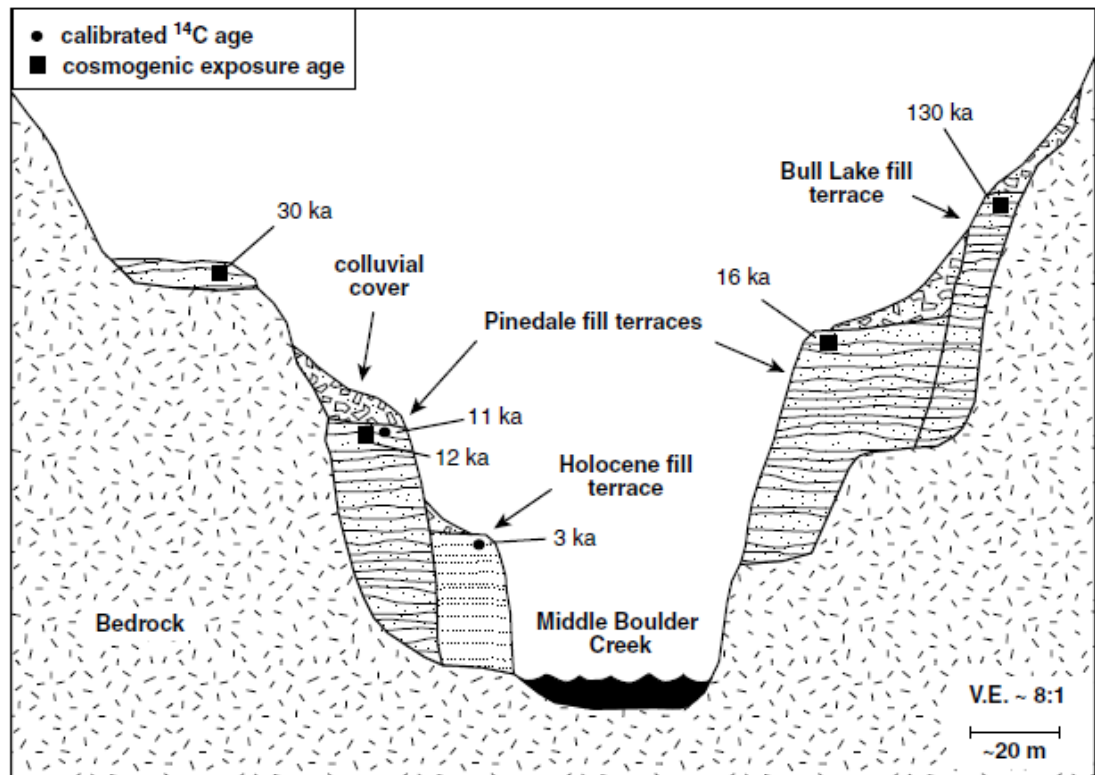
Figure 2.4 – Schematic cross-section of terraces in Middle Boulder Creek, Colorado. From Schildgen *et al*. (2002).

Alluviation phases largely corresponded to periods of ice retreat when the exposure of extensive tracts of unconsolidated sediments and heightened meltwater discharge led to sediment aggradation for up to 30 km downstream. The subsequent transition to full interglacial conditions was characterised by net incision and the isolation of terrace surfaces. The occurrence of deposition and incision during climatic transitional phases supports the notion that periods of morphogenesis are not always confined to phases of full glacial or interglacial conditions. Instead, longer-term fluctuations in the deposition and exposure of sediments may be important for the development of sedimentary records within glaciated basins.

2.2.2   South America: Patagonia

Patagonia contains some of the most complete Quaternary glacial sequences in the world (Clapperton, 1993). Recent investigation of Pleistocene glaciofluvial systems in the Lago Pueyrredón valley, Argentinean Patagonia (Hein *et al*., 2009; 2011) has considerably enhanced our understanding of headwater glacial dynamics within this region. During the Quaternary, this valley has been repeatedly glaciated by an outlet glacier of the Patagonian ice sheet, which has formed a series of moraines and outwash terraces. A lack of intact dateable material means that only limited data are available from the glacial record prior to the last glacial maximum. Instead ^{26}Al and ^{10}Be exposure techniques have been used to directly date outwash gravels deposited in association with headwater glaciation (Hein *et al*., 2009; 2011). Major advances of the Patagonian ice sheet have been identified within the fluvial record at c. 1.2 Ma, c. 600 ka (c. MIS 16), and c. 260 ka (MIS 8). Deposits from MIS 6 and MIS 4 have not been identified. The innermost moraine and outwash sediments, dated to c. 27-25 ka (MIS 3-2), were indicative of the local LGM, and slightly precede the global last glacial maximum of MIS 2 (Section 2.3). It is possible that glaciers from the local LGM were more extensive than the ice masses of MIS 6 and 4, and have destroyed the evidence of these previous cold stages. The excellent preservation of the fluvial record prior to MIS 6 highlights the potential of these sequences to allow us to understand Quaternary glacial activity more fully (Hein *et al*., 2011).

2.2.3   Asia: The Himalaya

The Quaternary glacial and hydrological history of the Himalaya-Tibetan orogen has been reviewed in detail by Owen *et al*. (2008). Considerable variation in the timing of Pleistocene glacial and fluvial activity is evident across the region, yet in many catchments geochronologies are currently poorly constrained (Benxing and Rutter, 1998; Owen *et al*., 2008). The increasing application of radiometric dating techniques, however, is helping to develop more comprehensive dating frameworks (see Owen *et al*., 2005; Kong *et al*., 2009; Xu and Zhou, 2009). For example, electron spin resonance (ESR) ages from moraines and river terraces (Fig. 2.5) in the Daocheng and Yazhe River Valleys, of the Haizi Shan in the south eastern Tibetan Plateau (Xu and Zhou, 2009) have allowed the glacial record to be securely correlated to the fluvial archive downstream. During the Quaternary, an ice cap of c. 3,600 km^2 was centred upon the Haizi Shan. Glacial deposits record a total of six major ice advances, each of decreasing extent, since the Mid-Pleistocene (MIS 16, 14/12, 6, 3, 3-2 and 2) and the fluvial records reflect four of these advances (MIS 16, 12, 6 and 2). Fluvial aggradational phases are

correlated with periods of deglaciation in the upper reaches of the Haizi Shan, and the heightened meltwater and sediment flux downstream. These landscape dynamics correspond to the geochronological evidence from glaciated catchments elsewhere (e.g. Amorosi *et al*., 1996; Schildgen *et al.,* 2002) that demonstrates the important influence of climatic transitional periods on the Quaternary morphosedimentary record.
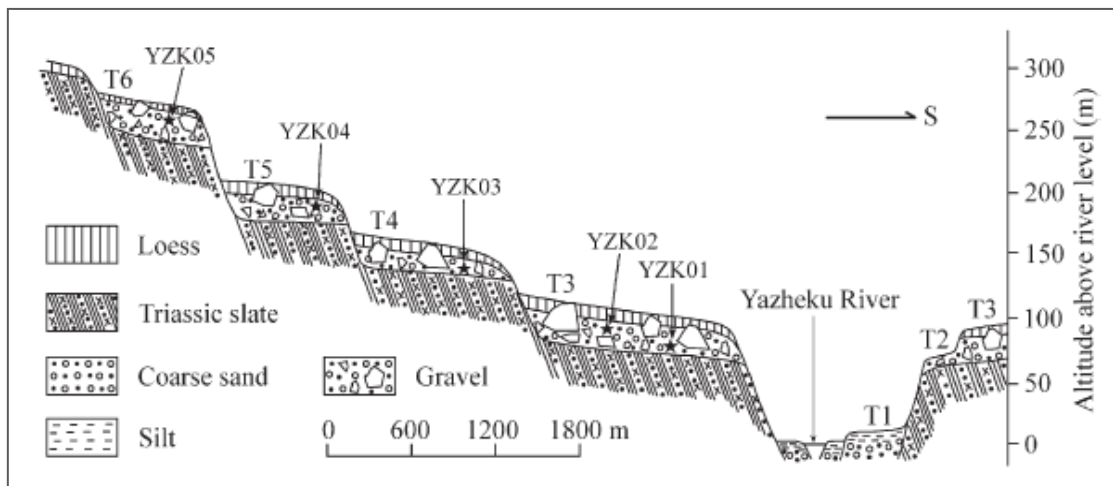
Figure 2.5 - Cross sectional profile of terraces in the Yazheku Valley. From Xu and Zhou (2009).

2.2.4 Australasia: New Zealand

The Pleistocene glacial record of New Zealand presents a valuable archive of mid-latitude environmental change in the Southern Hemisphere. During Pleistocene cold stages, mountain glaciers here frequently extended as far as the coastal zone (Suggate, 1990). In the Hope River Valley of the Southern Alps, for example, glaciers advanced up to 40 km from their headwall, reaching the coast of the Tasman Sea (Rother *et al.,* 2010). Postglacial fluvial incision has exposed a succession of glacial, glaciofluvial and lacustrine sediments (Fig. 2.6) from over nine depositional phases that reflect two major ice advances and one minor readvance.

Periods of glacial advance correspond to the deposition of extensive glaciofluvial sequences, whilst glacial retreat phases are linked to the deposition of proglacial fans, mass flow diamicts and glaciofluvial fines (Rother *et al*., 2010). Six IRSL dates from fluvial sands yield ages ranging from 197.7–164.9 ka to 124.9–105.1 ka and are correlated to MIS 6. Prior to the investigation of the palaeohydrological sequence within this valley (Rother *et al*., 2007; 2010), the glacial evidence alone was believed to reflect ice advance no earlier than the local LGM (Suggate, 1965). As observed elsewhere (see Woodward *et al*., 2008; Lewis *et al*., 2009), this study

presents evidence for the remobilisation of glacigenic sediment over multiple climatic cycles, and highlights the importance of integrating both glacial and fluvial records to develop a more comprehensive reconstruction of Quaternary landscape dynamics.
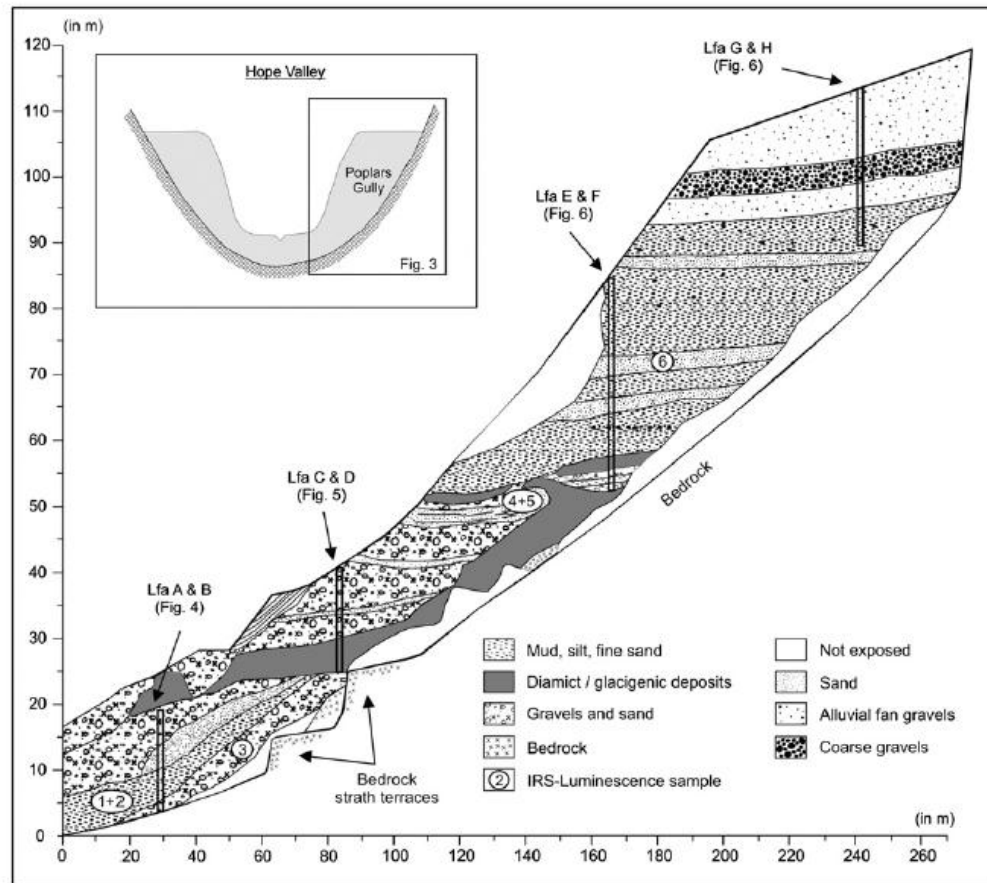
Figure 2.6 – Cross section of the lithofacies assemblage within the Hope River Valley, Southern Alps. From Rother *et al*. (2010).

2.2.5   A global geochronological framework

Using the geochronological data obtained from these selected glaciated catchments (Table 2.1) it is possible to explore the nature of glacial-fluvial interactions within a range of depositional settings. This also allows the geochronological data to be tested against current hypotheses of the timing of fluvial activity in response to glacial dynamics. Figure 2.7 displays the age indicators from glacial and fluvial deposits within each study region. It should be highlighted that the different dating techniques represent minimum or maximum ages and can therefore reflect phases of aggradation or quiescence. Cosmogenic methods, for example, provide minimum ages of exposure upon deglaciation. Similarly, U-series ages reflect periods of land

surface stability, rather than initial landform development. By contrast, ^{14}C and luminescence techniques (e.g. OSL, IRSL, and TL) more closely record the time of deposition. These distinctions are highlighted in Figure 2.7 through the use of open and opaque bars, for minimum and maximum ages, respectively. Data are plotted against an East Pacific $\delta^{18}O_{benthic}$ record and total arboreal pollen (TAP %) record from Tenaghi Philippon, Greece (Tzedakis, 2006) to indicate the broader, global and Mediterranean-scale Quaternary climatic cycles. For ease of analysis, the age indicators are displayed by date only and do not necessarily resemble the stratigraphic order in which they were initially studied. This allows the spatial patterns of glacial and fluvial dynamics to be more readily observed and correlated.

In many catchments, such as the Colorado Front Range and the Lago Pueyrredón valley, Argentina, the fluvial record has been used to more effectively constrain the timing of headwater glacial activity. Geochronological data from a number of valleys (Shaluli Mountains, Tibetan Plateau; Colorado Front Range) suggest that the dominant phases of meltwater and sediment flux occurred during glacial-interglacial transitions. These catchments track the idealised meltwater curve of Marren (2005) where maximum meltwater discharge occurs during deglaciation. Other catchments, such as the Hope Valley, New Zealand, instead indicate that thick glaciofluvial sequences are deposited during ice advance (Rother *et al*., 2010).

In the Colorado Front Range, morphosedimentary records suggest that the exposure of glacigenic sediments upon ice retreat can lead to an extended (i.e. paraglacial) period of sediment erosion and deposition. This highlights the importance of internal sediment stores within glaciated catchments in determining the nature of fluvial morphosedimentary response to glacial activity, when compared to ice-free basins (Dühnforth *et al*., 2008).

In the Southern hemisphere, ages obtained from the Lago Pueyrredón valley, Argentina, record a major ice advance during MIS 8 (Hein *et al*., 2009; 2011), whilst fluvial sediments in the Hope Valley, New Zealand represent glacial activity no earlier than MIS 6 (Rother *et al*., 2010). In the Northern Hemisphere, depositional phases dated to MIS 6, 3-2 and 2 are evident in both North America (Schildgen *et al*., 2002) and the Tibetan Plateau (Xu and Zhou, 2009). The discontinuous nature of glacial and fluvial records throughout the Middle to Late Pleistocene reflect both the spatially variable nature of global palaeoclimatic change, and the differential preservation of the glacial record within contrasting settings.
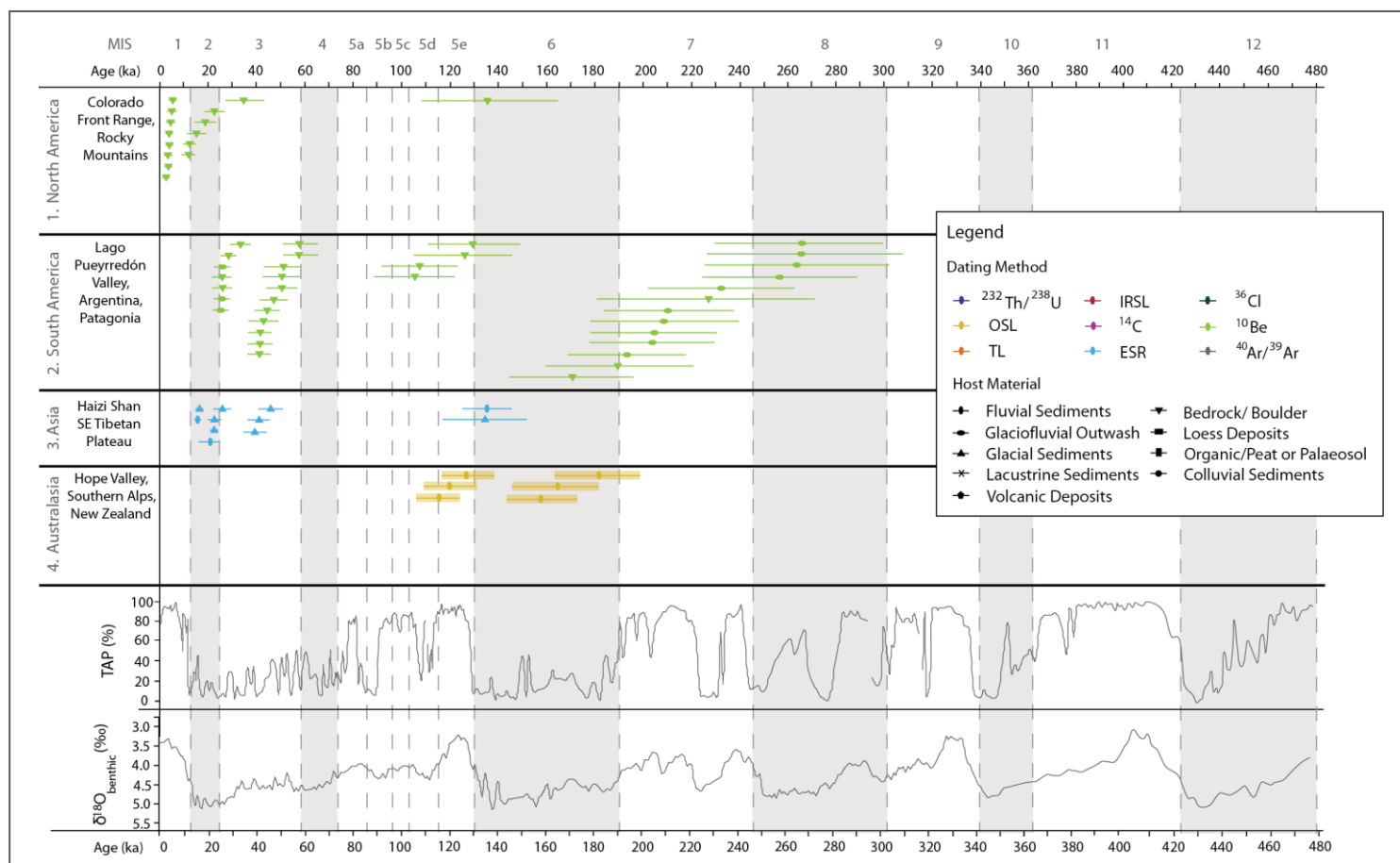
Figure 2.7 - Pleistocene glacial and fluvial geochronological records from selected glaciated catchments across the world. Dates are presented according to dating method and the host sediment body. Based on the published data outlined in Table 2.1. Correlation with global multi-proxy records is provided by an East Pacific $\delta^{18}O_{benthic}$ record and a total arboreal pollen (TAP %) record from Tenaghi Philippon, Greece (Tzedakis, 2006). Shaded bars are used to differentiate successive marine isotope stages (MIS).

2.3 Fluvial response to Pleistocene glaciation: Eurasian ice sheets

2.3.1 Pleistocene ice sheet dynamics

European fluvial systems have not only responded to mountain glaciation but have also been significantly influenced by large continental ice sheets that extended over the European mainland during the Middle and Late Pleistocene. These have altered the catchment dynamics and meltwater pathways of many fluvial systems draining into the Mediterranean (Arkhipov *et al*., 1995; Toucanne *et al*., 2009). As well as large scale transformations in meltwater and sediment supply routes between glacial phases, ice sheet margin fluctuations during individual glaciations, in the order of tens of hundreds of kilometres, also led to changes in drainage conditions. The glacial history of these continental-scale ice masses therefore provides important context for the landscape dynamics of southern Europe.

Ice sheets are defined as thick accumulations of glacier ice covering >50,000 km^2 and largely submerging the underlying topography (Sharp, 1988). During the Pleistocene an extensive Eurasian ice sheet complex developed from the advances of the Scandinavian, Barents and Kara ice sheets (Rinterknecht *et al*., 2006; Fig. 2.8). The extent and glacial regime of these ice masses varied considerably between glacial cycles. The Scandinavian ice sheet is considered to have broadly increased in size with each glaciation, whilst the Barents-Kara ice sheet progressively diminished in extent during the Middle and Late Pleistocene (Svendsen *et al*., 2004).

In the Middle Pleistocene two distinct drainage patterns developed from the Eurasian ice sheet. During the Drenthe substage, marking the Saalian (>130 ka, MIS 8 – 6) glacial maximum, the catchment area of the Mediterranean attained its maximum extent (Fig. 2.8d), with a total ice front of up to 5,000 km in length. The formation of several large proglacial lakes diverted drainage towards the River Danube and into the Black Sea, as well as southwards towards the Mediterranean (Arkhipov *et al*., 1995). A significant proportion of meltwater delivered to the Mediterranean region at this time was also supplied by fluvial systems to the east of the ice sheet, including the Ob, Irtysch, Yenisei and Tunguska catchments in Siberia (Arkhipov *et al*., 1995).
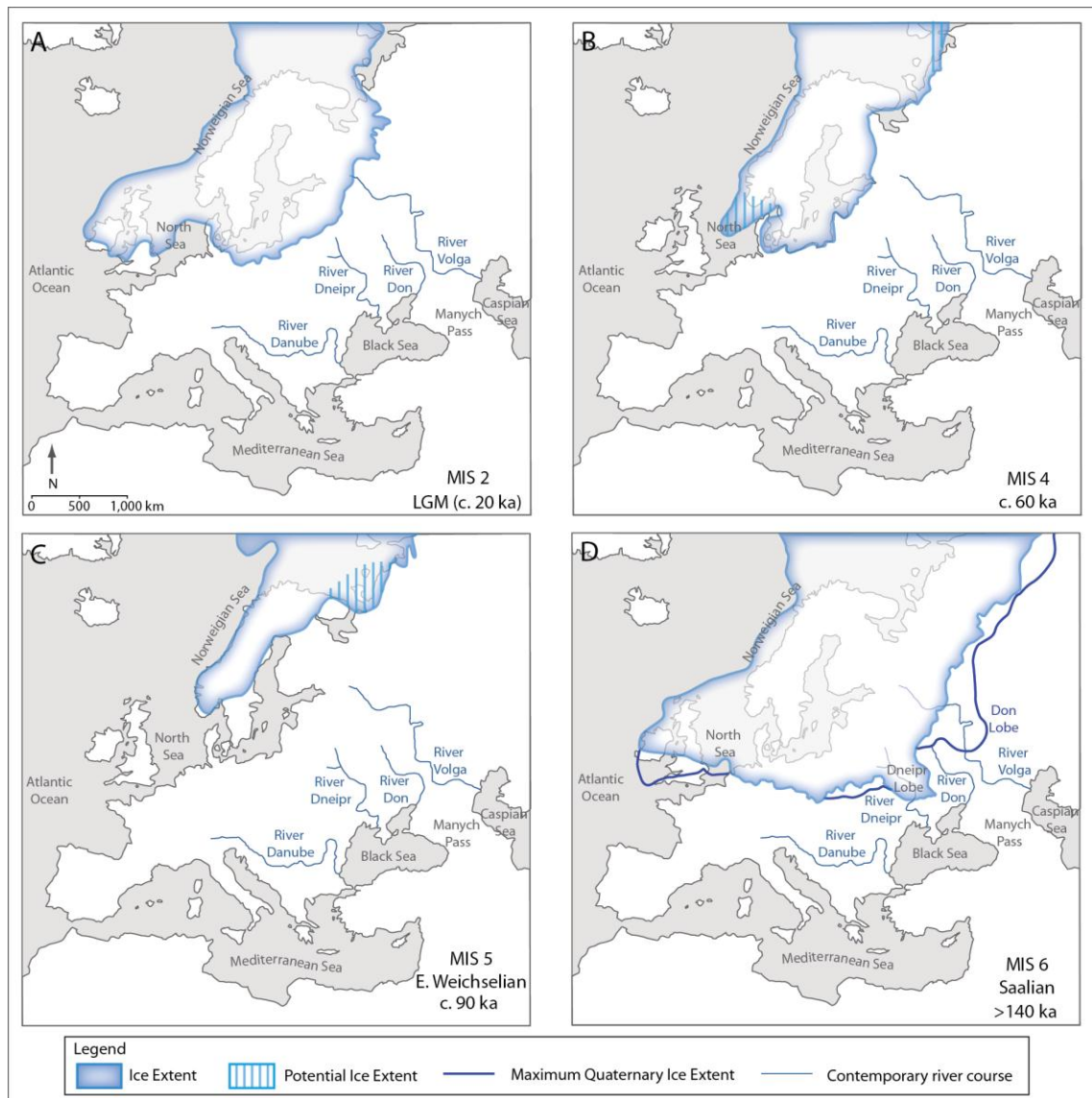
Figure 2.8 - Pleistocene ice sheet extent in Northern Europe at: A) c. 20 ka (LGM, MIS 2); B) c. 60 ka (MIS 4); C) c. 90 ka (Early Weichselian, MIS 5); and D) >140 ka (Saalian, MIS 6). Based on reconstructions discussed by Arkhipov *et al*. (1995); Mangerud *et al*. (2004); Rinterknecht *et al*. (2006).

During the Warthe substage of the late Saalian ice cover was less extensive and meltwater drainage was concentrated along the River Volga towards the Caspian Sea. Meltwater at this time may have also drained into the Black sea, via the Manytsh Depression (Manych Pass), before reaching the Mediterranean.

In the Late Pleistocene (Weichselian, MIS 5d-2) OSL ages from lacustrine sequences (Mangerud *et al*., 2004) indicate two intervals of meltwater diversion across mainland Europe and towards the Mediterranean. Extensive, ice-dammed, proglacial lakes also drained via the River Volga to

the Caspian Sea. The limited extent of the Scandinavian Ice Sheet under the interglacial climate of MIS 5 (Fig. 2.8c) meant that volumes of meltwater runoff were insufficient to reach the Black Sea, which itself remained isolated from the Mediterranean (Andersen and Mangerud, 1989; Arkhipov *et al.*, 1995).

The global last glacial maximum (LGM) is defined as the last period of maximum global ice volume and is approximated to a 6,000 year interval at c. 21 ± 3 ka BP (Bard, 1999). As will be discussed, in many mountainous regions of the Mediterranean, the local LGM, or the last local maximum ice volume, is not always synchronous with the global LGM (Section 2.4 and 2.5). Advance of the Scandinavian Ice Sheet during the global LGM (Late Weichselian, c. 18 ka) restricted drainage towards the Baltic Sea in the west (Fig. 2.8a). The River Volga became the primary meltwater pathway supplying the Caspian and Black Seas (Mangerud *et al.*, 2004). The development of 'urstromtäler' (drainage pathways situated parallel to the ice margin) was also instrumental in directing meltwater away from the Mediterranean basin. Instead, the Dneipr and Don River catchments, and to a lesser extent the River Danube, provided the main meltwater routes from the Scandinavian ice sheet to the Mediterranean basin at this time (Arkhipov *et al.*, 1995).

2.3.2   *Ice sheet geochronologies: comparisons with mountain glaciations*

Marine $\delta^{18}O$ records indicate that the large ice sheets of the Northern Hemisphere underwent a major period of advance from c. 115 ka and reached their maximum extent at c. 20 ka, during the global LGM (Gillespie and Molnar, 1995). Initial studies assumed that mountain glaciers and continental ice sheets advanced and retreated in synchrony, together with global sea level fluctuations. Continued investigation of Pleistocene ice caps and valley glaciers has, however, demonstrated that in many mountain regions, glaciers reached their maximum extent up to 20,000 years prior to the global LGM (Seret *et al.*, 1990; Gillespie and Molnar, 1995; Giraudi and Frezzotti, 1997; Woodward *et al.*, 2008; Lewis *et al.*, 2009). In a review of global glacial synchronicity during the Pleistocene, Gillespie and Molnar (1995) indicate that morphosedimentary features such as moraines, incised streams, and river terraces, which are frequently associated with the global LGM and last deglaciation, may in fact be much older. This suggests that in some regions, Pleistocene mountain glaciers were not entirely dependent on global climatic fluctuations, but also responded to regional palaeoenvironmental perturbations and catchment-specific boundary conditions. During Pleistocene cold stages, whilst mountain glaciers may have advanced at the same time as the larger continental ice

sheets, their maximum extent may have occurred independently of the global LGM (Gillespie and Molnar, 1995). This is demonstrated by evidence from the Rocky Mountains, the European Alps (Gillespie and Molnar. 1995) and northern Patagonia (Glasser *et al*., 2010) as well as basins across the Mediterranean (Section 2.4). Smaller-scale ice masses can respond more readily to short term climatic fluctuations than larger ice sheets. The observed asynchrony between continental ice sheets and many mountain glacial records may therefore be more widespread than initially assumed. The timing of ice advance within individual basins is investigated in more detail in the following sections using a regional synthesis of Pleistocene mountain glaciation and fluvial activity in the Mediterranean.

2.4   Fluvial response to Pleistocene glaciation: a Mediterranean perspective

As observed in many parts of the world, mountainous regions of the Mediterranean have undergone repeated phases of glaciation and periglaciation throughout the Quaternary. An early synthesis of Pleistocene glacial activity by Messerli (1967) provides one of the most comprehensive, yet undated, reviews of Mediterranean glaciation. More recently, the Quaternary glacial history of this region has been reviewed in detail by Hughes *et al*. (2006b), Hughes and Woodward (2008; 2009) and Hughes (2011). Mediterranean geomorphological processes are conditioned by: vegetation characteristics; the abundance of high relief catchments; glaciation; and widespread tectonic activity (Macklin *et al*., 2002). The strong climatic gradient across the Mediterranean, with regard to precipitation and temperature for example, has produced a regionally variable glacial history, which is reflected in the glacial and fluvial geomorphological records (Woodward *et al*., 2004; 2008). Pleistocene Mediterranean cold stages were largely characterised by cirque and valley glaciers, but in some regions larger ice caps and ice fields developed (Hughes and Woodward, 2009; Cowton *et al.*, 2009; Hughes *et al.*, 2010). These would have been more sensitive to Quaternary climatic perturbations than the larger continental ice sheets (Hughes and Woodward, 2009). These records of glacial activity therefore provide detailed insights into Quaternary palaeoenvironmental change. Hughes *et al*. (2006a) use palynological and sea surface temperature (SST) records to constrain the timing of climatic phases most favourable for glacial advance in Greece during the last interglacial and glacial cycle (Fig. 2.9). This can be used as a basis for comparing the timing of Pleistocene glacial advance across the Mediterranean, and in relation to the Eurasian ice sheet record. The following sections discuss the geochronological, geomorphological and sedimentological data from glaciated catchments in five Mediterranean regions (Fig. 2.10).
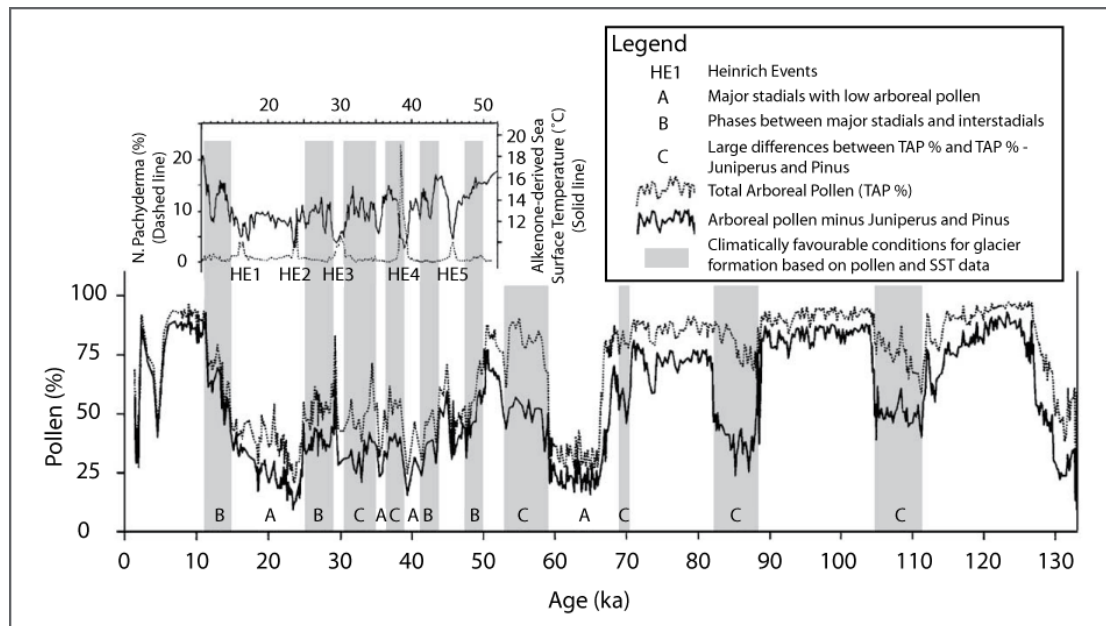
Figure 2.9 – Climatic phases potentially favouring Pleistocene glacial advance in Greece, highlighted by the letters A, B and C. Phases B and C (shaded) are more conducive to positive glacier mass balance. Adapted from Hughes *et al.* (2006a).
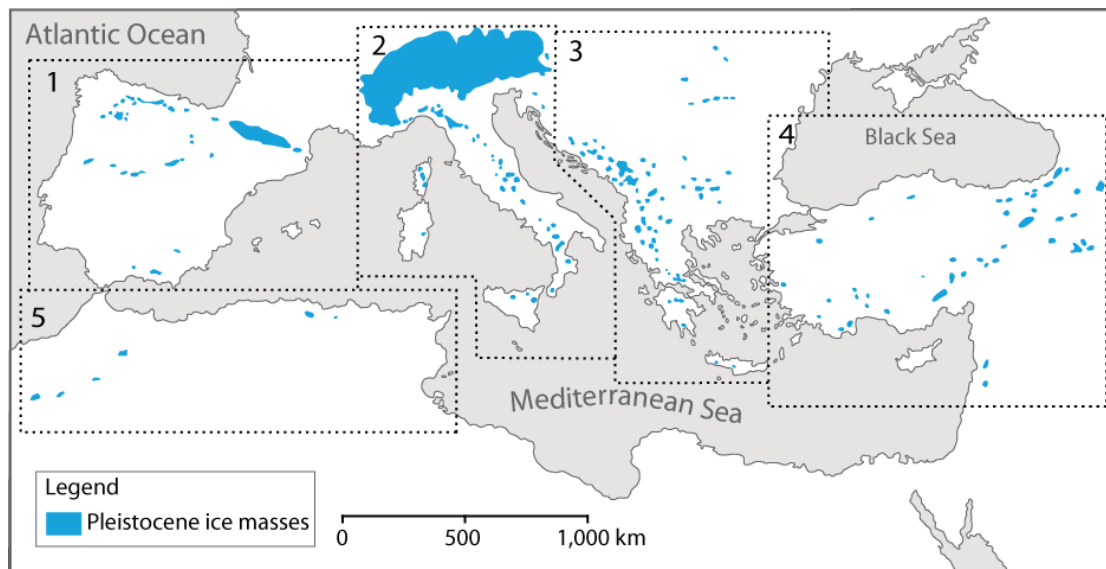
Figure 2.10 - Mediterranean zones discussed in the text indicating Pleistocene ice masses: 1) Iberian Peninsula; 2) Italian Peninsula; 3) Balkan Peninsula; 4) Anatolia; 5) North Africa. Based on: Messerli (1967); Demir *et al*. (2004); Hughes *et al.* (2006b).

A selection of the most securely dated sites is used to develop a detailed regional characterisation of Pleistocene glacial and fluvial activity. This is used to test current

hypotheses of fluvial system response to Pleistocene glaciation in the contrasting geomorphological settings observed across the Mediterranean basin and elsewhere.

2.4.1   Iberian Peninsula

The Iberian Peninsula, at the interface between Atlantic, Mediterranean, European and African climatic systems, has a highly diverse palaeoenvironmental history. During the Pleistocene, glaciers developed on many high mountain regions across Iberia (Hughes *et al*., 2006b) including the Pyrenees, the Picos de Europa and the Sierra Nevada, as well as the central mountain regions such as Peñalara, Sierra da Guadarrama and the Sierra de Gredos. The increasing application of radiometric dating techniques (notably ^{14}C, OSL, U-series, and cosmogenic dating) in a number of catchments has provided a more coherent framework into which relative chronologies have been incorporated (Goméz-Ortiz *et al*., 2000). In many cases across Iberia the absence of secure geochronological control on glacial and fluvial deposits (Hughes *et al*., 2006b; Hughes and Woodward, 2009) means that an understanding of Quaternary landsystem dynamics largely relies on morphostratigraphical correlations. For example, geomorphological evidence from the Parque Natural Lago de Sanabria, northwest Spain (Cowton *et al*., 2009) has identified three glacial phases. Although not directly dated, the onset of maximum glacial advance is correlated to MIS 2.

The Pyrenees contained some of the largest Quaternary ice masses of the Iberian Peninsula (Goméz-Ortiz *et al*., 2000). These transformed the meltwater and sediment supply characteristics of river systems draining into northern Spain and southern France. Geomorphological evidence suggests that glaciers in the northern Pyrenees reached a maximum thickness of c. 900 m and extended for up to 65 km downvalley (Pallás *et al*., 2006). In the southern Pyrenees, glaciers attained thicknesses of 600 m, and a maximum length of c. 30 km (Marti Bono and Garcia Ruiz, 1994). The timing and extent of Quaternary ice-masses in this region has been particularly well-resolved (e.g. Serrano-Cañadas, 1992; García-Ruiz *et al*., 2001; Lewis *et al*., 2009). The Ebro basin, for example, now contains one of the most comprehensive chronological frameworks of Pleistocene glacial and fluvial activity in the Iberian region (Santisteban and Schulte, 2007). Based on OSL ages from glacial and glaciofluvial sediments in the terminal reaches of the Gállego valley glacier, south central Pyrenees, three depositional phases were identified corresponding to MIS 7b, 5b, and 3 (Peña *et al*., 2004), with an additional, weaker signal attributed to MIS 4. No evidence of ice advance during the global LGM (MIS 2) was reported by Peña *et al*. (2004) from this catchment. In a more recent

study here, however, Lewis *et al*. (2009) use over 50 OSL dates from glacial and fluvial deposits to constrain periods of ice advance to 90-80 ka (MIS 5b-5a), 75-53 ka (MIS 4), 39-33 ka (MIS 3-2) and 23-17 ka (MIS 2). Corresponding alluvial phases in the Cinca and Gállego valleys are correlated to MIS 6, 5d-2, 4, 3 and 2-1. The robust glacial-fluvial correlations indicate a regional morphogenic synchronicity between Pleistocene glacial outwash and valley floor aggradation, deposited under high discharge conditions (Lewis *et al*., 2009). All records indicate a local glacial maximum several thousand years prior to the global LGM. This corresponds to other studies undertaken in the Pyrenees (e.g. Andrieu *et al*., 1988; García-Ruiz *et al*., 2003) and elsewhere (French Vosges - Seret *et al*., 1990; Pindus Mountains, Greece - Woodward *et al*., 2008; Picos de Europa – Moreno *et al*., 2009) which suggest that a number of mountain glaciers are out of phase with the larger continental ice sheets (Hughes and Woodward, 2008). Glaciated catchments in other areas of Iberia (such as the Sierra de Gredos, central Iberia - Palacios *et al*., 2010; and northwest Iberia – Fernandez Mosquera *et al*., 2000) do however record a glacial advance in phase with the global LGM.

Investigation into the Pleistocene karstification of the lower Gállego valley (Benito *et al*., 2010), suggests that alluvial deposition may be connected to solution-induced subsidence resulting from high meltwater discharge from the glaciated headwaters. These periods of enhanced streamflow have been linked to phases of decreased salinity within the Mediterranean basin, which had previously been attributed to Heinrich events within the North Atlantic (Sierro *et al*., 2005). Under this reappraisal, freshwater inputs are instead thought to be associated with seasonal meltwater from the glaciated uplands. This highlights the role of fluvial systems in transferring palaeoenvironmental signals from the glaciated uplands, and potentially as far as the sedimentary record offshore. Through analysing Pleistocene fluvial deposits it may therefore be possible to develop a more integrated reconstruction of Quaternary land surface dynamics from the terrestrial mountain regions to the offshore zone.

Cosmogenic exposure dating of moraines within the Querol and Malniu valleys of the south eastern Pyrenees (Pallàs *et al*., 2010) indicates that the oldest recorded glacial advance occurred during MIS 5. Unlike the Cinca and Gállego valleys of the northern Pyrnees, no evidence of glaciation from MIS 6 has been reported here. Records of glacial activity prior to MIS 6 on the Iberian Peninsula have, however, been identified by Fernandez Mosquera *et al.* (2000) in the Sierra de Queixa and the Sierra de Xúres, northwest Iberia. [12]Ne dating of moraines and glacially polished surfaces in these catchments indicates three glacial phases during MIS 8, 6 and 2. Elsewhere in Iberia, geomorphological evidence of Pleistocene glaciation

has been reported from MIS 3-2 and 2 (e.g. Delmas *et al.*, 2008; Palacios *et al.*, 2010). This highlights the fragmentary nature of glacial and fluvial landform development and preservation within both neighbouring catchments and mountain regions.

These spatial variations in glacial and fluvial dynamics have been tested by Pallás *et al*. (2006) in the Upper Noguera Ribagorçana Valley, south-central Pyrenees, using ^{10}Be dating of glacial erosion surfaces, moraines and erratics. The valley configuration here allowed the authors to explore potential asymmetries in the glacial records of neighbouring catchments. ^{10}Be ages indicated that, within adjacent basins, moraines corresponding to the same glacial pulse were formed at different heights and distances downvalley. Some valleys may have been deglaciated, whilst others were still occupied by valley or cirque glaciers. Rockglaciers were also found to have been active at different times within neighbouring valleys. This evidence is used to suggest that, rather than a local LGM several millennia prior to the global LGM, this part of the Pyrenees instead experienced a prolonged pleniglacial period, incorporating several glacier fluctuations recorded differently in contrasting topographic settings.

During the Holocene and historical periods (e.g. Little Ice Age - LIA), isolated glaciers have existed only in the highest cirques of the Pyrenees, the Picos de Europa and the summits of the Sierra Nevada (González Trueba *et al*., 2008). Until recently, the mountains of the Sierra Nevada contained the most southerly glacier in Europe, which had fully retreated by the early twentieth century (Messerli, 1967). At present, glaciers exist in the central Pyrenees, and are inherited forms from the LIA (Pallás *et al*., 2006; Grunewald and Sheithauer, 2010). Our understanding of these more recent glacial phases in Iberia, and their impacts on contemporary fluvial systems, is currently less well refined than our insights into Pleistocene glacial-fluvial systems (González Trueba *et al*., 2008).

2.4.2   *Italian Peninsula, Sardinia and Corsica*

The Italian Peninsula was extensively glaciated during the Quaternary, with glaciers present in the Alps and the Italian Apennines as well as the mountains of Sardinia and Corsica. The highly tectonically active setting of the Italian Peninsula (Vezzoli and Garzanti, 2009) means that relatively few studies have correlated the fluvial archive with headwater glacial records, and instead favour long-term tectonic and eustatic landscape controls (e.g. Amorosi *et al*., 1996; Wegmann and Pazzaglia, 2009). In regions such as Italy, discriminating the relative influence of

Quaternary climate change, glaciation and tectonic activity on long-term river system dynamics is important to the interpretation of Quaternary alluvial sequences.

In the Alps, large ice caps and outlet glaciers developed during the Pleistocene as well as smaller cirque glaciers confined to the higher peaks (Carraro and Giardino, 2004). Many of the meltwater pathways drained into the Mediterranean, and the Alps have therefore been incorporated into this section of the discussion. Late Pleistocene glacial activity is chronologically well-constrained, yet Middle Pleistocene records are comparatively poorly understood due to limited dating control. In the northern Alps the last maximum ice advance is dated using ^{14}C and ^{10}Be cosmogenic methods to 30 – 18 ka (e.g. Bini and Zuccoli, 2004). The last maximum advance of the Tagliamento glacier, on the southern slope of the Alps, is dated using ^{14}C to 26.5 - 23.0 ka (Monegato *et al*., 2007). These ages are consistent with evidence from elsewhere in the Mediterranean (Woodward *et al*., 2008; Lewis *et al*., 2009) of an early local glacial maximum. On the northern slopes of the Alps, however, there is no significant evidence that the local LGM preceded the global LGM (Ivy-Ochs, 2008). As observed in Iberia, this suggests that glacial advances were highly variable in timing and extent between valleys. Federici *et al*. (2008), however, use exposure ages of glacial landforms to suggest that glaciation during the Egesen Stadial (Younger Dryas) is synchronous across the Alps. As in many regions of the Mediterranean, the limited geochronological control in many Italian catchments means that interpretations currently rely heavily on morphostratigraphical correlations (Dehnert *et al*., 2010). Detailed geomorphological mapping of large areas of the Alps provides a comprehensive relative dating framework (Ivy-Ochs *et al*., 2008). For example, a recent study in the Castellamonte region of the western Alps used soil development indices as a relative age indicator of Plio-Pleistocene glacial and fluvial landforms (Forno and Ferrando, 2008). This was used alongside sedimentological and clast lithological analyses to delineate the catchment characteristics of localised, Middle Pleistocene glaciers.

The Po drainage network, which diverts meltwater from the Alps and Apennines towards the Adriatic Sea, contains a valuable record of Quaternary glacial-fluvial dynamics (Muttoni *et al*., 2003; Amorosi *et al*., 2008). A major structural boundary means that this region has also been influenced by Pleistocene tectonic activity (Amorosi *et al*., 1996). In a recent study of alluvial sequences across the foreland, Vezzoli and Garzanti (2009) use a quantitative sediment provenance method to track changes in Pleistocene drainage patterns across the Po Plain. Cores obtained from both ice proximal and distal locations present a varied history of meltwater and sediment provenance since the onset of Middle Pleistocene glaciation (MIS 22).

These records highlight the important interactions between regional tectonics, Quaternary climate change and glacial activity in conditioning long-term landscape processes. Detailed records of these landscape changes are often well-preserved within the alluvial sequences of large depocentres such as the Po Plain, and in some cases may also extend offshore. For example, detailed investigation of alluvial fan and megafan sequences on the Po Plain has revealed important sedimentary records of Pleistocene headwater glaciation (Ori, 1982; Amorosi *et al*., 1996; Guzzetti *et al*., 1997; Paiero and Monegato, 2003). In the eastern Southern Alps, Fontana *et al*. (2008) use 250 ^{14}C dates to correlate the glacial record of three major valleys with corresponding alluvial megafan deposits. During the global LGM large volumes of meltwater and sediment were delivered to the Po Plain and fluvial aggradation extended offshore onto the North Adriatic shelf. The glacial record here is not directly dated, but ^{14}C ages of the fan sediments were used to constrain the timing of maximum ice advance to c. 22 – 18 cal ka BP (Fontana *et al*., 2008). Upon deglaciation, the fans underwent a shift from net aggradation to incision, marking the onset of a major erosional phase from c. 14.5 cal ka BP, which continued into the Holocene. As observed in the western Alps (Bini and Zuccoli, 2004) and elsewhere (Pallás *et al*., 2006), the fluvial morphosedimentary evidence recorded highly irregular glacial advances in each of the feeder valleys.

The Italian Apennines also contain detailed records of Pleistocene glacial activity. The application of a range of dating techniques including ^{14}C, U-series and tephrochronology, means that this region contains some of the most securely dated Pleistocene glacial sequences of the Italian Peninsula. The most extensive glaciations are recorded within the northern and central Apennines and a series of glacial advances prior to the global LGM have been identified (Giraudi *et al*., 2011; Giraudi, 2012). The local LGM has been dated using ^{14}C ages of organic-rich colluvium, peat deposits and lacustrine sediments within the Campo Felice Basin, and the most recent estimates provide ages of c. 30-18 cal ka BP (Girauldi, 2004; Giraudi *et al*., 2011; 2012). These ages correspond to the local LGM of the southern Alps (Bini and Zuccoli, 2004; Granger *et al*., 2006; Monegato *et al*., 2007). Glaciers of the Gran Sasso massif, in the Apennines are also thought to have advanced in phase with the early local LGM of the Tagliamento glacier of the southern Alps (Giraudi and Frezzotti, 1997). [14]C ages from river terraces and alluvial fan sediments within river systems draining the northern Apennines indicate that floodplain aggradation here largely occurred at cold-warm transitions (Amorosi *et al*., 1996). This is observed elsewhere (e.g. Schildgen *et al*., 2002; Xu and Zhou, 2009) during high discharge conditions in association with glacial retreat. Widespread alluvial gravel deposition from c. 19.5 – 13.0 cal ka BP broadly corresponds to the onset of deglaciation in the

Apennines and the release of large volumes of clastic material into meltwater pathways. Subsequent incision here is attributed to tectonically-induced base level change, and highlights the interactions between glacial and tectonic activity in determining long-term fluvial characteristics (Amorosi *et al.*, 1996).

Within the Campo Felice Basin of the central Apennines, ^{14}C and ^{39}Ar-^{40}Ar ages indicate five glacial advances and corresponding fluvial depositional cycles (Giraudi *et al.*, 2011; Fig. 2.11). Age determinants from moraines, lacustrine sediments and alluvial fan deposits are used to develop a composite chronology of glacial activity from MIS 14, 10, 6, 4, 3 and 2 (Giraudi, 1998). Contrary to other studies across the Mediterranean (e.g. Hughes, 2004; Woodward *et al.*, 2008; Hughes *et al.*, 2010; 2011b) which record a major glacial phase during MIS 12, glacially-derived sediments dated to MIS 12 have not yet been reported from the Campo Felice system. Coarse sediments associated with the 5th depositional cycle (MIS 2) within the Campo Felice record closely resemble the sedimentary characteristics of previous cycles. This may be indicative of long-term paraglacial sediment remobilisation. The western Alps (Carraro and Giardino, 2004) and the Voidomatis Basin in Greece (Woodward *et al.,* 2008) also contain evidence for the inheritance of older glacial and fluvial sediments within more recent depositional settings. Intensive weathering, periglacial and glaciofluvial activity leads to the long-term reworking of glacial deposits (Bini and Zuccoli, 2004; Castiglioni, 2004). These processes continue in the Campo Felice system at the present day under the influence of modern fluvial systems (Carraro and Giardino, 2004). The preservation potential of both fluvial and glacial deposits is therefore ultimately conditioned by both the prevailing and preceding palaeoenvironmental regime (Clark, 1987; Vandenberghe, 2008; Lewin and Macklin, 2003; Gibbard and Lewin, 2009).

At present, 201 glaciers have been reported in the Italian Alps (Pelfini and Smiraglia, 1992), many of which have shown a broad trend of retreat throughout the historical period. The Ghiacciaio del Calderone is the only current glacier in the Italian Apennines, and is one of the southernmost glaciers in Europe (d'Orefice *et al.*, 2000). Current research in the Alps also monitors the present day meltwater and sediment supply characteristics to fluvial systems downstream (e.g. Bezinge *et al.*, 1989; Collins, 2007). These studies provide valuable opportunities to compare contemporary Mediterranean glacial-fluvial interactions with the Quaternary geological record. Field imagery of the Glacier de Tsanfleuron in the Swiss Alps, for example, demonstrates the importance of limestone karst sinkholes in channelling meltwater into the subterranean drainage network (Hambrey and Alean, 2009). This provides an

important analogue for the Pleistocene ice masses that developed within karstic terrain in Greece (Hughes 2004; 2006c) and Montenegro (Hughes *et al.*, 2010; 2011b) for example.
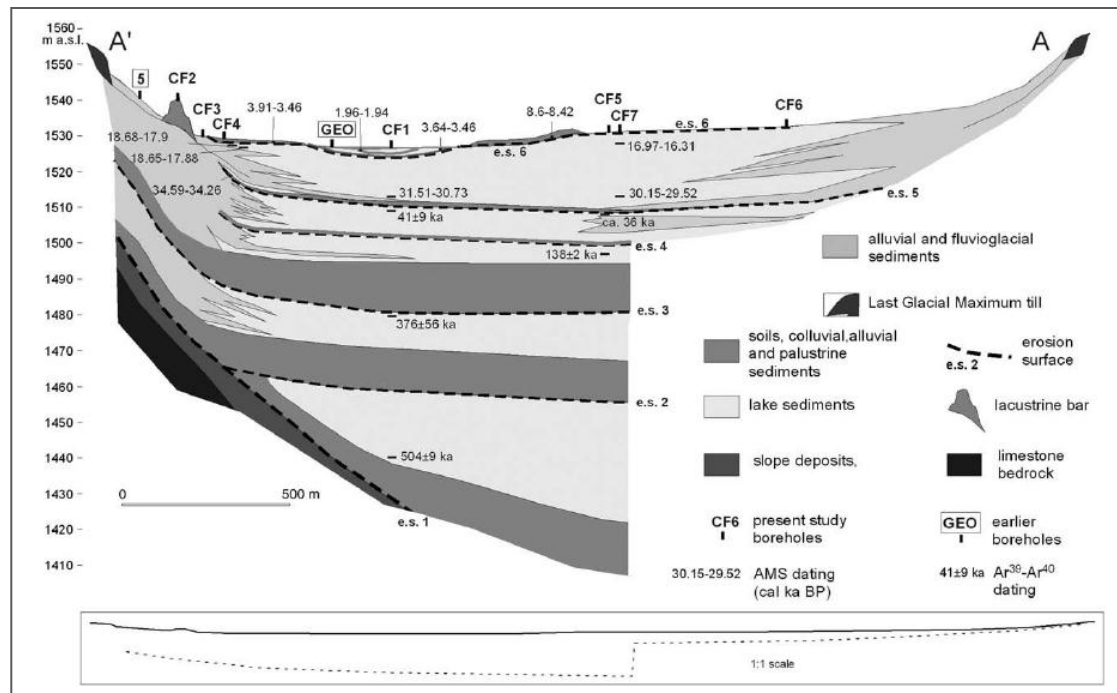
Figure 2.11 – Stratigraphic section of the coring locations in the Campo Felice Basin. [14]C and [39]Ar-[40]Ar dated horizons are indicated. From Giraudi *et al*. (2011).

2.4.3   Balkan Peninsula

The mountainous regions of the Balkan Peninsula were extensively influenced by Pleistocene glaciation (Hughes *et al*., 2006b). Ice caps and valley glaciers developed on numerous high altitude regions extending as far south as Greece. The elevated precipitation levels in this part of the Mediterranean meant that it contained some of the largest Pleistocene ice masses of the Mediterranean basin (Woodward *et al*., 2008; Hughes *et al*., 2010). Investigation into these glaciated mountains began over a century ago with the pioneering work of Civjić (1898; 1900). Since then, many studies have focused on the morphostratigraphical analysis of Pleistocene glacial deposits to establish the number and extent of glacial phases. In many areas, the increasing use of radiometric dating techniques has also allowed more robust geochronologies to be developed.

In the Julian Alps of Slovenia, ^{14}C, U-series and IRSL dates from fluvial and lacustrine deposits in the Upper Soča River region highlight two major depositional phases. The first correlates with

the penultimate glacial-interglacial transition (MIS 6-5), and the second corresponds to the last glacial-interglacial transition (MIS 2-1) (Bavec *et al.*, 2004). It is suggested that ice did not advance as far as the Soča River basin. Instead, diamicts reported in association with the alluvial record are thought to reflect mass flow sediments prepared and deposited under a previous glacial regime when glaciers were present at higher altitudes. Such large quantities of glacially-conditioned debris were then transported to the middle and lower reaches via braided river networks (Bavec *et al.*, 2004) and deposited under paraglacial mechanisms.

Further south, the Croatian Adriatic coast contains a series of Pleistocene glacial features of apparent Late Würmian (MIS 2) age. Sediments have undergone considerable post-depositional alteration and the age of the local LGM is currently unknown (Marjanac and Marjanac, 2004). Glacial and glaciofluvial deposits have been reported close to sea level, near the Velebit Mountains by Marjanac and Marjanac (2004). They argue that kame terraces have been deposited close to the present day shoreline within the Baška valley (Krk Island) and form part of an extensive Pleistocene glacial sedimentary archive that may extend offshore (Marjanac and Marjanac, 2004). This would have significant implications for our understanding of ice dynamics in this part of the Mediterranean and requires further investigation.

Several generations of research into the glaciated mountains of neighbouring Montenegro means that the extent of Pleistocene ice masses, particularly within the dominant glacial centres of Orjen, Durmitor and Prokletije, are now well constrained (Civjić, 1898; Sawicki, 1911; Menkovic *et al.*, 2004; Milevojević *et al.*, 2008; Kuhlemann *et al.*, 2009; Hughes *et al.*, 2010; 2011b). The Pleistocene glacial deposits and karstic landscape of Lovčen, southwest Montenegro, has also recently been discussed in detail by Stepišnik and Žebre (2011). The Pleistocene glacial record of Montenegro will be discussed in detail in Chapter 3, and will be only briefly summarised here. The most recent investigations by Hughes *et al.* (2010; 2011b) have provided detailed morphostratigraphical and geochronological reconstructions of Pleistocene ice caps in this part of the Balkans. In southeast Montenegro, a Pleistocene ice cap covering an area of 165 km^2 was centred on the coastal mountains of Orjen (1,894 m a.s.l.). Geomorphological evidence suggests three glacial phases, each of decreasing ice extent. These have been dated using 12 U-series ages and are correlated to: 480-430 ka (MIS 12), 190-130 ka (MIS 6) and 110-11.7 ka (MIS 5d-2). The extent of these glaciations is supported by evidence from the mountains of Lovčen (Stepišnik and Žebre, 2011), southwest of the Orjen massif, which also suggests that glaciers extended beyond the highest cirques during the major cold stages of the Pleistocene.

The Pleistocene glacial record of the central Montenegrin massifs (Durmitor, Sinjajevina, Moračke, Maganik and Prekornica) has recently been studied in detail by Hughes *et al*. (2011b). The glacial history of Sinjajevina has also recently been presented by Telbisz (2010a; 2010b). Using geomorphological evidence and U-series dating Hughes *et al.* (2011b) have identified four glacial phases correlated to MIS 12, MIS 8 and 6, MIS 5d-2, and the Younger Dryas. Holocene and recent glaciers have also been reported from further up valley. During the maximum ice extent at 470-420 ka (MIS 12) a series of coalescing ice caps covered an area of c. 1,483 km^2 over the adjacent massifs of Durmitor, Sinjajevina, Moračke, Maganik and Prekornica. This would have been one of the largest centres of Middle Pleistocene ice accumulation in Southern Europe. A present day glacier situated in one of the highest cirques of Durmitor measures 0.05 km^2. The Pleistocene fluvial records downstream of these glaciated regions have currently not been investigated and may provide greater detail to the existing glacial archives. Considerable opportunities therefore exist within this region of the Balkans to explore the interactions of glacial and fluvial systems, now that the glacial records have been documented in detail.

To the east of Montenegro, moraines within the Šara Mountains of Kosovo have been dated using [10]Be and correlated to the global LGM (Kuhlemann *et al.,* 2009). Contrary to other records across the Balkans, and much of the western Mediterranean (Giraudi, 1998; Peña *et al*., 2004; Hughes *et al*., 2006c), no evidence of earlier glaciation has been reported from this region. This may represent a true absence of glacial activity prior to the global LGM, but it may also be that morphosedimentary evidence of earlier glacial phases has not been preserved, or has not yet been identified.

The mountains of Greece contain some of the best preserved records of Pleistocene glacial activity in the Mediterranean (Woodward *et al*., 2004). Detailed research has been carried out on Mount Olympus by Smith *et al*. (1997) from a suite of glacial and fluvial deposits, each related to a distinct phase of headwater glaciation. Attempts to derive a radiometric chronology for this region have been problematic (Manz, 1998; Woodward *et al.,* 2004), and analysis has instead focused on more detailed sedimentological and pedological analyses. More recently, following three phases of research in the Pindus Mountains of northwest Greece (Lewin *et al*., 1991; Woodward *et al*., 1992; 1995; Woodward *et al*., 2004; Hughes *et al*., 2006c) the glacial and fluvial morphostratigraphical records have been successfully correlated using ^{14}C, ESR and U-series ages (Woodward *et al*., 2008). The glacial morphosedimentary record of Mount Tymphi in the Pindus Mountains presents three glacial

phases correlated to MIS 12, 6 and 5d-2, which correspond to those identified in the Montenegrin glacial records. The largest ice cap, correlated to MIS 12, covered an area of 72.6 km^2, which is considerably smaller than the MIS 12 ice masses of central Montenegro. A total of 28 U-series ages from the glacial and fluvial archives of the Voidomatis basin (Fig. 2.12) make this one of the most detailed chronologies of Pleistocene glaciation in the Mediterranean (Hughes *et al.*, 2006c; Woodward *et al.*, 2008). The slackwater record from the lower reaches of the Voidomatis basin (Woodward *et al*., 2001) has also been used to effectively infer sediment sources during the last glacial-interglacial transition (Woodward *et al*., 2008). Slackwater sediments are fine-grained alluvial deposits accumulating in zones of low flow velocity (Woodward *et al*., 2001) and provide valuable records of Pleistocene fluvial and palaeoflood dynamics (Baker *et al*., 1994; Rittenour *et al*., 2007).
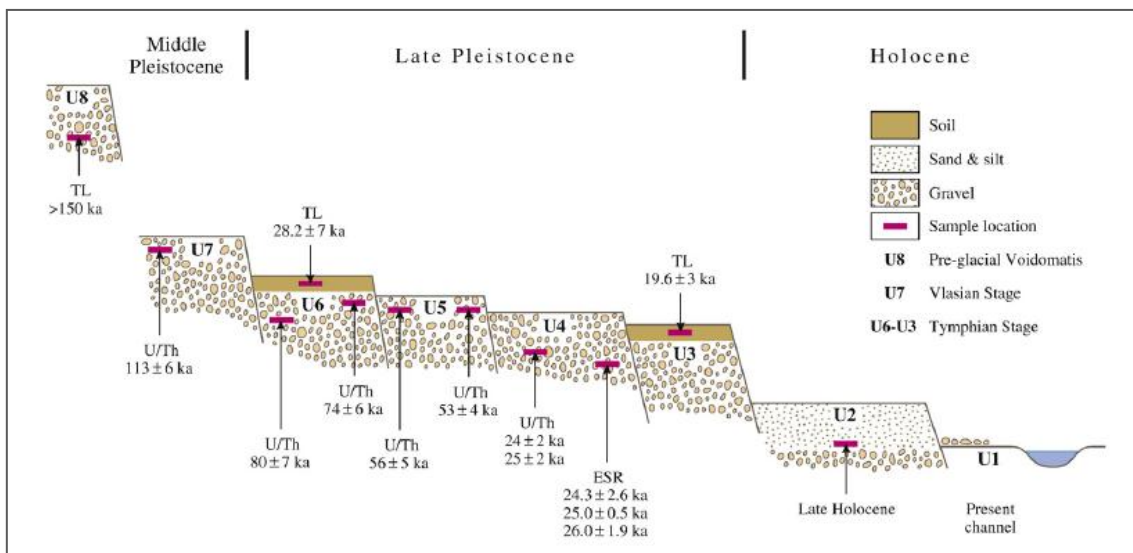
Figure 2.12 – Cross sectional schematic of the Voidomatis Basin, northwest Greece displaying U-series, ESR and TL ages from the fluvial archive. From Woodward *et al*. (2008).

River terrace records from the last cold stage in the Voidomatis basin (MIS 5d-2) reflect anomalously high sedimentation rates despite comparatively minor headwater glaciation at this time, when compared to the major glaciation of MIS 12. Aggradation of this magnitude was ascribed to the extensive volumes of glacigenic sediment supplied to the fluvial system during preceding glacial periods (MIS 12 and 6) and subsequently remobilised during MIS 5d-2. Late Pleistocene fluvial records may therefore, in part, reflect a cumulative signal of upland glaciation inherited from previous cold stages. A detailed analysis of the landscape-scale sedimentary context, alongside a coupled glacial-fluvial approach, is required to effectively constrain the temporal variations in Pleistocene sediment flux from glaciated headwaters.

Today, glaciers and snow patches exist on several of the highest peaks of the Balkan Peninsula, including the Triglav glacier, Slovenia (Gabrovec, 1998), the Debeli Namet glacier of Durmitor, Montenegro (Hughes, 2007), and four active glaciers in the Prokletije Mountains of Albania (Hughes, 2009). There are currently no available published data investigating the interactions between present day glacial activity in the Balkans and meltwater and sediment dynamics downstream.

2.4.4   Anatolia

The majority of fluvial studies in Anatolia focus on unglaciated catchments. The strong tectonic influence here, as well as across other parts of the Mediterranean, means that many studies explore the complex interactions between Quaternary climatic change, volcanism, long-term uplift rates and river terrace sequences (Demir *et al.* 2004; Westaway *et al.*, 2004; Collins *et al.*, 2005; Doğan, 2010). Increasingly, however, research has begun to address the Pleistocene glacial and fluvial records of Anatolia (e.g. Sarikaya *et al.*, 2009). In Turkey, Pleistocene glacial landforms are present within three key regions: The Taurus Mountains (southeast Turkey); The Pontic Mountain Range (eastern Black Sea coast); and independent mountain chains and volcanic centres across the Anatolian plateau (Çiner, 2004). Whilst little of Turkey was glaciated during the Pleistocene, much of its area was located close to the snowline during glacial maxima (Demir *et al.*, 2004) making it particularly sensitive to fluctuations in vegetation cover and landscape instability. Geochronological frameworks from glaciated Anatolian basins do not currently match the detail of those developed for parts of Spain (Lewis *et al.*, 2009) or Greece (Woodward *et al.*, 2008), for example. Studies have, however, begun to employ surface exposure dating of glacial deposits to more effectively constrain the timing of Pleistocene glacial activity (e.g. Zreda *et al.*, 2005; Akçar *et al.*, 2007; Sarikaya *et al.*, 2008; 2009; Zahno *et al.*, 2009; 2010). The local LGM in Anatolia has been dated using cosmogenic techniques (see Sarikaya *et al.*, 2009) and is considered to be broadly in phase with the global LGM.

In areas with a current absence of dating control, considerable attention has been focused on the morphostratigraphical correlation of glacial and fluvial records. A recent study by Altın (2009), for example, investigates the influence of Pleistocene glacial activity in the Aladağ Mountains on fluvial systems in the adjacent Ecemiş Valley, Central Anatolia. Five river terraces were recognised, reflecting three depositional phases (Fig. 2.13). Morphostratigraphical correlations of sedimentary sequences indicate an interposing of glacial, fluvial and colluvial deposits. This suggests that during the last cold stage periglacial

slope processes and glacial regime led to rapid runoff and the heightened erosion and transportation of clastic material within glaciofluvial systems (Altın, 2009). This system is a clear demonstration of the paraglacial hypothesis of Church and Ryder (1972), where climatic oscillations during the Pleistocene repeatedly destabilised slope and channel systems, maintaining high fluvial sediment loads during a period of prolonged paraglacial sedimentation (Church and Ryder, 1972; Gurnell, 1987). Several studies have indicated that alluvial deposition within Turkish river systems largely occurred during Pleistocene glacial maxima (Demir *et al.*, 2004; Westaway *et al.*, 2004). Terrace and valley floor sediments in the Kızılırmak valley, Central Anatolia, however, suggest that maximum aggradation is not always synchronous with the coldest climatic conditions (Doğan, 2010). The last major incisional phase here is dated using ^{14}C (18.96 - 18.52 cal ka BP) and ^{40}Ar-^{39}Ar (112.7 - 76.3 ka) to have occurred after the global LGM. This would suggest that the river was largely incisional throughout the global LGM due to low sediment yield and high discharge conditions (Doğan, 2010) as glaciers advanced in the high mountain regions of Turkey. The post-LGM period is believed to be characterised by extensive alluvial aggradation as ice masses retreated and the exposure of unconsolidated debris led to an increase in sediment yield. If these dates are reliable, this study presents a clear paradox to other glaciated basins in the Mediterranean, where the global or local LGM was characterised by fluvial deposition (Fontana *et al.*, 2008; Woodward *et al.*, 2008).
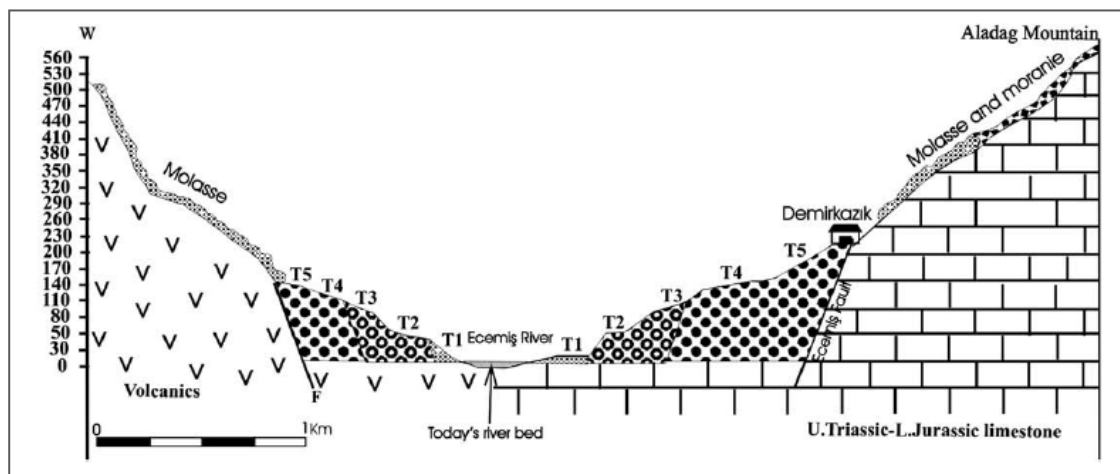
Figure 2.13 – Geomorphological cross section and terrace record of the Ecemiş Valley. From Altın (2009).

Today, glaciers occupy only the highest mountain peaks of Turkey and are largely concentrated in the southern Taurus Mountains. An ice cap of c. 10 km^2, the largest in Anatolia, is currently present on Mount Ağri (Ararat) (Kurter, 1991). As in many parts of the Mediterranean, there are currently no available published records of contemporary glacial and fluvial interactions.

2.4.5   North Africa

Quaternary glacial landforms are widespread throughout the Atlas Mountains of North Africa but research has been largely limited to geomorphological mapping or reconnaissance studies (Hughes *et al*., 2004). Both the timing and extent of Pleistocene glacial activity here is currently poorly understood. Preliminary results of an ongoing [10]Be dating programme have recently been published by Hughes *et al*. (2011a) which presents one of the first comprehensive research endeavours into the glacial history of this region. [10]Be ages from three stratigraphically distinct moraines in the High Atlas suggest at least three phases of Pleistocene glaciation. The lowest moraines are dated to 76.0 ± 9.4 ka. Moraines above these are dated to 24.4 ±3.0 ka. The highest moraines yield ages of 12.4 ± 1.6 ka, 12.2 ± 1.5 ka, and 11.1 ± 1.4 ka and correspond to the African humid period (14.8 – 5.5 ka) and the Younger Dryas (12.9 – 11.7 ka) (Hughes *et al*., 2011a). There are limited published data from the river systems draining the glaciated catchments of the Atlas Mountains. One of the first studies of the Pleistocene alluvial sequences in North Africa (Arboleya *et al*., 2008) relates fluvial depositional archives in the Ouarzazate foreland basin of Morocco to the Quaternary climatic record using cosmogenic dating techniques. The study reaches are, however, not derived from glaciated headwaters. As with many other regions of the Mediterranean, focus is frequently placed on the impacts of tectonism upon fluvial system dynamics (Stokes *et al*., 2008; Hssain and Bridgland, 2009). The study of glacial and fluvial systems here requires further investigation if it is to be effectively incorporated into the wider Mediterranean palaeoenvironmental record. Today, snow patches exist on the highest peaks, such as Mount Toubkal (4,167 m a.s.l.) in the High Atlas, but the true snowline is believed to be above this, at c. 4,200 m a.s.l. (Messerli, 1980; Hughes *et al*., 2006b) and glaciers do not exist under the current climatic regime.

2.4.6   A Mediterranean geochronological framework

Using published geochronological data from selected glaciated catchments across the Mediterranean a regional comparison of Pleistocene glacial and fluvial activity has been constructed. Over 200 dates from 12 of the most securely dated catchments described above have been selected for analysis (Table 2.2). These reflect a variety of glacial and fluvial depositional settings and dating techniques (Fig. 2.14). This allows us to explore the timing of Pleistocene Mediterranean glaciation, identify regional synchronicities in glacial activity, and investigate its impacts on fluvial systems downstream. This can be used to test current hypotheses on the response of fluvial morphosedimentary processes to Pleistocene glaciation

in the Mediterranean and assess the long-term impacts of glacial activity on fluvial dynamics and sediment transfer downstream. Comparisons can be drawn with the global examples presented in Section 2.2.5 (Fig. 2.7). The data in Table 2.2 are combined with the wider evidence discussed in the text to develop a synthesis of Pleistocene glacial phases represented within the Mediterranean glacial and fluvial geomorphological record (Fig. 2.15).

Glacial phases in the Mediterranean have been identified in the geomorphological record from MIS 14, 12, 10, 8, 6, 5d-2 and the Younger Dryas, as well as several Holocene and present day glaciers. These glacial advances track the large-scale glacial-interglacial cycles evident within other palaeoenvironmental archives (such as the East Pacific $\delta^{18}O_{benthic}$ and Tenaghi Philippon long pollen records). In many basins, fluvial systems respond in phase to glacial mass balance fluctuations and broadly demonstrate periods of alluviation during or shortly after Pleistocene cold stages, and incision during interglacials. Glacially-driven changes in meltwater and sediment flux are represented, and frequently well-preserved, in the fluvial morphosedimentary record downstream. Whilst fluvial archives are inherently fragmentary, they provide effective indicators of Pleistocene glacial activity and in many cases can contribute greater detail to an often incomplete glacial record.

In the catchments analysed here, glacial and fluvial archives reflect a highly fragmentary glacial history of the Mediterranean basin. Of the five Mediterranean regions in this study, no individual zone, or individual catchment, contains a full record of all Pleistocene glacial stages. During the Middle Pleistocene the Campo Felice Basin, on the Italian Peninsula, is the only location where glacial activity as early as MIS 14 has been suggested (Giraudi *et al*., 2011). This is based on indirect evidence of glaciation within a long lacustrine sequence. The earliest direct evidence of Middle Pleistocene glaciations, in the form of moraines, has been identified in catchments in Greece (Woodward *et al*., 2008) and Montenegro (Hughes *et al.,* 2010; 2011b) where a major glacial advance has been correlated with MIS 12. Evidence of glacial activity has been identified from MIS 10 in Italy (Giraudi *et al*., 2011) and MIS 8 in Spain and Montenegro (Fernandez Mosquera *et al*., 2000; Hughes *et al*., 2011b). However, where moraines have been dated using either U-series or cosmogenic dating, these geochronologies represent minimum ages and the glacial advance may be considerably older. During the Late Pleistocene, glacial and fluvial activity is reported from MIS 6 and 5d-2 from a series of catchments across the Mediterranean, yet records are spatially discontinuous.

Author	Location	Latitude, Longitude	Mountain Range	Max. Elevation (m a.s.l.)	Dominant Lithology	Valley	Max. Ice Extent	Dating Method	MIS
Lewis *et al.* (2009)	Northeast Spain	42.5866 N, 0.2196 E	Pyrenees	2,200	Gypsum, marine strata	Cinca and Gállego Valleys	35 km	OSL	2, 3-4, 5a, 5b-5c, 5e and 6
Benito *et al.* (2010)	Northeast Spain	42.5866 N, 0.2196 E	Pyrenees	2,200	Gypsum, marine strata	Gállego Valley	35 km	OSL	2, 3, 5b-5e, 6 and 7
Delmas *et al.* (2008)	Northeast Spain	42.5090 N, 2.0965 E	Pyrenees	2,921	-	Têt Basin	20 km	¹⁰Be	2
Monegato *et al.* (2007)	Northern Italy	46.3021 N, 13.6133 E	Alps	2,800	-	Tagliamento Valley	-	¹⁴C	2, 3
Giraudi *et al.* (2011)	Central Italy	42.2166 N, 13.4166 E	Apennines	> 2,200	Limestone	Campo Felice Basin	-	¹⁴C and ³⁹Ar-⁴⁰Ar	2, 3-4, 6, 10 and 14
Bavec *et al.* (2004)	Northwest Slovenia	46.4166 N, 13.7500 E	Julian Alps	2,864	Carbonate, Flysch	Upper Soča River	-	¹⁴C and IRSL	1-2 and 5-6
Hughes *et al.* (2010)	Western Montenegro	42.5666 N, 18.5333 E	Orjen Massif	1,894	Limestone	-	165 km²	U-series	2-5d, 6, and 12
Woodward *et al.* (2008)	Northwest Greece	20.7500 N, 40.6666 E	Pindus Mountains	2,400	Limestone, Flysch	Voidomatis Basin	60 km²	U-series and TL	2-5d, 6 and 12
Hughes *et al.* (2006c)	Northwest Greece	20.8333 N, 39.9166 E	Pindus Mountains	2,497	Limestone, Flysch	-	60 km²	U-series	2-5, 6 and 12
Doğan (2010)	Turkey	38.7960 N, 34.4566 E	-	-	-	Kızılırmak Valley	-	¹⁴C	2 and 5b
Sarikaya *et al.* (2009)	Central Turkey	38.5430 N, 35.4340 E	Mount Erciyes	3,917	-	Aksu and Üçker Valleys	5.8 km	³⁶Cl	1 and 2
Zahno *et al.* (2009)	Southwest Turkey	37.6185 N, 31.3283 E	Dedegöl Mountains	2,100	Sandstone, Schist, Carbonate	Muslu Valley	-	¹⁰Be	1, 2 and 3

Table 2.2 – Published Mediterranean geochronological records from Pleistocene glacial and fluvial deposits. These represent a selection of the most securely dated Pleistocene sedimentary records in the Mediterranean and are used to develop a regional correlation of glacial activity and river behaviour (Fig. 2.14). Dashed lines indicate unavailable data.
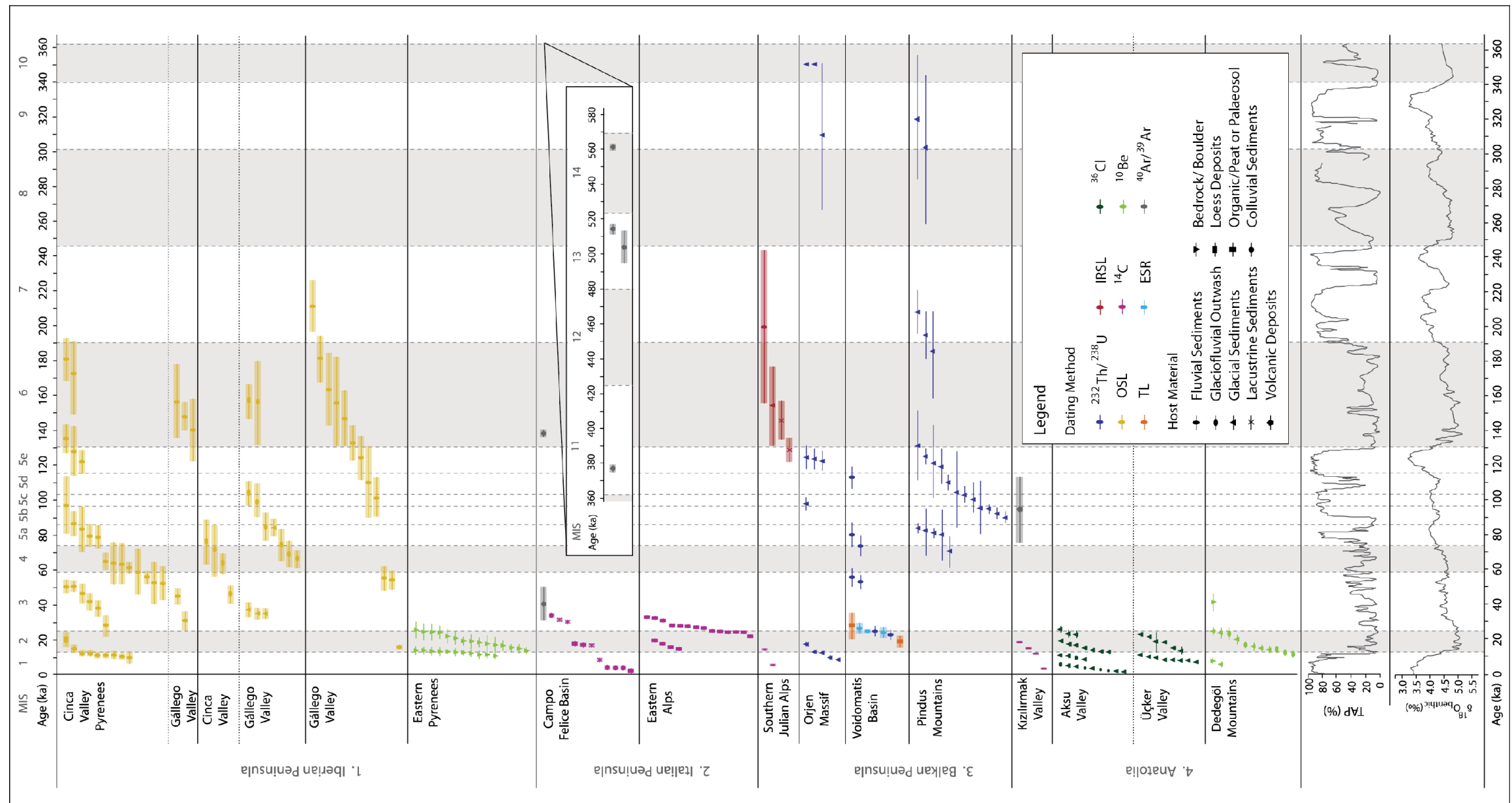
Figure 2.14 - Published geochronological data from the most securely dated glaciated Mediterranean catchments. Correlation with global multi-proxy records is provided by an East Pacific δ[18]O_benthic record and a total arboreal pollen (TAP %) record from Tenaghi Philippon, Greece (Tzedakis, 2006). Based on the published data outlined in Table 2.2.

In Anatolia, evidence of glacial activity prior to MIS 5b has not yet been reported. On the Italian Peninsula, there appears to be a hiatus within the glacial and fluvial morphosedimentary records from MIS 6-2. In some catchments, such as in Turkey, there is no reported evidence of glaciation prior to the global or local LGM (Kuhlemann *et al.*, 2009; Sarikaya *et al.*, 2009)

As well as the Mediterranean-wide variations in glacial and fluvial dynamics, local-scale contrasts are also evident within the morphosedimentary archives of neighbouring valleys. This reflects the localised climatic, atmospheric and topographic controls on glacial mass balance, meltwater and sediment dynamics. Such fragmentary records are associated not only with variations in landscape processes, but may also reflect the spatially variable preservation of the geomorphological record (see discussion in Lewin and Macklin, 2003). For example, the scarcity of glacial evidence prior to the LGM in Anatolia might be used to suggest that glacial activity at the local LGM was more extensive than earlier glacial phases, and has erased any evidence of previous glaciation. This is considered unlikely in the context of the extensive middle Pleistocene glacial advances of MIS 12 and MIS 6 that are preserved elsewhere in the Mediterranean. The suggestion of extensive glaciation in Turkey during the Early Holocene, extending to 1,510 m a.s.l. (Zreda *et al.*, 2005) may however limit the preservation of earlier landforms. Landscape-scale investigations, that incorporate multiple components of the glacial and fluvial landsystem, are therefore required to more fully understand the catchment-specific controls on the formation and preservation of Pleistocene morphosedimentary records.

Ages obtained from glacial and fluvial deposits in a number of catchments, such as the Têt basin in the Eastern Pyrenees (Delmas *et al.*, 2008) and the Aksu and Üçker valleys of Turkey (Sarikaya *et al.*, 2009), suggest a local glacial maximum in phase with the global LGM. In other catchments, such as in the French Vosges (Seret *et al.*, 1990), Northwest Greece (Woodward *et al.*, 2004), Northern Spain (Lewis *et al.*, 2009) and the Italian Apennines (Giraudi and Frezzotti, 1997; Kotarba *et al.*, 2001) morphosedimentary evidence indicate a local LGM several millennia prior to the global LGM. The deposits in the Cinca and Gállego Valleys of the Pyrenees, for example, suggest that the local LGM occurred during MIS 4.

Several basins record major depositional phases during climatic transitional periods (e.g. Bavec *et al.*, 2004; Monegato *et al.*, 2007; Woodward *et al.*, 2008; Lewis *et al.*, 2009). These largely occur during deglaciation phases, as large volumes of meltwater and unconsolidated sediment are released into glaciofluvial systems (Marren, 2005). This supports the hypothesis that geomorphological activity can be enhanced during periods of climatic instability and is not

always confined to full glacial and interglacial conditions (Vandenberghe, 1995; 2008). A number of Mediterranean catchments display evidence of the reworking of glacigenic sediment by paraglacial processes and fluvial systems long after glacial advance (e.g. Galicia, Spain - Vidal-Romani and Fernández Mosquera, 2006; the Voidomatis Basin, northwest Greece – Woodward et al., 2008; and the Ecemiş Valley, central Anatolia – Altın, 2009). Variations in the timing of glacial advance within individual basins means that depositional settings downstream may contain highly contrasting records of meltwater flux and sediment delivery from the ice margin. In some catchments, such as in Turkey (Demir et al., 2004; Westaway et al., 2004), peak sediment yield is synchronous with maximum glaciation and peak discharge (such as the idealised meltwater curve of Marren, 2005). In other basins, such as in Italy, (Amorosi et al., 1996) maximum sedimentation occurs during or shortly after deglaciation.
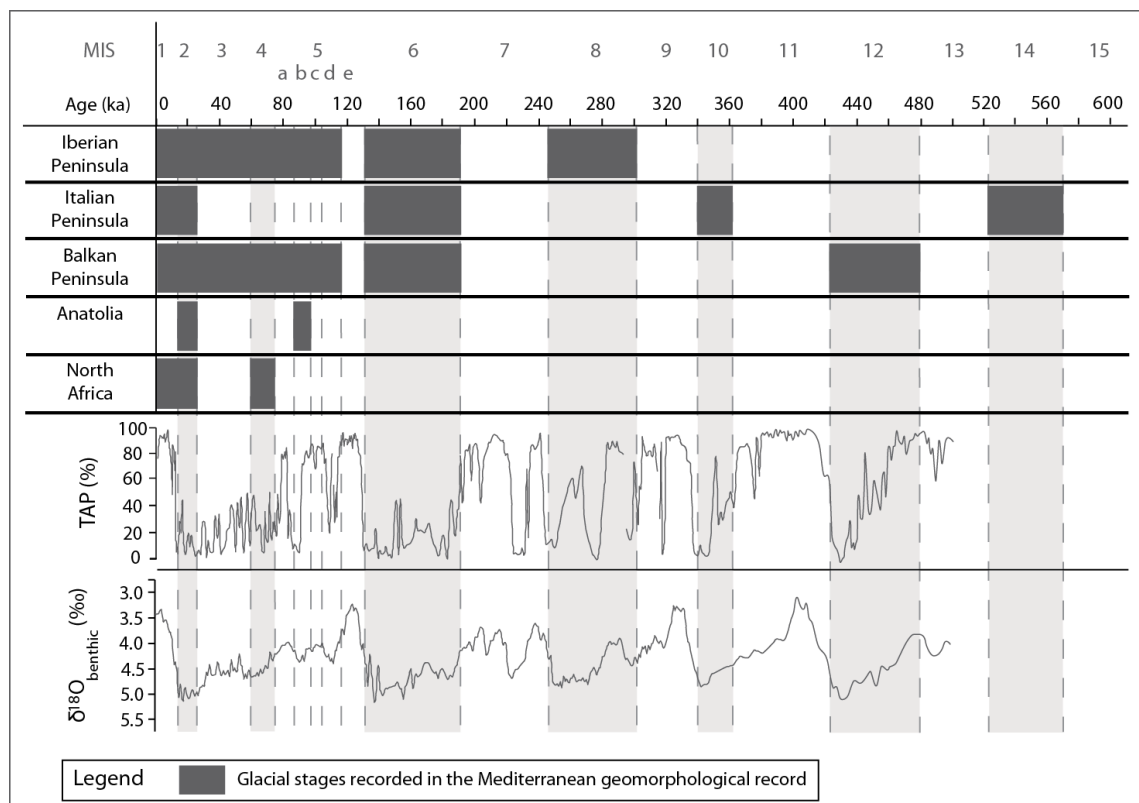
Figure 2.15 - Synopsis of glacial phases represented within the Mediterranean geomorphological record. Based on data used within Table 2.2 and studies discussed in the text. All records are plotted alongside an East Pacific δ[18]O_benthic record and total arboreal pollen (TAP %) data from Tenaghi Philippon, Greece (Tzedakis, 2006).

Analysis of the Mediterranean glacial and fluvial records has highlighted the importance of a landscape-scale approach to the study of Pleistocene glacial activity. Research undertaken in northwest Greece (Woodward et al., 2008) and northeast Spain (Lewis et al., 2009) are the

only Mediterranean studies to directly correlate Pleistocene glacial and fluvial archives. To more fully understand the drivers of landscape processes within glaciated basins, research should focus on the development of full landsystem models of Pleistocene glacial and fluvial interactions. Due to the fragmentary nature of many depositional archives, this approach must incorporate securely-dated morphosedimentary records from neighbouring valleys and within contrasting geomorphological settings.

2.5   Conclusions

This review aimed to investigate the impacts of Pleistocene Mediterranean glacial activity on long-term fluvial dynamics, and to test current hypotheses of glacial and fluvial landsystem interactions. Focus has been placed on the timing of glaciation and its representation in the morphosedimentary records downstream. Comparisons have also been drawn with selected glaciated basins from across the world.

River systems draining glaciated catchments have highly distinctive discharge and sediment regimes. Several hypotheses are currently used to understand and explain the long-term impacts of Pleistocene glacial activity on fluvial processes and sediment pathways. These relate to the timing of peak meltwater and sediment flux during an individual glacial cycle (such as Marren, 2005), as well as the sediment storage capacity of the landscape and its impacts on the long-term paraglacial redistribution of sediment (such as Church and Ryder, 1972; Dünforth *et al.*, 2008).

In the Mediterranean, morphosedimentary evidence of Pleistocene glaciation has been reported from MIS 14, 12, 10, 8, 6, 5d-2, the Younger Dryas and the Holocene. Ages obtained from glacial and fluvial archives in a number of Mediterranean catchments (such as northwest Greece and northeast Spain) suggest a local glacial maximum several millennia prior to the global LGM of the larger, continental ice sheets. The smaller size and higher sensitivity of these Mediterranean ice masses has led to variations in the timing of maximum ice advance between different mountain ranges and neighbouring basins. In several cases, major phases of geomorphological activity (aggradation or incision) have occurred during climatic transitional phases and are not always confined to full glacial or interglacial conditions.

Glacial and fluvial morphosedimentary records are highly fragmentary across the Mediterranean basin. For example, several regions do not contain evidence of Pleistocene glaciation earlier than the global LGM. No single basin records a complete succession of Pleistocene glacial cycles. This may be a function of: catchment-specific characteristics (such as topography, geology and local climatic regime) and their influence on glacial dynamics; localised variations in the development and preservation of the geomorphological record; or inconsistencies in dating techniques. The published studies analysed here represent a variety of depositional settings that often present unique sedimentary records and preservation styles.

This Mediterranean-wide synthesis has enhanced our understanding of the timing and nature of Pleistocene glaciation and its impacts on river systems downstream. In some instances, the fluvial archive has added considerable detail to the glacial record. Research should focus on the development of more integrated glacial and fluvial landsystem reconstructions. This would further our understanding of Quaternary landscape processes. Current research in the glaciated catchments of Orjen, Montenegro will address this research impetus through the detailed analysis of Pleistocene fluvial archives within contrasting depositional settings and in the context of a single, glaciated landsystem.

CHAPTER THREE

Study Area

Synopsis

The study region of Mount Orjen, western Montenegro is situated within a highly distinctive Mediterranean setting which is characterised by its intensively karstified limestone geology and a moist climatic regime. Today, the mountains of Orjen receive some of the highest recorded precipitation in Europe (4,962 mm/yr) and during the Pleistocene this upland region contained some of the largest ice masses in the Mediterranean (Hughes *et al.*, 2010; 2011b). The alluvial records of Pleistocene glaciation are preserved across the Orjen massif within a range of geomorphological settings. This provides a unique opportunity to explore the nature of fluvial response to Pleistocene glaciation within contrasting alluvial environments. Sections 3.1 – 3.4 explore the local and regional geological, climatic and geographical setting of Orjen within the wider Mediterranean landscape. Section 3.5 discusses the previous research undertaken on the Pleistocene glacial record of Orjen and the glaciated massifs of central Montenegro and the Prokletije, eastern Montenegro. The selected field sites surrounding Orjen, in relation to the existing glacial record of Hughes *et al.* (2010), are highlighted in Section 3.6.

3.1   Study region: Orjen, Montenegro

Orjen is a compact group of limestone mountains forming part of the Dinaric Alps (Fig. 3.1), on the border of western Montenegro, Croatia and Bosnia-Herzegovina. The mountain massif is situated northwest of the Bay of Kotor (Boka Kotorska), a coastal inlet of the Adriatic Sea (Plate 3.1; Fig. 3.2). The highest peak, Zubački kabao (1,894 m a.s.l.), and five additional summits exceeding 1,800 m a.s.l. are concentrated on the western margins of the massif (Hughes *et al.*, 2010). These are surrounded by a series of radially-draining valleys, deeply incised gorges and polje depressions (Plate 3.2). During the Pleistocene these would have formed the dominant meltwater pathways emanating from the Orjen ice cap, transporting sediments from the ice margin and ultimately offshore into the Bay of Kotor and the Adriatic Sea. Today, these meltwater routes contain well-preserved Pleistocene morphosedimentary records. These provide an unrivalled opportunity to study a variety of fluvial depositional settings (e.g. coastal

and upland alluvial fans, polje fills and river terraces) which are representative of many glaciated catchments across the Mediterranean and elsewhere. Their geographical proximity means that they can be studied alongside the glacial record in the context of a single landsystem (Evans, 2003). Whilst the glacial record of Orjen has recently been documented in detail (Hughes *et al.*, 2010; see Section 3.4), the fluvial archives downstream have not previously been investigated.
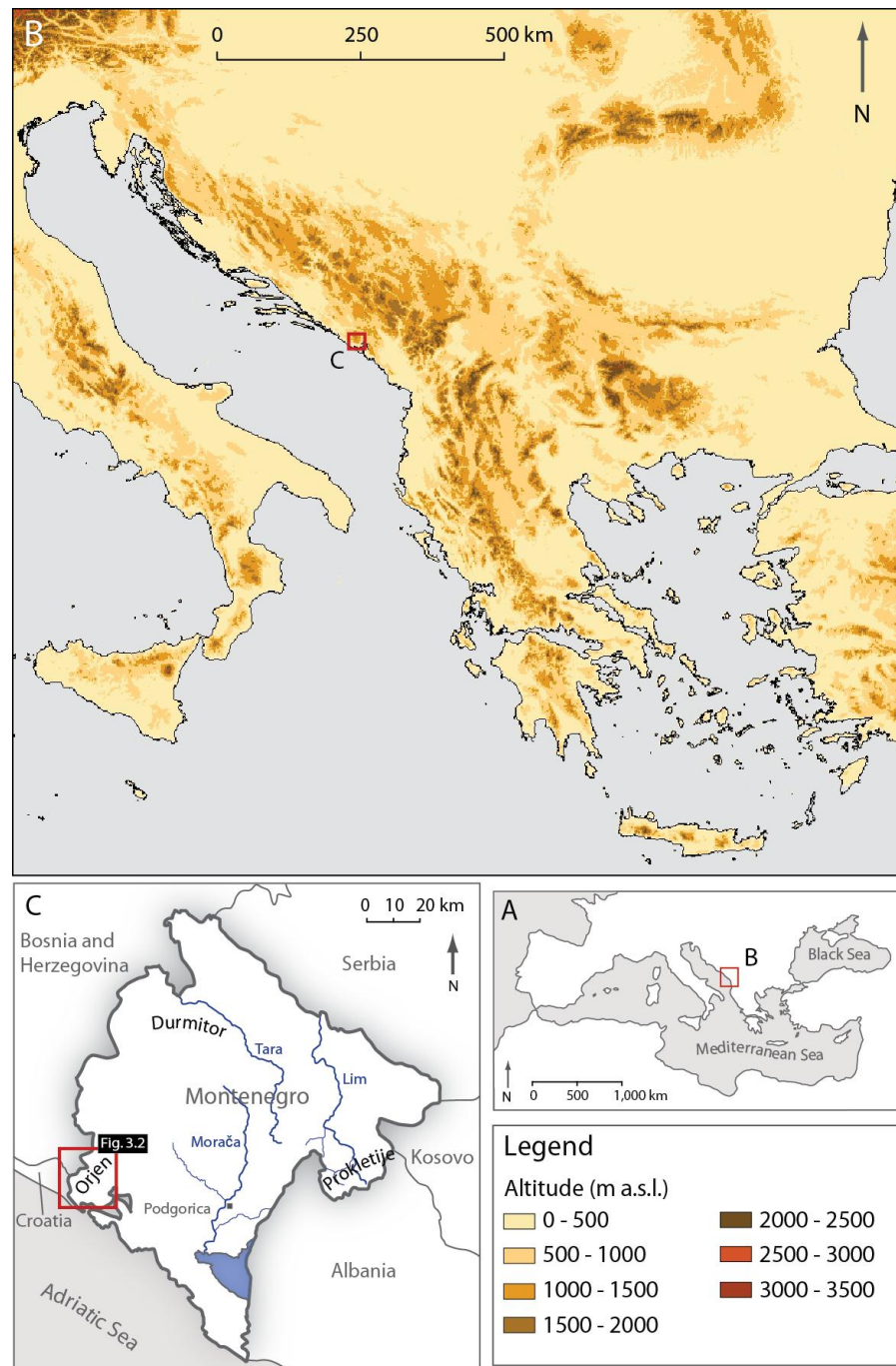
Figure 3.1 – The study region of Montenegro with: A) The Mediterranean context; B) Topographic map of the Balkan region; and C) Map of Montenegro indicating Mount Orjen.

Plate 3.1 – The study region of the Orjen massif: A) View from the town of Kotor, east of Perast (Fig. 3.2), looking northwest over the Bay of Kotor towards the mountains of Orjen; B) View eastwards, from the highest peak of the Orjen massif, Zubački kabao, overlooking the high altitude plateau of Reovci.
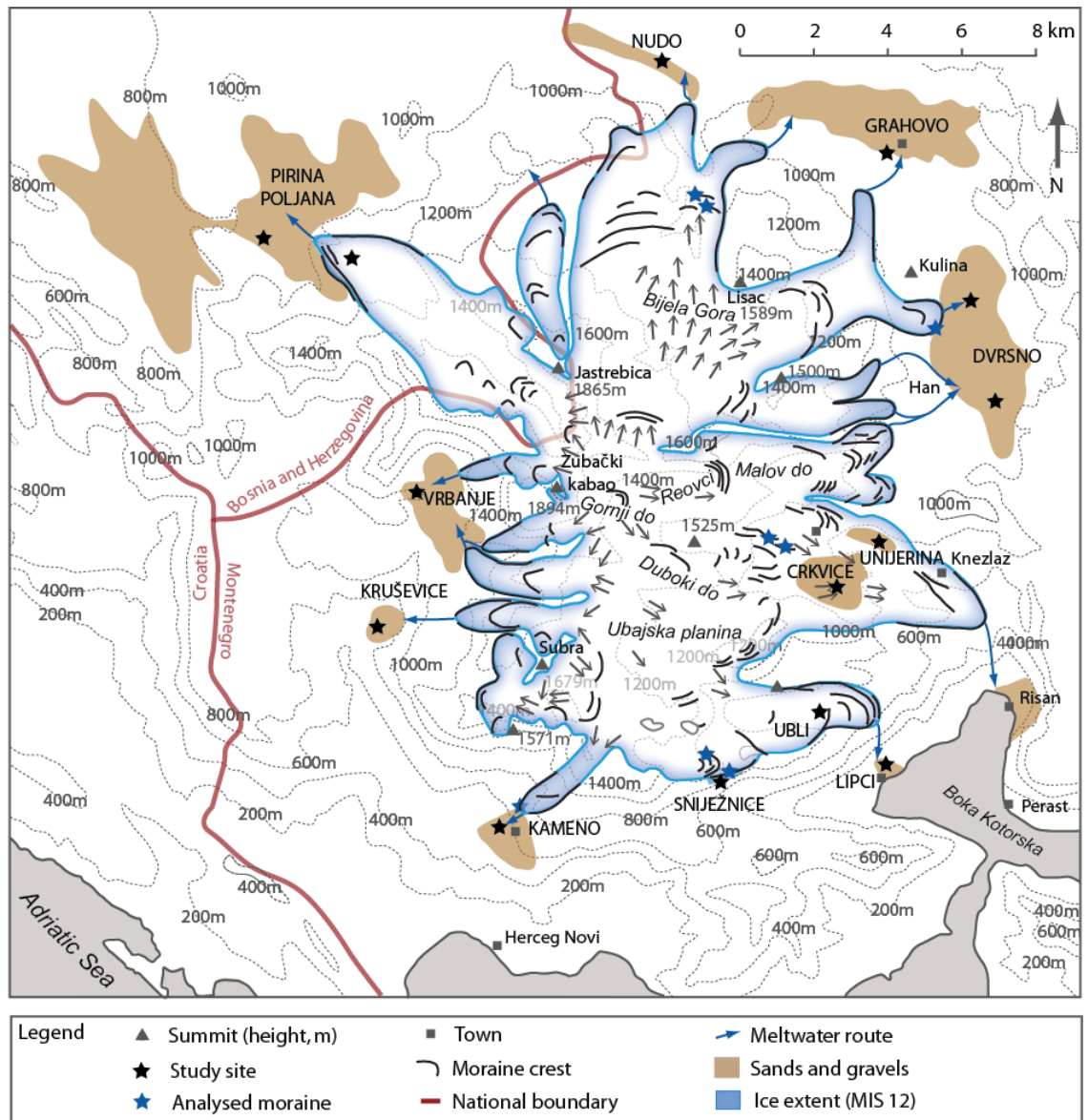
Figure 3.2 – The study region of Orjen, southwest Montenegro indicating the maximum Pleistocene ice margins (MIS 12) detailed by Hughes *et al*. (2010) and the field sites investigated in this study.

Plate 3.2 – Geomorphological environments of the Orjen massif: A) River terrace in the Nudo valley, north Orjen; B) Grahovo polje, west Orjen; C) Oblique view of the coastal alluvial fan at Lipci, southwest Orjen, taken from the fan apex downstream of a steep-sided bedrock ravine; D) Karstified limestone bedrock outcrops on the high altitude region of Sniježnice, south Orjen; E) Moraine at Sniježnice, correlated to MIS 6 (Hughes *et al*., 2010); F) Exposed bedrock on the steep valley sides at Kruševice, western Orjen.

3.2   Geology and karstic processes

3.2.1   Regional geology

The regional geology and surficial sediments are reported in a series of 1:100,000 geological maps by the Institute for Geological and Geophysical Research (IGGR), Belgrade (Izradio Zavod za geološka I geofizića istrazivanja, Beograd) 1962-69 (Fig. 3.3). Carbonate lithologies are

dominant throughout Montenegro, with non-carbonate (clastic, metamorphic and igneous) lithologies present only in isolated patches (Djurović and Petrović, 2007). The Orjen massif is formed in Jurassic and Cretaceous limestones and dolomites with Triassic and Eocene limestones, dolomites and flysch. The Pleistocene ice cap delineated by Hughes *et al*. (2010), covered Upper Cretaceous limestones and dolomite. Jurassic and Lower Cretaceous limestones are also present to the northern and southern extents of the maximum ice limits. Outside the former ice margins, Triassic and Jurassic limestones are present to the north; Upper Cretaceous and Eocene limestones and dolomites to the East; Cretaceous and Jurassic limestones to the west, and Eocene and Cretaceous flysch and conglomerates to the south. Extensive areas of unconsolidated Quaternary sediments have also been identified within and outside the former ice margins (IGGR, 1969). These are of variable origin including alluvial, glacial, lacustrine and colluvial deposits (Fig. 3.3).

The coastal region of Montenegro has undergone a long and intensive history of faulting and tectonic movement (Oluić *et al*., 1982). Plio-Pleistocene tectonic activity has led to considerable, uplift-dominated, vertical displacement along this region of the Adriatic coast (Djurović and Petrović, 2007). Current uplift rates of the highest mountain regions of Montenegro are estimated at 2-4 mm/yr. Evidence suggests that the Bay of Kotor itself and the Skadar Basin (southeast Montenegro and Albania) have been downthrown (Djurović and Petrović, 2007) and are currently subsiding.

3.2.2   Limestone karst

The dominance of limestone lithologies, often of considerable thickness and purity, means that large areas of Montenegro have been exposed to intense karstification during the Quaternary. Karst is a distinctive landscape formed within highly soluble rocks such as limestone, gypsum and marble (Ford and Williams, 2007). It contains a series of subterranean hydrological networks and surficial landforms, and is characterised by features such as sinking streams, caves, enclosed depressions, fluted rock outcrops and large springs. In regions of high rainfall, such as Montenegro, the elevated water flux generates a highly active karstic system, and karst relief forms a distinctive feature of the landscape (Lewin and Woodward, 2009; Telbisz, 2010a; 2010b). Djurović and Petrović (2007) have suggested that karstic processes also enhanced the incision of over 20 large canyons and gorges across Montenegro (such as the

Tare, Morača, and Grlye canyons), many of which drain the high mountain regions and may exceed 1,300 m depth (Djurović and Petrović, 2007).

A series of karstic landforms have developed across the high altitude areas of the Orjen massif as well as at lower elevations, including: dolines/sinkholes (e.g. Reovački Dolovi, Duboki Do, Crni Do, Vuči Do, Stjepov Do and Dubovi Do) and poljes (e.g. Pirina Poljana, Grahovo and Dvrsno) (Magaš, 2002). Of these, poljes are some of the largest karstic features of the Orjen landscape, often measuring up to several hundred square kilometres. A wide range of polje forms exist, and their origins are widely disputed in the literature (see Jennings, 1985; Gams 1978; Nicod, 2003). Three hydrogeological criteria are considered common to most poljes (Gams, 1978; Ford and Williams, 1989; 2007):

- The feature is flat bottomed and is situated on bedrock or unconsolidated sediment.
- The polje develops within a closed basin that is constrained on all sides by steeply rising slopes.
- The polje possesses a subterranean, karstic, drainage system.

The five polje forms identified by Gams (1978) have been simplified into three basic morphogenic types by Ford and Williams (1989). Border poljes are dominated by allogenic sediment inputs and develop where, during fluvial activity, lateral planation and alluviation dominate over incision. Baselevel poljes are controlled by water table fluctuations rather than allogenic mechanisms and occur where the epiphreatic zone intersects the surface. Structural poljes are geologically controlled and are associated with grabens and fault-angle depressions. This type of polje forms an important feature of the Dinaric karst landscape where polje morphology is conditioned by geological characteristics. The polje deposits of the region of Orjen have not been extensively researched.

The Eastern Adriatic coast comprises a Mesozoic-Early Palaeogene carbonate platform of up to 8,000 m thick that has also been extensively karstified during tectonic folding, faulting and uplift (Surić et al., 2005; 2009). Late Pleistocene-Holocene sea level rise has flooded the coastal region, submerging many karstic forms such as pits, caves and speleothems. Over 230 of these submerged features have now been identified along the Croatian coast alone (Surić et al., 2009). Here, the deepest recorded speleothem is now situated at a depth of 71 m below sea level (Garašić, 2006).
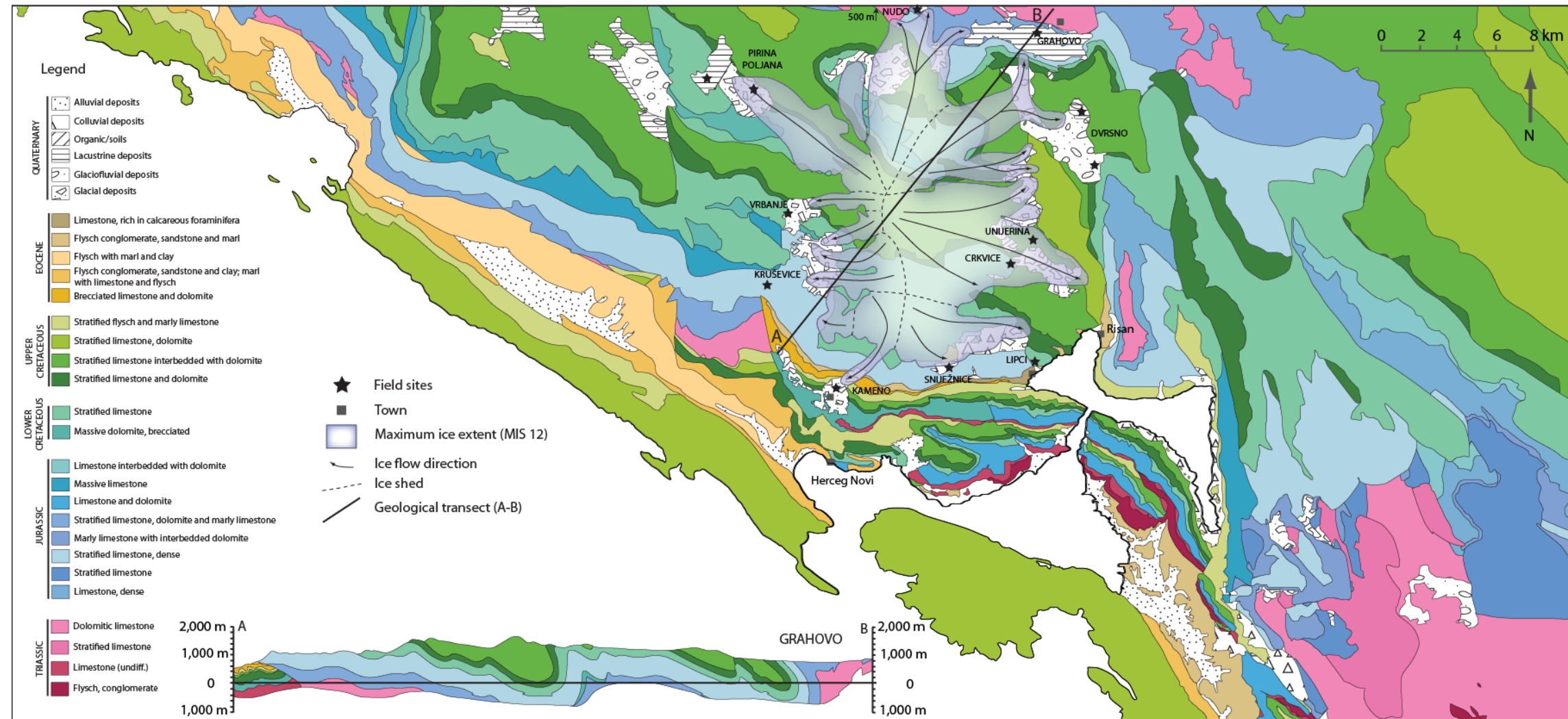
Figure 3.3 – Geological map of the Orjen massif and vicinity. The maximum (MIS 12) extent of the Pleistocene ice margins of Hughes *et al*. (2010) are indicated with ice shed boundaries and flow directions. Adapted from: Institute for Geological and Geophysical Research, Belgrade (1969).

Studies based on the mineralogy and U-series dating of submerged speleothems on the Krk Island of Croatia by Surić *et al.* (2009) suggest two periods of sea level highstand during MIS 5a (c. 87-77 ka) (Surić *et al.*, 2009). These ages are used to estimate a regional tectonic uplift rate of 0.15–0.25 mm/yr with episodic subsidence. On the neighbouring Pag and Brač islands of Croatia, ^{14}C ages from submerged speleothems (Surić *et al.*, 2005) suggest that speleothem formation persisted throughout the local last glacial maximum (c. 37 – 22 ka cal BP). Sea level inundation, rather than climatic conditions, was deemed the cause of the cessation of speleothem growth at c. 21.6 cal ka BP. This highlights the strong interactions between Quaternary climatic changes and regional tectonics in this part of the Mediterranean.

In the upland regions, karstic landscapes are frequently shaped by Pleistocene glacial activity, leading to the production of 'glaciokarst' (Smart, 1986; Bogdan and Leszek, 1999; Lewin and Woodward, 2009). This now forms the dominant landscape of many parts of the Dinaric Alps, such as Mount Orjen; the Cantabrian Mountains of Spain; and the Pindus Mountains of Greece (Hughes and Woodward, 2009). Many poljes within glaciokarst across the Balkans and elsewhere now contain detailed morphosedimentary records of Pleistocene glaciation, yet have received little research attention.

3.3   Modern climate

The climate of Montenegro is strongly influenced by its latitude, the orographic effects of its high mountain regions and its proximity to the large water bodies of the Adriatic Sea and Lake Skadar (Hydrological and Meteorological Service of Montenegro, 2006). Rainfall across Montenegro is markedly seasonal and is largely concentrated into the winter months, particularly November and December (Magaš, 2002) (Table 3.1). The cyclone of Genoa also has a strong influence on the regional climate, where low atmospheric pressure is established across the Balkan Peninsula, causing short-lived episodes of intensive precipitation (Hughes *et al.*, 2010). Montenegro is unique in that, despite its Mediterranean climate, it receives some of the highest recorded precipitation in Europe (Magaš, 2002). At Crkvice (940 m a.s.l.) in the mountains of Orjen and adjacent to the Bay of Kotor (Fig. 3.1), average annual precipitation between 1931 and 1960 was 4,962 mm/yr, with 8,063 mm recorded in 1937. This value is likely to be even greater at higher elevations. Average values of up to 7, 000 mm/yr have been reported by the Hydrological and Meteorological Service of Montenegro (2006). Frost, mist

and fog are also highlighted as key moisture sources in the Dinaric Alps and are likely to enhance precipitation values further (Kirigin, 1967; Mileta, 2005; Hughes *et al.*, 2010). During the Pleistocene, this elevated moisture supply would have had favourable impacts on karstic processes and the development of large ice masses in the mountains of Orjen. The development of a large ice cap here, at such low elevations (<2,000 m a.s.l.), probably reflects the high precipitation inputs to this region even during cold stages of the Pleistocene (Hughes *et al.*, 2010). Present-day glaciers in the Prokletije Mountains of eastern Montenegro and northern Albania are sustained at such low latitudes (42.5°N) and altitudes (1,980-2,410 m a.s.l.) through elevated inputs of avalanching and windblown snow. Glaciers at similar latitudes exist only at higher elevations, such as the North Cascade Range, North America (47-49°N) and the Caucasus of Russia/Georgia (41–44°N) (Hughes, 2009). Current glaciers at equivalent or lower latitudes to the Prokletije are found only in the Southern Hemisphere under maritime climates such as New Zealand (Braithwaite and Raper, 2007). The Franz Josef glacier in New Zealand (43.4°S) has an ELA of c. 1,500 m a.s.l. as a response to high annual precipitation inputs of c. 5,000 mm (Woo and Fitzharris, 1992). This supports the presence of glaciers in the high mountain regions of Montenegro under the estimated moisture supply conditions of the Pleistocene.

Month	Max. Temp (°C)	Min. Temp (°C)	Rainfall (mm)
Jan	4.9	-3.2	584
Feb	5.5	-2.6	474
Mar	8.1	-0.3	507
Apr	12.0	3.4	386
May	16.8	7.3	204
Jun	20.5	10.1	134
Jul	23.8	12.4	74
Aug	23.9	12.2	142
Sep	20.3	9.6	256
Oct	16.0	5.7	499
Nov	10.4	2.0	720
Dec	6.5	-1.5	642

Table 3.1 – Modern climate data by month for Crkvice, Orjen, southwest Montenegro. From Hydrological and Meteorological Service of Montenegro (2006).

At the national scale, surface runoff in Montenegro is channelled by a series of large rivers (Fig. 3.2): the River Lim, the River Tara and the River Morača. These watercourses drain in two dominant directions: northwards towards the Black Sea (over a total drainage area of 7,260

km^2), and south towards the Adriatic (6,560 km^2) (Hydrological and Meteorological Service of Montenegro, 2006). This is supplemented by an extensive subterranean karstic hydrological system which has not been extensively researched.

3.4   Soils

The soils of Montenegro are largely Entisols (containing only an A horizon) and Alfisols (A, E, Bt and Cox/C horizons) (see Fig. 4.4) which are typical of Mediterranean climates, and have developed on moraines, glaciofluvial outwash, river terrace surfaces and within karstic poljes (Magaš, 2002). Fluviosols (soils developed within waterlain sediments) are also common on younger deposits and lithosols (soils containing imperfectly weathered rock fragments) have developed within many karstic areas. Terra rossa has also been reported in regions of purer limestone and dolomite lithologies (Morley and Woodward, 2011). On the Orjen massif, soils have developed across the landscape except for at higher altitudes and on active and unconsolidated slopes.   In many areas of Orjen, particularly at higher elevations, extensive areas of exposed bedrock remain uncovered by Quaternary sediments or soil horizons (Plate 3.2). This reflects the stripping of the landscape by glacial action and surface runoff.

3.5   Previous research: Quaternary glaciation of Montenegro

Several generations of research into the Quaternary glacial history of Montenegro suggest at least three phases of Pleistocene glaciation (Sawicki, 1911; Roth von Telegd, 1923; Messerli, 1967; Hughes, 2007; Kuhlemann *et al*., 2009; Hughes *et al*., 2010; 2011b). These broadly reflect the Pleistocene glacial chronostratigraphy developed by Hughes (2004), Woodward *et al.* (2004) and Hughes *et al*. (2006c) for the Pindus Mountains of northwest Greece, which comprises: the Skamnellian (c. MIS 12), the Vlasian (c. MIS 6), and the Tymphian (c. MIS 5d-2) stages, as well as more recent glaciation during the Younger Dryas (Table 3.2). Some of the largest Quaternary ice masses of southern Europe developed in the mountains of Montenegro within three dominant glacial centres: Prokletije; Durmitor and adjacent massifs; and Orjen (Milivojević *et al*., 2008; Djurović, 2009). The lowest elevation Pleistocene glaciers developed in the coastal region of the Dinaric Alps at elevations below 1,000 m a.s.l. (Penck, 1900; Civjić,

1900). In some instances, such as the Krk islands of Croatia, Marjanac and Marjanac (2004) suggest that ice in this region of the Adriatic may have extended down to sea level.

Chronostratigraphy	Correlated Marine Isotope Stage (MIS)	Glacial Characteristics
Tymphian Stage	5d-2	Localised ice fields, valley and cirque glaciers
Vlasian Stage	10-6	Separate ice caps, valley and cirque glaciers
Skamnellian Stage	12	Conjoined ice caps and valley glaciers

Table 3.2 – Glacial chronostratigraphy developed for the Pindus Mountains, Greece (Hughes, 2004) and applied within the glaciated mountains of Orjen, southwest Montenegro (Hughes *et al*., 2010) and the upland massifs of central Montenegro (Hughes *et al*., 2011b).

3.5.1   Prokletije

In the Prokletije Mountains of eastern Montenegro and Albania, Milivojević *et al*. (2008) report a series of three moraines situated at 990 m, 1,350 m and 1,900 m a.s.l. No absolute ages are available for these records, but based on existing glacial deposits across the Mediterranean (Pindus Mountains, Greece; Mount Velebit, Croatia; Mount Retezat, Romania and the Pyrenees, Spain; see Hughes *et al*., 2006c) Milivojević *et al*. (2008) have tentatively correlated them to the pre-LGM period, the LGM and the Younger Dryas, respectively. Roth von Telegd (1923) reported the presence of '*firnmasse*' (mass of firn) in the Prokletije mountains during the early twentieth century. The largest of these extended for over 1 km from the highest cirque, Maja Jezerce (2,692 m a.s.l.). The nature of these snow/ice masses is unclear from the reports of Roth von Telegd and how many 'real' glaciers existed in the early twentieth century is unknown and little is known about the modern state of these *firnmasse* features. However Hughes (2009) confirmed the presence of at least four small active glaciers in the Prokletije.

3.5.2   Central massifs

The Pleistocene glacial record of the central Montenegrin massifs (Durmitor, Sinjajevina, Moračke Planine, Maganik, Prekornica and Vojnik) has been examined in detail by Hughes *et al*. (2011b). The Pleistocene glacial history and karstic landscape of Sinjajevina has also been discussed by Telbisz (2010a; 2010b). 31 U-series ages (Table 3.3) as well as morphostratigraphic and soil development data have been used by Hughes *et al*. (2011b) to highlight five glacial phases across this part of the Dinaric Alps. The largest glaciation occurred

before 350 ka, and is correlated to MIS 12 (470-420 ka). At this time, four coalescing ice caps covered an area of c. 1,483 km^2, making it the largest Pleistocene ice mass so far identified in the Balkans. This corresponds to the major, Skamnellian, glacial phase observed elsewhere in the Balkans, such as Greece (Hughes, 2004) and Orjen, Montenegro (Hughes *et al*., 2010). A subsequent glacial phase correlated to MIS 10-6 (360-130 ka) broadly corresponds with the Vlasian glaciation of MIS 6. The last cold stage (MIS 5d-2) in the Durmitor region corresponds to the Tymphian glacial phase (110-11.7 ka), and was characterised by cirque and valley glaciers covering an area of 49 km^2. Evidence of more recent, Younger Dryas (12.9-11.7 ka) and Holocene glaciation has also been identified in the highest cirques of central Montenegro. Recent investigation by Hughes (2007; 2008) has identified an active glacier in the Durmitor massif, central Montenegro. The Debeli Namet glacier (43.0139°N, 19.0736°E) is situated in the north-facing Karlica cirque of Mount Slijeme (2,455 m a.s.l.), Durmitor. It currently covers an area of 0.05 km^2 (Hughes, 2007; 2008) making it the largest active present day glacier of the Balkan Peninsula. The rapid growth and decay of this ice mass in response to annual climatic variability demonstrates the high sensitivity of these low latitude glaciers to environmental change, both under the current climatic regime and throughout the Quaternary. The survival of the Debeli Namet glacier is thought to be largely reliant upon the inputs of avalanching snow (Hughes, 2008) which highlights the importance of moisture availability for glacier development in the Balkan region.

3.5.3   Orjen

In the Orjen massif (1,894 m a.s.l.), Pleistocene glacial landforms were identified in the early 20th century by Grund (1910) and Sawicki (1911) extending as low as 500 m a.s.l. towards the Bay of Kotor. More recently the glacial history of Orjen has been reviewed by Marković *et al*. (2009) and discussions of the glaciokarst have been presented by Stepišnik *et al*. (2009). The Pleistocene glacial deposits of Lovčen, c. 25 km southeast of Mount Orjen, have been documented by Stepišnik and Žebre (2011). The most comprehensive investigation into the glacial history of the Orjen massif has been undertaken by Hughes *et al*. (2010) who used detailed geomorphological mapping, U-series dating (Table 3.3; Fig. 3.4) and soil development indices to determine the extent and timing of Pleistocene glacial activity. Three phases of Pleistocene glaciation have been identified on Mount Orjen, which correspond to the glacial evidence from central Montenegro (Hughes *et al*., 2011b) and further south in the Pindus Mountains of northwest Greece (Hughes, 2004). The most extensive ice cap on Orjen,

correlated to MIS 12, covered an area of 165 km^2 and up to 450 m thick, extending down to 500 m a.s.l. in some areas (Hughes *et al*., 2010). Under the current precipitation inputs of c. 5,000 mm/yr, a temperature depression of c. 5-6 °C would be required to maintain a glacier of this size. This further highlights the importance of a sustained moisture supply across the Balkan region during Pleistocene cold stages (Kuhlemann *et al*., 2009).

Member and Location	U-series age (ka)	Harden Soil Index	MIS Stages	Chronostratigraphy (after Hughes, 2004)	Glacial Characteristics
Debeli Namet Member Central Montenegro			AD 1850 to present		Modern glacier
Gornji do Member Orjen	9.6 ± 0.8 8.0 ± 0.2			Younger Dryas	Cirque glaciers
Karlica Member Central Montenegro	10.9 ± 0.3 10.5 ± 0.3 9.8 ± 0.3 9.1 ± 0.3 7.9 ± 0.3 2.2 ± 0.09	14.3			Valley and cirque glaciers
Reovci Member Orjen	17.3 ± 0.6 13.9 ± 0.4 12.5 ± 0.4		MIS 2	Tymphian	Valley and cirque glaciers
Meded Member Central Montenegro	13.4 ± 0.4	16.8			Valley glaciers
Crkvice Member Orjen	124.6 ± 5.7 124.5 ± 3.5 124.0 ± 3.4 102.4 ± 3.1		MIS 6	Vlasian	Ice caps and valley glaciers
Žabljak Member Central Montenegro	120.2 ± 6.4 105.4 ± 5.2 104.1 ± 2.9 88.1 ± 3.4	31.5			Ice caps and valley glaciers
Žabljak Member Central Montenegro (Absent from Orjen)	231.9 ± 17.5 162.7 ± 7.9 58.8 ± 2.0	32.7	MIS 8 or 10		Ice caps and valley glaciers
Knežlaz Member Orjen	>350 >350 309.3 ± 42.4		MIS 12	Skamnellian	Ice caps
Ninkovici Member Central Montenegro	>350 >350 396.6 ± 87.2 40.7 ± 1.2 38.8 ± 1.3	43.1			Ice caps

Table 3.3 – Summary of U-series ages from calcites cementing moraines in the coastal mountains of Orjen (southwest Montenegro) and the central massifs (Durmitor, Sinjajevina, Moračke Planine, Maganik, Prekornica and Vojnik). From Hughes *et al*. (2010; 2011b).
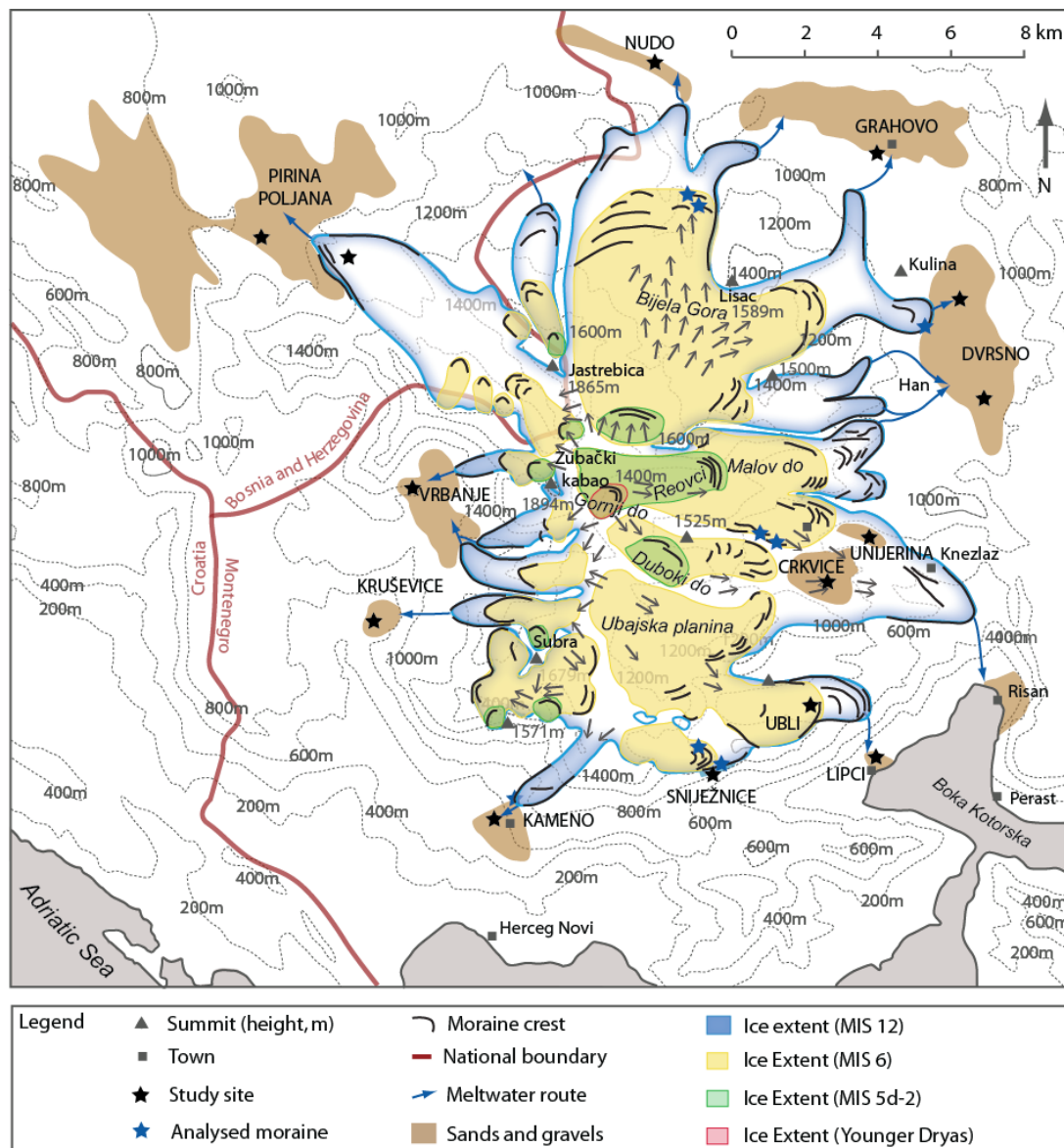
Figure 3.4 – The glacial record of the Orjen massif, adapted from Hughes *et al.* (2010). Ice margins from MIS 12, 6, 5d-2 and the Younger Dryas are indicated. The glacial chronostratigraphy is based on U-series ages and the Harden Soil Index (Table 3.3). The moraine positions (black outlines) reflect field-based evidence, whilst the intervening ice limits (blue, yellow, green and red outlines) represent the interpolated margin estimates.

Subsequent glaciations were less extensive, and largely comprised smaller ice caps (MIS 6) and more isolated cirque and valley glaciers (MIS 5d-2). As observed in other parts of Montenegro, the last glacier on Orjen formed during the Younger Dryas and covered an area of c. 1 km². The Pleistocene ice masses on Orjen advanced in an outward radiating nature from the central massif. The morphology of individual outlet glaciers is highly asymmetric, and reflects the spatial variability in ice mass dynamics over successive glacial cycles. In many valleys

surrounding the Orjen massif, the glacial records have been well preserved, and demonstrate clear geomorphological links to the fluvial archives downstream. The robust geochronology and detailed understanding of the glacial record here provides a valuable opportunity to investigate the interactions between Pleistocene glacial and fluvial systems.

3.6   Field sites

Twelve field sites have been selected for analysis. These are situated radially surrounding the Orjen massif, both within and outside the maximum Pleistocene ice margins (Fig. 3.2; 3.4; 3.5 Table 3.4). Eight moraines have also been selected for sedimentological and particle size analysis at: Lisac, Dvrsno, Crkvice, Sniježnice and Kameno. Together, these sites reflect a variety of alluvial depositional environments. Their analysis in conjunction with the existing glacial record of the Orjen massif (Hughes *et al*., 2010) can be used to considerably enhance our understanding of Pleistocene landsystem dynamics both within Montenegro and elsewhere.
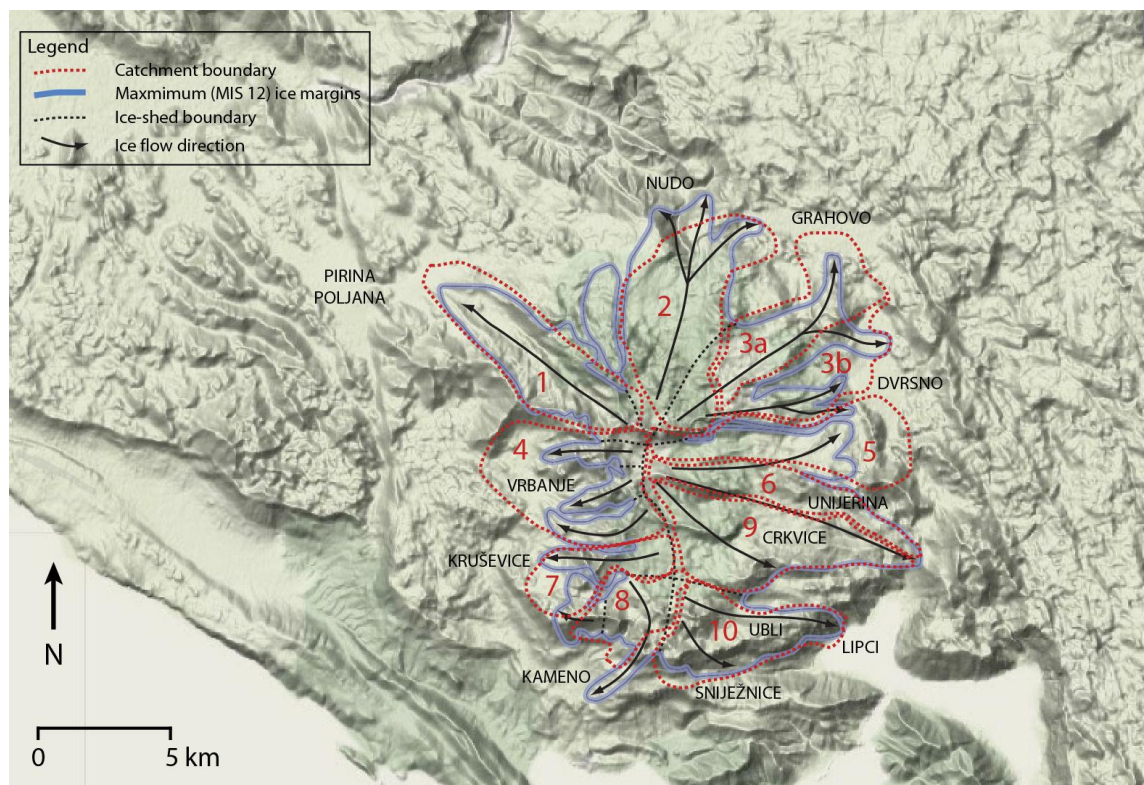
Figure 3.5 – Study sites and catchment boundaries (red outlines). Ice-sheds (black outlines), ice flow directions (black arrows) and the maximum Pleistocene ice margins of MIS 12 (blue outlines) from Hughes *et al.* (2010) are also delineated. See table 3.4 for catchment areas (km^2). Base map source: Google Earth.

Site Name	Geomorphological Context	Latitude, Longitude	Catchment Number and (Area, km^2)	Elevation (m a.s.l.)	Minimum Distance from Pleistocene ice margin (m)	Number logged sections	Number U-series ages	Number thin sections
Grahovo	Polje	42.6492°N 18.6512°E	3a and 2* (14.25 and 24.25*)	722	1,390	2	1	-
Dvrsno	Polje	42.6130°N 18.6795°E	3b and 5† (11.25 and 17.00)	623	950	9	-	-
Kruševice	Polje	42.5307°N 18.4910°E	7 (8.50)	632	2,000	2	-	-
Vrbanje	Polje	42.5663°N 18.4954°E	4 (21.25)	982	1,400	4	1	-
Pirina Poljana	Polje	42.6152°N 18.4127°E	1 (19.75)	677	4,360	3	2	-
Crkvice	Polje	42.5406°N 18.6378°E	9 (18.75)	848	2,200	2	2	-
Lipci	Alluvial Fan	42.4981°N 18.6556°E	10 (15.25)	40	980	4	7	-
Kameno	Alluvial Fan	42.4904°N 18.5363°E	8 (8.00)	622	150	8	3	-
Nudo	River Terraces	42.6736°N 18.5704°E	2 (24.25)	407	500	8	6	9
Unijerina	Proglacial/Lacustrine	42.5505°N 18.6512°E	6 (10.00)	627	1,900	3	4	2
Ubli	Proglacial	42.5119°N 18.6326°E	10 (12.00)	785	1,500	1	-	-
Sniježnice	Ice Marginal Glaciofluvial	42.4971°N 18.5979°E	10 (6.75)	1,044	100	2	1	-

Table 3.4 – Field sites surrounding the Orjen massif selected for analysis in this study. Sites reflect polje, alluvial fan, river terrace and ice marginal morphosedimentary environments. Site locations in relation to the Pleistocene ice margins are displayed in Figure 3.4. Ice sheds and catchment areas are delineated in Fig. 3.5. *Grahovo is supplied by two ice sheds, one of which also supplies Nudo. †Dvrsno is also supplied by two ice sheds.

CHAPTER FOUR

Field and Laboratory Methods

Synopsis

A series of field and laboratory methods have been used in this study to investigate the depositional history of the alluvial sequences surrounding Orjen. In the field, geomorphological maps and sediment logs were produced, including secondary carbonate macromorphological descriptions. Field analysis was supplemented in the laboratory with detailed particle size analysis and measurement of the insoluble residue/carbonate content ($CaCO_3$) of the fine matrix fraction. Secondary carbonates were also analysed in the laboratory using micromorphology to investigate their formation mechanisms in more detail. Two geochronological techniques have been used at the sites surrounding Orjen. The Harden Soil Index is used as a relative geochronometer and was completed both in the field and the laboratory. U-series dating of secondary carbonates selected in the field provides radiometric age indicators, and was completed in the laboratory at the Open University Uranium Isotope Facility. This chapter details the procedures undertaken in the field and laboratory, and is categorised by method. More detailed descriptions of the complex chemical preparation procedures used within U-series dating are provided in Appendix A. The calculation procedures used to determine soil profile development indices within the Harden Index are presented in Appendix B.

4. 1   Geomorphological mapping

A full understanding of Quaternary landscape dynamics relies on the detailed geomorphological description of individual landforms and landform assemblages (Chorley *et al*., 1984). The reconstruction of glacial landsystems over complete climatic cycles requires a holistic assessment of both the nature and distribution of glacial landforms and sediments (Evans, 2003; Evans and Benn, 2007). A detailed understanding of the geomorphological system provides a robust framework through which smaller scale sedimentological, geochronological and micromorphological analyses can be integrated.

At all study sites on the Orjen massif, fluvial and glaciofluvial landforms were mapped onto 1:25,000 base maps from the Vojnogeografski Institut (Military Geographical Institute, Belgrade) and referenced against existing glacial geomorphological maps developed by Hughes *et al.* (2010). A handheld Garmin ETrex global positioning system (GPS) was used to record site location and surface altitude. Locational accuracy was typically ± 3 m, whilst altitudinal accuracy varied from ± 3 m to ± 11 m within areas of high vegetation density. All field mapping was supplemented using satellite imagery and aerial photography from the Vojnogeografski Institut (Military Geographical Institute, Belgrade) as well as satellite imagery from Google Earth. This increased the accuracy and resolution of the mapped areas.

A total of 14 field sites within 12 areas surrounding Orjen were surveyed over 2 field seasons (2010 and 2011) to provide a comprehensive geomorphological appraisal of the major meltwater routes emanating from the Orjen massif and their fluvial depositional contexts. Three broad geomorphological environments are represented here: river terraces, polje fills, and alluvial fans. Ice marginal and proglacial settings were also identified and logged in the field as individual exposures.

4.1.1 Field methods

4.1.1.1 River terraces

Fluvial terraces represent abandoned floodplains that have been isolated from the present channel by uplift and/or incision (Merritts, 2007). In many river valleys, flights of several terraces have been preserved and provide a long history of Quaternary river dynamics (Macklin *et al.*, 2002; Lewin and Macklin, 2003; Schildgen *et al.,* 2002; Starkel, 2003; Gibbard and Lewin, 2009). Their geomorphology, sedimentology and geochronology can be readily investigated to develop a valuable archive of Quaternary climate change, tectonics, glacial activity and landscape processes.

A suite of river terraces is preserved within the Nudo Valley, on the northern side of Orjen. Base maps of this region are of insufficient resolution to capture the geomorphological complexity of discrete terrace surfaces. Detailed geomorphological maps were produced by traversing the longitudinal valley axis to map the extent and altitude of each terrace surface

using a handheld GPS. GPS data were combined with terrain and satellite imagery to produce the final geomorphological map.

4.1.1.2 Poljes

The formation mechanisms and geological characteristics of poljes have been discussed in Section 3.2. A series of poljes have developed across the Orjen region. They are constrained by the surrounding topography and range in size from 0.6 m to 50 km in length. Poljes were initially identified using satellite imagery, aerial photographs and 1:25,000 base maps. Field observations and GPS points were used to confirm the extent and elevation of each polje.

4.1.1.3 Alluvial fans

Alluvial fans are sedimentary landforms that develop where a channel emerges from an upland catchment (Bull, 1977). They are frequently conical in shape and typically comprise coarse grained, poorly sorted sediments, becoming finer with distance from the fan apex. Their role as a sediment storage component, or buffer, means that they play an important part in mountain geomorphological systems and sediment transfer dynamics (Harvey *et al*., 2005). Within glaciated regions, they can provide a valuable sedimentary record of Quaternary glacial history (Ritter and Ten Brink, 1986). Two alluvial fans emanating from the Orjen massif, at Kameno and Lipci, were mapped onto a 1:25,000 base map. Field observations and GPS points were taken at the fan surface to constrain the depositional extent and surface elevation of each fan deposit.

4.2   Sedimentology and stratigraphy

Sedimentological methods focus on describing the physical properties of sedimentary successions (textures and structures) to investigate their transportation and depositional processes (Reading, 1996). To draw together the relationships between different sediment bodies over wider areas and through time, stratigraphy is used as a system of classification and correlation (Jones *et al*., 1999). Sedimentology and stratigraphy should be considered together (Nichols, 2009) as a method through which Quaternary environmental change and landscape processes can be more fully understood. Sedimentological analysis of Quaternary sequences

(lithostratigraphy) often involves the analysis of the associated landforms (morphostratigraphy). In this regard, morpholithostratigraphy, as a combination of these methods, forms a robust basis for the investigation of Quaternary landscape dynamics, and is adopted here (Hughes, 2010).

4.2.1 Field methods

4.2.1.1 Field descriptions and logging

Access to sedimentary sections was largely provided through quarry exposures, road cuttings, and stream-cut sections. A total of 48 logs were recorded in the field at alluvial sites across Orjen. Sedimentary units were systematically logged using standard procedures noting all changes in texture, grain size and bedding characteristics (see Jones *et al.*, 1999; Evans and Benn, 2004) using the sedimentological symbols displayed in Figure 4.1. Clast density estimates followed the methods of Hambrey (1994) where clast content of <40% is deemed matrix-supported and >40% is clast-supported. Colour changes were assessed using the Munsell Colour notation system (Munsell, 1975). Where calcite profiles had developed, carbonate macromorphology was described in the field following the framework of Netterberg (1969) and Machette (1985). All notes were accompanied by detailed field sketches and photographs taken using a reference object for scale (Fig. 4.1).

Eight moraines, deemed representative of the outlet glaciers emanating from Orjen, were also logged and sampled in the field. These were previously mapped and described by Hughes *et al.* (2010) and have been correlated to either MIS 12 or MIS 6 on the basis of U-series and morphostratigraphy. In this study, their sedimentological analysis is used as an indicator of the glacial sediment sources at selected sites. This provides context for the glacigenic origins of the fine matrix component that is subsequently transported and deposited within the fluvial environment.

4.2.1.2 Matrix and clast sampling

Approximately 100 g of matrix sediment and a selection of clasts (pebble sized) were extracted from key units within each lithofacies and analysed in the laboratory for particle size distribution and determination of $CaCO_3$/insoluble residue content (Section 4.2.2.1). Where

present, clasts were also extracted and their morphology (striations, faceting, and shape) described in the field.

Figure 4.1 – Example of an exposure at Unijerina, western Orjen and a sediment log with clast fabric and roundness data taken in the field. Sedimentological symbols used in this study are indicated in the legend. Full details of lithofacies codes and sample locations are given in Chapter 5.
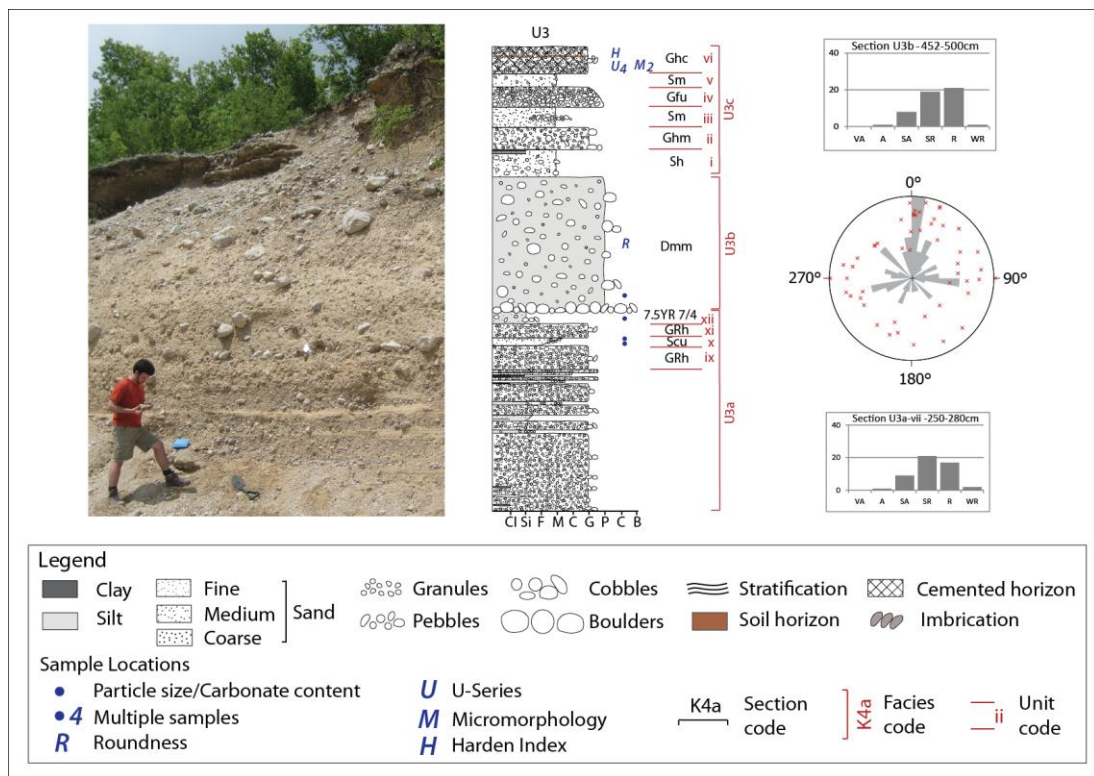
4.2.1.3 Clast roundness

Clast roundness was established using the qualitative sphericity index of Krumbein (1941) and Benn and Ballantyne (1994) based on the visual descriptive appraisal of ≥50 clasts, located *in situ* within each section (Fig. 4.1). The index comprises six categories of increasing roundness: *very angular, angular, sub-angular, sub-rounded, rounded and well rounded*. Roundness ratings were completed by a single operator to maintain internal consistency and minimise the subjectivity inherent to this method (Evans and Benn, 2004). Due to this potential subjectivity, and high spatial variability in clast roundness (Benn and Ballantyne, 1993; 1994), this technique should be used alongside other sedimentological and geomorphological analyses to ensure accurate interpretations of the morphosedimentary record.

4.2.1.4 Clast fabric

Clast fabric measurements were taken using a compass-clinometer to analyse the a-axis dip and azimuth of elongate clasts preserved *in situ* (see Evans and Benn, 2004). A minimum sample size of 50 clasts was used to reduce statistical variance.

4.2.2   Laboratory methods

4.2.2.1 Particle size analysis and carbonate content

A number of particle size analysis (PSA) techniques are available, and each of these has been extensively reviewed in the literature (see McCave and Syvitski, 1991; Syvitski *et al*., 1991; Michoel *et al*., 1994; Konert and Vandenberghe, 1997; McCave *et al*., 2006; Goossens, 2008). Laser diffraction techniques are widely regarded as providing the greatest reproducibility (Sperazza *et al.,* 2004; Goossens, 2008). In this study, particle size distributions were generated using a Malvern Mastersizer 2000 laser diffraction particle size analyser using a standard operating procedure (SOP) developed for the carbonate-rich samples typical of the Orjen study region. The Orjen SOP consists of an automated four-step procedure to ensure robust internal consistency of sample measurements:

1. System alignment and measurement of background obscuration/residual noise.
2. Manual introduction of the sample in solution and application of 25 seconds of pre-treatment ultrasound to disaggregate the sample.
3. Samples passed through the detection lens. Three repeat measurements are taken and a mean value calculated. Values are reported as percentage volume concentrations.
4. The system is cleaned and refilled between sample runs to minimise cross contamination.

PSA was undertaken on a total of 170 sediment matrix (clay-sand horizon) samples from key lithofacies within glacial and fluvial sequences. These were analysed at two size classes and for two lithological fractions:

- <2 mm – bulk (all lithologies)
- <63 μm – bulk (all lithologies) and insoluble residue (non-carbonate lithologies)

PSA was also completed for the insoluble residue component of 16 bedrock clast samples from 11 sites surrounding the Orjen massif. These were analysed at <2 mm:

- <2 mm – insoluble residue (non-carbonate lithologies)

These samples were used to generate detailed particle size distributions (PSD) of both the total sediment sample (<2 mm) and the fine grained component (<63 µm) (Fig. 4.2). Analysis of the two lithological fractions (bulk and residual) allowed the transition of limestone clasts to be analysed during their transformation in the glacial and fluvial environment. Bulk and residual samples required different preparation and analytical procedures:
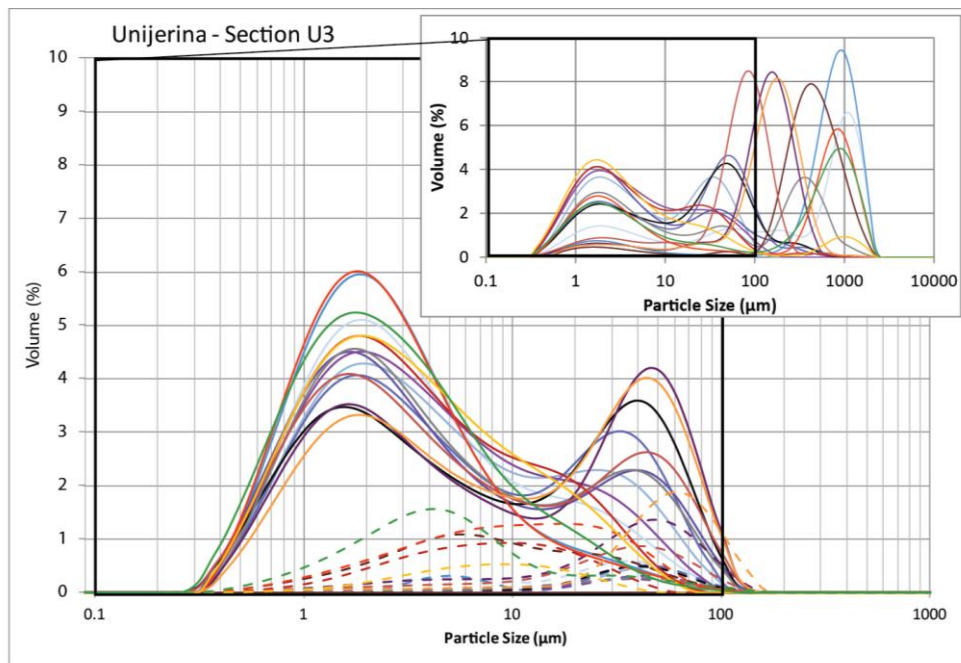
Figure 4.2 – Example of PSA data generated using the Malvern Mastersizer for sediment samples from Unijerina, western Orjen, screened at <2 mm and <63 µm. Full details of the data and sampled horizons are provided in Chapters 5 and 6.

Bulk sample preparation and analysis: Sediment matrix <2 mm and <63 µm

Approximately 5-6 g of each sample was oven dried at 60°C for 12 hours and reweighed to determine the dry sample weight. Samples analysed at <2 mm were dry sieved through a 2 mm sieve mesh. Particles retained in the sieve were weighed and set aside. Samples analysed for the <63 µm fraction were screened through a 63 µm (4ϕ) sieve mesh using deionised

water. Samples retained within the sieve were dried and reweighed to give the >63 μm fraction as a percentage of the total dry weight.

The use of separate samples allows the fine sediment fraction to be analysed without the potential obscuration of larger (>63 μm) particles. This method also minimises the potential inaccuracies in separating the <63 μm fraction from a previously analysed <2 mm sample. In such instances particles >63 μm, yet incorporated into the <63 μm sample, may be quantified multiple times.

Samples were taken into solution using deionised water and 5 ml dilute (5 % v/v) sodium hexametaphosphate. Solutions were agitated into suspension and set aside for 24 hours to ensure full disaggregation and minimise particle flocculation (Konert and Vandenberghe, 1997) prior to laser particle analysis. Samples were analysed using a 2,000G dispersant unit suitable for standard sample concentrations (>10% laser obscuration) and following the Orjen SOP.

Residual sample preparation and analysis: Sediment matrix <63 μm and bedrock <2 mm

To assess the calcium carbonate ($CaCO_3$) content (% mass) of each sample, sediments were digested in 10% HCl. The insoluble residue was then used to generate a particle size distribution of the non-carbonate lithologies, to be compared with the bulk sediment PSD.

Samples were prepared following the methodology outlined in Woodward (1990). Approximately 8-10 g of each sample was oven dried at 60°C for 12 hours and reweighed. 10 ml distilled water and 10 ml HCl was added to each sample, left to settle and the supernatant decanted. The process was repeated until no further reaction occurred. Each sample was washed with deionised water to remove excess HCl and decanted. The remaining sediment was oven dried at 60°C and reweighed to calculate the $CaCO_3$ content as a percentage of the dry bulk sample weight. The dry samples were screened through a 63 μm sieve mesh using deionised water and washed into a 50 ml centrifuge tube. 5 ml dilute sodium hexametaphosphate was added to each sample and agitated. The coarse grained fraction (>63 μm) was retained, dried and reweighed.

Three limestone clasts from 11 sites were weighed and digested in 10% HCl and reweighed, following the methods outlined above. The insoluble residue was analysed at the <2 mm size fraction.

Following acid digestion, residual sample weights (<1 g) were insufficient for analysis using the standard dispersal unit. Samples were analysed manually, following the Orjen SOP, using a 2,000µp nano sample dispersal unit, suitable for samples of <10% laser obscuration using the 2,000G dispersal unit.

4.2.2.2 Laser particle size analysis: system calibration

To ensure internal consistency and comparability of results a series of calibrations were undertaken using the standard (2,000G) and nano (2,000µp) sample dispersal units. Matrix samples were randomly selected from ten sites and screened at both 2 mm and 63 µm. Samples <2 mm were analysed using the standard sample dispersal unit. Samples <63 µm were analysed using both the standard and nano sample dispersal units. The results of this calibration (Appendix C) suggest that the <2 mm and <63 µm data are directly compatible and can be interpreted as a single dataset.

4.3   Secondary carbonates: field macromorphology and thin section micromorphology

4.3.1   Field methods

4.3.1.1 Carbonate macromorphology and field sampling

Secondary carbonate macro- and micromorphological studies are widespread within arid regions both in the Mediterranean (see Candy *et al*., 2003; 2005; 2012; Alonso-Zarza *et al*., 2004; Eren *et al*., 2008; Candy and Black, 2009) and elsewhere (see Rossinsky and Swart, 1993; Khadkikar *et al*., 1998; 2000), but have not been widely undertaken within more humid or moist climate regions (Andrews *et al*., 1998). Since the original definition of the term *calcrete* by Lamplugh (1902) a number of carbonate cement forms have been described in the literature using a range of terminology. These are summarised in Table 4.1. These terms are often used interchangeably with a great deal of overlap and little formal nomenclature (Candy

et al., 2011). The term *calcrete* is now more specifically regarded as a secondary carbonate developed in association with pedogenic processes. In this study, to avoid confusion of terminology, all carbonate cements will be referred to as *secondary carbonates* or *calcites* to avoid any genetic interpretations. Secondary carbonates were classified using the morphogenic framework of Candy *et al.* (2011) (Fig. 4.3).

Secondary Carbonate Terminology	Classification of Candy *et al.* (2011)	Formation and Description
Calcrete (soil/pedogenic) Also termed *Caliche*	Weathering-zone carbonates	Formed within a soil profile due to biogenic activity. Forms discrete nodules coalescing to form indurated hardpan and laminar crusts (Braithwaite, 1983; Wright and Tucker 1991; Candy *et al.*, 2003).
Vadose zone carbonate		Formed above the water table by the downward leaching or dissolution of carbonate, and not necessarily in association with an overlying soil profile. Forms as coatings on clasts or as infills within larger void spaces of clasts (Aber, 1979).
Phreatic (groundwater) zone carbonate		Formed at or below the water table, often within the small pore spaces between detrital grains (Arakel and McConchie, 1982; Nash and Smith, 1998; Kelly *et al.*, 2000).
Tufa	Flowing-water carbonates	Formed in association with cool-water springs and riverine environments through degassing as groundwater flows into the subaerial environment. Forms as overgrowths on clasts and as laminated carbonates (Pentecost, 1993; Andrews *et al.*, 2006; Candy *et al.*, 2011).
Travertine		Formed in association with hot-water springs through degassing as groundwater flows into the subaerial environment. Forms as overgrowths on clasts and as laminated carbonates (Pentecost, 2005; Andrews *et al.*, 2006; Candy *et al.*, 2011).
Lacustrine carbonate	Still-water carbonates	Forms by abiogenic precipitation due to modifications in water chemistry. Carbonate precipitates in the water column and is deposited from suspension at the lake bed (Candy *et al.*, 2011).

Table 4.1 – A selection of the most widely used secondary carbonate terminology. These are referenced against the simplified framework developed by Candy *et al.* (2011).

All secondary carbonates are formed through the dissolution and reprecipitation of calcium carbonate ($CaCO_3$) within an unconsolidated, host sediment body. Calcite precipitation occurs at sedimentary horizons where surface evaporation is in equilibrium with the percolation of $CaCO_3$-rich water (Wright and Tucker, 1991; Wright, 2007). Secondary carbonate formation is widespread within Quaternary sedimentary sequences of Mount Orjen due to the limestone-

dominated bedrock, the abundance of glacially-eroded fine sediments, and the high precipitation totals.

Secondary carbonates suitable for micromorphological and U-series analysis were identified in the field on the basis of several criteria (Plate 4.1):

- Calcites are representative of the sampled exposure/horizon.
- Calcites have developed *in situ* within a sedimentary sequence.
- There is limited evidence of recent disturbance to, and exposure of, calcite surfaces.
- Where possible, calcite profiles contain detrital clasts/grains to allow calcite-grain interactions to be assessed.

Calcite macromorphology, stratigraphic position and orientation were detailed following the descriptive framework of Netterberg (1969) and Machette (1985). This system was developed for pedogenic carbonates, but is applicable to a range of weathering zone carbonate forms. Samples were extracted using a geological hammer.
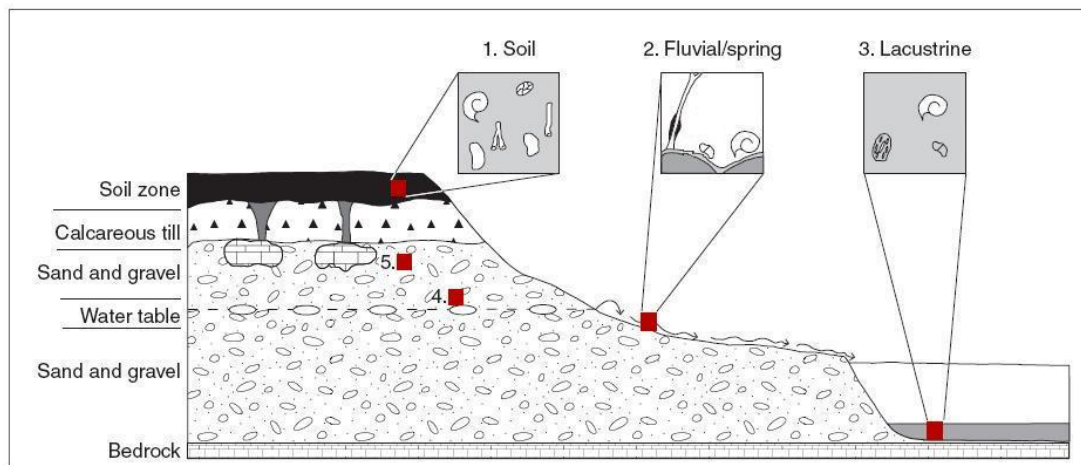
Figure 4.3 – The dominant types of terrestrial and freshwater carbonates. Their formation position within a sedimentary body is indicated: 1) Weathering-zone - pedogenic/soil carbonates (containing, clockwise: terrestrial mollusc shells, earthworm granules, calcified root systems and carbonate nodules); 2) Flowing-water – fluvial/spring carbonates (containing, clockwise: chara precipitates, freshwater mollusc shells, ostracods, and clast coatings); 3) Still-water – lacustrine carbonates (containing, clockwise: freshwater mollusc shells, ostracods, and chara fragments); 4) Weathering-zone – phreatic zone carbonates; 5) Weathering-zone – vadose zone carbonates. Adapted from Candy *et al*. (2011).

Plate 4.1 – A secondary carbonate profile at Kameno. This profile contains large, detritus-free calcite crystals suitable for U-series analysis, it is representative of the carbonate sequence here, it has developed *in-situ,* and it contains multiple large clasts – the grain: calcite contacts of which can be analysed using micromorphology.

4.3.2 Laboratory methods

4.3.2.1 Sample preparation and thin section manufacture

Micromorphological analysis has been widely applied to secondary carbonate (calcite) horizons within Quaternary sedimentary sequences (Calvet and Julià, 1983; Bain and Foos, 1993; Alonso-Zarza and Arenas, 2004; Candy *et al.*, 2005; 2012). Thin section analysis can reveal considerable complexity in secondary calcite formation mechanisms that are otherwise overlooked at the macro scale. Variations in microstructure can provide significant detail on the prevailing climatic and vegetation conditions as well as characteristics of the host sediment and the duration of carbonate accumulation (Wright and Tucker, 1991; Alonso-Zarza and Arenas, 2004). This has considerable implications for our understanding of Quaternary land surface developments and for the use of secondary carbonates within U-series and relative dating techniques. Calcite samples were prepared for micromorphological analysis at the Earthslides thin section laboratory, Cambridge. Samples were impregnated in Polylite clear casting resin and mounted onto large format glass slides.

4.3.2.2 Microscopy

Slides were analysed using a petrographic microscope under plane and cross polarised light at 40x and 100x magnification. Microfacies were delineated across each thin section profile, and microfabrics were described in detail to reflect variations in cement/groundmass, grain abundance and microstructures, following examples outlined by *inter alia* Alonso *et al*. (2004) and Wright (2007). Calcite cements (micrite, microspar, and spar) and detrital grain components were quantified as a percentage areal cover of individual microfacies following the methodology of Kemp (1985). Each microstructure was quantified on the basis of percentage areal cover following a four-fold classification devised for this study (Table 4.2; adapted from Kemp, 1985) and assigned a corresponding score. Scores were collated to aid comparisons between samples (Chapter 9).

Microstructure abundance – % areal over			
Abundance	**Code**	**Description of areal cover**	**Score**
Absent	A	0%	0
Present	P	<30%	1
Frequent	F	30-60%	2
Dominant	D	>60%	3

Table 4.2 – Frequency groupings of microstructure abundance based on areal percentage cover. Adapted from Kemp (1985).

4.4   Harden Index of soil development

Soil profiles have been widely used in the Mediterranean and elsewhere to construct relative geochronologies and to correlate across landform surfaces (e.g. Harden, 1982 in California; van Andel, 1998; Hughes *et al*., 2006c; and Woodward *et al*., 1994 in Greece; Hughes *et al*., 2010 in Montenegro; Pallàs *et al*., 2010 in Spain). The use of soil development indices, recording physical and chemical changes within a soil profile, means that this method can be applied in a series of geomorphological environments. This is particularly valuable as a complement to, or in the absence of, radiometric age indicators.

Within the Mediterranean, soils are dominantly Alfisols (Birkeland, 1999; Soil Survey Staff, 1999), which contain an organic-rich A horizon, an underlying leached E horizon, and a clay-rich Bt horizon (Fig. 4.4). In regions of carbonate-rich substrate or percolating waters a Bk or K horizon may develop, which itself comprises a series of time-dependent secondary carbonate

morphological stages (Gile *et al.*, 1965; 1966). The underlying, unmodified host substrate is termed the C horizon (van Andel, 1998).
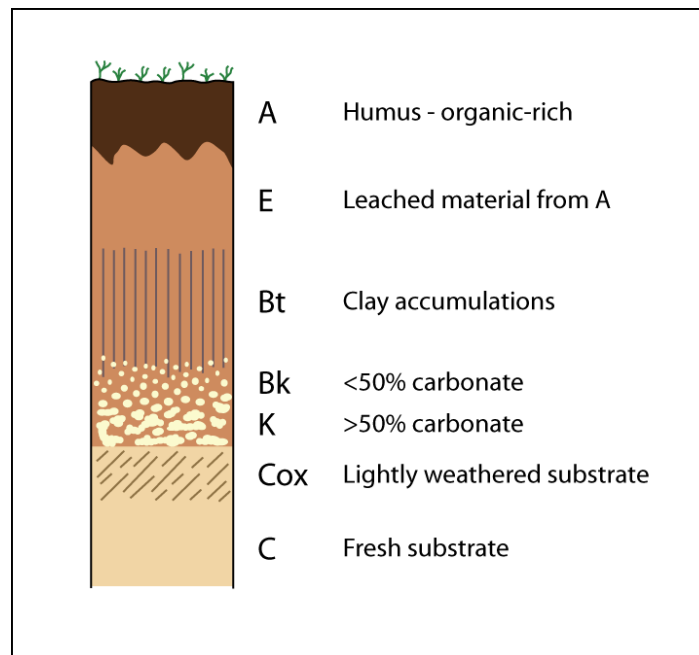
Figure 4.4 – Idealised profile of a Mediterranean Alfisol. Adapted from van Andel (1998).

In this study, the Harden Soil Index has been used to correlate landform surfaces and provide a degree of relative age control. This method was developed by Harden (1982) in the Merced River system of central California. It has been successfully applied by Hughes *et al.* (2010) to soils developed on the glacial landforms of Orjen. The Index comprises nine parameters that can be determined in the field and are used to characterise the soil profile (Harden, 1982):

- Rubification (colour hue and chroma)
- Colour Paling (colour hue and chroma)
- Melanisation (colour value)
- Structure
- Wet consistency and total texture
- Dry consistency
- Moist consistency
- Clay films
- pH

For internal consistency, field observations from this study were supported by additional investigation under controlled laboratory conditions. Results from each profile were normalised and summed (Appendix B; Birkeland, 1999) to provide a combined profile development index (PDI). The greater the PDI value, the more mature the soil profile.

4.4.1 Field methods

4.4.1.1 Soil profile sampling

In the field, soil profiles and parent material were described in detail noting horizon thickness, texture, Munsell colour and visual attributes. Unless soil stratigraphy determined otherwise, profiles were sampled at 10 cm increments (c. 200 g air-dry weight) extending from the surface (A horizon) to the underlying substrate (C horizon). The remaining parameters were analysed in the laboratory following the methods outlined by Harden (1982) and adapted by Birkeland (1999).

4.4.2 Laboratory methods

Samples were air dried for 48 hours to remove excess moisture, and screened through a 2 mm sieve mesh to remove granular material. Each of the Harden Index parameters were determined for all soil horizons. Organic content (loss on ignition) was also measured to further investigate the degree of soil profile development (after Woodward *et al*., 1994; Hughes, 2004).

4.4.2.1 Rubification, colour paling and colour value/melanisation

Soil colour can provide a valuable indication of soil maturity (van Andel, 1998). Colour hues and chromas often become redder and brighter with age, through the process of rubification (Kubiëna, 1970; Harden, 1982). Colour values tend to decrease with age as the A horizon becomes darker through the accumulation of organic matter (melanization) (Harden, 1982). The colour of each soil horizon within the study region was assessed in the field when moist and after air drying in the laboratory using a Munsell soil colour chart (Munsell, 1975).

4.4.2.2 Structure: grade and aggregate

Soil structure is assessed using classifications of grade and aggregate type (Harden, 1982). Over time, soil aggregates progress from unconsolidated peds, forming a *granular* horizon, increasing in size and cohesion to form *platey*, *prismatic*, *columnar* and finally *blocky* profile structures (van Andel, 1998; Birkeland, 1999). Soil grade is classified as: *weak*, *moderate*, or *strong* reflecting the aggregation of peds within the soil profile. This was evaluated in the field using visual characterisation of *in situ* soil profiles, and confirmed in the laboratory.

4.4.2.3 Consistency and total texture

Consistency is based on the wet, moist and dry consistencies of the soil profile. Consistency is thought to become harder and firmer with increasing age, as the soil profile becomes more strongly bound by clays, oxides and organic compounds (Harden, 1982). Moist consistency is determined using a scale of friability (*loose, very friable, friable, firm, very firm, extremely firm*). Dry consistency is assessed by hardness ratings (*loose, soft, slightly hard, hard, very hard, extremely hard*).

Soil texture is determined by particle size distribution of sand, silt and clay assessed by hand using a texture triangle. This parameter is combined with measurements of wet consistency. This is assessed using the methods outlined by Birkeland (1999), through the progression of stickiness (*non-sticky, slightly sticky, sticky, very sticky*) and plasticity (*non-plastic, slightly plastic, plastic, very plastic*).

4.4.2.4 Clay films

The development of a clay-rich argillic (B) horizon, with relatively low clay content in the A and C horizons, is indicative of a comparatively mature soil profile. This reflects extensive periods of mineral breakdown and clay translocation (Birkeland, 1999). The clays may also form *in situ* due to mineral weathering within the B horizon (Hubble *et al.*, 1983). Clay films are evaluated on the basis of frequency (*very few, few, common, many*), thickness (*faint, distinct, prominent*) and location (*ped faces, pores bridges, coats, coats and bridges*), following the classifications outlined by Birkeland (1999).

4.4.2.5 pH

Soil pH is largely dependent on the extent of leaching of basic cations through the soil profile, and thus decreases through time (Harden, 1982). The difference in the pH value between the soil and underlying substrate may therefore be used as an indicator of soil maturity. The pH of each soil sample was measured in the laboratory using a desktop pH meter – calibrated using buffer solutions at pH4 and pH7. Samples were analysed in solution using deionized water. Three repeat measurements were undertaken and the mean value was used in the PDI calculations.

4.4.2.6 Organic content – loss on ignition

Loss on ignition (LOI) is a measure of the organic content within a sediment or soil sample. Samples were prepared following the standard procedure (e.g. Dean, 1974; Heiri *et al*., 2001) using approximately 1-2 g of air dried sample. Samples were oven dried for 12 hours at 105°C, reweighed (DW_{105}) and fired at 550°C for two hours, and finally reweighed (DW_{550}). The weight lost on ignition is calculated as a percentage of the original dry weight using equation 4.1.

LOI = [(dry weight – weight after ignition)/dry weight) x 100

or   LOI = [(DW_{105} – DW_{550})/DW_{105}] x 100   [4.1]

4.5   Uranium series geochronology

Uranium-series (U-series) dating is one of the most widely employed geochronological methods in Quaternary science and is particularly effective for dating Quaternary sequences in areas dominated by carbonate-rich lithologies. It has been successfully applied across the Mediterranean in regions containing carbonate-rich bedrock such as the Pindus Mountains of Greece (Hughes, 2004; Hughes *et al*., 2006**c**; Woodward *et al*., 2008), the Italian Apennines (Kotarba *et al*., 2001) and southeast Spain (Candy *et al*., 2005) as well as on the glacial deposits of Orjen (Hughes *et al*., 2010) and across the upland massifs of central Montenegro (Hughes *et al*., 2011b). The limited abundance of quartz- or feldspar-rich lithologies means that optically stimulated luminescence (OSL) or [10]Be cosmogenic dating techniques would not be appropriate for the alluvial deposits of Orjen. The use of [36]Cl has not been tested at the field

site, and may be influenced by the degree of surface weathering of the limestone. U-series has been used across the limestone-rich terrain of the Balkans (see Woodward *et al.,* 2008; Hughes *et al.,* 2010; 2011b) and is therefore the most effective dating technique within this study. A full detailing of U-series systematics is provided in Chapter 8.

4.5.1   Field methods

4.5.1.1 Carbonate sampling

A total of 35 carbonates suitable for U-series analysis were selected in the field based on several criteria:

- Carbonates have developed *in-situ* within a sedimentary sequence.
- There is limited evidence of recent disturbance to, and exposure of, calcite surfaces.
- There is no visible evidence of open system behaviour (i.e. overprinting or recementation of calcite macrofabrics), or multiple macrofabrics can easily be separated (Smart, 1991).
- Carbonates are densely cemented and free from detrital clasts/grains, or detrital clasts/grains can be readily separated.

The macromorphology and stratigraphic position of each calcite was recorded in the field using the methods and nomenclature outlined in Chapter 4.3.1.1 and samples were extracted using a geological hammer.

4.5.2   Laboratory methods

4.5.2.1 Sample pre-clean

In the laboratory, surficial debris was removed using a handheld drill. All sample surfaces were cleaned in dilute hydrochloric acid (10% HCl v/v) and deionised water and then air dried. Where several carbonate fabrics were present, samples were extracted from one fabric only to avoid the homogenisation of carbonate cements potentially spanning multiple precipitation phases. Samples containing macroscopic calcite crystals (>1 mm) were lightly disaggregated using an agate pestle and mortar. Uncontaminated crystals were identified under a light microscope and crushed to a fine powder. Within samples containing smaller calcite crystals

(i.e. <1 mm and not manually separable), or a high detrital grain or clast content, interstitial calcite was directly extracted using a 5 mm drill bit and crushed to a fine powder. For samples prepared for detrital Th correction (Chapter 8) surfaces were cleaned with a handheld drill, but not subjected to HCl washing. This ensured that the detrital matrix component of the secondary carbonate remained intact.

4.5.2.2 Chemical preparation – sample dissolution and spiking

Samples were prepared for analysis by the author alongside staff at the Open University Uranium-Isotope Facility in Milton Keynes (NERC Grant reference: IP/1140/1109) over a total of five weeks. Samples were prepared following the chemical procedures outlined by Edwards *et al.* (1987) using approximately 0.5-1.0 g powdered calcite. Nitric acid (TD 7M HNO_3 and TD 15M HNO_3) was used for sample dissolution, and detritus-rich calcites were further treated with hydrofluoric acid (HF). All samples were spiked with a ^{229}Th/^{236}U solution and equilibrated overnight. Two total procedural blank (TPB) samples and young speleothem (YS) samples were also prepared using the same procedure to assess background contamination and internal consistency. The chemical preparation methods used in this study are fully outlined in Appendix A and are briefly summarised here.

4.5.2.3 Separation of Th and U – anion exchange columns

The Th and U were purified using 10 ml anionic resin columns. Columns were washed in hydrochloric acid (TD 6M HCl), distilled water (MQ H_2O) and nitric acid (TD 7M HNO_3). Th was extracted from the sample using hydrochloric acid (TD 6M HCl) and collected in savillex vials. U was then eluted with hydrobromic acid (TD 1M HBr) and collected in separate vials (Plate 4.2). Samples were evaporated to dryness, and redissolved in nitric acid (TD 14M HNO_3) and distilled water (MQ H_2O).

4.5.2.4 Sample analysis – mass spectrometry

Samples were analysed using a Nu Instruments multi-collector inductively coupled plasma-ionisation mass spectrometer (MC-ICPMS). The MC-ICPMS has high ionisation efficiency and has greater sensitivity than other methods, such as thermal ionisation mass spectrometry (TIMS). Whilst TIMS is frequently the preferred method to achieve high-precision age

determinations, MC-ICPMS was used for the samples in hand for a number of reasons. Several of the Orjen calcites contained high detrital components, providing comparatively small amounts of pure calcite for analysis. The uranium content of the samples was also previously unknown, and the use of MC-ICPMS ensured that potential problems of low calcite concentration and sample availability could be overcome.
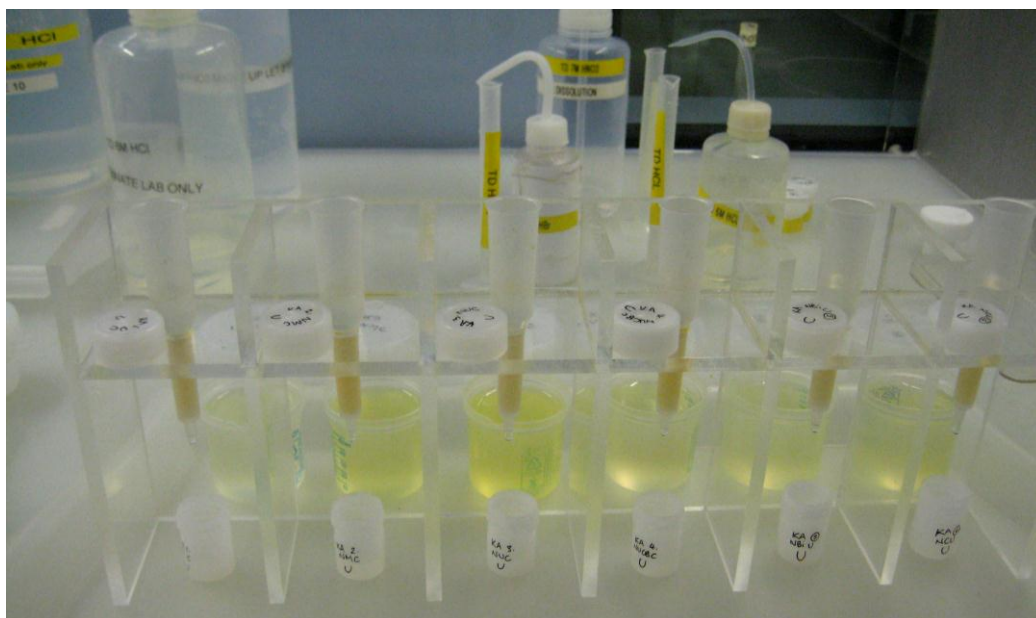
Plate 4.2 – Chemical preparation of U-series samples at the Open University. Here samples are undergoing U-Th separation in anionic resin columns. The sample (in this case, Uranium) is collected in small vials (base of the image) and retained for analysis using the MC-ICPMS.

Samples were run with bracketing standards and cleaning cycles to monitor cross contamination and drift. Each sample reading was then normalised using the two bracketing standards. The detritus, TPB and YS samples were analysed alongside the carbonate samples and standards to cross check for internal consistency.

4.6   Summary

The use of a wide range of field and laboratory techniques allows the nature and timing of fluvial response to Pleistocene glaciation, within a range of geomorphological settings, to be investigated in detail. The results of the analytical methods outlined here are presented in the following chapters.

CHAPTER FIVE

Results – Field Evidence: Geomorphology and Sedimentology

Synopsis

Field analysis of the fluvial geomorphology and sedimentology of the study sites surrounding Mount Orjen provides the key data for exploring the interactions between Pleistocene glacial and fluvial environments. A detailed understanding of Pleistocene landsystem dynamics relies heavily on a thorough examination of morphosedimentary archives. This is particularly significant within the current study as it is based upon a large-scale landsystems approach (see Evans, 2003). Morphosedimentary observations are used to inform the sampling of sedimentary sequences for particle size, micromorphology and U-series analysis. This chapter discusses the key morphosedimentary evidence from alluvial depositional sites, and a selection of moraines, surrounding the Orjen massif. The observed sediments are used to develop facies models of fluvial sedimentary response to glacial activity (Section 5.14; Chapter 9). Sediment logs presented in the following sections record the horizons sampled for particle size analysis, micromorphological analysis, U-series and Harden Index soil development characteristics. The results of these analyses are fully discussed in chapters 6, 7 and 8, respectively.

5.1   Introduction

A total of 14 field sites, within 12 study areas, have been selected from both within and outside the former ice margins identified in Hughes *et al.* (2010) (Figure 5.1). These are situated radially around the Orjen massif and broadly correspond to the major outlet glaciers and meltwater routes downstream of the former ice cap. These sites reflect a variety of depositional environments including: six poljes, two alluvial fans, a river terrace sequence, an ice marginal zone and a proglacial low energy/shallow lacustrine setting. This chapter details the geomorphological and sedimentological records at each of these environmental setting surrounding Mount Orjen (Sections 5.2 – 5.14). Detailed sedimentary logs were recorded at 48 exposures across the field sites. Sedimentological symbols, facies and unit codes follow those outlined by Benn and Evans (1998); Jones *et al.* (1999) and Evans and Benn (2004) (Table 5.1) using the legend displayed in Figure 5.2. Section altitude is levelled at the surface of each exposure and displayed adjacent to the section logs. Roundness data are presented alongside

the sediment logs and in Appendix D (supplementary data disc). The spatial variability of clast roundness characteristics (Benn and Ballantyne, 1994) means that these data should be considered alongside the morphosedimentary context and not as independent datasets. Full field descriptions of individual sedimentological units are provided in Appendix D.
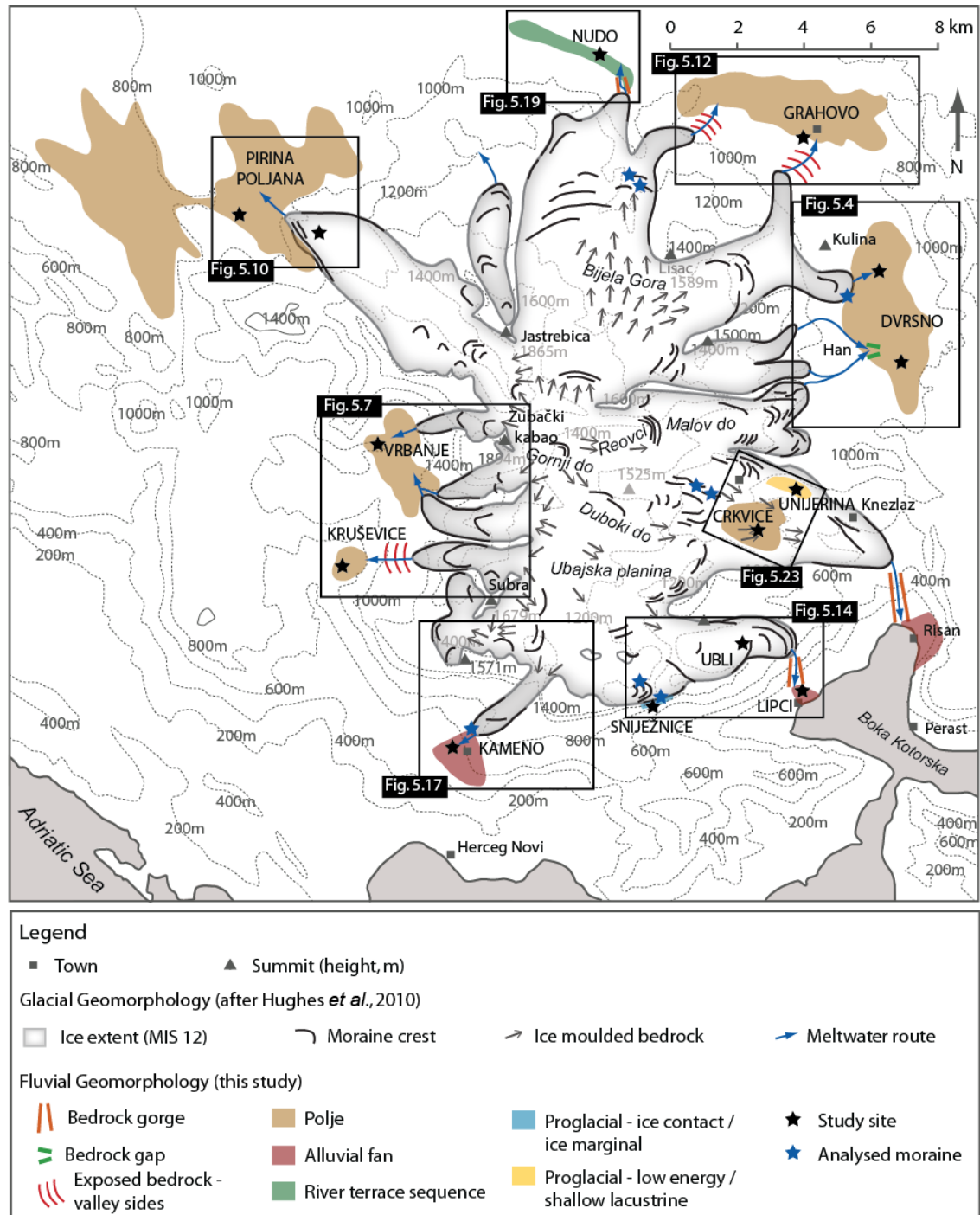
Figure 5.1 - Geomorphological map of the Orjen massif with the glacial record of Hughes *et al*. (2010) and fluvial landforms and depositional environments identified in this study. Features were mapped using 1:25,000 base maps and field GPS coordinates. Observations were verified using Google Earth. Inset labels highlight the expanded maps presented in this chapter.

Facies Code	Description
Dcm	Diamicton, clast supported, massive
Dmm	Diamicton, matrix supported, massive
Fm	Fine sand/silty layer, massive
Fs	Fines, interstratified
Gcu	Gravels, coarsens upwards
Gfu	Gravels, fining upwards
Ghc	Gravels, horizontally bedded, clast supported
Ghf	Gravels, horizontally bedded, fine layers
Ghi	Gravels, horizontally bedded, imbrication
Ghm	Gravels, horizontally bedded, matrix supported
Gmc	Gravels, massive, clast supported
Gmi	Gravels, massive, imbrication
GRc	Granules, clast supported
GRcu	Granules, coarsening upwards
GRfu	Granules, fining upwards
GRh	Gravels, horizontally bedded/plane bedded
GRhc	Gravels, horizontally bedded, clay layers
GRm	Granules, matrix supported
Scu	Sand coarsening upwards
Sgm	Sand, granular, massive
Sh	Sand, horizontally bedded
Shf	Sand, horizontally bedded, fine layers
Sm	Sand, massive
Ssf	Sand, interstratified fine layers
Sx	Sand, cross bedded

Table 5.1 - Lithofacies codes used to describe the key characteristics of sedimentary units within the logged sections. After Benn and Evans (1998) and Evans and Benn (2004).
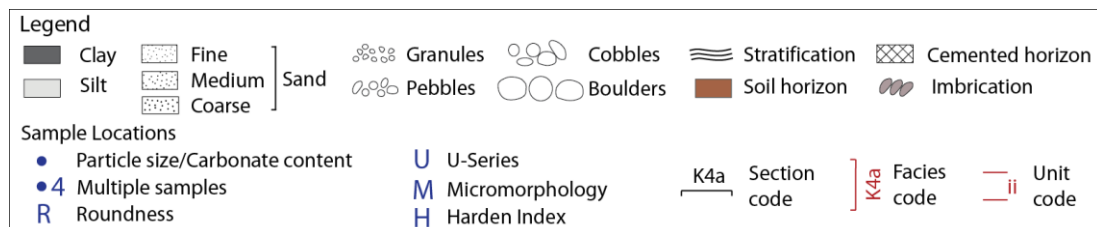
Figure 5.2 – Legend of sedimentological and sampling symbols used within this study.

5.2   Glacial landforms - moraines

The morphosedimentary characteristics of eight moraines (Fig. 5.1) have been described in the field. These moraines have been mapped and U-series dated by Hughes *et al*. (2010) and are correlated to either MIS 12 or MIS 6 (Fig. 5.3). Sedimentological analysis of these moraines provides context for understanding the changing characteristics of glacially-comminuted limestone bedrock and sediments downstream over multiple glacial-interglacial cycles. The moraines surrounding Orjen are classic lateral and terminal moraine features (Hughes *et al*.,

2010) and form arcuate ridges of diamicton deposits. Sediments typically contain a fine silt and clay matrix, indicative of the glacial comminution of limestone clasts (Boulton *et al.,* 1978), with abundant subangular cobbles and boulders (Plate 5.1; Fig. 5.3). The moraine sediments are poorly sorted, matrix- to clast-supported (clast density typically 30-70%) and contain a large granular component. Clasts are angular to rounded and frequently blocky and/or faceted. These characteristics are typical of glacially moulded clast forms (Benn and Ballantyne, 1993; 1994). This suggests a combination of both active and passive transport within the glacier as well as the input of angular scree material from the steep limestone valley sides (Fig. 5.3 Plate 5.2). These observations are consistent with the variety of clast angularity observed within moraines and glacial till deposits (Benn and Ballantyne, 1993).
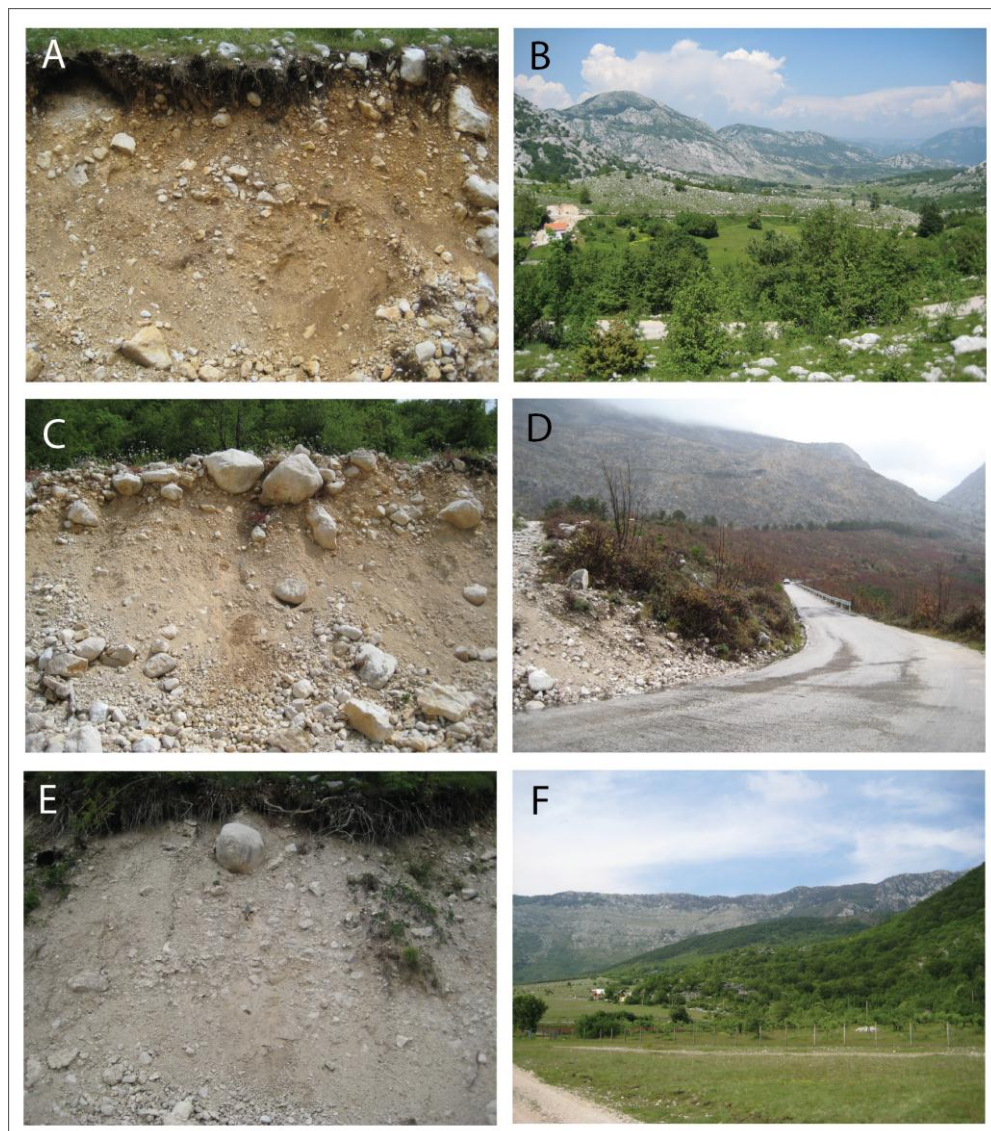
Plate 5.1 – Selected moraines identified by Hughes *et al*. (2010) at : A) Sniježnice (MIS 6); B) Sniježnice (MIS 6) looking downvalley to Ubli; C) Dvrsno (MIS 12); D) Kameno (MIS 12) looking upvalley; E) Lisac (MIS 6) and F) Vrbanje (MIS 12) .
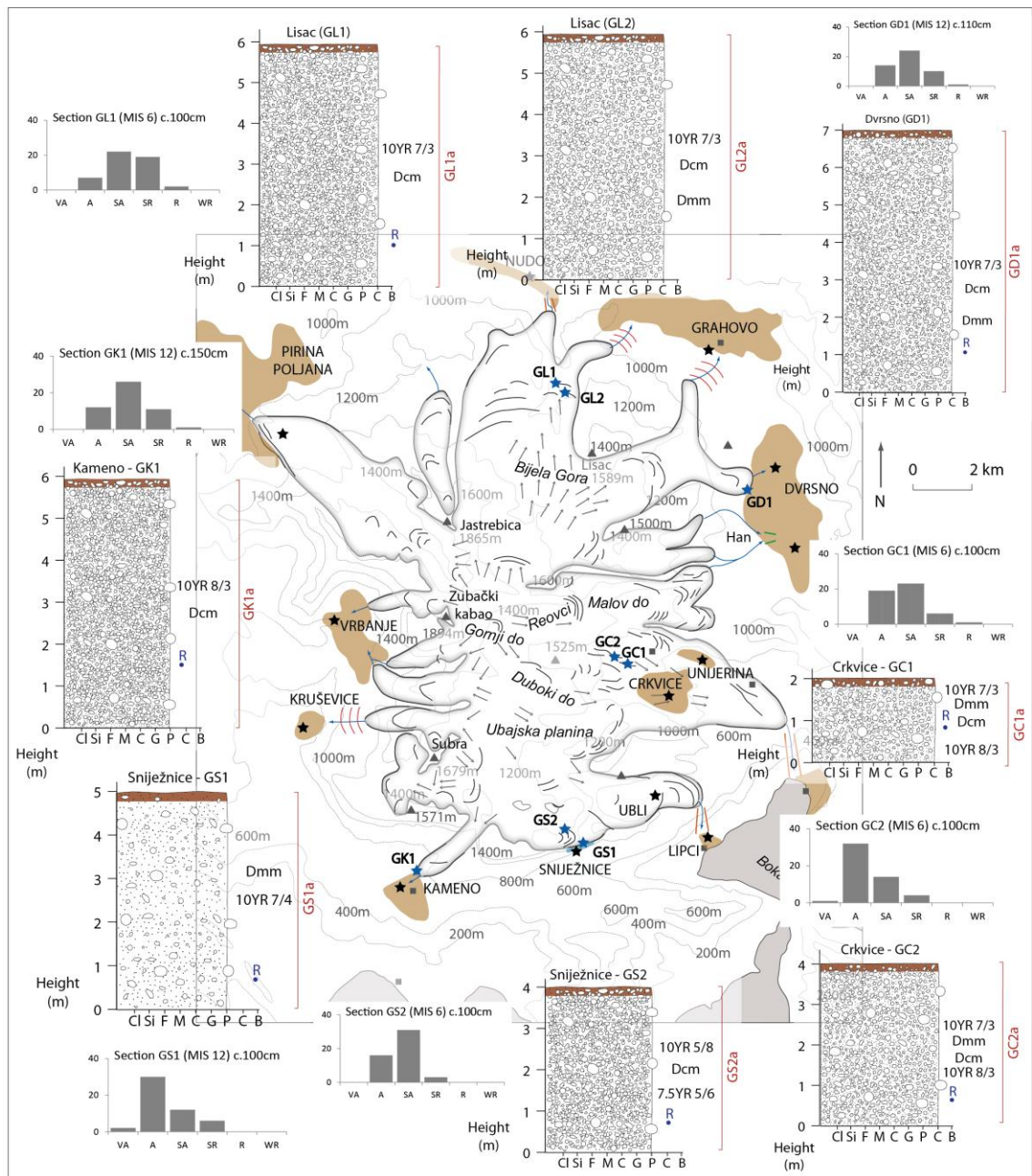
Figure 5.3 – Sedimentary logs and clast roundness data from selected moraines surrounding Orjen. Hughes *et al*. (2010) have correlated the moraines at Lisac (GL1 and GL2), Crkvice (GC1 and GC2) and Sniježnice (GS2) to MIS 6; and the moraines at Dvrsno (GD1), Sniježnice (GS1) and Kameno (GK1) to MIS 12. Legend: Figure 5.2.
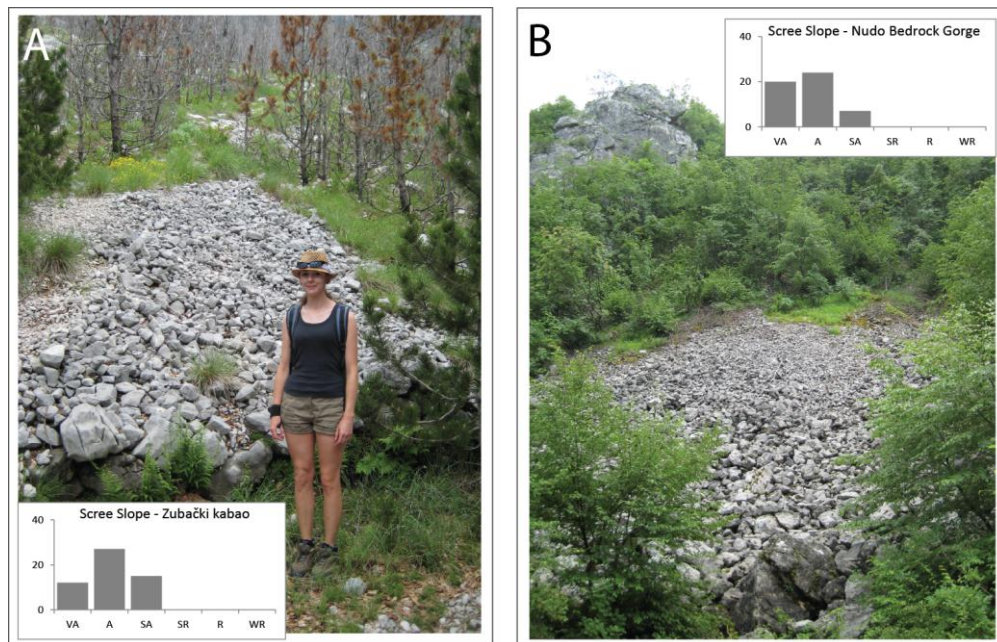
Plate 5.2 - A) Angular limestone scree on the slopes of Zubački kabao (1,894 m), east Orjen.
B) Angular to very angular limestone scree within the steep-sided limestone gorge feeding the
Nudo valley, north Orjen.

5.3   Dvrsno

The Dvrsno polje (42.6130°N, 18.6795°E, c. 630 m a.s.l.) is situated outside the eastern margin
of the former ice cap, trending north-south over an area of 4.6 km x 2 km (Fig. 5.1; 5.4). The
polje surface has a shallow eastwards sloping gradient from 640 to 620 m a.s.l.

Meltwater and sediment has been supplied to Dvrsno by two outlet glaciers from the east of
the Orjen ice cap during MIS 12. The northern ice lobe emanates from the same outlet glacier
that has supplied Grahovo (Section 5.7), but at Dvrsno the ice terminated within the polje and
is marked by a large moraine within the northern sector of the polje depression (Fig. 5.4). The
second outlet glacier, that supplied meltwater and sediment to the southern margins of
Dvrsno, was situated c. 2.5 km from the polje, and the main meltwater route would have
drained through a bedrock gap at Han (Hughes *et al*., 2010). The polje sediments are well
exposed within several quarries to depths of up to 10 m, though the true depth of the polje,
which is currently unknown, is likely to be considerably greater than this (Gams, 2005). Two
transects of sedimentary logs have been analysed downstream of both the northern (Transect
1) and southern (Transect 2) meltwater pathways (Fig. 5.4).
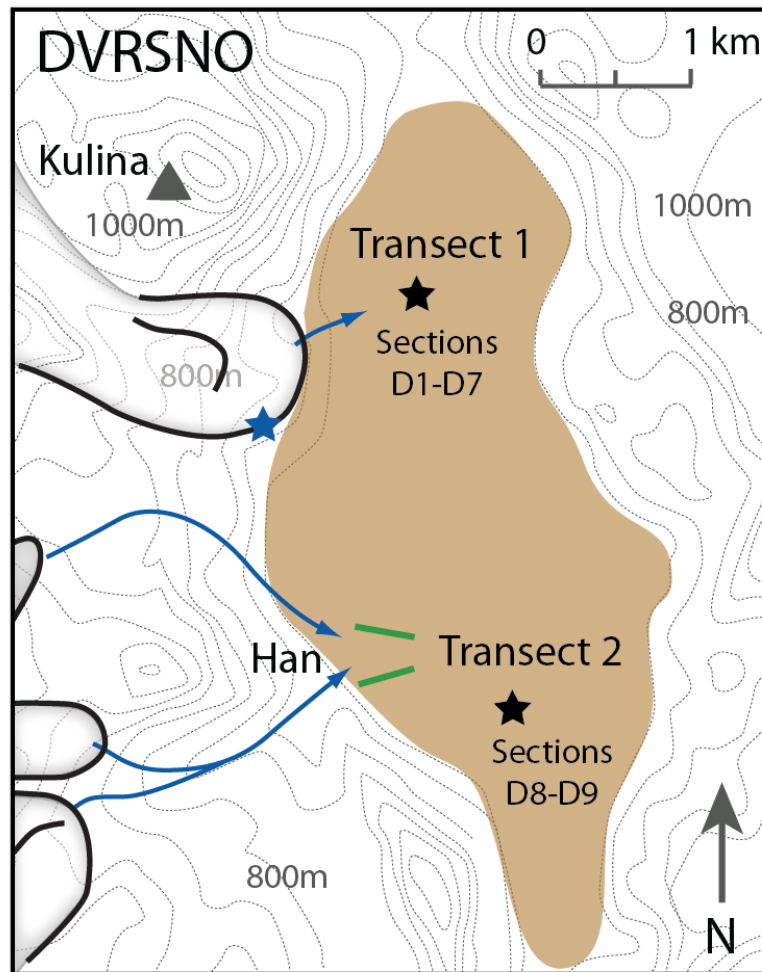
Figure 5.4 – Geomorphological map of Dvrsno polje, east Orjen indicating the maximum Pleistocene ice margins (MIS 12) presented by Hughes *et al*. (2010). Legend: Figure 5.1

Transect 1 (Fig. 5.5) contains seven exposures extending from close to the terminal moraine (Section D1) to 1.3 km from the ice margin (Section D7). Sections D1 and D2, up to 953 m from the ice margin, display massive and poorly-stratified, clast-supported limestone cobbles to granules with a granular and coarse sandy matrix (Plate 5.3). Clasts are subangular to subrounded with a minor angular component and show little variation in angularity across the transect (Fig. 5.5). Sediments become increasingly stratified and finer with distance from the ice margin and clast density decreases from 60% (Section D1) to 30% (Section D6). Sequences contain an increasing abundance of medium sandy lenses as well as clay and silt horizons. At Section D7 (1,350 m) the sequence presents a more complex stratigraphy of interstratified fines, granules and pebbles within a medium sandy matrix (Plate 5.3). A 50 cm-thick soil horizon has developed across the polje surface and has been sampled from Section D5.
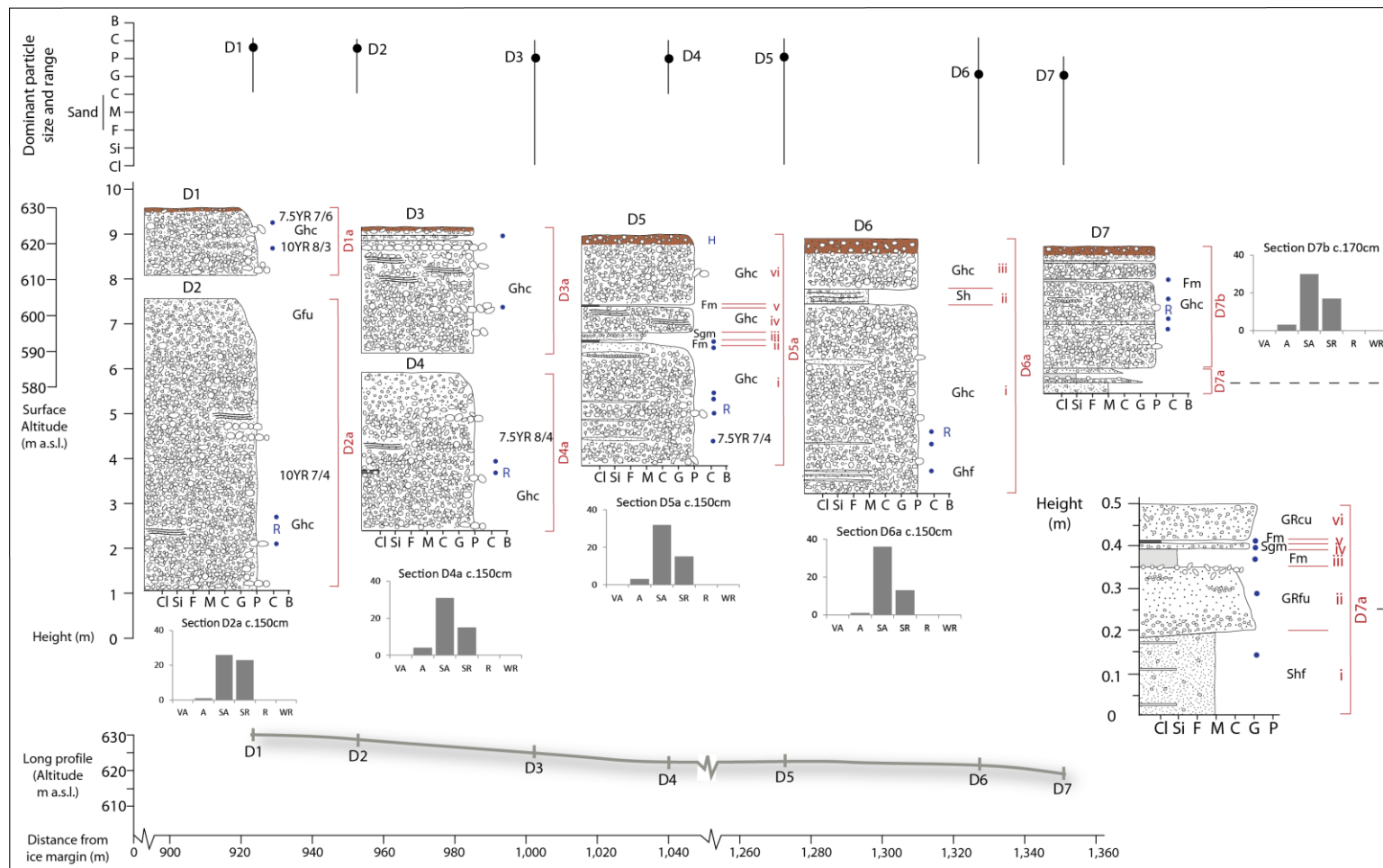
Figure 5.5 – Sedimentary logs at Dvrsno polje, Transect 1, draining the northern meltwater pathway. Sections D1-D2 and D3-D4 have been used to develop two composite logs. Dominant particle size and range with increasing distance downstream is indicated by site. Legend: Figure 5.2
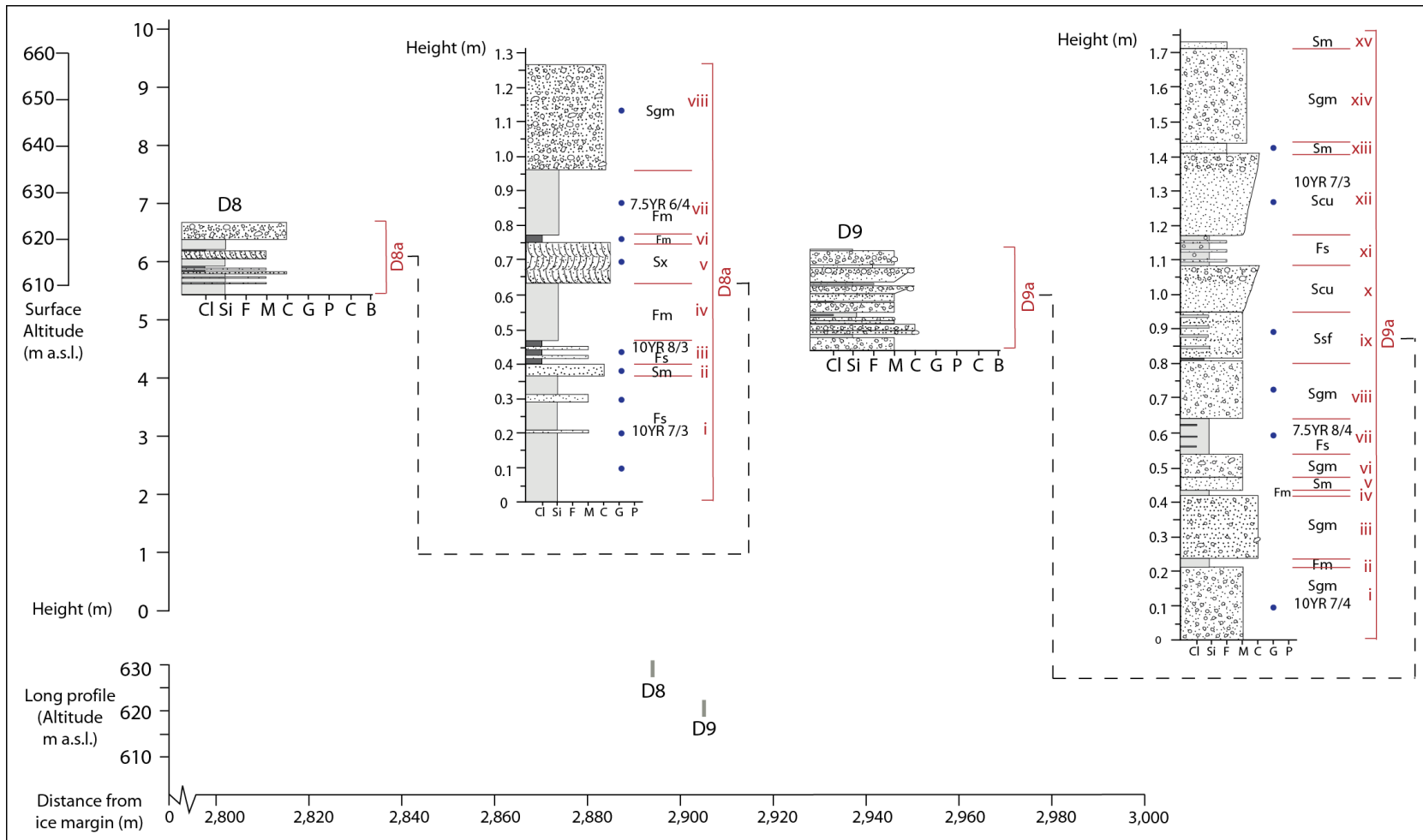
Figure 5.6 - Sedimentary logs at Dvrsno polje, Transect 2, draining the southern meltwater pathway. Legend: Figure 5.2.

Dvrsno Transect 2 is located at the southern end of the polje (42.5858°N, 18.6882°E, 624 m a.s.l.), downstream of the bedrock gap at Han, and presents two shallow exposures. The sediments here are situated c. 3 km from the MIS 12 ice margins and reflect those observed within the ice distal environment at Dvrsno Transect 1 (Section D8; Plate 5.3c). The sequences are dominated by medium sands and granules with abundant silt horizons (up to 20 cm thick) and interstratified clays (clast density 20%) (Fig. 5.6). Evidence of cross bedding (Section D8a-v) and well-stratified granules (Section D9a) is also present.
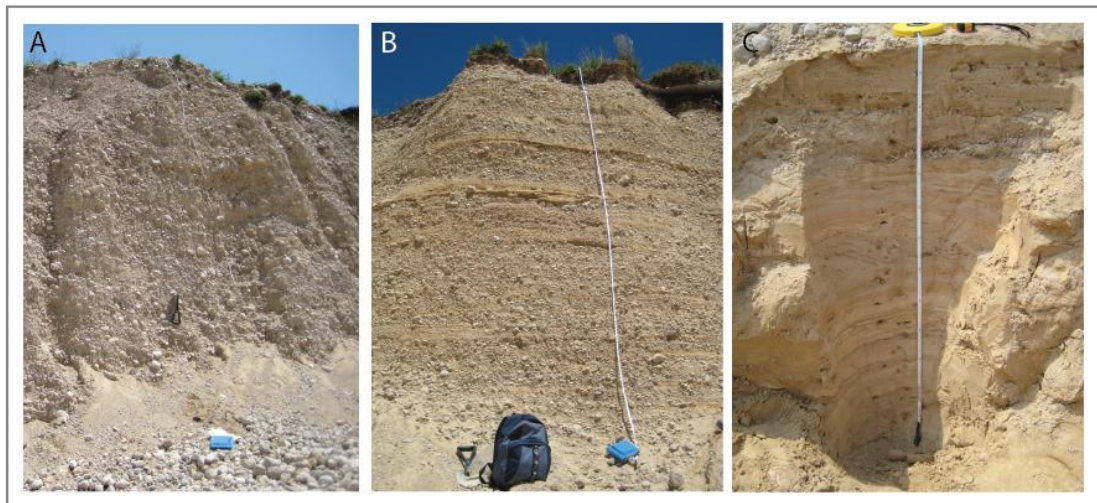
Plate 5.3 – Sedimentary exposures at Dvrsno demonstrating the progressive down-polje fining and increase in stratification: A) Section D1 – Transect 1 (note the entrenching tool and munsell colour chart for scale); B) Section D5 – Transect 1; C) The 1.7 m exposure at Section D8 – Transect 2 - indicating cross bedding.

5.4   Kruševice

The polje at Kruševice (42.5307°N, 18.4910°E, 641 m a.s.l.) is situated to the west of the Orjen massif covering an area of 1 km x 0.6 km (Fig. 5.7). The polje is bounded by steep sided mountainous terrain, including the high altitude plateau of Subra (1,679 m a.s.l.) to the east of the site, where the Pleistocene ice margin terminated at an elevation of c. 1,400 m and approximately 2 km due east of the polje (Plate 5.4). Sediments are exposed here within c. 9 m deep quarry cuttings (Fig. 5.8; Plate 5.5).
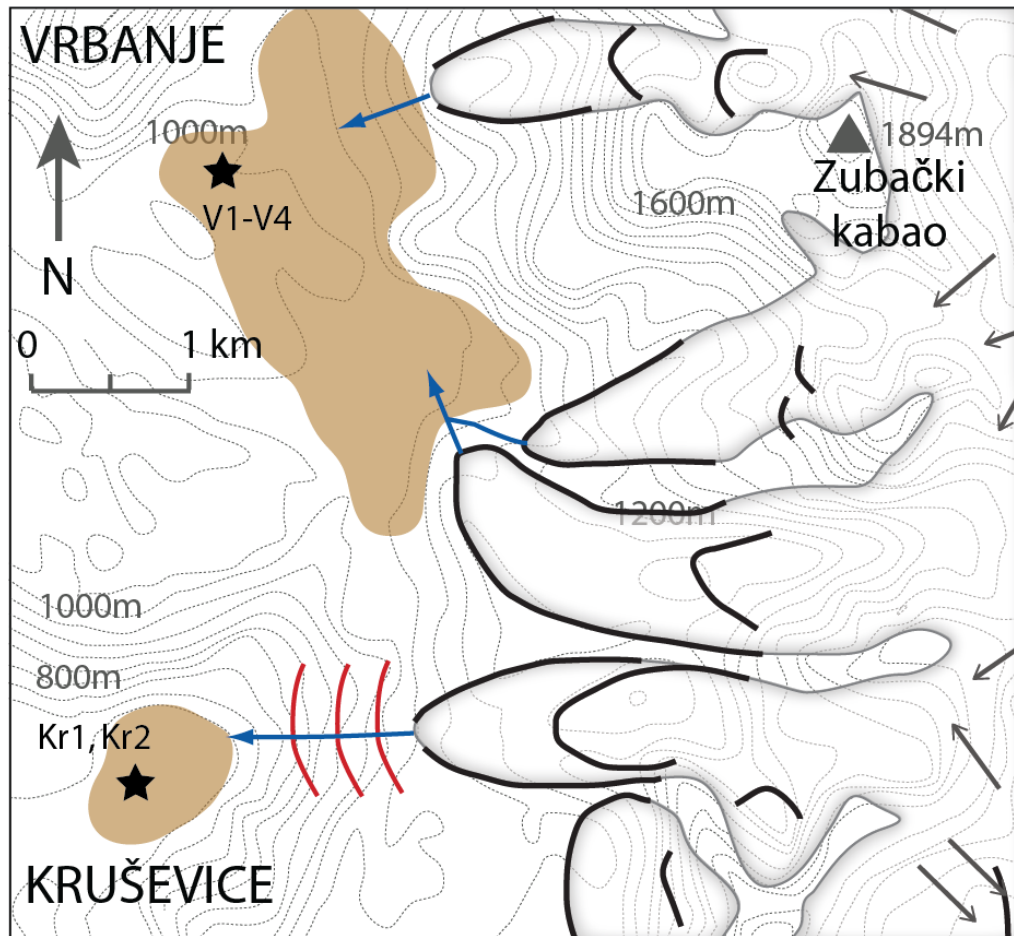
Figure 5.7 - Geomorphological map of Kruševice and Vrbanje poljes, west Orjen indicating the maximum Pleistocene ice margins (MIS 12) presented by Hughes *et al*. (2010). Legend: Figure 5.1.

Plate 5.4 – Panoramic image looking southwest over the polje at Kruševice. The Pleistocene ice margin would have been situated to the left hand side of the image on the upland plateau. The highest peak of this plateau is Subra (1,697 m a.s.l.) (see Fig. 5.1).

The ice proximal side of the polje (Section Kr1 at 1.9 km from the ice margin) contains stratified sands and silts with abundant limestone pebbles and granular horizons (clast density 30-60%) (Plate 5.5; Fig. 5.8). Gravel and sandy-silt lenses are abundant throughout the exposure and many are laterally continuous over several metres. Larger, more massive sand horizons are also present close to the base of the exposure (Kr1a-ii). At section Kr2 (2 km from the ice margin) sediments are well-stratified and demonstrate a considerable increase in the abundance of fine sand and silt horizons (Plate 5.5; Fig. 5.8). Within the lower units (Kr2a-i) thin clay veneers are evident on clast surfaces and incipient calcite development is present. Clast roundness increases with distance from the ice margin, with a dominance of subangular and subrounded clasts within Section Kr2 in contrast to the broader range of angularity within Section Kr1 (Fig. 5.8). Clast density here is typically 50%. A 60 cm-thick, yet frequently disturbed, soil horizon has developed across the polje surface. This has been sampled from Section Kr1 and is discussed more fully in Chapter 8.2.
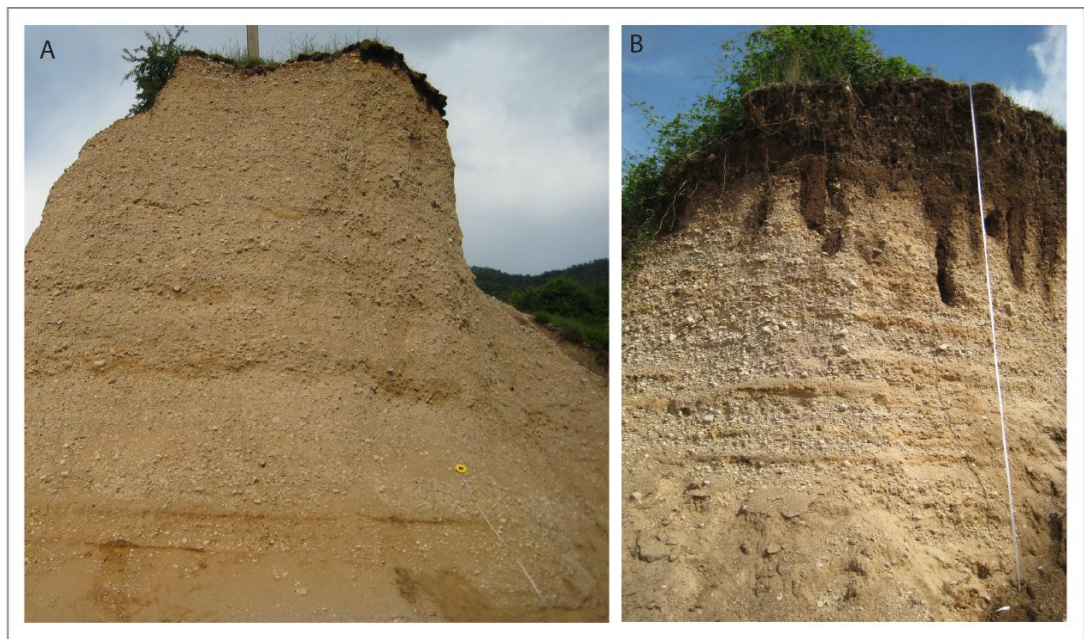
Plate 5.5 – Sedimentary exposures at Kruševice: A) Section Kr1 (note the 2 m tape measure for scale) and B) The 4 m exposure at Section Kr2.
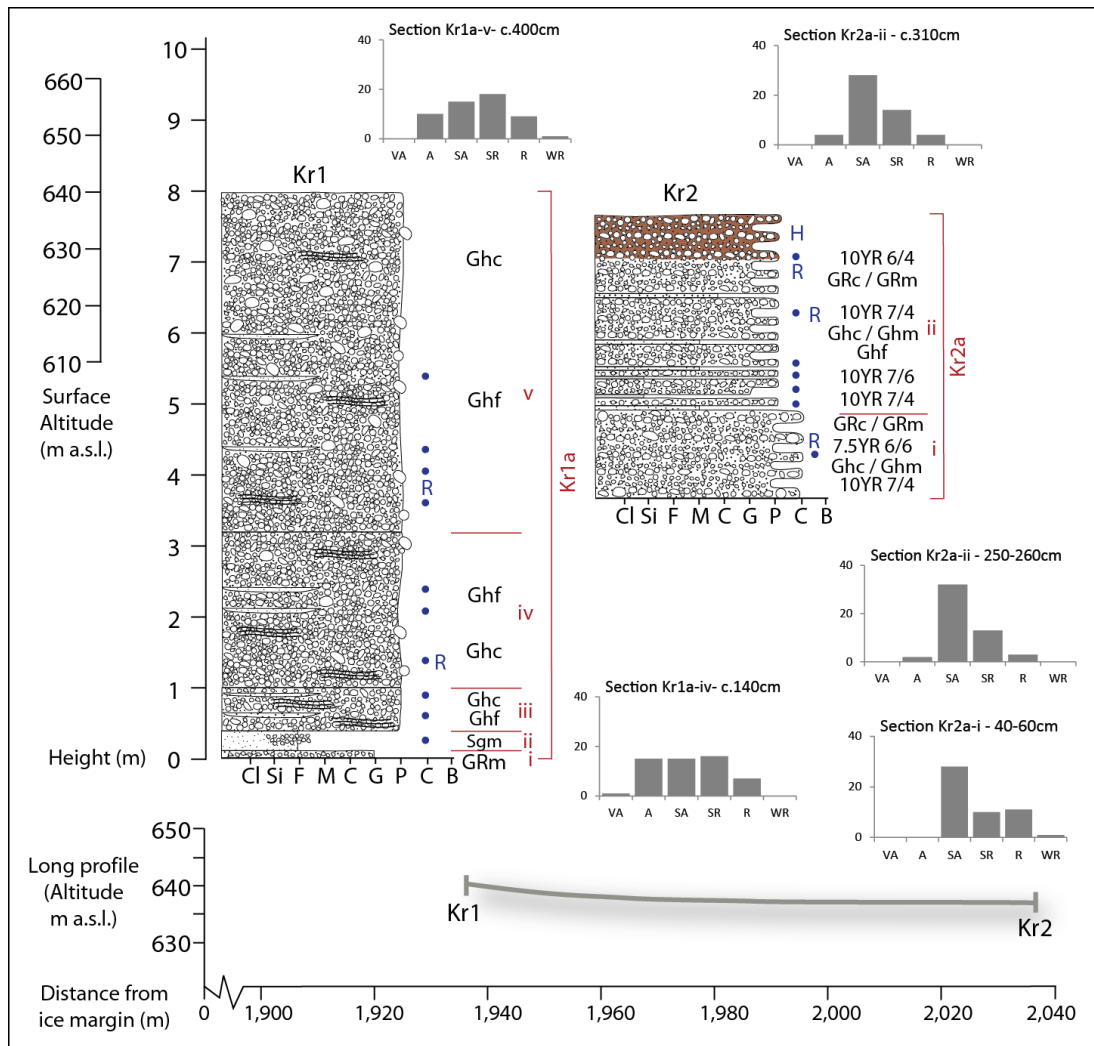
Figure 5.8 – Sedimentary logs at Kruševice polje, west Orjen. Legend: Figure 5.2.

5.5   Vrbanje

The polje at Vrbanje (42.5663°N, 18.4954°E, 982 m a.s.l.) on the western side of the former ice cap is one of a series of partially coalescing karstic depressions, separated by low-lying bedrock ridges (Fig. 5.1; 5.7). Here, the Pleistocene ice margin extended down to the polje and a large moraine, correlated to MIS 12 by Hughes *et al*. (2010), is situated to the northeast of the site. Polje sediments are exposed within a shallow quarry (up to 7 m deep) approximately 1.4 km from the ice margin (Fig. 5.9). Sediments are largely stratified to well-stratified clast- and matrix-supported sands and limestone gravels (Plate 5.6). A matrix of coarse-medium sand with a minor silty component is present throughout the exposure, with granules in the interstices of larger clasts. Some imbrication structures are present in a number of units (V1a-iii; V2a; V3a-v and vi; and V4a-iii and iv) and indicate a north eastern flow direction. Clasts are

dominantly subangular to subrounded with a minor increase in roundness with distance from the ice margin (Fig. 5.9). Clast density throughout the exposure is 20% (Section V1) to 60% (Sections V2-V4). In some horizons clasts are blocky and faceted in morphology (V4a-i and ii) which is deemed indicative of a glacial origin (Benn and Ballantyne, 1993; 1994). Thin clay drapes are present on clast surfaces within the ice proximal side of the quarry (V1a-iii). These are similar in texture to the clay horizons observed at Kruševice. A granular and unconsolidated soil horizon, of variable thickness, is present across the polje surface and has been sampled at Section V4.
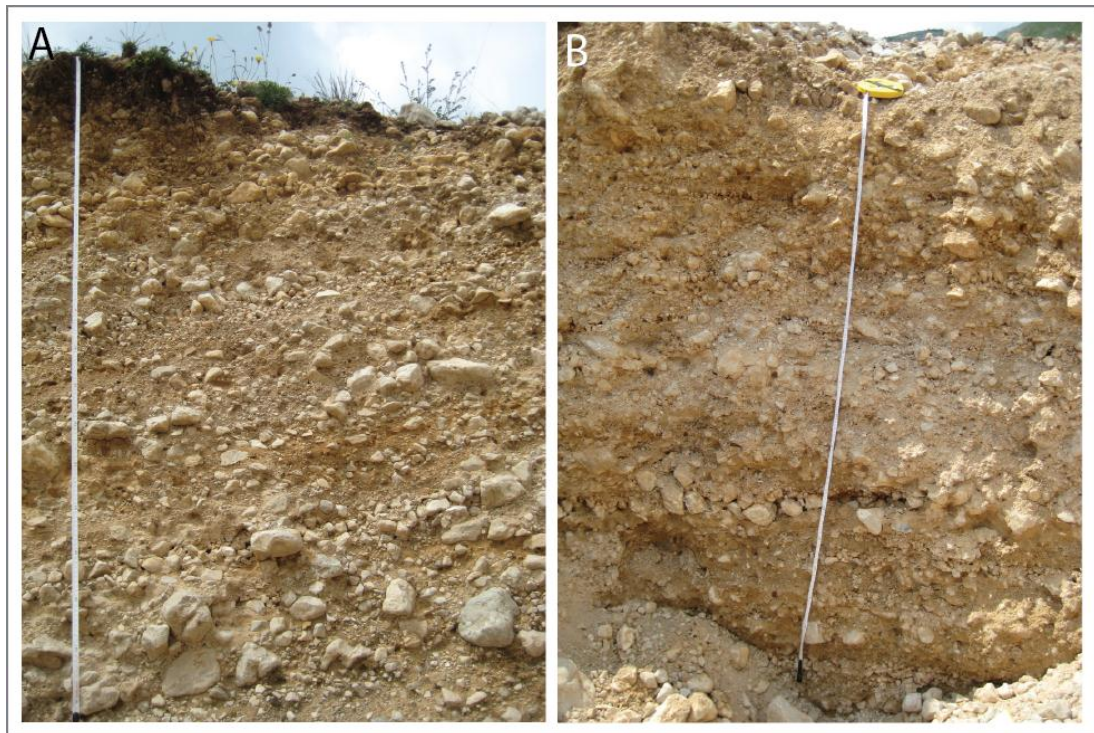
Plate 5.6 – Sedimentary exposures at Vrbanje: A) A 2 m exposure at Section V4 indicating the vague stratification and evidence of imbrication; B) A 1.5 m exposure at Section V2 indicating the well-stratified horizons and clay accumulations (darker in colour, to the right of the tape measure).
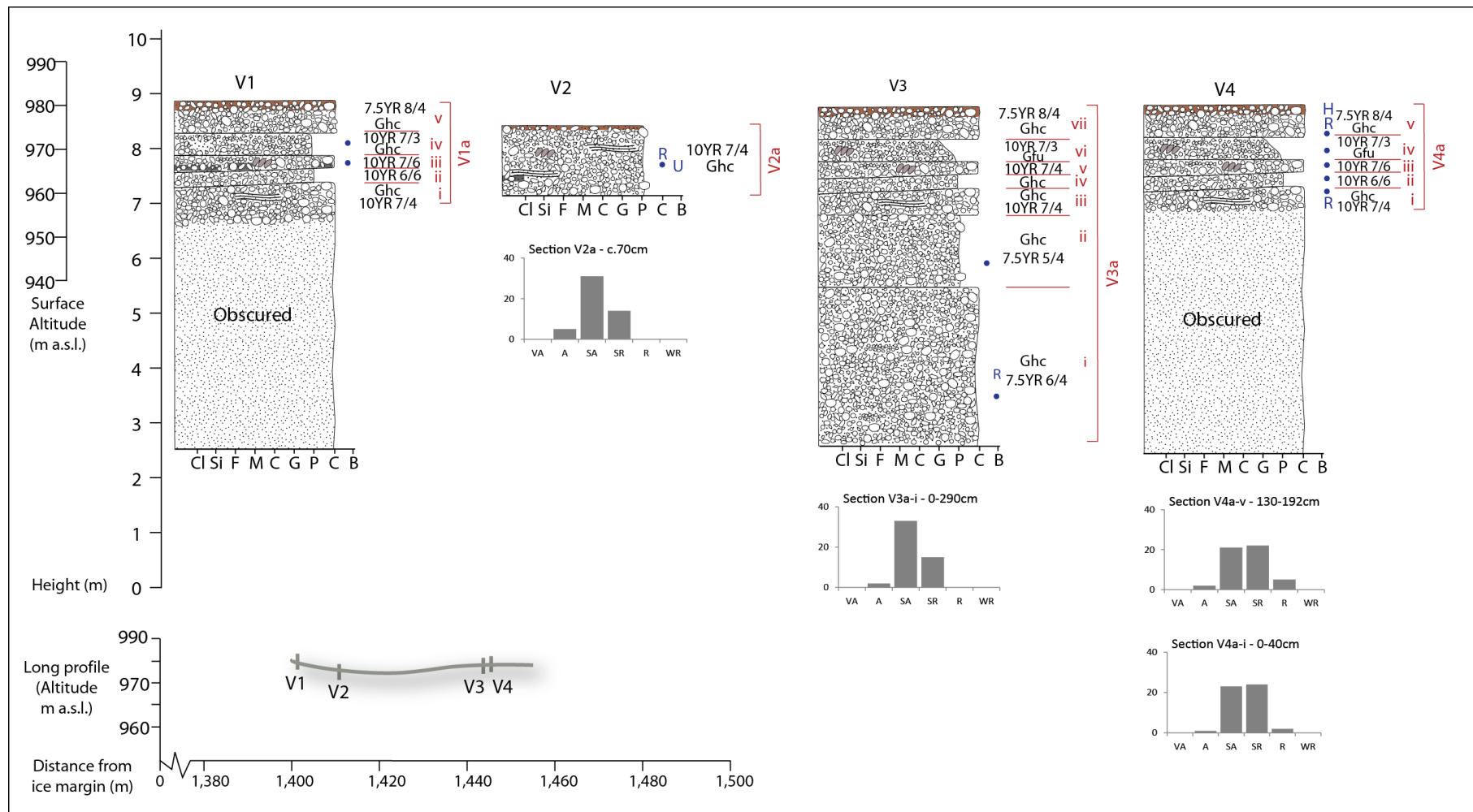
Figure 5.9 - Sedimentary logs at Vrbanje polje, west Orjen. Legend: Figure 5.2.

5.6   Pirina Poljana

The polje at Pirina Poljana (42.6152°N, 18.4127°E) is located within Bosnia-Herzegovina, downstream of one of the largest ice lobes emanating from the northwest of the Orjen ice cap (Fig. 5.1; 5.10). Here, the ice limits extended as far as the polje and a series of moraines are preserved at its eastern margin. The polje is partially divided by a bedrock gap, forming a western and an eastern sector (Fig. 5.1), the latter of which is analysed here. Combined, these sectors span an area of 50 km x 5.5 km. Quaternary sediments are exposed within small road cuttings inside the former MIS 12 ice margins (Section P1) and within large quarries beyond the ice limits (Section P2 and P3) (Fig 5.11; Plate 5.7).
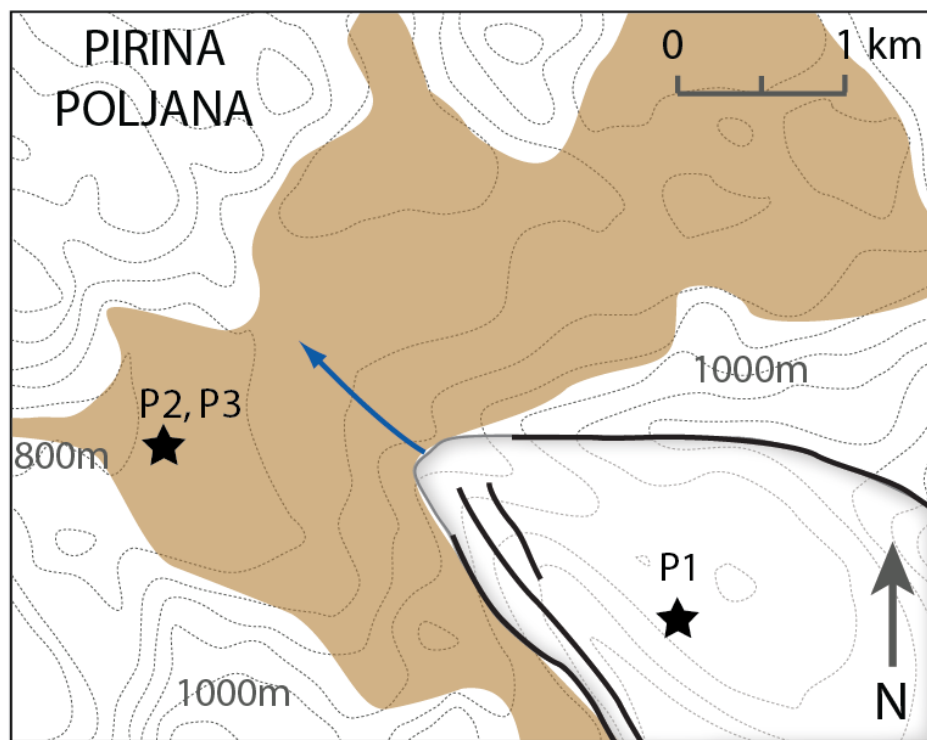
Figure 5.10 – Geomorphological map of Pirina Poljana polje, northwest Orjen indicating the maximum Pleistocene ice margins (MIS 12) presented by Hughes *et al*. (2010). Legend: Figure 5.1.

Section P1 (42.6202°N, 18.4805°E) is situated approximately 1.5 km up-valley of the MIS 12 end moraines at (42.6202N, 18.4805E, 1,018 m a.s.l. and 42.6217°N, 18.4772°E, 1,011 m a.s.l.) and up to 4 km from the MIS 6 moraines. Sediments here contain interstratified sands and gravels with a dominant silt component (P1a-iv) (clast density 0-30%). A c. 30 cm-thick, friable and granule-rich soil horizon has developed across the land surface (Fig. 5.11).

Outside the MIS 12 ice margins (42.6152°N, 18.4127°E, 677 m a.s.l.) exposures P2 and P3 (c. 2 km from the MIS 12 moraines) contain well-cemented and crudely-stratified sands and gravels (clast density 60%) (Fig. 5.11). Clasts are largely subangular to subrounded, with negligible variation in roundness characteristics across the polje (Fig. 5.11). The coarse-medium sandy matrix present throughout the polje is almost entirely weakly cemented with phreatic carbonate development (Plate 5.7b) and Section P2 contains a densely-cemented bench of detritus-rich calcite (P2a). A series of calcite 'clasts' are present within the overlying facies here (P2b), and may reflect the reworking and moulding of carbonate accumulations from underlying deposits, or elsewhere in the catchment. Section P3 is better stratified and gravel deposits are interbedded with finer, sand and silt horizons or lenses (P3a). A 60 cm-thick soil horizon has developed at the surface of this exposure, and is laterally continuous across this part of the polje.

Plate 5.7 – The large polje at Pirina Poljana, northwest Orjen indicating: A) The view down-polje taken from the Montenegro - Bosnia-Herzegovina border, indicating the location of sections P2 and P3 (arrowed) within the extensive polje. The maximum Pleistocene ice margins, delineated by large moraines (Hughes *et al.*, 2010), were to the right of the image; B) Well-stratified and cemented sediments at Section P2; and C) Well-stratified and well-cemented sands and gravels adjacent to Section P3.
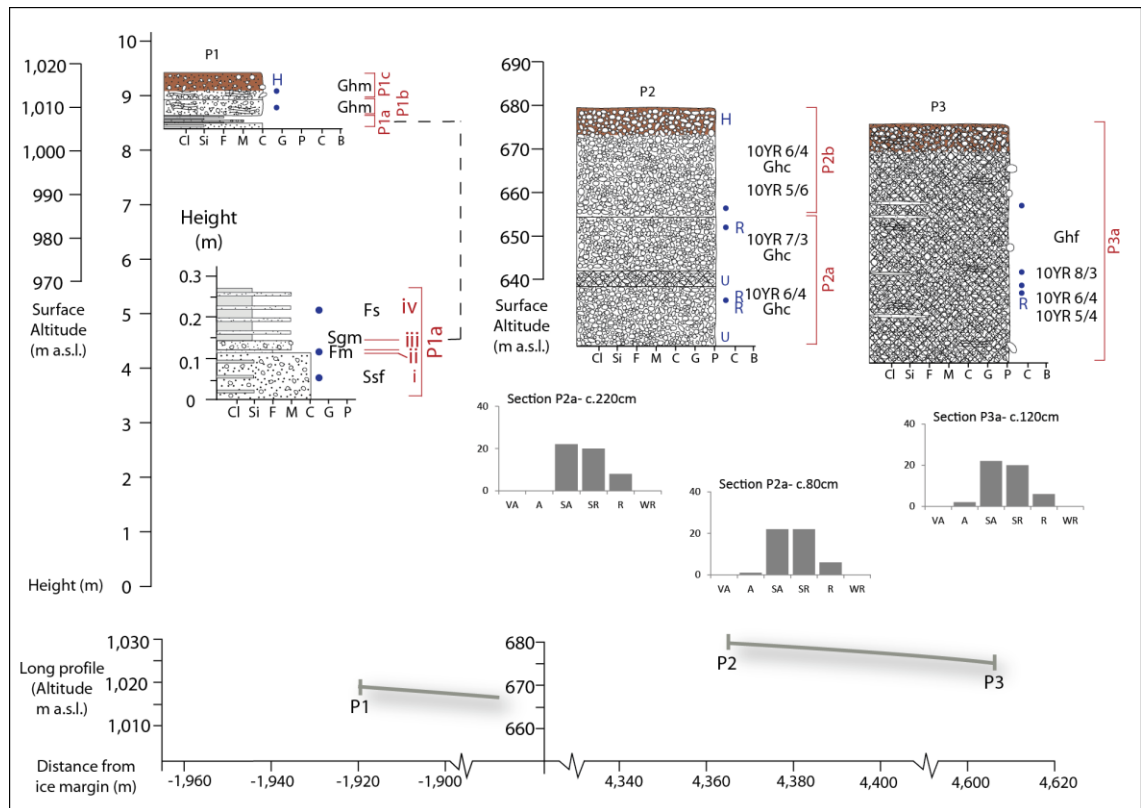
Figure 5.11 - Sedimentary logs at Pirina Poljana polje, northwest Orjen. Distance from the ice margin is referenced against the MIS 12 moraine position of Hughes *et al*. (2010). Legend: Figure 5.2.

5.7   Grahovo

The polje at Grahovo is situated to the northeast of the former Orjen ice cap (42.6492°N, 18.6512°E, 722 m a.s.l.). The shallow gradient depression broadly trends west-east over an area of 5.8 km x 1.5 km and is constrained by steeply inclined bedrock on all sides (Fig. 5.12; Plate 5.8). The ice proximal side of the polje is located around 1.4 km from the MIS 12 moraines delineated by Hughes *et al*. (2010). Two meltwater pathways, emanating from two ice lobes, have delivered sediment and meltwater to the polje (Fig. 5.12). These ice masses did not reach as far as the polje, and were separated from the depression by a series of bedrock ridges. Sedimentary exposures here are limited to two sections within a small road cutting (Section G1 at c. 1.4 km from the ice margin) and a stream bank (Section G2 at c. 2.8 km) (Fig. 5.13).

Sediments at section G1 contain stratified, clast-supported sands and gravels with lenses of medium to coarse sand throughout the sequence. Clasts are largely sub-angular to rounded

pebbles and cobbles (Fig. 5.13; Plate 5.8) (clast density 50-60%). Weak vadose carbonate accumulations have developed on the underside of clasts within facies G1a-ii. Sediments display a general fining and greater stratification with increasing distance from the ice margin, and section G2 comprises well-stratified pebbles and granules (Fig. 5.13). A thin and sandy soil horizon has developed across the polje surface (see Chapter 8.2).
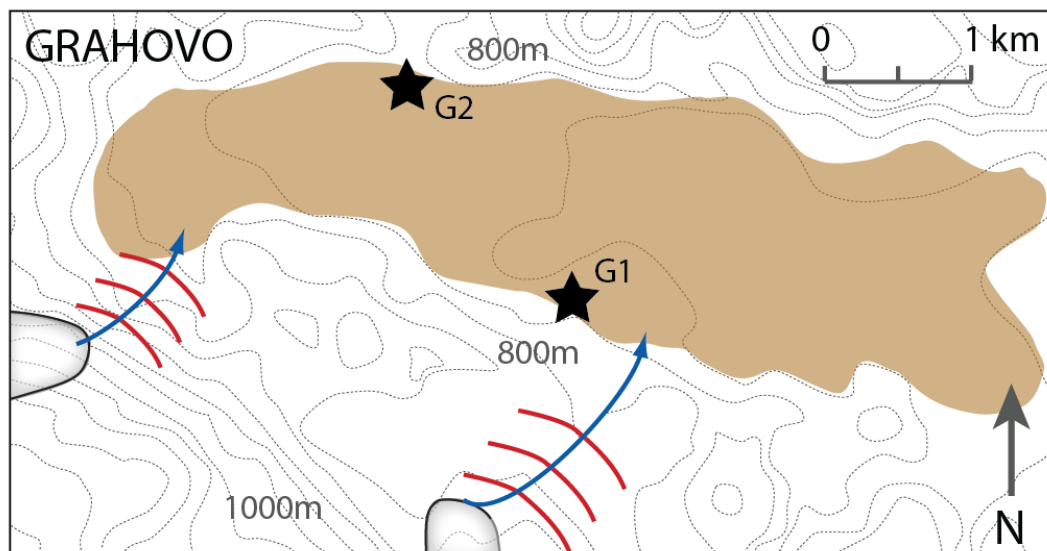
Figure 5.12 - Geomorphological map of Grahovo polje, northeast Orjen indicating the maximum Pleistocene ice margins (MIS 12) presented by Hughes *et al*. (2010). Legend: Figure 5.1.
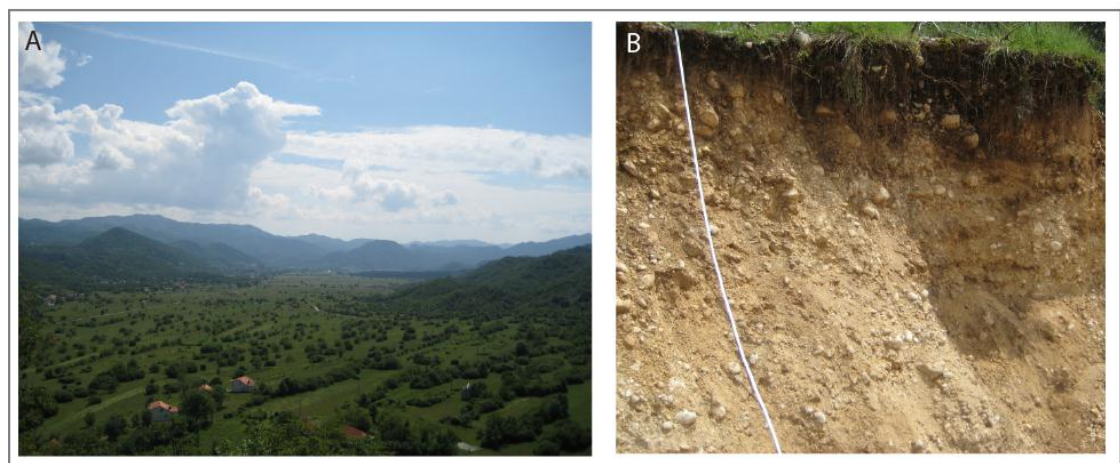
Plate 5.8 – Grahovo Polje, northeast Orjen indicating: A) The view west-east across the polje from the higher terrain close to Nudo. The study sites are to the right of the image, behind the bedrock outcrop; B) The sedimentary exposure at Section G1 indicating the stratified sands and gravels and clay accumulations (darker horizons at the centre of the section).
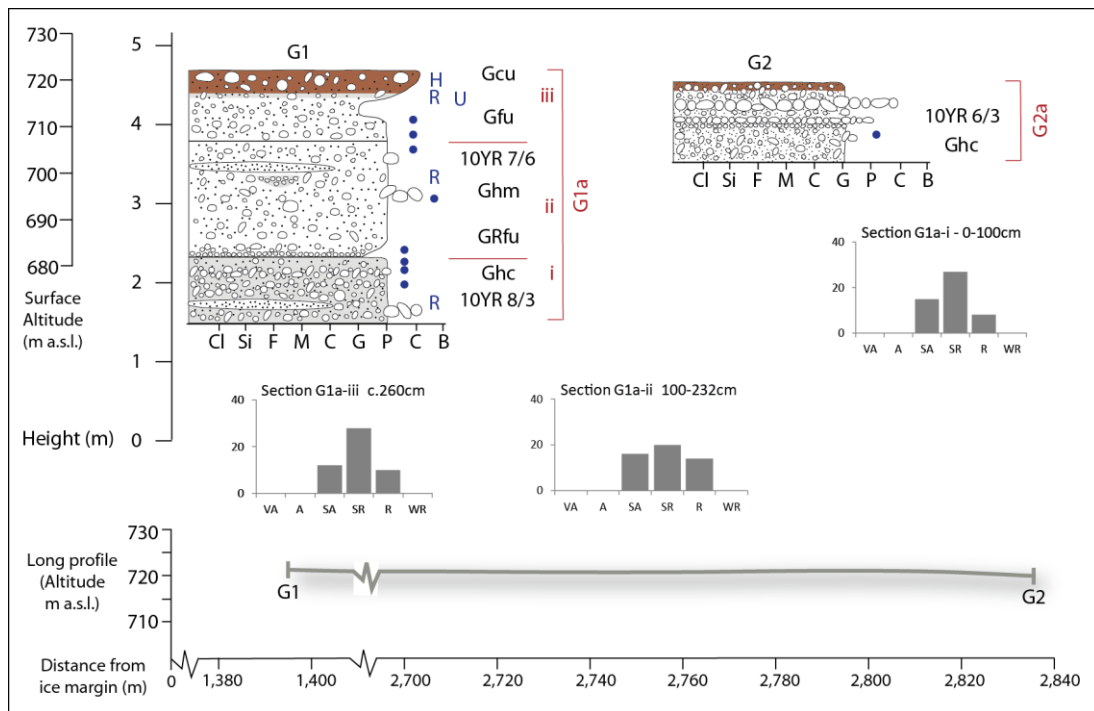
Figure 5.13 – Sedimentary logs at Grahovo, northeast Orjen. Legend: Figure 5.2.

5.8   Lipci

Lipci is a large, relatively shallow gradient alluvial fan downstream of the southern margin of the former Orjen ice cap (42.4981°N, 18.6556°E) (Fig. 5.14). The fan is deposited at the outflow of a steep sided limestone ravine which drained the southern margins of the ice mass. Its apex is situated at c. 50 m a.s.l. and the lower portion of the fan, which is now below sea level, extends to >600 m offshore (Giglio, 2012 pers. comm.). The submarine topography of the Bay of Kotor has recently been investigated by Bortoluzzi *et al*. (2009). The modern bay reaches average depths of 20-40 m and bathymetric data have revealed a series of submerged karstic depressions, submarine springlines and karstic aquifers discharging below sea level (Fig. 5.15). Since deposition, the Lipci fan has been incised by a series of small channels. Submarine topographic imagery (Giglio, 2011 pers. comm.) indicates that these continue along the length of the fan and have migrated laterally over time, incising up to 10 m deep (Fig. 5.15). These submerged channels are well preserved, which may reflect a strong degree of secondary carbonate cementation prior to submersion. In the terrestrial part of the fan, the contemporary channel bed contains abundant sub-angular to sub-rounded cobbles and boulders with angular pebbles and granular material.
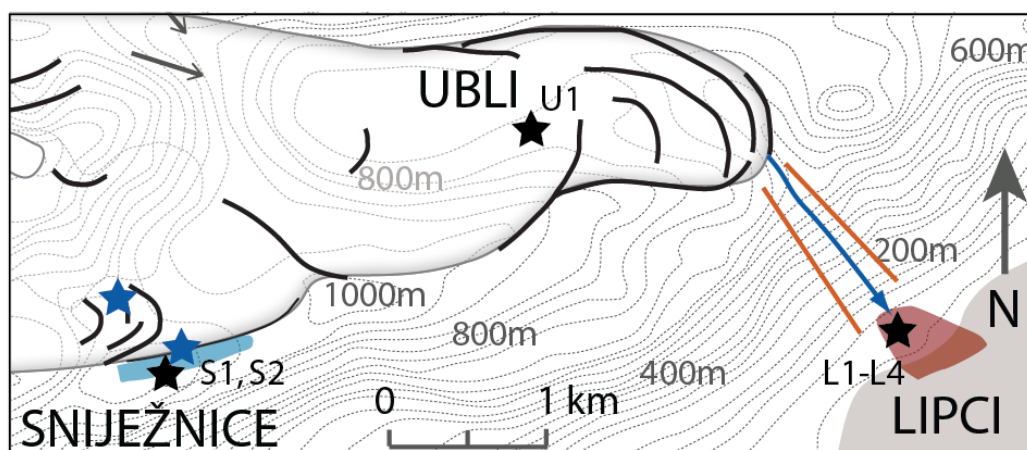
Figure 5.14 - Geomorphological map of Lipci Fan, Ubli and Sniježnice, south Orjen indicating the maximum Pleistocene ice margins (MIS 12) presented by Hughes *et al*. (2010). Legend: Figure 5.1.

A series of exposures are accessible along the length of the terrestrial part of fan extending from close to the fan apex (c. 41 m a.s.l.) to near sea level (c. 23 m a.s.l.) (Fig. 5.16). Fan sediments comprise massive to coarsely-stratified open framework gravels (cobbles with pebbles and occasional boulders) (clast density 70-80%) (Plate 5.9). Clasts are dominantly sub-angular with abundant angular and sub-rounded clasts. Minor increases in roundness are observed with distance down-fan (Fig. 5.16). The fan sequence is now well-cemented by vadose zone carbonates (Sections L1 – L3) and flowing water carbonates (Section L4) and the majority of the fine unconsolidated sediment matrix has been displaced by indurated and often sparitic calcite crystals.

Plate 5.9 – Lipci fan, south Orjen indicating: A) The exposure at Section L1 with an abundance of angular and sub-angular clasts (note tape measure for scale); B) An oblique view of the Lipci fan taken from the steep sided limestone ravine and demonstrating its proximity to the Bay of Kotor; C) The exposure at Section L3 indicating the clast-supported pebbles and cobbles.
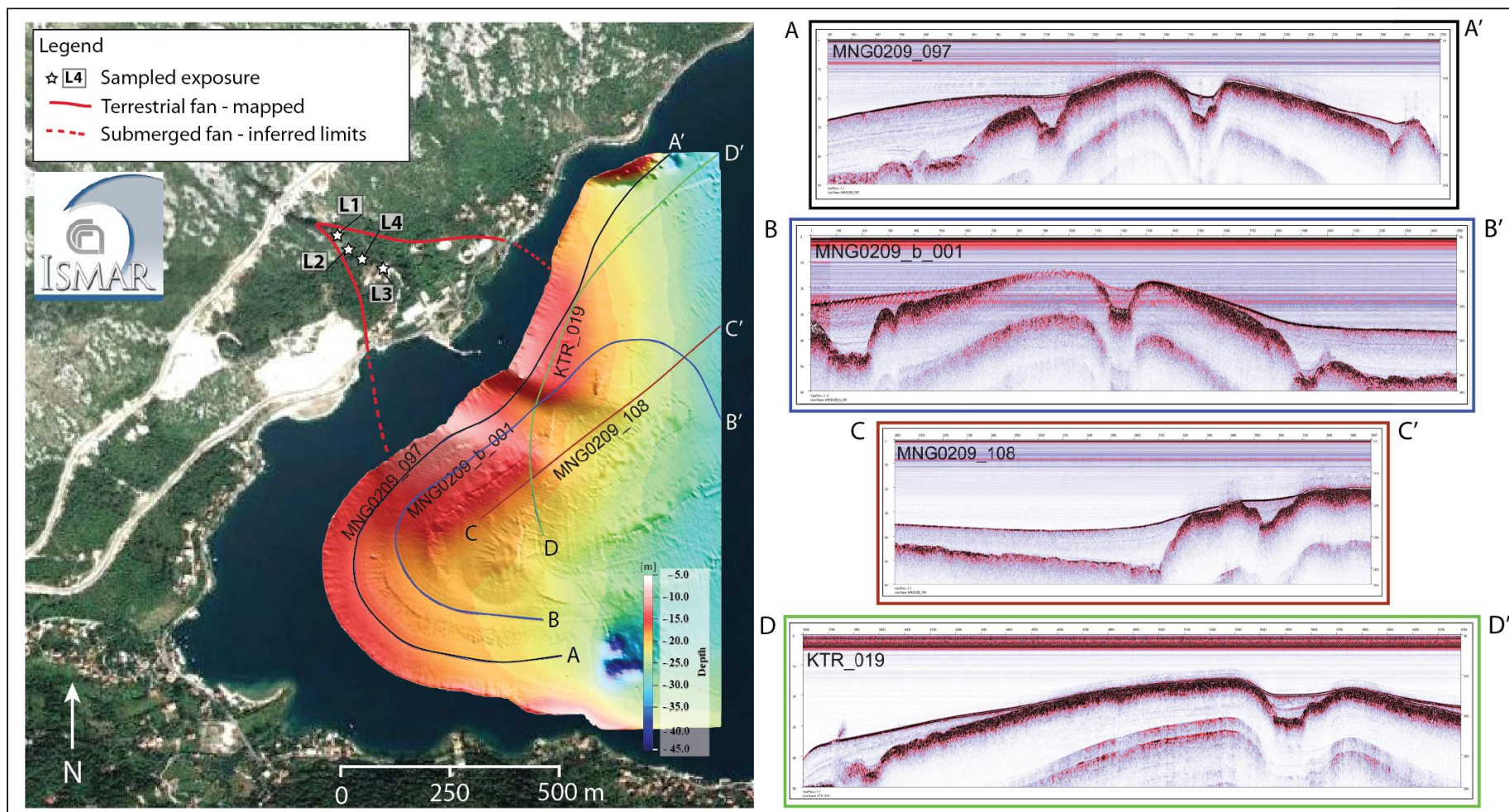
Figure 5.15 – Submarine topographic imagery and location of terrestrial sampled exposures of the Lipci fan. Submarine profiles (transects A-A', B-B', C-C' and D-D') demonstrate the channel cuttings into the now submerged portion of the fan. Submarine imagery: Giglio (2012 pers. comm.); Base map: Google Earth.
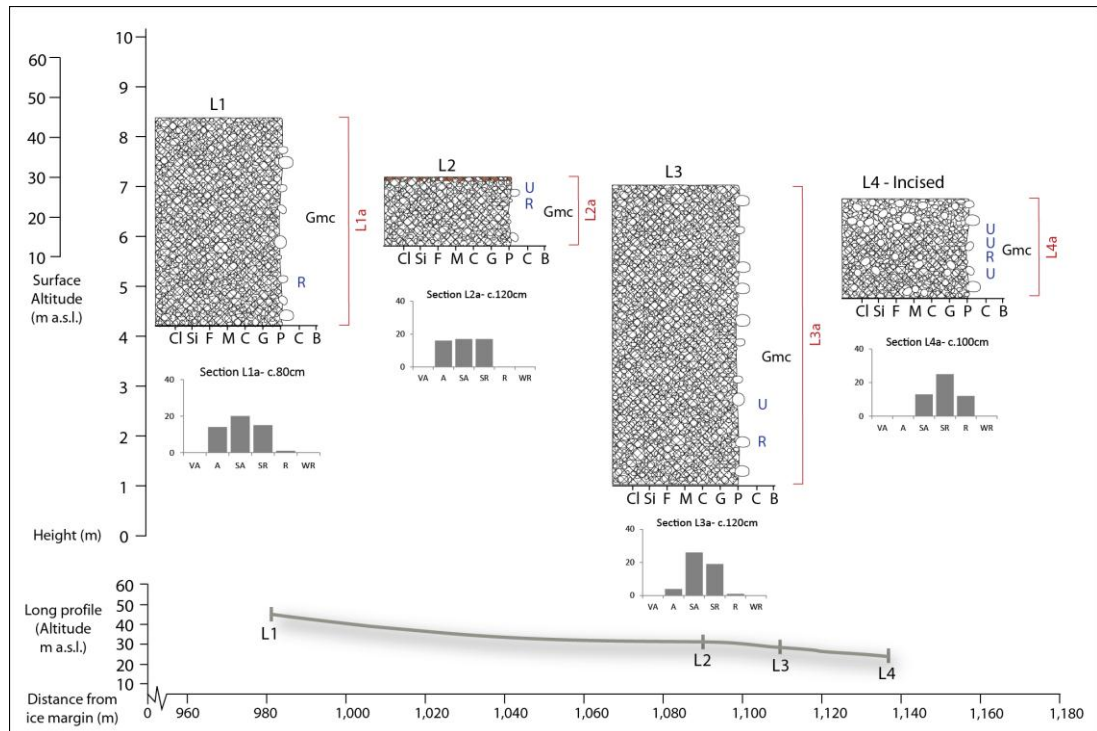
Figure 5.16 - Sedimentary logs at Lipci alluvial fan, south Orjen. Legend: Figure 5.2.

5.9 Kameno

A proglacial fan of 1,380 m length is located at Kameno, to the southwest of the Orjen massif at 42.4904°N, 18.5363°E, 565 m a.s.l. (Fig. 5.1). The fan is situated downstream of a large lateral moraine (42.4924°N, 18.5355°E) correlated to MIS 12, associated with a small outlet glacier draining the south western margins of the Orjen ice cap (Fig. 5.17). The fan surface grades from its apex at 565 m a.s.l. to 501 m a.s.l. A transect of eight sections was analysed from the moraine extending down-fan over a distance of almost 900 m (Fig. 5.18; Plate 5.10).

Section K1 (42.4904°N, 18.5363°E) is situated 150 m downvalley from the moraine, and contains massive, open framework and clast-supported cobbles and boulders (clast density 80%). Pebbles and granules are present in the interstices of larger clasts and the sequence contains only a limited matrix component. The sequence is crudely stratified and contains a series of well-cemented horizons as well as a densely cemented vadose carbonate unit at the surface (K1b). Clasts are dominantly subangular to subrounded cobbles and pebbles, with occasional boulders, set within a coarse-medium sandy matrix. Roundness measurements

demonstrate little variance downfan, with only minor changes in the abundance of angular and rounded clasts (Fig. 5.18).
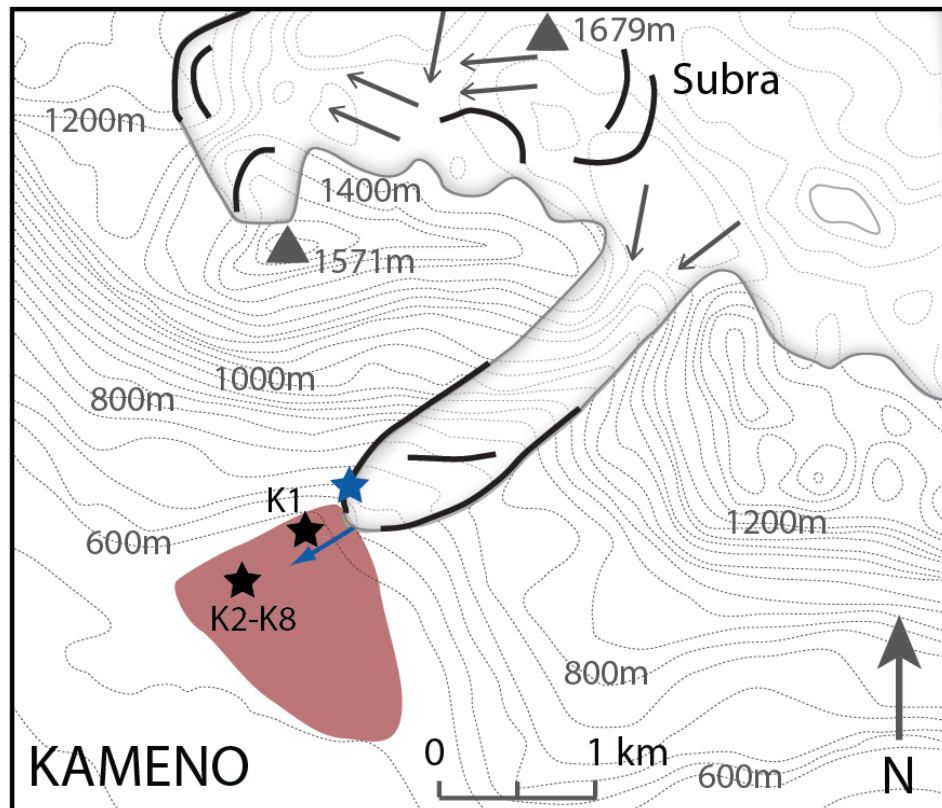
Figure 5.17 - Geomorphological map of Kameno fan, southwest Orjen indicating the maximum Pleistocene ice margins (MIS 12) presented by Hughes *et al*. (2010). Legend: Figure 5.2.
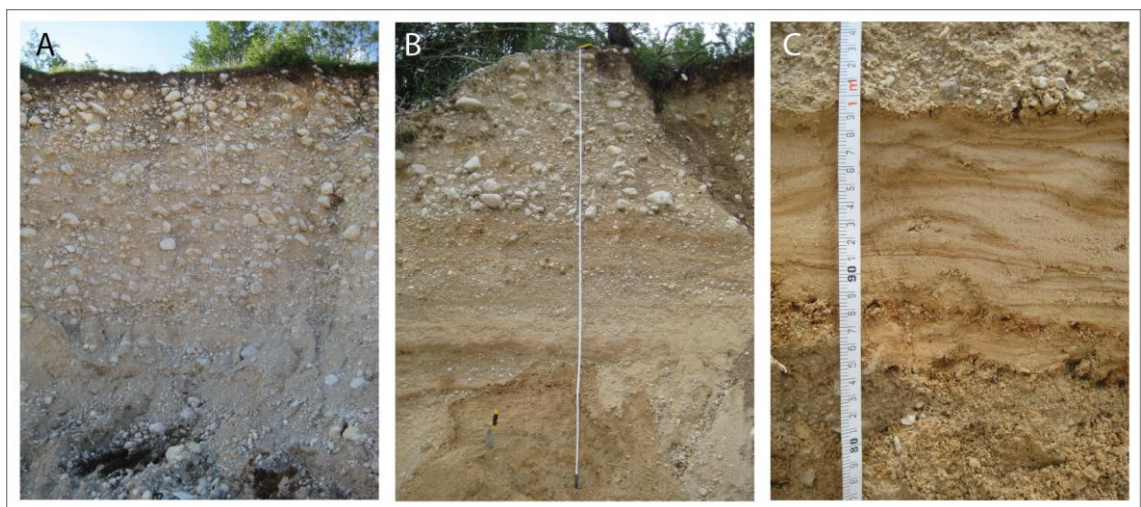
Plate 5.10 – Sedimentary exposures at Kameno alluvial fan, southwest Orjen indicating: A) The 7 m section of massive, crudely-stratified sediments at Section K2 (note the tape measure for scale); B) The increasing down-fan stratification and fining of sediments at Section K6; and C) The finely interstratified sands and silts within Section K8.

The fan sediments become increasingly stratified with distance from the ice margin (Plate 5.10) and contain a greater proportion of the fine matrix component, as well as interstratified silts and clays within the ice distal exposure (Section K8; Fig. 5.18). Clast density progressively decreases from 80%, close to the fan apex, to 60% within Section K6. Evidence of weak imbrication is apparent in the ice medial part of the fan (Sections K4 and K5) and indicates a north easterly flow origin. Sand lenses and matrix-rich horizons become increasingly abundant within sedimentary sequences from Section K4 – K8 (>c. 800 m from the ice margin) but are also present within the basal units of Section K3. Clay drapes on the upper surfaces of clasts within Unit K6a-i, are similar in texture and morphology to those identified within the polje fills at Grahovo, Kruševice and Vrbanje. Within the ice distal part of the fan, at Section K8, c. 1 km from the ice margin, the sedimentary sequence is well-stratified with a dominance of the finer sediment matrix as well as silt and clay horizons (K8a-ii; iv; vi) (clast density 0-50%). Section K7 contains a series of stacked, inversely graded sequences. These are diagnostic of sediments deposited by meltwater draining a retreating ice margin (Miall, 1983; 1985). An organic-rich soil horizon has developed in the upper 30 cm of the fan sequence and samples have been obtained from Section K3.
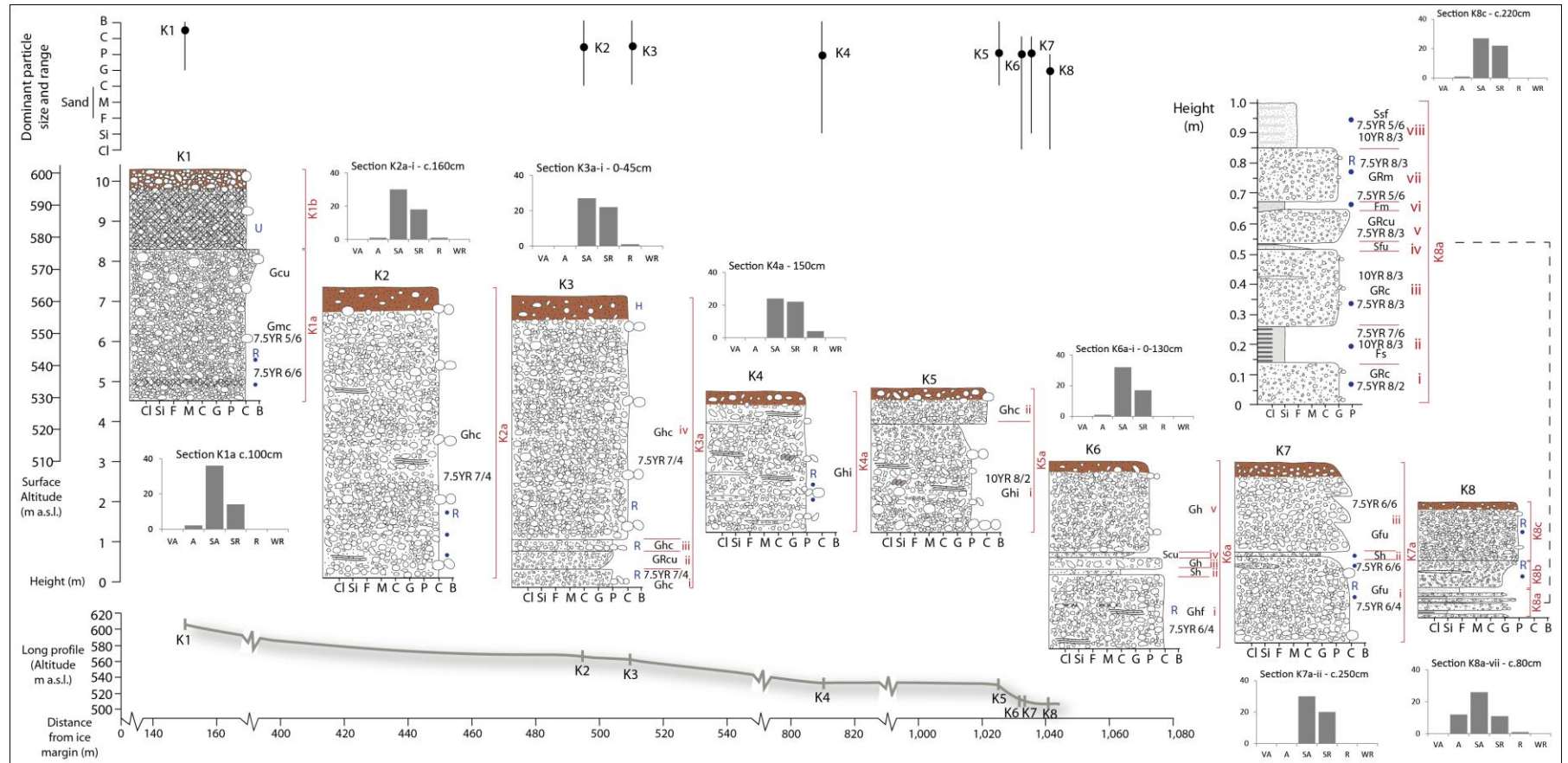
Figure 5.18 - Sedimentary logs at Kameno alluvial fan, south Orjen. Dominant particle size and range with increasing distance downstream is indicated by site. Legend: Figure 5.2.

5.10   Nudo

The Nudo valley (42.6736°N, 18.5704°E, c. 410 m a.s.l.) is situated to the north of the Orjen massif, draining broadly southeast-northwest (Fig. 5.19). The valley is a steep sided limestone gorge and is fed by a narrow ravine at its south eastern extent, and is also supplemented by a small tributary (River Jenkov). The present day river, the River Zaslapnica, joins the River Sušica close to the village of Vućija, before continuing its course into Bosnia-Herzegovina (Fig. 5.20). The stream is seasonal and reaches high flow conditions following snow melt, during winter due to high seasonal precipitation, or after high intensity or prolonged rainfall events during the summer months. The channel contains both boulder bed and incised bedrock reaches (Plate 5.11b).
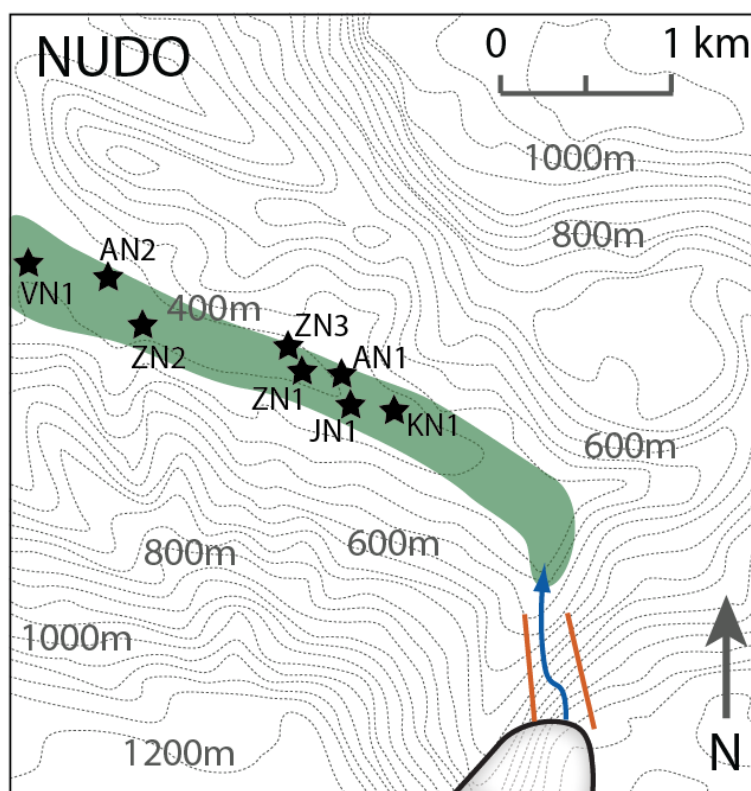
Figure 5.19 - Geomorphological map of the Nudo valley, north Orjen indicating the maximum Pleistocene ice margins (MIS 12) presented by Hughes *et al*. (2010). Legend: Figure 5.1.

During the Pleistocene, the valley would have been the main meltwater conduit from the northern sector of the Orjen ice sheet, draining a large ice lobe that formed over the high altitude region of Bijela Gora (Hughes *et al*., 2010). The alluvial sediments have undergone progressive incision since their deposition during the Pleistocene and a sequence of five river

terraces has been preserved (albeit discontinuously) along the valley axis (Fig. 5.20; Plate 5.11). The depositional history of the Nudo valley is discussed in detail in Chapter 9. A potential sixth terrace has also been tentatively identified at higher altitudes but is currently inaccessible for field sampling due to farming and limited exposures. Soil profiles have developed at the surface of each terrace, and many of the sediments contain phreatic secondary carbonates. Terrace units are discussed here with increasing altitude from the present day channel (Fig. 5.21).

5.10.1 *Zaslap Unit*

The Zaslap unit is exposed within a series of terraces along the length of the valley axis. These are particularly well-preserved on the northern side of the channel within the upper reaches of the valley, close to the village of Zaslap. The terrace surface is typically situated c. 2-3 m above the present day channel (Plate 5.11b). Two exposures were logged and sampled: Section ZN1 (42.6739°N, 18.5691°E, 394 m a.s.l.) and Section ZN2 (42.6750°N, 18.5663°E, 384 m a.s.l.). These units comprise crudely stratified matrix- to clast-supported sands and limestone gravels (clast density 50-60%). Clasts are dominantly subangular to subrounded pebbles (Fig. 5.21) with abundant granules and cobbles. The medium sandy matrix is weakly cemented by a phreatic carbonate horizon at the base of Section ZN1, forming laminar yet friable and detritus-rich calcite infills.

A small tributary, the River Jenkov, supplies the trunk stream from the northern valley side. Sediments here are exposed adjacent to Section ZN1 within Section ZN3 (42.6741°N, 18.5691°E, 398 m a.s.l.). This unit contains matrix- to clast-supported limestone granules and abundant pebbles within a coarse sand-silt matrix (clast density 50%) (Plate 5.11c). Discrete cobble-rich horizons are present throughout the sequence. Clasts are more angular than those observed within Section ZN1, from the trunk stream, and reflect a colluvial origin delivered to the fluvial system from the steep valley sides.
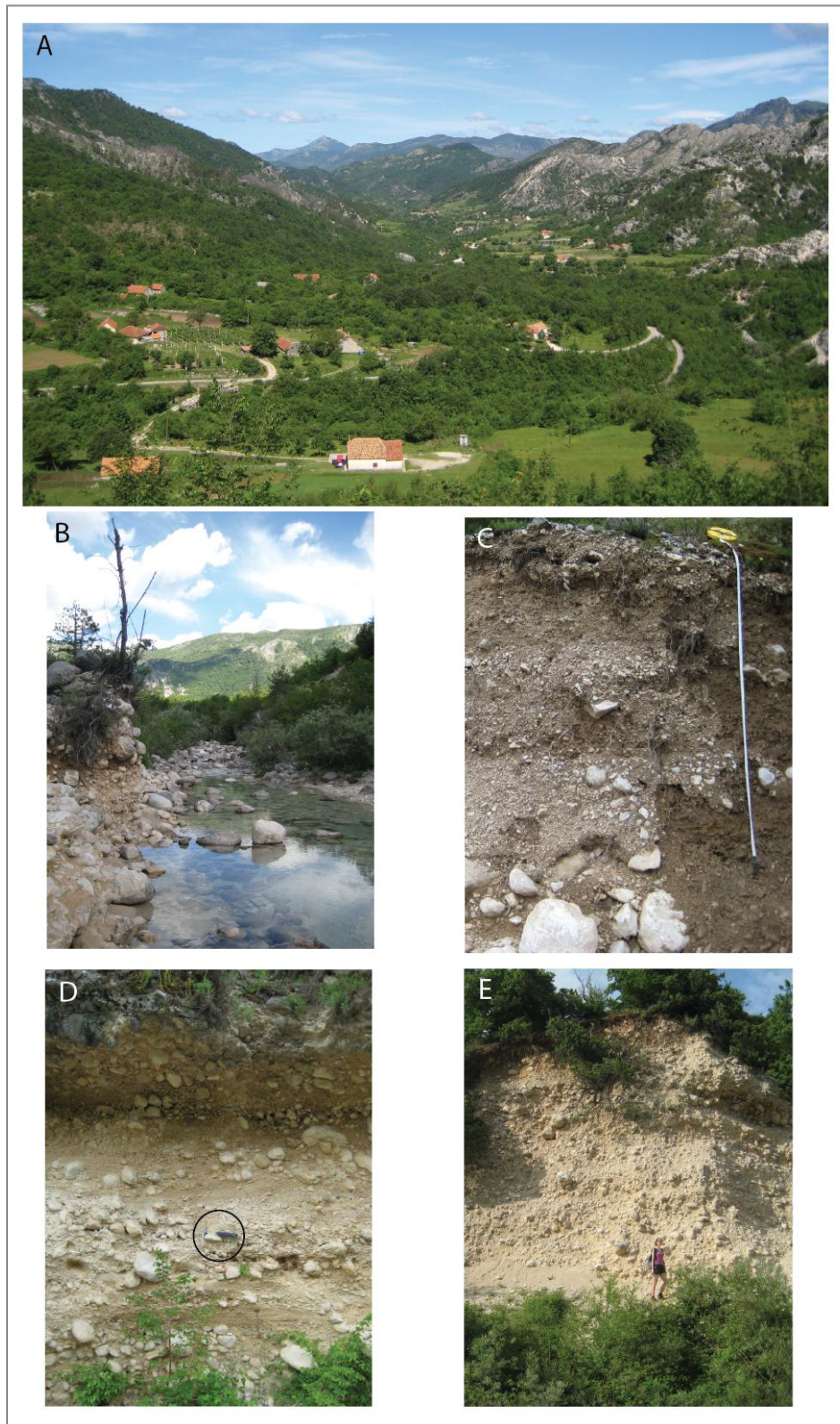
Plate 5.11 – The Nudo valley, north Orjen indicating: A) The view down-valley from the bedrock gorge; B) The 3 m exposure of the Zaslap Unit (Section ZN1) with the stream in flow; C) Angular colluvial clasts within the River Jenkov tributary (Section ZN3); D) Sediments of the Javora Unit (Section JN1) (note the hammer for scale, circled); and E) Sediments of the Arandelovo Unit (Section AN1).
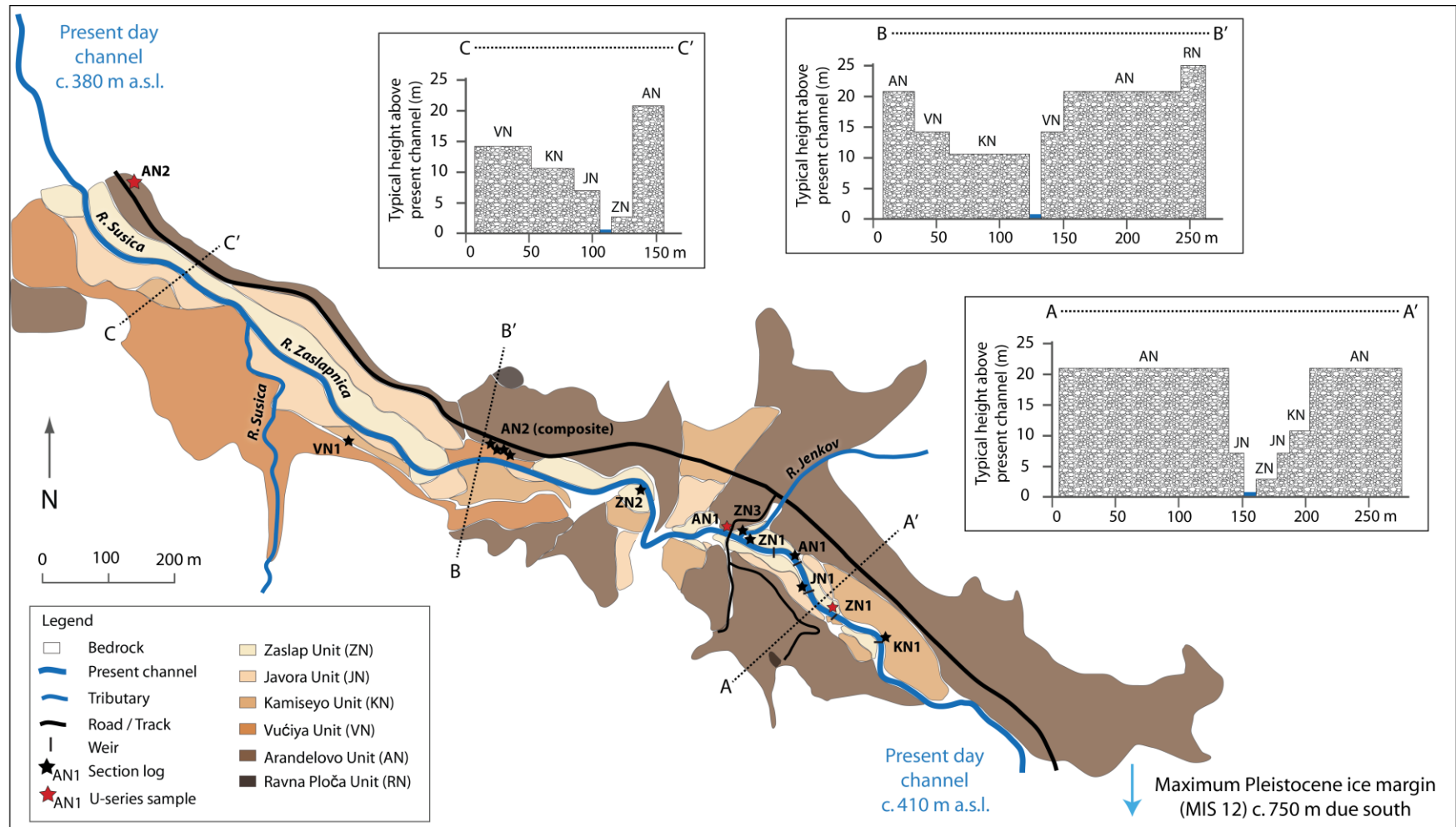
Figure 5.20 – Geomorphological map and terrace record of Nudo. Terraces were mapped using field evidence, GPS coordinates and Google Earth.

Figure 5.21 - Sedimentary logs from river terraces within the Nudo valley, north Orjen. Legend: Figure 5.2.

5.10.2 Javora Unit

The Javora unit is well-preserved throughout the valley and the terrace surface is typically situated 5-7 m above the present channel. Exposures in this unit are scarce, as sections are largely inaccessible or have been altered for agriculture. The sampled exposure (Section JN1) is located in the upper reaches of the valley on the southern side of the present channel (42.6729°N, 18.5707°E, 403 m a.s.l.). The section is obscured at the base by c. 2 m of slumped material, leaving an exposure of 5 m (Plate 5.11d). Sediments are dominated by matrix- to clast-supported, rounded to subrounded limestone pebbles to boulders within a medium sandy matrix (Fig. 5.21). Granules are present within the interstices of larger clasts (clast density 50%) and some evidence of weak imbrication is visible throughout the sequence. As observed in several other terrace exposures, the fine sediment matrix is very weakly cemented, but the thicker phreatic carbonate infills, evident in the Zaslap unit, are not observed here. A thin soil horizon has developed in the upper 20 cm of the exposure.

5.10.3 Kamiseyo Unit

The Kamiseyo Unit is particularly well preserved on the south side of the valley, and the terrace surface is situated c. 10-11 m above the present day channel (Fig. 5.20). Section KN1 (42.6719°N, 18.5730, 404 m a.s.l.) presents a 6.5 m exposure above 4 m of slumped material. Sediments are massive and crudely-stratified clast-supported limestone boulders to granules (clast density 70%) containing dominantly subangular to subrounded cobbles (Fig. 5.21). The coarse sandy matrix is weakly cemented and carbonate rinds have also developed as densely-cemented veneers on most clast surfaces. Gravel lenses (dominantly pebbles) are evident throughout the section as well as several discrete, sandy lenses. A thin soil horizon (c. 20 cm) has developed at the terrace surface and demonstrates a degree of leaching/mineral translocation down the profile to depths of 40-60 cm.

5.10.4 Vućiya Unit

The Vućiya unit is well-preserved within the lower reaches of the valley, particularly on the south side of the channel close to the Kamiseyo unit, but has not been identified in the upper reaches (Fig. 5.20). The terrace surface is typically 12-13 m above the present channel and a granular yet organic-rich soil horizon has developed at the terrace surface. Section VN1

(42.6760°N, 18.5580°E, 384 m a.s.l.) displays crudely stratified, clast-supported limestone granules-pebbles with frequent cobbles and boulders (clast density 60%). Clasts are dominantly subrounded to subangular (Fig. 5.21). The coarse sandy matrix of the Vućiya unit contains a minor silty component and can be differentiated from the Kamiseyo unit by an absence of fine sand lenses and well-stratified gravel horizons.

5.10.5 Arandelovo Unit

The Arandelovo unit is the most extensively preserved terrace unit in the valley (Fig. 5.20). The terrace surface is c. 20 m above the present day channel. A soil horizon has developed in the upper 50 cm of the sediments and a series of cemented benches are exposed in section. Two exposures have been sampled: Section AN1 in the valley's upper reaches (42.6736°N, 18.5704°E, 410 m a.s.l.) and AN2 downstream (42.6757°N, 18.5625°E, 394 m a.s.l.). The sediments display crudely-stratified, clast-supported subangular to rounded limestone cobbles and boulders, with pebbles and granules (clast density 60%) (Fig. 5.21; Plate 5.11b). This unit contains a greater abundance of boulders and large cobbles than have been observed in other terrace units, and boulder-rich horizons are frequent at Section AN1. The fine-medium sandy matrix is weakly cemented throughout the exposure and calcite accumulations are common on the underside of clasts, often forming laminated rinds. Densely cemented, yet detritus-rich, phreatic carbonate benches are also present throughout the exposure. It is likely that these have formed periodically in association with groundwater levels; however it is unclear whether this process has occurred during either sediment aggradation or incision. Section AN2 is a composite log of four adjacent sequences exposed in a track cutting over a distance of 20 m. In comparison to Section AN1, the matrix here is typically a coarse limestone sand with abundant granules and intraclast pockets of fine sand and silt. The cemented benches here are accessible within a track cutting and samples from 4 carbonate horizons have been taken for micromorphological analysis (Chapter 7) and U-series dating (Chapter 8).

5.11   Sniježnice

The site at Sniježnice (42.4971°N, 18.5980°E, 1,066 m a.s.l.) is located within a high altitude basin, up valley of Ubli, and adjacent to the MIS 12 ice margins (Plate 5.12; Fig. 5.14). During MIS 12, the ice here coalesced to form the southern extent of the ice mass. In MIS 6 a smaller,

isolated ice mass developed, also along this southern margin (Fig. 5.1). A complex of moraines from MIS 12 and MIS 6 is now well preserved and the glaciofluvial sediments at Sniježnice are exposed within shallow quarry cuttings in the ice marginal zone, immediately outside the former ice margins (Fig. 5.22).
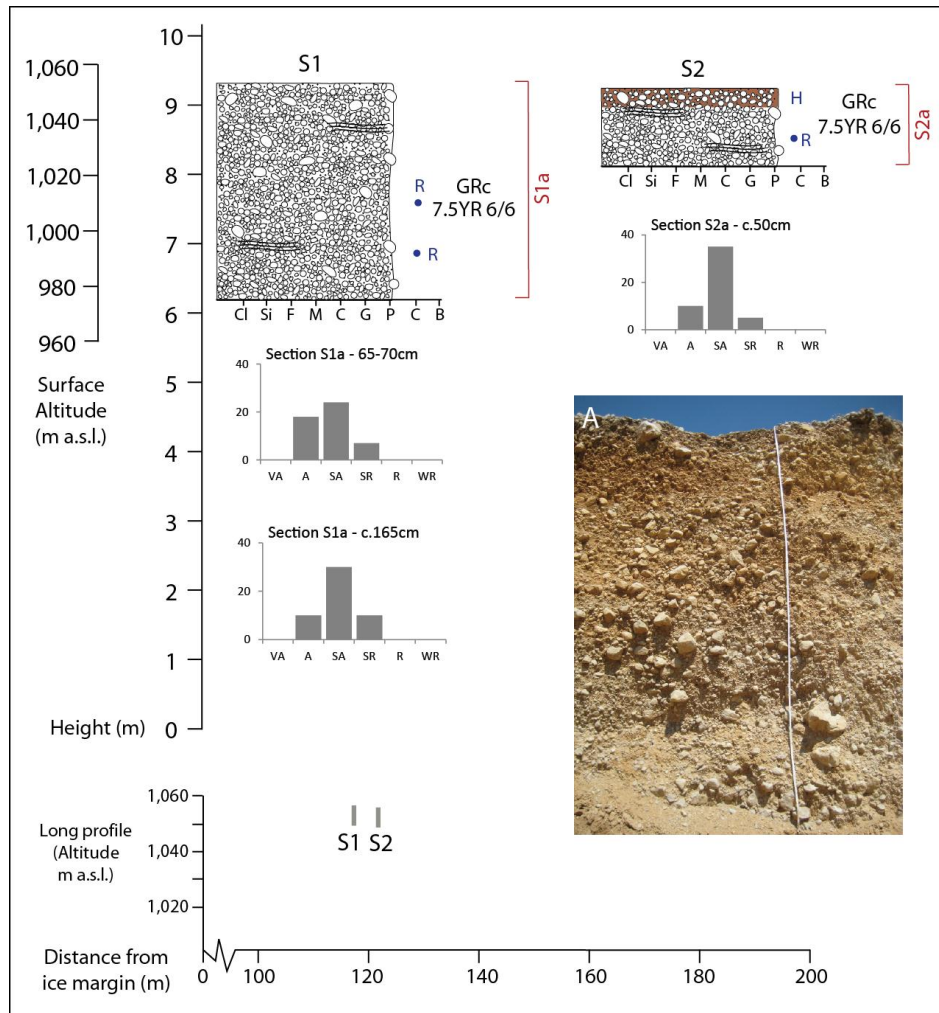
Figure 5.22 – Sediment logs at Sniježnice, south Orjen. Inset A) Sediments exposed at Section S1 demonstrating their coarse grained and crudely-stratified characteristics. Legend: Figure 5.2.

Sections S1 (42.4971°N, 18.5980°E) and S2 (42.4951°N, 18.5960°E) are situated c. 120 m from the MIS 12 ice margin and present a sequence of massive, clast-supported, crudely-stratified sands and gravels (clast density 60%) (Fig. 5.22). Clasts are dominantly angular to subrounded limestone pebbles-cobbles with granules and occasional boulders (Fig. 5.22). Horizons of well-stratified material, which become increasingly abundant with distance from the ice margin, distinguish these deposits from the adjacent glacial diamict (Plate 5.1). A series of vadose zone

calcites have been sampled from the edge of the largest MIS 12 moraine at this site. This moraine surface grades into the sampled ice marginal sediments, and its age is therefore closely linked to the deposition of both sequences. A 40 cm-thick poorly developed and granule-rich soil horizon has developed across the land surface.

Plate 5.12 – Sniježnice, south Orjen indicating: A) The field site (arrowed) and moraines identified by Hughes *et al*. (2010) and correlated to MIS 12 (adjacent to the field site) and MIS 6 (left of the image).

5.12   Unijerina

Unijerina is located on the south eastern side of the Orjen massif, inside the former MIS 12 ice margins and downstream of the moraines at Crkvice which have been U-series dated and correlated on the basis of morphostratigraphy to MIS 6 (Hughes *et al*., 2010). During the Pleistocene, both Unijerina and Crkvice (Section 5.13) would have been fully overrun by ice. The site at Unijerina is situated within a shallow valley system (Fig. 5.23) that drains towards the coastal fan at Risan, in the Bay of Kotor (Fig. 5.1). Three lithofacies are exposed within a stacked sequence at Section U3 (42.5501°N, 18.6553°E; 730 m a.s.l.). These also correlate to exposures at Section U1 and U2 (Fig. 5.24). The lowest facies (U3a) contains a 4.5 m sequence of stratified alluvial sands and gravels. These are interpreted as alluvial deposits due to their well-sorted characteristics and interstratifications of fine silts and clays as well as coarser, granular and sandy horizons. Sedimentary units are often laterally discontinuous and largely display gradational contacts with the overlying deposits. Units vary throughout the facies from matrix- to clast-supported (clast density 0-40%), and typically contain medium-coarse limestone sand, granules and pebbles. Clasts throughout this facies are dominantly sub-rounded to rounded, with inputs of well-rounded and angular material (Fig. 5.24). The

sequence is capped by a c. 30 cm-thick horizon of massive sandy silt with pebble to cobble sized dropstone features (U3a-xii) that have deformed the underlying sediments (Plate 5.13). This may be indicative of a proglacial shallow lacustrine environment (e.g. Rother *et al.*, 2010; Alberti *et al.*, 2011) or a slow-flowing fluvial setting.
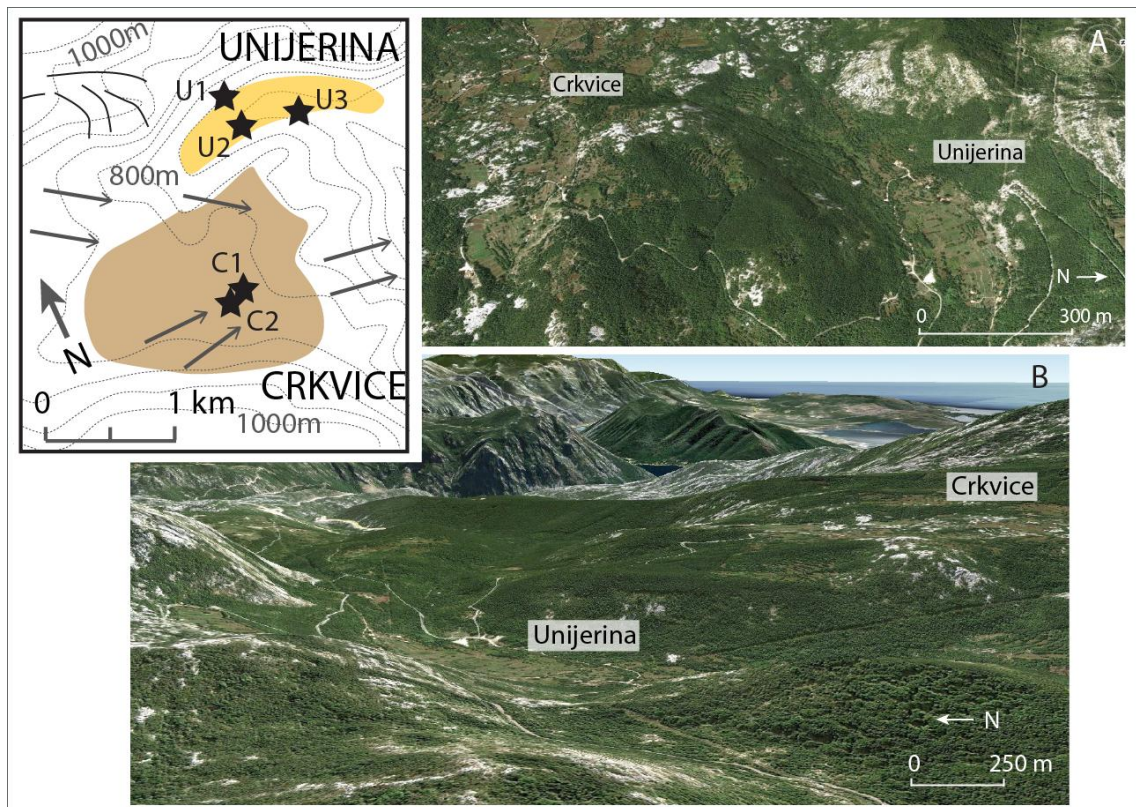
Figure 5.23 - Geomorphological map of Unijerina and Crkvice, east Orjen indicating the Pleistocene glacial landforms presented by Hughes *et al*. (2010) Legend: Figure 5.1. A) Aerial image of east Orjen indicating the valley at Unijerina and shallow polje at Crkvice; B) View down-ice from the moraines at Crkvice towards the Bay of Kotor indicating the Unijerina valley and the adjacent polje at Crkvice. Source: both Google Earth.

The basal facies is overlain by 3 m of massive, matrix-supported (clast density 30-40%), silt-rich diamicton (U3b). The gradational lower boundary is discontinuously defined by a cobble lag, which is often deposited as dropstone features into the underlying silt unit (U3a-xii). Clasts are dominantly subangular to rounded limestone pebbles and cobbles (Fig. 5.24), with granules and boulders throughout the unit. Clasts are often blocky in morphology and macrofabric measurements indicate a weak northeast-southwest orientation (Fig. 5.24). These characteristics suggest a glacial origin of this diamicton (Benn and Ballantyne, 1993; 1994), yet the weak fabric data are more indicative of slumping. This may indicate the redeposition of an existing glacial diamict by mass movement processes. The uppermost facies (U3c) contains a c.

3 m sequence of stratified, weakly-cemented, matrix- to clast- supported (clast density 30-70%) sands and gravels (pebbles and cobbles) within a coarse sand and granular matrix. These are similar in character to the lowest facies (U3a) and are also interpreted as fluvial deposits. This upper facies is correlated with a shallow exposure of stratified sands and gravels at Section U1 (42.5505°N, 18.6512°E), which is situated 322 m further upvalley from Section U3, and shares the same land surface. A 60 cm-thick, granule-rich soil horizon has developed across the surface of the deposits (Chapter 8.2).
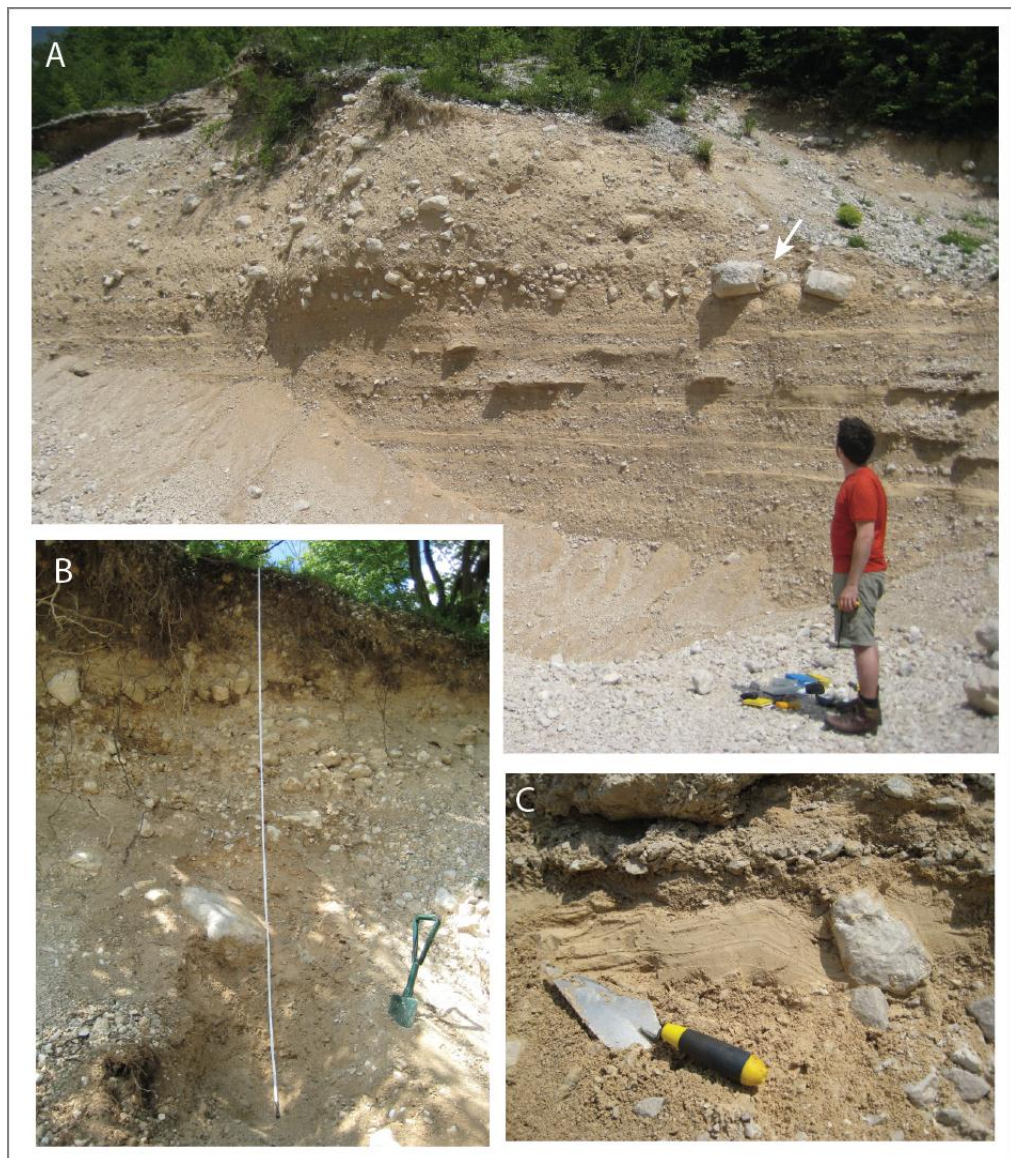
Plate 5.13 – Unijerina, east Orjen, indicating: A) The sedimentary exposure at Section U3 demonstrating the three facies (lower stratified fluvial sediments, diamicton, and capping fluvial deposits). The cobble-sized 'dropstone' features are arrowed; B) The stratified diamict at Section U2; and C) Detailed image of the dropstones into the massive silt horizon at the contact between Facies U3a and U3b.
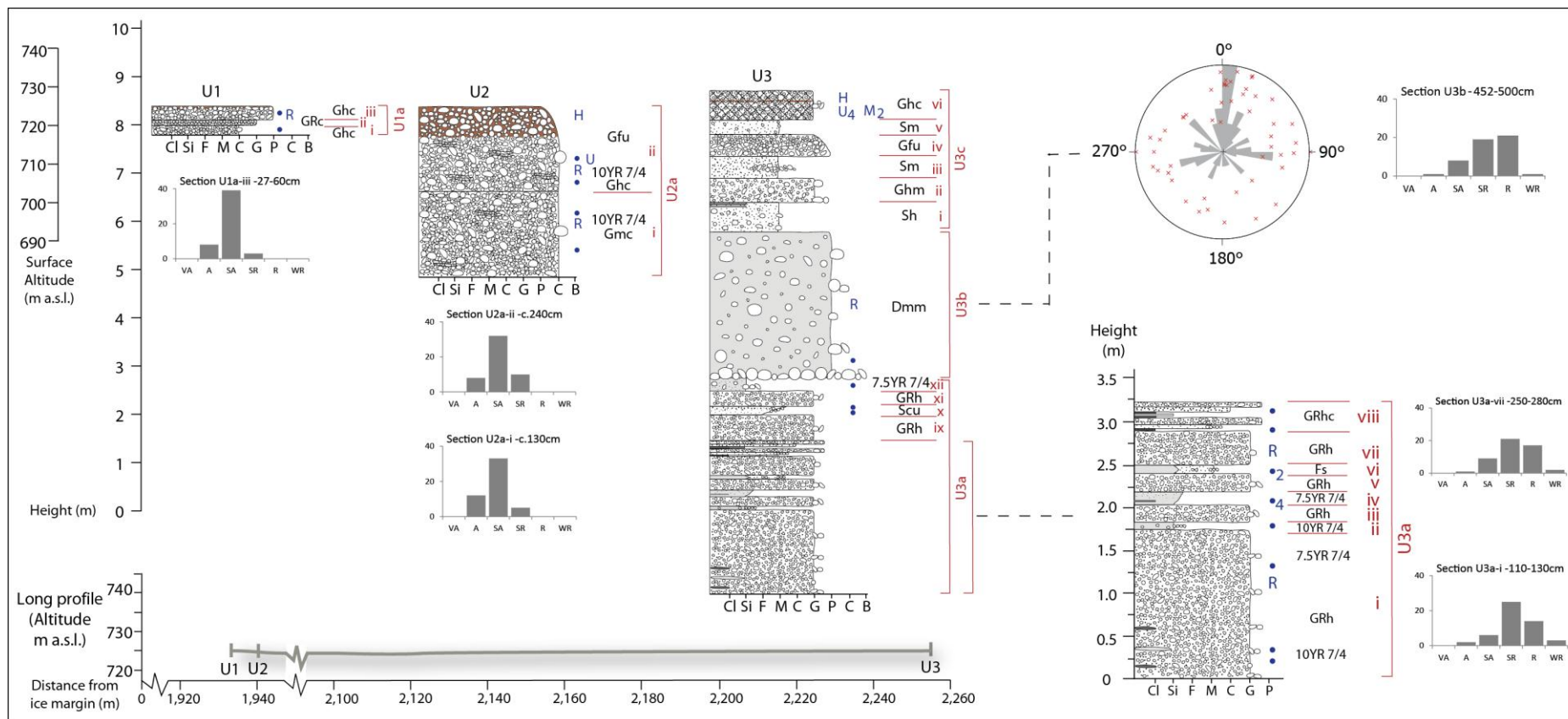
Figure 5.24 - Sedimentary logs at Unijerina, east Orjen. Legend: Figure 5.2.

Section U2 (42.5501°N, 18.6509°E) is 315 m up valley from Section U3 and reveals a matrix- to clast-supported (clast density 50%), stratified diamicton. The coarse sandy matrix has a dominant silt component. As observed in facies U3b, clasts are frequently blocky in texture, yet are largely subangular here compared to the abundance of subrounded and rounded clasts within facies U3b. More detailed particle size analysis and U-series dating will more fully constrain the correlations between these individual facies (Chapters 6 and 8).

5.13   Crkvice

The exposures at Crkvice (42.5406°N, 18.6378°E, 850 m a.s.l.), southwest of Unijerina, are also within the MIS 12 ice margins and downstream of the MIS 6 moraines at Crkvice (Fig. 5.1; 5.23). The area forms a small polje enclosed by glacially-scoured bedrock (Fig 5.23). Sediment exposures here are scarce in comparison to the larger poljes outside the ice margins and isolated patches of sediments are exposed within roadside cuttings (Plate 5.14; Fig. 5.25).
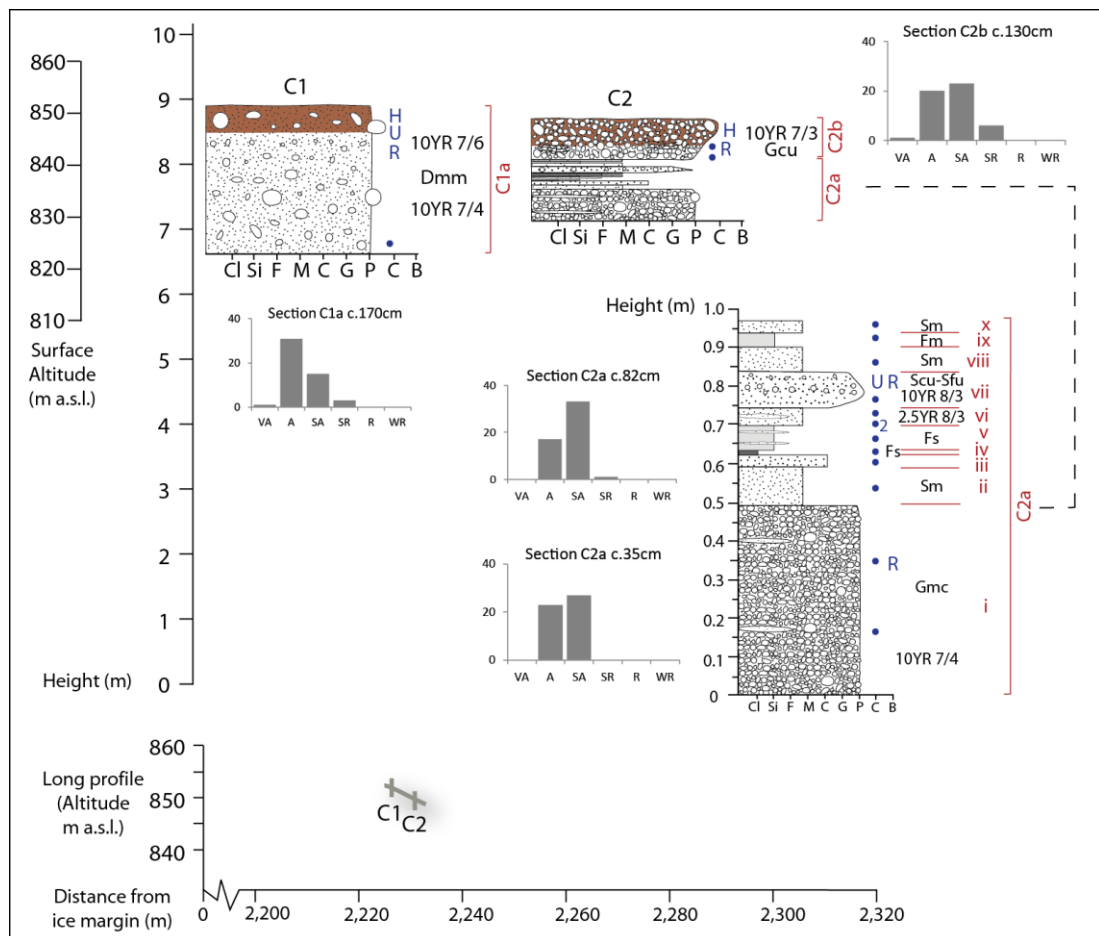
Figure 5.25 - Sedimentary logs at Crkvice, east Orjen. Legend: Figure 5.2.

Section C1 (42.5406°N, 18.6378°E) is situated c. 2.2 km from the MIS 6 ice margin and presents a massive, matrix-supported diamicton (clast density 35%) (Plate 5.14). Clasts are dominantly angular and subangular limestone granules and pebbles, with cobbles and boulders throughout the sequence (Fig. 5.25). Faceting of clasts is common, particularly on the larger pebbles and cobbles, and suggests a glacial origin (Benn and Ballantyne, 1993; 1994). The matrix of coarse-medium sand contains a strong silty component. Weakly developed phreatic carbonates are present within some horizons, and a calcite 'clast' was extracted from c. 200 cm. This possibly reflects the reworking, remoulding and subsequent redeposition of a previously-formed calcite deposit, but U-series analysis would serve as a maximum age constraint on this sequence. As observed at Unijerina, this may reflect the slumping of glacial sediment into the polje depression.
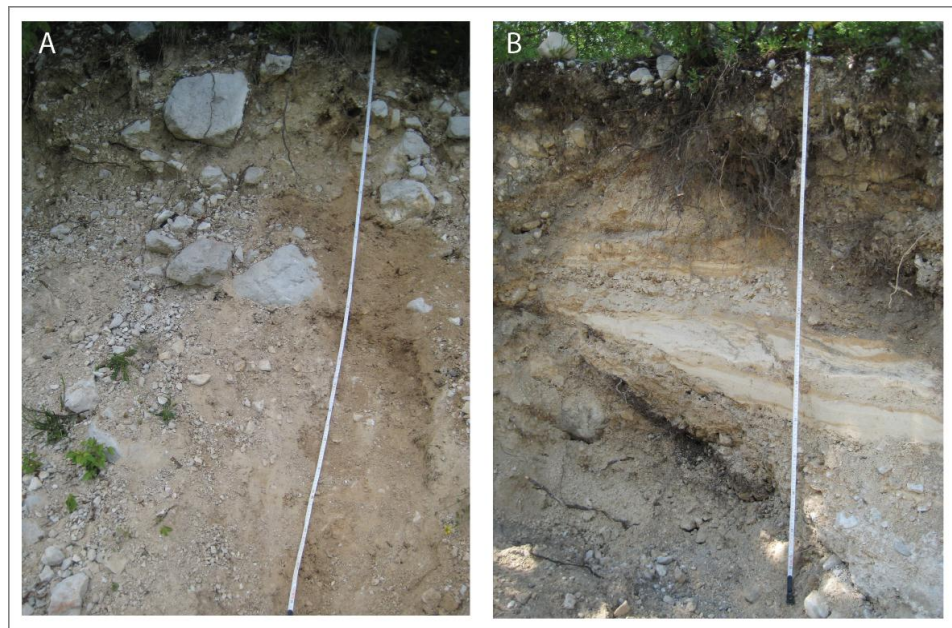
Plate 5.14 – Sedimentary exposures at Crkvice, east Orjen indicating: A) The massive diamicton at Section C1; and B) The finely interstratified sands and gravels at Section C2.

Section C2 is adjacent to Section C1 within the polje, at a lower elevation. The sedimentology here contrasts markedly with Section C1, and presents a series of interstratified sands, gravels and fines (clast density typically 0% and occasionally 60%). Within the lowest unit (C2a-i) clasts are largely subangular and angular pebbles with granules and cobbles (Fig. 5.25), and are frequently blocky and faceted in texture and resemble those observed within Section C1. The coarse sandy matrix contains a dominant silt component and silty drapes are present on the

upper surfaces of clasts, particularly at c. 80 cm (C2a-vii). The sedimentary characteristics here resemble the ice distal exposures of Dvrsno polje. A 50 cm-thick, yet weakly developed and granule-rich soil horizon has developed across the land surface at Sections C1 and C2.

5.14   Ubli

The exposure at Ubli (42.5120°N, 18.6326°E, 785 m a.s.l.) is located 1.5 km from the MIS 6 moraines of Hughes *et al*. (2010) within a wide and shallow gradient valley, constrained by limestone bedrock (Fig. 5.14; Plate 5.15). This valley is distinct from the poljes due to its shallow gradient rather than flat valley floor, comparatively gentle valley sides, and outflow below the MIS 12 moraines close to Lipci. This valley would have formed the dominant meltwater route draining the southern margin of the Orjen ice cap, entering the Bay of Kotor via a large, steep sided ravine at Lipci, where an extensive alluvial fan is now preserved (Fig. 5.1; Section 5.8).
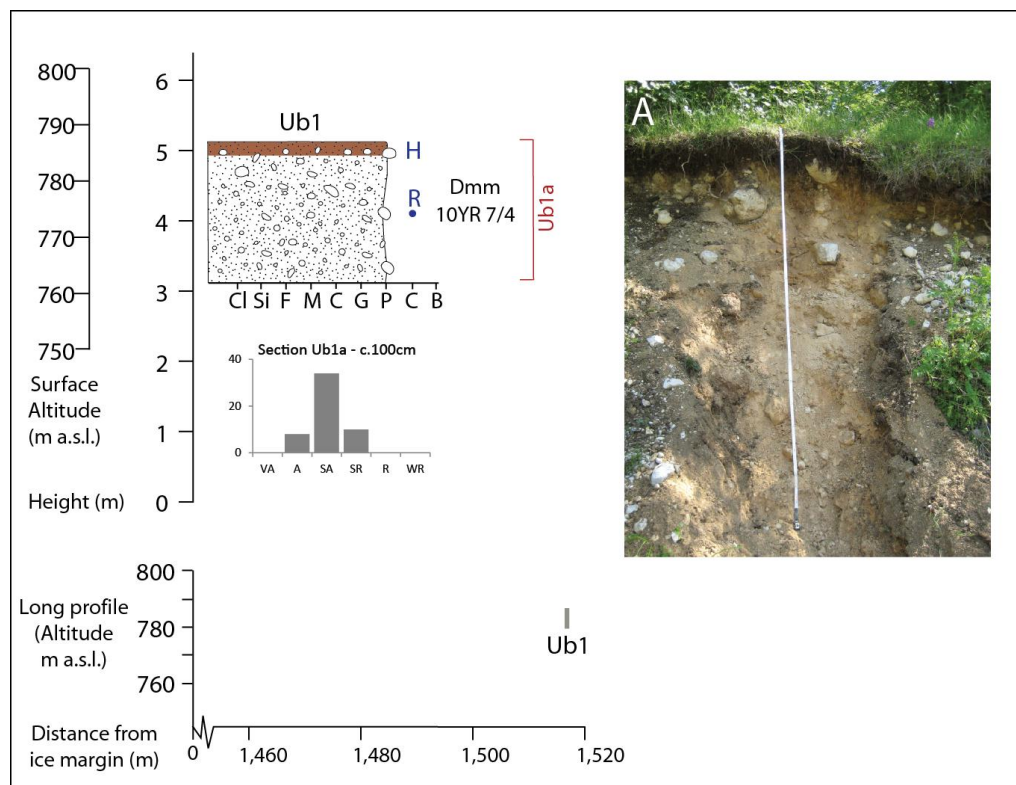
Figure 5.26 – Sedimentary logs and the exposure (inset, A) at Ubli, southwest Orjen. Legend: Figure 5.2.

The sedimentary record is generally poorly preserved within the valley at Ubli apart from infrequent exposures of sediment perched on the valley sides. The analysed exposure, Section Ub1 (Fig. 5.26), is situated on the up-ice face of a small bedrock knoll (600 m x 300 m) in the centre of the valley. Terrain imagery indicates that this bedrock outcrop has a steep stoss face and shallow lee side. The sediments here present a massive, matrix-supported diamicton (clast density 30%) with a coarse sand- sandy silt matrix (Fig. 5.26a). Clasts are dominantly subangular blocky and faceted limestone pebbles-cobbles with granules and occasional boulders (Fig. 5.26). These are indicative of a glacial rather than fluvial origin (Benn and Ballantyne, 1993; 1994). This indicates that fluvial sediments are poorly preserved within this valley, and may have instead been transported further downstream and deposited at the Lipci fan. The sediments at Ubli can, however, help to constrain the depositional history within this valley. A 30 cm-thick soil horizon has developed at the land surface and has been sampled to determine the relative age of this deposit.
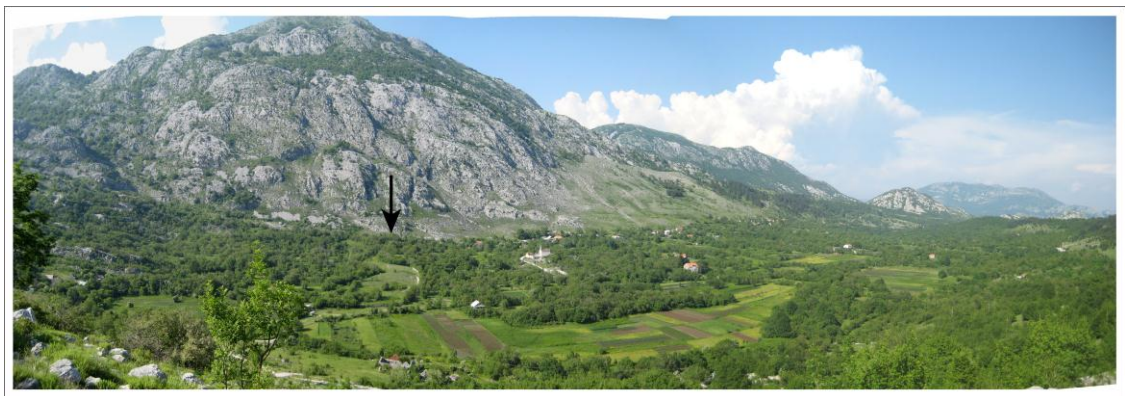
Plate 5.15 – Panoramic image of Ubli, southwest Orjen. Pleistocene ice flow direction was left to right across the image, emanating from Ubajska planina and Sniježnice. The MIS 6 moraines are situated towards the centre of the image (arrowed) and larger MIS 12 moraines are situated downvalley close to a steeply incised gorge at the apex of the Lipci alluvial fan.

5.15   Summary and facies model

The fluvial deposits analysed in this study highlight the contrasting sedimentological characteristics of the different geomorphological settings surrounding Mount Orjen. These data can be used to develop facies models to assess the transformation of sedimentary sequences from the ice margins to the depocentres downstream. Six facies types are exposed within the fluvial environments of Orjen (types a-c). Alluvial fan (type a) and polje (type b) facies contain a further three sub-facies types (i – iii) (Table 5.2). The morphosedimentary

analyses can be used alongside detailed particle size analysis (Chapter 6) and dating techniques (Chapter 8) to develop a more integrated and quantified model of fluvial response to Pleistocene glaciation surrounding the Orjen massif, within Chapter 9.

	Facies Type			Description	Exposed at facies:
a.	**Alluvial fan**				
	Increasing distance downstream	Ice Proximal	i	Massive, clast-supported crudely stratified gravels (dominantly cobbles and pebbles with boulders).	L1a, L2a, L3a, L4a; K1a, K1b, K2a, K3a
		Ice Medial	ii	Stratified clast- to matrix- supported gravels (dominantly pebbles and granules) with sand lenses. Some evidence of imbrication.	K4a, K5a, K6a, K7a, K8b, K8c
		Ice Distal	iii	Interstratified fine sands, silts and clays with stratified sands and granules.	K8a
b.	**Polje**				
	Increasing distance downstream	Ice Proximal	i	Massive, clast-supported stratified gravels (dominantly cobbles and pebbles with some boulders). Some sand lenses are present.	D1a, D2a, D3a, D4a
		Ice Medial	ii	Massive, stratified gravels (pebbles and granules) with some cobbles. Sand lenses and well-stratified horizons are abundant.	D5a, D6a, D7a; Kr1a, Kr2a; V1a, V2a, V3a, V4a; P1b, P2a, P2b, P3a; G1a, G2a; C2b
		Ice Distal	iii	Interstratified silts, clays and fine sands with coarse sands and granules. Some evidence of cross stratification.	D8a, D9a; P1a; C2a
c.	**River terrace - alluvium**				
				Massive, crudely-stratified to stratified, clast- to matrix- supported, sands and gravels (dominantly pebbles with cobbles and granules). Some sand lenses and well-stratified gravels are present.	AN1a, AN2a, VN1a, KN1a, JN1a, ZN1a, ZN2a, ZN3a
d.	**Diamict**				
				Massive, often crudely-stratified silty sand with cobbles and boulders with some pebbles and granules.	U2a; U3b; C1a; Ub1a
e.	**Proglacial - Ice marginal glaciofluvial**				
				Massive, crudely-stratified and clast-supported sands and gravels (dominantly pebbled and cobbles with boulders).	S1a, S2a
f.	**Proglacial - Glaciofluvial and low energy/shallow lacustrine**				
				Finely interstratified sands, silts, clays and gravels (granules with pebbles). Some thick horizons of silt (20-30 cm) are present.	U1a, U3a, U3c

Table 5.2 – Facies types exposed within the fluvial sequences surrounding Mount Orjen.

Synopsis

This chapter presents data on the particle size characteristics and carbonate content of bedrock clasts (Section 6.2) and sediment samples from glacial (Section 6.3) and fluvial (Sections 6.4 - 6.15) contexts across Mount Orjen. This aspect of the Pleistocene sediment record has been explored in detail to establish the nature of the fine sediment fraction in the glacial environment and how this has been modified downstream by fluvial processes such as abrasion and sorting. In a wider Mediterranean context, it is important to characterise the nature of the fine sediment fraction from glaciated limestone terrains because this material can be transported to a range of depositional settings downstream and it may have considerable palaeoenvironmental significance. Glacially-sourced limestone-rich fine sediment has been recorded in coarse-grained flood deposits (Lewin *et al*., 1991), in slackwater sediment records (Woodward *et al*., 2008), in lacustrine settings (Giraudi *et al*., 2011), and in Pleistocene rockshelter sediment records (Woodward and Bailey, 2000). Many of the loess deposits on the Balkan Peninsula have significant calcium carbonate components (Marković *et al*., 2009) and some of this material may have been entrained from alluvial basins fed by glaciated catchments. It is also likely that these sediments were delivered in significant quantities to marine environments during Pleistocene cold stages. It is therefore important to better understand how the characteristics of these sediments may change during fluvial transport so that this material can be identified with confidence.

6.1   Introduction

A total of 170 samples of the fine sediment matrix have been collected from moraines and fluvial sediments in a wide range of depositional contexts both proximal and distal to the MIS 12 and MIS 6 ice margins (Fig. 6.1). A selection of limestone clasts from each study site (Section 6.2) has also been analysed to characterise the carbonate composition and particle size of the limestone bedrock before it is transformed by glacial and fluvial processes.
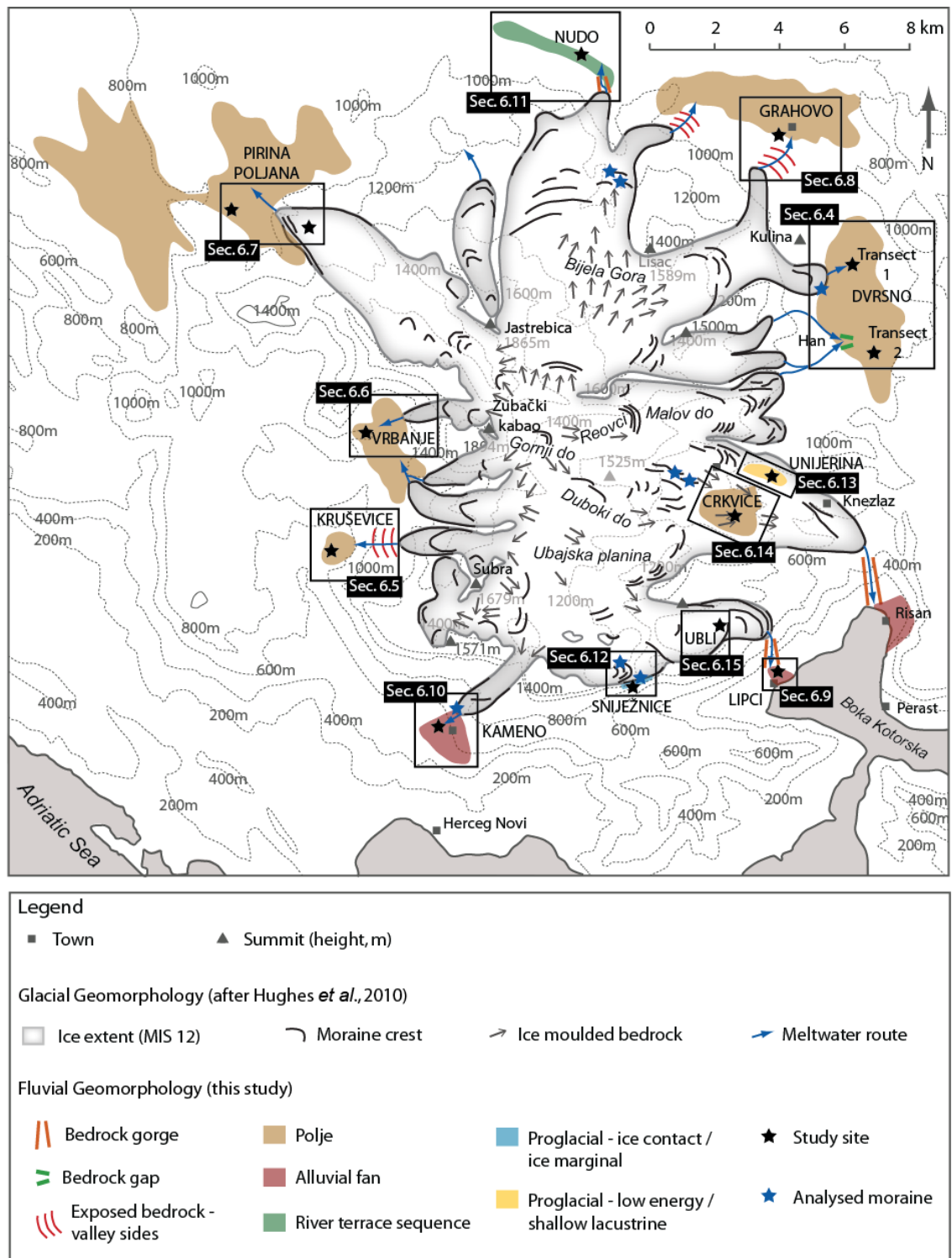
Figure 6.1 – Map of the Orjen massif indicating the sampled locations. Insets indicate the relevant sections of this chapter that discuss the sediment particle size and carbonate content at each site.

Horizons that were sampled for analysis are indicated on the sediment logs in Chapter 5. Samples were screened at both 2 mm, to characterise the full particle size range of the bulk

sediment, and at 63 μm, to investigate the finest sediment fraction in detail. The carbonate content of the <63 μm fraction was also determined, and the particle size of the remaining insoluble residue (non-carbonate) component was analysed. These data are presented as percentages of the bulk sediment matrix within a series of pie charts alongside mean particle size distributions (PSD) of the <63 μm matrix component.

The most representative PSDs, at <2 mm and <63 μm, at each site are presented in this chapter, whilst a full record of all PSA results is provided in Appendix E (supplementary data disc). PSA data are recorded as volume (%) and plotted on a logarithmic scale of particle size in microns (μm). Bulk sample and corresponding residual sample PSA data are displayed as a solid and dashed line, respectively. This allows the changing nature of fine matrix sediments to be assessed with distance from the ice margin.

6.2   Limestone bedrock calcium carbonate content and particle size analysis

Carbonate content and particle size (<2 mm) of the residual lithologies of a selection of clasts from 11 sites across the study area has been used to infer bedrock characteristics. These data are used to provide indicators of the transportation and depositional processes operating within the glacial and fluvial environments, as the fine particles of the bedrock sources are transformed downstream (see Nesbitt and Young, 1996; Garzanti *et al*., 2008; 2009; 2010; Eynattan *et al*., In Press). As will be discussed, these processes may include both chemical and physical weathering mechanisms.

The spatial variations in source bedrock characteristics are presented in Figure 6.2. Within all bedrock samples, the <2 mm fraction of the insoluble residue is dominated by medium-fine silts, with some inputs of coarser silts and clays (Fig. 6.2; 6.3). The PSD is largely unimodal, and often contains a sharp peak within the fine silt size fraction. The insoluble residue typically accounts for less than 1.5% of the bulk bedrock sample (Table 6.1). Samples from Pirina Poljana (3.6%) and the Vućiya Unit of the Nudo valley (3.3%) present the highest values of insoluble residue and may reflect localised sources of non-limestone lithologies (Chapter 3). The bedrock data are presented within the following sections alongside particle size and carbonate content data from glacial and fluvial sediments from catchments surrounding the Orjen massif. These are used to explore the ways in which limestone bedrock, and its

constituent minerals, can become progressively comminuted and sorted within the glacial and fluvial environments downstream.
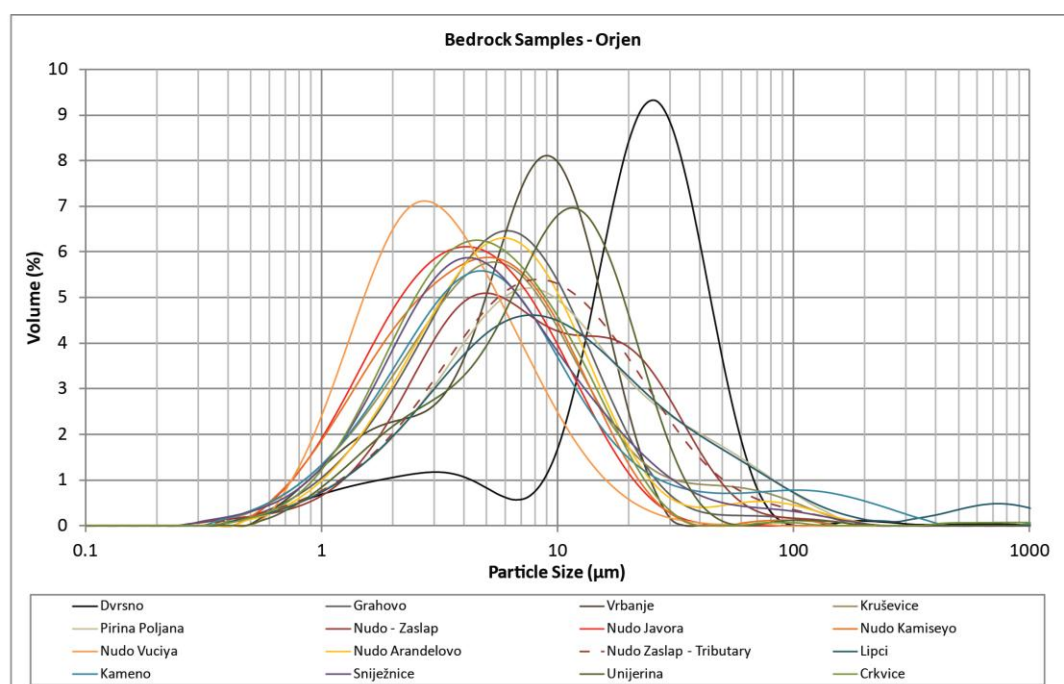
Figure 6.2 – Particle size distribution of the insoluble residue (non-carbonate) component of bedrock clast samples at <2 mm.

Sample	<2 mm % non-carbonate (NC)	<2 mm % carbonate (C)
Dvrsno	0.9	99.1
Grahovo	1.5	98.5
Kruševice	1.0	99.0
Vrbanje	1.9	98.1
Pirina Poljana	3.6*	96.4
Kameno	0.4	99.6
Lipci	1.5	98.5
Sniježnice	1.3	98.7
Crkvice	1.1	98.9
Unijerina	1.2	98.8
Nudo Zaslap	1.5	98.5
Nudo Javora	0.8	99.2
Nudo Kamiseyo	2.0	98.0
Nudo Vućiya	3.3	96.7
Nudo Arandelovo	0.5	99.5
Nudo - Zaslap Tributary	1.2	98.8
Nudo Average	**1.5**	**98.5**

Table 6.1 – Clast lithological data for bedrock clast samples obtained from across Orjen displayed as % non-carbonate (NC) and carbonate (C) of the bulk sample (<2 mm). * Following acid digestion, the sample at Pirina Poljana contained a granule-sized insoluble clast that was not included in the particle size measurements.
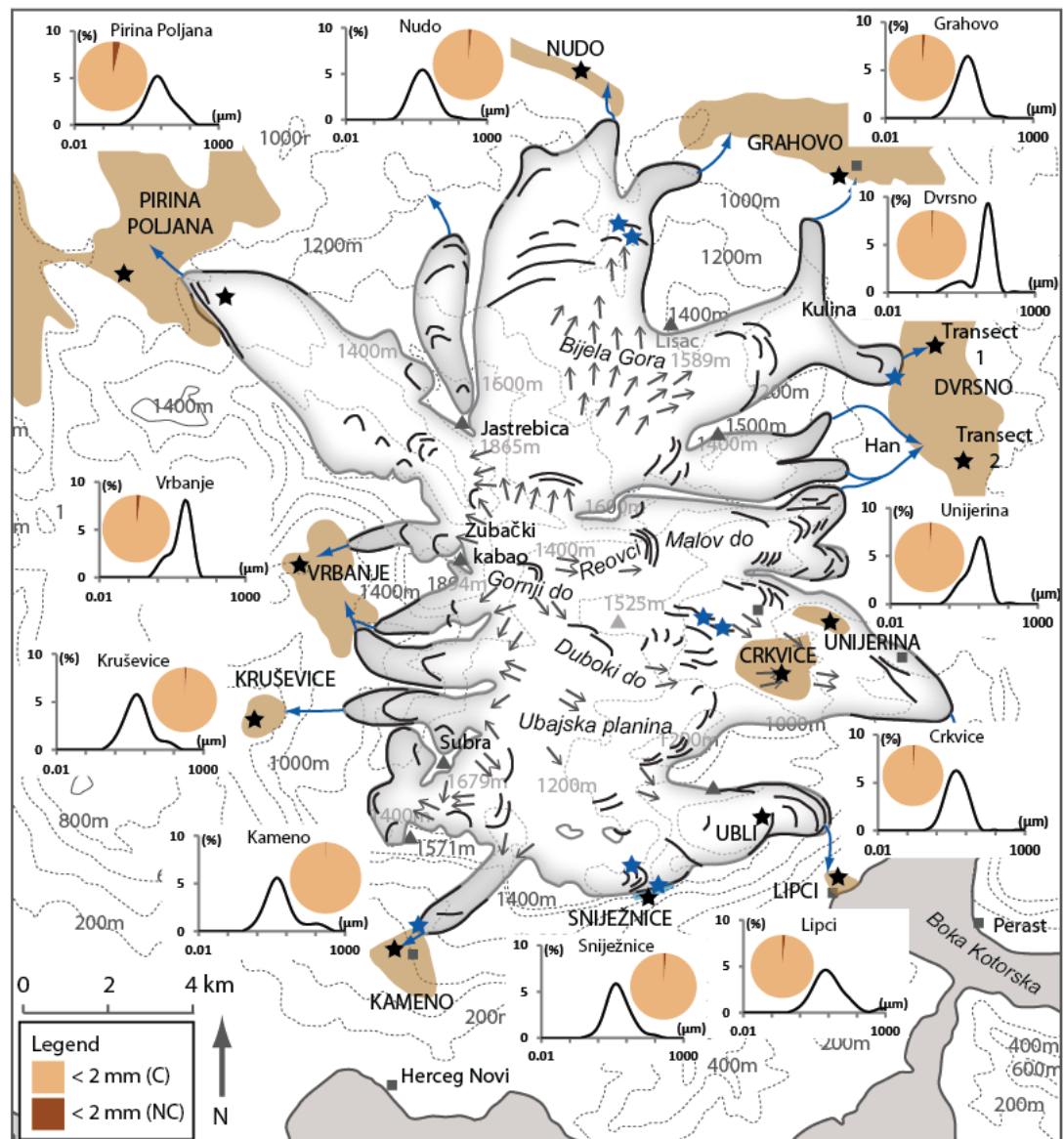
Figure 6.3 – Clast lithological data and particle size distribution of the insoluble residue component (<2 mm) from bedrock clast samples taken from across the Orjen massif.

6.3   Glacial sediments

The glacial sediments of seven moraines on Mount Orjen display a largely bimodal particle size distribution with peaks centred on 1 to 10 μm and 1,000 μm (Fig. 6.4 inset), reflecting the high granular content within a silt-rich matrix. The <63 μm fraction is dominated by clay and very fine silt (<8 μm) (Fig. 6.4). These observations are similar to the particle size data obtained from the limestone-rich glacial sediments of Mount Tymphi, northwest Greece (Woodward *et al.*, 1995), where 40% of the bulk matrix sediments are <10 μm.
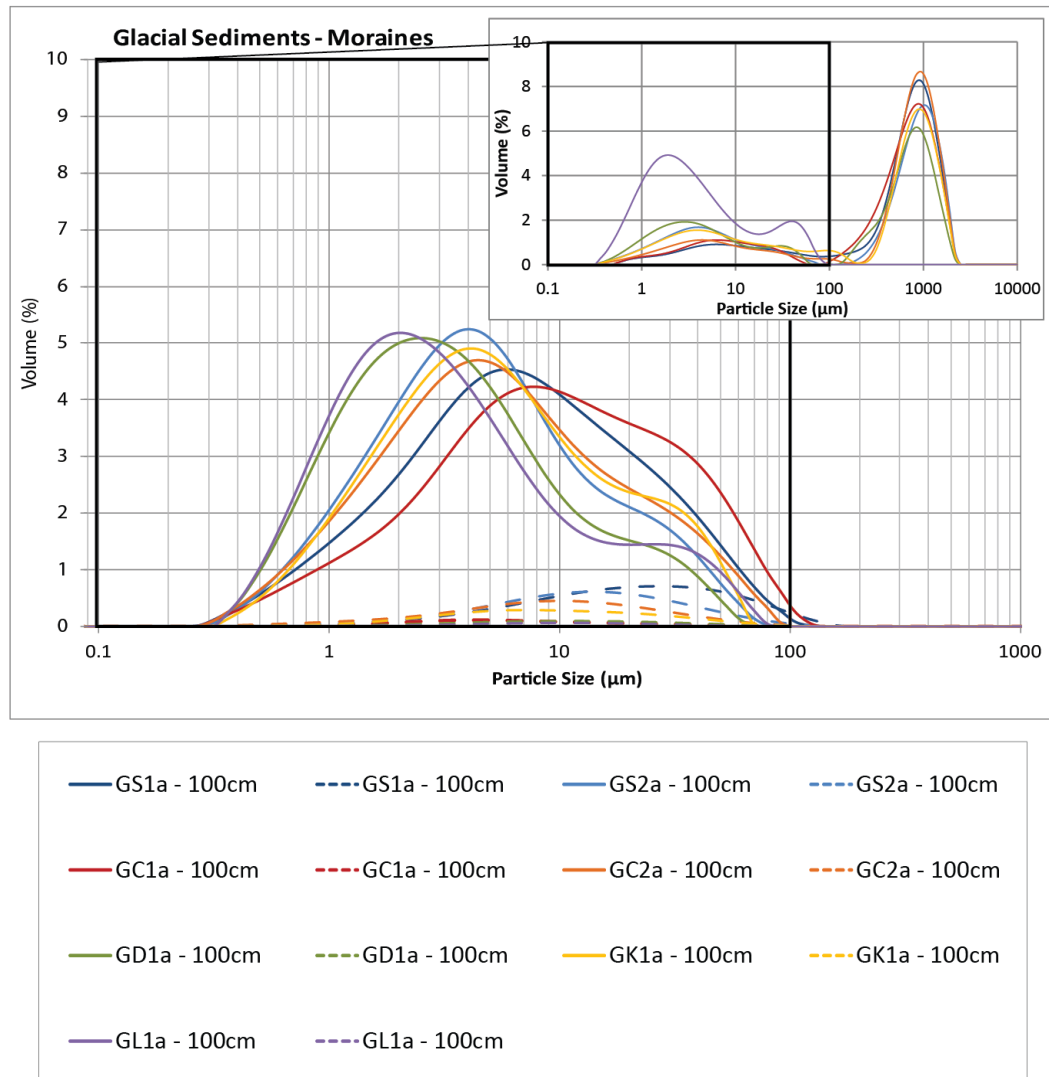
Figure 6.4 – Particle size distribution of glacial till samples from moraines surrounding the Orjen massif at <2 mm (inset graph) and <63 μm (main graph). Hughes *et al*. (2010) have correlated the moraines at Lisac (GL1), Crkvice (GC1 and GC2) and Sniježnice (GS2) to MIS 6; and the moraines at Dvrsno (GD1), Sniježnice (GS1) and Kameno (GK1) to MIS 12.

The non-carbonate lithologies occupy a coarser particle size range (9 – 60 μm) than the limestone-rich fines, and account for 2.1% to 15.5% of the <63 μm sediment content (Table 6.2). These values are highest at Sniježnice, south Orjen (9.9% and 15.5%) which may reflect the presence of flysch outcrops close to the ice terminus here (Chapter 3, Fig. 3.2; Section 6.1). The mean particle size and carbonate content statistics for the moraines of Orjen are presented within the following sections alongside the fluvial records.

Moraine (MIS)	Height up profile (cm)	Unit/Facies Description	<2mm >63µm % non-carbonate (NC %)	<2mm >63µm % carbonate (C %)	<63µm % non-carbonate (NC %)	<63µm % carbonate (C %)
GLACIAL SEDIMENTS - MORAINES						
Lisac (MIS 6)	100	Matrix	0.1%	68.6%	5.0%	26.3%
Dvrsno (MIS 12)	100	Matrix	0.2%	54.7%	4.8%	40.3%
Crkvice 1 (MIS 6)	100	Matrix	0.2%	81.9%	2.1%	15.8%
Crkvice 2 (MIS 6)	100	Matrix	0.3%	74.6%	7.3%	17.8%
Sniježnice 1(MIS 12)	100	Matrix	0.3%	57.1%	15.5%	27.1%
Sniježnice 2 (MIS 6)	100	Matrix	0.1%	66.3%	9.9%	23.7%
Kameno (MIS 12)	100	Matrix	0.1%	72.0%	2.1%	25.7%

Table 6.2 – Carbonate content data from the fine sediment matrix of moraines across the Orjen massif displayed as % non-carbonate (NC) and carbonate (C) of the bulk sediment by size fraction: <2 mm >63µm and <63 µm.

6.4   Dvrsno

Two transects of Pleistocene sediments have been analysed from the northern (Transect 1) and southern (Transect 2) sectors of the Dvrsno polje (Figure 6.1). Transect 1 extends from 950 to 1,350 m from the MIS 12 moraine. The <2 mm particle size distribution is dominated by the <63 µm sediment fraction (Fig. 6.5) at distances of <1,040 m from the ice margin. Beyond this, inputs of coarser sediments (100 to 2,000 µm) lead to a quasi-bimodal particle size distribution (Fig. 6.6). The mean particle size characteristics of the sediment matrix indicate that the <63 µm fraction itself is dominated by the finest clays (1 to 4 µm) and displays a fining with distance from the ice margin (Fig. 6.6). Non-carbonate lithologies are concentrated in the <63 µm size fraction (Fig. 6.6) where they typically contribute up to 20% of the finest clay horizons (Table 6.3). These values are particularly high for a region dominated by limestone bedrock (0.9% non-carbonate bedrock lithologies; Table 9.1). This may be due to the chemical weathering and concentration of insoluble lithologies within the clay size fraction. Alternatively, this accumulation of clay and silt-sized insoluble residue may represent the flocculation of glacially comminuted fines within the fluvial environment. Within low energy flow regimes, these non-carbonates may preferentially settle from suspension as carbonate grains are transported, or winnowed, further downstream. Both of these processes have been observed within a number of meltwater studies within the Mediterranean and elsewhere (Reynolds and Johnson, 1972; Nesbitt and Young, 1996; Woodward *et al.,* 2002; Tranter, 2003; Garzanti *et al*., 2008; 2009; 2010; von Eynattan *et al*., In Press) and will be discussed in more detail, in light of the sedimentary evidence from across the Orjen massif, within Chapter 9.

Figure 6.5 – Particle size distribution for Dvrsno polje, Transect 1 at <2 mm (inset graph) and <63 μm (main graph).

Facies Code	Height up profile (cm)	Unit/Facies Description	<2mm >63µm % non-carbonate (NC %)	<2mm >63µm % carbonate (C %)	<63µm % non-carbonate (NC %)	<63µm % carbonate (C %)
DVRSNO - TRANSECT 1						
Section D1						
D1a	0 - 50	Matrix	0.0%	92.8%	2.9%	4.2%
D1a	50 - 100	Matrix	0.2%	82.3%	2.8%	14.7%
	Section D1 mean matrix values		0.1%	87.6%	2.9%	9.5%
Section D2						
D2a	100.0 - 150.0	Matrix	0.1%	88.0%	6.9%	5.0%
D2a	150	Matrix	0.0%	90.0%	1.6%	8.3%
	Section D2 mean matrix values		0.0%	89.0%	4.3%	6.7%
Section D3						
D3a	100	**Matrix**	**0.1%**	**90.3%**	**3.3%**	**6.4%**
D3a	250 - 255	Sandy horizon	0.0%	89.8%	2.0%	8.1%
Section D4						
D4a	130	Clay clast coatings	1.0%	3.5%	20.0%	75.4%
D4a	150	**Matrix**	**0.9%**	**89.1%**	**4.7%**	**5.3%**
Section D5						
D5a-i	55 - 63	Medium sand horizon	0.4%	87.6%	2.0%	10.1%
D5a-i	106- 108	Medium sand horizon	0.2%	86.6%	2.9%	10.3%
D5a-i	150	**Matrix**	**0.1%**	**84.5%**	**5.2%**	**10.1%**
D5a-i	161 - 163	Medium-Coarse sand	0.1%	88.0%	5.0%	6.8%
D5a-i	272 - 276	Sand underlying clay	0.5%	81.8%	7.0%	10.8%
Section D6						
D6a-i	55 - 56	Sandy lenses	5.1%	84.2%	6.2%	4.5%
D6a-i	110 - 114	Matrix	0.3%	87.7%	3.5%	8.5%
D6a-i	140	Matrix	0.1%	83.7%	2.9%	13.3%
	Section D6 mean matrix values		0.2%	85.7%	3.2%	10.9%
Section D7						
D7a-i	44105	Fine sand	0.5%	53.1%	1.8%	44.6%
D7a-ii	20 - 35	Coarse sand	0.1%	91.4%	8.2%	0.3%
D7a-iii	35 - 39	Clayey silt	0.0%	4.4%	7.1%	88.6%
D7a-iv	39 - 41	Coarse sand	0.1%	87.3%	7.3%	5.3%
D7a-v	41 - 42	Silty clay	0.0%	13.9%	13.1%	73.0%
D7b	157 - 161	Sandy horizon	0.3%	81.0%	5.0%	13.7%
D7b	170	**Matrix**	**0.1%**	**94.0%**	**5.8%**	**0.1%**
D7b	204 - 212	Sandy horizon	0.1%	94.1%	5.4%	0.4%
D7b	246 - 250	Silty sand	0.6%	70.1%	9.3%	20.0%

Table 6.3 – Sediment sample data from Dvrsno polje Transect 1, east Orjen displayed as % non-carbonate (NC) and carbonate (C) of the bulk sediment by size fraction: <2 mm >63µm and <63 µm. Matrix samples used to generate mean particle size distribution of the <63 µm fraction and calcium carbonate content of the bulk sediment matrix are highlighted in bold.
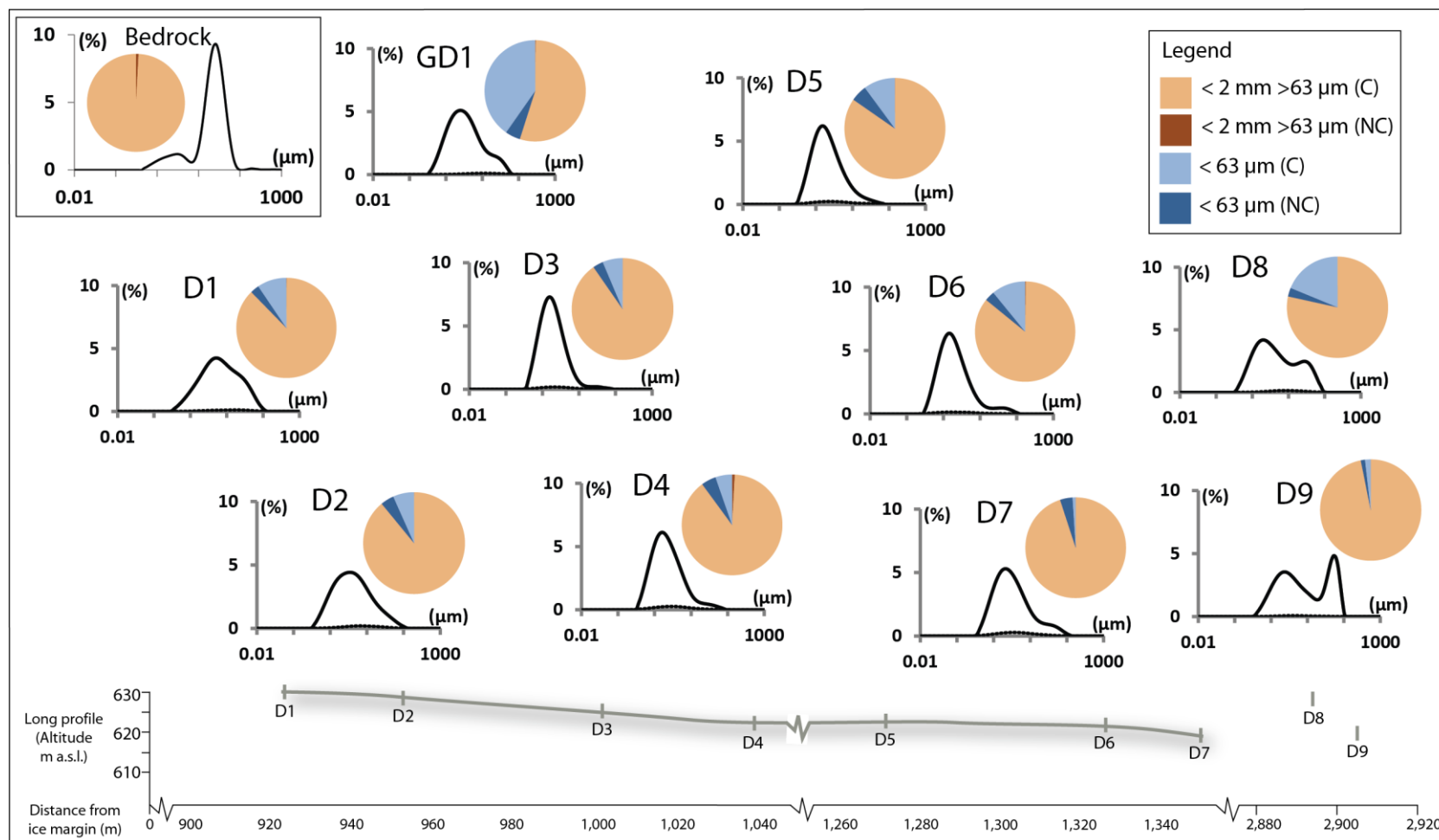
Figure 6.6 – Mean particle size distribution of the fine (<63 μm) sediment matrix and sediment lithological composition of the <2 mm matrix component at Dvrsno polje, Transects 1 and 2 east Orjen. Based on matrix samples emboldened in Tables 6.3 and 6.4. Glacial matrix PSA and clast lithology (sample GD1) data are displayed for comparative purposes. Bedrock samples represent the <2 mm fraction (Section 6.1).

Transect 2 (Sections D7 and D8) begins 2,900 m from the Pleistocene ice margin and displays a similar sedimentological record to the ice distal side of Transect 1 (Section D7 - 1, 350 m from the moraine; Fig. 6.5). The <2 mm PSD is highly variable (Fig. 6.7) and also closely resembles the PSD and insoluble residue contents of the distal sites of Transect 1 (Tables 6.3; 6.4). The fine matrix component (<63 μm) at Transect 2 displays a distinctly bimodal particle size distribution which is considerably more pronounced than Transect 1. This may reflect the variations in sediment transport pathways between Transect 1 (where sediment was delivered directly to the polje from the ice margin) and Transect 2 (which was fed via the bedrock gap at Han). Transect 2 is also situated further from the maximum ice margins than Transect 1 (950 m) and the greater transport distance may also explain the increased sediment sorting.
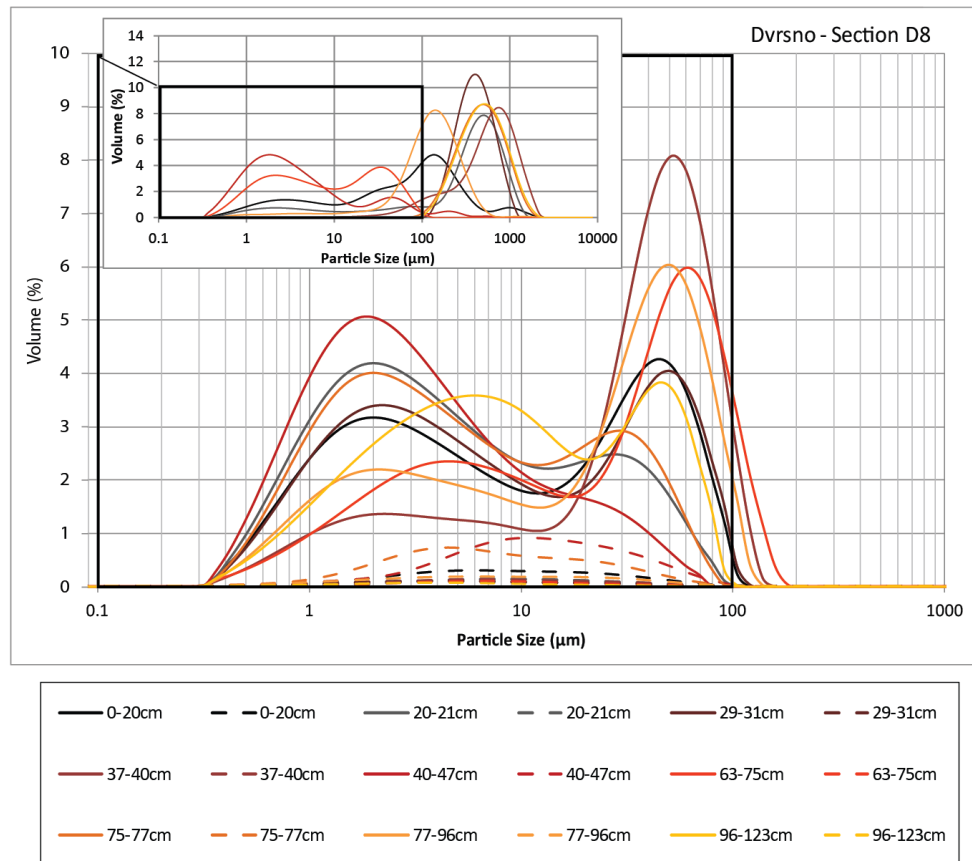
Figure 6.7 – Particle size distribution for Dvrsno polje, Transect 2 at <2 mm (inset graph) and <63 μm (main graph).

Clay horizons throughout both transects 1 and 2 contain a greater proportion of residual lithologies (Section D4, 20% and Section D8, 16.9%) than the matrix, silt or sand samples (Section D8, 14.6%) (Fig. 6.6). This may be due to the accumulation of higher density, non-carbonate fine sediments, derived from impure limestone or dolomite lithologies within the

catchment. Studies have indicated that higher density minerals can become concentrated into the finer silt and clay fractions due to preferential weathering from the host bedrock and settling from suspension (Nesbitt and Young, 1996; Woodward *et al.*, 2002; Garzanti *et al.*, 2008; 2009; 2010; Eynattan *et al.*, In Press). These similarities suggest that the 'ice distal' depositional environment at Dvrsno, characterised by the deposition and interstratification of fine sediments within a fully fluvial setting is attained at distances of c. 1, 300 m from the ice margin. The presence of gravel-rich horizons draped with clay coatings on clasts (Chapter 5) highlights the variable discharge regime of proglacial streams. Such environments can be characterised by both high-energy sediment-charged meltwater pulses as well as lower-energy conditions and the deposition of finer particles from suspension.

Facies Code	Height up profile (cm)	Unit/Facies Description	<2mm >63µm % non-carbonate (NC %)	<2mm >63µm % carbonate (C %)	<63µm % non-carbonate (NC %)	<63µm % carbonate (C %)
DVRSNO - TRANSECT 2						
Section D8						
D8a-i	0 - 20	Silt	0.1%	56.4%	6.8%	36.8%
D8a-i	20 - 21	**Matrix**	**0.0%**	**78.4%**	**2.8%**	**18.8%**
D8a-i	29 - 31	Medium sand	0.0%	93.6%	2.2%	4.2%
D8a-ii	37 - 40	Coarse sand	0.0%	86.4%	2.6%	11.0%
D8a-iii	40 - 47	Clay and sand	0.1%	16.2%	16.9%	66.8%
D8a-v	63 - 75	Cross stratified sands	0.1%	28.9%	14.6%	56.5%
D8a-vi	75 - 77	Clay and silt	0.0%	97.8%	2.0%	0.1%
D8a-vii	77 - 96	Silt	0.1%	66.7%	4.7%	28.5%
D8a-viii	96 - 123	Coarse sand	0.0%	98.0%	1.3%	0.7%
Section D9						
D9a-i	0 - 21	**Matrix**	**0.1%**	**96.8%**	**1.4%**	**1.8%**
D9a-vii	54 - 64	Silt and clay	0.1%	64.2%	2.4%	33.2%
D9a-viii	64 - 81	Medium-coarse sand	0.1%	97.1%	0.9%	1.9%
D9a-ix	82 - 95	Interstratified sands/silts	0.1%	68.5%	4.1%	27.3%
D9a-xii	117 - 141	Medium-coarse sand	0.0%	97.9%	1.5%	0.6%
D9a-xiii	141 - 144	Fine sand and silt	0.1%	82.5%	2.4%	15.1%

Table 6.4 – Sediment sample data from Dvrsno polje Transect 2, east Orjen displayed as % non-carbonate (NC) and carbonate (C) of the bulk sediment by size fraction: <2 mm >63µm and <63 µm.

6.5   Kruševice

The PSD data at Kruševice (Fig. 6.1) are comparable to the particle size characteristics of the ice distal side of Dvrsno polje, east Orjen (c. 1,300 m from the MIS 12 ice margin). The <2 mm PSD of the sediment matrix at Kruševice is broadly unimodal and is dominated by sands and granules (Fig. 6.8). Bulk matrix samples typically contain less than 8% of the <63 µm size

fraction (Table 6.5) which is lower than that observed at Dvrsno and more closely resembles the coarser sediment characteristics at Grahovo polje (Section 6.8).

As observed at Grahovo and Dvrsno, the non-carbonate lithologies are concentrated in the finer silt and clay horizons (<63 μm) which contain up to 45.7% insoluble residue (Table 6.5; Fig. 6.9). These values are an order of magnitude higher than the mean non-carbonate content of the bulk matrix at Kruševice (4.3% at Section Kr1 and 2.3% at Section Kr2). This may reflect the presence of dolomite and other non-limestone lithologies high within the glacier source area and the continual comminution of these less pure carbonates during transportation to the lower elevation poljes. This mineralogical pattern is seen within a number of fluvial environments across Orjen, and may indicate the chemical and/or mechanical concentration of non-limestone lithologies within the <63 μm size fraction (Nesbitt and Young, 1996; Woodward *et al*., 2002; Garzanti *et al*., 2008; 2009; 2010).
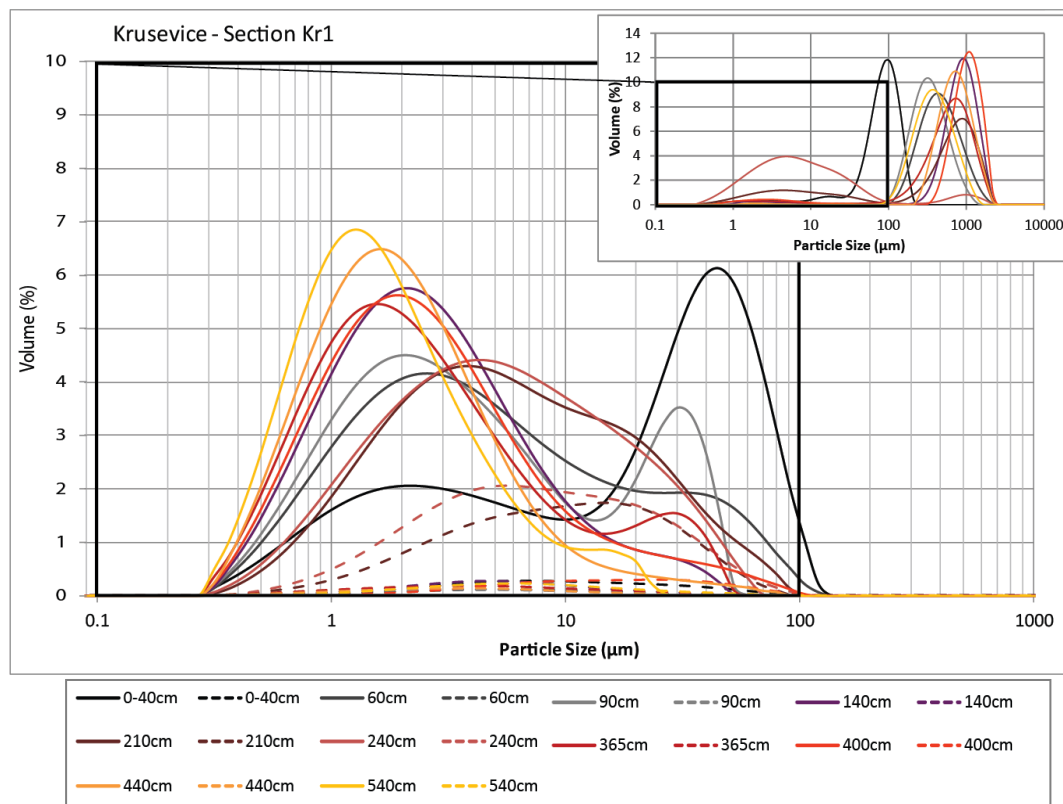
Figure 6.8 - Particle size distribution for Kruševice polje, southwest Orjen at <2 mm (inset graph) and <63 μm (main graph).

Figure 6.9 – Mean particle size distribution of the fine (<63 μm) sediment matrix and sediment lithological composition of the <2 mm matrix component at Kruševice polje, southwest Orjen. Based on matrix samples emboldened in Table 6.5. Bedrock samples represent the <2 mm fraction (Section 6.1).

Facies Code	Height up profile (cm)	Unit/Facies Description	<2mm >63μm % non-carbonate (NC %)	<2mm >63μm % carbonate (C %)	<63μm % non-carbonate (NC %)	<63μm % carbonate (C %)
			KRUŠEVICE			
			Section Kr1			
Kr1a-ii	0-40	Silty sand	0.2%	49.0%	5.6%	45.1%
Kr1a-iii	60	Matrix	0.1%	95.1%	2.3%	2.6%
Kr1a-iii	90	Medium sand	0.1%	95.6%	2.9%	1.4%
Kr1a-iv	140	Matrix	0.1%	93.4%	4.6%	2.0%
Kr1a-iv	210	Silty lens	0.2%	55.5%	36.5%	7.8%
Kr1a-iv	240	Silty lens	0.3%	37.9%	45.7%	16.1%
Kr1a-v	365	Sand lens	0.1%	87.8%	4.2%	7.9%
Kr1a-v	400	Matrix	0.0%	88.3%	6.1%	5.6%
Kr1a-v	440	Sand lens	0.1%	93.3%	2.9%	3.7%
Kr1a-v	540	Sand lens	0.0%	93.0%	4.4%	2.5%
		Section Kr1 mean matrix values	**0.1%**	**92.2%**	**4.3%**	**3.4%**
			Section Kr2			
Kr2a-i	60	Matrix	0.0%	92.4%	2.5%	5.0%
Kr2a-ii	124-129	Sandy horizon	0.1%	90.2%	3.8%	5.8%
Kr2a-ii	141-145	Medium sand horizon	0.1%	46.6%	10.5%	42.9%
Kr2a-ii	167-171	Medium sand horizon	0.1%	79.6%	7.0%	13.3%
Kr2a-ii	181-184.5	Medium sand horizon	0.1%	79.9%	5.1%	14.9%
Kr2a-ii	250	Matrix	0.1%	92.8%	2.1%	5.0%
Kr2a-ii	310	Matrix	0.0%	91.8%	2.1%	6.1%
		Section Kr2 mean matrix values	**0.0%**	**92.3%**	**2.3%**	**5.4%**

Table 6.5 - Sediment sample data from Kruševice polje, southwest Orjen displayed as % non-carbonate (NC) and carbonate (C) of the bulk sediment by size fraction: <2 mm >63μm and <63 μm. Matrix samples used to generate mean particle size distribution of the <63 μm fraction and calcium carbonate content of the bulk sediment matrix are highlighted in bold.

6.6   Vrbanje

Vrbanje polje is situated to the north of Kruševice (Fig. 6.1) and forms one of a series of partially coalescing karstic depressions. The MIS 12 ice margins here terminated within the north eastern margin of the polje and the sampled exposures are situated c. 1,400 m from MIS 12 moraine. Both the <2 mm and mean <63 μm particle size distributions of the sediment matrix are broadly unimodal and contain up to 36% silts and clays (Fig. 6.10; Fig. 6.11). In comparison to other polje sites, bulk matrix samples at Vrbanje contain elevated concentrations of non-carbonate lithologies (up to 15.1%) (Table 6.6). These are concentrated into the <63 μm sediment fraction and may reflect the outcrop of dolomite close to the ice terminus (Chapter 3) and the preferential accumulation and/or deposition of these non-carbonate lithologies within the low energy fluvial environment (Nesbitt and Young, 1996; Woodward *et al.,* 2002; Garzanti *et al*., 2008; 2009; 2010).

Facies Code	Height up profile (cm)	Unit/Facies Description	<2mm >63μm % non-carbonate (NC %)	<2mm >63μm % carbonate (C %)	<63μm % non-carbonate (NC %)	<63μm % carbonate (C %)
			VRBANJE			
			Section V1			
V1a-iii	67	Sandy horizon	0.7%	87.4%	6.9%	5.0%
V1a-iv	110	Sand lens	0.0%	87.5%	7.5%	5.0%
			Section V2			
V2a	50	**Matrix**	**0.0%**	**64.0%**	**15.1%**	**20.8%**
			Section V3			
V3a-i	90	Matrix	0.1%	87.4%	12.5%	0.1%
V3a-ii	330	Matrix	0.0%	84.7%	6.2%	9.1%
	Section V3 mean matrix values		**0.0%**	**86.0%**	**9.3%**	**4.6%**
			Section V4			
V4a-i	0-40	Matrix	0.0%	84.2%	3.4%	12.4%
V4a-ii	40-63	Matrix	0.0%	85.3%	3.8%	10.8%
V4a-ii	63-92	Matrix	0.0%	90.7%	3.6%	5.6%
V4a-iv	92-130	Matrix	0.0%	96.2%	1.8%	2.0%
V4a-v	130-192	Matrix	0.0%	77.6%	7.2%	15.2%
	Section V4 mean matrix values		**0.0%**	**86.8%**	**4.0%**	**9.2%**

Table 6.6 - Sediment sample data from Vrbanje polje, west Orjen displayed as % non-carbonate (NC) and carbonate (C) of the bulk sediment by size fraction: <2 mm >63μm and <63 μm. Matrix samples used to generate mean particle size distribution of the <63 μm fraction and calcium carbonate content of the bulk sediment matrix are highlighted in bold.
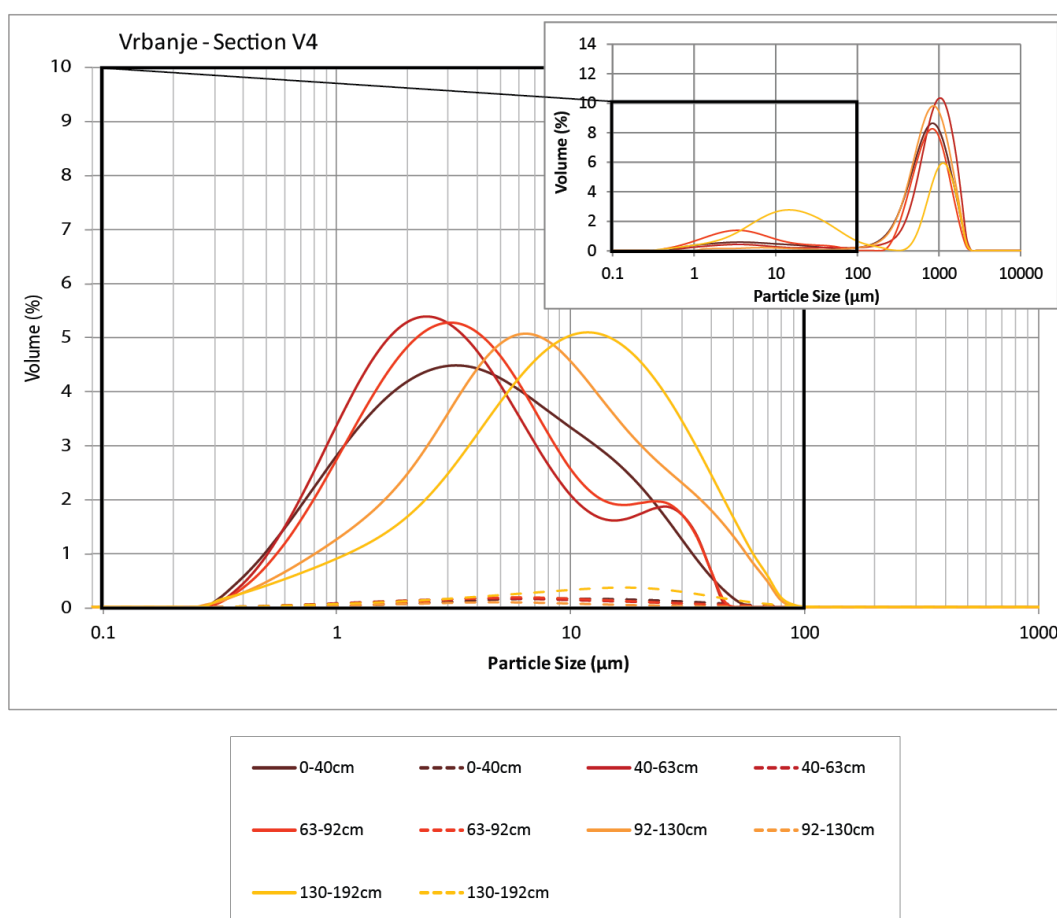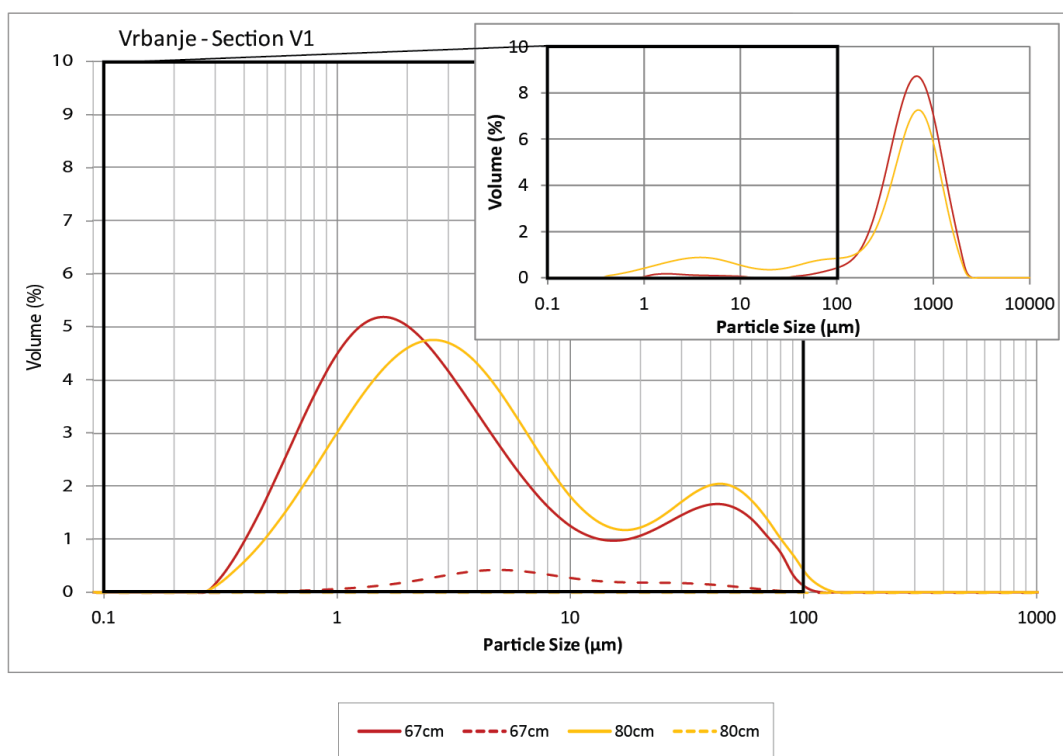
Figure 6.10 - Particle size distribution for Vrbanje polje, western Orjen at <2 mm (inset graph) and <63 μm (main graph).
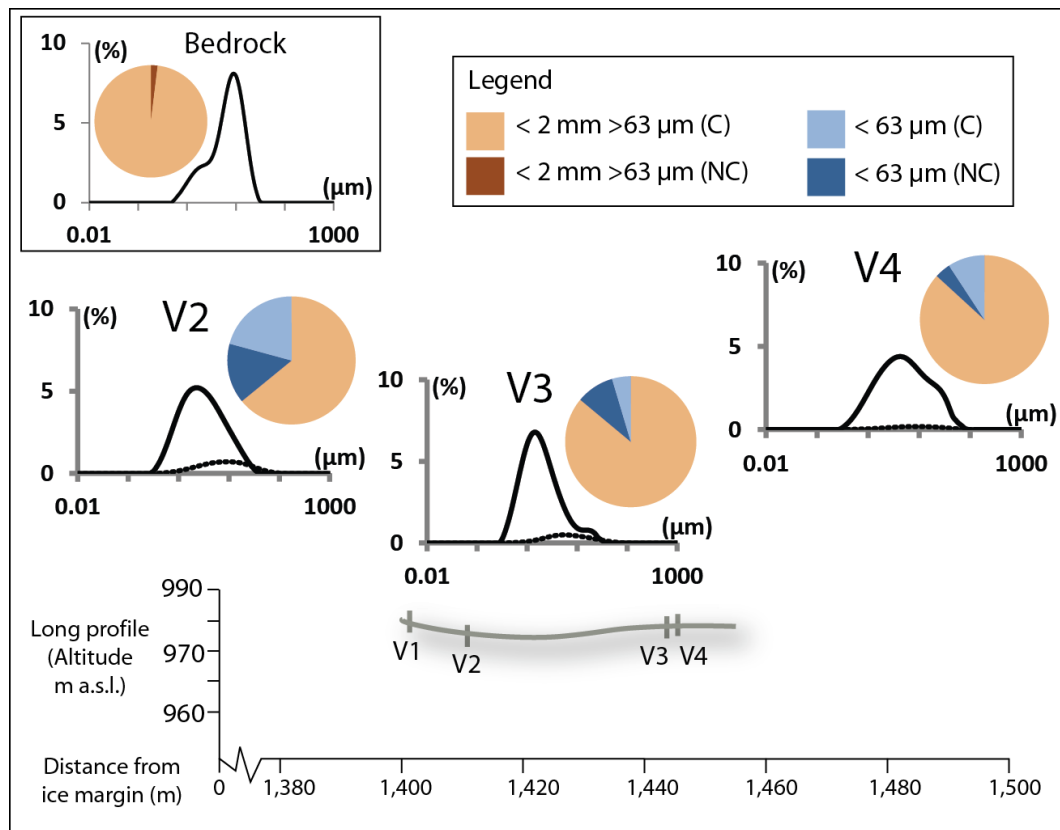
Figure 6.11 – Mean particle size distribution of the fine (<63 μm) sediment matrix and sediment lithological composition of the <2 mm matrix component at Vrbanje, west Orjen. Based on matrix samples emboldened in Table 6.6. Bedrock samples represent the <2 mm fraction (Section 6.1).

6.7   Pirina Poljana

Sediment samples from both within (Section P1) and outside (Sections P2 and P3) the former MIS 12 ice margins have been analysed at Pirina Poljana (Table 6.7). Sediment matrix samples at Section P1, 1,500 m upstream of the MIS 12 moraines, are dominated by coarse sands and granules with a subordinate silt and clay (<63 μm) component (typically less than 10% of the bulk matrix) (Table 6.7; Fig. 6.12; 6.13). Residual lithologies contribute less than 1.5% of the bulk sediment matrix and are concentrated into the <63 μm fraction. These lithologies may originate from the dolomite bedrock underlying a large portion of the source area of this outlet glacier (Chapter 3). Sections P2 and P3 are situated c. 4,300 m from the MIS 12 moraines and display a strong, unimodal PSD dominated by coarse sands and granules with only a limited <63 μm component, which is also normally distributed. In this part of the polje, the <63 μm fraction consists of <5% insoluble residue (Table 6.7; Fig 6.12). This concentration of non-limestone lithologies within the fine sediments is observed within the other polje

environments across Orjen, and may be indicative of the chemical dissolution or density settling of non-carbonate lithologies from an otherwise limestone-rich meltwater environment (Nesbitt and Young, 1996; Woodward *et al.*, 2002; Garzanti *et al.*, 2008; 2009; 2010).

Facies Code	Height up profile (cm)	Unit/Facies Description	<2mm >63µm % non-carbonate (NC %)	<2mm >63µm % carbonate (C %)	<63µm % non-carbonate (NC %)	<63µm % carbonate (C %)
			PIRINA POLJANA			
			Section P1			
P1a-i	0-11	Coarse sand	0.1%	86.8%	1.7%	11.5%
P1a-ii	11-12	Sand and silt	0.1%	71.5%	4.1%	24.3%
P1a-iv	16-27	Interstratified silt	0.1%	28.2%	10.8%	61.0%
P1b	27-54	Matrix	0.1%	94.4%	1.2%	4.3%
P1c	54-104	Matrix	0.1%	85.1%	1.4%	13.4%
Section P1 mean matrix values			**0.1%**	**89.7%**	**1.3%**	**8.9%**
			Section P2			
P2a	80	Matrix	0.0%	91.6%	2.1%	6.3%
P2a	200	Matrix	0.1%	96.2%	1.9%	1.8%
P2b	220	Matrix	0.1%	90.7%	1.8%	7.4%
Section P2 mean matrix values			**0.1%**	**92.9%**	**1.9%**	**5.2%**
			Section P3			
P3a	120	Sand lens	0.0%	88.0%	3.6%	8.4%
P3a	120	**Matrix**	**0.1%**	**92.1%**	**2.5%**	**5.4%**
P3a	163	Silt	0.1%	50.3%	4.4%	45.1%
P3a	286-290	Sand	0.1%	92.6%	1.4%	6.0%

Table 6.7 - Sediment sample data from Pirina Poljana polje, northwest Orjen displayed as % non-carbonate (NC) and carbonate (C) of the bulk sediment by size fraction: <2 mm >63µm and <63 µm. Matrix samples used to generate mean particle size distribution of the <63 µm fraction and calcium carbonate content of the bulk sediment matrix are highlighted in bold.
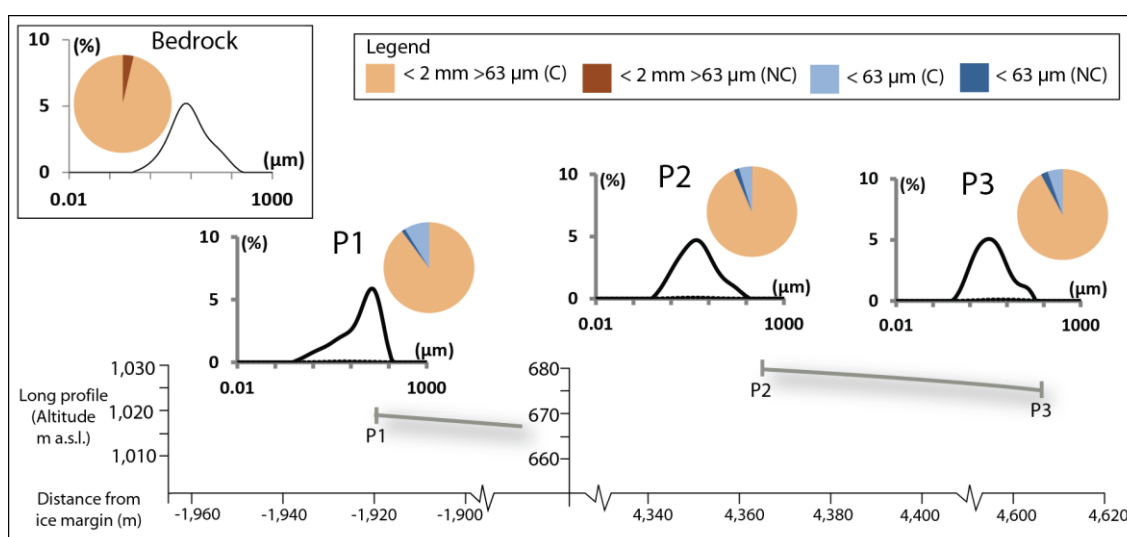
Figure 6.12 – Mean particle size distribution of the fine (<63 µm) sediment matrix and sediment lithological composition of the <2 mm matrix component at Pirina Poljana polje, northwest Orjen. Based on matrix samples emboldened in Table 6.7. Bedrock samples represent the <2 mm fraction (Section 6.1).
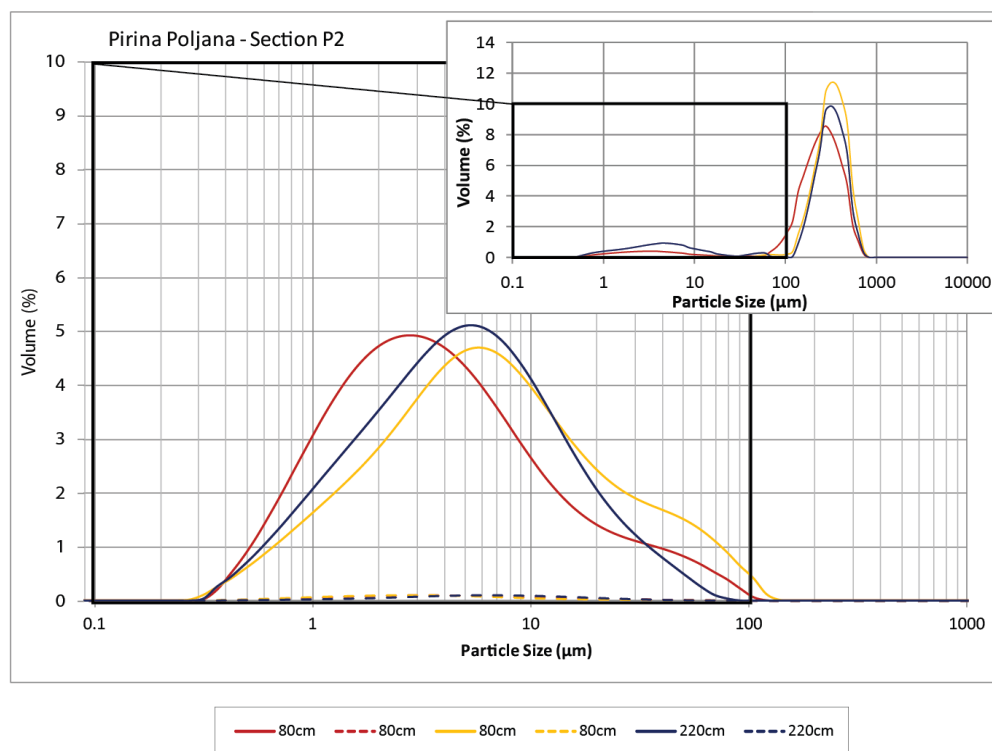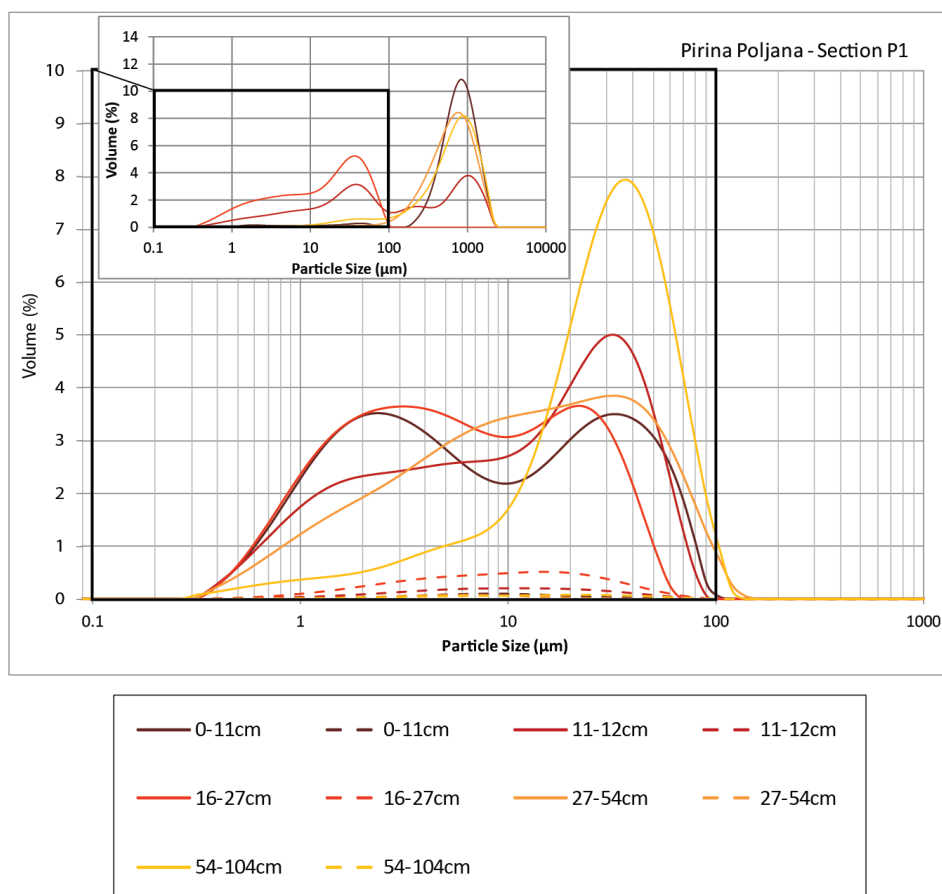
Figure 6.13 - Particle size distribution for Pirina Poljana polje, northwest Orjen at <2 mm (inset graph) and <63 μm (main graph).

6.8   Grahovo

Grahovo polje, on the north eastern side of the Orjen massif, is situated 1,400 m outside the maximum Pleistocene ice margins of MIS 12. At sections G1 and G2 the <2 mm PSD of the sediment matrix is bimodal and the sequence is dominated by coarser (sand and granule) material (Fig. 6.14). The <63 µm fraction typically contributes below 7% of the bulk sediment matrix (Table 6.8) and is strongly unimodally distributed (Fig. 6.14). Non-carbonate lithologies are limited in abundance within Grahovo polje, which may indicate the dominance of dolomite and purer limestone within the catchment (Chapter 3). As observed at Dvrsno (Section 6.4), silt coatings on clast surfaces contain the greatest proportion of non-carbonate material at Grahovo (5.9%), whilst matrix samples typically contain <2% insoluble residue (Table 6.8, Fig. 6.15). This supports the evidence from elsewhere surrounding Mount Orjen that suggests that these sediments may reflect the preferential accumulation of non-limestone clays (Section 6.4).

Facies Code	Height up profile (cm)	Unit/Facies Description	<2mm >63µm % non-carbonate (NC %)	<2mm >63µm % carbonate (C %)	<63µm % non-carbonate (NC %)	<63µm % carbonate (C %)
GRAHOVO						
Section G1						
G1a-i	50	Matrix	0.0%	92.6%	4.9%	2.6%
G1a-i	60 - 70	Silt coatings on clasts	0.0%	20.1%	5.9%	74.0%
G1a-i	70 - 83	Matrix	0.0%	94.2%	0.9%	4.9%
G1a-ii	87 - 100	Matrix	0.0%	94.9%	0.2%	4.8%
G1a-ii	160	Matrix	0.0%	94.4%	1.3%	4.2%
G1a-ii	216	Matrix	0.0%	93.1%	2.8%	4.1%
G1a-iii	240	Matrix	0.0%	91.0%	1.5%	7.5%
G1a-iii	260 - 350	Matrix	0.1%	93.2%	1.9%	4.8%
Section G1 mean matrix values			0.0%	93.3%	1.9%	4.7%
Section G2						
G2a	20.0 - 30.0	**Matrix**	**0.0%**	**95.6%**	**1.0%**	**3.4%**

Table 6.8 – Sediment sample data from Grahovo polje, northeast Orjen displayed as % non-carbonate (NC) and carbonate (C) of the bulk sediment by size fraction: <2 mm >63µm and <63 µm. Matrix samples used to generate mean particle size distribution of the <63 µm fraction and calcium carbonate content of the bulk sediment matrix are highlighted in bold.
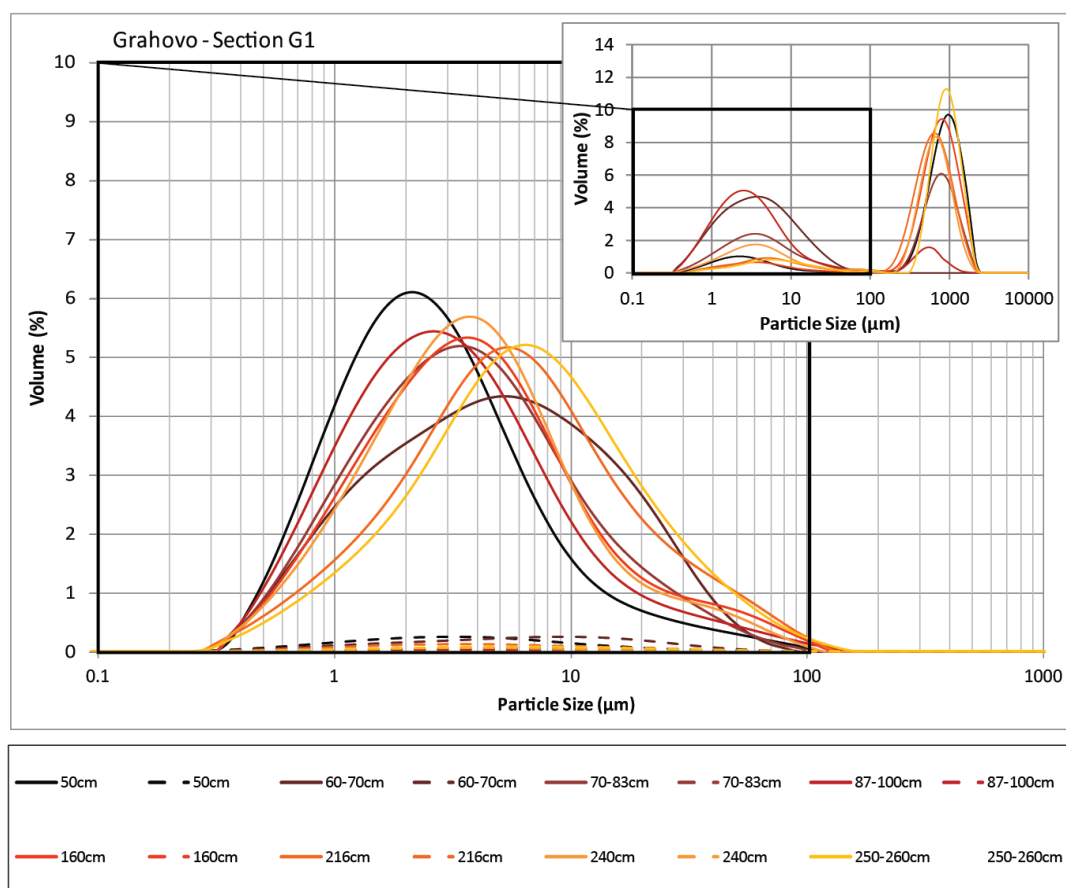
Figure 6.14 – Particle size distribution for Grahovo polje, northeast Orjen at <2 mm (inset graph) and <63 µm (main graph).
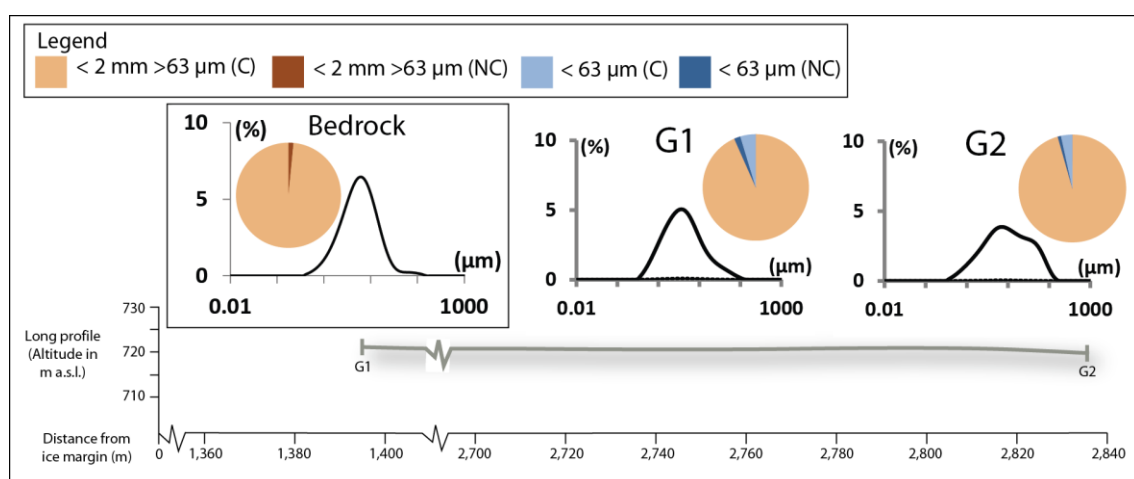
Figure 6.15 – Mean particle size distribution of the fine (<63 µm) sediment matrix and sediment lithological composition of the <2 mm matrix component at Grahovo polje, north east Orjen. Based on matrix samples emboldened in Table 6.8. Bedrock samples represent the <2 mm fraction (Section 6.1).

6.9 Lipci

The strongly cemented nature of the fan sediments at Lipci meant that it was not possible to collect unconsolidated matrix samples at this site. In many instances, the calcite has entirely replaced the fine matrix component, leaving only open framework gravels cemented by sparitic calcite crystals (Chapter 5.8).

6.10 Kameno

Sediment samples have been obtained from a transect of exposures at Kameno (Fig. 6.1) extending down-fan from c. 150 to 1,000 m from the MIS 12 moraines. Particle size data display a clear progression from ice proximal to ice distal depositional environments (Fig. 6.16; Fig. 6.17). Matrix samples from Section K1, closest to the ice margin, show a strong unimodal PSD within both the <2 mm (dominantly coarse sand and granules) and <63 μm (dominantly silt) fractions (Fig. 6.17). Further down fan (Section K2) the fine sediment component becomes dominated by clays and very fine silts (1 to 4 μm) with only negligible contributions of non-carbonate lithologies (less than 3.6%) (Table 6.9). The central, or 'ice medial', portion of the fan at Section K4 contains a greater concentration of these non-carbonate lithologies within the sand fraction of the sediment matrix (up to 1% of the bulk matrix sample) compared with the negligible (0.1%) concentrations observed elsewhere across the fan. This distribution is also evident within the matrix samples at Dvrsno polje, northeast Orjen, which contain an increase in sand-sized insoluble residue within the central portion of the polje. This spatial pattern in the concentration of non-carbonate lithologies may be indicative of the changing depositional environments with distance down-fan/down-polje, and the preferential accumulation of non-carbonate lithologies within the fluvial environment and their deposition as the meltwater streams lose competence (Nesbitt and Young, 1996; Garzanti *et al*., 2008; 2009; 2010).

The fine sediment matrix samples of the ice distal deposits, such as at Section K8, display a weak bimodal distribution (Fig. 6.17). Despite the overall down fan sediment fining, the clay content of the matrix remains elevated throughout the transect and may reflect the high inputs of glacigenic clays due to the proximity of the fan to the glacier front. At this site, non-

carbonate lithologies (Table 6.9; Fig. 6.17) contribute 12.7% of the sediment matrix and 22.1% of the clay horizons, but only 0.4% of the bedrock (Table 6.1; Fig. 6.17). The insoluble residue is thought to originate from an area of flysch bedrock, mapped by the Institute for Geological and Geophysical Research, Belgrade (1969), close to the terminal reaches of the outlet glacier (Chapter 3). Non-carbonate lithologies are particularly concentrated in the <63 µm fraction of the most distal exposure (K8, 1,040 m from the ice margin; Table 6.9). This supports the particle size evidence from elsewhere within the fluvial settings surrounding Mount Orjen and suggests that these non-limestone lithologies become concentrated within the sediment matrix with distance downvalley. At this site, this may suggest that the accumulation of non-carbonate minerals, possibly due to density settling and or/flocculation of non-limestone clays within the low energy fluvial environment occurs at distances of over 1 km from the ice margin.

Facies Code	Height up profile (cm)	Unit/Facies Description	<2mm >63µm % non-carbonate (NC %)	<2mm >63µm % carbonate (C %)	<63µm % non-carbonate (NC %)	<63µm % carbonate (C %)
KAMENO						
Section K1						
K1a	35 - 39	Sand pocket	0.1%	81.9%	5.9%	12.1%
K1a	100	**Matrix**	**0.1%**	**78.9%**	**6.1%**	**14.9%**
Section K2						
K2a	60	Matrix - Granular horizon	0.0%	89.2%	3.4%	7.5%
K2a	71-120	Matrix - pebble horizon	0.1%	80.0%	3.5%	16.4%
K2a	150	Matrix	0.0%	83.2%	1.8%	15.0%
Section K2 mean matrix values			**0.0%**	**84.1%**	**2.9%**	**12.9%**
Section K4						
K4a	75 - 88	Fine sand lens	0.0%	68.1%	6.3%	25.5%
K4a	120	**Matrix**	**1.0%**	**77.0%**	**1.2%**	**20.9%**
Section K7						
K7a-i	100	**Matrix**	**0.1%**	**88.2%**	**1.8%**	**9.9%**
K7a-i	189-199	Fine sand lens	0.1%	77.8%	3.7%	18.4%
K7a-ii	230-246	Medium sand horizon	0.1%	64.8%	5.7%	29.4%
Section K8						
K8a-i	0-14	Coarse sand and granules	0.1%	94.0%	1.6%	4.3%
K8a-ii	14-26	Clays and silts	0.2%	46.7%	6.8%	46.3%
K8a-iii	26-52	Matrix	0.1%	86.1%	2.5%	11.3%
K8a-vi	64-67	Clayey silt	0.2%	44.8%	22.1%	32.8%
K8a-vii	67-85	Matrix	0.2%	94.1%	1.3%	4.4%
K8a-viii	85-100	Interstratified sands	0.2%	63.6%	6.0%	30.3%
K8b	100-190	Matrix	0.0%	70.9%	12.7%	16.4%
K8c	190-390	Matrix	0.1%	79.0%	4.3%	16.6%
Section K8 mean matrix values			**0.1%**	**82.5%**	**5.2%**	**12.2%**

Table 6.9 - Sediment sample data from Kameno alluvial fan, south Orjen displayed as % non-carbonate (NC) and carbonate (C) of the bulk sediment by size fraction: <2 mm >63µm and <63 µm. Matrix samples used to generate mean particle size distribution of the <63 µm fraction and calcium carbonate content of the bulk sediment matrix are highlighted in bold.
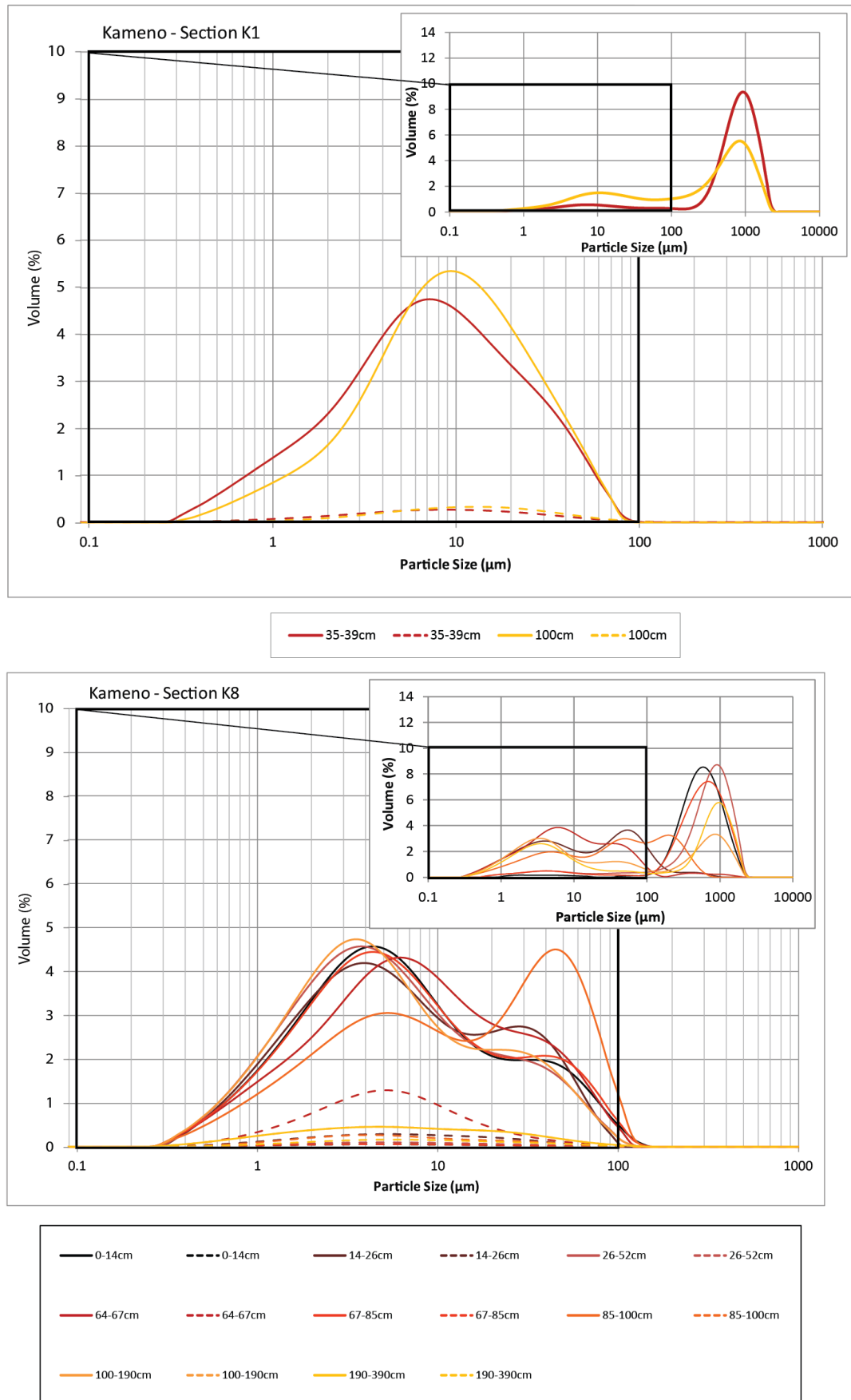
Figure 6.16 – Particle size distribution for Kameno alluvial fan, south Orjen at <2 mm (inset graph) and <63 μm (main graph).
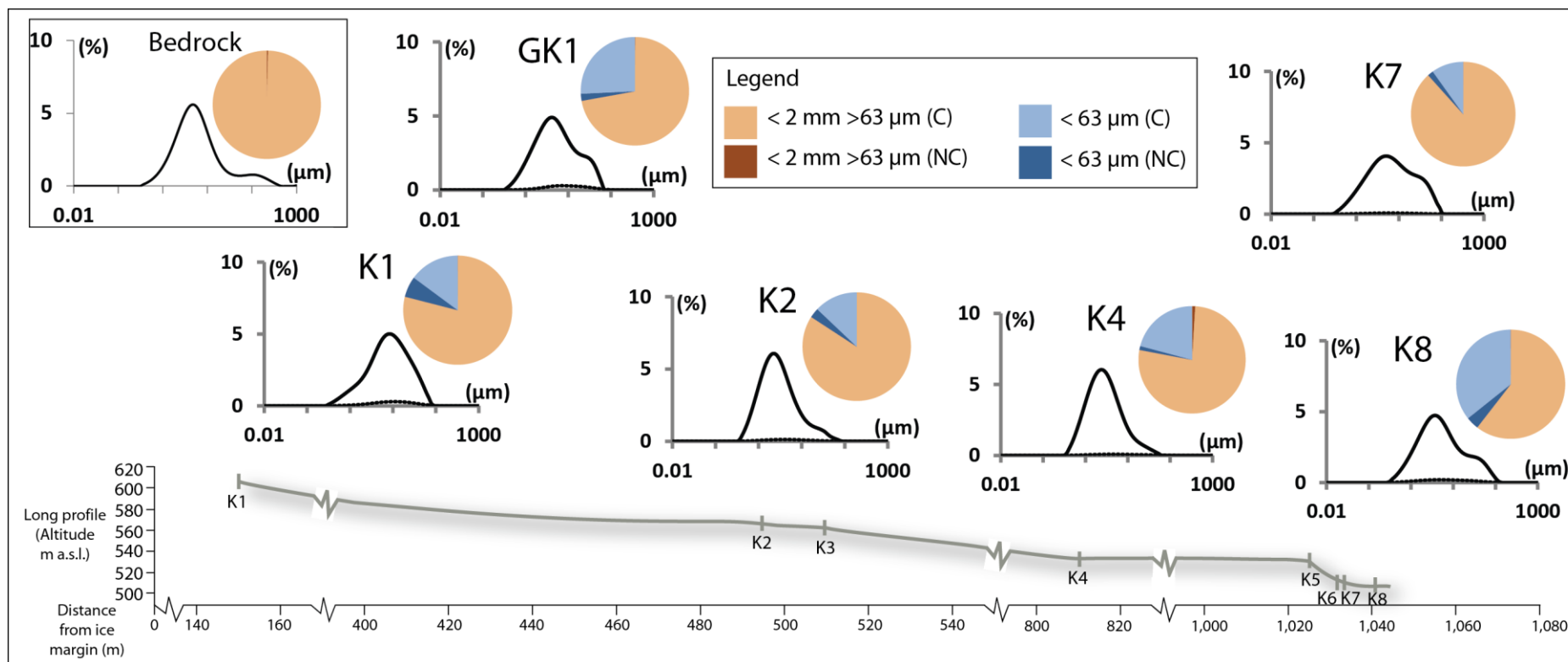
Fig. 6.17 – Mean particle size distribution of the fine (<63 μm) sediment matrix and sediment lithological composition of the <2 mm matrix component at Kameno alluvial fan, southwest Orjen. Based on matrix samples emboldened in Table 6.9. Glacial matrix PSA and clast lithology (sample GK1) data are displayed for comparative purposes. Bedrock samples represent the <2 mm fraction (Section 6.1).

6.11   Nudo

A sequence of five terrace units has been identified and sampled within the Nudo valley (Fig. 6.1). Particle size data of the <2 mm sediment matrix indicate a weak bimodal distribution (Fig. 6.18) with dominant inputs of coarse sand to granules (200 to 2,000 μm) and silts to fine sands (1 to 100 μm). The <63 μm fraction typically contributes below 20% of the bulk matrix sediment (Table 6.10); and contains a broadly unimodal PSD (Fig. 6.19).

Facies Code	Height up profile (cm)	Unit/Facies Description	<2mm >63μm % non-carbonate (NC %)	<2mm >63μm % carbonate (C %)	<63μm % non-carbonate (NC %)	<63μm % carbonate (C %)
NUDO						
Arandelovo Unit						
AN1a	50	Matrix	0.1%	84.3%	2.2%	13.4%
AN1a	100	Matrix	0.1%	75.4%	2.1%	22.5%
AN2a	30	Matrix	0.1%	87.2%	1.7%	11.1%
AN2a	60	Matrix	0.1%	54.4%	6.1%	39.4%
AN2a	150	Matrix	0.1%	82.2%	2.7%	14.9%
AN2a	490	Matrix	0.1%	82.4%	1.8%	15.7%
AN2a	705	Matrix	0.1%	85.0%	1.1%	13.8%
AN2a - not logged		Matrix - not logged	0.0%	80.8%	1.5%	17.6%
Section AN mean matrix values			**0.1%**	**79.0%**	**2.4%**	**18.5%**
Vućiya Unit						
VN1a	100	**Matrix**	**0.0%**	**84.8%**	**1.6%**	**13.5%**
Kamiseyo Unit						
KN1a	400	**Matrix**	**0.1%**	**79.2%**	**2.2%**	**18.4%**
Javora Unit						
JN1a	220	**Matrix**	**0.1%**	**89.2%**	**0.9%**	**9.8%**
Zaslap Unit						
ZN1a	100-120	Matrix	0.1%	91.4%	1.0%	7.4%
ZN1a - correlated		Matrix	0.0%	94.4%	1.7%	3.9%
ZN2a	170	Matrix granular horizon	0.0%	81.5%	2.5%	16.0%
Section ZN1 and ZN2 mean matrix values			**0.1%**	**89.1%**	**1.7%**	**9.1%**
Zaslap Unit - Tributary						
ZN3a	80	**Matrix**	**2.6%**	**78.6%**	**17.9%**	**0.9%**

Table 6.10 - Sediment sample data from terrace units of the Nudo valley, north Orjen displayed as % non-carbonate (NC) and carbonate (C) of the bulk sediment by size fraction: <2 mm >63μm and <63 μm. Matrix samples used to generate mean particle size distribution of the <63 μm fraction and calcium carbonate content of the bulk sediment matrix are highlighted in bold.

The bimodal distribution of the <63 μm fraction observed within the polje and alluvial fan settings is not evident at Nudo. This may reflect the type of Pleistocene meltwater pathway here, where surface runoff and sediments would have been delivered via a steep sided limestone gorge. This high energy environment may have been less conducive to the sorting

and deposition of fine sediments that is observed within the lower gradient, and lower energy, poljes and alluvial fan settings. Samples at Nudo do, however, display a concentration of non-limestone lithologies within the <63 µm size fraction (Table 6.10), that is evident elsewhere.

Sediments within the tributary exposure to the north of the Nudo valley (R. Jenkov; Section ZN3a) contain over 20% insoluble residue. Unlike many other sedimentary sequences across Orjen, this is present both within the <63 µm and <2 mm size fractions (Table 6.10; Fig. 6.19). The elevated values of non-carbonate lithologies within the tributary sediments (ZN3a) may reflect a localised source of non-carbonate or impure limestone lithologies on the northern valley flanks. The occurrence of sand-sized, insoluble residue (2.6% of the bulk matrix sample) may be indicative of the short transportation distances of this tributary, and the settling of residual material, from the steep valley sides.
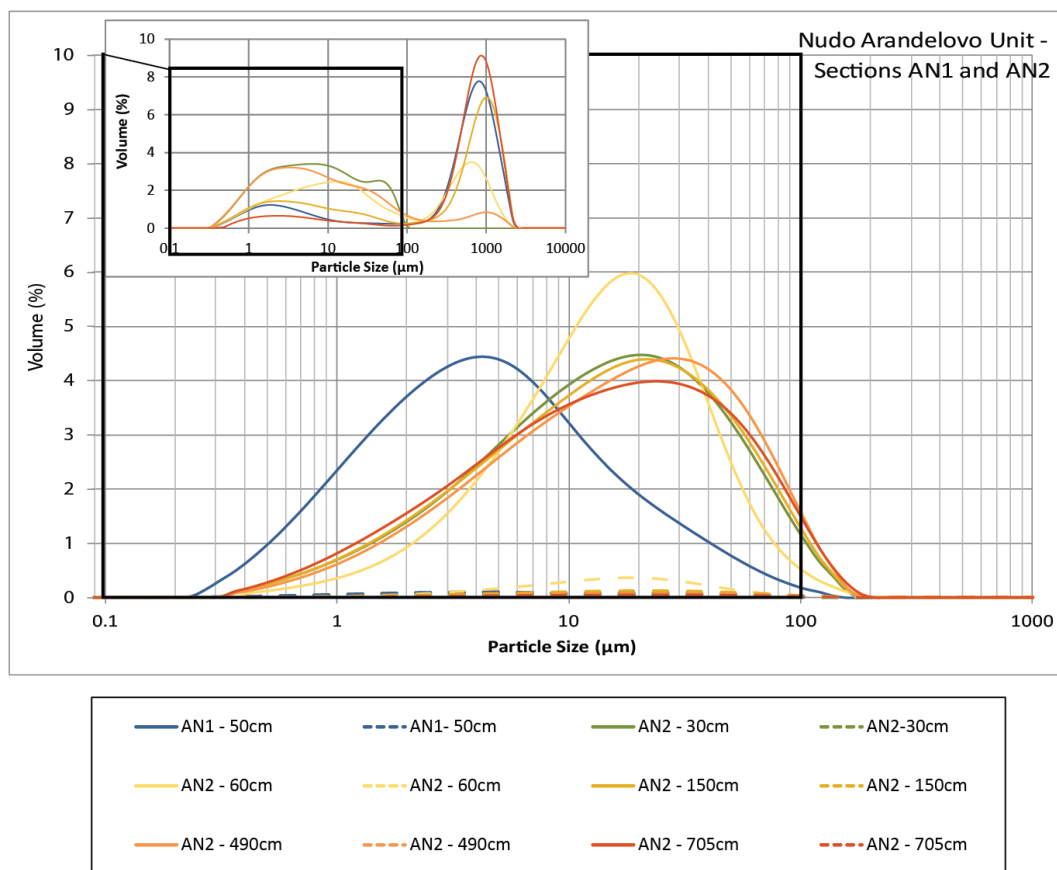
Figure 6.18 – Particle size distribution for terrace units of the Nudo valley, north Orjen at <2 mm (inset graph) and <63 µm (main graph).
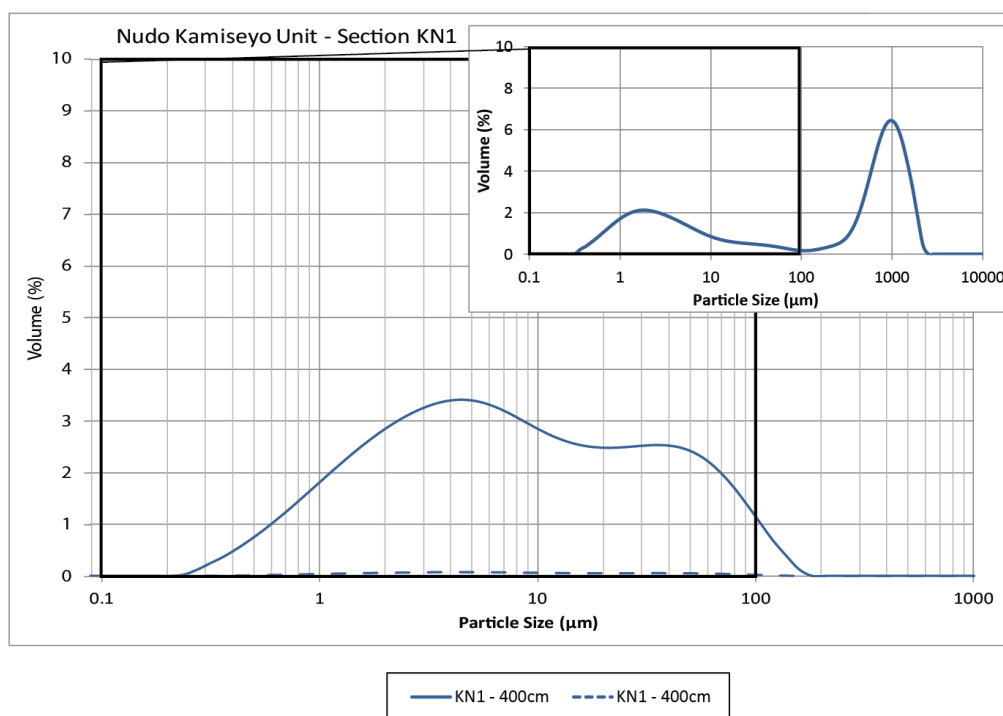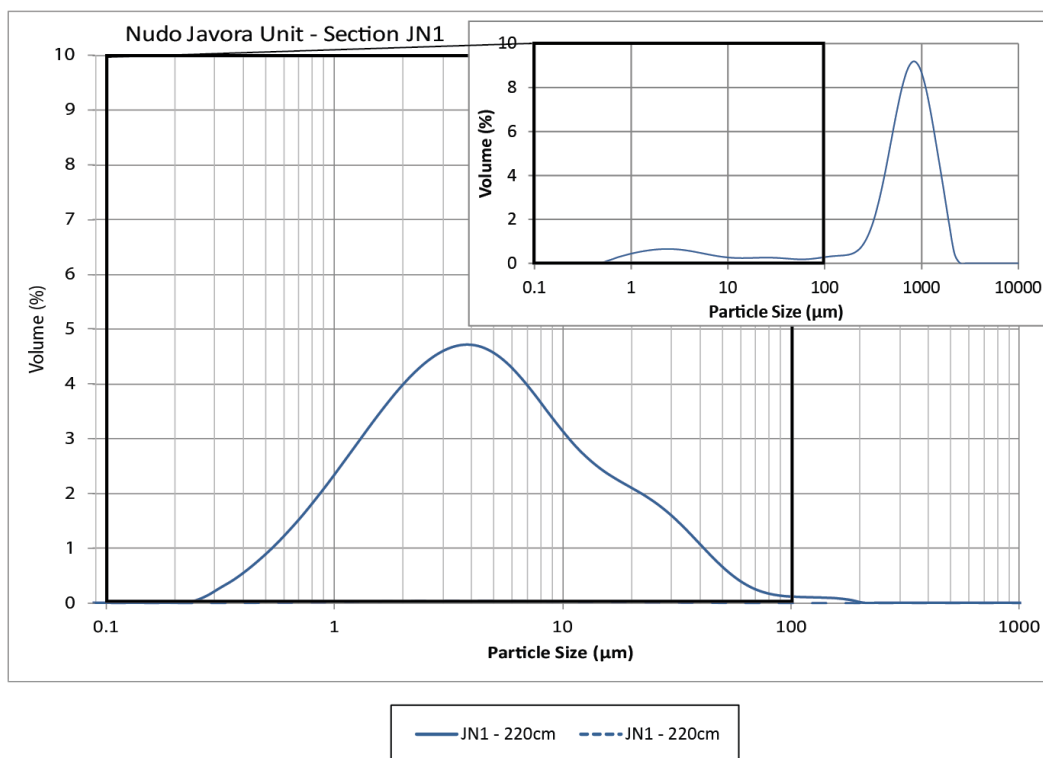
Figure 6.18 continued – Particle size distribution for terrace units of the Nudo valley, north Orjen at <2 mm (inset graph) and <63 µm (main graph).
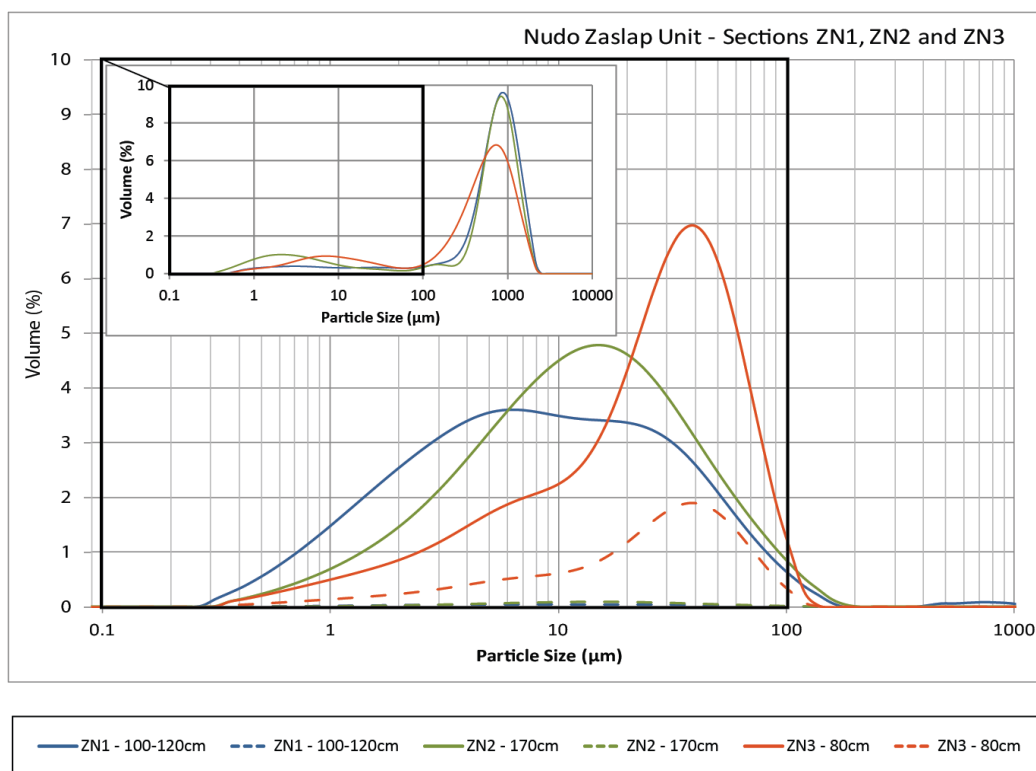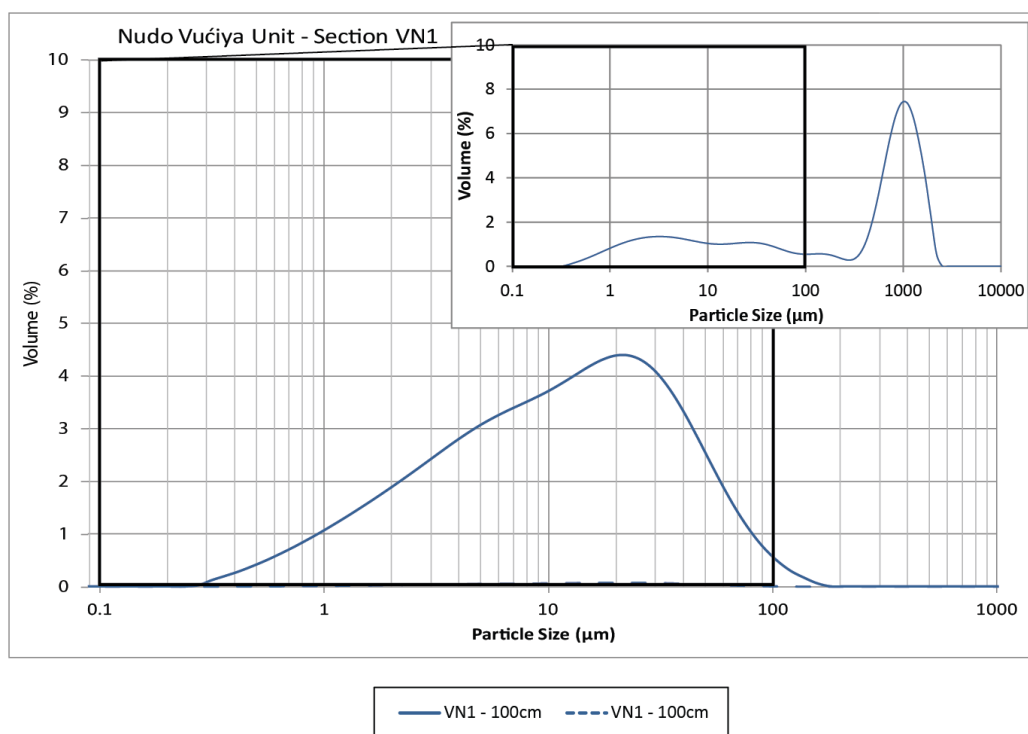
Figure 6.18 continued – Particle size distribution for terrace units of the Nudo valley, north Orjen at <2 mm (inset graph) and <63 μm (main graph).
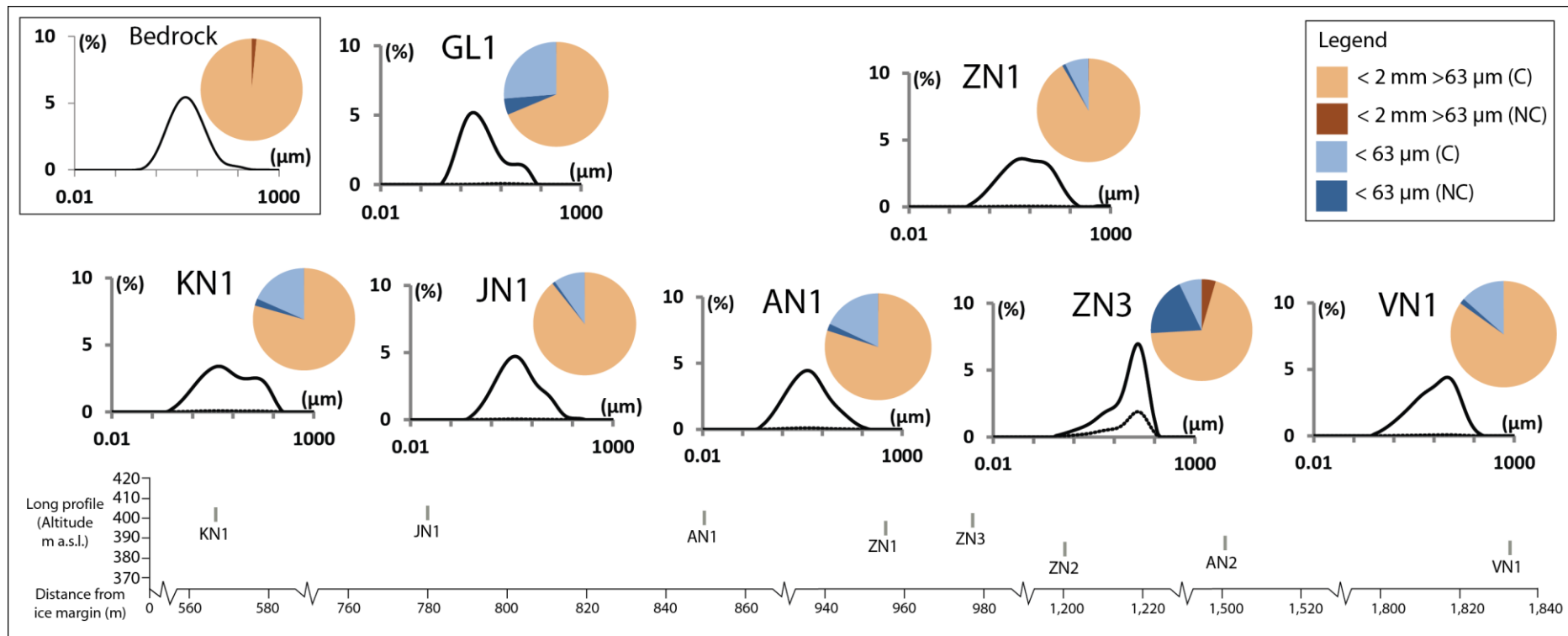
Figure 6.19 - Mean particle size distribution of the fine (<63 μm) sediment matrix and sediment lithological composition of the <2 mm matrix component of the Nudo valley, north Orjen. Data are also provided for the moraine at Lisac (GL1), which are situated upstream of Nudo and have been correlated to MIS 6 by Hughes *et al*. (2010). Based on matrix samples emboldened in Table 6.10. Glacial matrix PSA and clast lithology (sample GL1) data are displayed for comparative purposes Bedrock samples represent the <2 mm fraction (Section 6.1).

6.12   Sniježnice

The sedimentary records at Sniježnice represent an ice marginal depositional environment adjacent to a large moraine correlated to MIS 12 (Hughes *et al.*, 2010). The sediment matrix contains coarse sand and granules (Fig. 6.20) with a <63 µm component of up to 33% (Table 6.11). This closely resembles the PSD of both the MIS 12 (Section GS1) and MIS 6 (Section GS2) moraines (Fig. 6.20; Fig. 6.21). This elevated clay and silt component is considerably higher than the fine sediment matrix of many other fluvial sediments across Orjen. This may reflect its typical ice marginal sedimentary signature (Miall, 1983; 1985) which contains both glacigenic fines and coarser, clastic material (>100 µm). The proximity of this site to the ice margins is likely to have considerably influenced the sedimentary characteristics over successive glacial cycles. Within glaciated catchments, a location that was situated within an ice 'proximal' setting during MIS 12 for example, would be transformed into an ice 'distal' depositional environment as ice retreated, such as during MIS 6 (Miall, 1996). The close spacing of the moraines at Sniježnice therefore means that these fluctuations may be compounded by a greater potential for sediment reworking within a zone characterised by landscape instability.
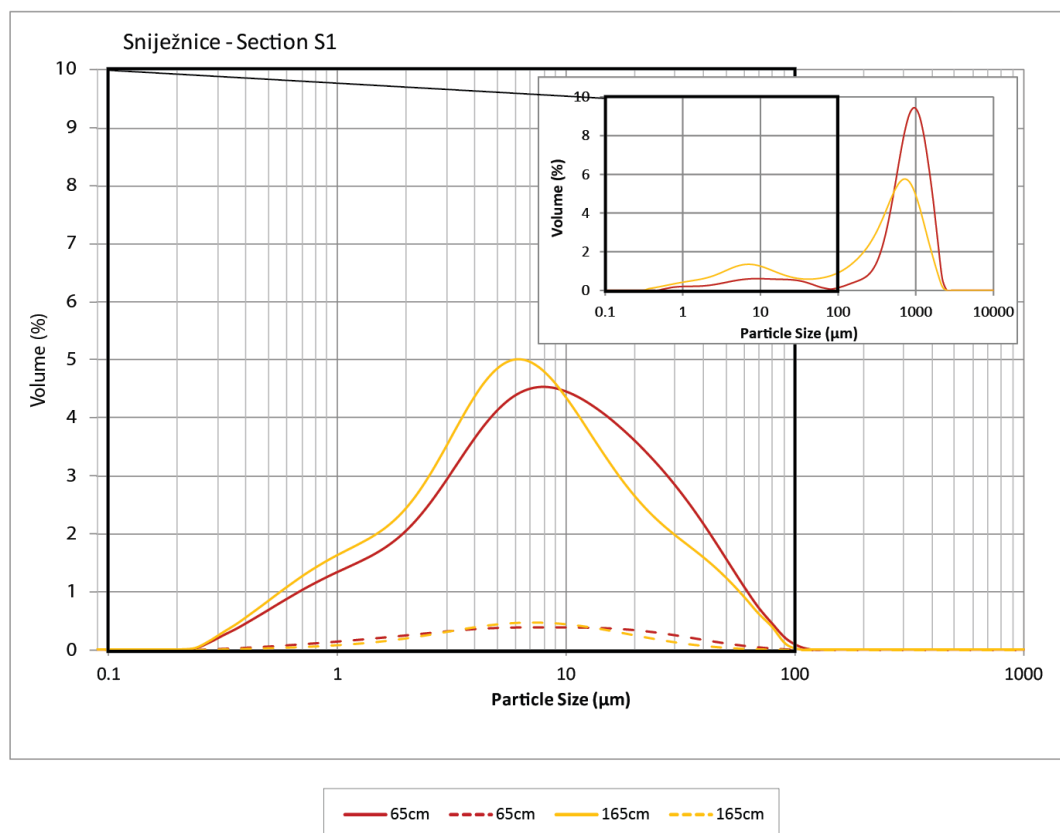
Figure 6.20 - Particle size distribution for Sniježnice, south Orjen at <2 mm (inset graph) and <63 µm (main graph).

Facies Code	Height up profile (cm)	Unit/Facies Description	<2mm >63μm % non-carbonate (NC %)	<2mm >63μm % carbonate (C %)	<63μm % non-carbonate (NC %)	<63μm % carbonate (C %)
SNIJEŽNICE						
Section S1						
S1a	65	Matrix	0.1%	66.9%	9.2%	23.8%
S1a	165	Matrix	0.1%	83.9%	7.9%	8.1%
Section S1 mean matrix values			**0.1%**	**75.4%**	**8.6%**	**16.0%**
Section S2						
S2a	40	**Matrix**	**0.1%**	**78.1%**	**5.7%**	**16.1%**

Table 6.11 - Sediment sample data from Sniježnice, south Orjen displayed as % non-carbonate (NC) and carbonate (C) of the bulk sediment by size fraction: <2 mm >63μm and <63 μm. Matrix samples used to generate mean particle size distribution of the <63 μm fraction and calcium carbonate content of the bulk sediment matrix are highlighted in bold.
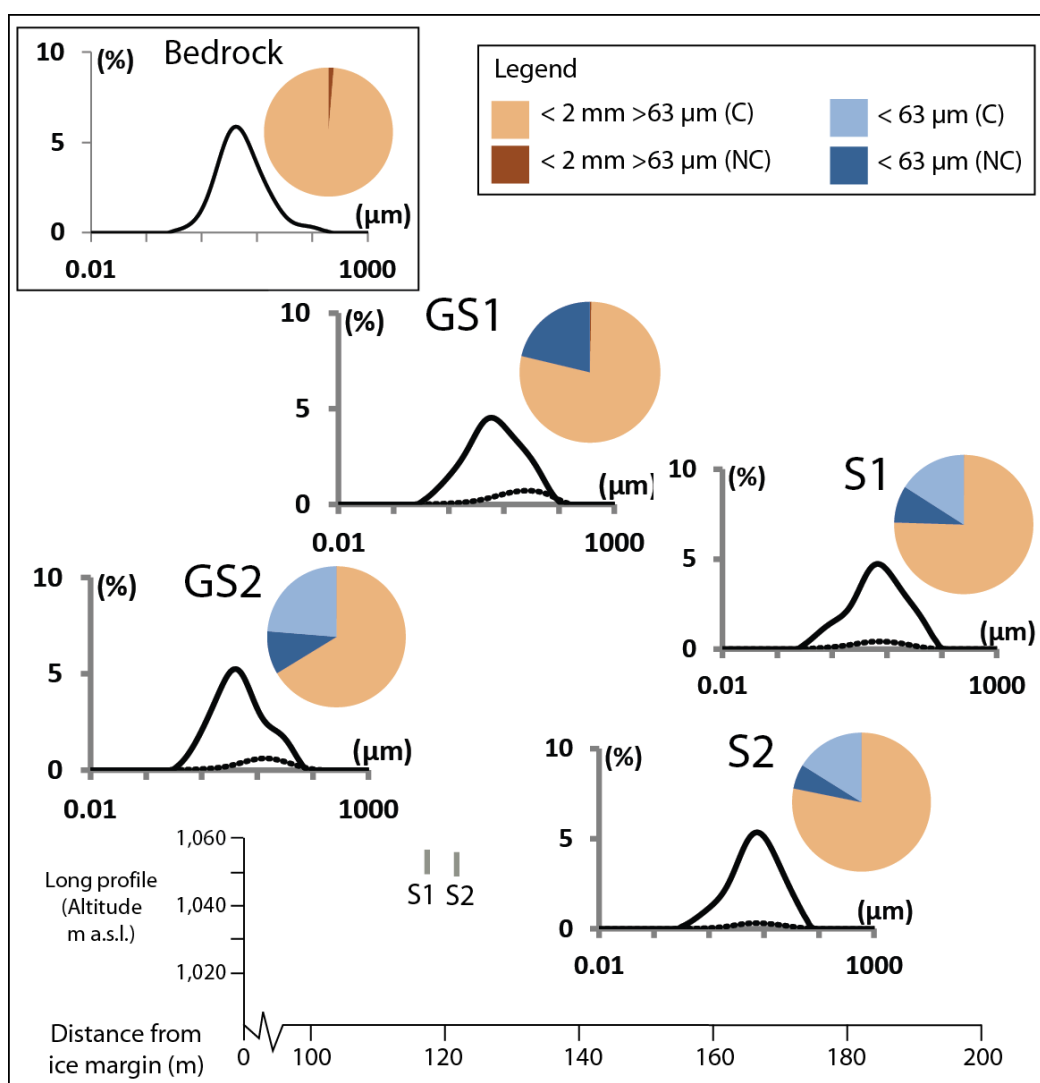
Figure 6.21 – Mean particle size distribution of the fine (<63 μm) sediment matrix and sediment lithological composition of the <2 mm matrix component at Sniježnice, south Orjen. Based on matrix samples emboldened in Table 6.11. Glacial matrix PSA and clast lithology (samples GS1 and GS2) data are displayed for comparative purposes. Bedrock samples represent the <2 mm fraction (Section 6.1).

6.13   Unijerina

The exposures at Unijerina are situated c. 1,900 – 2,200 m downstream of the MIS 6 ice margins at Crkvice (Hughes *et al.*, 2010) and upstream of the MIS 12 moraines (Fig. 6.1). The sediments are exposed in a sequence of 3 stacked lithofacies at Section U3 (Chapter 5). Section U1 is correlated to the upper fluvial deposits of Section U3 (U3c). Matrix sediments here contain coarse sands and granules (Fig. 6.22) and a limited <63 μm component (9%) (Table 6.12). This contrasts with the diamicton sediments at Section U2 and U3b (Fig. 6.22). Both of these diamict units contain a greater <63 μm component than the fluvial deposits at Section U1 and range from 18.8% (Section U2) to 42.1% (Section U3).

Importantly, the diamict at Section U3 contains an insoluble residue content of 26.2% (Table 6.12; Fig. 6.23), which is considerably higher than the diamict (4.8% matrix mean, Section U2) and fluvial deposits (2.2% matrix mean, Section U1) further upvalley (Fig. 6.23). At Section U3, these non-carbonate lithologies occupy both the <2 mm and < 63 μm size fractions and are also evident within the fluvial deposits at Section U3. This may indicate a localised source of non-carbonate bedrock that becomes eroded and introduced into the fluvial sediments downstream of Sections U1 and U2, and reworked into the glacial till during the deposition of facies U3b.

The fluvial deposits at the base of Section U3 (Facies U3a) display a complex PSD within both the <2 mm and <63 μm fractions. This reflects the detailed stratification of fine silt and clay horizons with coarser, granule-rich sediments (Chapter 5). The <63 μm PSD is quasi-bimodal (Fig. 6.22 and 6.23), and shows similarities with the particle size characteristics of several ice distal sites within the polje environments (Dvrsno and Kruševice) and the alluvial fan at Kameno. The 32 cm-thick silt unit (100% <63 μm) capping the fluvial facies (U3a-xii) contains 9% residual lithologies. This further supports the evidence of a localised, non-limestone source lithology and the concentration of these residual minerals into the finest sediment size fractions as they are deposited from suspension. This may be indicative of a low energy, proglacial lacustrine or slow-flowing fluvial environment. Dropstone features have also been observed at the contact with the overlying diamicton (Chapter 5) which may suggest the input of larger clasts into a lower energy proglacial setting.
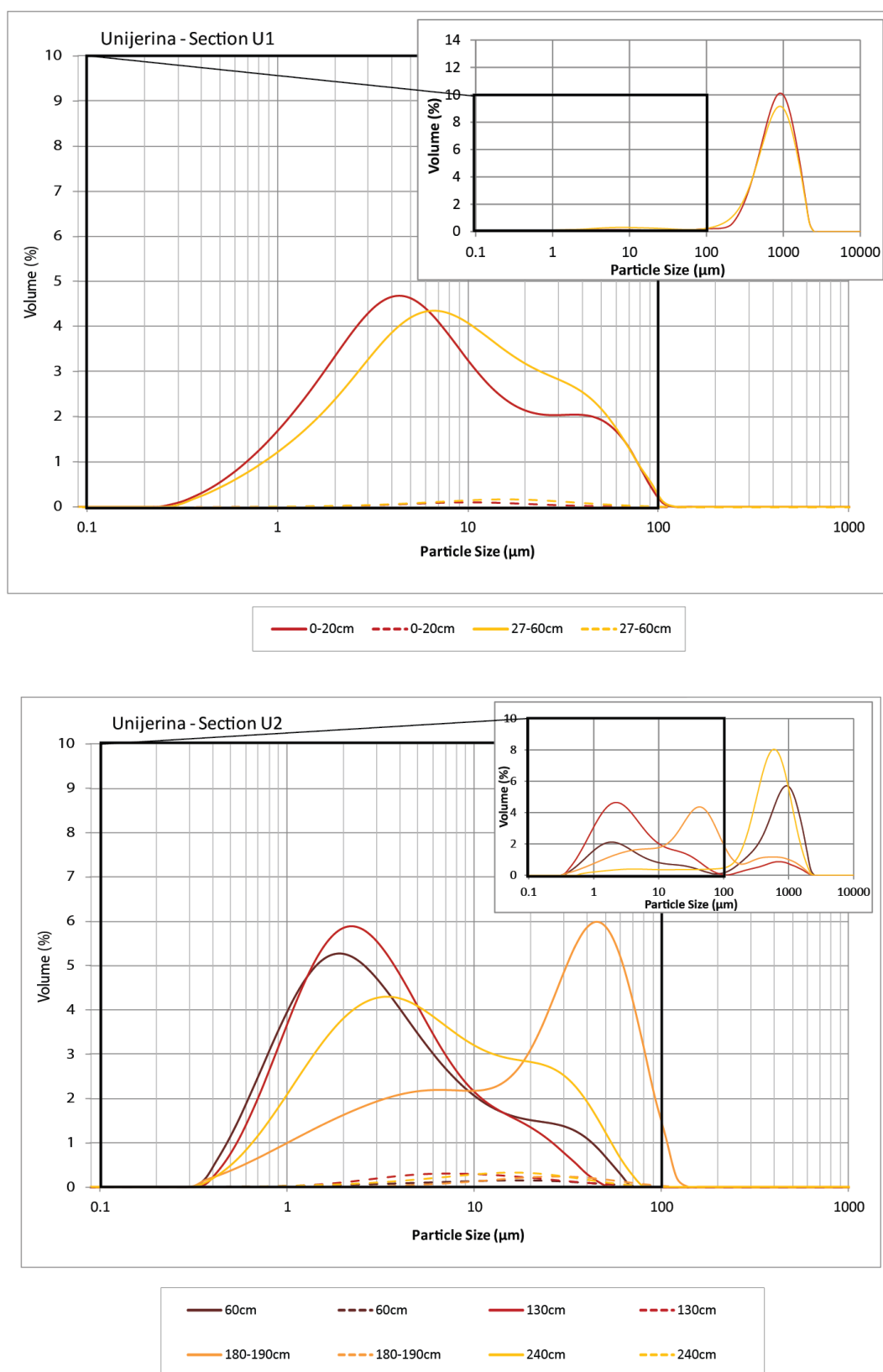
Figure 6.22 – Particle size distribution for Unijerina, east Orjen at <2 mm (inset graph) and <63 µm (main graph).
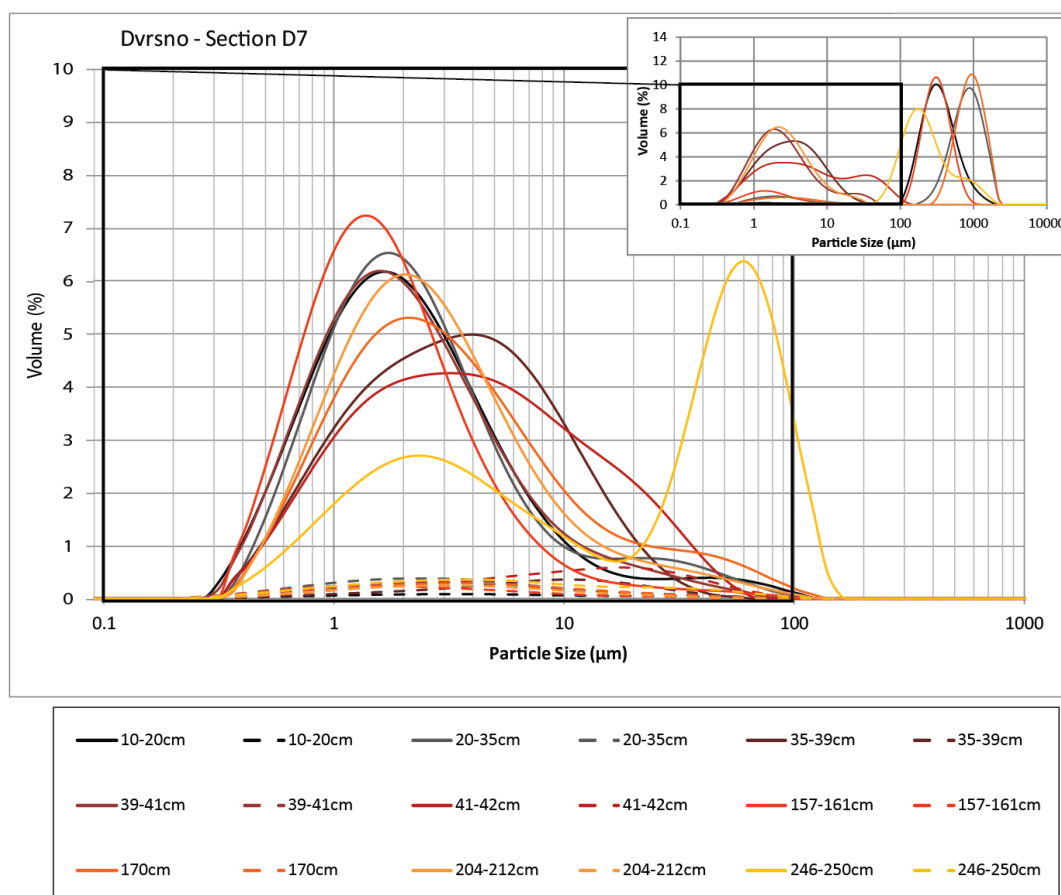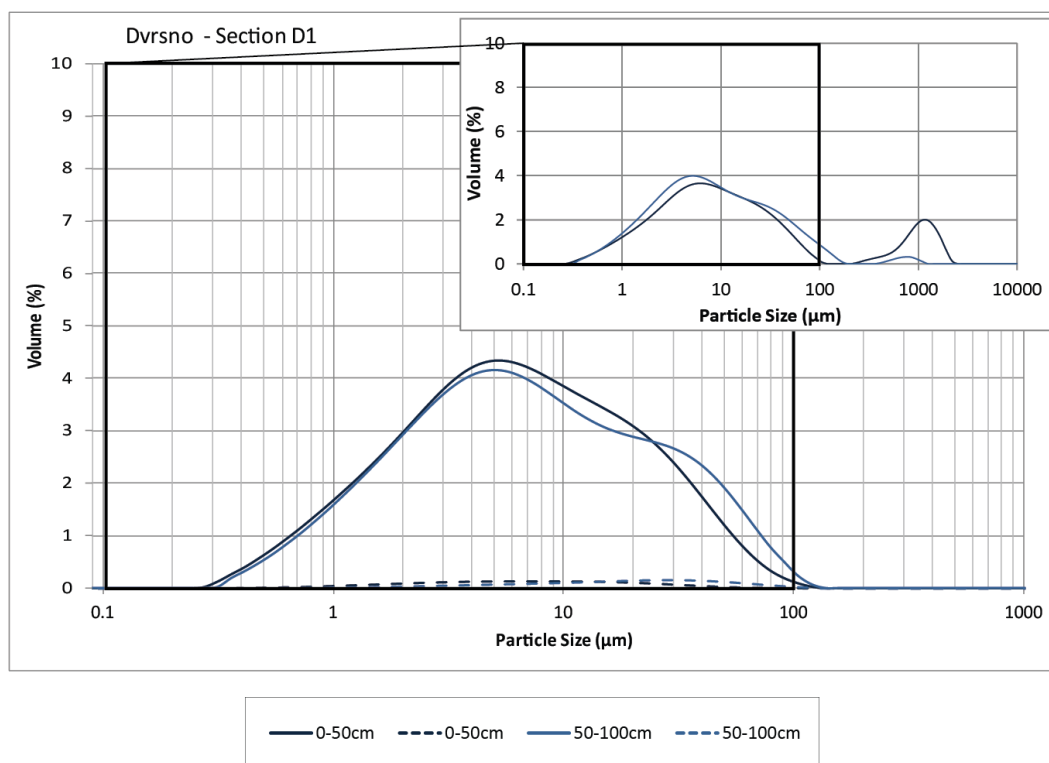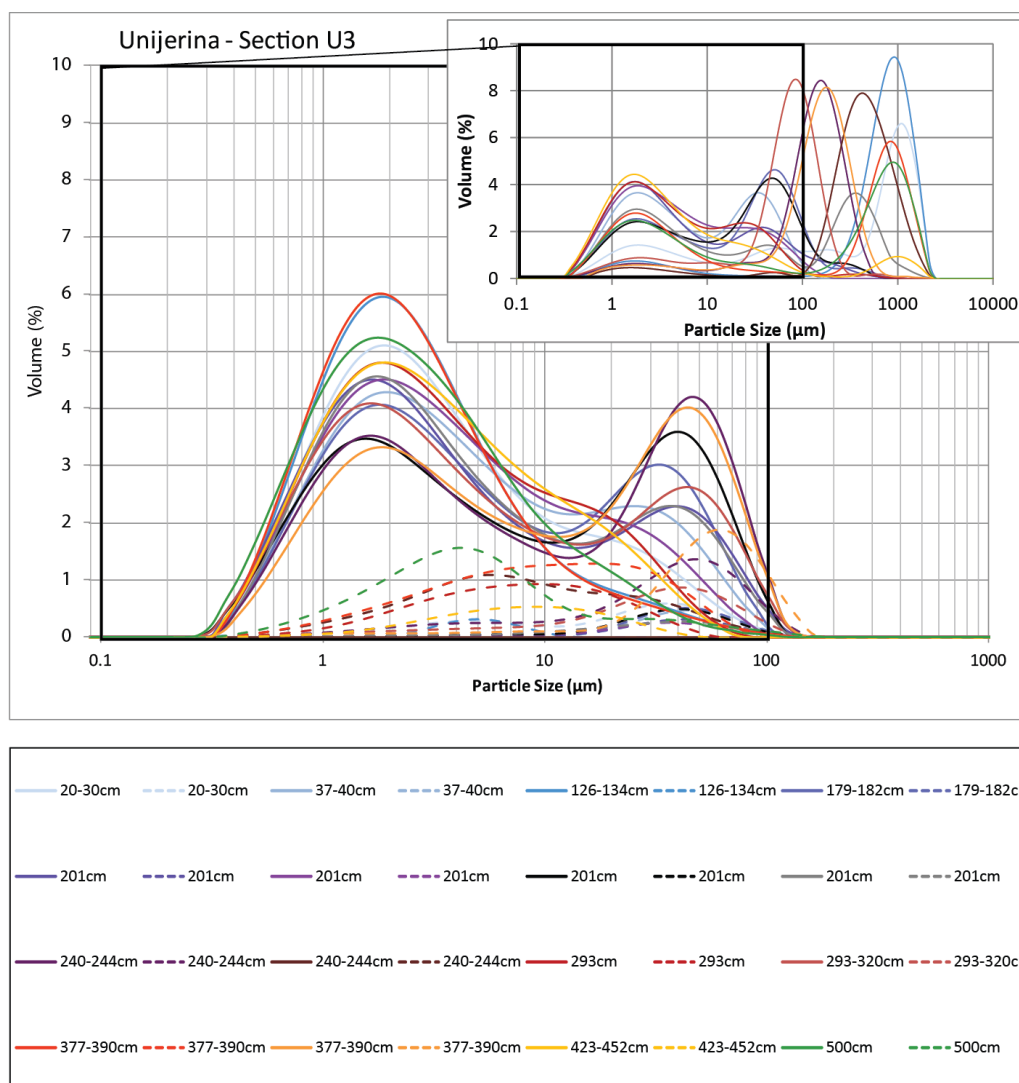
Figure 6.22 continued – Particle size distribution for Unijerina, east Orjen at <2 mm (inset graph) and <63 μm (main graph).

Facies Code	Height up profile (cm)	Unit/Facies Description	<2mm >63μm % non-carbonate (NC %)	<2mm >63μm % carbonate (C %)	<63μm % non-carbonate (NC %)	<63μm % carbonate (C %)
			UNIJERINA			
			Section U1			
U1a-i	0-20	Matrix	0.2%	93.8%	1.3%	4.7%
U1a-iii	27-60	Matrix	0.1%	90.9%	2.7%	6.3%
	Section U1 mean matrix values		**0.2%**	**92.4%**	**2.0%**	**5.5%**
			Section U2			
U2a-i	60	Matrix	0.1%	78.4%	3.0%	18.5%
U2a-i	130	Matrix	0.1%	81.2%	5.7%	13.1%
U2a-ii	180-190	Silty horizon	0.3%	55.5%	3.2%	41.0%
U2a-ii	240	Matrix	2.2%	85.0%	3.2%	9.6%
	Section U2 mean matrix values		**0.8%**	**81.5%**	**4.0%**	**13.7%**

Table 6.12- Sediment sample data from Unijerina, east Orjen displayed as % non-carbonate (NC) and carbonate (C) of the bulk sediment by size fraction: <2 mm >63μm and <63 μm.

Facies Code	Height up profile (cm)	Unit/Facies Description	<2mm >63µm % non-carbonate (NC %)	<2mm >63µm % carbonate (C %)	<63µm % non-carbonate (NC %)	<63µm % carbonate (C %)
			Section U3			
U3a-i	20-30	**Matrix**	**7.0%**	**71.1%**	**3.3%**	**18.5%**
U3a-i	37-40	Silty lens	0.1%	9.3%	4.7%	86.0%
U3a-i	126-134	Gravel-rich sand horizon	0.0%	89.5%	2.8%	7.6%
U3a-ii	179-182	Silt horizon	0.1%	27.5%	5.1%	67.2%
U3a-iv	201	Silt horizon	0.2%	49.9%	3.3%	46.6%
U3a-iv	201	Clay horizon	0.1%	13.1%	3.0%	83.9%
U3a-iv	201	Silty sand	0.2%	61.9%	5.2%	32.7%
U3a-iv	201	Silty sand	0.2%	82.2%	3.8%	13.8%
U3a-vi	240-244	Silty horizon	6.0%	69.0%	6.5%	18.5%
U3a-vi	240-245	Medium sand and silt	16.9%	67.7%	6.2%	9.2%
U3a-viii	293	Silty clay	6.5%	5.0%	11.5%	77.1%
U3a-viii	293-320	Sand horizon	8.6%	69.4%	3.9%	18.0%
U3a-x	377-390	Coarse sand	23.3%	64.7%	6.1%	5.9%
U3a-x	377-391	Silty sand	13.9%	56.0%	4.9%	25.1%
U3a-xii	423-452	Sandy silt	0.0%	0.0%	9.0%	91.0%
U3b	500	**Matrix**	**20.6%**	**37.3%**	**5.6%**	**36.5%**

Table 6.12 continued - Sediment sample data from Unijerina, east Orjen displayed as & non-carbonate (NC) and carbonate (C) of the bulk sediment by size fraction: <2 mm >63µm and <63 µm. Matrix samples used to generate mean particle size distribution of the <63 µm fraction and calcium carbonate content of the bulk sediment matrix are highlighted in bold.
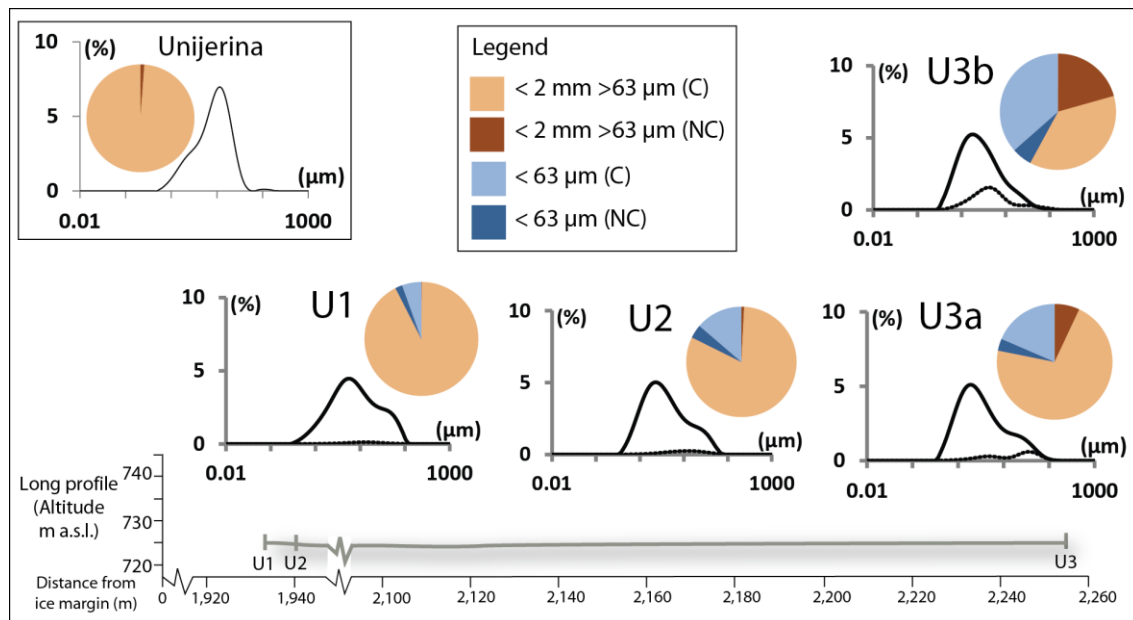
Figure 6.23 – Mean particle size distribution of the fine (<63 µm) sediment matrix and sediment lithological composition of the <2 mm matrix component at Unijerina, east Orjen. Based on matrix samples emboldened in Table 6.12. Bedrock samples represent the <2 mm fraction (Section 6.1).

6.14   Crkvice

The exposures at Crkvice are also located downstream of the MIS 6 ice margins (c. 2,200 m) within a small polje adjacent to Unijerina (Fig. 6.1). Two facies are exposed here on adjacent land surfaces: a diamicton (Section C1) and stratified alluvial deposits (Section C2). The bulk matrix samples of the diamicton at Section C1 has a broadly bimodal PSD (Fig. 6.24) with a dominant <63 μm component (24.7%) (Table 6.13). The <63 μm fraction itself displays a broad PSD (1 to 60 μm) which closely resembles the PSD and insoluble residue concentrations of the till sediments at Crkvice Section GC2 (Table 6.13; Fig. 25). The fluvial deposits at Section C2 are also similar in particle size characteristics to the glacial sediments upstream at Sections GC1 and GC2 (Fig. 6.25). The weakly bimodal PSD of these fluvial sediments reflects the PSD observed at Unijerina (Section 6.13). Sediments at Crkvice, however, contain much lower insoluble residue concentrations (6.2%). This may be due to localised factors at Unijerina such as a local source of non-limestone lithologies, or the preferential deposition of non-carbonate lithologies within a low energy proglacial setting. More detailed Harden Index and U-series analyses are required to more securely constrain the timing of sediment deposition at these sites.

Facies Code	Height up profile (cm)	Unit/Facies Description	<2mm >63μm % non-carbonate (NC %)	<2mm >63μm % carbonate (C %)	<63μm % non-carbonate (NC %)	<63μm % carbonate (C %)
			CRKVICE			
			Section C1			
C1a	170	**Matrix**	**0.2%**	**75.1%**	**6.0%**	**18.7%**
			Section C2			
C2a-i	17	Sandy lens	0.3%	83.7%	4.8%	11.2%
C2a-i	35	Matrix	0.1%	81.4%	2.6%	15.9%
C2a-ii	49-59	Fine-Medium sand	0.4%	82.7%	1.8%	15.0%
C2a-iii	59-62	Medium-Coarse sand	0.2%	96.9%	1.1%	1.8%
C2a-iv	62-63	Silty clay	0.3%	6.1%	92.7%	0.9%
C2a-v	63-69	Silt and fine sand	0.5%	66.2%	2.3%	31.0%
C2a-vi	69.5 - 74	Fine-Medium sand	0.4%	86.0%	1.7%	11.9%
C2a-vi	69.5 - 74	Medium sand	0.4%	78.7%	5.8%	15.1%
C2a-vii	76	Coarse sand	0.1%	96.4%	1.0%	2.5%
C2a-viii	84 - 90	Medium sand	0.1%	90.1%	3.3%	6.5%
C2a-ix	90 - 92	Silt	0.3%	50.4%	2.7%	46.6%
C2a-x	92 - 97	Medium Sand	0.3%	65.9%	3.3%	30.5%
C2b	110	Sand pocket	0.1%	91.3%	2.4%	6.3%
C2b	130	Matrix	0.1%	87.3%	2.0%	10.5%
Section C2 mean matrix values			0.1%	84.4%	2.3%	13.2%

Table 6.13 - Sediment sample data from Crkvice, east Orjen displayed as % non-carbonate (NC) and carbonate (C) of the bulk sediment by size fraction: <2 mm >63μm and <63 μm. Matrix samples used to generate mean particle size distribution of the <63 μm fraction and calcium carbonate content of the bulk sediment matrix are highlighted in bold.
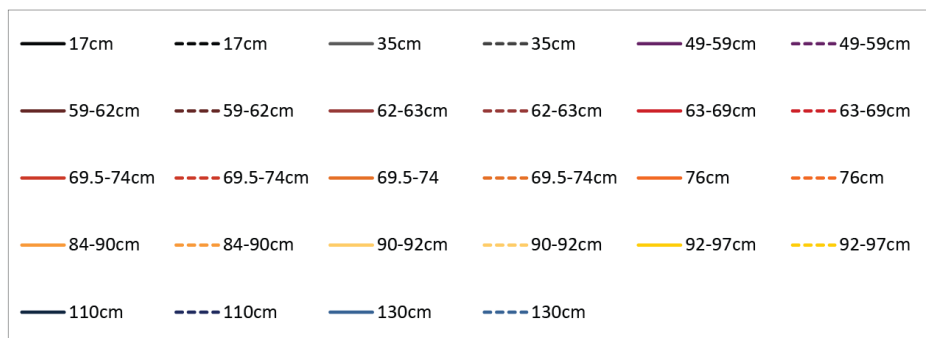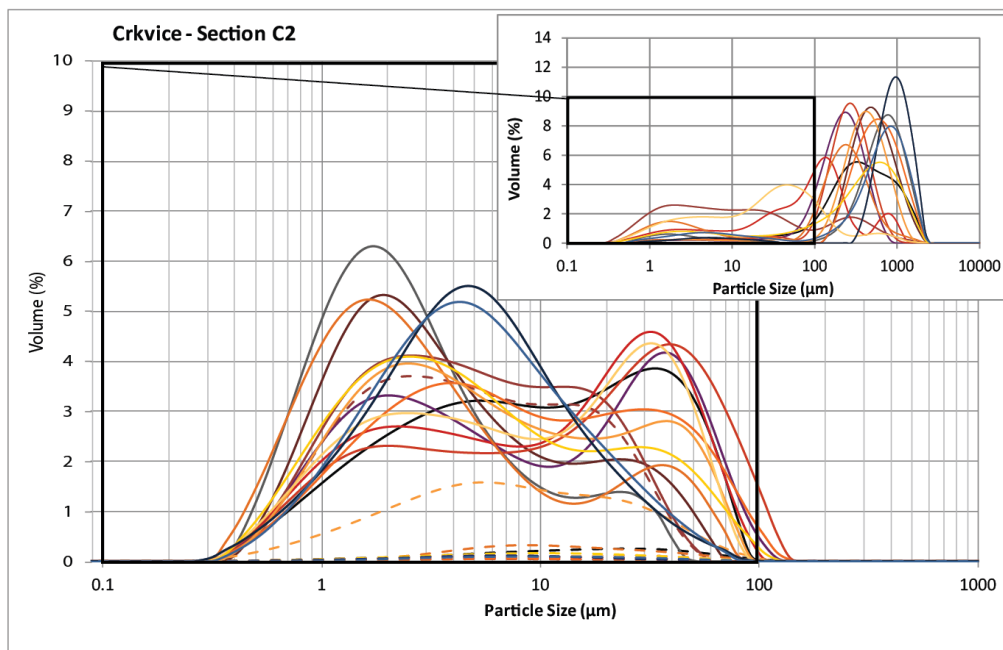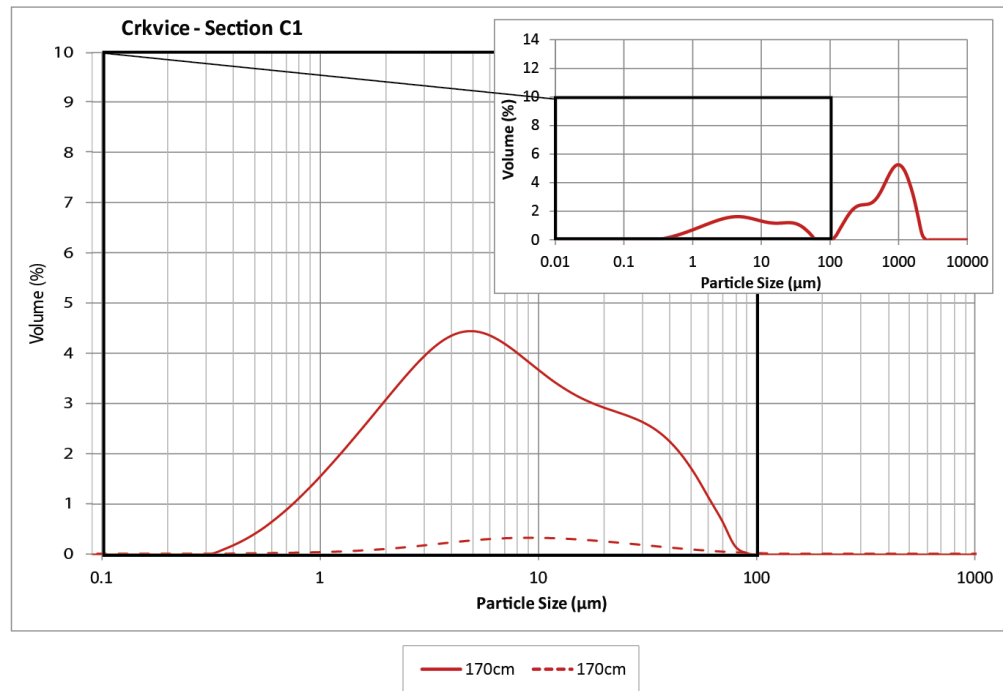
Figure 6.24 - Particle size distribution for Crkvice, east Orjen at <2 mm (inset graph) and <63 µm (main graph).
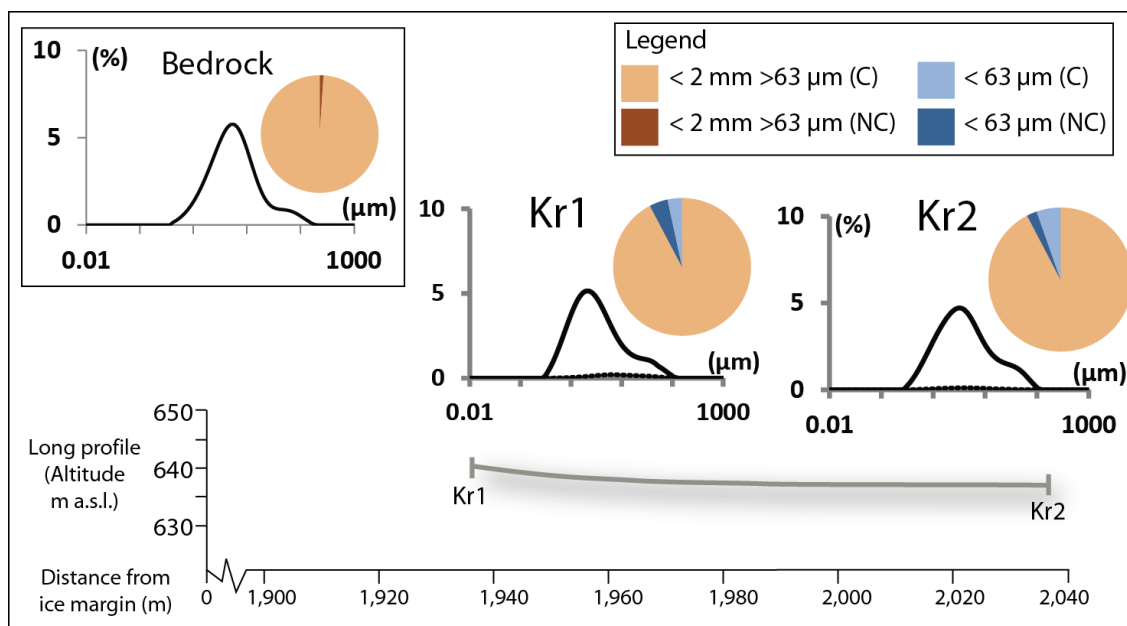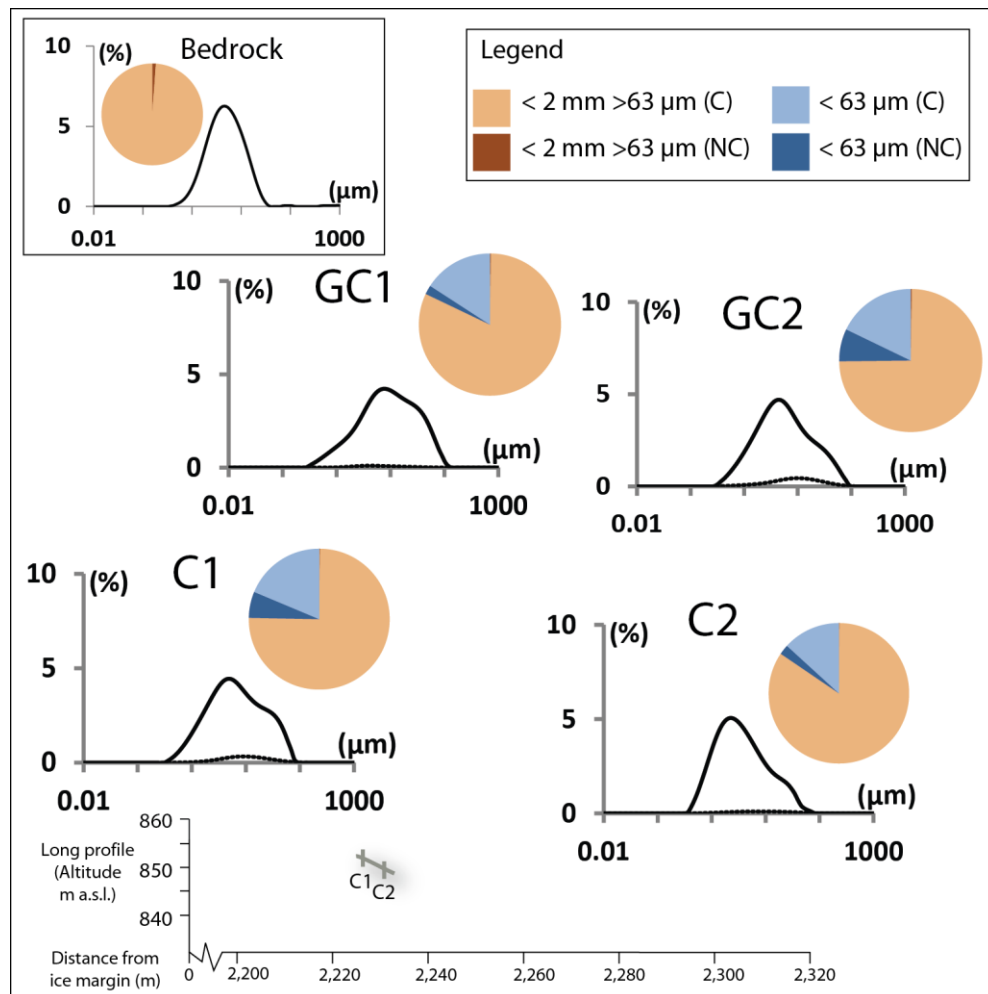
Fig 6.25 – Mean particle size distribution of the fine (<63 μm) sediment matrix and sediment lithological composition of the <2 mm matrix component at Crkvice, east Orjen. Based on matrix samples emboldened in Table 6.13. Glacial matrix PSA and clast lithology (sample GC1 and GC2) data are displayed for comparative purposes. Bedrock samples represent the <2 mm fraction (Section 6.1).

6.15   Ubli

Ubli is also situated downstream of the MIS 6 ice margins, and upstream of a series of MIS 12 moraines, at the southern extent of the Orjen ice cap (Fig. 6.1). The PSD of the fine <2 mm sediment fraction shows a dominance of coarse sands and granules (Fig. 6.26) with a <63 μm component of 14.6% (Table 6.14). This <63 μm fraction is normally distributed and closely resembles the particle size characteristics of the moraines at Sniježnice (Fig. 6.27). The insoluble residue within the sediment matrix at Ubli contributes 2.4% of the bulk sediment sample (Table 6.14; Fig. 6.27), in comparison to 15.8% (GS1) and 10.0% (GS2) within the till sediments further up valley at Sniježnice. This may be indicative of the transformation of till

sediments with distance downstream. It is likely that this sequence was deposited during a period of ice advance, as the outlet glacier reached its maximum extent during MIS 12, approximately 2 km downvalley from this site. Harden Index soil analysis, and the integration of morphosedimentary evidence from Lipci, downstream of the site, and Sniježnice, upvalley, may constrain the depositional history of this valley. This site therefore provides a strategic tie point between the glacigenic sediment source at Sniježnice and the redistribution and deposition of these sediments downstream towards Lipci and offshore into the Bay of Kotor.
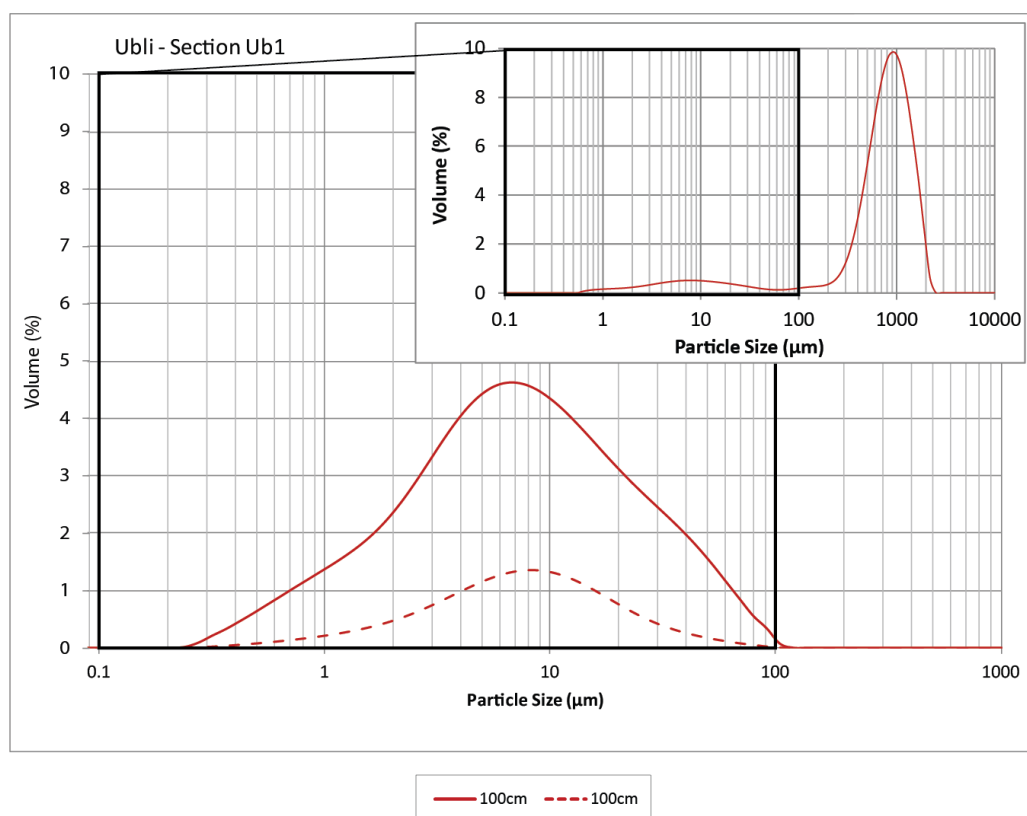
Figure 6.26 - Particle size distribution for Ubli, southeast Orjen at <2 mm (inset graph) and <63 µm (main graph).

Facies Code	Height up profile (cm)	Unit/Facies Description	<2mm >63µm % non-carbonate (NC %)	<2mm >63µm % carbonate (C %)	<63µm % non-carbonate (NC %)	<63µm % carbonate (C %)
			UBLI			
			Section Ub1			
Ub1a	100	**Matrix**	0.1%	85.3%	2.3%	12.3%

Table 6.14 - Sediment sample data from Ubli, southeast Orjen displayed as % non-carbonate (NC) and carbonate (C) of the bulk sediment by size fraction: <2 mm >63µm and <63 µm. Matrix samples used to generate mean particle size distribution of the <63 µm fraction and calcium carbonate content of the bulk sediment matrix are highlighted in bold.
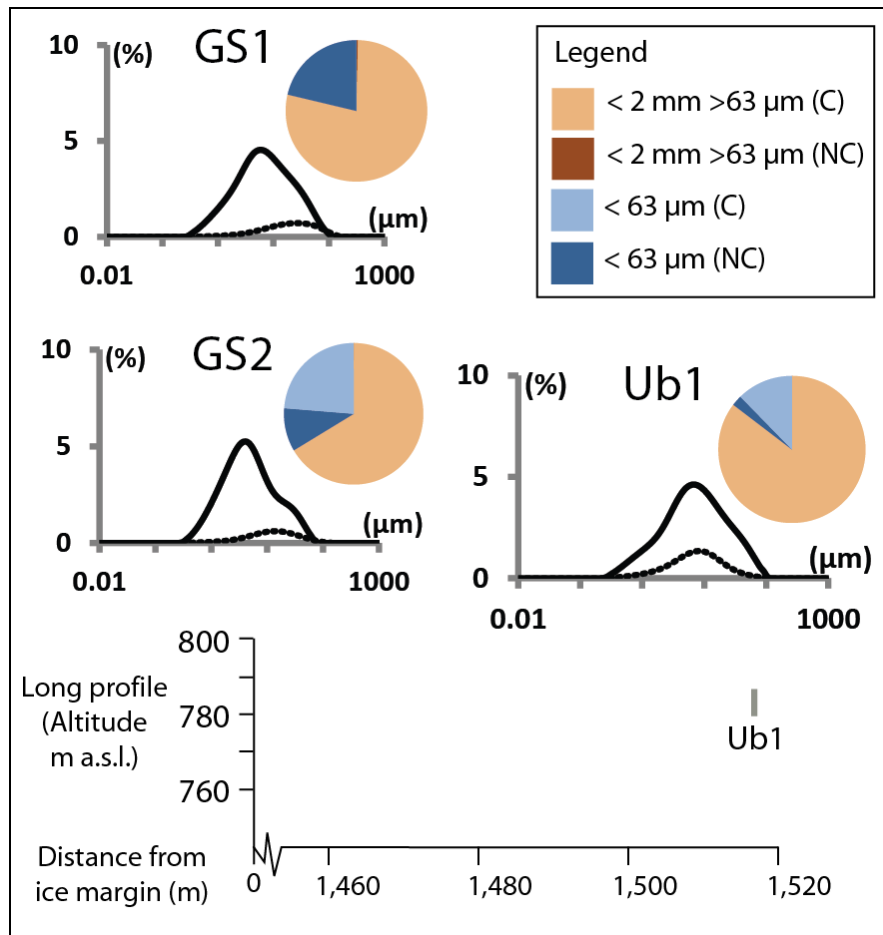
Figure 6.27 – Mean particle size distribution of the fine (<63 μm) sediment matrix and sediment lithological composition of the <2 mm matrix component at Ubli, southeast Orjen. Based on matrix samples emboldened in Table 6.14. Glacial matrix PSA and clast lithology (sample GS1 and GS2) data are displayed for comparative purposes. Bedrock samples represent the <2 mm fraction (Section 6.1).

6.16   Summary

Detailed particle size measurements and carbonate content determinations have been used in this study to assess the transformation of limestone bedrock and glacigenic sediments within the fluvial environment. These data provide important insights into the long-term landscape processes operating within glaciated catchments. A combination of chemical and mechanical weathering as well as fluvial sorting processes may contribute towards the distinct sedimentary signatures observed within the contrasting fluvial geomorphological settings of the Orjen massif. These data will be discussed further in Chapter 9, alongside the larger scale geomorphological and morphostratigraphical framework (Chapter 5) and the geochronological indicators (Chapters 7 and 8).

CHAPTER SEVEN

Results: Secondary Carbonates

Field Macromorphology and Thin Section Micromorphology

Synopsis

Secondary carbonates (calcites) have been used within this study for two key reasons: to investigate the factors controlling carbonate development over time using micromorphology (Section 7.2); and to develop a detailed U-series chronology of alluvial depositional phases surrounding Mount Orjen (Chapter 8). Within sedimentary sequences containing secondary carbonates, an understanding of calcite development at both the macromorphological (Section 7.1) and micromorphological (Section 7.2) scale is important for the accurate reconstruction of Quaternary landscape processes. Secondary carbonate profiles often contain detailed microfabrics, many of which are diagnostic of specific climatic regimes or environmental conditions. The analysis of calcite profiles can therefore also serve as a valuable relative age tool (Section 7.3).

In this study, all secondary carbonates were identified and described in section using the nomenclature outlined in Chapter 4.3.1. This has been used as a basis for the extraction of calcites for micromorphological and U-series analysis. Micromorphology samples have been extracted from carbonate horizons at Unijerina, west Orjen and from river terraces of the Nudo valley, north Orjen. These are used to develop a qualitative model of calcite development (Chapter 9). U-series samples were obtained in the field from 35 calcite horizons from 10 sites surrounding Orjen and will be discussed in Chapter 8.

7.1   Secondary carbonate macromorphology

Secondary carbonate profiles within the alluvial deposits of Orjen reflect a variety of calcite formation mechanisms from the *weathering-zone* classification of Candy *et al*. (2011). These include vadose zone carbonates, formed within the interstices of open framework gravels (such as at Kameno and Lipci) as well as phreatic zone calcites developed in association with groundwater (such as at Nudo, Pirina Poljana, Vrbanje, and Unijerina) (Table 7.1; Plate 7.1).

The formation of vadose zone calcites relies upon a sustained moisture input (through precipitation) and an abundant supply of calcium carbonate ($CaCO_3$) from the limestone-rich bedrock and sediments (Hughes, 2004). This $CaCO_3$ is dissolved and translocated within percolating waters and reprecipitated within the sediment profile. Vadose zone calcites frequently form large sparitic cements within the void spaces of clasts and in many cases contain calcite crystals suitable for U-series dating. Unlike many secondary carbonate forms, the reliance of vadose zone carbonates on augmented moisture supplies means that they are unlikely to be formed under arid or semi-arid conditions and are often more closely associated with wetter climatic periods (Wright and Tucker, 1991; Hughes, 2004).

In contrast, phreatic zone cements can form under both moist and arid environmental conditions, and instead rely on sufficiently high evaporation rates to induce calcite precipitation (Wright and Tucker, 1991). This is because the groundwater is already abundant in dissolved $CaCO_3$ and requires little further moisture input to promote carbonate percolation (Hughes, 2004). Phreatic carbonates form within existing sediment bodies meaning that they are frequently rich in detrital sediments and often contain small calcite crystals surrounding clasts and grains. This type of secondary carbonate is abundant in many of the alluvial sequences of Orjen. The presence of detrital material makes the extraction of secondary carbonate from the sediment matrix problematic and can lead to the contamination of U-series samples (Chapter 8). Where possible, vadose type carbonates were extracted for U-series analysis. At sites where these were not present, care was taken to select and extract phreatic zone calcites from the surrounding sediment matrix (Chapter 8). In the field, samples were examined for multiple cement layers and re-crystallisation to avoid carbonates that showed evidence of overprinting and open-system behaviour (Smart, 1991).

Study Site	Secondary Carbonate Type	Description	Horizon thickness (cm)	Sampled Facies/Units	U-series Analysis	Micromorph. Analysis
Grahovo	Incipient vadose carbonate	Large sparitic and detritus-free calcite crystals in a thin, discontinuous horizon at 285-290 cm, situated in the Bk horizon.	5	G1a-iii	✓	✗
Dvrsno	-	No observed secondary carbonate development.	-	-	-	-
Kruševice	Incipient phreatic carbonate	Detritus-rich carbonate coating on clasts at 250-260 cm. Very friable. Otherwise no secondary carbonate development present.	n/a	Kr2a-ii	✓	✗
Vrbanje	Incipient vadose carbonate	Sparitic crystal coatings on a clast within a discontinuous, yet densely cemented horizon at 65-70 cm, situated within the Bk horizon.	5	V2a	✓	✗
Pirina Poljana	Phreatic carbonate	1) A 30 cm thick cemented bench at c. 100 cm containing a densely-cemented yet detritus-rich phreatic zone carbonate. 2) A carbonate rind surrounding a clast below the cemented bench.	5 - 30	P2a	✓	✗
Lipci	Vadose zone and flowing water carbonates	1) Large sparitic and detritus-free vadose zone carbonates developed within clast void spaces in sections L2a and L3a. 2) Sparitic calcite crystals developed as a flowing water carbonate and exposed within a tributary cutting at L4.	10 - 20	L2a, L3a, L4a	✓	✗
Kameno	Vadose zone carbonate	Sparitic calcite crystals developed within the void spaces of open framework gravels within the Bk horizon.	50	K1b	✓	✗
Nudo	Phreatic carbonate	Friable and detritus-rich phreatic carbonates formed within river terrace sequences, frequently as cemented benches (sections AN1 and AN2) and as incipient coatings around clasts (sections ZN1 and JN1)	5 - 50	AN1a, AN2a, VN1a, KN1a, JN1a, ZN1a	✓	✓
Unijerina	Vadose and Phreatic zone carbonates	1) Large, sparitic calcite crystals forming a vadose zone cement in the capping fluvial deposits of Section U3 (Facies U3c). 2) Detritus-rich phreatic carbonates within Facies U2a-ii and U3c.	60	U2a-ii; U3c	✓	✓
Crkvice	Phreatic zone carbonate	1) Thin, friable phreatic carbonate rinds on the surface of clasts at 80 cm in Section C2a within a discontinuous zone of carbonate accumulation 2) Sparitic calcite clast at 200 cm. Potentially a reworked calcite.	5	C1a, C2a-vii	✓	✗
Ubli	-	No observed secondary carbonate development	-	-	–	-
Sniježnice	Vadose zone carbonate	Large, sparitic carbonate developed within the near-surface, vadose, zone of a moraine/ice marginal fluvial deposit.	10	Correlated with S1	✓	✗

Table 7.1 – Secondary carbonate macromorphological descriptions and horizon thickness based on field observations. Samples obtained for U-series and micromorphological laboratory analysis are indicated and referenced to the sedimentary logs, facies and unit codes defined in Chapter 5.

Plate 7.1 – Secondary carbonate horizons from alluvial sedimentary sequences at sites surrounding the Orjen massif. These are representative of the variety of calcite textures observed across the study region: A) Vadose zone and flowstone carbonates exposed within the tributary cutting of the Lipci fan (Section L4); B) Phreatic carbonates within the capping fluvial deposits at Unijerina (Section U3); C) Vadose zone, sparitic calcite coatings on clasts at Kameno (Section K1); D) Phreatic carbonate, cemented bench at Pirina Poljana (Section P2); E) Incipient carbonate coatings on clasts (arrowed) in the Zaslap Unit of the Nudo Valley (correlated to Section ZN1); F) Phreatic, detritus-rich carbonates within the Arandelovo Unit of the Nudo Valley (correlated to Section AN1).

7.2   Secondary carbonate micromorphology

Micromorphology has been used within this study to gain a more detailed insight into the palaeoenvironmental factors that have influenced alluvial environment calcite development. A total of 11 thin sections have been analysed from secondary carbonate profiles within fluvial deposits at Unijerina, west Orjen (Sections 7.2.1 – 7.2.2) and from cemented benches within river terraces of the Nudo valley, north Orjen (Sections 7.2.3 – 7.2.11). These samples are representative of the range of vadose and phreatic secondary carbonate forms at sites surrounding Orjen (Plate 7.1). Samples have not been obtained from other study sites due to either a limited abundance of secondary carbonate accumulations which were preferentially analysed for U-series, or due to time constraints in the manufacture of thin section slides. The samples from Unijerina have been successfully dated by U-series methods, whilst those from terraces of the Nudo valley have not all yielded secure ages (Chapter 8). Micromorphological analysis may therefore also serve as a relative age tool and as a method for investigating the suitability of calcites for U-series dating. Alongside qualitative descriptions of calcite texture and appearance, more quantitative estimates are also made of: percentage areal cover by cement type (spar, >30 μm; microspar, 30 - 4 μm; and micrite <4 μm); and percentage areal cover of calcite and detrital grains/clasts. Pebble sized clasts are excluded from this latter value as they may lead to unrepresentative estimates of the overall calcite content. These microfabric statistics are used to develop a qualitative index of carbonate development over time (Chapter 9).

7.2.1   Sample 1 - Unijerina (Section U3)

This sample is taken from the capping fluvial deposits at Unijerina within Facies U3c. Secondary carbonates here are visible in section as a 60 cm-thick, detritus-rich and partially-indurated phreatic carbonate horizon. In thin section, the carbonate is rich in detrital grains ranging in size from 300 – 1,400 μm   (50% calcite, 50% grains). The cements are dominated by sparitic cements (95% calcite area) throughout the section, with smaller patches of dense micrite (5%) (Fig. 7.1). Microsparitic cements have not been observed within this microfacies.

The section is largely homogenous, as a single microfacies, with no distinct shifts in cement type or texture. Calcite typically forms in rinds around detrital grains and as infills within void spaces. Here, spar crystals are smallest around the void periphery, coalescing to form larger

crystals within the central void space. Spar crystals are frequently bladed in appearance, and often form meniscus cements between grains. Bioclasts (n=5) are present in localised clusters towards the top and base of the section, but no other biological evidence or beta fabric development is present.

7.2.2   Sample 2 – Unijerina (Section U3)

This sample is also obtained from Section U3 and presents features typical of a vadose zone calcite forming as rinds at the surface of a large clast. In thin section, three distinct microfacies are evident (*microfacies a - c*), developing around a limestone clast (*microfacies d*) (Fig. 7.2):

Microfacies a

Developed at the outer edge of the clast, this microfacies is a very pure (99% calcite, 1% grains) and dominantly sparitic (90% spar, 10% micrite) cement forming elongate, needle-spar crystals. These crystals frequently have no preferred orientation, but are occasionally oriented perpendicular to the clast, particularly towards the base of the microfacies. Thin micritic coatings are also present on the very limited number of detrital grains present within this microfacies.

Microfacies b

This microfacies has developed on the upper surface of the clast and contains needle-spar calcite crystals similar to *microfacies a* (70% spar, 30% micrite). Detrital grains are not present within this microfacies (100% calcite). The carbonate here is often interspersed with more dendritic micrite cements, particularly towards the outer edge of the microfacies, where there is also evidence of pelleted micrite. These features are frequently deemed indicative of biogenic activity (of macro- and micro-organisms) within the overlying horizons (Calvet and Julià, 1983; Bain and Foos, 1993; Alonso-Zarza *et al.*, 1998; Wright, 2007) and reflect beta fabric development (Fig. 7.2).

Micromorphology

- Spar
- Microspar
- Micrite
- Variable groundmass
- Dense calcite
- Distinct microfacies boundary
- Diffuse microfacies boundary
- Voids/fractures
- Infilled voids/fractures
- Cracks (empty) and crystallaria (infilled)
- Calcite patches (diffuse and distinct boundaries
- Sediment grains
- Meniscus cements
- Etched grains
- Bladed calcite coronas
- Needle spar crystals (and growth direction)
- Laminar calcite
- Dendritic micrite
- Peloids (pelleted micrite)
- Bioclast (mollusc shells)

Groundmass statistics (% cover)

- Spar
- Microspar
- Micrite
- Calcite cement
- Grains

Sample 1
Unijerina Section U3c

A) Micromorphology schematic, reflecting percentage areal cover of cement type and grain:cement ratio.

B) Characteristic microfabrics.
i) Meniscus cements between grains (arrowed); ii) Spar and microspar infilling of void spaces.

Fig. 7.1 – Sample 1 - Micromorphology of secondary carbonate accumulations at Unijerina Section U3, facies U3c: A) Micromorphology schematic and groundmass statistics; B) Plates of characteristic microfabrics.
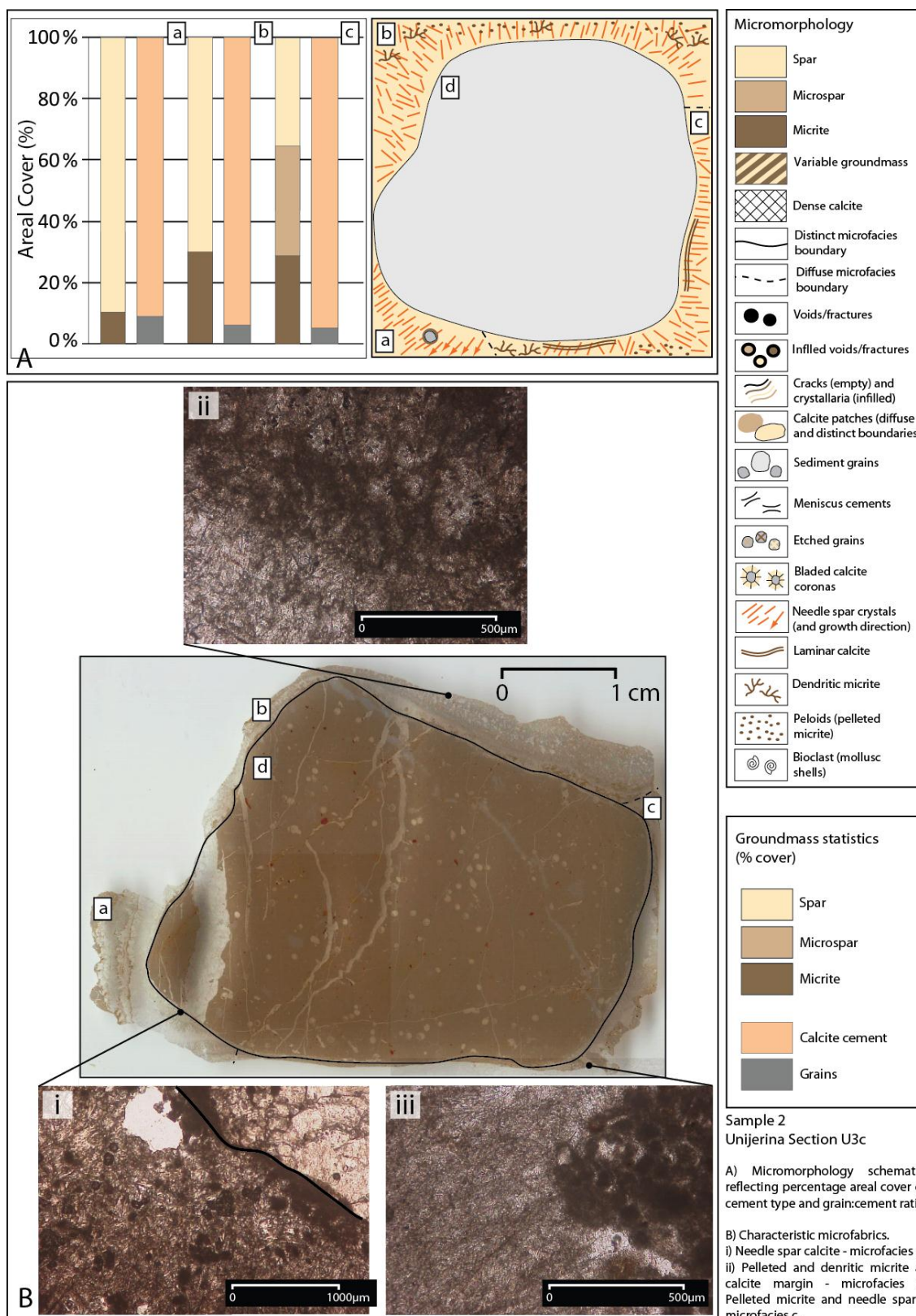
Fig. 7.2 – Sample 2 - Micromorphology of secondary carbonate accumulations at Unijerina Section U3, facies U3c: A) Micromorphology schematic and groundmass statistics; B) Plates of characteristic microfabrics.

Microfacies c

Microfacies c has gradational contacts with adjacent *microfacies a* and *b*. The needle-spar fabric is similar in composition to *microfacies a*, yet grades towards microsparitic cements towards the base (Fig. 7.2). Pelleted micrite is also interspersed with larger spar crystals here (35% spar, 35% microspar, 30% micrite). Laminar spar-micrite structures are evident at the underside of the clast, and dendritic micrite has also developed along the contact with *microfacies a*. These micritic structures reflect those present in *microfacies b*, and are indicative of carbonate formation in association with biogenic activity within the overlying weathering zone. Calcite crystals from this microfacies have been submitted for U-series analysis (Chapter 8).

7.2.3   Sample 3 – Nudo Zaslap Unit (Section ZN1)

This calcite is taken from the lowest terrace unit in the Nudo valley, the Zaslap Unit (Section ZN1). Secondary carbonates here form laminar yet friable and poorly-cemented phreatic calcites within the basal 70 cm of the terrace exposure. In thin section, the calcite presents a single microfacies dominated by dense, often laminated, microsparitic and micritic groundmass with incipient spar infilling within void spaces (3% spar, 50% microspar, 47% micrite) (Fig. 7.3). Detrital grain content here is limited (80% calcite, 20% grains) and void spaces are smaller than those observed at Unijerina. Detrital grains/clasts are small and measure 65 – 1,400 µm. Beta fabric microstructures such as pelleted micrite, spar-infilled root pathways, and incipient alveolar septal fabric are present in the central portion of the sample. One etched grain is visible towards the right hand side of the microfacies, yet these are otherwise absent from the section.

7.2.4   Sample 4 - Nudo Arandelovo Unit (correlated to Section AN1)

The Arandelovo Unit represents the highest accessible river terrace surface of the Nudo valley. Sediments of this unit contain a series of stacked, phreatic-zone cemented benches interspersed with unconsolidated alluvial sediments. This sample is obtained from an exposure of the Arandelovo Unit that is situated adjacent to, and has been correlated with, the highest cemented bench of Section AN1 (Chapter 5). The carbonate here is densely-cemented, yet contains a high detrital grain component (50% calcite and 50% grains) as well as large, granule-

pebble sized clasts (grain sizes of 100 – 2,000 µm) (Fig. 7.4). The calcite cement is dominantly sparitic with gradational contacts to patches of microspar and micrite (60% spar, 15% microspar, 25% micrite). Spar crystals are larger towards the base of the section, forming bladed calcite coronas around detrital grains and as infills within voids. These sparitic microtextures grade upwards towards much smaller crystals where they form only thin grain coatings. A series of dense, reddened microspar horizons are present throughout the sample, frequently accompanied by pelleted micrite and dense micritic patches. In many locations, this microspar has overprinted the sparitic groundmass. The gradational contacts between cement types suggest a degree of ingrowth of the cement into the detrital grains. Void spaces are present throughout the sample, and many of these have been infilled with spar crystals. Within numerous voids, the infilling propagates from the centre of the void space, rather than as initial coatings on the void wall. This may suggest that the initial coatings have since been removed, by dissolution processes for example. Cracks within the groundmass are less abundant than the void spaces, but are also infilled with small spar crystals. These features may reflect a greater degree of carbonate complexity, possibly due more than one carbonate precipitation phase.
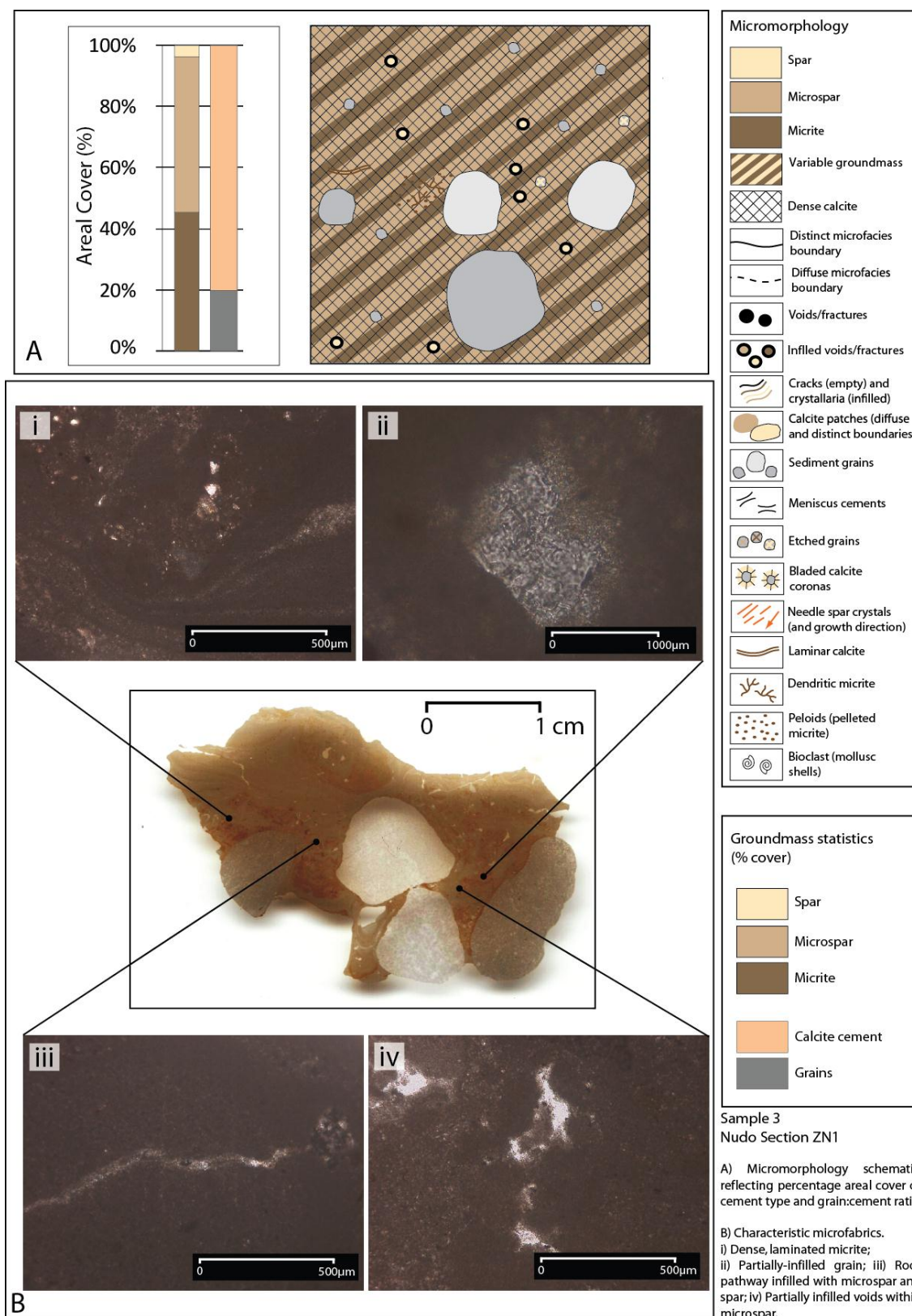
Fig. 7.3 – Sample 3 - Micromorphology of secondary carbonate accumulations at Nudo Section ZN1: A) Micromorphology schematic and groundmass statistics; B) Plates of characteristic microfabrics.

Micromorphology (legend)
- Spar
- Microspar
- Micrite
- Variable groundmass
- Dense calcite
- Distinct microfacies boundary
- Diffuse microfacies boundary
- Voids/fractures
- Inflled voids/fractures
- Cracks (empty) and crystallaria (infilled)
- Calcite patches (diffuse and distinct boundaries
- Sediment grains
- Meniscus cements
- Etched grains
- Bladed calcite coronas
- Needle spar crystals (and growth direction)
- Laminar calcite
- Dendritic micrite
- Peloids (pelleted micrite)
- Bioclast (mollusc shells)

Groundmass statistics (% cover)
- Spar
- Microspar
- Micrite
- Calcite cement
- Grains

Sample 4
Nudo Section AN1

A) Micromorphology schematic, reflecting percentage areal cover of cement type and grain:cement ratio.

B) Characteristic microfabrics.
i) Insipient spar infilling; ii) Spar infilling voids in microspar; iii) Dense microspar with spar-infilled cracks; iv) large spar crystals.

Fig. 7.4 – Sample 4 - Micromorphology of secondary carbonate accumulations at Nudo Section AN1: A) Micromorphology schematic and groundmass statistics; B) Plates of characteristic microfabrics.

7.2.5   Sample 5 – Nudo Arandelovo Unit (correlated to Sections AN1 and AN2)

This sample is obtained from a cemented bench at the surface of the Arandelovo Unit, close to the border of Montenegro and Bosnia- Herzegovina. This phreatic carbonate horizon can be traced along the terrace surface and correlates with the logged sections AN1 and AN2. In thin section, this calcite presents a single, yet highly heterogeneous microfacies, with a variable micrite-spar groundmass interspersed with microsparitic patches (45% spar, 10% microspar, 45% micrite) (Fig. 7.5). The carbonate groundmass contains abundant detrital grains (50% calcite, 50% grains) ranging from coarse sand and granules (100 – 1,800 µm) to pebble sized clasts. Void spaces are abundant throughout the sample and many have been infilled by spar, microspar or micrite. Unlike the other samples from Unijerina and Nudo, spar crystal size and infill pattern are highly variable throughout the sample. For example, micrite is dominant in several areas of this profile with spar as a secondary infill. In other samples analysed from Orjen spar forms the dominant cement type with secondary infills of micrite or microspar. Occasional spar-micrite laminae are present at clast surfaces here, and a number of grains have been partially infilled by microsparitic cements. The majority of the minor microsparitic component (10%) forms a series of reddened microspar-micrite horizons. This complex interposing of microstructures is indicative of at least two phases of carbonate development.

The following sections (7.2.6 – 7.2.11) discuss the micromorphology of Samples 6 – 11 which are taken from a stacked sequence of cemented benches within Section AN2 of the Nudo valley, Arandelovo Unit. These are exposed within a track cutting and present thick (up to 50 cm) phreatic carbonates. The section has been logged as a continuous sequence from the base of Bench 1 (Sample 6) to the top of Bench 6 (Sample 11) (Chapter 5).

Legend entries (Micromorphology):
- Spar
- Microspar
- Micrite
- Variable groundmass
- Dense calcite
- Distinct microfacies boundary
- Diffuse microfacies boundary
- Voids/fractures
- Infilled voids/fractures
- Cracks (empty) and crystallaria (infilled)
- Calcite patches (diffuse and distinct boundaries
- Sediment grains
- Meniscus cements
- Etched grains
- Bladed calcite coronas
- Needle spar crystals (and growth direction)
- Laminar calcite
- Dendritic micrite
- Peloids (pelleted micrite)
- Bioclast (mollusc shells)

Groundmass statistics (% cover):
- Spar
- Microspar
- Micrite
- Calcite cement
- Grains

Sample 5
Nudo Section AN2 and AN1

A) Micromorphology schematic, reflecting percentage areal cover of cement type and grain:cement ratio.

B) Characteristic microfabrics.
i) Laminated spar and micrite (arrowed); ii) Spar-infilled void within micrite.

Fig. 7.5 – Sample 5 - Micromorphology of secondary carbonate accumulations at Nudo Section AN1: A) Micromorphology schematic and groundmass statistics; B) Plates of characteristic microfabrics.

7.2.6   Sample 6 – Nudo Arandelovo Unit (Section AN2)

This carbonate is taken from the lowest bench of the exposure at Section AN2 (Bench 1) and is dominated by coarse sand grains (30% calcite, 70% grains) and granules (80 – 1,900 µm) (Fig. 7.6). The calcite groundmass contains sparitic cements of a range of crystal size, with micrite patches and infills, and a minor microspar component (50% spar, 10% microspar, 40% micrite).

The grain-calcite boundaries throughout this section are often diffuse and suggest a degree of passive, calcite ingrowth onto detrital grains. The degree of this ingrowth is not dependent on grain size, and both small and larger grains have undergone infilling. There is only limited evidence of etched grains. This suggests that alpha fabric environments have not dominated the formation mechanisms of this carbonate. This is supported by the presence of meniscus cements and bridges formed between detrital grains and the laminated coatings around larger grains/clasts, which are indicative of passive, phreatic carbonate precipitation.

7.2.7   Sample 7 – Nudo Arandelovo Unit (Section AN2)

This sample, from Bench 2 (Sample 7), contains very limited calcite content (30% calcite, 70% grains) with a dominance of larger detrital clast sizes (50 – 2,000 µm) (granule to small pebbles) in comparison with the lower cemented bench (Fig. 7.7). Calcite has dominantly formed as thin micritic coatings on detrital grains (70%), with a small input of microspar (10%) and spar (20%) forming as elongate fronds around larger grain surfaces. As observed in the lower cemented bench, there is some evidence of micritic and sparitic meniscus cements forming between detrital grains. Carbonate characteristics largely resemble the features observed within Bench 1 and are indicative of a single phase carbonate, or a more complex profile that has become homogenised. The formation history of these calcite profiles is discussed in detail in Chapter 9.
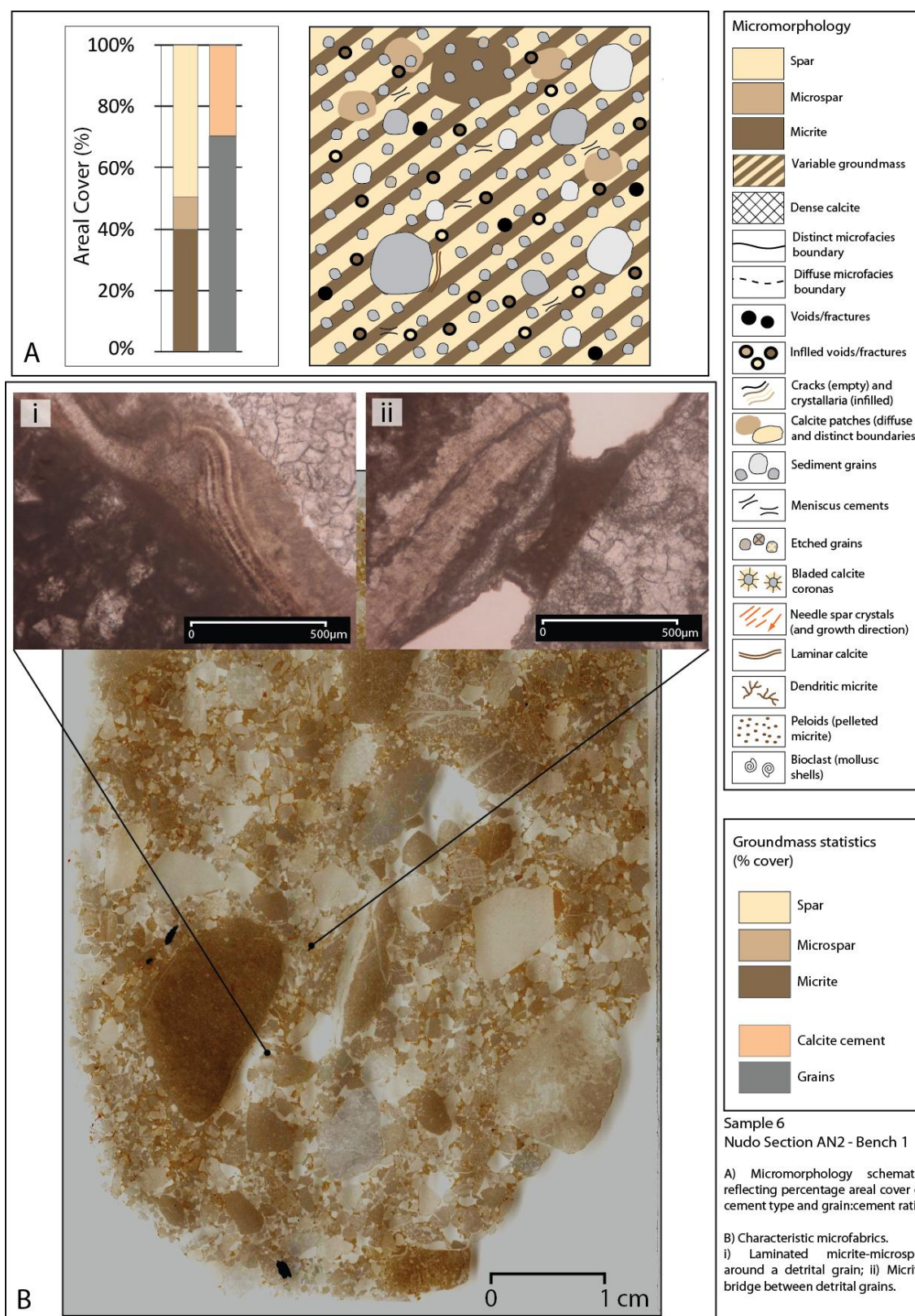
Fig. 7.6 – Sample 6 - Micromorphology of secondary carbonate accumulations within Bench 1 at Nudo Section AN2: A) Micromorphology schematic and groundmass statistics; B) Plates of characteristic microfabrics.
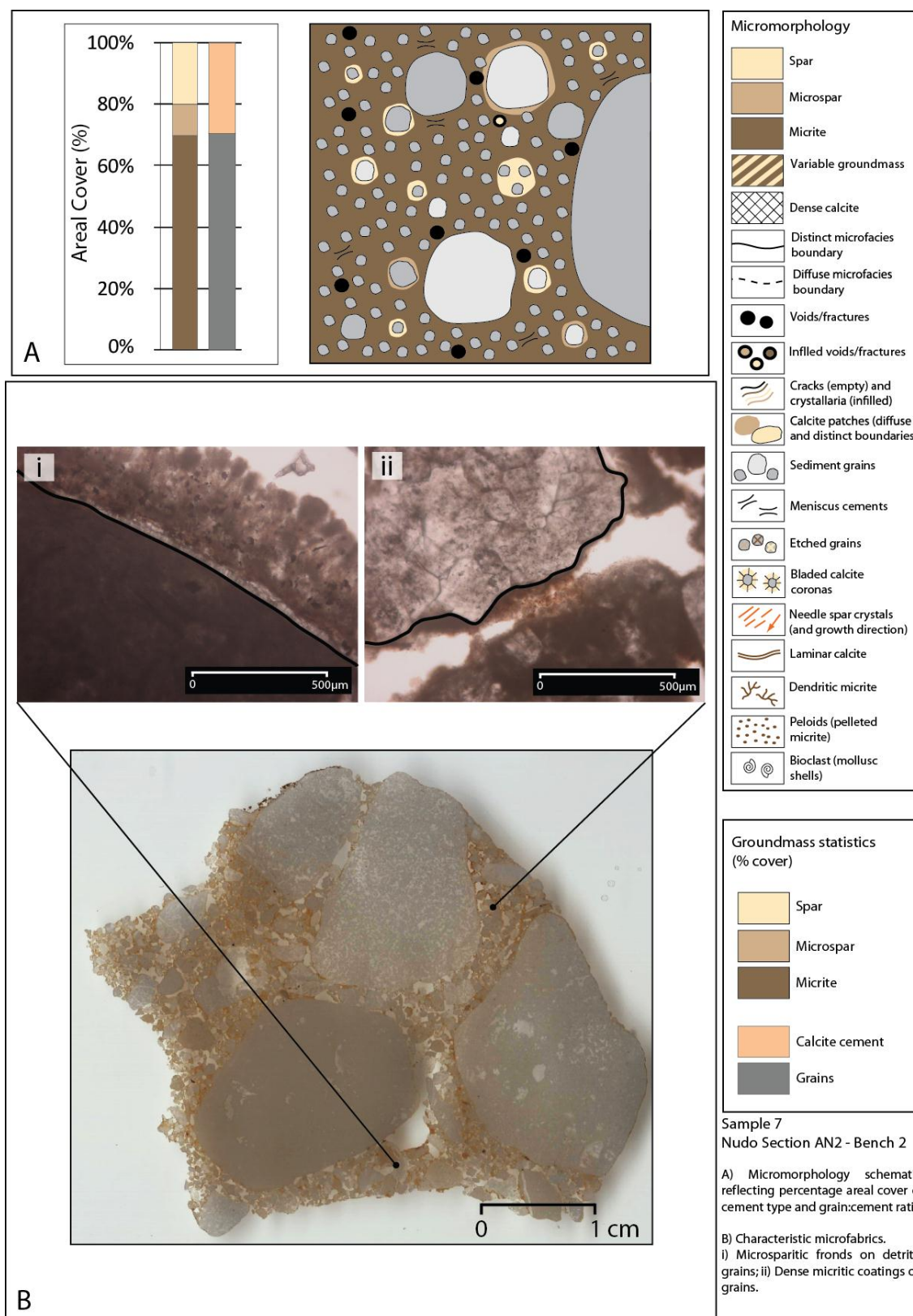
Fig. 7.7 – Sample 7 - Micromorphology of secondary carbonate accumulations within Bench 2 at Nudo Section AN2: A) Micromorphology schematic and groundmass statistics; B) Plates of characteristic microfabrics.

7.2.8 Sample 8 – Nudo Arandelovo Unit (Section AN2)

Similar to the lower cemented benches, Bench 3 (Sample 8) contains abundant detrital grains (85 – 1,600 µm), with only limited calcite precipitation (10% calcite, 90% grains) (Fig. 7.8). Where cements *are* present they are dense and strongly developed within grain interstices. Grains typically have sharp contacts with the surrounding groundmass and do not display the gradational encroachment of the groundmass onto the grain boundary that is observed within the lower benches. Instead, calcite here has largely formed as microsparitic coatings around clasts (80%) and as sparitic (10%) and micritic (10%) infills within voids. Such void spaces are present throughout the section, and many show no evidence of infilling. Microspar also forms as meniscus cements and bridges between detrital grains, as well as laminations at the base of the sample. As observed within Sample 5 (Fig. 7.5), this microfacies also contains patches of reddened microspar and pelleted micrite, as well as dense areas of micritic groundmass, that may be indicative of beta microfabrics. The uniform development of this microfacies reflects a single phase, or highly overprinted, calcite profile.

7.2.9 Sample 9 – Nudo Arandelovo Unit (Section AN2)

Calcites from Bench 4 (Sample 9) present a highly variable microfacies when compared to the lower cemented horizons (Fig. 7.9). The section contains a large clast towards the base surrounded by coarse sand and granular detrital grains (50 – 2,600 µm) set within a calcite cement. This texture grades towards a dense calcite cement with a negligible grain content in the upper horizons (overall 60% calcite, 40% grains). Throughout the sample, the groundmass is dominated by dense microspar (25% spar, 70% microspar, 5% micrite) with sparry infills within voids, and small patches of pelleted micrite. Within the lower horizons, grain-cement boundaries are frequently diffuse. This is indicative of the ingrowth of calcite onto the smaller (sand) detrital grains. Voids and cracks within the lower horizons are infilled with large, often elongate spar crystals. Some evidence of very dense microspar and reddened pelleted micrite is also present (see also samples 5 and 8). The upper horizons also contain these very dense microsparitic cements, with few detrital grains. Here grain-cement contacts remain sharp, and there is no evidence of ingrowth or infilling. Void spaces here are limited, and are largely infilled with microspar. Pelleted micrite is also present throughout these upper horizons. The complex micromorphology within this sample may be indicative of multiple, overprinted phases of carbonate development.
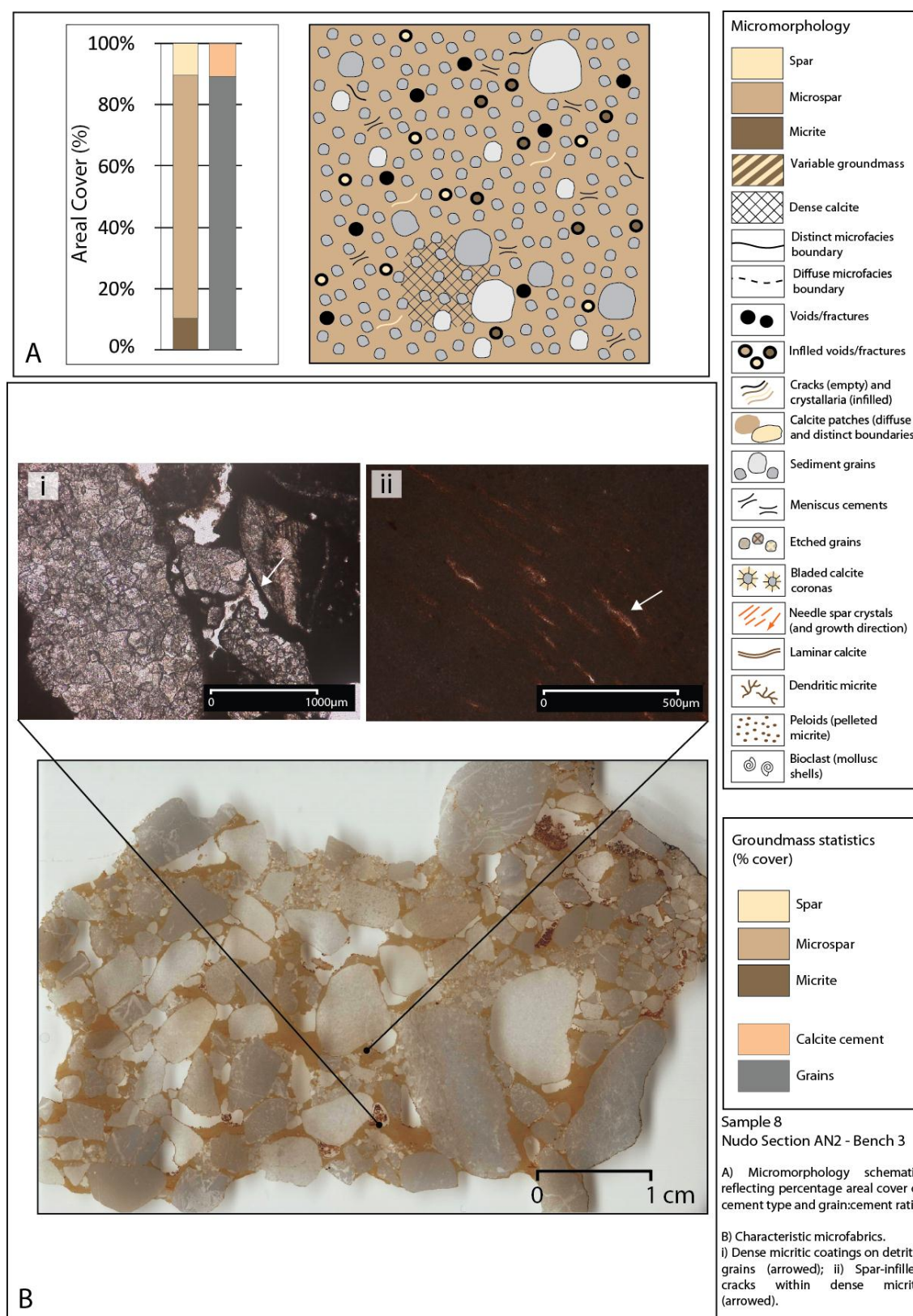
Fig. 7.8 – Sample 8 - Micromorphology of secondary carbonate accumulations within Bench 3 at Nudo Section AN2: A) Micromorphology schematic and groundmass statistics; B) Plates of characteristic microfabrics.
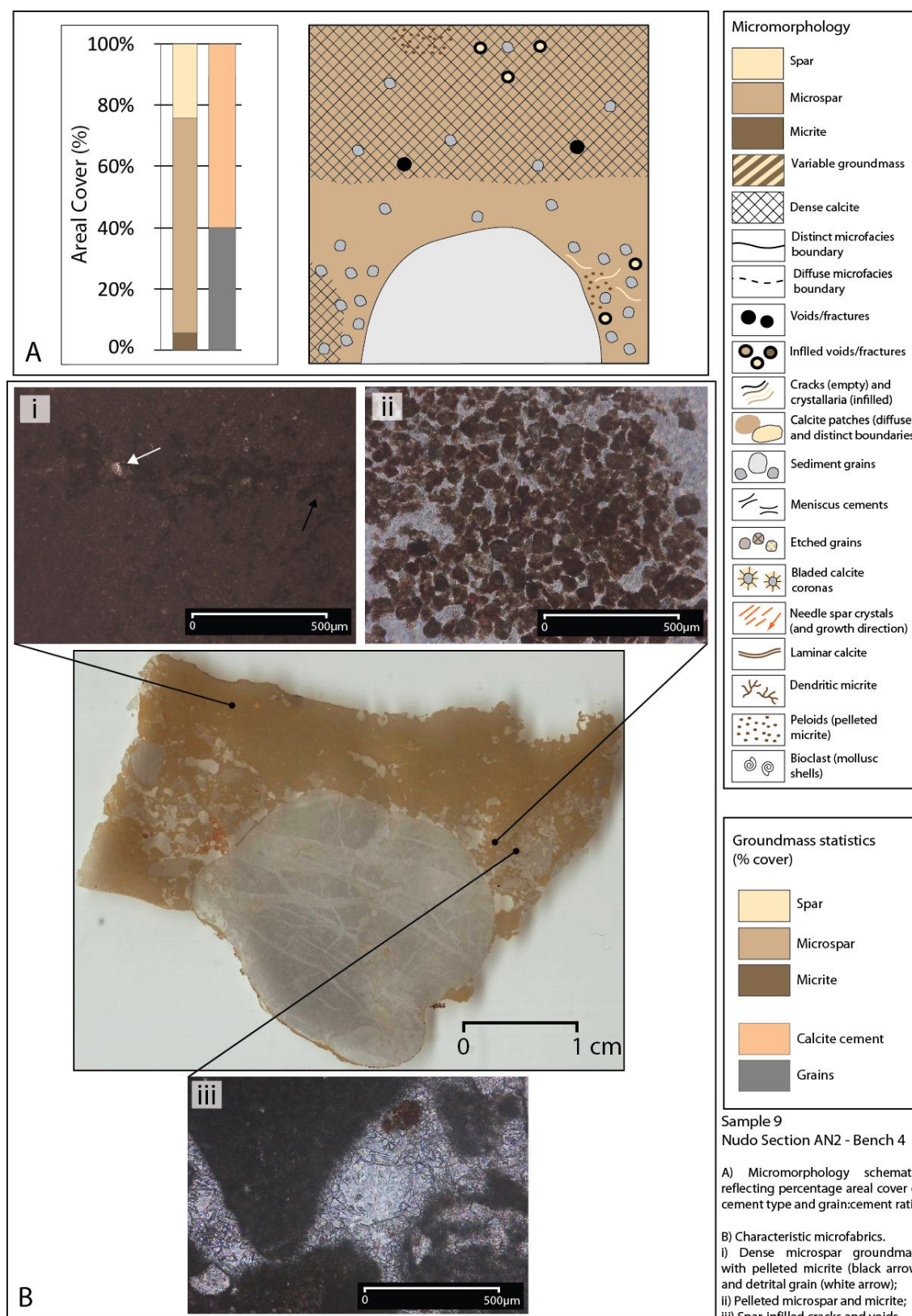
Fig. 7.9 – Sample 9 - Micromorphology of secondary carbonate accumulations within Bench 4 at Nudo Section AN2: A) Micromorphology schematic and groundmass statistics; B) Plates of characteristic microfabrics.

7.2.10 Sample 10 –Nudo Arandelovo Unit (Section AN2)

This calcite, within Bench 5, contains a very densely cemented carbonate with only limited evidence of microstructure development (Fig. 7.10). This sample is abundant in detrital grains (40% calcite, 60% grains) which display sharp contacts with the surrounding groundmass. Cements are predominantly microsparitic, with abundant micrite throughout the sample, and sparry infills within voids and cracks (5% spar, 55% microspar, 40% micrite). Unlike other cemented benches from this terrace exposure, void spaces within this profile are largely empty or fringed with small spar crystals or microspar. This may reflect the dissolution of existing infills and the ingrowth of calcite within void spaces. The section is broadly homogenous with no significant development of either alpha or beta microfabrics. The density of the cements within this horizon suggests that successive phases of overprinting may have altered the micromorphological characteristics towards a uniform profile that does not necessarily resemble the original microtextures. This is discussed in detail in Chapter 9.

7.2.11 Sample 11 – Nudo Arandelovo Unit (Section AN2)

This sample is taken from the highest cemented bench within this terrace exposure and contains microfabrics representative of those observed within the lower cemented horizons (Sample 6) (Fig. 7.11). Detrital grain content is high (30% calcite, 70% grains) with abundant sand to granule sized clasts (60 – 1,600 µm). The surrounding groundmass contains densely cemented microspar and micrite cements with sparry infills within void spaces (10% spar, 50% microspar, 45% micrite). Cement crystal sizes frequently fall between the microspar and micrite size fractions (microspar: 30 - 4 µm; micrite: <4 µm). This forms a distinctive feature of this sample that is not evident in other calcites analysed here. As has been observed in the underlying cemented horizon (Sample 10), this microfacies is uniformly developed with very limited evidence of alpha or beta microstructure development. This may be due to the exposure of this carbonate to multiple phases of dissolution and or (re)precipitation. Over several climatic cycles, this would cause the carbonate horizon to bear the imprint of multiple calcite precipitation phases. In effect, this may produce a broadly homogenous sample that does not necessarily reflect the complexity of individual calcite precipitation phases.
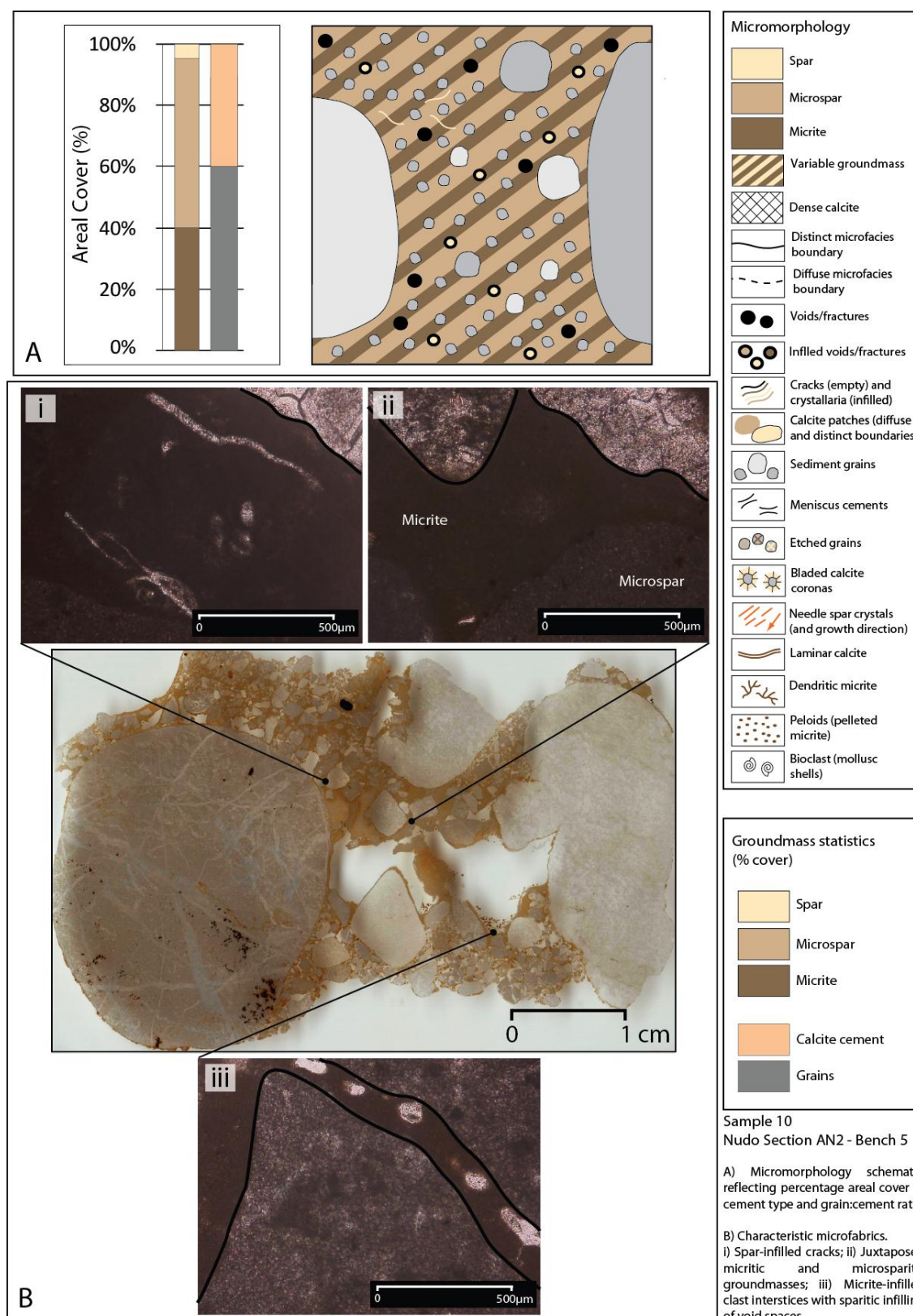
Fig. 7.10 – Sample 10 - Micromorphology of secondary carbonate accumulations within Bench 5 at Nudo Section AN2: A) Micromorphology schematic and groundmass statistics; B) Plates of characteristic microfabrics.
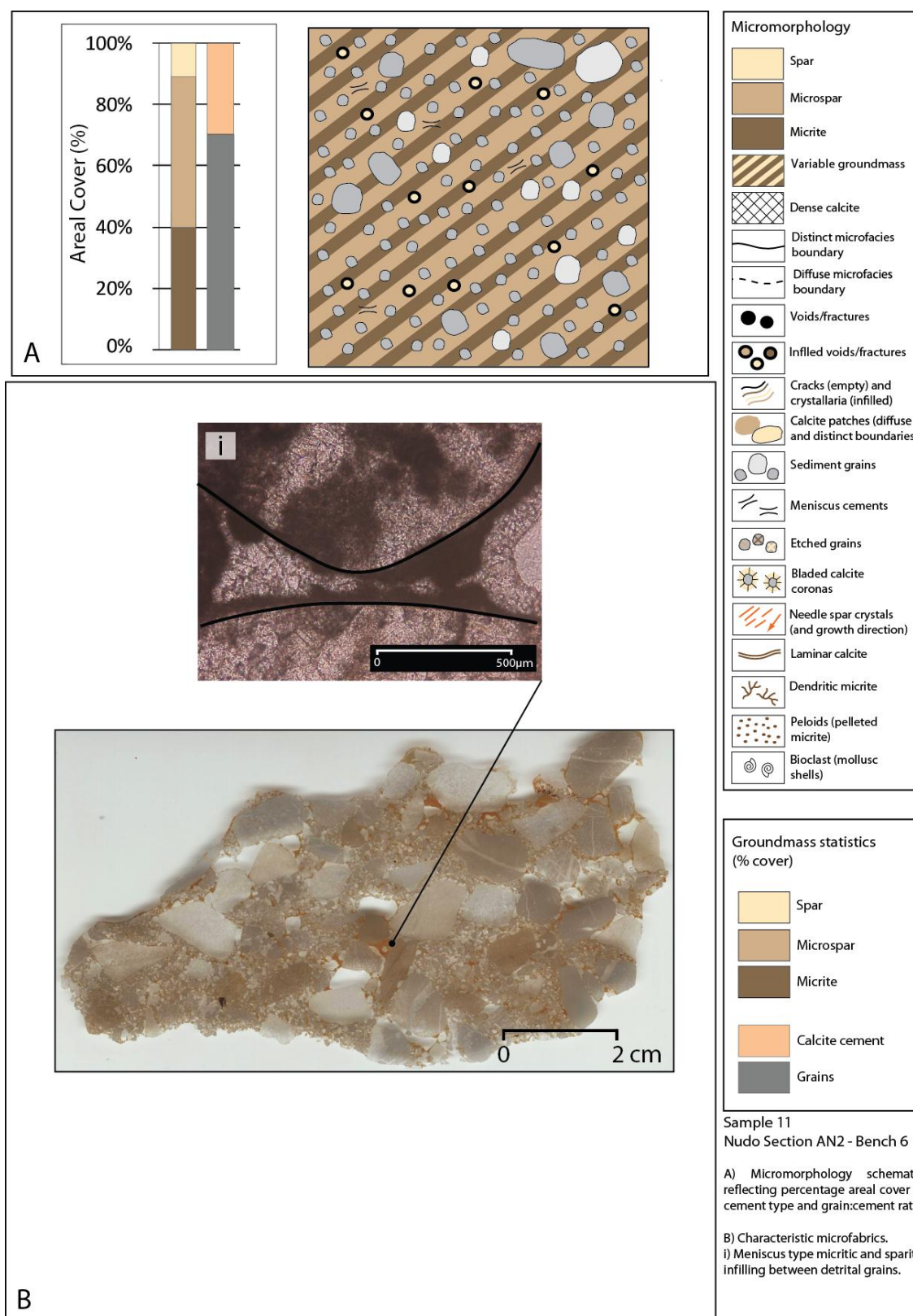
Fig. 7.11 – Sample 11 - Micromorphology of secondary carbonate accumulations within Bench 6 at Nudo Section AN2: A) Micromorphology schematic and groundmass statistics; B) Plates of characteristic microfabrics.

7.3   Summary and carbonate development statistics

Table 7.2 presents the summary statistics of micromorphological features and groundmass observations within the sampled calcite horizons (see methods in Chapter 4). These values are summed to provide an overall score of carbonate complexity for each profile. Groundmass type (S – Spar; MS – Microspar; M - Micrite), grain:cement ratios (%), and detrital grain sizes (µm) are also presented here to aid comparisons between samples.

At Unijerina (Table 7.2), the data suggest that the phreatic carbonate horizon (Sample 1) contains a greater complexity of microfabrics (a total of 6 features) than Sample 2, and a greater abundance of alpha (non-biogenic) fabrics. The vadose zone carbonate (Sample 2) forms three calcite rinds around a limestone clast. These cements contain multiple microfacies, yet each with lower complexity (total features of 2 and 3) than the phreatic carbonate of Sample 1 (6 features). These microfacies contain a greater abundance of biogenic (beta) microstructures than Sample 1, and a limited occurrence or absence of void spaces, cracks, and detrital grains which are indicative of alpha fabric environments. The Nudo terraces (Table 7.2) contain a series of phreatic carbonate benches. Calcites within Section AN2 are characterised by meniscus cements, infilled cracks/voids and high grain:cement ratios (>40:60). These features are typical of carbonate precipitation in association with groundwater and contrast with the vadose zone cements at Unijerina. The phreatic carbonates of the Zaslap Unit (ZN1) also contain biogenic microstructures (such as dendritic micrite and pelleted micrite). This is deemed indicative of multiple carbonate formation mechanisms; both passively in association with groundwater, and through biogenic activity within the host sediments/soil. This is reflected within the comparatively high total carbonate complexity score for the Zaslap Unit, the lowest terrace surface within the Nudo valley (score of 7) in comparison with cemented benches of the higher altitude Arandelovo Unit (scores of 4-9). It may be that the exposure of the higher terrace surfaces for greater periods of time may have led to the overprinting and homogenisation of existing microfabrics (see Chapter 9).

The microfacies data from these samples provide an insight into the micromorphological characteristics of vadose and phreatic carbonates within the alluvial sediments of Orjen. This can be used to develop a more detailed qualitative model of the palaeoenvironmental factors influencing carbonate development (Chapter 9) and inform the selection of secondary carbonates for U-series analysis (Chapter 8).

Sample Number (Sampled facies)		1 (UN3c)	2 (UN3c - a)	2 (UN3c - b)	2 (UN3c - c)	3 (ZN1a)	4 (AN1)	5 (AN1+2)	6 (AN2)	7 (AN2)	8 (AN2)	9 (AN2)	10 (AN2)	11 (AN2)
Feature	**Content**													
Dominant Groundmass	*S/MS/M*	S	S	S	MS/M	S	S/M	S/M	M	MS	MS	MS/M	MS/M	S
Grain:Cement Ratio (%)	*Grain*	50	1	0	20	60	50	70	70	90	40	60	70	0
	Cement	50	99	100	80	40	50	30	30	10	60	30	30	100
Grains (μm)	*Min.*	300	-	-	65	100	100	80	50	85	50	60	60	-
	Max.	1,400	-	-	1,480	2,000	1,800	1,900	2,000	1,600	2,600	2,800	1,600	-
Etched Grains	*P*	-	-	-	-	●	●	●	●	-	-	-	-	-
	F	-	-	-	-	-	-	-	-	-	-	-	-	-
	D	-	-	-	-	-	-	-	-	-	-	-	-	-
Voids (empty)	*P*	●	●	●	●	●	●	-	●	-	●	●	-	●
	F	-	-	-	-	-	-	●	-	●	-	-	●	-
	D	-	-	-	-	-	-	-	-	-	-	-	-	-
Infilled Voids	*P*	-	-	-	-	●	●	●	●	●	●	●	●	-
	F	●	-	-	-	-	-	-	-	-	-	-	-	●
	D	-	-	-	-	-	-	-	-	-	-	-	-	-
Cracks (empty)	*P*	-	-	-	-	-	●	●	-	-	●	●	-	-
	F	-	-	-	-	-	-	-	-	-	-	-	-	-
	D	-	-	-	-	-	-	-	-	-	-	-	-	-
Infilled Cracks	*P*	●	-	-	●	●	●	●	-	-	●	●	●	-
	F	-	-	-	-	-	-	-	-	-	-	-	-	-
	D	-	-	-	-	-	-	-	-	-	-	-	-	-
Calcite Patches	*P*	●	●	-	-	-	●	-	●	●	-	-	-	-
	F	-	-	-	-	-	-	●	-	-	-	-	-	-
	D	-	-	-	-	-	-	-	-	-	-	-	-	-
Bladed Calcite Corona	*P*	-	-	-	-	-	●	-	-	-	-	-	-	-
	F	-	-	-	-	-	-	-	-	-	-	-	-	-
	D	-	-	-	-	-	-	-	-	-	-	-	-	-
Dendritic Micrite	*P*	-	-	●	-	●	-	-	-	-	-	-	-	-
	F	-	-	-	-	-	-	-	-	-	-	-	-	-
	D	-	-	-	-	-	-	-	-	-	-	-	-	-
Pelleted Micrite	*P*	-	-	-	●	●	-	-	-	-	●	●	-	-
	F	-	-	●	-	-	●	-	-	-	-	-	-	-
	D	-	-	-	-	-	-	-	-	-	-	-	-	-
Meniscus Cement	*P*	●	-	-	-	-	-	-	●	-	●	-	-	●
	F	-	-	-	-	-	-	-	-	●	-	-	-	-
	D	-	-	-	-	-	-	-	-	-	-	-	-	-
Laminated Micrite	*P*	-	-	-	-	●	-	●	●	-	-	-	-	-
	F	-	-	-	-	-	-	-	-	-	-	-	-	-
	D	-	-	-	-	-	-	-	-	-	-	-	-	-
Bioclast	*P*	●	-	-	-	-	-	-	-	-	-	-	-	-
	F	-	-	-	-	-	-	-	-	-	-	-	-	-
	D	-	-	-	-	-	-	-	-	-	-	-	-	-
Total Score		7	2	4	3	7	9	9	6	6	6	5	4	4
No. Features Present		6	2	3	3	7	8	7	6	4	6	5	3	3

Table 7.2 – Micromorphological summary statistics for secondary carbonate samples from Unijerina. Dominant groundmass types are classified as S (spar); MS (microspar); M (micrite). Microstructure/feature abundance is categorised as P (present, score: 1); F (frequent, score 2); D (dominant, score 3).

CHAPTER EIGHT

Results – Geochronology: U-series and Harden Index Dating Techniques

---

Synopsis

Chapters 5 – 7 have discussed the geomorphological, sedimentological and secondary carbonate characteristics of the alluvial sequences surrounding Mount Orjen. These have provided an understanding of the depositional environment within each fluvial setting. Establishing a robust chronology for these deposits is fundamental for their correlation, both between contrasting fluvial records and with the glacial record of Mount Orjen presented by Hughes *et al*. (2010). This also enables them to be placed within a wider context of Mediterranean Quaternary environmental change. In this study, U-series analysis is used as a radiometric dating technique to assess the timing of fluvial activity in response to Pleistocene glaciation (Section 8.1). The Harden Index provides a relative age indicator of soil horizon development (Section 8.2). This technique is particularly effective where U-series dating has not been possible or where differentiation and correlation between land surfaces is otherwise complicated.

8.1 U-series dating: radiometric age indicators

U-series methods are used to date the timing of secondary carbonate (calcite) formation. When these calcites form within Quaternary sediments, U-series dating provides minimum ages of landform/land surface development. This can allow fluvial morphosedimentary records to be accurately correlated between neighbouring valleys. U-series dating has also been used on the Pleistocene glacial deposits of Mount Orjen (Hughes *et al*., 2010). This means that the U-series geochronology for the alluvial deposits can be directly correlated with the glacial record to form a fully integrated reconstruction of glacial and fluvial landsystem dynamics surrounding the Orjen massif.

8.1.1 U-series dating theory

U-series dating is based on the measurement of three naturally occurring radioactive decay series of uranium (U) and thorium (Th): ^{238}U (half-life of 4.49 x 10^9 years), ^{235}U (7.13 x 10^8

years) and ^{232}Th (1.14 x 10^{10}), each decaying to a stable isotope of lead (^{206}Pb, ^{207}Pb and ^{208}Pb, respectively) (Bourdon *et al.*, 2003) (Fig. 8.1). The short half-lives of the daughter isotopes of ^{232}Th make this unsuitable as a geochronological indicator. As will be discussed, this isotope does, however, play an important role in U-series dating as it can be used to correct for detrital contamination (Walker, 2005). Of the uranium isotopes, ^{238}U is the most abundant, making it the most appropriate for use within geological research. ^{235}U is much less abundant, with ^{238}U: ^{235}U activity ratios of 21.7:1, making its measurement more difficult (Schwarcz, 1989). The ^{238}U decay series is therefore the most effective for U-series within Quaternary geochronology (Smart, 1991). This method uses the ^{230}Th/^{234}U daughter/parent combination of the ^{238}U decay chain (Fig. 8.1). The ^{230}Th/^{234}U method is based on the daughter-deficiency technique, where the parent nuclide (^{234}U) is deposited free of its daughter (^{230}Th) and the age of the deposit is determined by the degree of ingrowth of the daughter towards secular equilibrium (Ku, 2000).
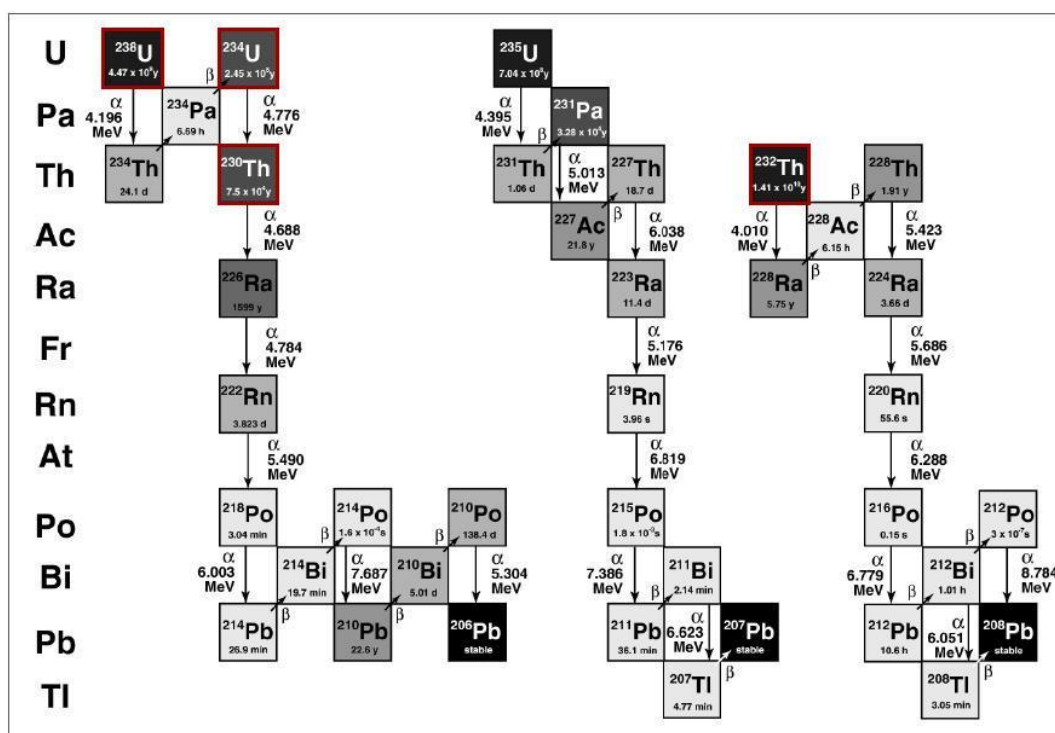
Fig. 8.1 – Schematic diagram of the ^{238}U, ^{235}U and ^{232}Th decay chains. Vertical lines reflect alpha (α) decay whilst diagonal lines indicate beta (β) decay mechanisms. Darker grey boxes indicate longer half-lives. Isotopes pertinent to the use of U-series within Quaternary research are indicated in red. Adapted from Bourdon *et al*. (2003).

Uranium is highly soluble, and readily transported, in natural waters. Th is comparatively insoluble or becomes quickly scavenged out of solution, rendering it broadly immobile in the near surface environment (Langmuir and Herman, 1980; Ku, 2000). When a mineral such as

calcite precipitates from an aqueous solution, it will contain U (at the parts per million, ppm, level) but negligible quantities of Th. As secondary carbonates accumulate within a sedimentary body, they contain ^{234}U but not the daughter isotope, ^{230}Th. Over time, this disequilibrium is altered by the ingrowth of the daughter isotope, ^{230}Th. Measuring the extent of this ingrowth, via U-series methods, serves as an indicator for the time that has elapsed since carbonate precipitation (Walker, 2005). This disequilibrium is compounded by the preferential release of ^{234}U from mineral surfaces, leading to disequilibrium between ^{238}U and ^{234}U within natural waters (Ku, 2000; Hughes, 2004; Fig. 8.2). Recently-precipitated secondary carbonates may therefore be enriched in ^{234}U, which decays over time within a closed system in accordance with its half-life (2.5×10^5 years) (Ku, 2000). This decay of excess ^{234}U increases the $^{230}Th/^{234}U$ ratio at any given time and must be corrected for during U-series age calculations.
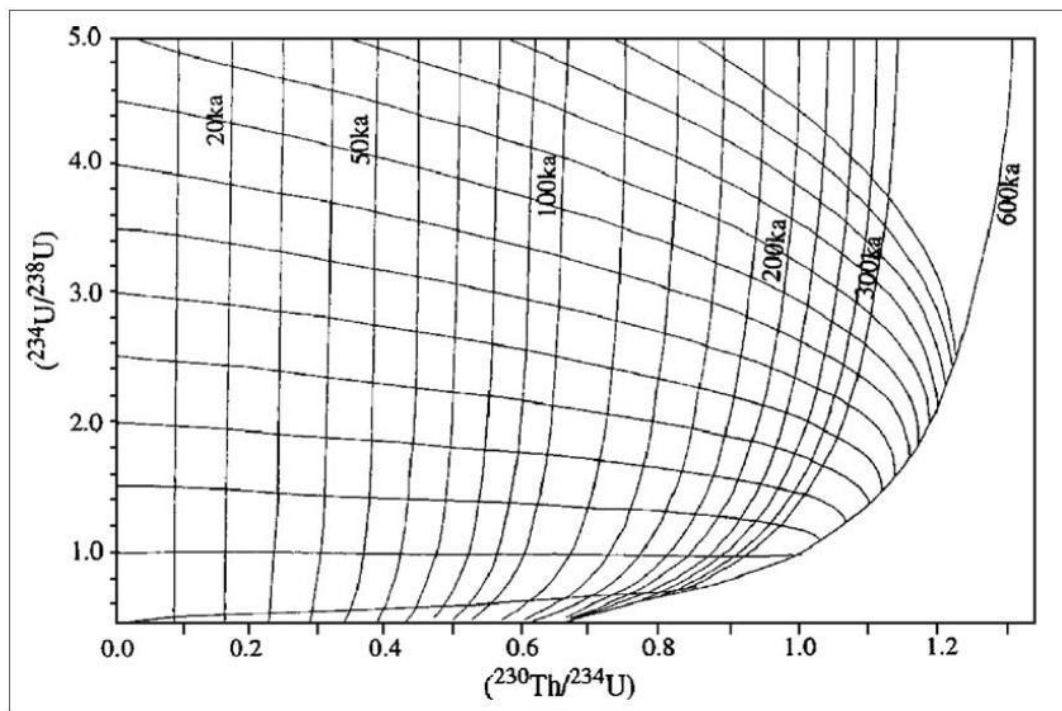
Figure 8.2 – Variations in $^{230}Th/^{234}U$ and $^{234}U/^{238}U$ activity ratios over time, and within a closed system, assuming no initial ^{230}Th and for varying initial $^{234}U/^{238}U$. The (sub-) vertical lines are isochrons (of constant age). The (sub-) horizontal lines are growth curves, reflecting change in nuclide activity ratios as age increases for various $^{234}U/^{238}U$ activity ratios. The area outside the graph (>600 ka) represents an infinite age determination. From Ku (2000); Walker (2005); Techer *et al.* (2006).

U-series ages are determined using measured $^{230}Th/^{234}U$ and $^{234}U/^{238}U$ ratios. The feasible dating range of the $^{230}Th/^{234}U$ U-series method is <100 years to 600, 000 years (Ku, 2000),

though incorporating analytical error, this is optimised at <350,000 years (Ku, 2000). Ages greater than this are subject to large error margins and are not always deemed reliable. In this thesis samples that have yielded ages older than 350,000 years are cited as '>350 ka' as the precision of these older samples is not always consistent with that of the younger carbonates.

The accurate dating of secondary carbonates using U-series methods relies heavily upon a series of assumptions. These inform the selection and sampling of calcites and must be considered during isotopic measurement and age calculation. They are based on the inferences that:

1. The secondary carbonate is free of detrital ^{230}Th, which can be incorporated into the cement via silicate or organic material. The presence of detrital ^{230}Th within a sample can be determined through measurements of ^{232}Th and is deemed to significantly reduce the quality of the sample when ^{230}Th/^{232}Th ratios are below 300 (Hellstrom, 2006). This is particularly important within phreatic carbonates, where the precipitation of calcite within small void spaces between sediment grains makes the extraction of pure carbonate crystals problematic. Detrital contamination can be corrected by measuring detritus samples separately (Chapter 4; Section 8.2). Uncorrected contaminated samples yield apparent ages older than the real U-series age as excess ^{230}Th suggests that the sample is closer to secular equilibrium than is actually the case.

2. U and Th have not migrated into or out of the sample since initial formation of the secondary carbonate, and a closed system has been maintained. This can be problematic where carbonate dissolution, reprecipitation and overprinting have occurred and can be avoided by thorough examination of the carbonate structure (in the field and using micromorphology) prior to U-series analysis.

8.1.2   U-series dating of fluvial sediments of the Orjen massif: determined ages

35 samples have been analysed from fluvial sequences surrounding the Orjen massif. These are derived from a range of carbonate forms from the weathering zone carbonate category of Candy *et al*. (2011) (Table 8.1). Eight of these samples have not yielded ages, and will be discussed in Section 8.1.3.

Two samples from the alluvial fans at Lipci and Kameno were used to assess the detrital contribution of U and Th to the calcites (Table 8.2). These correspond to U-series samples Kameno 2 and Lipci 4 (Table 8.1) and are deemed representative of the variety of detritus source areas of the secondary carbonates analysed from across Mount Orjen. This technique measures the ^{232}Th/^{238}U detrital molecular ratios of the two secondary carbonates, with the detrital component isolated, assuming that: all ^{232}Th is detrital in origin; the detritus is in secular equilibrium, and the isolated detrital material is representative of the likely contamination for all secondary carbonates used within the study. The two detritus samples provided detrital molecular ratios (^{232}Th/^{238}U) of 3.35 at Kameno and 2.80 at Lipci. These values reflect those observed within the glacial deposits of Mount Orjen (2.47) (Hughes *et al*., 2010) and within the central massifs of Montenegro (3.21) (Hughes *et al*., 2011b). They also bracket the global mean value for continental crust (3.12) (van Calsteren 2012, pers. comm.). The lithological similarity of the catchments surrounding Orjen supports the use of this global mean value for detrital correction at all sites. By using this standard, the correlation of these samples with wider U-series datasets, both in Montenegro and elsewhere, is deemed to be more robust. The higher detrital molecular ratio observed at Kameno reflects the outcrops of flysch within this catchment, in comparison to the catchment area of Lipci, which is almost entirely dominated by limestone lithologies (Chapter 3).

U-series ages require correction when ^{230}Th/^{232}Th ratios are <300 (Hellstrom, 2006). The secondary carbonates from Orjen largely yield ^{230}Th/^{232}Th ratios between 1.31 and 175.31 and there is no relationship between carbonate type (phreatic or vadose) and ^{230}Th/^{232}Th ratio. Only three samples exceed a value of 300 (Lipci 6, 325.91; Kameno 2, 420.81; Grahovo 1, 1540.44). All samples have been corrected here, including those with ratios >300, for consistency. Corrected and uncorrected ages are presented in Table 8.2. In the following discussion, U-series ages are quoted as uncorrected ages. This follows the methods outlined by Hughes *et al*. (2010; 2011b) on the glacial deposits of Mount Orjen and within the central massifs of Montenegro where corrected values are within the error margins of uncorrected ages.

Sampled Facies	U-series Sample	Secondary Carbonate Description	Age Determined? (Age, years)
Grahovo			
G1	Grahovo 1	Grahovo Section G1a, vadose carbonate at 285-290 cm	✓ (>350,000)
Kruševice			
Kr2b	Kruševice 1	Kruševice Section Kr2b, very friable clast coating at 250-260 cm	✗
Vrbanje			
V2a	Vrbanje 1	Vrbanje Section V2a, densely cemented, pure sparitic calcite coating on clast at 60-70 cm	✓ (126,552 ± 4,530)
Pirina Poljana			
P2a	Pirina Poljana 1	Pirina Poljana Section P2a, phreatic carbonate at c. 90 cm (below cemented bench)	✓ (213,467 ± 11,853)
P2a	Pirina Poljana 2	Pirina Poljana Section P2a, phreatic carbonate forming a cemented bench	✓ (77,162 ± 1,961)
Lipci			
L2a	Lipci 1	Lipci Section L2a, vadose carbonate at 96-106 cm	✓ (94,930 ± 2,949)
L2a	Lipci 2	Lipci Section L2a, vadose carbonate at 96-106 cm	✓ (99,336 ± 3,005)
L3a	Lipci 3	Lipci Section L3a, vadose carbonate at 170-180 cm	✓ (47,287 ± 1,237)
L4a	Lipci 4	Lipci incised tributary at Section L4a, large sparitic crystals within a flowing water carbonate at 54-68 cm	✓ (239,201 ± 14,203)
L4a	Lipci 5	Lipci incised tributary at Section L4a, large sparitic crystals within a flowing water carbonate at 54-68 cm	✓ (320,630 ± 33,381)
L4a	Lipci 6	Lipci incised tributary at Section L4a, large sparitic crystals within a flowing water carbonate at 100-120 cm	✓ (196,604 ± 10,685)
L4a	Lipci 7	Lipci incised tributary at Section L4a, large sparitic crystals within a flowing water carbonate at 140 cm	✓ (292,511 ± 26,580)
Kameno			
K1b	Kameno 1	Kameno Section K1b, large sparitic, vadose calcites forming a cemented bench at c. 430 cm	✓ (>350,000)
K1b	Kameno 2	Kameno Section K1b, large sparitic, vadose calcites forming a cemented bench at c. 430 cm	✓ (>350,000)
K1b	Kameno 3	Kameno Section K1b, large sparitic, vadose calcites forming a cemented bench at c. 430 cm	✓ (>350,000)

Table 8.1 – U-series sample locations and facies codes. Samples that yielded undeterminable ages are discussed in Section 8.1.3.

Sampled Facies	U-series Sample	Secondary Carbonate Description	Age Determined? (Age, years)
Nudo			
AN1 - correlated	Nudo 1 - A	Exposure adjacent to, and downstream of, Section AN1. A phreatic cemented bench at c. 850 cm	✗
AN1 - correlated	Nudo 2 - A	Exposure adjacent to, and downstream of, Section AN1. A phreatic cemented bench at c. 850 cm	✗
AN2 - Bench 1	Nudo 3 - A	Section AN2, friable phreatic carbonate within the lowest cemented bench at c. 120 cm	✓ (65,855 ± 5,165)
AN2 - correlated	Nudo 4 - A	Exposure downstream of Section AN2, correlates to surficial phreatic carbonate of this unit	✗
AN2 - correlated	Nudo 5 - A	Nudo Section AN2 correlated - taken from capping carbonate near border c. 200 cm	✓ (56,525 ± 1,340)
VN1	Nudo 6 - V	Section VN1, very friable phreatic calcite coating on clasts at c. 100 cm	✓ (>350,000)
KN1	Nudo 7 - K	Section KN1, friable phreatic calcite forming incipient coatings around clasts at c. 400 cm	✗
JN1	Nudo 8 - J	Section JN1, friable phreatic calcite as incipient coatings around clasts at c. 400 cm	✓ (>350,000)
JN1	Nudo 9 - J	Section JN1, friable and detritus-rich phreatic calcite at c. 100 cm	✗
ZN1	Nudo 10 - Z	Section ZN1, phreatic carbonate at base of section, sample obtained at its surface, from c. 100 cm	✗
ZN1 - correlated	Nudo 11 - Z	Exposure upstream of Section ZN1, sparitic calcite crystals as clast coatings at c. 250 cm	✓ (146,778 ± 9,092)
ZN1 - correlated	Nudo 12 - Z	Exposure upstream of Section ZN1, densely-cemented and sparitic, vadose cement, not *in-situ* but has been dislodged from a surficial cemented horizon at c. 300 cm (above Nudo 11 - Z)	✓ (>350,000)
Unijerina			
U2a-ii	Unijerina 1	Section U2a, friable phreatic carbonate within the diamicton, at c. 270 cm	✓ (>350,000)
U3c	Unijerina 2	Section U3c, sparitic phreatic carbonate within the capping fluvial deposits	✓ (80,256 ± 5,863)
U3c	Unijerina 3	Section U3c, sparitic phreatic carbonate within the capping fluvial deposits	✓ (16,577 ± 360)
U3c	Unijerina 4	Section U3c, sparitic phreatic carbonate within the capping fluvial deposits	✓ (248,628 ± 16,690)
U3c	Unijerina 5	Section U3c, detritus-rich phreatic carbonate within the capping fluvial deposits	✗
Crkvice			
C1a	Crkvice 1	Section C1a, sparitic carbonate 'clast' (potentially reworked) at 200 cm	✓ (144,153 ± 5,067)
C2a	Crkvice 2	Section C2a, incipient phreatic carbonate accumulations on clasts at 80 cm	✓ (18,547 ± 409)
Sniježnice			
S1a - correlated	Sniježnice 1	Surficial, sparitic vadose carbonates on moraines grading into the surface of section S1a	✓ (268,253 ± 22,201)

Table 8.1 continued – U-series sample locations and facies codes. Samples that yielded undeterminable ages are discussed in Section 8.1.3.

U-Series Sample	Lipci 1	Lipci 2	Lipci 3	Lipci 4	Lipci 5	Lipci 6	Lipci 7	Kameno 1	Kameno 2	Kameno 3
^{238}U ppm	0.035141	0.048254	0.040645	0.044960	0.093720	0.069504	0.054392	0.172717	0.107043	0.186572
uncertainty	0.000138	0.000142	0.000116	0.000169	0.000273	0.000177	0.000116	0.000499	0.000287	0.000617
$(^{234}$U/^{238}U)	1.065922	1.045114	1.043621	1.069242	1.039572	1.074016	1.042278	1.001775	0.986860	0.990173
uncertainty	0.006056	0.004719	0.004590	0.006305	0.004923	0.004188	0.003870	0.004445	0.003932	0.004604
^{234}U ppm	0.000002	0.000003	0.000002	0.000003	0.000005	0.000004	0.000003	0.000009	0.000006	0.000010
uncertainty	0.000000	0.000000	0.000000	0.000000	0.000000	0.000000	0.000000	0.000000	0.000000	0.000000
^{230}Th ppb	0.000359	0.000496	0.000245	0.000711	0.001529	0.001036	0.000875	0.003195	0.001776	0.004064
uncertainty	0.000004	0.000005	0.000003	0.000007	0.000015	0.000011	0.000009	0.000030	0.000017	0.000047
^{232}Th ppb	1.446345	17.297911	37.096290	0.976989	5.408715	0.601300	9.338422	44.714100	0.794020	39.670412
uncertainty	0.261469	3.126954	6.705850	0.176665	0.977727	0.108732	1.688098	8.082852	0.143565	7.171244
$(^{230}$Th/^{232}Th)	48.248427	5.526309	1.306583	138.813735	53.358399	325.906693	17.802572	13.413989	420.810674	19.200662
uncertainty	2.081015	0.235034	0.056713	5.903630	2.274448	13.973645	0.759053	0.562676	17.680394	0.851279
$(^{230}$Th/^{234}U)	0.585289	0.600765	0.352549	0.903919	0.958987	0.848237	0.943124	1.128067	1.027084	1.343797
uncertainty	0.006127	0.005927	0.003787	0.008907	0.009555	0.008641	0.009403	0.010472	0.009586	0.015682
AGE UNCORRECTED (years)	94,930	99,336	47,287	239,201	320,630	196,604	292,511	>350,000*		
2 * uncertainty	2,918	2,972	1,231	13,488	29,499	10,685	23,995			
2 * uncertainty	- 2,949	- 3,005	- 1,237	- 14,203	- 33,318	- 10,170	- 26,580			
% Error	3.09	3.01	2.61	5.79	9.80	5.30	8.65			
Corrected values using ^{232}Th/^{238}U detrital molecular ratio 3.12										
$(^{230}$Th/^{234}U) Corr	0.579956	0.550013	0.091213	0.903273	0.958225	0.847834	0.939867	1.139960	1.027151	1.369917
uncertainty	0.008644	0.008138	0.001607	0.012632	0.013631	0.012232	0.013632	0.015615	0.013575	0.023413
$(^{234}$U/^{238}U) Corr	1.066827	1.051142	1.062326	1.069741	1.040337	1.074227	1.044807	1.001940	0.986828	0.989434
uncertainty	0.008631	0.007119	0.007664	0.008953	0.007034	0.005933	0.005643	0.006560	0.005568	0.006737
AGE CORRECTED (years)	93,551	86,455	10,434	238,310	318,427	196,317	286,675	No age	>350,000	No age
2 * uncertainty	4,059	3,652	383	18,720	40,191	13,691	32,385	All correlated to >350,000		
2 * uncertainty	- 4,119	- 3,703	- 384	- 20,095	- 47,462	- 14,471	- 37,228			
% Error	4.37	4.25	3.67	8.14	13.76	7.17	12.14			

Table 8.2 – U-series ages for secondary carbonates within the alluvial deposits surrounding the Orjen massif. Corrected and uncorrected ages are highlighted. *Sample Kameno 2 yielded an age of >350,000 years. Samples Kameno 1 and 3 yielded undetermined ages but have been correlated to >350,000 years on the basis of high ^{230}Th/^{232}Th ratios and similar U and Th isotope ratios between all samples from Kameno – see discussion for details.

U-Series Sample	Grahovo 1	Vrbanje 1	Pirina Poljana 1	Pirina Poljana 2	Nudo 3 - A	Nudo 5 - A	Nudo 6 - V	Nudo 8 - J	Nudo 11 - Z	Nudo 12 - Z
^{238}U ppm	3.299652	0.057041	0.608197	0.494590	0.891523	0.620712	0.849318	1.026203	0.586691	0.328534
uncertainty	0.011805	0.000152	0.001768	0.001518	0.003036	0.001980	0.001194	0.003452	0.001854	0.001089
(^{234}U/^{238}U)	0.995051	1.005732	1.022929	1.018683	1.017869	1.002395	0.994524	0.998719	1.003992	1.005662
uncertainty	0.005328	0.004243	0.004664	0.005493	0.005077	0.004931	0.004172	0.005001	0.004591	0.004927
^{234}U ppm	0.000177	0.000003	0.000034	0.000027	0.000049	0.000034	0.000046	0.000055	0.000032	0.000018
uncertainty	0.000001	0.000000	0.000000	0.000000	0.000000	0.000000	0.000000	0.000000	0.000000	0.000000
^{230}Th ppb	0.053350	0.000645	0.008791	0.004188	0.006738	0.004195	0.014187	0.016688	0.007133	0.005761
uncertainty	0.001811	0.000006	0.000084	0.000039	0.000194	0.000042	0.000139	0.000451	0.000109	0.000053
^{232}Th ppb	6.467664	29.049695	81.214448	48.925047	65.642251	286.131453	64.184684	34.340062	249.381977	36.519369
uncertainty	1.169149	5.251233	14.680911	8.844061	11.866407	51.723070	11.602457	6.209217	45.080171	6.601527
(^{230}Th/^{232}Th)	1540.438851	4.158727	20.245668	16.044804	19.193550	2.743638	41.298423	90.821308	5.350506	29.536650
uncertainty	102.634402	0.174564	0.855687	0.673089	1.179555	0.117023	1.754760	5.423918	0.256620	1.237108
(^{230}Th/^{234}U)	0.992674	0.686823	0.863272	0.507855	0.453634	0.411891	1.026098	0.994726	0.739851	1.065251
uncertainty	0.033718	0.006395	0.008289	0.004720	0.013061	0.004115	0.010087	0.026899	0.011318	0.009823
AGE UNCORRECTED (years)	**>350,000**	**126,552**	**213,467**	**77,162**	**65,855**	**56,525**	**>350,000**	**>350,000**	**146,778**	**>350,000**
2 * uncertainty		**4,530**	**10,853**	**1,948**	**5,057**	**1,333**			**8,768**	
2 * uncertainty		**- 4,148**	**- 11,337**	**- 1,961**	**- 5,165**	**- 1,340**			**- 9,092**	
% Error		**3.43**	**5.20**	**2.53**	**7.76**	**2.36**			**6.08**	
Corrected values using ^{232}Th/^{238}U detrital molecular ratio 3.12										
(^{230}Th/^{234}U) Corr		0.624260	0.857140	0.491622	0.440322	0.307118		0.994667	0.697777	1.067712
uncertainty		0.008935	0.011898	0.006568	0.018147	0.004680		0.038249	0.016185	0.014181
(^{234}U/^{238}U) Corr		1.006886	1.023982	1.019311	1.018313	1.002823		0.998705	1.004641	1.005877
uncertainty		0.006529	0.006750	0.007901	0.007271	0.007523		0.007112	0.006966	0.007098
AGE CORRECTED (years)	**>350,000**	**106,635**	**208,739**	**73,634**	**63,234**	**40,057**	**>350,000**	**>350,000**	**130,459**	**>350,000**
2 * uncertainty		**4,787**	**14,820**	**2,628**	**6,838**	**1,432**			**10,823**	
2 * uncertainty		**- 4,874**	**- 15,729**	**- 2,653**	**- 7,036**	**- 1,438**			**- 11,320**	
% Error		**4.53**	**7.32**	**3.59**	**10.97**	**3.58**			**8.49**	

Table 8.2 continued – U-series ages for secondary carbonates within the alluvial deposits surrounding the Orjen massif. Corrected and uncorrected ages are highlighted.

U-Series Sample	Unijerina 1	Unijerina 2	Unijerina 3	Unijerina 4	Crkvice 1	Crkvice 2	Sniježnice 1		Detritus Sample	Kameno 2	Lipci 4
^{238}U ppm	1.178867	0.334505	0.541709	0.294718	0.179441	1.081247	0.073100		^{238}U ppm	1.330900	0.965400
uncertainty	0.003646	0.001151	0.001708	0.000724	0.000476	0.004055	0.000203		uncertainty	0.006700	0.003100
$(^{234}$U/^{238}U)	1.005373	1.009957	0.969782	1.008743	1.006803	1.024392	1.010549		$(^{234}$U/^{238}U)	0.784700	1.106100
uncertainty	0.004523	0.005531	0.004648	0.004170	0.004000	0.005157	0.004237		uncertainty	0.005700	0.005300
^{234}U ppm	0.000064	0.000018	0.000028	0.000016	0.000010	0.000060	0.000004		^{234}U ppm	6.00E-0.5	0.000060
uncertainty	0.000000	0.000000	0.000000	0.000000	0.000000	0.000000	0.000000		uncertainty	3.00E-0.7	0.000000
^{230}Th ppb	0.020278	0.002881	0.001210	0.004378	0.002170	0.002834	0.001110		^{230}Th ppb	0.001300	0.001800
uncertainty	0.000281	0.000072	0.000012	0.000042	0.000020	0.000029	0.000011		uncertainty	2.00E-0.5	0.000020
^{232}Th ppb	206.633313	17.207791	4.354443	38.902517	2.326448	35.792257	7.757910		^{232}Th ppb	4574.300000	2771.500000
uncertainty	37.352759	3.110615	0.787142	7.032261	0.420558	6.470095	1.402383		uncertainty	826.890000	501.000000
$(^{230}$Th/^{232}Th)	18.336884	31.440809	52.741709	21.090755	175.307302	14.867744	27.086721		$(^{230}$Th/^{232}Th)	0.100900	0.236000
uncertainty	0.853089	1.814506	2.258482	0.891933	7.324785	0.637815	1.143315		uncertainty	0.004600	0.010700
$(^{230}$Th/^{234}U)	1.045235	0.521029	0.140747	0.899563	0.733849	0.156331	0.917883		$(^{230}$Th/^{234}U)	0.075200	0.104200
uncertainty	0.014485	0.013054	0.001430	0.008659	0.006688	0.001600	0.008760		uncertainty	0.001000	0.001300
AGE UNCORRECTED (years)	>350,000	80,256	16,577	248,628	144,153	18,547	268,253		^{232}Th/^{238}U DETRITAL MOLECULAR RATIO	3.35	2.80
2 * uncertainty		5,725	360	15,598	4,969	408	18,128				
2 * uncertainty		- 5,863	- 360	- 16,690	- 5,067	- 409	- 22,201				
% Error		7.22	2.17	6.49	3.48	2.20	7.52				

Corrected values using ^{232}Th/^{238}U detrital molecular ratio 3.12							
$(^{230}$Th/^{234}U) Corr	1.047986	0.512870	0.138399	0.895047	0.732717	0.147270	0.914946
uncertainty	0.021139	0.018326	0.001991	0.012452	0.009464	0.002143	0.012566
$(^{234}$U/^{238}U) Corr	1.005701	1.010128	0.969702	1.009140	1.006832	1.024660	1.010931
uncertainty	0.006586	0.007889	0.006582	0.006030	0.005670	0.007334	0.006100
AGE CORRECTED (years)	>350,000	78,416	16,279	243,876	143,675	17,381	265,428
2 * uncertainty		7,871	499	21,268	6,971	541	25,499
2 * uncertainty		- 8,138	- 500	- 23,301	- 7,165	- 542	- 28,448
% Error		10.21	3.07	9.14	4.92	3.12	10.16

Table 8.2 continued – U-series ages for secondary carbonates within the alluvial deposits surrounding the Orjen massif. Corrected and uncorrected ages and detrital samples are highlighted.

The corrected and uncorrected U-series ages demonstrate a close agreement, and only four samples provide corrected ages outside the uncorrected error margins (Nudo 5 – A, Vrbanje 1, Lipci 2 and Lipci 3). Ages from the fluvial record closely reflect the dating framework of the Orjen glacial deposits developed by Hughes *et al*. (2010) (Fig. 8.3). As will be discussed, in some instances, ages derived from the fluvial archive have provided greater detail to parts of the glacial record that were previously correlated by morphostratigraphy alone. The following discussion briefly summarises the ages obtained from each of the sampled sites. A full detailing of the stratigraphic significance of the U-series samples will be provided in Chapter 9, which develops a formalised morphostratigraphical and geochronological framework for the alluvial environments of Mount Orjen.

Carbonates within the polje sediments at Grahovo yield an age of >350 ka, which corresponds to the U-series ages providing minimum ages for the glacial moraines at the northern extent of the polje (324.0 ± 31.4 ka; MIS 12). The U-series age of the fluvial deposits at the southern edge of the polje also supports the morphostratigraphical correlation of the glacial moraines at Dvrsno to MIS 12. Both poljes are situated outside the ice margins of the major MIS 12 glaciation here and were supplied by meltwater routes draining the same ice lobe.

Calcites from the sediments at Vrbanje polje, western Orjen, provide an age of 126.6 ± 4.1 ka. This postdates the large moraine at Vrbanje, which has been correlated to MIS 12. The dated polje sediments may therefore reflect a more recent sediment pulse, deposited in association with the MIS 6 glaciation. Moraines correlated with MIS 6 are present in several tributary valleys feeding into this polje (Fig. 8.3). If the analysed sediments were deposited during MIS 6, it is likely that they overlie older deposits, delivered to the polje during the major cold stage of MIS 12. Alternatively, the calculated age may reflect calcite formation during MIS 6 within pre-existing sediments. Morphosedimentary and particle size evidence can be used alongside the U-series data to potentially differentiate these depositional phases (Chapter 9).
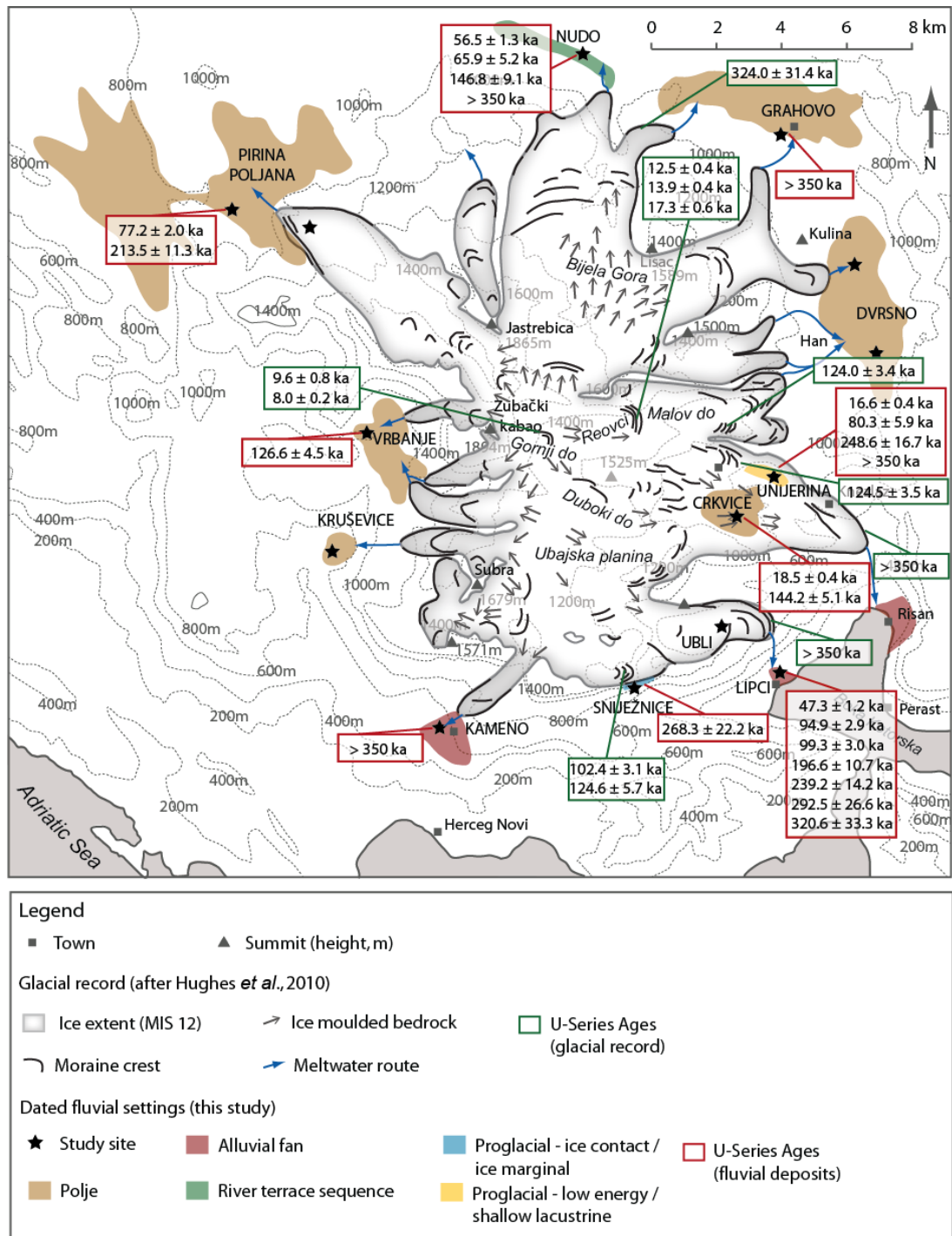
Figure 8.3 – Map of Orjen indicating the U-series ages from fluvial deposits (this study) and the corresponding glacial landforms (dated by Hughes *et al.*, 2010).

Calcites from the polje at Pirina Poljana yield minimum ages of 77.2 ± 2.0 ka and 213.5 ± 11.3 ka, and are correlated to MIS 7. The large moraines here remain undated but have been correlated using morphostratigraphy to MIS 12 (Hughes *et al.,* 2010) and delineate one of the largest ice lobes emanating from Mount Orjen. It is possible that an ice advance of this

magnitude is associated with the MIS 8 glacial phase, which has been tentatively suggested for the Durmitor massif in central Montenegro (Hughes *et al.*, 2011b). However, the presence of large volumes of sediment within Pirina Poljana, which is the largest polje of Mount Orjen (50 km x 5.5 km), suggests that these deposits may have been delivered to the site during the major glacial phase of MIS 12. The only dated evidence of glaciation during MIS 8 in the Mediterranean has been identified in Iberia by Fernandez-Mosquera *et al.* (2000), but this is based on very few radiometric ages. Though morphosedimentary evidence from MIS 8 has not yet been identified within the glacial record of Mount Orjen it is likely that glaciers were present here during all Pleistocene glacial cycles. It may however be that glaciers during MIS 6 were more extensive than the MIS 10 and MIS 8 ice masses and have overrun previous glacial evidence. Due to its situation outside the maximum ice margins of MIS 12, the polje at Pirina Poljana is therefore likely to contain meltwater deposits from the MIS 12 glaciation, as well as sediments derived from later glacial phases. It is unlikely that the younger U-series age of 77.2 ± 2.0 ka (MIS 4) reflects the advance of meltwater sediments into the polje during the last glacial cycle (MIS 5d-2). The position of the MIS 5d-2 moraines, up to 10 km from the site at Pirina Poljana (Fig. 8.3), means that it is improbable that meltwater would have delivered such large volumes of sediment as far downstream as Pirina Poljana (Chapter 9). This age may therefore reflect the prolonged redistribution of sediments from MIS 12-8, or a more recent phase of calcite formation within existing sediments.

River terraces of the Nudo valley yield U-series ages from 56.5 ± 1.3 ka (Arandelovo Unit) to >350 ka (Vućiya, Javora and Zaslap Units). Calcites from the highest sampled terrace surface, the Arandelovo Unit, yield some of the youngest ages (56.5 ± 1.3 ka and 65.9 ± 5.2 ka) whilst three ages associated with the lower terraces are dated at >350 ka. This suggests that the entire sequence was deposited in association with the major glaciation of the Orjen massif, and elsewhere in the Balkans, during MIS 12. This is in accordance with the morphostratigraphical evidence from the fluvial settings surrounding Orjen, which suggests that large volumes of glacigenic sediment were delivered to the river systems downstream during MIS 12. Since then, the sequence at Nudo has undergone progressive downcutting. This may reflect changing sediment supply dynamics during the Pleistocene. It may also be, in part, due to the tectonic regime of the Balkan region which comprises a complex interaction of uplifting high altitude terrain (2-4 mm/yr) and subsiding basins (Oluić *et al.*, 1982; Djurović and Petrović, 2007). These landscape interactions are discussed in Chapter 9. The younger U-series ages here are thought to be associated with later phases of carbonate development as the

system was incising. These precipitation phases possibly occurred in association with a localised springline, and/or during periods when climatic conditions were favourable for secondary carbonate development (Chapter 9). It is not possible to further distinguish the age of terrace development with the U-series ages alone. The Harden Index relative age indicators (Section 8.2) and the sedimentological data (Chapter 5) could allow the depositional phases within the Nudo valley to be more fully understood. This is discussed in detail in Chapter 9.

At Unijerina, eastern Orjen, the diamict at Section U2 is dated to >350 ka. The samples from the overlying fluvial horizons, exposed at Section U3, are dated to 248.6 ± 16.7 ka, 80.3 ± 5.9 ka and 16.6 ± 0.4 ka. This suggests that the diamicton unit was deposited in association with the extensive MIS 12 glaciation, whilst the overlying fluvial deposits were deposited earlier than 248.6 ± 16.7 ka (MIS 8). This means that they were not deposited in association with the moraines upstream of the site which have been correlated on the basis of minimum U-series ages and morphostratigraphy to MIS 6 (Hughes *et al*., 2010). The younger ages here are obtained from calcites within the same carbonate bench as those that yield older ages. Whilst they may reflect a thin veneer of more recent sediment deposition, it is highly likely that they represent later calcite development within existing (MIS 12-8) sediments.

The exposures at Crkvice are also situated within close proximity of the MIS 6 moraines. The diamict unit at Section C1 has been dated within this study to 144.2 ± 5.1 ka. The calcite sample here, which may reflect a reworked carbonate deposit (Chapter 5) serves as a maximum age indicator at this site, and supports the morphostratigraphical correlation of these moraines to MIS 6. The adjacent fluvial deposits (Section C2) are dated to 18.5 ± 0.4 ka, which broadly corresponds to the youngest age at Unijerina (16.6 ± 0.4 ka). This may reflect the more recent deposition of meltwater sediments into these basins during MIS 5d-2, when a valley glacier existed upvalley at Reovci (Hughes *et al*., 2010). Alternatively, these ages may reflect calcite development within existing sediments deposited during MIS 12-6.

At Sniježnice the secondary carbonate capping the outermost moraine and ice marginal fluvial sequence has been dated to 268.3 ± 22.2 ka (MIS 8). This provides a minimum age for the moraine landform here. Moraines at this site yielded calcite ages of 102.4 ± 3.1 ka and 124.6 ± 5.7 ka and on the basis of morphostratigraphy these dates were ascribed to MIS 6. The older age of 268.3 ± 22.2 ka obtained in this study is interesting because the sample was obtained from the distal side of the moraines. The geomorphology at this site suggests that the MIS 6

glacier here is likely to have had distal margins close to the older MIS 12 glacial limits (Chapter 3; Fig. 3.4). The younger age of these calcites (268.3 ± 22.2 ka as opposed to >350 ka) may reflect the prolonged instability of the landscape or the lack of a springline (or both) until MIS 8 (the age of the calcite).

The U-series ages from sites across Orjen can be used alongside the sedimentological and carbonate analyses (Chapters 5-7) as well as the Harden Index relative age indicators (Section 8.2) to devise a more comprehensive morpholithostratigraphical framework for the fluvial deposits surrounding the Orjen massif.

8.1.3   U-series dating of fluvial sediments of the Orjen massif: undetermined ages

Eight of the secondary carbonate samples extracted in the field have not provided secure U-series ages (Table 8.3). Secondary carbonate systems, and the inherent U-series decay chains, are susceptible to open system behaviour through carbonate dissolution, reprecipitation and overprinting. This means that it is often difficult to identify the causes of sample contamination (Villemant and Feuillet, 2003). This section considers some of the potential sources of detritus within the samples at Orjen, and discusses the implications of this for the use of these indeterminable ages within the wider dating framework for the fluvial settings in this study.

Contamination of secondary carbonates can arise through several processes, both within the sedimentary sequence and during laboratory analysis. In the laboratory, the indeterminable samples were analysed simultaneously with other samples from Orjen that have successfully provided U-series ages and have all undergone rigorous preparation and analytical procedures. It is therefore unlikely that laboratory analytical error is the cause of these undetermined ages. Instead, these calcites may have developed under open system conditions. Secondary carbonates formed within sedimentary sequences are exposed to three main sources of disturbance to closed system conditions:

- The input of high levels of initial detrital ^{230}Th (not produced by *in-situ* decay) upon carbonate formation. This produces initial ^{230}Th/^{234}U and ^{230}Th/^{232}Th ratios >0.
- The redistribution, by either input or extraction, of isotopes (^{238}U, ^{234}U, ^{234}Th or ^{230}Th) due to alpha (α)–recoil processes over multiple timescales of calcretisation.

- The input of detrital ^{230}Th from allogenic sources, such as within detrital silicates, during later phases of carbonate formation or dissolution/reprecipitation.

Secondary carbonate samples contaminated with high levels of initial detrital ^{230}Th usually also display a large quantity of ^{232}Th (Hellstrom, 2006), but low ^{230}Th/^{232}Th ratios (<1 for example). The undetermined ages from Orjen are characterised by high ^{232}Th values (99.319 − 1515.648 ppb) but also high ^{230}Th/^{232}Th ratios of 2.573 − 162.001 (Table 8.3). This suggests that initial detrital ^{230}Th, at the time of calcite formation, is not the dominant source of contamination here. Instead, contamination within these samples may be due to the development of open system behaviour during a later phase of carbonate accumulation, through either α–recoil or allogenic inputs after initial calcite formation.

To distinguish between these types of open systems, a simplified inversion model has been used here, following the methods of Villemant and Feuillet (2003). This model uses ^{230}Th/^{234}U and ^{234}U/^{238}U ratios within the contaminated samples, plotted with reference to open- and closed-system isochrons (Fig. 8.4). The ^{230}Th/^{234}U and ^{234}U/^{238}U data from the determined ages has also been plotted for reference. The sub-horizontal (f) lines within the model represent the fraction of the daughter isotope that has been lost or gained relative to a closed system (^{230}Th = 0), and essentially reflects the degree of open system behaviour. Graph A reflects the autogenic contribution of U whilst Graph B constrains the allogenic input of U, enabling the distinction between detritally contaminated and uncontaminated samples. The sub-vertical lines are isochrons, varying according to the degree of open system behaviour. Using the clustering of samples along these isochrons it is possible to estimate the 'model age' of otherwise undetermined samples that were initially isotopically homogenous, but have evolved in an open system (Villemant and Feuillet, 2003). The model makes the following five assumptions (Villemant and Feuillet, 2003):

- The samples formed contemporaneously with the same initial ^{234}U/^{238}U and ^{230}Th/^{232}Th ratios.
- The initial $(^{230}\text{Th}/^{238}\text{U})_0$ ratios may vary between samples, and are dependent on the ability of the secondary carbonates to incorporate U or adsorb Th at the surface of sediment grains.
- The samples may evolve in an open system with mobility of the daughter isotopes of ^{238}U.

- Mobility of ^{234}Th and ^{230}Th are determined by time-dependent recoil processes.
- ^{238}U and ^{232}Th are not affected by these processes as they are not radiogenic.

The model effectively distinguishes between the determined and undetermined ages from Orjen, as calcites not yielding age information plot outside the autogenic isochrons (Fig. 8.4). Determined ages are plotted within the field of carbonate contribution, which is based upon the idealised isotopic ratios of carbonates of variable age, based on Villemant and Feuillet (2003). Consistent with the model assumptions, if α–recoil was driving these open system processes, ^{230}Th/^{234}U ratios within the age-undetermined samples would be increased, yet ^{232}Th levels would remain unaffected (as ^{238}U and ^{232}Th are not radiogenic), and should resemble the ^{232}Th values measured in the dated samples (Table 8.2). The undetermined samples at Orjen, however, yield ^{232}Th values much greater than those observed in the age-determined calcites (Table 8.2 and 8.3). Villemant and Feuillet (2003) also indicate that high ratios of ^{230}Th/^{234}U (i.e. >1) cannot be explained by α–recoil alone as they would require f-values (and therefore ^{234}U/^{238}U ratios) of up to 2.8; a value that is not observed within natural systems. These model parameters therefore suggest that the detrital component of these samples originates from allogenic input of silicates after initial calcite formation, derived from impure limestone lithologies within the catchments of Orjen.

Based on ^{230}Th/^{234}U and ^{234}U/^{238}U ratios, the determined U-series ages (Section 8.1.2) yield broadly comparable modelled ages, and suggest that the inversion model delivers reliable age estimates. Using this model it is therefore also possible to estimate the ages of several of the undetermined samples. The sample analysed from Kruševice is not included in the model as its ^{230}Th/^{234}U and ^{230}Th/^{232}Th values defy the isochron parameters and it continues to yield unsuitable age information. It can be inferred that this sample is contaminated beyond the levels feasible for U-series dating. Samples from Nudo (N1, N2, N4, N7 and N10) provide an inferred age of >100 ka. Sample N9, also from Nudo, can be constrained by the isochrons to >50 ka (c. 100 ka). These values are consistent with the other ages obtained from terrace units of the Nudo valley (Table 8.2). At Unijerina, sample U5 is constrained to >200 ka, which is also consistent with the determined ages of >350 ka for the glacial diamict at Section U2 and 248.6 ± 16.7 ka for the capping fluvial deposits at Section U3.

U-Series Sample	Kruševice 1	Nudo 1 - A	Nudo 2 - A	Nudo 4 - A	Nudo 7 - K	Nudo 9 - J	Nudo 10 - Z	Unijerina 5
^{238}U ppm	0.397573	2.010574	2.335642	2.058249	1.531213	0.235259	1.511642	2.928981
uncertainty	0.001103	0.006530	0.008078	0.005973	0.004507	0.000676	0.005529	0.011009
(^{234}U/^{238}U)	0.952482	1.007624	1.010394	0.951593	1.007745	0.963388	1.003112	1.025632
uncertainty	0.004428	0.004722	0.005369	0.005019	0.004750	0.004218	0.005377	0.005448
^{234}U ppm	0.000020	0.000109	0.000127	0.000106	0.000083	0.000012	0.000082	0.000162
uncertainty	0.000000	0.000000	0.000001	0.000000	0.000000	0.000000	0.000000	0.000001
^{230}Th ppb	0.086165	0.056310	0.058868	0.047733	0.046020	0.007082	0.047003	0.059759
uncertainty	0.052580	0.000543	0.000545	0.000427	0.000424	0.000085	0.000428	0.000537
^{232}Th ppb	99.319126	1515.647802	891.471744	1028.867672	825.845064	515.612976	1195.719799	341.569480
uncertainty	17.953649	273.995353	161.147968	187.182594	149.285328	93.207958	216.146743	61.744648
(^{230}Th/^{232}Th)	162.005503	6.940407	12.333172	8.666468	10.409858	2.572579	7.340959	32.684716
uncertainty	104.154256	0.293737	0.517191	0.364297	0.436074	0.114851	0.306702	1.361570
(^{230}Th/^{234}U)	13.900800	1.698042	1.523936	1.488857	1.821969	1.908893	1.893692	1.215293
uncertainty	8.482882	0.016395	0.014136	0.013336	0.016815	0.022865	0.017270	0.010933
AGE UNCORRECTED (years)	No age	No age	No age	No age	No age	No age	No age	No age
2 * uncertainty								
2 * uncertainty								
%err 2se								

Corrected values using ^{232}Th/^{238}U detrital molecular ratio 3.12								
(^{230}Th/^{234}U) Corr	15.118387							
uncertainty	13.593848							
(^{234}U/^{238}U) Corr	0.948230							
uncertainty	0.006496							
AGE CORRECTED (years)	No age	No age	No age	No age	No age	No age	No age	No age
2 * uncertainty								
2 * uncertainty								
%err 2se								

Table 8.3 – Analytical data for secondary carbonates within the alluvial deposits surrounding the Orjen massif that have not provided U-series ages. These data are used to develop the inversion model presented in Figure 8.4, based on the methods of Villemant and Feuillet (2003).
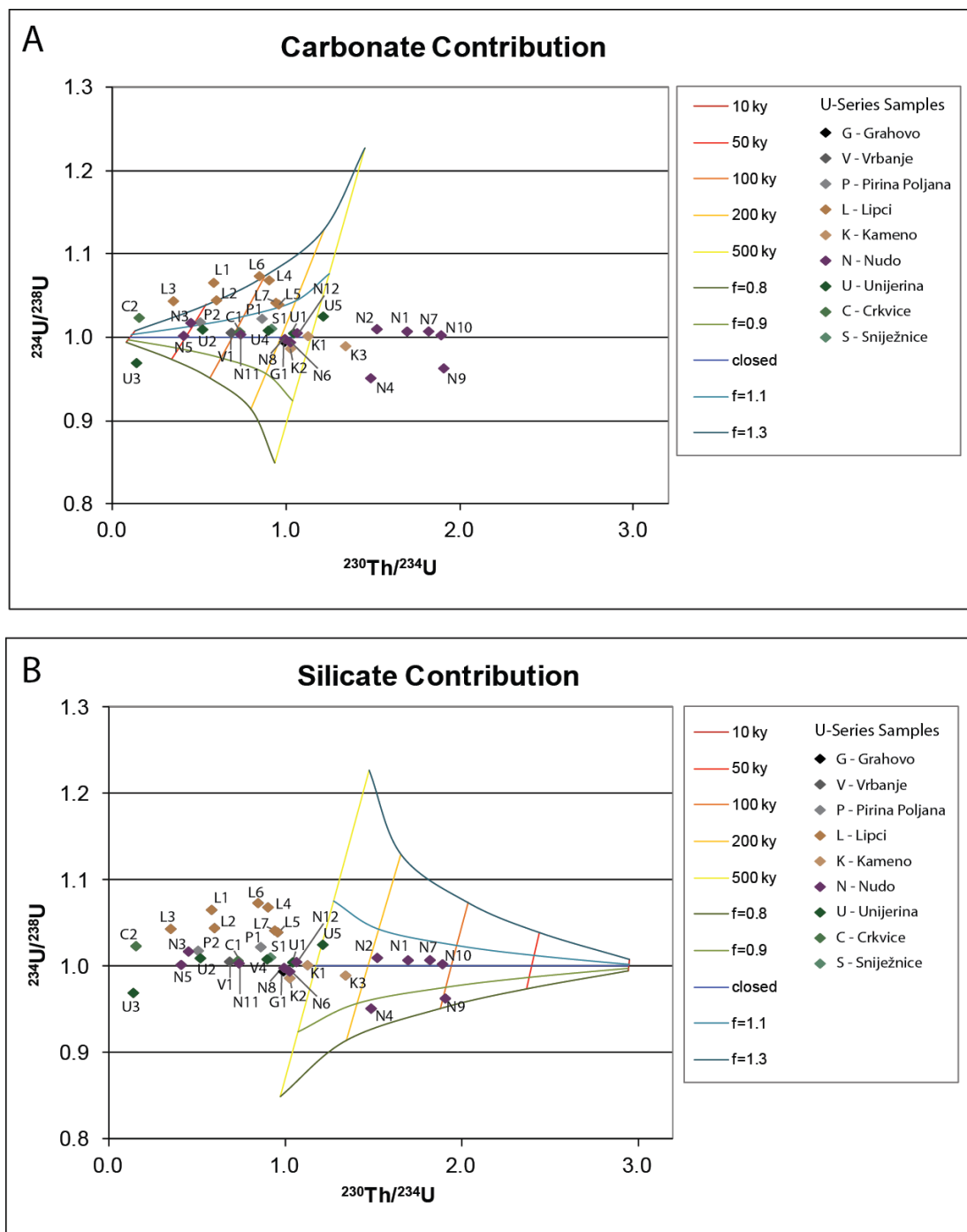
Figure 8.4 – Inversion model used to assess the detrital contamination of calcite samples at Orjen. Samples N1, N2, N4, N7, N9, N10 and U5 have not provided U-series ages using standard techniques. All calculations follow the methods and model outlined by Villemant and Feuillet (2003). A) U-series sample isotopic ratios plotted with the idealised isotopic envelope and isochrons of carbonate-rich calcites. Data plotting outside the isochrons are indicative of calcites that are not rich in carbonate B) U-series isotopic ratios plotted with the isotopic envelope of silicate-rich samples at a range of isochrons.

The isochron model also enables the ages from the alluvial fan at Kameno to be further refined. Samples K1 and K3 did not provide suitable age information due to levels of detrital input on the threshold of dating suitability. These samples were instead correlated on the basis of similar isotopic ratios to sample K2, which was successfully dated to >350 ka. The isochron model here confirms that these samples can be correlated with ages >200 ka and are therefore ascribed on the basis of stratigraphical correlations to the determined age of >350 ka.

8.2   Harden Index of soil profile development: relative age indicators

The Harden Index is used within this study as a relative age tool to complement the radiometric ages derived from U-series methods and to develop more robust morphostratigraphical correlations between catchments. The technique has been applied to 18 soil horizons from across the study region, such as those displayed in Plate 8.1. The Harden Index uses physical characteristics of the soil profile to distinguish between land surfaces of different age. Nine parameters are used to calculate the profile development index (PDI): rubification, colour paling, melanisation, structure, texture, moist consistency, dry consistency, clay films and pH, following the methods outlined in Chapter 4. Greater soil PDI values indicate more mature soil profiles, whilst lower values suggest more recent soil development. The Harden Index technique has been successfully applied to soil profiles on the glacial landforms of Orjen by Hughes *et al*. (2010) and can be used to explore the relationships between soil profiles within glacial and fluvial depositional environments.

8.2.1   Soil profile development indices: relative age indicators from the fluvial deposits of Mount Orjen

Table 8.4 and Figure 8.5 present the profile development indices for the soil profiles analysed within this study. Data tables containing all measured parameters are provided in Appendix B. The soils observed at the study sites were largely thin (<60 cm-thick), unconsolidated and granular in texture due to an abundance of sands and gravels from the underlying substrate. These soils are typical of Mediterranean Alfisols (van Andel, 1998; Birkeland, 1999) which, at Orjen, comprise a thin organic horizon at the surface (A Horizon or O Horizon of Birkeland, 1999) and an underlying leached (E) horizon. At two sites, the E horizon was underlain by a clay-rich Bt horizon (e.g. Grahovo and Nudo Vućiya Unit), but elsewhere this was absent and

the profile graded into the underlying weathered substrate (Cox Horizon) and unweathered substrate (C Horizon) (Plate 8.1).

Plate 8.1 – Soil profiles developed on the fluvial landforms surrounding Orjen: A) Dvrsno, Section D1; B) Grahovo, Section G1; C) Unijerina, Section U3; D) Kameno, Section K2.

Sampled Section	Soil Thickness (cm)	Soil Description	PDI	LOI (%) Profile Mean	U-series Age (years)
Grahovo					
G1	30	Granular, yet moderately developed soil horizon. Granules and pebbles throughout.	**9.91**	**1.56**	>350,000
G2	20	Granular, yet moderately developed soil horizon.	**4.76**	**1.00**	-
Dvrsno					
D1	40	Granular and gravel-rich soil with little organic content, evidence of significant leaching down the profile. Horizons become more clast-rich with depth.	**11.80**	**1.44**	-
D5	20	Platey and dark coloured soil horizon with no clasts within the upper 20 cm, becoming more granular with depth.	**7.35**	**1.20**	-
Kruševice					
Kr2	50	Fissile and organic-rich soil horizon, with a desiccated appearance.	**13.75***	**1.91**	-
Vrbanje					
V4	30	Unconsolidated, weakly-developed and granule-rich soil.	**4.88***	**2.09**	126,552 ± 4,530
Pirina Poljana					
P1	30	Sandy, granular and weakly-developed soil horizon.	**5.59***	**1.62**	-
P2	50	Sandy and granular soil horizon. Weakly-moderately developed.	**9.12**	**2.93**	77,162 ± 1,961 213,467 ± 11,853
Kameno					
K2	60	Granular to blocky soil containing large clasts. The organic component is largely concentrated into the upper 40 cm, and leached down the profile.	**15.97**	**1.49**	>350,000
Nudo					
ZN1	10	Granular and weakly developed soil horizon.	**1.84**	**0.82**	146,778 ± 9,092 >350,000
ZN2	10	Granular and weakly developed soil horizon.	**3.10**	**0.69**	-
VN1	30	Granular, yet organic-rich soil horizon. Dark in colour and generally well-developed	**6.29**	**1.20**	>350,000
Unijerina					
U2	55	Granular and poorly-developed soil horizon.	**6.29***	**1.05**	>350,000
U3	10	Granular, weakly developed soil horizon, grading into host substrate	**1.43***	**0.81**	16,577 ± 360 80,256 ± 5,863 248,628 ± 16,690
Crkvice					
C1	30	Sand and granule-rich, weakly-developed soil.	**3.92**	**1.31**	144,153 ± 5,067
C2	40	Granular and weakly-developed soil horizon.	**4.12**	**0.66**	18,547 ± 409
Ubli					
Ub1	20	Granular, sandy and weakly-developed soil horizon.	**7.21**	**2.75**	-
Sniježnice					
S2	25	Very granular and poorly-developed. Organic component concentrated in upper 5 cm.	**2.51**	**2.49**	268,253 ± 22,201

Table 8.4 – Harden Index soil development indices (PDIs) from sites across Orjen. PDI values marked with an asterisk indicate profiles where Colour Paling values were omitted from the final PDI calculations (Appendix B) following the methods of Birkeland (1999). Associated U-series ages are also displayed (see Table 8.2).
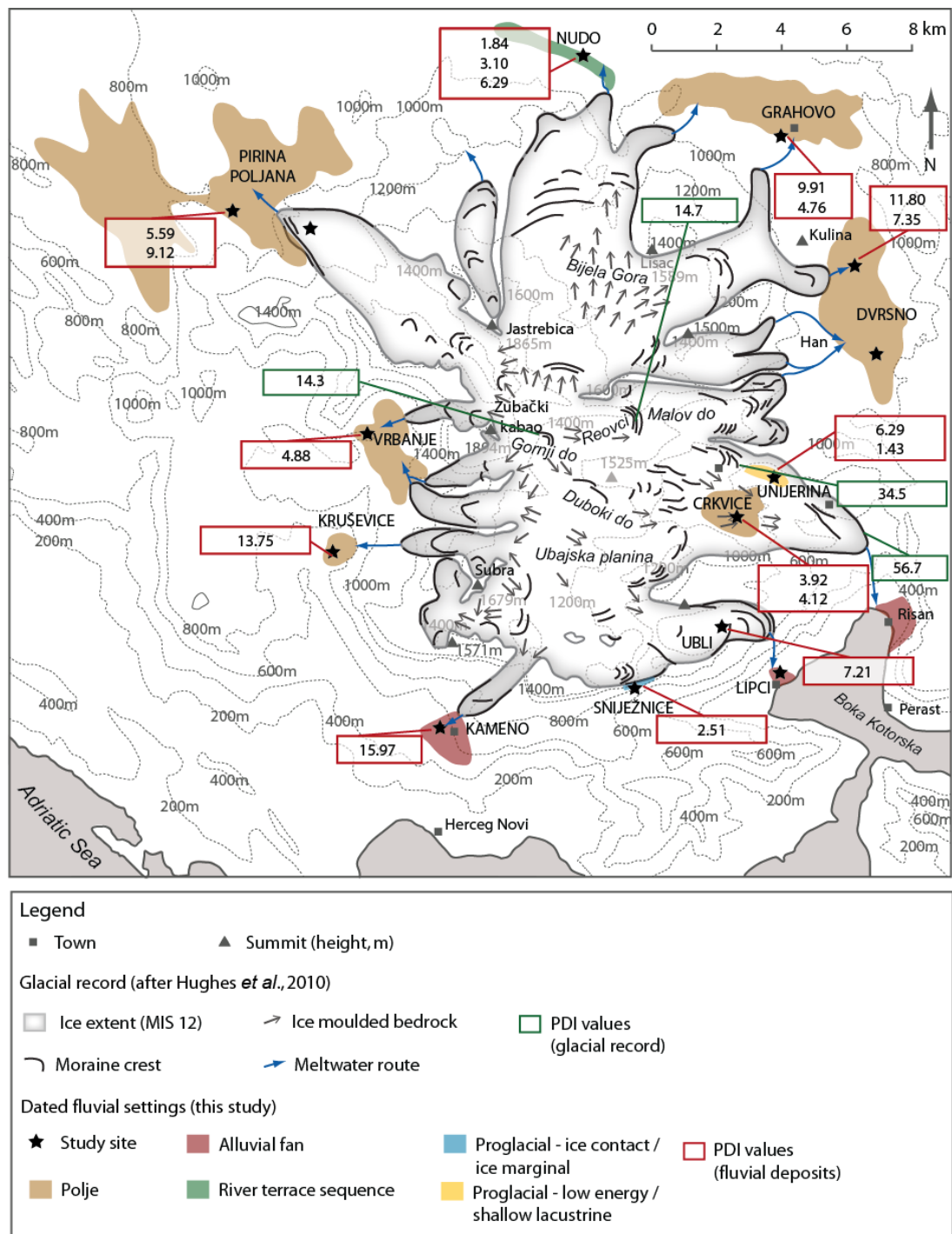
Figure 8.5 – Harden Index values for soil profiles within fluvial deposits surrounding Orjen (red boxes, this study) and associated glacial landforms (green boxes) after Hughes *et al*. (2010).

The PDI values indicate that the Harden Index technique is able to successfully distinguish relative land surface age within the alluvial environments of Orjen (see Chapter 9 for more detailed discussion of the relationship between Harden Index values and morphostratigraphy). Soil profiles formed on land surfaces correlated to MIS 12 (such as Grahovo, Dvrsno, Pirina

Poljana and Kameno) largely present higher PDI and LOI (%) values than those associated with more recent glacial depositional phases. PDI values of soils within the poljes broadly range from 4.76 (Grahovo, Section G2) to 13.75 (Kruševice, Section Kr2). The low soil PDI at Vrbanje (4.88; Section V4) reflects the younger U-series age obtained from these sediments (126.6 ± 4.5 ka, correlated to MIS 6), and further suggests that this unit may represent a meltwater and sediment pulse associated with MIS 6 (Chapter 9). LOI values typically range from 0.82% (Nudo, Section ZN1) to 2.93% (Pirina Poljana, Section P2) within land surfaces correlated to MIS 12, and from 0.66% (Crkvice, Section C2) to 0.81% (Unijerina, Section U3) within profiles correlated to younger depositional phases. All LOI values in this study are particularly low (<3%) and reflect the granular and friable nature of the soils that have developed across the gravel-rich fluvial sediments.

The soil profile at Kameno, a large alluvial fan deposited in front of a lateral moraine correlated to MIS 12, presents the highest PDI score of the sampled horizons (15.97; Section K2). This reflects the thickness of the soil profile (60 cm). The soil PDI here is of a similar order of magnitude to those calculated for Dvrsno (11.80) and Kruševice (13.75) which are also associated with sediment deposition during MIS 12.

The river terraces of the Nudo valley, north Orjen, provide several U-series ages of > 350 ka. Assuming that this sequence was deposited in association with the major glacial advance of MIS 12, constraining the timing of incision, and formation of these individual terraces, is not possible using U-series methods alone. Soil profiles from these terrace surfaces were largely inaccessible, yet PDI values from the Zaslap Unit and the Vućiya Unit suggest that it is possible to differentiate the relative timing of land surface stability and soil profile development. The lowest terrace surface of the valley (Zaslap Unit) presents soil PDIs of 1.84 (Section ZN1) and 3.10 (Section ZN2), whilst the value obtained from the higher terrace surface (Vućiya Unit, Section VN1) is calculated as 6.29, over twice that of the lower terraces. This supports the geomorphological and sedimentological (Chapter 5) data, and suggests that the sediments within this valley were deposited in association with the extensive glaciation of MIS 12, before being incised. This would lead to a progressive reduction in soil maturity with decreasing terrace altitude.

The Harden Index values at Unijerina support the morphostratigraphical and U-series data presented both in this study and by Hughes *et al*. (2010). The diamict unit at Section U2, dated

to >350 ka, presents a soil PDI of 6.29 compared to a value of 1.43 within the overlying fluvial deposits (Section U3), dated to (248.6 ± 16.7 ka). These values are considerably lower than those associated with other soil profiles of similar age at Grahovo, Pirina Poljana and Kameno. This may reflect a degree of land surface instability following deposition of the diamict deposit (correlated to MIS 12) and limited preservation of soil horizons until the ice had retreated from this site to the position of the MIS 6 moraines, upstream of Unijerina. Similar PDI values are also calculated for the diamict and fluvial deposits at Crkvice (3.92 at Section C1 and 4.12 at Section C2), and suggest a much later age of stabilised pedogenesis as the ice retreated to its MIS 6 margins.

Soil PDI values at Ubli (7.21; Section U1) are within the range of values observed at Grahovo, Dvrsno and Pirina Poljana. This suggests that soil horizons developed here prior to the MIS 6 glacial phase, and that this land surface is instead correlated to deposition during the extensive MIS 12 glaciation within this valley. The lower PDI value here, in comparison to MIS 12 sediments outside the maximum ice margins, is explained by the location of this site several kilometres upstream of the MIS 12 moraines. This may indicate that the soil profile developed here as ice retreated upstream towards Sniježnice.

The poorly developed soils in the ice proximal deposits at Sniježnice present a low PDI value of 2.51 (Section S2), despite a U-series age of 268.3 ± 22.2 ka from calcites at this land surface. This value is comparable with the youngest units of the Nudo valley, and the fluvial deposits at Unijerina and Crkvice. This might be explained by decreased land surface stability due to the ice marginal position of this deposit and prolonged disturbance of the sedimentary sequence.

8.2.2   Comparisons with soil PDIs associated with the glacial record

The Harden Index values calculated from the fluvial sites are considerably lower, in some cases by an order of magnitude, than those of equivalent age from the glacial landforms of Hughes *et al*. (2010). For example, the maximum PDI value from the fluvial deposits correlated to MIS 12 is 15.97 (Kameno), whilst the value obtained for the MIS 12 glacial deposits at Knezlaz is 56.7 (Figure 8.5). This relationship is also evident within soils correlated to MIS 6 where those developed on fluvial deposits present much lower values (3.92, Crkvice) than those from the glacial record (34.5, Crkvice). The lowest PDIs within the glacial record are derived from the soils at Reovci (14.7), and are correlated to MIS 5d-2 (Hughes *et al*., 2010). Despite the

variations in calculated PDIs, the values from the fluvial deposits broadly track the *relative* changes observed within the glacial sediments over successive glacial cycles, where older soils present higher PDI values. As will be discussed, these differences in PDI score may be a product of several factors that influence soil development within fluvial and glacial sediments. Table 8.5 presents a comparison of PDI values for corresponding soil horizons from fluvial (Kameno) and glacial deposits (Knezlaz) that have both been correlated using morphostratigraphy to MIS 12 (Hughes *et al.*, 2010; Hughes, 2012 pers. comm.). This is used to explore the observed variations in soil PDI values and the environmental influences on soil development within glacial and fluvial settings. The normalised values for each of the parameters contributing to the final PDI calculation are displayed.

Soil Depth (cm)	R	CP	M	S	T	MC	DC	CF	pH	Index	% Profile	Profile PDI
Fluvial Soil Profile - Kameno (Section K2)												
0-10	0.05	0.83	0.71	0.50	0.33	0.20	0.10	0.46	0.23	0.38	3.79	
10-20	0.00	0.33	0.71	0.50	0.33	0.20	0.00	0.46	0.22	0.31	3.06	
20-30	0.00	0.33	0.71	0.50	0.33	0.20	0.00	0.46	0.20	0.30	3.04	**15.97**
30-40	0.00	0.00	0.71	0.33	0.33	0.00	0.00	0.54	0.11	0.22	2.24	
40-50	0.11	0.17	0.47	0.33	0.22	0.00	0.00	0.54	0.13	0.22	2.19	
50-60	0.11	0.00	0.35	0.33	0.11	0.00	0.00	0.54	0.04	0.16	1.64	
Glacial Soil Profile - Knezlaz												
0-50	0.37	-	0.47	0.50	0.44	0.20	0.20	0.38	0.31	0.36	17.94	**54.51**
50-120	0.37	-	0.71	1.00	0.67	0.30	0.30	0.46	0.37	0.52	36.58	

Table 8.5 – Soil PDI values for soil profiles from glacial deposits at Knezlaz and fluvial deposits at Kameno, southeast Orjen. Both land surfaces are correlated using morphostratigraphy to MIS 12. R – Rubification; CP – Colour Paling; M – Melanisation; S – Structure; T – Texture; MC – Moist Consistency; DC – Dry Consistency; CF – Clay Films. Colour Paling has been removed from the calculations at Knezlaz due to value inversions (after Birkeland, 1999).

The data in Table 8.5 highlight the large discrepancy between the PDI values of soils of inferred comparable age (based on morphostratigraphy) from fluvial and glacigenic sediment substrates. This may be due to several parameters influencing soil development. Soil profile thickness forms an important component in the calculation of Harden Index PDI values. Each of the other normalised parameters is multiplied by the overall soil thickness, meaning that soil PDI values are intrinsically linked to the depth of soil development. At Knezlaz for example, soil profiles measure 120 cm thick, whilst those within the fluvial sediments at Kameno are typically 60 cm thick. Comparisons of the glacial and fluvial datasets also suggest that soil structure, texture and consistence can lead to differences in soil PDI values between glacial and fluvial settings (Table 8.5). Each of these PDI parameters can be explained by the

contrasting physical characteristics of the glacial and fluvial sediment substrates. Glacial sediments at Orjen are dominated by fine silt and clay material whilst alluvial deposits are typically coarse sands and gravels (Chapters 5 and 6). The presence of clay particles within a soil profile influences the nature of pedogenic processes due to its impacts on internal soil surface area and to a lesser degree, soil aeration, organic and nutrient contents. Soil profiles with greater internal surface area (i.e. elevated clay contents within glacial till) are considered more chemically active than those with lower surface area (such as coarse grained alluvium) (Birkeland, 1999). It is therefore likely that the observed variation between the soils developed on glacial and fluvial landforms surrounding Orjen is linked to the parent material. This in turn determines the degree of soil development and profile thickness, and may lead to the observed variations in Harden Index PDI values. This forms a limitation of the Harden Index method, and means that soils formed in different parent materials and within contrasting geomorphic surfaces may not always be directly compared. This also been observed within soil profiles developed on Pleistocene outwash terraces in the Ljubljana Basin, Slovenia by Vidic (1998). The author highlights that individual soil properties can develop at different rates due to factors such as parent material and climate. Duplicate PDI measurements, on multiple profiles from each surface, would be required to reduce statistical variance. At Orjen, however, by understanding these limitations and using the glacial and fluvial soil datasets alongside each other, the Harden Soil Index can be successfully used as a relative age tool. The systematic offset between glacial and fluvial soil PDIs at Orjen has important implications for the use of soil profiles as relative age indicators. It may indicate that some earlier studies using soil development methods, on soils with different parent materials, require a degree of revision.

8.3   Summary

The radiometric (U-series) and relative dating (Harden Index) techniques used within this study have yielded robust geochronological indicators from the fluvial settings surrounding Mount Orjen. These provide minimum ages of land surface stability, and relative ages of soil development and can be used to more securely constrain the timing of fluvial deposition. In the following discussion (Chapter 9), the geochronological results can be combined with the morphosedimentary data and U-series ages to develop a formal model of Quaternary landscape evolution surrounding the Orjen massif.

CHAPTER NINE

Discussion and Implications: Fluvial Response to Pleistocene Glaciation at Orjen

___

Synopsis

The key findings of this research are presented in Chapters 5 - 8. This chapter synthesises these data to develop a model of fluvial response to Pleistocene glaciation of the Orjen massif and explore its wider implications for Pleistocene glacial and fluvial interactions elsewhere. This study integrates morphosedimentary records from a range of fluvial depositional settings that are representative of glaciated catchments across the Mediterranean. The fluvial sedimentary signatures surrounding the Orjen massif vary both through time over successive glacial-interglacial cycles, and spatially within neighbouring depositional settings.

Section 9.1 presents a formal stratigraphical framework for the alluvial deposits of Mount Orjen. This is used within Sections 9.2 and 9.3 to investigate the timing and nature of Pleistocene fluvial activity within contrasting geomorphological contexts. Section 9.4 presents an index of secondary carbonate development which describes the history of pedogenic and land surface processes at the study sites. Section 9.5 integrates all of these data to test current hypotheses of the timing and nature of fluvial geomorphological and sedimentological response to Pleistocene glacial activity. This is achieved by comparing the Orjen fluvial record to wider Mediterranean and global morphosedimentary archives.

9.1   Fluvial morphostratigraphical and geochronological framework

The morphosedimentary data from the 12 field sites analysed in this study have been used to develop a formal fluvial morphostratigraphical framework for Mount Orjen (Table 9.1). Stratigraphical units are defined following standard nomenclature (Rose and Menzies, 1996) using morphosedimentary records and soil development indices, and have been verified using U-series ages. The framework contains two Members: Kotorska-Sušica Member and Krivošije Member. These correlate to the Knezlaz (MIS 12) and Crkvice (MIS 6) Members of the Orjen glacial stratigraphy, respectively (Hughes *et al.*, 2010). Sub-Members are defined on the basis of geomorphology and lithostratigraphy and reflect the variety of fluvial depositional environments surrounding Mount Orjen.

The Kotorska-Sušica Member represents the most extensive fluvial depositional phase of Mount Orjen, and has been correlated with the major glaciation of Mount Orjen and elsewhere in the Mediterranean during MIS 12. During this phase, ice often extended far beyond the high altitude plateau of Orjen and many of the sedimentary records are now situated within the depocentres downstream. The excellent preservation of these deposits means that it is unlikely that these landforms are associated with MIS 16 glaciation. Morphosedimentary data, soil profile indices and U-series ages suggest that this Member is likely to contain a collection of diachronous sedimentary units potentially spanning MIS 12, 10 and 8 (see Table 9.1 and text; Section 9.2). The Kotorska-Sušica Member has therefore been correlated to MIS 12-8 to account for this chronological complexity. This Member contains five Sub-Members, each corresponding to a distinct depositional environment (Table 9.1). The Nudo Sub-Member is further divided into six Beds, each reflecting an individual terrace surface within the Nudo valley. These are arranged in Table 9.1 by descending surface altitude (Ravna Ploča Bed to Zaslap Bed).

The Krivošije Member represents the fluvial morphosedimentary evidence correlated to MIS 6. The glacial record of Mount Orjen suggests that during MIS 6 ice was less extensive than MIS 12 and was largely confined to the higher altitude plateau (Hughes *et al*., 2010). The analysed fluvial records are therefore largely situated inside the MIS 12 moraines, and only limited alluvium from MIS 6 is observed beyond the MIS 12 ice limits. The Crkvice Sub-Member of the Krivošije Member (MIS 6) corresponds to polje sediments at Crkvice and Vrbanje. Sediments at Crkvice reflect an ice distal polje setting and present interstratified sands and silts. At Vrbanje, sediments are coarser and reflect its ice proximal location. As both of these polje depositional environments are also observed within the large polje at Dvrsno (Kotorska-Sušica Member; MIS 12) the sediments at Vrbanje and Crkvice are classified as the same stratigraphical unit (the Crkvice Sub-Member) and are not distinguished as different morphological settings.

Morphostratigraphical evidence of fluvial deposition during MIS 5d-2, including the Younger Dryas, has not yet been observed within the fluvial record of Mount Orjen. Two U-series ages (Table 9.1) dated to 18.5 ± 0.4 (Crkvice) and 16.6 ± 0.4 (Unijerina) may reflect MIS 5d-2 deposition (correlated to the Gornji do and Reovci Members of the glacial record (Hughes *et al*., 2010). However, it is also possible that these ages represent calcite development within pre-existing fluvial sediments. This chronological unit is therefore not assigned a morphostratigraphical subdivision within the formal fluvial stratigraphy of Mount Orjen.

| Stratigraphical Unit | Orjen Formation | | | Soil PDI | U-series Age (ka) | Exposed At | Correlations | | |
	Member	Sub-Member	Bed				MIS	Glacial Record Orjen (Hughes et al., 2010)	Glacial Record Mount Tymphi (Hughes, 2004)
2	Krivošije Member	Crkvice Sub-Member (Polje sediments)	-	4.88	126.5 ± 4.5	Vrbanje	6	Crkvice Member	Vlasian[‡] Stage
				3.92	144.2 ± 5.1	Crkvice			
				4.12	18.5 ± 0.4				
1	Kotorska-Sušica Member	Dvrsno Sub-Member (Polje sediments)	-	7.35 - 11.80	-	Dvrsno	12 – 8[†]	Knezlaz Member	Skamnellian Stage
				4.76 - 8.91	>350	Grahovo			
				13.75	-	Kruševice			
				4.88	-	Vrbanje*			
				5.59 - 9.12	213.5 ± 11.3 / 77.2 ± 2.0	Pirina Poljana			
		Nudo Sub-Member (River terraces)	Ravna Ploča	-	-	Nudo			
			Arandelovo	-	65.9 ± 5.2 / 56.5 ± 1.3				
			Vućiya	6.29	>350				
			Kamiseyo	-	-				
			Javora	-	>350				
			Zaslap	1.84 / 3.10	>350 / 146.8 ± 9.1				
		Kameno Sub-Member (Alluvial fans)	-	15.97	>350	Kameno			
				-	320.6 ± 33.4 / 292.5 ± 26.7 / 239.2 ± 14.2 / 196.6 ± 10.8 / 99.3 ± 3.1 / 94.9 ± 2.10 / 47.3 ± 1.3	Lipci			
		Unijerina Sub-Member (Proglacial - shallow lacustrine)	-	6.29	>350	Unijerina			
				1.43	248.6 ± 16.7 / 80.3 ± 5.9 / 16.6 ± 0.4				
		Sniježnice Sub-Member (Proglacial - ice marginal)	-	2.51	268.3 ± 22.2	Sniježnice			

Table 9.1 – Morphostratigraphical framework for the alluvial deposits of Orjen defined by: stratigraphical unit; Formation (Member, Sub-Member, Beds); study/exposure sites, Harden Soil Index PDI and U-series ages. Correlations with the Marine Isotope Stratigraphy (MIS), the glacial record of Orjen (after Hughes *et al.*, 2010) and the Pindus Mountains, Greece (Hughes, 2004) are also provided. *The sediments at Vrbanje polje have been dated using U-series and correlate with the Krivošije Member. It is likely, however that sediments underlying the dated horizon were deposited during MIS 12. This site has therefore been correlated to both the Krivošije and Kotorska-Sušica stratigraphical units. [†] Note that the units that make up the Orjen Formation may be diachronous. In particular, it is possible that different morphological units (poljes, river terraces, alluvial fans, etc.) of each Member may not always be time-equivalent (see text for more detailed discussion). [‡] The Vlasian Stage of the glacial chronostratigraphy of Mount Tymphi has been correlated to MIS 10-6 by Hughes (2004).

Two types of surface meltwater pathways have been observed surrounding Mount Orjen (Figure 9.1; see Section 9.3 for more detailed discussion). At some locations, the ice front was situated on the high altitude plateau or within high elevation valley systems (such as Kruševice, Lipci and Nudo) and meltwater was supplied to the depocentres downstream via bedrock gorges (Type 1). At other sites, the ice terminated within the polje (such as Vrbanje, Pirina Poljana and Dvrsno) or at the fan apex (Kameno) and sediment was delivered directly to the lower altitude depressions (Type 2).
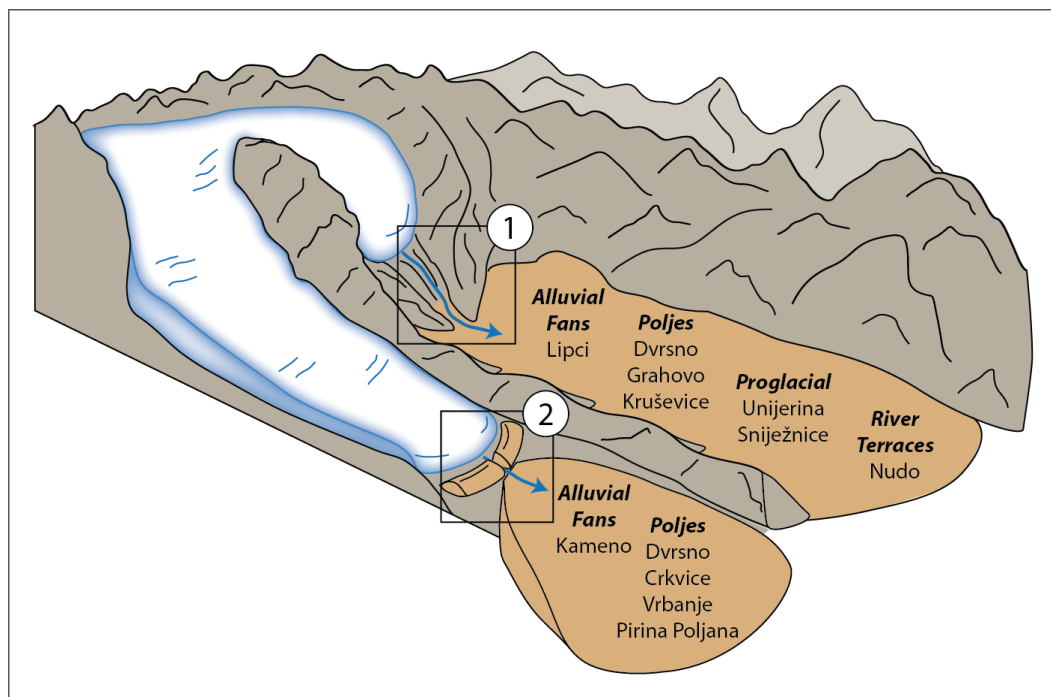
Fig. 9.1 – Schematic representation of the two types of surface meltwater pathways surrounding Mount Orjen and the types of depositional settings observed downstream. See Section 9.3 for a full discussion. 1) Meltwater pathway Type 1 reflects a steep sided, limestone gorge, often situated several kilometres from the depositional environment and draining the former ice cap situated on the high altitude plateau area. 2) Meltwater pathway Type 2 represents the termination of an outlet glacier within the depocentre downstream (such as within the polje depression). This may provide a lower energy meltwater environment than the steep sided ravines observed within Type 1 meltwater pathways.

Woodward *et al*. (2008) also describe similar types of meltwater pathways in the limestone-dominated Voidomatis Basin in Northwest Greece. In their study, meltwater route 1 (MR1) drained the high altitude plateau directly into the Vikos Gorge through the Megas Laccos Canyon. This system resembles meltwater pathway Type 1 at Mount Orjen. Meltwater route 2 (MR2) of Woodward *et al*. (2008) represents the termination of Pleistocene glaciers within the Voidomatis Valley, and more closely resembles the Type 2 meltwater pathway of Mount Orjen.

Differences in these meltwater and sediment transportation routes, as well as the contrasting depositional settings within neighbouring basins, may have led to variations in the timing of sediment delivery and landscape stability downstream. The Harden Index PDI values suggest that different land surfaces within the stratigraphical units defined in Table 9.1 have not stabilised simultaneously. The poljes of the Dvrsno Sub-Member, for example, present soil PDI values ranging from 4.76 (Grahovo) to 13.75 (Kruševice). This may reflect the 'asymmetrical' and 'asynchronous' nature of glacial activity within the individual basins (Gillespie and Molnar, 1996), whereby during any given glacial cycle, the outlet glaciers surrounding Orjen may reach different maximum extents at different times. These factors may have led to variations in the timing of peak meltwater discharge within different basins. This has been suggested by Gillespie and Molnar (1996) for glaciated catchments in The European Alps and the Rocky Mountains of North America. The absence of buried soil horizons within the fluvial sequences of Orjen also alludes to a degree of prolonged landscape instability between glacial phases. At Orjen, the karstic landscape also provides an important control on meltwater and sediment delivery downstream, and has led to considerable variations in landscape dynamics during successive glacial cycles. The significance of subterranean karstic meltwater flow at Mount Orjen is discussed in detail in the following sections.

9.2 Fluvial morphostratigraphical and geochronological framework: complex morphostratigraphical records

Four main fluvial settings surround Mount Orjen: river terraces in the Nudo valley; the ice proximal/shallow lacustrine environment at Unijerina; the coastal alluvial fan at Lipci; and the ice marginal setting at Sniježnice. These sites contain interesting morphosedimentary records that are worthy of more detailed discussion beyond the morphostratigraphical framework presented in Table 9.1. The depositional history of each of these settings is explored in the following sections.

9.2.1 Nudo: river terrace sequence

Five terrace surfaces have been sampled in the Nudo valley, and a sixth surface has been identified. The alluvial sediments are dominated by massive to crudely-stratified and coarse grained limestone sands and gravels. Terraces were mapped as individual sedimentary units

using standard field techniques and are represented within the Orjen fluvial morphostratigraphical framework (Section 9.1) as 'Beds' (Table 9.1). In the field, it was not possible to observe the contacts between individual units due to an absence of exposures. Differentiating between a single valley fill and multiple depositional phases therefore relies on the available morphosedimentary evidence as well as U-series and Harden Index data.

Many of the exposures in the Nudo valley contain thick calcite horizons and cemented benches, and six of these have been dated using U-series methods (Fig. 9.2). Three of these ages, from sediments beneath three of the lowest terrace surfaces (Zaslap, Javora and Vućiya units), are dated to >350 ka (Figure 9.2). A second sample from the Zaslap unit yields a minimum age of 146.8 ± 9.1 ka. Calcites from two of the highest terrace surfaces (Arandelovo Unit) have been dated to 56.5 ± 1.3 and 65.9 ± 5.2 ka. Harden Index PDI values for soils of the Vućiya (6.29) and Zaslap (3.10 and 1.84) units suggest that land surface stability, and the onset of pedogenesis, within the higher terrace surfaces preceded that of the lower units.
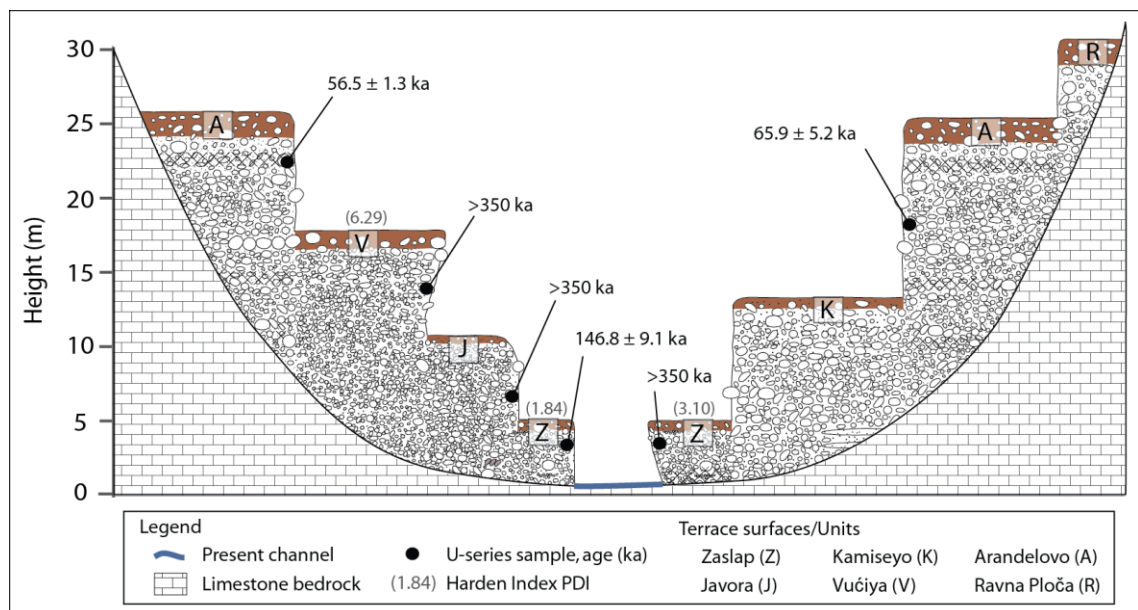
Figure 9.2 – Idealised cross sectional representation of the terraces of the Nudo valley, north Orjen, displaying U-series ages and sample locations. Height (m) represents the height of the terrace surface above the present day channel. U-series ages are uncorrected (see Chapter 8). Harden Index PDI values are indicated in parentheses for the Vućiya and Zaslap Units.

The U-series ages provide strong evidence to suggest that the bulk of the alluvial sedimentary sequence within the Nudo valley was deposited before 350 ka. This is thought to correlate with the major glaciation of Mount Orjen during MIS 12, when large volumes of glacigenic sediment would have been delivered to the fluvial system and deposited within the valley. This is

supported by the three U-series ages from the lowest terraces within the valley that are dated to >350 ka. If the validity of the U-series ages is accepted, and there is no reason to assume otherwise, the record at Nudo appears anomalous in that the lowest terraces yield the oldest ages whilst the highest terraces provide the youngest ages. It is important to reiterate that the U-series ages date phases of calcite formation and therefore represent minimum ages for the host alluvium. In key respects the record at Nudo is broadly consistent with the morphosedimentary and U-series data from other fluvial settings surrounding Mount Orjen (such as Grahovo polje, Pirina Poljana polje and Kameno alluvial fan) which suggest that the period of maximum alluvial deposition took place prior to 350 ka, and is correlated to MIS 12.

In contrast to other river basins in the Mediterranean region (Macklin and Woodward, 2009) the terrace sequence at Nudo contains only limited evidence of deposition since MIS 12. The U-series age of 146.8 ± 9.1 ka from calcites within the Zaslap surface may reflect a thin veneer of sediments deposited during MIS 6. This is consistent with the evidence of MIS 6 aggradation observed at Vrbanje polje and Lipci alluvial fan that are also situated beyond the MIS 12 ice margins. The highest terrace surface (Arandelovo unit) of Nudo yields U-series ages of 56.5 ± 1.3 ka and 65.9 ± 5.2 ka. It is possible that these ages represent a more recent phase of alluviation correlated to MIS 5d-2. It is also possible, however, that the younger ages within Nudo reflect phases of calcite formation within pre-existing sediments that were deposited during MIS 12. In this respect, the youngest ages obtained from Nudo, from the surface of the Arandelovo unit may reflect more recent calcite formation, possibly in association with localised springs along the valley sides.

The Nudo record shown in Figure 9.2 indicates that the system has been subsequently dominated by incision (perhaps during interglacial stages) and the morphosedimentary units, or beds, identified in the field actually reflect terrace *surfaces*, or straths, that have been cut into the main valley fill. The abundance of strongly cemented benches may help to preserve the incised terrace morphology. The similarities in sedimentology between all mapped exposures (Chapter 5; Plate 5.11) and the dominance of limestone lithologies means that it is not possible to distinguish between depositional phases on the basis of sedimentology alone. To further investigate the age of the deposits, and the onset of incision, within the Nudo valley further radiometric dating techniques should be applied. Several studies have used cosmogenic age-depth profiles within fluvial terraces to successfully establish terrace surface age (e.g. Carcaillet *et al*., 2009 - in Albania; Hein *et al*., 2009 - in Patagonia; and Egli *et al*., 2010

– in the Swiss and Italian Alps). This provides a valuable opportunity to more securely constrain the age of former floodplain levels and the pace of incision both within the Nudo valley, and elsewhere surrounding Mount Orjen. The feasibility of using these methods at Orjen requires further investigation.

The observed terrace sequence within the Nudo valley and the dominance of MIS 12 aggradation can be explained through changing sediment supply characteristics during the cold stages of the Middle to Late Pleistocene (Fig. 9.3). Three glacial phases have been identified by Hughes *et al*. (2010) in the glacial morphosedimentary record. These have been correlated to MIS 12, MIS 6, and MIS 5d-2 and the Younger Dryas and are in good agreement with the records from northwest Greece (e.g. Hughes, 2004; Woodward *et al*., 2008) and the glacial record of central Montenegro (Hughes *et al*., 2011b). The fluvial archives from elsewhere surrounding Orjen also record the impacts of these glacial phases, as well as tentative evidence of deposition during MIS 10-8. The magnitude of the MIS 12 glaciation means that in many instances the ice mass extended beyond the upland plateau (c. 1,000 m a.s.l.) and often reached the depocentres downstream (such as at Vrbanje, Kameno, Dvrsno and Pirina Poljana). This strong coupling of the glacial and fluvial systems meant that meltwater and glacigenic sediment were readily delivered directly to the fluvial environment and formed the thick sedimentary sequences within the poljes and alluvial fan settings. During MIS 6 the maximum ice margins were largely situated on the upland plateau whilst during MIS 5d-2 moraines indicate that ice was confined to the highest peaks. Ice masses during MIS 10 and 8 are likely to have been situated upvalley of the MIS 6 ice limits (Hughes *et al*., 2010). The progressive decrease in the magnitude of glaciation from the Middle to Late Pleistocene meant that since MIS 12 the coupling between the glacial and fluvial systems have become weaker, leading to a less efficient sediment delivery system (Fig. 9.3). This is compounded by the well-developed karstic terrain of the Orjen massif. When ice was restricted to the high altitude plateau extensive areas of karstic depressions and pathways into subterranean channel networks would have been exposed. Some sediment would have been retained within the surface dolines or poljes, whilst meltwater would have been preferentially channelled into the underground drainage system, and not necessarily as surface runoff. This phenomenon is observed at the present day in the limestone karst foreland of the Glacier de Tsanfleuron in the Swiss Alps (Hambrey and Alean, 2009). Sinkholes channel meltwater into the subterranean karst drainage network, and surface runoff is limited in comparison to non-karstic basins.

The extent of the incision within the alluvial fill of the Nudo valley suggests that this location may have formed one of the main subaerial meltwater conduits, emerging from the karstic system, since the major aggradational phase of MIS 12. The steep-sided limestone gorge setting of Nudo also favours the channelling of high-energy meltwaters and incision of the MIS 12 sediments. This meltwater would have been progressively starved of sediment as ice became constrained to the plateau and glacigenic material was deposited into the higher altitude surface depressions. There is evidence from the plateau area of Lisac, above the Nudo valley, of dolines filled with alluvium, yet these are currently not exposed for sampling (Chapter 5). Tectonic activity within this part of Montenegro may have also influenced the degree of incision within the Nudo valley. The estimated uplift rate of the Orjen massif is 2-4 mm/yr, but it has also been suggested that the Bay of Kotor is subsiding (Djurović and Petrović, 2007). This therefore creates a complex tectonic scenario for this region. The extent of incision at Nudo is not observed in any of the other fluvial settings surrounding Orjen. This suggests that tectonics play a minor role here, and the Orjen landsystem is instead driven by a changing meltwater and sediment supply regime during the Middle to Late Pleistocene. This would have been complicated by the karstic terrain, which has created variable sediment supply characteristics within neighbouring basins. Beyond Nudo, other sites such as Dvrsno, Pirina Poljana and Kameno display limited incision since MIS 12, which suggests that meltwater has been predominantly channelled within the subterranean karst. What is more, in contrast to the Nudo valley, these shallow gradient polje and fan settings favour the attenuation of any surface runoff and promote the long-term deposition of glacigenic sediment.

The river terrace sequence at Nudo contains some of the only evidence within the Mediterranean basin of alluvial deposition during MIS 12 (Section 9.5.3) (Macklin *et al.* 2002; Macklin and Woodward, 2009). This contrasts markedly with the fluvial record of the Voidomatis Basin in northwest Greece which presents one of the closest analogues to the Nudo valley and the wider Orjen landsystem. In the Voidomatis Basin, U-series ages (supported by ESR, ^{14}C and TL dates) provide evidence for fluvial deposition during MIS 5d-2. There are no sediments directly dated to MIS 12, although there is evidence to suggest that the oldest and thickest Pleistocene alluvial unit (U7) in the Voidomatis may be related to the largest glaciation in that catchment. More dates are needed to test this idea. It has been argued that the Late Pleistocene fluvial record in the Voidomatis in part represents the redistribution of large volumes of glacigenic and fluvial sediment that were delivered to the

system during MIS 12 (Woodward *et al.*, 2008). The contrasts in sediment delivery and preservation between Nudo and the Voidomatis records are therefore rather striking.
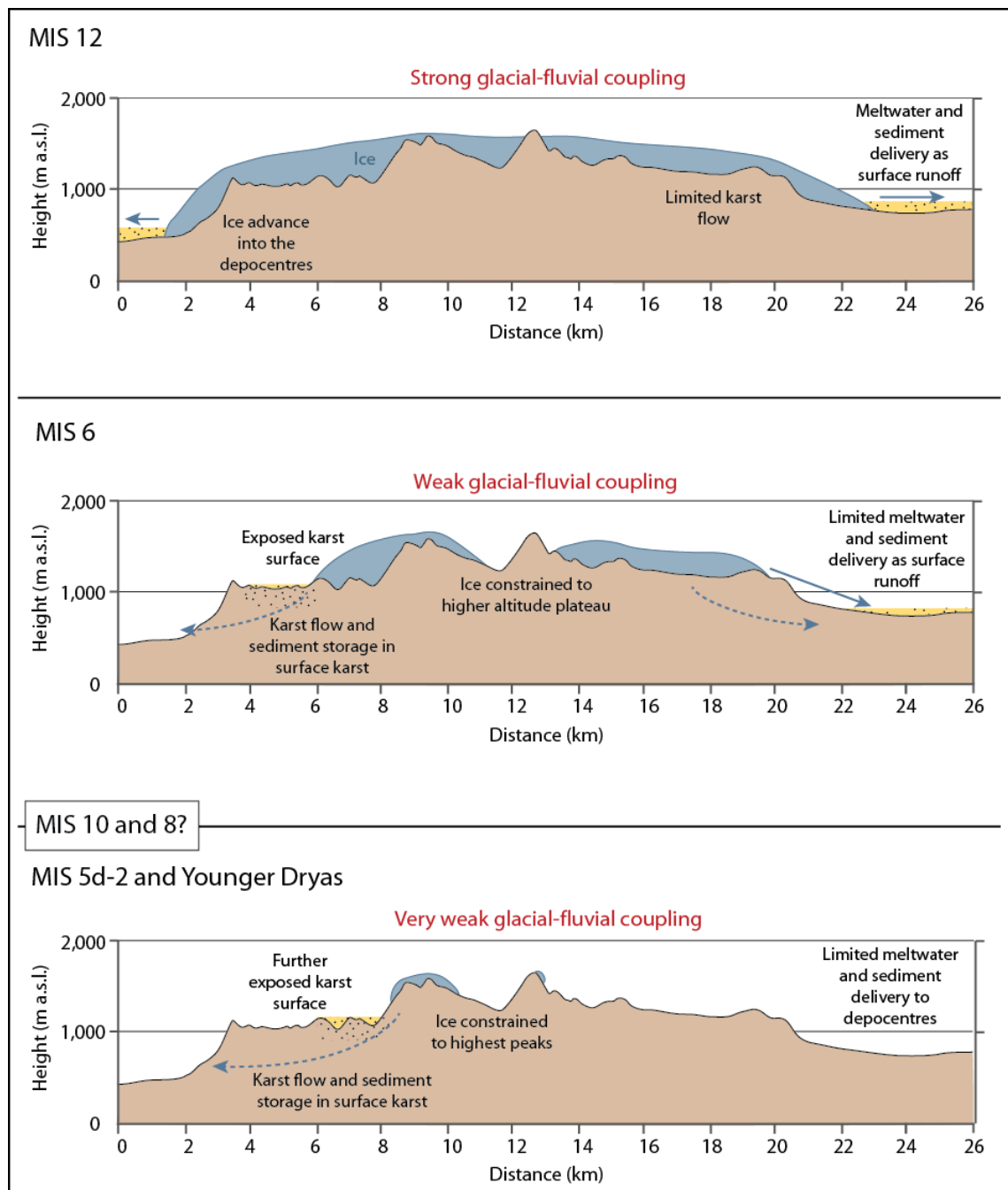
Figure 9.3 – Schematic representation of the influence of karstic terrain on the Pleistocene glacial and fluvial dynamics of the Orjen massif. Meltwater and sediment delivery pathways over successive glacial cycles are indicated. The glacial limit of the Orjen ice cap during MIS 10 and 8 has not been identified in the field, but it is likely to be situated between the MIS 6 and MIS 5d-2 margins.

The exceptional preservation of some of the oldest parts of the Pleistocene glacial and fluvial records at Orjen may be, in part, due to the dominance of the karstic system and the upland plateau setting of the Orjen massif, described above. This may have limited the degradation of the MIS 12 records and the supply of sediment in later cold phases. The depositional history within the Nudo valley therefore provides an important component to aid our understanding of Pleistocene landscape dynamics. This is significant not only for the wider region surrounding the Orjen massif, but also the glaciated Mediterranean uplands more generally.

9.2.2   *Unijerina: proglacial/shallow lacustrine setting*

The exposures at Unijerina are some of the few locations to contain evidence of at least three depositional phases (Chapter 5; Fig. 9.4). The lowest facies (U3a) contains interstratified fluvial sands and gravels. The capping silt unit contains dropstones, indicative of a proglacial lacustrine setting (e.g. Rother *et al*., 2010). Shallow proglacial lakes are also observed within present day karstic terrains, such as in the foreland of the Glacier de Tsanfleuron in the Swiss Alps (Hambrey and Alean, 2009). The fluviolacustrine sediments at Orjen are overlain by a diamicton (U3b). The sedimentological characteristics of this diamict may reflect the slumping of glacial sediments from the higher altitude valley sides, into a shallow proglacial lake or glaciofluvial setting (Fig. 9.4). The excellent preservation and undeformed nature of the underlying interstratified fluvial deposits indicates that both the fluvial sediments and the diamicton were deposited during a phase of ice retreat, or stabilisation, rather than ice advance. The diamicton at Unijerina and moraines further down valley, considered to be contiguous with Unijerina in the maps of Hughes *et al*. (2010), have both yielded U-series ages of >350 ka. The fluviolacustrine and glacial diamict facies are therefore correlated to the Kotorska-Sušica Member of the Orjen fluvial stratigraphy and the Knezlaz Member of the glacial framework (MIS 12). The upper facies presents a return to fluvial depositional processes and secondary carbonates here have been dated to 248.6 ± 16.7 ka (MIS 8/7). It is possible, however, that these sediments were deposited during the same depositional phase as the lower facies (MIS 12), or during MIS 10 or MIS 8, but reflect a much later phase of carbonate development during MIS 7 when climatic conditions would favour calcite formation. The sedimentary sequence here is significant in that it contains evidence of the localised deposition and reworking of sediments over multiple morphogenic phases. This provides insights into the contrasting sediment dynamics and variations in the preservation of the morphosedimentary record within neighbouring basins.
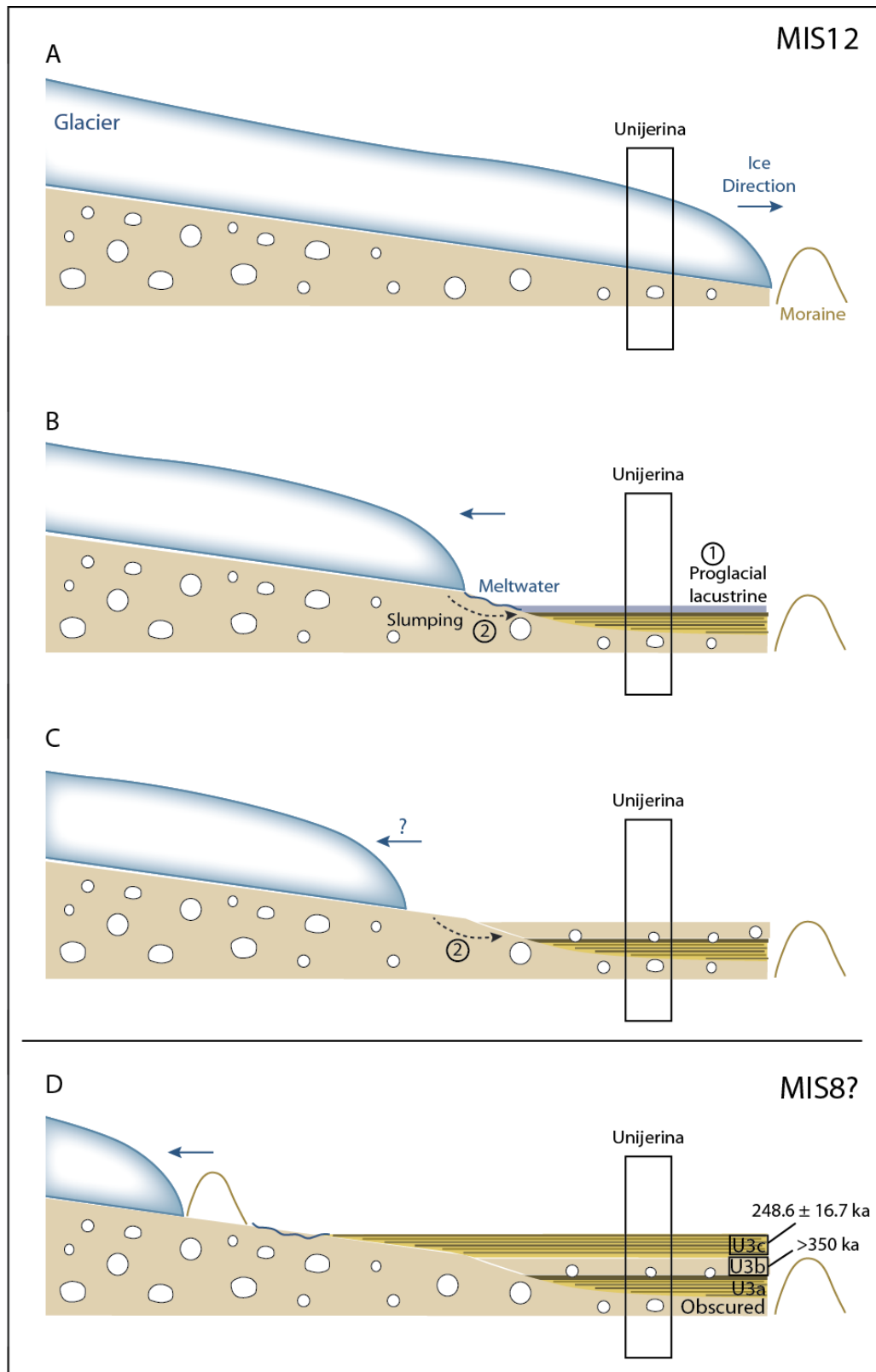
Figure 9.4 – Schematic model of the depositional setting at Unijerina, east Orjen, and the accumulation of the exposed stratigraphy. A) Ice advance during MIS 12 depositing a large end moraine. B) Ice retreat, the deposition of fluvial sediments, and 1 - the formation of a proglacial lake, before 2 – slumping of diamicton material. C) Possible ice retreat alongside slumping of diamicton from the surrounding terrain during MIS 12. D) Further ice retreat and/or stabilisation and the deposition of fluvial sediments, tentatively correlated to MIS 8.

9.2.3   Lipci: coastal alluvial fan

For at least two sites within the fluvial environment surrounding Orjen, there is evidence of deposition extending offshore; at the alluvial fans at Lipci and Risan. There are no sedimentary exposures at Risan, and the large alluvial fan here is mantled with unconsolidated limestone scree. The alluvial fan at Lipci contains evidence of several phases of deposition, as well as incision (Figure 9.5). Depositional phases are correlated on the basis of sedimentology and U-series analysis to MIS 12, MIS 10-8 and MIS 6, which broadly correspond to the phases of headwater glaciation (Hughes *et al.*, 2010). Submarine topography (Bortoluzzi *et al.,* 2009) indicates that the now submerged portion of the fan surface contains deeply incised channels (up to 10 m deep) which are similar in morphology to those exposed at Section L4. This suggests that these channels were incised subaerially, after the deposition of alluvium during MIS 6, and have since been submerged by rising sea level and subsidence of the Bay of Kotor since MIS 5e (Lambeck and Purcell, 2005; Djurović and Petrović, 2007; Surić *et al.*, 2009). This corresponds to the relative sea level curve derived from speleothem records in submerged caves along the Croatian coast (Lambeck and Purcell, 2005; Surić *et al.*, 2009). The U-series dated calcites from the Lipci fan (Sections L2-4) show no evidence of dissolution or detrital contamination, either in section or from isotopic indicators. This suggests that sea level has not submerged this part of the fan since the time of subaerial calcite precipitation, and maximum sea level highstand during MIS 5e within the Bay of Kotor can be constrained using the model of Surić *et al*. (2009) to <20 m a.s.l. Their model, however, was developed for the coastal region of Croatia, and may be complicated in this part of Montenegro by the complex tectonic regime which is characterised by uplift of the Orjen massif and subsidence of the Bay of Kotor (Djurović and Petrović, 2007).

The alluvial fan at Lipci provides an important link between the terrestrial glacial and fluvial records and the offshore marine record within the Bay of Kotor. This represents an important aspect for future research; to test the ways in which the sedimentological signal of Pleistocene glaciation in the Mediterranean is transformed not only downstream, but also offshore. This approach has been successfully applied in the Bay of Biscay by Toucanne *et al*. (2012), and would form a major research development within the Mediterranean region (Macklin *et al.,* 2012).
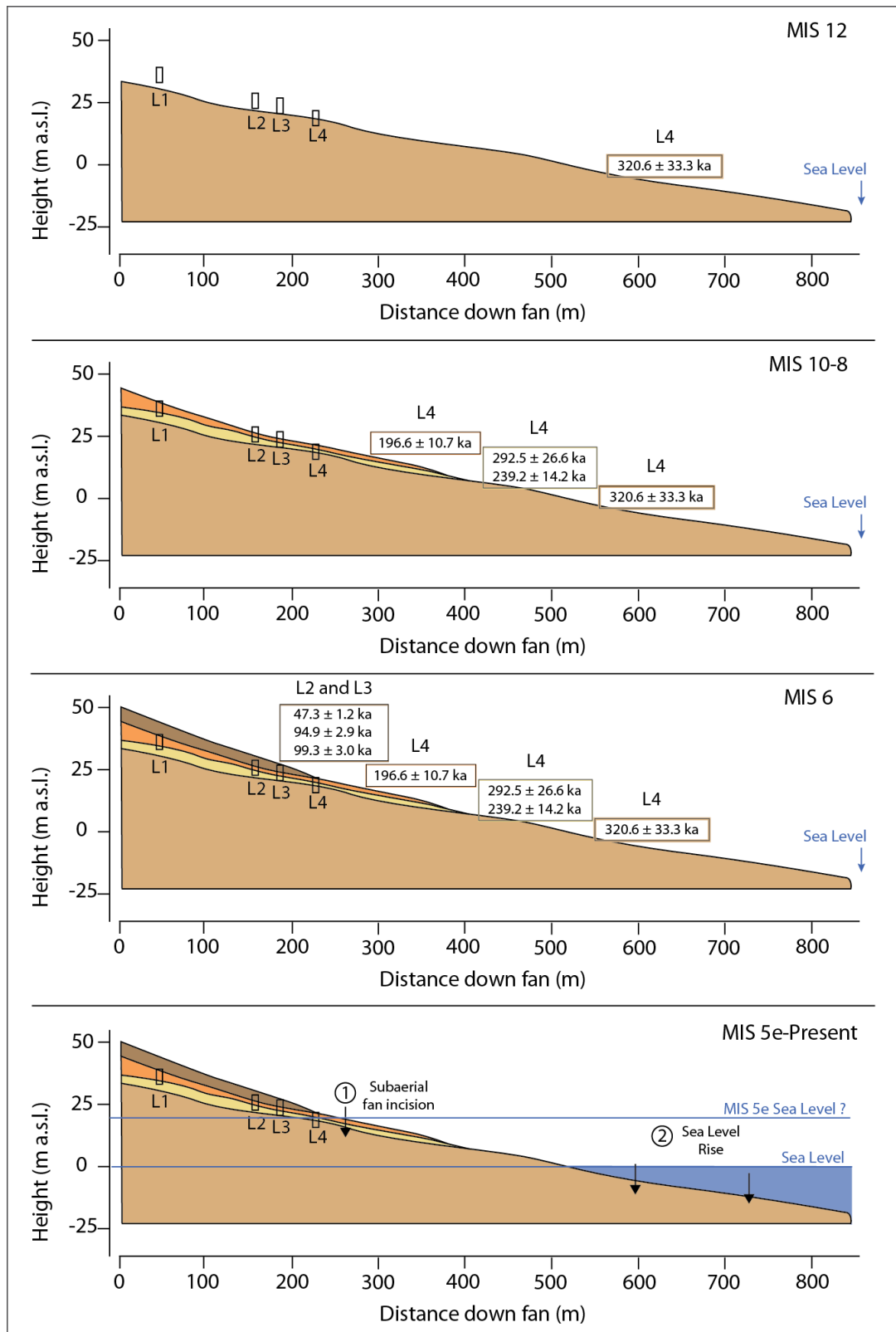
Figure 9.5 – Schematic representation and U-series ages of the development of the Lipci alluvial fan. Sea level below 0 m a.s.l. (present day sea level) is arbitrary, and reflects the present average depth of the Bay of Kotor (20-40 m). Sea level during maximum glacial stages would have been considerably lower (-100 m a.s.l.). The Lipci fan extends for up to 600 m offshore, and the x axis scale beyond 500 m is used as a guide only. The maximum suggested sea level highstand for MIS 5e follows Surić *et al*. (2009).

9.2.4   Sniježnice: ice marginal glaciofluvial setting

Alluvial sediments at Sniježnice (Fig. 9.6), south Orjen also contain evidence of multiple depositional phases within the Kotorska-Sušica Member (MIS 12-8). The outermost moraines in this valley are morphostratigraphically correlated to MIS 12. A series of inset moraines have been U-series dated to 124.6 ± 5.7 ka and 102.4 ± 3.1 ka and are correlated to MIS 6 (Hughes *et al*., 2010). Secondary carbonates capping the outermost moraine and adjacent fluvial deposits are dated to 268.3 ± 22.2 ka. These ages may represent more recent carbonate development within pre-existing (MIS 12) sediments (Chapter 8). It is also possible, however, that the moraines here form a palimpsest of glacial depositional phases during MIS 12-8. This has been suggested for the glacial deposits of Durmitor, in the central massifs of Montenegro (Hughes *et al*., 2011b), where closely spaced moraines from MIS 12-6 are often difficult to separate on the basis of morphostratigraphy. The fluvial record at Orjen, used together with the glacial framework, may therefore allow the timing of glacial activity to be more securely constrained.

9.3   Landsystem controls on Quaternary sedimentary records: the alluvial depositional settings of Orjen

9.3.1   Pleistocene fluvial behaviour: the contrasting morphosedimentary environments of Orjen

The sub-members of the Orjen fluvial stratigraphy have been categorised on the basis of morphosedimentary environment into: poljes, river terraces, alluvial fans, lacustrine and ice marginal settings. As will be discussed, these records, from variable topographic settings and meltwater pathways, display contrasting depositional histories of fluvial response to Pleistocene glacial activity. Figure 9.6 presents the dominant sedimentary characteristics of the fluvial depositional environments surrounding Mount Orjen. This has been developed using the facies model presented in Chapter 5, typical sedimentary logs, and idealised PSA data.

The large poljes situated outside the maximum ice margins contain thick sequences of stratified fluvial sands and gravels that are correlated to the Kotorska-Sušica Member (MIS 12-8). These sediments would have been delivered to the depocentres downstream as ice extended from the Orjen massif into the lower lying basins. The strong glacial-fluvial system

coupling during MIS 12 meant that large volumes of sediment were deposited at this time (Section 9.2.1). These sediments have been observed to depths of up to 10 m, but it is likely that many of these poljes are considerably deeper (Gams, 2005). In several poljes (Dvrsno, Kruševice and Pirina Poljana) the deposits become increasingly well-stratified and dominated by finer grained sediments with distance from the ice margin. Alluvial fan sediments at Lipci and Kameno, south Orjen, display a rapid downstream fining during the shift from ice-proximal to ice distal locations. The polje and alluvial fan settings are comparable in that many of the poljes, where ice terminates within the depression itself, resemble low angle alluvial fan depositional environments (such as at Vrbanje, Pirina Poljana and Dvrsno). The alluvial fans at Orjen, however resemble much steeper settings, and are often situated downstream of high-energy meltwater pathways (Type 1, bedrock gorges) such as at Lipci and Risan. The coastal fan at Lipci provides an important link between the Pleistocene terrestrial glacial archive and the submarine record within the Bay of Kotor (Section 9.2.3). The Nudo valley, north Orjen contains a suite of five river terraces, with a sixth terrace more tentatively identified at higher elevations (over 410 m a.s.l.). The sediments here are coarse grained, sandy, massive and stratified alluvium. These terrace surfaces have been U-series dated to >350 ka and are correlated to the Kotorska-Sušica Member and the major glacial advance during MIS 12 (Knezlaz Member of the glacial stratigraphy). The sediments at Sniježnice reflect the ice marginal characteristics defined by Fraser and Cobb (1982), and contain massive to stratified sands and gravels, with clays/silts and boulder sized clasts.

Lying within the maximum ice limits, the polje at Crkvice is correlated to the Krivošije Member (MIS 6) and contains stratified sands and silts typical of the ice distal deposits found within the larger poljes at Dvrsno and Grahovo. No other exposures of fluvial sediments have been identified within the maximum ice margins from MIS 6, 5d-2 or the Younger Dryas. It is likely, however, that at least some of the surface karstic depressions on the higher altitude plateau are filled with sediments from MIS 6 and MIS 5d-2, but are currently not exposed (Section 9.2.1). The deposits at Unijerina, within a neighbouring valley of Crkvice, have been correlated to the Kotorska-Sušica Member (MIS 12-8) (Section 9.1). It is possible, however, that a veneer of sediments from MIS 6 are also present here but have not yet been identified.

An important characteristic of the alluvial sedimentary archive of Orjen is that at no one location is the entire sequence of Pleistocene glacial and fluvial activity fully recorded. Fluvial depositional settings may, however, contain more detailed archives of landscape dynamics

than the glacial records, which are often more fragmentary (Giraudi, 1998; Fontana *et al.*, 2008; Rother *et al.*, 2010). This is particularly true in the case of poljes, which form extensive sediment depocentres. At Orjen, many of these poljes are situated downstream of the maximum ice margins, meaning that they have not been overrun by subsequent ice advance and the sedimentary sequence often remains intact. However, many of these poljes became infilled with sediments during MIS 12 and contain comparatively limited evidence of subsequent depositional phases. This may be due to the contrasting meltwater and sediment delivery pathways between glacial stages. As ice became constrained to the higher altitude plateau after MIS 12, evidence suggests that subterranean karst flow assumed a more dominant role in meltwater transfer from the ice margins, whilst sediments were deposited more locally and not necessarily transported to the larger depocentres outside the MIS 12 ice limits (Section 9.2.1; Fig. 9.3). The glacial and fluvial systems effectively became progressively decoupled. Within the MIS 12 ice margins, at sites such as Unijerina, evidence of sediment reworking means that constraining the timing of primary deposition is complex (Section 9.2.2). This suggests that sedimentary records of Pleistocene fluvial behaviour are preserved in different ways within contrasting topographic settings. Fluvial sedimentary records must therefore be considered at the landscape scale (Glasser *et al.*, 2009) and not as isolated landscape components. The variety of depositional settings surrounding Mount Orjen means that, in some ways, this system may be used as a model for the depositional scenarios observed within other glaciated basins across the Mediterranean and elsewhere. It is important to consider that the landscape-scale approach adopted in this study inherently sacrifices a certain degree of the spatial resolution of the fluvial record. The locations of the analysed exposures have been largely dictated by quarries, road cuttings and stream cut sections. This means that in some instances, such as the large poljes at Dvrsno and Grahovo, only a small portion of the sedimentary sequence was examined. Proglacial environments are characterised by the development and lateral migration of multiple braided and anastomosing streams (Anderson, 1989). These produce a highly diverse sedimentology containing vertical and lateral successions of coarse grained sediments as well as finer, clay and silt-rich alluvium. An individual quarry section within a vast polje may expose only one of these stream pathways. Through combining these fragmentary records, and understanding their limitations, it is possible to develop a more complete understanding of Pleistocene landscape history (Macklin *et al.*, 2012). Sections 9.3.2 and 9.3.3 will explore in more detail the processes operating at the glacial-fluvial interface and their impacts on morphosedimentary records through time.
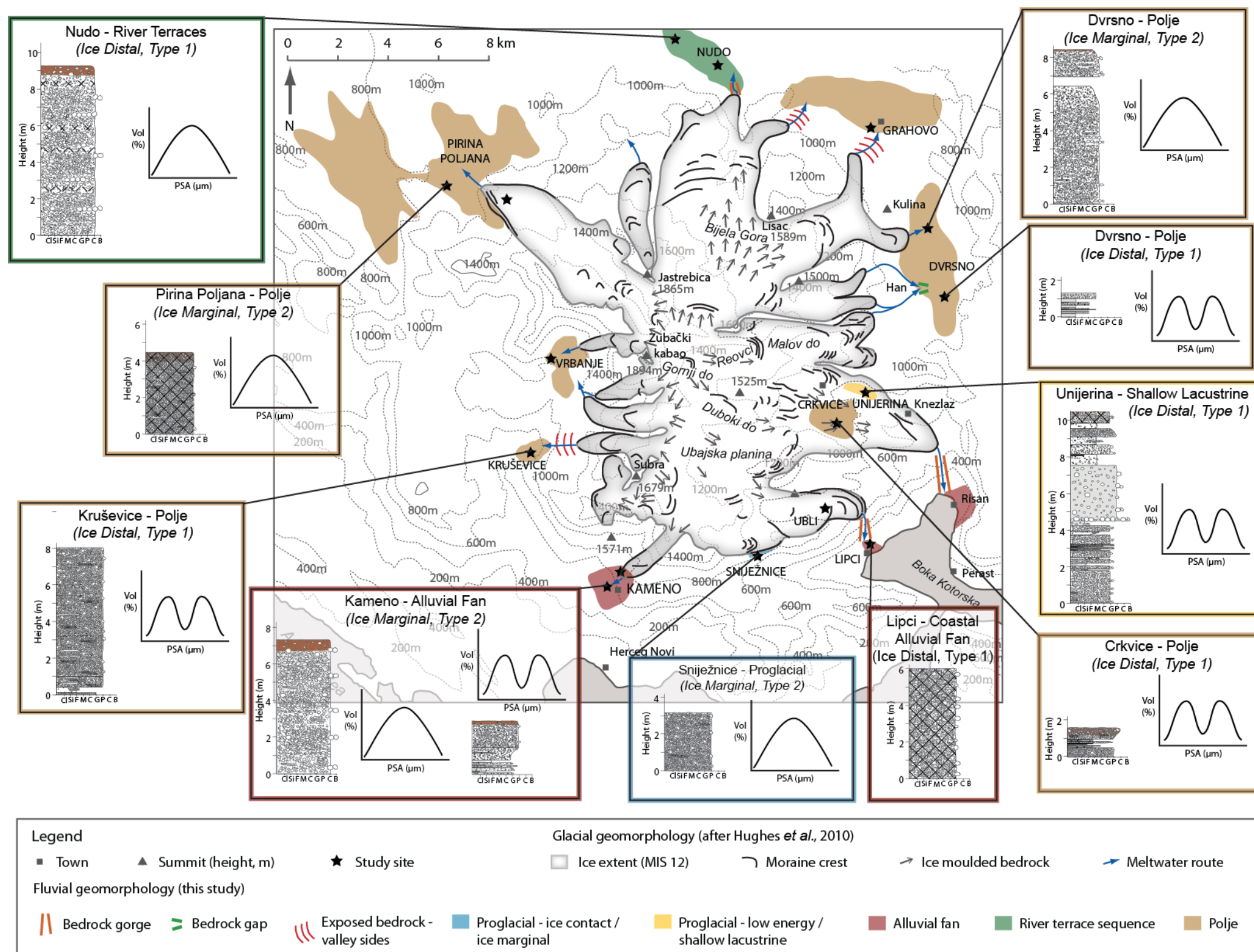
Figure 9.6 – Summary of the key alluvial morphosedimentary evidence at selected study sites, from sub-members of the Kotorska-Sušica (MIS 12-8) and Krivošije (MIS 6) members. Each site is representative of the sedimentological characteristics from each depositional setting: poljes, river terraces, alluvial fans, ice marginal and proglacial lacustrine. Schematic representations of the average dominant particle size distributions (PSD) of the fine sediment matrix are also provided. See Section 9.3.2 for a more detailed discussion of the fine sediment fraction PSD. Meltwater pathway types (1 and 2) follow the discussion in Section 9.2.2; Table 9.3).

9.3.2   Pleistocene fluvial behaviour: impacts of ice margin dynamics on the alluvial sedimentary record

The relative position of the Pleistocene ice margins exerts an important influence upon fluvial sedimentary characteristics at Mount Orjen. As has been discussed through the karst–meltwater model (Section 9.2.1; Fig. 9.3), evidence suggests that during MIS 12, when the karst plateau of Orjen was largely overrun by ice, surface meltwater channels formed the dominant pathway from the glacigenic sediment source areas to the depocentres downstream. After MIS 12 meltwater was largely channelled within the subterranean karstic network. In many of the analysed fluvial settings there is only limited evidence of deposition or incision since MIS 12-8. This provides an exceptional opportunity to examine the role of these surface meltwater pathways upon sediment characteristics.

Two dominant types of surface meltwater pathways have been identified (Type 1 – bedrock gorges, and Type 2 – alluvial channels from the ice margin, Figure 9.1). The sedimentary records downvalley of these contrasting pathways broadly reflect the facies models of meltwater outwash defined by Fraser and Cobb (1982), Miall (1983; 1985) and Anderson (1989) (Table 9.2), where sediments become finer with distance downstream.

Outwash Environment	Sedimentological Characteristics
Ice Marginal	Immediately adjacent to the ice margin. Contains clay-rich gravels (dominantly cobbles), laminated fines, cross stratified sand and gravel and massive cobble units reflecting sediment deposition directly from the ice margin.
Ice Proximal	Massive gravel units (typically >95% of the sequence) interstratified with sand lenses or thin sand horizons reflecting minor channels within a braided river environment.
Ice Medial	Interstratified sands and gravels with minor components of overbank fines. Evidence of wedge-shaped gravel point bars may also be present. Some exposures may consist of several courses of fining upwards sequences (reflecting a retreating ice margin) or coarsening upward sequences (indicating an advancing ice margin).
Ice Distal	Interstratified sand and finer material demonstrating considerable lateral variability and reflecting more of a meandering or anastomosing regime. This contrasts with the braided river environment closer to the ice margin.

Table 9.2 – Generalised model of the sedimentary characteristics of glacial meltwater, categorised by relative distance from the ice margin. Distance in this model is not quantified. After Miall (1983; 1985) with further discussion by Anderson (1989). The *Ice Marginal* facies model is defined by Fraser and Cobb (1982).

Analysis of the fine sediment matrix component (<63 μm) reveals several important distinctions between the alluvial depositional settings surrounding Orjen. Figure 9.6 and Table 9.3 present a summary of the dominant PSD at each site referenced against relative distance from the former ice margin, moraine location (terminating at the site or constrained to higher altitudes), and meltwater pathway (Type 1 and Type 2). Alongside field sedimentology, these contrasting particle size distributions can be used to propose a model framework of the depositional settings at Orjen using the classifications of Miall (1983) (Table 9.3). Sites situated <1,500 m from the Pleistocene ice margin are classified as *Ice Marginal-Proximal* whilst those located >1,500 m from the ice front are termed *Ice Medial-Distal* settings. Deposits in the *Ice Marginal-Proximal* zone largely contain massive, crudely- to well-stratified gravels. The fine sediment fraction (<63 μm) of these deposits displays a unimodal PSD. *Ice Medial-Distal* sediments comprise interstratified gravels, sands and fines, typical of the ice medial and distal environments of Miall (1983). The fine sediment fraction (<63 μm) at these sites is dominated by a bimodal PSD, which contrasts with the unimodal distribution observed upstream. These contrasting environments are highlighted in Figure 9.7, which presents a schematic representation of the neighbouring depositional settings surrounding the Orjen massif. The main exceptions to this relationship are the deposits within the Nudo valley. Sediments here are not formed by the alluvial fan-type sedimentation processes observed in the poljes or at Kameno. The terrace sequence at Nudo instead represents sediments delivered by an ice distal, Type 1 meltwater pathway, but highlights the influence of karstic processes on meltwater, sediment supply characteristics, and incisional processes MIS 12 (Section 9.2.1).

The exposures within the large polje at Pirina Poljana present a strong unimodal PSD despite their position >4,300 m from the maximum Pleistocene ice margins. The main difference between this site and others within the *Ice Medial-Distal* category is that the outlet glacier here terminated within the polje. This feature is otherwise only observed at sites within the *Ice Marginal-Proximal* zone (Table 9.3) at Dvrsno, Vrbanje and Kameno. This suggests that the transportation pathway (Type 1 or Type 2) of glacially-derived meltwater and sediment can have considerable impacts on the nature of the fine sediment matrix. Fluvial sediments that have been transported via bedrock gorges or across the higher altitude plateau (Type 1) tend to present a bimodal particle size distribution. Fine sediments delivered directly from the ice margin (Type 2; such as at Vrbanje, Dvrsno Transect 1, and Sniježnice) more closely resemble the normally distributed PSD of the glacial tills. This downstream shift towards bimodal sediments suggests the selective winnowing of specific fractions of the fine sediment

component (notably 6 – 20 μm, fine silts) and the concentration of clay sized non-carbonate particles during fluvial transport, as the limestone bedrock and glacigenic sediments are transformed within the fluvial environment. These particle size distributions have been observed within several studies of meltwater environments and have been attributed to chemical weathering (Reynolds and Johnson, 1972; Nesbitt and Young, 1996; Tranter, 2003) and/or mechanical sorting processes (Garzanti et al., 2009).
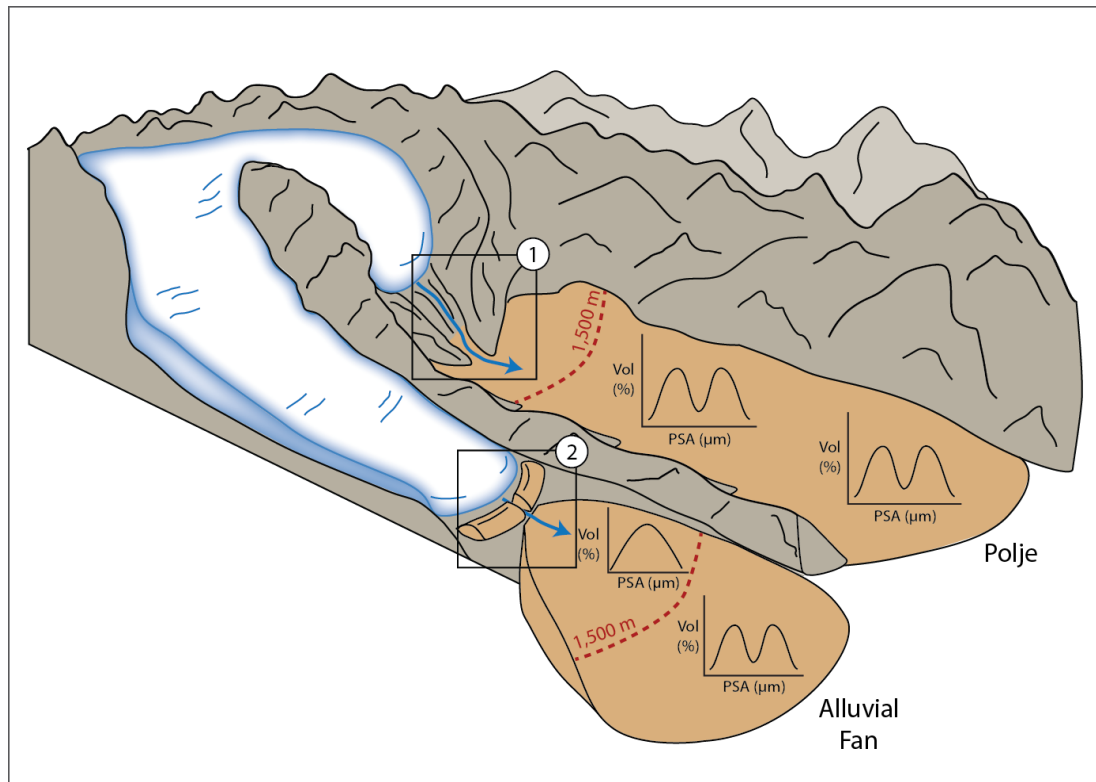
Figure 9.7 – Schematic diagram of surface meltwater pathways and depositional environments typical of the Orjen landscape. Meltwater pathway Type 1 depicts ice constrained at higher elevations, and the delivery of sediment to the polje via bedrock gorges (such as Dvrsno, Transect 2). Here the depocentre is situated >1, 500 m downstream of the ice margin (ice medial-distal) and the fine matrix component (<63 μm) displays a bimodal PSD. Meltwater pathway Type 2 reflects an ice terminus close to the depocentre, and sediment delivery directly into the polje/alluvial fan (such as Kameno). The fine sediment fraction displays a transition from unimodal to bimodal PSD at a threshold of 1,500 m from the ice front.

Proglacial environments are conducive to chemical weathering for a number of reasons. The high discharge regime and continual aeration of meltwater streams replenishes the acidity of these surface waters (Reynolds and Johnson, 1972; Tranter, 2003). The abundant supply of recently comminuted material from the glacier front means that mineral surfaces are freshly exposed, and more susceptible to chemical erosion (Reynolds and Johnson, 1972).

Geochemical studies have indicated that the preferential dissolution of carbonates, through hydrolysis, forms a meltwater solution at near saturation with calcite and aragonite. These solutions provide the necessary conditions for the dissolution of other, detrital, minerals (Tranter, 2003) that become concentrated within the clay size fraction (Nesbitt and Young, 1996). Evidence from the limestone-dominated catchments of Svalbard suggests that chemical weathering is particularly prevalent in the proglacial zone due to the abundance of carbonate lithologies and the colonisation of vegetation (Tranter, 2003).

Ice Marginal and Ice Proximal (<c. 1,500 m)				
Site	Distance from ice margin (m)	Moraine Position	Meltwater Source/Pathway	Dominant PSD
Dvrsno (Transect 1)	900 - 1,300	**At polje**	**Type 2**	Unimodal
Grahovo	1,400	Plateau	Type 1	Unimodal
Vrbanje	1,400 - 1,450	**At polje**	**Type 2**	Unimodal
Sniježnice	100	**Adjacent to site**	**Type 2**	Unimodal
Kameno	150 - 1,050	**At fan apex**	**Type 2**	Uni-/Bimodal
Lipci	950 - 1,150	Up valley	Type 1	-
Ubli	1,500	-	Type 1	Unimodal

Ice Medial and Distal (>c. 1,500 m)				
Site	Distance from ice margin (m)	Moraine Position	Meltwater Source/Pathway	Dominant PSD
Dvrsno (Transect 2)	2,900	Up valley	Type 1	Bimodal
Pirina Poljana	4,300	**At polje**	**Type 2**	Unimodal
Kruševice	1,900 - 2,000	Plateau	Type 1	Bimodal
Crkvice	2,200	Up valley	Type 1	Bimodal
Unijerina	1,900 - 2,250	Up valley	Type 1	Bimodal
Nudo	750 - 1,800	Up valley	Type 1	Unimodal

Table 9.3 – Depositional environments and dominant particle size distribution (PSD) of the fine sediment fraction at fluvial sites surrounding Mount Orjen (<63 μm). Values are referenced against ice margin position and meltwater pathways. **Type 1** meltwater pathways: steep sided, limestone gorge, often situated several kilometres from the depositional environment. **Type 2** meltwater pathways: the development of an alluvial channel directly from the ice margin, which terminates within the depocentre. Sites where moraines and meltwater pathways are situated at/within close proximity of the depositional site (Type 2 pathways) are emboldened.

It is likely that the non-limestone lithologies within the sediment samples from Orjen also reflect the mechanical sorting processes operating within the fluvial environment. Woodward *et al.* (2002) and Garzanti *et al*. (2009) suggest that denser grains are systematically concentrated into the finer fractions of sorted sediments as they preferentially settle from suspension. At Orjen, the bimodal PSD of the fine sediment matrix is apparent within almost all geomorphological contexts. It is therefore likely that in these systems, the observed particle

size distributions and lithological contributions are a combination of *both* the chemical preparation of non-carbonate lithologies, and their mechanical concentration within the fluvial environment through size-density sorting. Lighter, limestone and dolomite lithologies may have been transported further downstream and potentially offshore.

The contrasting meltwater pathways and observed particle size characteristics surrounding Mount Orjen can be used as a model to more fully understand the fluvial sedimentary environments in relation to the Pleistocene ice margins. At Pirina Poljana for example, the bimodal distribution of fine sediments at Section P1, inside the MIS 12 moraines, contrasts with the normally distributed fine sediment fraction beyond the ice limits. This suggests that these sediments were deposited at distances >1, 500 m from the ice front. This means that they may correlate with either a retreat phase of the MIS 12 glaciation (Crkvice Sub-Member), placing them within the Kotorska-Sušica Member, or downstream of the less extensive glaciation of MIS 6 as part of the Krivošije Member. The insoluble residue component of the fine sediment fraction here is similar to the sediments at Crkvice, which are correlated to the Krivošije Member (MIS 6). It can therefore be suggested that these sediments reflect deposition within the ice distal zone of the polje during MIS 6, and are not outwash sediments from a retreating MIS 12 ice front (Fig. 9.6).

9.3.3   River system response to glaciation of the Orjen massif over multiple glacial cycles

As well as the spatial variations in the nature of Pleistocene alluvial records surrounding Mount Orjen, fluvial system behaviour has also varied over successive glacial cycles. This has led to contrasting histories of fluvial dynamics within neighbouring catchments (Section 9.3.1). As will be discussed in Section 9.5, the alluvial archives of Mount Orjen reflect several aspects of the idealised theoretical models of sediment flux within glaciated basins (e.g. Church and Ryder, 1972; Church and Slaymaker, 1989; Marren, 2005; Dühnforth *et al*., 2008). These models are applicable over timescales of individual glacial cycles. When considered over multiple glacial-interglacial fluctuations since MIS 12, however, the glacial and fluvial dynamics of the Orjen massif are complicated by karstic processes. The role of karstic terrain in Pleistocene meltwater and sediment dynamics has previously received little research attention. The depositional settings surrounding Orjen, however, allow these long-term landscape processes to be explored in detail.

The karstic landscape of Orjen contains networks of subterranean channels and cave systems, as well as poljes and dolines at the surface. Based on the morphosedimentary evidence from the Nudo valley and elsewhere surrounding Orjen, a model of karstic and glacial-fluvial interactions has been discussed in detail in Section 9.2.1 and is briefly summarised here. The model suggests that during MIS 12 the karstic plateau was overrun by ice and the close coupling of the glacial and fluvial systems meant that sediment was delivered directly to the depocentres downstream. This has led to the deposition of thick sequences of MIS 12 alluvium. During MIS 6 the ice cap was constrained to the higher plateau, exposing large areas of karstic depressions and sinkholes at the surface which promoted subterranean meltwater flow. The limited evidence of MIS 6 sediments further downstream of the MIS 12 ice limits suggests that sediments may have been deposited within depressions of the high altitude karst. As the ice masses retreated further during MIS 5d-2, and were also constrained to the higher peaks during MIS 10 and 8, the karstic system played an increasing role in meltwater and sediment delivery downstream. The glacial and fluvial systems became progressively poorly coupled and there is only limited evidence of fluvial deposition from MIS 5d-2 downstream of the ice margins.

The karstic terrain of the Orjen massif reflects the classic karst landscapes described by Gams (1969; 1978) for the Dinaric region, and Lewin and Woodward (2009) for the wider Mediterranean. The landscape surrounding the Orjen massif also closely resembles the karstic setting of the Sinjajevina Mountains, central Montenegro (Telbisz, 2010a; 2010b) and the Voidomatis Basin in northwest Greece (Woodward *et al*., 2008). It is likely that many other karstic depressions across the Mediterranean also contain thick sequences of Pleistocene alluvium that have so far not been investigated. Within glaciated regions, these settings could provide valuable records of Quaternary landscape change.

The large poljes situated outside the MIS 12 ice margins, such as Dvrsno, Grahovo and Pirina Poljana, are considered to have formed prior to the onset of Pleistocene glaciations. They have since been filled with large volumes of glacigenic sediment delivered via meltwater from the Orjen ice cap. Within the maximum ice margins, the karstic landscape has been overrun and moulded by glaciation during Pleistocene cold stages since MIS 12. These ice masses would have transformed the existing accommodation spaces and karstic hollows. These hollows, both inside and outside the maximum MIS 12 ice margins, therefore form important areas of sediment storage or 'accommodation space' (Dühnforth *et al*., 2008) during subsequent glacial

advances. The proglacial alluvial fan at Kameno and the river terraces at Nudo also present thick and spatially extensive sedimentary sequences outside the ice margins and are correlated with the Kotorska-Sušica Member (MIS 12; Knezlaz Member of the glacial framework). These settings form important stores of fluvial sediments that have not subsequently been overrun and destroyed by ice. This provides a valuable opportunity to investigate the Pleistocene glacial and fluvial history of these contrasting settings. Outside the MIS 12 ice margins, at Grahovo, Nudo and Kameno for example, near-surface calcite deposits have yielded U-series ages of >350 ka. These cemented horizons (often up to 1 m thick) reflect extended periods of landscape stability. Their development close to the sediment surface, often beneath soil horizons indicates that in some settings there has been little deposition and/or preservation of alluvial sediments beyond the maximum ice front since MIS 12. It also suggests that the MIS 12 sediments remain largely intact. These records therefore provide some of the best preserved evidence of fluvial deposition during MIS 12 within the Mediterranean basin.

The sediments at Vrbanje, on the western side of Orjen, are dated to 126.6 ± 4.5 ka and present some of the only evidence beyond the maximum ice margins that bears the sedimentological imprint of MIS 6 deposition (Chapter 5). The dated sediments represent only a thin veneer (observed to depths of 6 m) at the polje surface and it is likely that these deposits are underlain by thick sequences of MIS 12 sediments. This site highlights the temporal variability in sediment distribution across the Orjen landsystem. Three other sites outside the MIS 12 ice margins (Pirina Poljana, Lipci, and Sniježnice) also yield U-series ages that correlate to depositional phases after MIS 12. It is also possible, however, that these dates represent calcite formation within pre-existing, MIS 12, sediments. The sediments at the surface of Pirina Poljana polje are dated to 213.5 ± 11.3 ka (MIS 7) and 77.2 ± 1.9 ka (MIS 5a). The MIS 12 moraines (Knezlaz Member) extend into the polje depression here and it is likely that these sediments are also underlain by MIS 12 alluvium. Calcites from the alluvial fan at Lipci have been dated from 320.6 ± 33.3 ka to 47.3 ± 1.2 ka, and are discussed in detail in Section 9.2.3 (Fig. 9.5). At Sniježnice, calcites dated to 268.3 ± 22.2 ka correlate to MIS 8, and may indicate a palimpsest of glacial deposits due to the close spacing of the moraines. This scenario has been suggested by Hughes *et al.* (2011b) for the Pleistocene glacial record of central Montenegro, where closely-spaced moraines have been correlated on the basis of morphostratigraphy and U-series ages to MIS 12-8 (Hughes *et al.*, 2011b) and provide some of the strongest evidence of glacial activity during MIS 8 in Montenegro. Within the glacial record of Mount Orjen, there is limited morphostratigraphical evidence from MIS 10-8 (Hughes *et al.*,

2010) and this signal is muted or absent within many glaciated catchments across the Mediterranean (Bavec *et al.*, 2004; Hughes *et al.*, 2006c; Woodward *et al.*, 2008). Within the fluvial record of Orjen, the close similarities in the sedimentary signatures of records dated to MIS 12-8 (Kotorska-Sušica Member) may suggest that the large volumes of sediments prepared during the major glaciation of MIS 12 are likely, in some settings, to have been reworked during subsequent meltwater phases (Church and Ryder, 1972; Church and Slaymaker, 1989). This has been observed within a number of catchments across the Mediterranean, such as the limestone-dominated Voidomatis Basin of northwest Greece (Woodward *et al.*, 2008). Detailed morphosedimentary analysis in the Voidomatis system suggested that sediments prepared during MIS 12 were redistributed within the fluvial environment during subsequent cold stages, notably MIS 5d-2.

At sites within the MIS 12 ice limits (such as Unijerina and Crkvice), the boundary conditions at the onset of MIS 10-8, MIS 6 and MIS 5d-2 would have been considerably different to those outside the maximum ice margins, which have not been covered by ice. Unlike the MIS 12 glaciation, later ice margins (MIS 6 and MIS 5d-2) were confined to cirques, valleys and plateaux areas at higher altitudes (Hughes *et al.*, 2010). Evidence of these glaciations is well-preserved in the moraines identified by Hughes *et al.* (2010). Meltwater sediments from these less extensive cold stages are, however, comparatively limited since MIS 12. In particular, there are only small remnants of MIS 6 alluvium outside the MIS 12 ice margins. As demonstrated in the karst-meltwater model detailed in Section 9.2.1, evidence suggests that glacigenic material may have been deposited within the dolines/hollows of the upland plateau whilst sediment-poor meltwaters were channelled through the subterranean karst and discharged elsewhere. It is also possible that in some instances, such as at Lipci, sediments from these later glacial phases have been transported further downstream or offshore and are not currently exposed.

At some sites within the maximum MIS 12 ice margins deposits represent primary sedimentation from MIS 10-8 and MIS 6, as well as the more localised reworking of MIS 12 deposits by fluvial action in front of the retreating MIS 12 glaciers. The glaciofluvial/shallow lacustrine setting at Unijerina, for example, contains primary alluvial deposition during MIS 12, the reworking of MIS 12 glacial sediment and the deposition of later alluvium, perhaps during MIS 8. There is no evidence of MIS 8 sediments further downstream of Unijerina. This suggests that these sediments have either not been extensively preserved within the valley at Unijerina or are not currently exposed in section. Alternatively, given the potential for deeply scoured

karstic depressions following the major glaciations of MIS 12, these sediments may not yet have been transported from their existing storage space upstream.

The neighbouring site of Crkvice represents a polje depression downstream of the MIS 6 ice front. Sediments here have been dated to 144.2 ± 5.1 ka and 18.5 ± 0.4 ka and have been correlated to MIS 6 (Krivošije Member). The younger age here may reflect sediment deposition from meltwater during MIS 5d-2, but is more likely to correspond to a more recent phase of calcite development within existing sediments (Chapter 8.1.2). It is likely that this polje also contains sediments from MIS 12-8 that were deposited during ice retreat. As observed at Unijerina, there is no evidence downstream of this site to suggest that these sediments have been transported downvalley or reworked since MIS 6.

Importantly, the fluvial records at Orjen do not reflect the glacial-interglacial fluctuations of aggradation and incision seen within other fluvial archives (Macklin *et al.*, 2002; Fontana *et al.*, 2008; Dühnforth *et al.*, 2008; Rother *et al.*, 2010). Many of the sites outside the maximum ice margins, such as the extensive poljes and the terraces at Nudo, contain calcite horizons from the sediment surface dated to >350 ka. This suggests that these depocentres filled with sediment during MIS 12 and there has been only limited deposition outside the maximum ice margins since this time (during the cold stages of MIS 10-8, 6, 5d-2, and the Younger Dryas). There is also little evidence of incision into these polje fills, and even at the present day Grahovo presents the only evidence of a shallow stream cutting into a polje surface. This suggests that Pleistocene interglacial phases were not characterised by net incision, and instead runoff may have been channelled through the subterranean karstic system. During the cold stages of the Pleistocene it is likely that a proportion of the void spaces within the karstic terrain of Orjen were filled with ice (Spektor and Spektor, 2009) and meltwater was channelled as surface runoff. During interglacial phases, the melting of this interstitial ice would have allowed meltwater to infiltrate the subterranean karst network. Surface runoff at these times may have been greatly reduced, therefore limiting the potential for incision. The long-term distribution of sediment across the landscape surrounding Orjen is therefore considerably more complicated due to the well-developed karstic landscape (Section 9.2.1).

The alluvial records surrounding Orjen demonstrate that neighbouring basins often contain contrasting histories of sediment deposition, storage, and reworking over successive glacial-interglacial cycles. In many settings, deposition largely occurred during MIS 12 and evidence of

later alluviation has not been observed. In other environments, there is more tentative evidence of deposition during MIS 8, 6 and 5d-2. In glaciated regions, the nature of these sedimentary records is conditioned by ice dynamics, meltwater pathways and the sediment storage capacity of the landscape. These parameters vary both spatially across an individual landsystem and through time over multiple glacial-interglacial cycles. Alluvial archives can considerably enhance our understanding of Pleistocene landscape processes, both on and offshore, but should be considered as a single landsystem, and not as individual depositional records.

Whilst the fluvial depositional phases surrounding Mount Orjen largely correspond to the timing of glacial activity (Table 9.1), that has been correlated by Hughes *et al.* (2010) to MIS 12, 6 and 5d-2, the U-series ages from the fluvial deposits suggest a more complex response of river system dynamics to headwater glaciation. It should be remembered that U-series ages reflect minimum ages of landsurface stability, and the onset of calcite formation is assumed to occur soon after landform genesis. Given the current evidence from calcites at Mount Orjen, it is not possible to further refine the timing of carbonate formation. Future research on Quaternary calcites should focus on the use of stable isotopic indicators from secondary carbonates as a means to understand the environmental conditions at the time of calcite precipitation. Comparison with other palaeoenvironmental archives (such as pollen, stable isotopes and macrofossils) would allow the timing of U-series dated calcites to be constrained more securely. In particular, this would further strengthen the correlations between glacial and fluvial systems through the use of U-series techniques.

9.4 Calcite micromorphology development index

The complex alluvial depositional history at Mount Orjen means that resolving the record of land surface stability is important for the accurate understanding of landscape dynamics. Using the carbonate micromorphological data from Unijerina and Nudo a qualitative model of calcite development is presented here. This sets out the formation processes of alluvial environment calcites at Mount Orjen and is used to discuss the application of secondary carbonate micromorphology and isotopic analysis as a relative age tool. This also has wider implications for the use of secondary carbonates for U-series dating.

The qualitative carbonate development index has been devised using the micromorphology parameters discussed in Chapter 7. The Carbonate Development Score reflects the relative abundance of microstructures within each microfacies; the Number of Features indicates the variety of calcite microstructures (Table 9.4; Figure 9.8). The qualitative model also accounts for any observed microfeatures that are indicative of overprinting, and therefore more mature, calcite profiles (including: infilled voids and infilled cracks). These observations are used to develop an indication of the degree of carbonate micromorphological development at Orjen. This is tested against the U-series ages from the calcite deposits themselves (Chapter 8). Through developing this model, it is intended to investigate the use of micromorphological analysis as a relative age tool, in instances where U-series ages are unobtainable, or present large error margins.

Sample	Age (years)*	Carbonate Development Score	Total Carbonate Development Score	Number of Features
1	248,628	7	7	6
2a		2		2
2b	248,628*	4	9	3
2c		3		3
3	146,778*	7	7	7
4	56,525	9	9	8
5	56,525*	9	9	7
6	65,855*	6	6	6
7	350,000	6	6	4
8	350,000	6	6	6
9	350,000	5	5	5
10	350,000	4	4	3
11	350,000	4	4	3

Table 9.4 – Micromorphology samples and secondary carbonate development values used within the calcite development model. * indicates samples that have been directly U-series dated. Other ages are inferred from morphostratigraphical correlations to U-series dated horizons elsewhere, and may not reflect the true age of the sample. See text for further discussion. Samples 2a-2c have been combined to reflect the complexity of the full profile within this carbonate sample.

Fig 9.8a shows a good positive correlation (R^2 = 0.8782) between the Carbonate Development Score and the Number of Features. This indicates that carbonates containing a greater abundance of microstructures also contain a greater variety of features. The U-series ages, however, do not show a clear relationship between calcite age and the relative degree of carbonate development (Fig 9.8b). The oldest dated calcite (sample 2c: 248.6 ± 16.7 ka) has a carbonate complexity comparable to the youngest sample (sample 5: 56.5 ± 1.3 ka).

In Figure 9.8b, the Carbonate Development Scores (Table 9.4) are plotted against U-series age to explore the distribution between calcite age and the degree of micromorphological complexity. Ages are based on the directly dated microfacies (samples 2c, 3, 5 and 6). Calcites that have not been directly dated (ie: are assigned ages on stratigraphic correlations alone) have been omitted from this graph. This is due to the fact that it is possible that these correlated ages do not reflect the true age of the sample. For example, the undated terraces of the Nudo valley have here been correlated to >350 ka on the basis of U-series ages elsewhere in the catchment. It is, however, likely that some of these carbonates are considerably younger than this, given the U-series ages from samples 5 and 6. Although there are currently only a limited number of dated samples, the age-calcite complexity distribution suggests that microfacies complexity does not linearly increase with progressive age. To explore this further, the qualitative micromorphological observations can be used to develop a schematic model of fluvial environment carbonate formation at Orjen.

It is unlikely that the observed relationship is a product of the prevailing environmental conditions at the time of calcite formation. The minimum U-series ages correspond to both cold stage (such as sample 3, 146,778 ± 9.1 ka correlated to MIS 6) and warm phase (such as sample 2c, 248.6 ± 16.7 ka correlated to MIS 7/8) carbonate formation. Groundmass crystal size (spar, microspar, micrite) has been used as an indicator of past moisture regime, where larger crystal sizes (such as spar) are formed under wetter conditions (Adamson *et al.*, In Prep.). In the Orjen calcites, however, there is no evidence to suggest that the presence or absence of a groundmass type is related to the sample age or Carbonate Development value. This suggests that calcite formation during climatically distinct periods does not control the patterns of profile complexity. More detailed U-series, micromorphological and stable isotopic (C and O) analysis of the calcite microfabrics would be required to further investigate such climatic controls. In particular, the use of combined micromorphological and isotopic analysis of secondary carbonates has recently been used at other sites across Europe by Candy *et al*. (2011). Their analysis provided detailed indications of the palaeoenvironmental conditions at the time of calcite formation (Candy *et al.*, 2011). By applying these methods in humid environments, this would allow research efforts to focus on the timing of calcite formation in relation to landform genesis and landsurface stability. This would contribute a major advance in the use of U-series analysis and allow more secure geochronological interpretations.
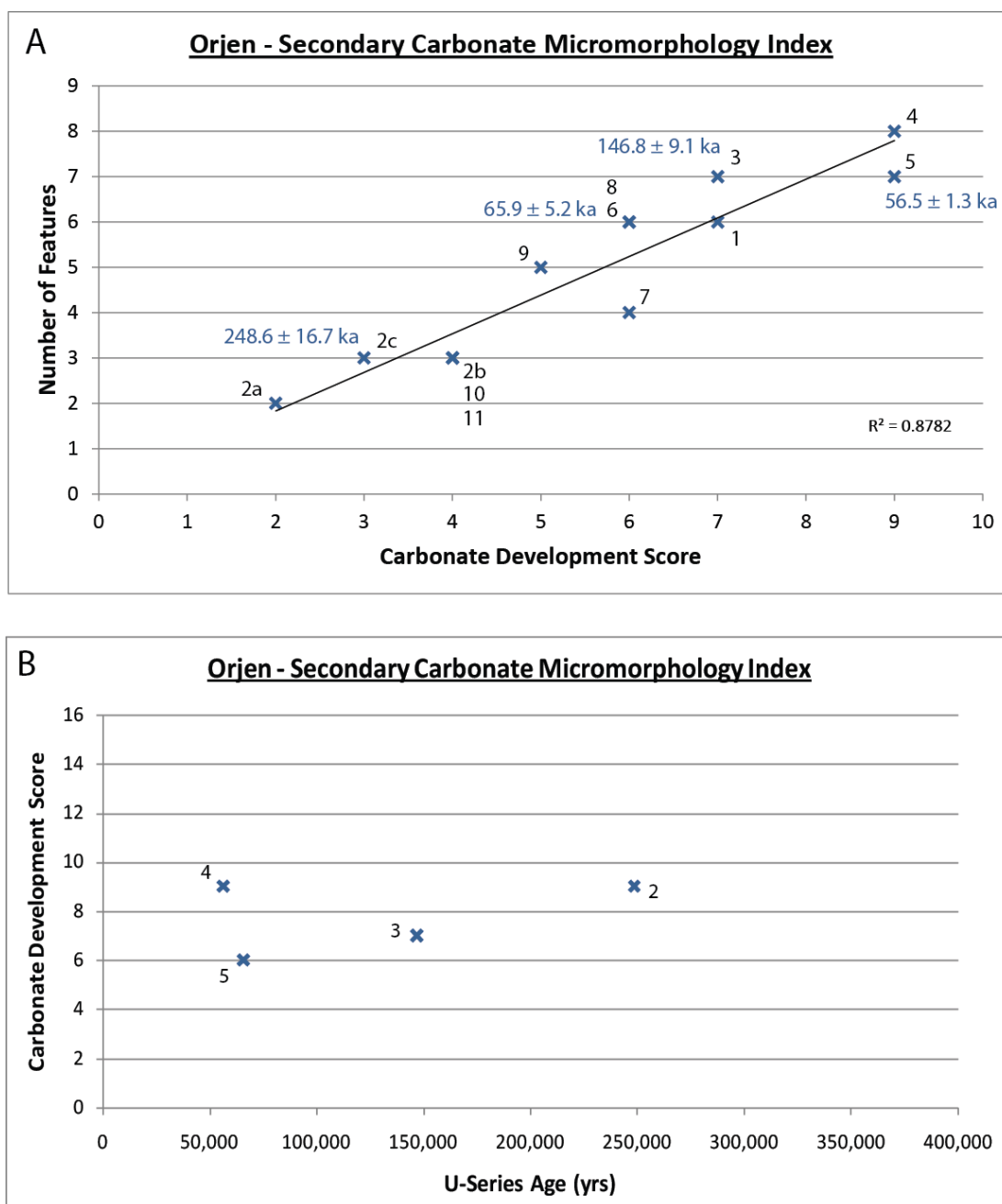
Figure 9.8 – Carbonate Development Index from samples detailed in Table 9.4. A) Carbonate Development Score (relative abundance of microstructures) and the Number of Features are plotted with U-series ages for reference. B) U-Series Age and Carbonate Development Score (Table 9.4).

The absence of a clear relationship between age and complexity may instead be explained by processes of time-dependent diagenetic alteration. The nature of secondary carbonate formation, by dissolution and precipitation, makes them highly susceptible to post-depositional transformation (Wright and Tucker, 1991). In the fluvial environment calcites of

Mount Orjen, carbonate profiles increase in complexity from c. 100 - 225 ka, before demonstrating a decline in microfabric variability. At this time, neomorphic processes such as replacement (dissolution of one mineral and formation of another) and recrystallisation (changes in crystal size through aggrading or degrading neomorphism) may lead to the development of 'pseudofabrics' (Flügel, 2004). This may homogenise the observed microfacies. In these instances microstructures are not necessarily contemporaneous, and may reflect a cumulative fabric of multiple precipitation phases. This calcite development history is presented in Figure 9.9 which provides a three phase qualitative model of secondary carbonate formation at Orjen. This model is in broad agreement with the developmental history of weathering zone calcites observed elsewhere in the Mediterranean (Alonso-Zarza *et al.*, 1998; Alonso-Zarza and Arenas, 2004; Candy *et al.*, 2005; 2009; 2011) which display increasing complexity with increasing age. It is likely, however, that calcite development at Orjen is more complex due to the humid climatic regime.

Phase 1 calcite development is correlated to calcites dated to <100 ka. These profiles reflect single phase calcite precipitation, and comparatively simple microfabrics. Phase 2 calcites are dated to 100 – 225 ka and display increasing microfabric complexity, characterised by multiple phase calcites, overprinting and the onset of neomorphism. Stage 3 profiles demonstrate negligible variance between 225-250 ka. This corresponds to the suggested maximum timescale of carbonate formation, of up to 250,000 years (Candy *et al.*, 2005).

Over time, the carbonates are transformed from dominantly spar–microspar cements to micritic cements, indicating degrading neomorphism (reduction in crystal size). After c. 225 ka, the calcites at Orjen cease to display any significant changes in microfabric content. After c. 225-250 ka microfabrics indicate a decrease in complexity. This marks the upper age limits on the capabilities of the qualitative model to predict relative age. The patterns at Orjen can be explained by the sustained high moisture input to this part of the Mediterranean, with Orjen receiving some of the highest precipitation totals in Europe (up to 7,000 mm/yr, Magaš, 2002; Hydrological and Meteorological Service of Montenegro, 2006). These conditions would promote the dissolution and overprinting of samples over several climatic cycles. The abundant carbonate supply, from glacigenically-prepared limestone bedrock, also means that calcite formation may continue during both warm and cold climate conditions (Candy and Black, 2009).

	A	B	C
Model Age	0 - 100 ka	100 - 225 ka	>225 ka (to 250 ka)
Typical Microfabrics	Sparitic groundmass Microspar/Micrite patches Infilled voids and cracks Laminated calcite Pelleted micrite	Microspar groundmass Micrite patches (some spar) Infilled voids Meniscus cements Alveolar septal fabric Etched grains	Micrite groundmass Microspar patches Meniscus cements Infilled voids
Processes	Phase 1 Single phase calcites Increasing microfabric complexity	Phase 2 Multiple phase calcites Overprinting Onset of neomorphism	Phase 3 Homogenised calcites Advanced neomorphism and homogenisation of fabrics
Examples			

Figure 9.9 – Three-phase relative age model of secondary carbonate micromorphology at Mount Orjen based on the qualitative observations of micromorphological development. The projected decrease in calcite complexity after c. 250 ka marks the upper age limits of the model functionality. Examples of dated microfacies from each development phase at Mount Orjen are presented.

In other areas of the Mediterranean, cold stage calcite profiles are rare (Martín-Algarra *et al.*, 2003; Woodward and Hughes, 2011) due to increased landscape instability and reduced biogenic soil activity during glacial periods (Candy and Black, 2009; Tzedakis *et al.*, 2001; Martín-Algarra *et al.*, 2003). The calcite profiles at Orjen provide an important insight into the palaeoenvironmental processes governing calcite formation under moist climates. The micromorphological model developed in this study (Fig 9.9) has the potential to be used as a relative age indicator over periods of up to 250 ka in humid parts of the Mediterranean, subject to further testing and refinement. Further U-series dating of calcite microfabrics as well as stable isotopic analysis is required to more securely constrain the timing of carbonate formation processes which would allow the model to be further refined. This model highlights the importance of microfacies analysis prior to U-series dating in environments where calcite overprinting is prevalent.

9.5   Summary and palaeoenvironmental implications: testing hypotheses of fluvial response to Pleistocene glaciation

9.5.1   Fluvial activity over multiple glacial-interglacial cycles

The Pleistocene fluvial record examined here closely reflects the glacial archive of Mount Orjen presented by Hughes *et al*. (2010). The most extensive fluvial depositional phase is correlated to the major glaciation of MIS 12, when the large poljes outside the maximum ice margins were filled with thick sequences of alluvium. At this time, the glacial and fluvial systems were well-coupled and meltwater and sediment were delivered downstream via surface runoff. After MIS 12, some settings display evidence of localised redistribution of sediment, potentially during MIS 10-8. This adds important detail to the glacial record of Mount Orjen, which contains limited evidence of glaciation from that period. Instead, the alluvial record here is similar to the glacial archive of the central massifs of Montenegro, where the MIS 12 moraines are accompanied by more muted morphosedimentary evidence of glacial advance during MIS 10-8 (Hughes *et al.,* 2011b). Less extensive evidence of fluvial deposition surrounding Mount Orjen during MIS 6 is also present at several sites downstream of both the MIS 6 and MIS 12 moraines. Morphostratigraphical evidence of fluvial deposition during MIS 5d-2 or the Younger Dryas has not yet been identified. Two U-series ages, at Unijerina (16.6 ± 0.4 ka) and Crkvice (18.5 ± 0.4 ka) (Table 9.1), may however represent a thin veneer of alluvium over the pre-existing (MIS 12-8 and/or MIS 6) sediments. However it is also possible that these ages reflect more recent calcite development within older sediments. The limited evidence of fluvial deposition since MIS 12-8 therefore suggests that younger sediments have not been preserved, or have been deposited within the glacially-scoured karstic hollows of the Orjen plateau area and are not currently exposed in section. This is reflected in the karst-meltwater model presented in Section 9.2.1. This model uses morphostratigraphical evidence from the Nudo valley and other depositional settings surrounding Orjen to suggest that subterranean meltwater pathways assumed greater dominance, at the expense of surface runoff, as the karstic terrain was exposed during less extensive glaciations. It is also possible, given the evidence from the coastal alluvial fans at Lipci and Risan, that at least part of the Pleistocene fluvial record is now located offshore.

The fluvial archives of Mount Orjen do not contain widespread evidence of the glacial-interglacial fluctuations of aggradation and incision that have been suggested for other

glaciated river systems (Dühnforth *et al*., 2008; Chapter 2). The alluvial fan at Lipci, the terrace sequence within the Nudo valley and the shallow stream cutting at Grahovo are the only sites to display unequivocal evidence of incision since MIS 12. At the present day, Nudo is the only setting where full stream flow conditions are reached, after periods of prolonged or intense rainfall, for example. Other evidence of surface runoff is limited given that Montenegro, and this part of Orjen in particular, is one of the wettest parts of Europe. It is therefore likely that this runoff is channelled into the subterranean karstic system where it discharges below ground or via the submarine springlines identified within the Bay of Kotor by Bortoluzzi *et al*. (2009). This is also likely to have been the case during previous Pleistocene interglacial phases, when the karstic system would have thawed and surface runoff could infiltrate the subterranean channel network.

The deposits at Unijerina present an important record of landscape processes in response to changing ice marginal position. In the depositional model outlined in Figure 9.4, it is possible that the slumping of glacial diamict into the glaciofluvial/shallow lacustrine environment at lower elevations occurred during a period of ice retreat from the maximum Pleistocene ice extent of MIS 12. This reflects a number of glacial and fluvial records from across the Mediterranean and elsewhere (Bavec *et al*., 2004; Carraro and Giardino, 2004; Woodward *et al.*, 2008; Giraudi *et al.*, 2011), where previously deposited sediments are reworked during phases of landscape instability. It is possible that such surface reworking can occur within a karstic landscape due to the presence of ice within bedrock void spaces during Pleistocene cold stages (Spektor and Spektor, 2009). Unconsolidated sediments may be reworked by surface runoff, during periods of climatic transition and landscape instability, but before the karstic system has fully thawed and subterranean discharge has been fully established.

Phases of maximum alluvial deposition do not always correspond with periods of maximum ice advance. They may instead reflect lags in landscape relaxation times and the exposure of glacially-prepared, unconsolidated sediment for transportation and deposition downstream during a subsequent climatic phase. For this reason, the thick alluvial sequences have been correlated to MIS 12-8 within the Kotorska-Sušica Member, to reflect this prolonged landscape adjustment. This corresponds to observations within the glaciated catchments of northwest Greece (Woodward *et al*., 2008), the Pyrenees in northern Spain (Lewis *et al*., 2009) and the Southern Julian Alps in Slovenia (Bavec *et al*., 2004), where sediments prepared by glacial action during MIS 12 were redistributed within the fluvial environment and delivered to the

lower valley reaches during later cold stages. This appears to be the case at Unijerina and Sniježnice on Mount Orjen, where evidence of deposition during MIS 12-8 (Kotorska-Sušica Member) is in some instances complex and overprinted.

9.5.2   A landsystem approach to understanding long-term landscape processes

Fluvial response to Pleistocene glaciation of the Orjen massif has varied between neighbouring basins through both the timing and nature of deposition. In many catchments, this has formed an 'asynchronous' and 'asymmetric' morphosedimentary record that reflects the complexities of landscape-scale glacial and fluvial dynamics. At some sites, such as Nudo, Dvrsno, and Lipci, glacially-sourced fluvial sediments have been transported well beyond the maximum ice margins and in some cases are now situated offshore. In other settings, such as Unijerina and Crkvice, sediments have been deposited and reworked more locally. These variations in landscape dynamics reflect: the production of glacially-comminuted limestone sediments during Pleistocene cold stages; the sediment accommodation space and storage capacity of the landscape; the dominant types of surface meltwater pathways (Types 1 and 2 identified in this study); the extent of subsurface karst meltwater flow; and the depositional setting. These catchment-specific conditions lead to the observed spatial patterns in both the characteristics of fluvial activity and the preservation of the morphosedimentary record (Lewin and Macklin, 2003).

Evidence from the large poljes and alluvial fans surrounding Mount Orjen, and the thick river terrace sequences within the Nudo valley indicate that large quantities of sediment were deposited during the major glaciation of MIS 12. These are now exposed to thicknesses of at least 20 m (Chapter 5) and would have formed major sediment sources during later glacial stages. The Pleistocene landscape dynamics of the Orjen massif reflect the observations of Dühnforth *et al*. (2008) in the glaciated basins of the Sierra Nevada, North America. This study suggested that glacial moulding of a catchment produces internal sediment storage space (within hollows and fans, for example) which, in part, also sustains the long-term redistribution of sediment through glacial and fluvial reworking over multiple climatic cycles. This is evident at Unijerina, where phases of sediment deposition and reworking have been correlated to MIS 12-8. In many cases surrounding Orjen, however, there has been only limited sediment delivery downstream of the maximum ice margins since MIS 12.

As well as the spatial variations in the depositional settings surrounding Orjen, meltwater routes and catchment size can have important impacts on sediment transportation processes. Detailed sedimentological and particle size analysis of bedrock, glacial tills and fluvial sediments (Chapters 5 and 6) has revealed a number of spatial patterns in the transformation of limestone bedrock with distance downstream. As discussed in detail in Section 9.3.2, the two types of surface meltwater pathways observed surrounding Mount Orjen (Type 1 - bedrock gorges; and Type 2 – alluvial channels from the ice margin) produce contrasting particle size distributions of the fine matrix fraction. The sedimentological signatures of the analysed samples may therefore be diagnostic of sediment transportation history and meltwater dynamics. Whilst the evidence suggests that post-MIS 12 alluvium was largely deposited within depressions on the karst plateau, it is unclear with the available sedimentary data what influence the subterranean karstic flow might have had on sedimentary signatures downstream.

In broad terms, sedimentary records downstream of small basins (<c. 20 km^2) preserve evidence of several alluvial depositional phases (Table 9.5). Sites such as Lipci (15.25 km^2) and Unijerina (10.00 km^2), for example, contain sediments correlated to MIS 12-8 (Kotorska-Sušica Member) and, more tentatively, MIS 6 (Krivošije Member). Larger drainage basins (>c. 20 km^2) record fewer phases of glacial-fluvial deposition, as observed at Grahovo (28.25 km^2) and Dvrsno (38.50 km^2), which are situated outside the maximum Pleistocene ice margins and contain sediments correlated only to MIS 12. These larger basins that were filled with vast quantities of alluvium during MIS 12 have since displayed a more attenuated signal of sediment delivery downstream. This may be due to the capacity of these larger systems to buffer the morphosedimentary signals of transportation and long-term redistribution of sediments since MIS 12. In contrast, smaller steep-sided basins (such as Unijerina and Lipci) may be more sensitive to meltwater and sediment supply variations, due to the comparatively limited availability of accommodation space to process large volumes of glacigenic sediment. This in part reflects the paraglacial theory of Church and Ryder (1972) and Church and Slaymaker (1989) which suggests that within smaller upland basins, maximum sediment yield is concentrated at the time of deglaciation and rapidly declines to background levels. In larger basins sediment yield may be sustained for several thousand years after deglaciation. These systems do not necessarily display the distinct peaks in sediment flux that are observed within smaller catchments.

Site	Basin Area (km²)	Total Basin Area (km²)	Depositional Phases Observed	Total Phases
Kameno	8.00	8.00	MIS 12	1
Kruševice	8.50	8.50	MIS 12	1
Unijerina	10.00	10.00	MIS 12-8 and 6	2+
Lipci	15.25	15.25	MIS 12, 10-8, 6	3+
Sniježnice	15.25	6.75	MIS 12-8	1+
Ubli	15.25	12.00	MIS 12	1
Crkvice	18.72	18.72	MIS 6	1
Pirina Poljana	19.75	19.75	MIS 12 and 8	2
Vrbanje	21.25	21.25	MIS 12 and 6	2
Nudo	24.25	24.25	MIS 12	1
Dvrsno	11.25	28.25	MIS 12	1
	17.00			
Grahovo	24.25	38.50	MIS 12	1
	14.25			

Table 9.5 – Drainage basin area by site with the number of observed depositional phases based on U-series ages and morpholithostratigraphy.

At Mount Orjen, the relationship between drainage basin area and sediment delivery is complicated by the karstic terrain. This means that throughout the Pleistocene it is likely that runoff has been periodically channelled via subterranean karstic networks, and has not always transferred sediment across the land surface. Idealised models of landscape dynamics (such as Church and Ryder, 1972; Dühnforth *et al*., 2008) may therefore not be directly applicable to karstic terrain. What is more, fluvial records are inherently fragmentary and individual geomorphological settings surrounding the Orjen massif do not record a full history of Pleistocene glacial and fluvial activity. This is true for fluvial archives both across the Mediterranean and elsewhere. The fragmentary nature of these records does not necessarily indicate that the palaeoenvironmental signal has been 'shredded', as has recently been suggested by Jerolmack and Paola (2010). Although the fluvial records of Orjen are discontinuous, the exposed sediments represent valuable 'time slices' that often preserve detailed palaeoenvironmental signals. When these individual sedimentary archives are combined, however, it is possible to develop a more complete understanding of long-term Pleistocene landscape dynamics (Macklin *et al*., 2012).

9.5.3   Comparisons with wider Mediterranean glacial and fluvial records

The Pleistocene fluvial characteristics observed at Mount Orjen are broadly representative of Pleistocene glacial and fluvial records across the Mediterranean. The alluvial records of Mount Orjen correspond to the timing of glacial advance and meltwater activity within the glaciated massifs of Montenegro (Hughes *et al*., 2010; 2011b), as well as several glaciated mountain regions of the Mediterranean (Fig. 9.10). The fluvial archive of the Orjen massif, however, is distinctive in that it contains one of the best-preserved Mediterranean alluvial records from MIS 12. Evidence of more recent fluvial activity, from MIS 6 and MIS 5d-2 is limited in comparison to other records from Mediterranean glaciated basins (Woodward *et al*., 2008; Lewis *et al*., 2009; Giraudi *et al*., 2011). The Pleistocene morphosedimentary records of the Voidomatis Basin and the Pindus Mountains of northwest Greece have been documented in detail by Hughes *et al*. (2004; 2006c), Woodward (1991), and Woodward *et al*. (1992; 1995; 2001; 2004; 2008). The limestone karst setting of the Voidomatis provides an important comparison to the glacial and fluvial systems of Mount Orjen. Three Pleistocene glacial phases have been identified in the Pindus Mountains (Fig. 9.10) and are correlated to MIS 12, MIS 10-6 and MIS 5d-2. In the Voidomatis basin downstream, fluvial sediments from MIS 12 have not been preserved and morphosedimentary records instead suggest that this material was reworked and deposited during MIS 5d-2. As observed in other Mediterranean catchments (Cararro and Giardino, 2004; Giraudi *et al*., 2011) fluvial archives within the Voidomatis basin display evidence for the prolonged reworking or 'inheritance' of this sediment over multiple glacial cycles. At Mount Orjen, however, there is little evidence of widespread alluvial deposition from the cold stages of MIS 6 or MIS 5d-2. Instead, redistribution of sediment within the Orjen landscape appears to have occurred more locally, as observed at Unijerina and Crkvice.

In Iberia, sedimentary evidence from the Trevinca Mountains (Alberti *et al*., 2011) and the south central Pyrenees (Pallás *et al*., 2006) indicates that records of Pleistocene glaciation are often highly contrasting between adjacent catchments. This is due to catchment-specific parameters such as: ice-shed/drainage basin area; bedrock lithology; and topographic characteristics. These often lead to spatial variations in both Pleistocene ice mass dynamics, and the preservation potential of the sedimentary record within contrasting geomorphological settings. Some valleys may undergo deglaciation whilst neighbouring basins are contemporaneously occupied by ice (Gillespie and Molnar, 1995). This phenomenon may help

to explain the variations in glacial and alluvial records across Orjen and elsewhere (Lewis *et al*., 2009; Glasser *et al*., 2010; Rother *et al*., 2010).

As well as local-scale variations in Pleistocene morphosedimentary records, evidence from a number of Mediterranean catchments also indicates that periods of maximum ice extent are often out of phase with the maximum ice advances of the Eurasian Ice Sheet during the global LGM (Woodward *et al*., 2008; Lewis *et al*., 2009; Hughes *et al*., 2010). Although this phenomenon is not recorded within the fluvial sediments of Mount Orjen it provides an important consideration for the understanding of landscape-scale glacial and interglacial interactions. It is necessary to consider the localised landscape processes that influence the development and preservation of the Pleistocene morphosedimentary record, and may or may not be tied to wider scale Quaternary palaeoenvironmental changes (Lewin and Macklin, 2003). The detailed investigation of the contrasting fluvial geomorphological settings of Mount Orjen highlights the importance of adopting a 'landsystem' approach in order to gain such understanding (Evans, 2003). Using Orjen as a landsystem model, it is therefore possible to more fully understand glacial and fluvial system interactions, both across the Mediterranean and within glaciated basins elsewhere.
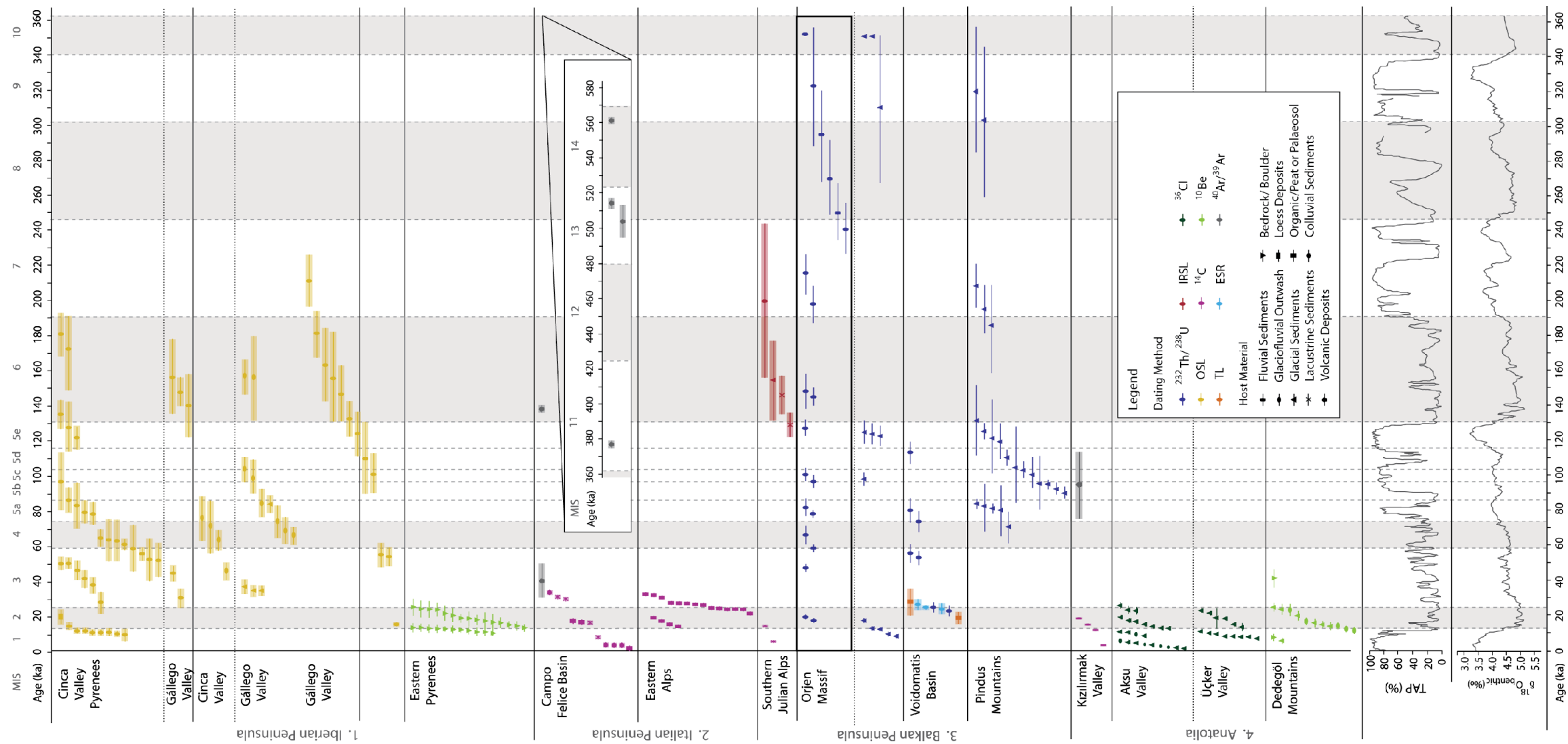
Fig. 9.10 - U-series ages from the Pleistocene fluvial records of Orjen (emboldened) with published geochronological data from selected glaciated Mediterranean catchments (Chapter 2). Correlation with global multi-proxy records is provided by an East Pacific δ^{18}O$_{benthic}$ record and a total arboreal pollen (TAP %) record from Tenaghi Philippon, Greece (Tzedakis, 2006).

CHAPTER TEN

Conclusions and Further Research

- This study provides one of the first, integrated, landscape-scale investigations of Pleistocene glacial and fluvial dynamics with a robust geochronological framework. This follows the classic, yet undated models of Penck and Brückner (1909). Using 12 field sites surrounding the Orjen massif in western Montenegro, it has been possible to develop a 'landsystem' approach to the study of formerly glaciated catchments. This study is unique in that it explores the morphosedimentary records of a range of depositional settings including: poljes, alluvial fans, river terraces, ice marginal environments and proglacial/shallow lacustrine settings. These are broadly representative of the depositional environments that may be found within glaciated basins across the Mediterranean and elsewhere.

- Detailed field mapping and sedimentological analysis has revealed several phases of alluvial deposition during the Middle and Late Pleistocene. The most extensive fluvial depositional phase has been correlated to MIS 12-8 (Kotorska-Sušica Member). This corresponds to the major glaciation of Mount Orjen during MIS 12 (Hughes *et al*., 2010; Knezlaz Member). Less extensive evidence of fluvial activity during MIS 6 (Krivošije Member) is preserved on the high altitude plateau, and more tentatively at sites downstream of the MIS 12 moraines. This corresponds to the Crkvice Member of the glacial record of Hughes *et al*. (2010). There is limited morphosedimentary evidence of fluvial deposition during MIS 5d-2 in the study area. Late Pleistocene deposits may have been reworked and/or transformed further downstream.

- The timing of fluvial activity surrounding the Orjen massif has been determined using U-series ages from calcites cementing the fluvial deposits and relative age indicators from soil horizons at each site. These ages are in good agreement with the morphostratigraphical sub-divisions. U-series ages from fluvial deposits outside the maximum ice margins yield ages of >350 ka and are correlated to MIS 12. At some locations, such as Pirina Poljana (213.5 ± 11.3 ka) and Vrbanje (126.5 ± 4.5 ka), sediments close to the surface also yield ages that correlate to fluvial deposition during MIS 10-8 and MIS 6. Inside the ice margins, the ages indicate fluvial deposition

during MIS 12-8 (Unijerina, 248.6 ± 16.7 ka) and MIS 6 (Crkvice, 144.2 ± 5.1 ka). Harden Index soil development indices are in agreement with the morphostratigraphical and U-series data, and indicate that deposits correlated to MIS 12 contain more mature soil profiles than sediments ascribed to MIS 6.

- The different fluvial settings surrounding Mount Orjen often contain contrasting records of Pleistocene meltwater and sediment dynamics. Within neighbouring basins and reaches there may be considerable variations in both the timing of fluvial activity and/or the preservation of the morphosedimentary record. This has been observed in many other Pleistocene glacial and fluvial archives across the Mediterranean (e.g. Lewin *et al.*, 1991; Hughes and Woodward, 2009). Whilst all of the fluvial records surrounding Mount Orjen are inherently fragmentary, they provide important information on the nature of the glacial-sediment system in each catchment. Individual catchments should be considered as part of a wider landscape system, and not as isolated components.

- The extensive karstic poljes surrounding Mount Orjen are considered to be pre-Pleistocene features that became filled with large volumes of glacigenic sediment during MIS 12. They therefore provide an important record of Pleistocene glacial and fluvial activity in this part of the Mediterranean. It is likely that other poljes within karstic terrains across the Balkans, and the wider Mediterranean also contain thick sequences of Pleistocene alluvium, but have not yet been adequately dated.

- The river valley at Nudo, north Orjen, presents one of the best-preserved river terrace sequences within the Mediterranean that has been correlated to MIS 12. This record suggests that the valley was filled with alluvium during the major glaciation of MIS 12 and has since been progressively incised. The available morphosedimentary evidence is unable to further constrain the timing of incision after MIS 12. Future research in this valley should use cosmogenic depth profiles of terrace surfaces to provide minimum ages of terrace exposure. This method has been successfully applied on fluvial terraces within glaciated catchments by Carcaillet *et al.* (2009) in Albania, Hein *et al.* (2009) in Patagonia and Egli *et al.* (2010) in the Swiss and Italian Alps.

- The coastal alluvial fan at Lipci, south Orjen provides an important link between the terrestrial glacial record and the offshore record within the Bay of Kotor. During the cold stages of the Pleistocene, when the sea level was considerably lower, the alluvial fan would have been deposited subaerially. Sea level rise means that much of this fan is now submerged. Recent investigation of the submarine topography within the Bay of Kotor (Bortoluzzi *et al.*, 2009; Giglio, pers. comm.) reveals a series of channels with well-developed channel margin berms on the now submerged portion of the fan. The sea floor is also characterised by karstic depressions and submarine springlines. Reconciling the Pleistocene terrestrial record with the offshore archive therefore presents an important opportunity to more fully understand landscape processes within this part of the Mediterranean.

- The limestone karst terrain of Mount Orjen offers some important insights into the interactions between glacial, fluvial and karstic processes. During MIS 12, as the ice advanced beyond the karstic plateau, the glacial and fluvial systems were well-coupled and meltwater and sediments (coarse and fine) were delivered via surface channels to the large depocentres downstream. During MIS 6 and MIS 5d-2, when ice masses were increasingly constrained to higher altitudes (Hughes *et al.*, 2010), extensive areas of karst were exposed and the glacial and downstream fluvial systems became progressively decoupled as meltwater was channelled via the subterranean karst network. It could therefore be argued that sediments would have been deposited more locally on the karstic plateau, and only limited volumes of sediment were transported beyond the maximum ice margins. Alternative explanations for the limited evidence of Late Pleistocene alluvial sediments observed in this investigation are: i) the sampling framework, which was commonly constrained by the presence of quarries, means that these deposits may have been overlooked, or ii) these sediments have been transported downstream to distal areas beyond the depocentres in the immediate vicinity of Orjen due to the limited accommodation space following the major filling events of MIS 12. These records might therefore now be situated offshore within the Bay of Kotor. Further research, both on and offshore, would be required to test these ideas. The topography of Mount Orjen, which comprises a high altitude plateau and radial depocentres, means that it is possible to observe landscape changes over successive glacial-interglacial cycles. Further investigation in glaciated karst

terrains should expand upon these observations to explore the influence of karst on Pleistocene glacial and fluvial landscape processes within other settings.

- Two types of surface meltwater pathways have been identified at Mount Orjen: Type 1 (steep, limestone bedrock gorges) and Type 2 pathways (alluvial channels draining directly from the ice margin). These different meltwater routes appear to exert considerable control on the <63 μm sediment characteristics further downstream. Sediments delivered via Type 1 meltwater pathways demonstrate a largely bimodal particle size distribution. Type 2 pathways are characterised by unimodal sediment distributions. Unimodal particle size distributions are dominant at distances of <1.5 km from the ice margin whilst bimodal particle size distributions are developed at distances of >1.5 km from the ice front. These bimodal particle size characteristics are thought to be due to the winnowing of limestone sediments and the preferential concentration of non-limestone lithologies, within the silt to clay size fraction. This is ascribed to a combination of both chemical weathering within the proglacial meltwater environment and the preferential settling of denser lithologies from suspension in the fluvial environment.

- Micromorphological analysis of the secondary carbonate horizons of Mount Orjen provides an insight into the formation mechanisms of humid climate calcites. A three-phase development model has been devised using calcite microfabrics and U-series ages. Phase 1 profiles (c. 0 - 125 ka) reflect single stage calcite development. Phase 2 profiles (c. 125 – 250 ka) are characterised by an increasing complexity, overprinting and the onset of neomorphism. Phase 3 calcites (c. 250 – 300 ka) contain considerable evidence of overprinting and microfabric homogenisation, and mark the upper age limit of the model feasibility. This corresponds to the suggested timescale of carbonate formation observed elsewhere across the Mediterranean over periods of c. 250 ka (Candy *et al.*, 2005). Further investigation into the isotopic signals of each of the profiles used within the model as well as more detailed U-series analysis of individual microfacies would be required to better constrain the timing of calcite precipitation.

- The distinctive geomorphological setting of Mount Orjen, and the variety of morphosedimentary records, can be used as a model to more fully understand Pleistocene glacial and fluvial interactions within glaciated basins across the

Mediterranean and elsewhere. The dominance of the karst terrain also means that this system provides important insights, and raises important questions, into the influence of karstic processes on landscape dynamics.

- The fluvial record of Mount Orjen is distinct in that it contains one of the best-preserved records of glacial and fluvial activity during MIS 12 within the Mediterranean. Interestingly, evidence of later glaciations, during MIS 6 or MIS 5d-2, which are well-preserved within the glacial record, is muted within the fluvial record of Orjen. Unlike the large scale phases of Pleistocene alluviation from MIS 6 and 5d-2 evident within other Mediterranean basins (e.g. Carraro and Giardino, 2004; Woodward *et al.*, 2008; Giraudi *et al.*, 2011), there is only limited evidence of localised fluvial sediment deposition at that time within the catchments of the Orjen massif.

REFERENCES

Aber, J. S. (1979) 'Glacial conglomerates of the Appalachian Plateau, New York' in *Quaternary Research* 11 185-196

Adamson, K. R., Candy, I. and Whitfield, L. (2012) 'Calcrete development and palaeoenvironmental analysis: a coupled micromorphological and stable isotope approach' In Prep

Akçar, N., Yavuz, V., Ivy-Ochs, S., Kubik, P. W., Vardar, M. and Schlüchter, C. (2007) 'Paleoglacial records from Kavron Valley, NE Turkey: Field and cosmogenic exposure dating evidence' in *Quaternary International* 164–165 170–183

Alberti, A. P., Díaz, M. V., Martini, I. P., Pascucci, V. and Andreucci, S. (2011) 'Upper Pleistocene glacial valley-junction sediments at Pias, Trevinca Mountains, NW Spain' in *Geological Society, London, Special Publications* 354 93-110

Allen, H. D. (2003) 'Response of past and present Mediterranean ecosystems to environmental change' in *Progress in Physical Geography* 27(3) 359-377

Allen, J. R. M., Brandt, U., Brauer, A., Hubberten, H.W., Huntly, B., Keller, J., Kraml, M., Mackensen, A., Mingram, J., Negendank, J. F. W., Nowaczyk, N. R., Oberhansli, H., Watts, W. A., Wulf, S. and Zolitschka, B. (1999) 'Rapid environmental changes in southern Europe during the last glacial period' in *Nature* 400 740-743

Allen, J. R. M., Watts, W. A. and Huntley, B. (2000) 'Weichselian palynostratigraphy, palaeovegetation and palaeoenvironment; the record from Lago Grande di Monticchio, southern Italy' in *Quaternary International* 73-74 91-110

Alonso, P., Dorronsoro, C. and Egido, J. A. (2004) 'Carbonation in palaeosols formed on terraces of the Tormes river basin (Salamanca, Spain)' in *Geoderma* 118, 261-276

Alonso-Zarza, A. M. and Arenas, C. (2004) 'Cenezoic calcretes from the Teruel Graben, Spain: microstructure, stable isotope geochemistry and environmental significance' in *Sedimentary Geology* 167 91-108

Alonso-Zarza, A. M., Silva, P. G., Goy, J. L. and Zazo, C. (1998) 'Fan-surface and biogenic calcrete development: interactions during ultimate phases of fan evolution in the semiarid SE Spain (Murcia) *Geomorphology* 24 147-167

Altın, T. (2009) 'Pleistocene and Holocene fluvial development of the Ecemiş Valley (Central Anatolia, Turkey)' in *Quaternary International* 204 76-83

Amorosi, A., Forina, M., Severi, P., Preti, D., Caporale, L. and Di Dio, G. (1996) 'Genetically related alluvial deposits across active fault zones: an example of alluvial fan-terrace correlation from the upper Quaternary of the southern Po Basin, Italy' in *Sedimentary Geology* 102 275-295

Amorosi, A., Pavesi, M., Lucchi, M. R., Sarti, G. and Piccin, A. (2008) 'Climatic signature of cyclic fluvial architecture from the Quaternary of the central Po Plain, Italy' in *Sedimentary Geology* 209 58-68

Andersen, B. G. and Mangerud, J. (1989) 'The last interglacial-glacial cycle in Fennoscandia' in *Quaternary International* 3/4 21-29

Anderson, M. P. (1989) 'Hydrogeologic facies models to delineate large-scale spatial trends in glacial and glaciofluvial sediments' in *Geological Society of America Bulletin* 101 501-511

Andrews, J. E. (2006) 'Palaeoclimate records from stable isotopes in riverine tufas: synthesis and review' in *Earth Science Reviews* 75 85-104

Andrews, J. E., Singhvi, A. K., Kailath, A. J., Kuhn, R., Dennis, P. J., Tandon, S. K. and Dhir, R. P. (1998) 'Do stable isotope data from calcrete record Late Pleistocene monsoonal climate variation in the Thar Desert of India?' in *Quaternary Research* 50 240-251

Andrieu, V., Hubschman, J., Jalut, G. and Herail, G. (1988) 'Chronologie de la deglaciation des Pyrénées françaises, Dynamique de sedimentation et contenu pollinique des paléolacs: application à l'interpretation du retrait glaciaire' in *Bulletin Association Française pour l'Etude du Quaternaire* 2/3 55–67

Arakel, A. V. and McConchie, D. (1982) 'Classification and genesis of calcrete and gypsite lithofacies in palaeo-drainage basins of inland Australia and their relationship to carnotite mineralisation' in *Journal of Sedimentary Petrology* **52** 1149-1170

Arboleya, M. L., Babault, J., Owen, L. A., Teixell, A. and Finkel, R. C. (2008) 'Timing and nature of Quaternary fluvial incision in the Quarzazate foreland basin, Morocco' in *Journal of the Geological Society, London* 165 1059-1073

Arkhipov, S. A., Ehlers, J., Johnson, R. G. and Wright Jr., H. E. (1995) 'Glacial drainage towards the Mediterranean during the Middle and Late Pleistocene' in *Boreas* 24 196-206

Avouac, J. P., Tapponnier, P., Bai, M., You, H. and Wang, G. (1993) 'Active thrusting and folding along the Northern Tien Shan and Late Cenozoic rotation of the Tarim relative to Dzungaria and Kazakhstan' in *Journal of Geophysical Research* 98(B4) 6755–6804

Bain, R. J. and Foos, A. M. (1993) 'Carbonate microfabrics related to subaerial exposure in palaeosols formation' in Rezak, R. and Lanoie, D. L. (Eds) *Carbonate Microfabrics* Springer-Verlag, Berlin

Baker, V. R. (1994) 'Glacial to modern changes in global river fluxes' in National Research Council (Ed.) *Material Fluxes on the surface of the Earth: Studies in Geophysics* Washington: National Academy Press

Ballantyne, C. K. (2002) 'Paraglacial Geomorphology' in *Quaternary Science Reviews* 21 1935-2017

Bard, E. (1999) 'Ice age temperatures and geochemistry' in *Science* 5417 1133-1134

Bavec, M., Tulaczyk, S. M., Mahan, S. A. and Stock, G. M. (2004) 'Late Quaternary glaciation of the Upper Soča River Region (Southern Julian Alps, NW Slovenia)' in *Sedimentary Geology* 165 265-283

Benito, G., Sancho, C., Peña, J. J., Machado, M. J. and Rhodes, E. J. (2010) 'Large-scale karst subsidence and accelerated fluvial aggradation during MIS 6 in NE Spain: climatic and palaeohydrological implications' in *Quaternary Science Reviews* 29 2694-2704

Benn, D. I. and Ballantyne, C. K. (1993) 'The description and representation of particle shape' in *Earth Surface Processes and Landforms* 18 665-672

Benn, D. I. and Ballantyne, C. K. (1994) 'Reconstructing the transport history of glacigenic sediments: a new approach based on the co-variance of clast form indices' in *Sedimentary Geology* 91 215-227

Benn, D. I. and Evans, D. J. A. (1998) *Glaciers and Glaciation* London: Arnold

Benxing, Z. and Rutter, N. (1998) 'On the problem of Quaternary glaciations, and the extent and patterns of Pleistocene ice cover in the Quinghai-Xizang (Tibet) plateau' in *Quaternary International* 45/56 109-122

Berger, A. and Loutre, M-F (2007) 'Milankovitch theory and paleoclimate' in Elias, S. (Ed.) *Encyclopedia of Quaternary Science* London: Elsevier

Bezinge, A., Clark, M. J., Gurnell, A. M. and Warburton, J. (1989) 'The management of sediment transported by glacial melt-water streams and its significance for the estimation of sediment yield' in *Annals of Glaciology* 13 1-5

Bini, A. and Zuccoli, L. (2004) 'Glacial history of the southern side of the central Alps, Italy' in Ehlers, J. and Gibbard, P. L. (Eds.) *Quaternary Glaciations – Extent and chronology Part 1: Europe* Amsterdam: Elsevier

Birkeland, P. W. (1999) *Soils and Geomorphology* 3rd Edn. New York: Oxford University Press

Bogdan, G. and Leszek, L. (1999) 'Glaciokarst of subalpine and alpine zone of the Mała Łąka valley, Tatra mts., Poland' in *Acta Carsologica* 28(1) 5 71-89

Bortoluzzi, G., Del Bianco, F., D'Oriano, F., Giglio, F., Borgia, T. T. M., Santi, D., Bulatović, A., Dević, N., Radojević, D., Matović, M., Sretenović, A., Diaconov, A. and Tola, M. (2009) 'Report on the morphobathymetric, oceanographic, geological and geophysical investigations during cruise MNG01 09 (19-27 April 2009, R/V Urania)' *ISMAR-CNR Interim Technical Cruise Report* Bologna

Boulton, G.S. (1978) 'Boulder shapes and grain-size distributions of debris as indicators of transport paths through a glacier and till genesis' in *Sedimentology* 25 773-799

Boulton, G. S. and Eyles, N. (1979) 'Sedimentation by valley glaciers: a model and genetic classification' in Schlücter, C. (Ed.) *Moraines and Varves* Rotterdam: A. **A.** Balkema

Bourdon, B., Henderson, G. M., Lundstrom, C. C and Turner, S. P. (Eds.) (2003) *Uranium-Series Geochemistry Reviews in Mineralogy and Geochemistry Volume 52* Mineralogical Society of America

Bowen, D. Q. (1978) *Quaternary Geology: a stratigraphic framework for multidisciplinary work* Oxford: Pergamon

Braithwaite, C. J. R. (1983) 'Calcrete and other soils in Quaternary limestones: structures, processes and applications' in *Journal of the Geological Society of London* 140 351 – 363

Braithwaite, R. J., and Raper, S. C. B. (2007) 'Glaciological conditions in seven contrasting regions estimated with the degree-day model' in *Annals of Glaciology* 46 296–302

Brardinoni, F. and Hassan, M. A. (2006) 'Glacial erosion, evolution of river long profiles, and the organization of process domains in mountain drainage basins of coastal British Columbia' in *Journal of Geophysical Research* 111, F01013, doi:10.1029/2005JF000358

Bridgland, D. R. (1994) 'The Pleistocene of the Thames' In Bridgland, D. R. (Ed.) *Quaternary of the Thames* London: Chapman and Hall

Bridgland, D. R. (2000) 'River terrace systems in north-west Europe: an archive of environmental change, uplift and early human occupation' in *Quaternary Science Reviews* 19 1293-1303

Bridgland, D. R. and Westway, R. (2008) 'Climatically controlled river terrace staircases: A worldwide Quaternary phenomenon' in *Geomorphology* 98 285-315

Bull, W. (1977) 'The alluvial fan environment' in *Progress in Physical Geography* 1 222-270

Cacho, I., Grimalt, J. O. and Canals, M. (2002) 'Response of the Western Mediterranean Sea to rapid climatic variability during the last 50,000 years: a molecular biomarker approach' in *Journal of Marine Systems* 33– 34 253– 272

Cacho, I., Grimalt, J. O., Pelejero, C., Canals, M., Sierro, F. J., Flores, J. A. and Shackleton, N. J. (1999a) 'Dansgaard–Oeschger and Heinrich event imprints in the Alboran Sea paleotemperatures' in *Paleoceanography* 14 (6) 698–705

Cacho, I., Pelejero, C., Grimalt, J. O., Calafat, A. M. and Canals, M. (1999b) 'C$_{37}$ alkenone measurements of sea surface temperature in the Gulf of Lions (NW Mediterranean)' in *Organic Geochemistry* 33 557– 566

Calvet, F. and Julià, R. (1983) 'Pisoids in the caliche profiles of Tarragona (N. E. Spain)' in Pryt, T. (Ed.) *Coated Grains* Berlin: Springer-Verlag

Candy, I., (2009) 'Terrestrial and freshwater carbonates in Hoxnian interglacial deposits, UK: micromorphology, stable isotopic composition and palaeoenvironmental significance' in *Proceedings of the Geologists' Association* 120 49–57

Candy, I. and Black, S. (2009) 'The timing of Quaternary calcrete development in semi-arid southeast Spain: investigating the role of climate on calcrete genesis' in *Sedimentary Geology* 218 1-4 6-15

Candy, I., Adamson, K. R., Gallant, C. E., Maher, L. and Pope, R. (2011) 'Oxygen and carbon isotopic composition of Quaternary meteoric carbonates from western and southern Europe: their role in palaeoenvironmental reconstruction' in *Palaeogeography, Palaeoclimatology, Palaeoecology* 1–11 326–328

Candy, I., Black, S. and Sellwood, B. W. (2003) 'Calcrete profile development in Quaternary alluvial sequences, southeast Spain: implications for using calcretes as a basis for landform chronologies' in *Earth Surface Processes and Landforms* 28 169 – 185

Candy, I., Black, S. and Sellwood, B. W. (2005) 'U-series isochron dating of immature and mature calcretes as a basis for constructing Quaternary landform chronologies for the Sorbas basin, southeast Spain' in *Quaternary Research* 64 100-111

Candy, I., Stephens, M., Hancock, J. and Waghorne, R. (2011) 'Palaeoenvironments of Ancient Humans in Britain: The Application of Oxygen and Carbon Isotopes to the Reconstruction of Pleistocene Environments' in Ashton, N. M., Lewis, S. G. and Stringer, C. B (Eds) *The Ancient Human Occupation of Britain Developments in Quaternary Science 14* London: Elsevier

Carcaillet, J., Mugnier, J. L., Koçi, R. and Jouanne, F. (2009) 'Uplift and active tectonics of southern Albania inferred from incision of alluvial terraces' in *Quaternary Research* 71 465–476

Carraro, F. and Giardino, M. (2004) 'Quaternary glaciations in the western Italian Alps – a review' in Ehlers, J. and Gibbard, P. L. (Eds.) *Quaternary Glaciations – Extent and chronology Part 1: Europe* Amsterdam: Elsevier

Castiglioni, G. B. (2004) 'Quaternary glaciations in the eastern sector of the Italian Alps' in Ehlers, J. and Gibbard, P. L. (Eds.) *Quaternary Glaciations – Extent and chronology Part 1: Europe* Amsterdam: Elsevier

Chedadi, R. and Rossignol-Strick, M. (1995) 'Eastern Mediterranean Quaternary paleoclimates from pollen and isotope records of marine cores in the Nile cone area' in *Palaeoceanography* 10(2) 291-300

Chorley, R. J., Schumm, S. A. and Sugden, D. E. (1984) *Geomorphology* London: Methuen & Co

Church, M. and Ryder, J. M. (1972) 'Paraglacial sedimentation: a consideration of fluvial processes conditioned by glaciation' in *Geological Society of America Bulletin* 83 3059-3072

Church, M. and Slaymaker, O. (1989) 'Disequilibrium of Holocene sediment yield in glaciated British Columbia' in *Nature* 337 452–454

Çiner, A. (2004) 'Turkish glaciers and glacial deposits' in Ehlers, J. and Gibbard, P. L. (Eds.) *Quaternary Glaciations – Extent and chronology Part 1: Europe* Amsterdam: Elsevier

Clapperton, C. M. (1993) *Quaternary geology and geomorphology of South America* Amsterdam: Elsevier

Clark, M. J. (1987) 'The alpine sediment system: a context for glaciofluvial processes' in Gurnell, A. M. and Clark, M. J. (Eds.) *Glacio-fluvial Sediment Transfer: an alpine perspective* Chichester: John Wiley

Cohen, K. M. and Gibbard, P. L. (2010) *Global chronostratigraphical correlation table for the last 2.7 million years* Subcommission on Quaternary Stratigraphy
Available at: http://www.quaternary.stratigraphy.org.uk/charts/
Last Accesed: 11th August 2012

Collins, D. N. (2007) 'Changes in quantity and variability of runoff from Alpine basins with climatic fluctuation and glacier decline' in Ginot, P. and Sicart, J. E. (Eds.) *Glacier Mass Balance Changes and Meltwater Discharge (selected papers from sessions at the IAHS Assembly in Foz do Iguaçu, Brazil, 2005)* IAHS 318 75-85

Collins, P. E. F., Rust, D. J., Bayraktutan, M. S. and Turner, S. D. (2005) 'Fluvial stratigraphy and palaeoenvironments in the Pasinler Basin eastern Turkey' in *Quaternary International* 140–141 121–134

Cordier, S., Hammond, D., Frechen, M. and Beiner, M. (2006) 'Fluvial system response to Middle and Upper Pleistocene climate change in the Meurthe and Moselle valleys (Eastern Paris Basin and Rhenish Massif' in *Quaternary Science Reviews* 25 1460-1474

Cowton, T., Hughes, P. D. and Gibbard, P. L. (2009) 'Palaeoglaciation of Parque Natural Lago de Sanabria, northwest Spain' in *Geomorphology* 108 282–291

Civjić, J. (1898) 'Das Rilagebirge und seine ehemalige Vergletscherung' in *Zeitschrift der Gesellschaft für Erdkunde zu Berlin* 33 200-253

Civjić, J. (1900) 'L'Époque Glaciaire dans la Péninsule des Balkans' in *Annales de Géographie* 9 359-372.

Dean, W. E. (1974) 'Determination of carbonate and organic matter in calcareous sediments and sedimentary rocks by loss on ignition: comparison with other methods' in *Journal of Sedimentary Petrology* 44 242–248

Dehnert, A., Preusser, F., Kramers, J. D., Akçar, N., Kubik, P. W., Reber, R. and Schlüchter, C. (2010) 'A multi-dating approach applied to proglacial sediments attributed to the Most Extensive Glaciation of the Swiss Alps' in *Boreas* 39 620–632

Delmas, M., Gunnell, Y., Braucher, R., Calvet, M. and Bourlès, D. (2008) 'Exposure age chronology of the last glaciation in the eastern Pyrenees' in *Quaternary research* 60 231-241

Demir, T., Yeşilnacar, İ. and Westaway, R. (2004) 'River terrace sequences in Turkey: sources of evidence for lateral variations in regional uplift' in *Proceedings of the Geologists' Association* 115 289–311

Desloges, J. R. (1990) 'Sources for valley-fill alluvial sediments: Bella Coola River Basin, British Columbia' in *The Canadian Geographer* 34(2) 98-109

Djurović, P. (2009) 'Reconstruction of the Pleistocene glaciers of Mt. Durmitor in Montenegro' in *Acta Geographica Slovenica* 49(2) 263-289

Djurović, P. and Petrović, A. (2007) 'Large canyons in the Dinaric and Prokletije Mountains region of Montenegro' in *Geographica Panoramica* 11

Doğan, U. (2010) 'Fluvial response to climate change during and after the Last Glacial Maximum in Central Anatolia, Turkey' in *Quaternary International* 222 (1-2) 221-229

d'Orefice, M., Pecci, M., Smiraglia, C. and Ventura, R. (2000) 'Retreat of Mediterranean glaciers since the Little ice Age: Case Study of Ghiacciaio del Calderone, Central Apennines, Italy' in *Arctic, Antarctic, and Alpine Research* 32(2) 197-201

Dühnforth, M., Densmore, A. L., Ivy-Ochs, S. and Allen, P. A. (2008) 'Controls on sediment evacuation from glacially modified and unmodified catchments in the eastern Sierra Nevada, California' in *Earth Surface Processes and Landforms* 33(10) 1602–1613

Edwards, R. L., Chen, H. and Wasserburg, G. J. (1987) '^{238}U- ^{234}U- ^{230}Th- ^{232}Th systematics and the precise measurement of time over the past 500,000 years' in *Earth and Planetary Science Letters* 81 175-192

Egli, M., Brandová, D., Böhlert, R., Favilli, F. and Kubik, P. W. (2010) '^{10}Be inventories in Alpine soils and their potential for dating land surfaces' in *Geomorphology* 119 62-73

Elias, S. (2007) 'History of Quaternary Science' in Elias, S. (Ed.) *Encyclopedia of Quaternary Science* London: Elsevier

Eren, M., Kadir, S., Hatipoĝlu, Z. and Gül, M. (2008) 'Quaternary calcrete development in the Mersin area, Southern Turkey' in *Turkish Journal of Earth Sciences* 17 763-784

Evans, D. J. A. (Ed.) (2003) *Glacial Landsystems* London: Arnold

Evans, D. J. A. and Benn, D. I. (2004) *A practical guide to the study of glacial sediments in the field* London: Arnold

Evans, D. J. A. and Benn, D. I. (2007) 'Glacial Landforms' in Elias, S. (Ed.) *Encyclopedia of Quaternary Science* London: Elsevier

Federici, P. R., Granger, D. E., Pappalardo, M., Risolini, A., Spagnolo, M. and Cyr A. J. (2008) 'Exposure age dating and Equilibrium Line Altitude reconstruction of an Egesen moraine in the Maritime Alps, Italy' in *Boreas* 37 245-253

Fernandez Mosquera, D., Marti, K., Vidal Romani, J. R. and Weigel, A. (2000) 'Late Pleistocene deglaciation chronology in the NW of the Iberian Peninsula using cosmic-ray produced ^{21}Ne in quartz' in *Nuclear Instruments and Methods in Physics Research B* 832-837

Fisk, H. N. (1951) 'Loess and Quaternary geology of the Lower Mississippi Valley' in *Journal of Geology* 59 333–356

Fletcher, W. J. and Sanchez Goñi, M. F. (2008) 'Orbital- and sub-orbital-scale climate impacts on vegetation of the western Mediterranean basin over the last 48,000 yr' in *Quaternary Research* 70 451–464

Fletcher, W. J., Sanchez Goñi, M. F., Peyron, O. and Dormoy, I. (2010) 'Abrupt climate changes of the last deglaciation detected in a Western Mediterranean forest recording' in *Climate of the Past* 6 245–264

Fontana, A., Mozzi, P. and Bondesan, A. (2008) 'Alluvial megafans in the Venetian-Friulian Plain (north-eastern Italy): evidence of sedimentary and erosive phases during the Late Pleistocene and Holocene' in *Quaternary International* 189 71-90

Ford, D. and Williams, P. (1989) *Karst Geomorphology and Hydrology* London: Unwin Hyman

Ford, D. C. and Williams, P. (2007) *Karst Hydrogeology and Geomorphology* Oxford: Wiley

Forno, M. G. and Ferrando, S. (2008) 'Plio-Quaternary continental deposits of the Castellamonte area, between Orco and Dora Baltea Basins (Torino Province, Italy)' in *Quaternary International* 190 103-111

Fraser, G. S. and Cobb, J. C. (1982) 'Late Wisconsinan proglacial sedimentation long the West Chicago Moraine in northeaster Illinois' in *Journal of Sedimentary Petrology* 52(2) 473-491

Fuller, I. C., Macklin, M. G., Lewin, J., Passmore, D. G. and Wintle, A. G. (1998) 'River response to high-frequency climate oscillations in southern Europe over the past 200 k.y.' in *Geology* 26 275-278

Gabrovec, M. (1998) 'The Triglav glacier between 1986 and 1998' in *Geografski zbornik, XXXVIII* 90-110

Gams, I. (1969) 'Some morphological characteristics of the Dinaric Karst' in *The Geographical Journal* 135(4) 563-572

Gams, I. (1978) 'The polje: the problem of its definition'in *Zeitschrift für Geomorphologie* 22 170-181

Gams, I. (2005) 'Tectonics impact on poljes and minor basins (case studies of Dinaric karst)' in *Acta Carsologica* 34 (1) 25-41

Garašić, M. (2006) 'Found and documented deepest speleothems in the sea' (in Croatian) in *Spelaeolog. Croat.* 7 58

García-Ruiz, J. M., Valero-Garcés, B. L., Martí-Bono, C. and González-Sampériz, P. (2001) 'La evolución de los glaciares del Pleistoceno Superior en el Pirineo Central Español. El ejemplo de los glaciares de Escarra y Lana Mayor, Alto Valle de Gállego' in *Cuaternario y Geomorfología* 15 (1-2) 103-119

García-Ruiz, J. M., Valero-Garcés, B. L., Martí-Bono, C. and González-Sampériz, P. (2003) 'Asynchroneity of maximum glacier advances in the central Spanish Pyrenees' in *Journal of Quaternary Science* 18(1) 61-72

Garzanti, E., Andò, S., France-Lanord, C., Vezzoli, G., Censi, P., Galy, V., and Najman, Y (2010) 'Mineralogical and chemical variability of fluvial sediments 1. Bedload sand (Ganga–Brahmaputra, Bangladesh)' in *Earth and Planetary Science Letters* 299 368–381

Garzanti, E., Andò, S. and Vezzoli, G. (2008) 'Settling equivalence of detrital minerals and grain-size dependence of sediment composition' in *Earth and Planetary Science Letters* 273 138–151

Garzanti, E., Andò, S. and Vezzoli, G. (2009) 'Grain-size dependence of sediment composition and environmental bias in provenance studies' *in Earth and Planetary Science Letters* 277 422–432

Gibbard, P. L. and Cohen, K. M. (2008) 'Global chronostratigraphical correlation table for the last 2.7 million years' in *Episodes* 31(2) 243-247

Gibbard, P. L. and Lewin, J. (2009) 'River incision and terrace formation in the Late Cenozoic of Europe' in *Tectonophysics* 474 41–55

Gile, L. H., Peterson, F. F. and Grossman, R. B. (1965) 'The K horizon: a master soil horizon of carbonate accumulation' in *Soil Science* 99(2) 71-82

Gile, L. H., Peterson, F. F. and Grossman, R. B. (1966) 'Morphological and genetic sequences of carbonate accumulation in desert soils' in *Soil Science* 101 347–360

Gillespie, A. and Molnar, P. (1995) 'Asynchronous maximum advances of mountain and continental glaciers' in *Reviews of Geophysics* 33 3 311-364

Giraudi, C. (1998) 'The Late Quaternary geologic evolution of Campo Felice (Abruzzo—Central Italy)' in *Giornale di Geologia* 60 67–82

Giraudi, C. (2012) 'The Campo Felice Late Pleistocene Glaciation (Apennines, Central Italy)' in *Journal of Quaternary Science* 27(4) 432–440

Giraudi, C. and Frezzotti, M. (1997) 'Late Pleistocene glacial events in the Central Apennines, Italy' in Q*uaternary Research* 48 280–290

Giraudi, C., Bodrato, G., Ricci Lucchi, M., Cipriani, N., Villa, I. M., Giaccio, B. and Zuppi, G. M. (2011) 'Middle and Late Pleistocene Glaciations in the Campo Felice basin (Central Apennines-Italy)' in *Quaternary Research* 75 219–230

Girauldi, C. (2003) 'Middle Pleistocene to Holocene Appenine Glaciation (Italy)' in *Il Quaternario* 16 37-48

Girauldi, C. (2004) 'The Apennine glaciations in Italy' in Ehlers, J. and Gibbard, P. L. (Eds.) *Quaternary Glaciations – Extent and chronology Part 1: Europe* Amsterdam: Elsevier

Glasser, N. F., Harrison, S. and Jansson, K. N. (2010) 'Topographic controls on glacier sediment-landform associations around the temperate North Patagonian Icefield' in *Quaternary Science Reviews* 28 2817-2832

Gómez-Ortiz, A., Martí-Bono, C. and Salvador-Franch, F. (2000) 'Evolución reciente de los estudios de geomorfología glaciar y periglaciar en España (1980-2000): balance y perspectivas' in *Revista Electrónica de Geografía y Ciencias Sociales* 4 (77)

González Trueba, J. J., Martín Moreno, R., Martínez de Pisón, E. and Serrano, E. (2008) ''Little Ice Age' glaciation and current glaciers in the Iberian Peninsula' in *The Holocene* 18 (4) 551-568

Goossens, D. (2008) 'Techniques to measure grain-size distributions of loamy sediments: a comparative study of ten instruments for wet analysis' in *Sedimentology* 55 65-96

Grund, A. (1910) 'Beiträge zur Geomorphologie des Dinarischen Gebirges' in *Geographische Abhandlungen* 7 (H.3) 121-125

Grunewald, K. and Sheithauer, J. (2010) 'Europe's southernmost glaciers: response and adaptation to climate change' in *Journal of Glaciology* 56 195 129-142

Gurnell, A. M. (1987) 'Fluvial sediment yield from alpine, glacierized catchments' in Gurnell, A. M. and Clark, M. J. (Eds.) *Glacio-fluvial Sediment Transfer: an alpine perspective* Chichester: John Wiley

Guzzetti, F., Marchetti, M. and Reichenbach, P. (1997) 'Large alluvial fans in the north-central Po Plain (Northern italy) in *Geomorphology* 18 119-136

Hagg, W., Brown, L. N., Kuhn, M. and Nesgaard, T. I. (2007) 'Modelling of hydrological response to climate change in glacierized Central Asian catchments' in *Journal of Hydrology* 332 40-53

Hambrey, M. J. (1994) *Glacial Environments* London: UCL Press

Hambrey, M. J. and Alean, J. (2009) *Glaciers Online*
Available at: http://www.swisseduc.ch/glaciers/
Last Accessed: 10th August 2012.

Hamilton, T. D. (2001) 'Quaternary glacial, lacustrine, and fluvial interactions in the western Noatak basin, Northwest Alaska' in *Quaternary Science Reviews* 20 371-391

Hanson, P. R., Mason, J. A. and Goble, R. J. (2006) 'Fluvial terrace formation along Wyoming's Laramie Range as a response to increased late Pleistocene flood magnitudes' in *Geomorphology* 76 12-25

Harden, J. W. (1982) 'A quantitative index of soil development from field descriptions: examples from a chronosequence in central California' in *Geoderma* 28 1-28

Harding, A., Palutikof, J. and Holt, T. (2009) 'The Climate System' in Woodward, J. C. (Ed.) *The Physical Geography of the Mediterranean* Oxford: Oxford University Press

Hartman, G. M. D. and Clague, J. J. (2008) 'Quaternary stratigraphy and glacial history of the Peace River valley, northeast British Colombia' in *Canadian Journal of Earth Sciences* 45(5) 549-564

Harvey, A. M. and Wells, S. G. (1987) 'Response of Quaternary fluvial systems to differential epeirogenic uplift: Aguas and Feos river systems, southeast Spain' in *Geology* 15 689-693

Harvey, A. M., Mather, A. and Stokes, M. (2005) 'Alluvial Fans: Geomorphology, Sedimentology, Dynamics' in *Geological Society, London: Special Publications* 251 (1-7)

Hays, J. D., Imbrie, J. and Shackleton, N. J. (1976) 'Variations in the Earth's orbit: Pacemaker of the ice ages' in *Science* 194 1121-1132

Hein, A. S., Dunai, T. J., Hulton, N. R. and Xu, S. (2011) 'Exposure dating outwash gravels to determine the age of the greatest Patagonian glaciations' in *Geology* 39 2 103–106

Hein, A. S., Hulton, N. R. J., Dunai, T. J., Schnabel, C., Kaplan, M. R., Naylor, M. and Xu, S. (2009) 'Middle Pleistocene glaciation in Patagonia dated by cosmogenic-nuclide measurements on outwash gravels' in *Earth and Planetary Science Letters* 286 184-197

Heiri, O., Lotter, A. F. and Lemcke, G. (2001) 'Loss on ignition as a method for estimating organic and carbonate content in sediments: reproducibility and comparability of results' in *Journal of Paleolimnology* 25 101–110

Hellstrom, J. (2006) 'U–Th dating of speleothems with high initial [230]Th using stratigraphical constraint' *in Quaternary Geochronology* 1 289–295

Hssain, A. A. and Bridgland, D. (2009) 'Pliocene-Quaternary fluvial and aeolian records in the Souss Basin, southwest Morocco: a geomorphological model' in *Global and Planetary Change* 68 288-296

Hubble, G. D., Isbell, R. F. and Northcote, K. H. (1983) 'Features of Australian soils' in Division of soils CSIRO *Soils: An Australian Viewpoint* Melbourne: CSIRO

Hughes, P. D. (2004) *Quaternary Glaciation in the Pindus Mountains, Northwest Greece* Unpublished PhD Thesis. University of Cambridge

Hughes, P. D. (2007) 'Recent behaviour of the Debeli Namet glacier, Durmitor, Montenegro' in *Earth Surface Processes and Landforms* 192 1593-1602

Hughes, P. D. (2008) 'Response of a Montenegro glacier to extreme summer heatwaves in 2003 and 2007' in *Geografiska Annaler* 90 (4) 259-267

Hughes, P. D. (2009) 'Twenty-first Century Glaciers in the Prokletije Mountains, Albania' in *Arctic, Antarctic and Alpine Research* 4 455-459

Hughes, P. D. (2010) 'Geomorphology and Quaternary stratigraphy: the roles of morpho-, litho- and allostratigraphy' in *Geomorphology* 123 189-199

Hughes, P. D. (2011) 'Glacial History of the Mediterranean Mountains' in Vogiatzakis, I.N. and Tzanopoulos, J. (Eds) *Mediterranean Mountain Environments*. Wiley-Blackwell.

Hughes, P. D., Fenton, C. R. and Gibbard, P. L. (2011a) 'Quaternary Glaciations of the Atlas Mountains, North Africa' in Ehlers, J., Gibbard, P. L. and Hughes, P. D. (Eds.) *Quaternary Glaciations - Extent and Chronology: A Closer Look* London: Elsevier

Hughes, P. D. and Woodward, J. C. (2008) 'Timing of glaciation in the Mediterranean mountains during the last cold stage' in *Journal of Quaternary Science* 23(6-7) 575-588

Hughes, P. D. and Woodward, J. C. (2009) 'Glacial and Periglacial Environments' in Woodward, J. C. (Ed.) *The Physical Geography of the Mediterranean* Oxford: Oxford University Press

Hughes, P. D., Woodward, J. C. and Gibbard, P. L. (2006a) 'Late Pleistocene glaciers and climate in the Mediterranean' in *Global and Planetary Change* 50 83-98

Hughes, P. D., Woodward, J. C. and Gibbard, P. L. (2006b) 'Quaternary glacial history of the Mediterranean mountains' in *Progress in Physical Geography* 30 (3) 334–364

Hughes, P. D., Woodward, J. C., Gibbard, P. L., Macklin, M. G., Gilmour, M. A. and Smith, G. R. (2006c) 'The glacial history of the Pindus Mountains, Greece' in *Journal of Geology* 114 413-434

Hughes, P. D., Woodward, J. C., van Calsteren, P. C., Thomas, L. E. and Adamson, K. R. (2010) 'Pleistocene ice caps on the coastal mountains of the Adriatic Sea' in *Quaternary Science Reviews* 29(27-28) 3690-3708

Hughes, P. D., Woodward, J. C., van Calsteren, P. C. and Thomas, L. E. (2011b) 'The glacial history of the Dinaric Alps, Montenegro' in *Quaternary Science Reviews* 30 23-24 3393-3412

Hydrological and Meteorological Service of Montenegro (2006) Available at: http://www.meteo.co.me/ Last Accessed: (May 18th 2012)

Imbrie, J., Hays, J. D., Martinson, D. G., MacIntyre, A., Mix, A. C., Morlet, J. J., Pisias, N. G., Prell, W.L. and Shackleton, N.J. (1984) 'The orbital theory of Pleistocene climate: support from a revised chronology of the marineδ^{18}O record' in Berger, A. Imbrie, J. Hays, J., Kukla, G. and Saltzman, B. (Eds) *Milankovitch and Climate*. Dordrecht: Reidel

Ivy-Ochs, S., Kerschner, H., Reuther, A., Preusser, F., Heine, K., Maisch, M., Kubik, P. W. and Schlüchter, C. (2008) 'Chronology of the last glacial cycle in the European Alps' in *Journal of Quaternary Science* 23 (6-7) 559-573

Jennings, J. N. (1985) *Karst Geomorphology* Oxford: Blackwell

Jerolmack, D. J. and Paola, C. (2010) 'Shredding of environmental signals by sediment transport' in *Geophysical Research Letters* 37 doi:10.1029/2010GL044638

Jones, A. P., Tucker, M. E. and Hart, J. K. (1999) *QRA Technical Guide No.7 - Description & Analysis of Quaternary Stratigraphic Field Sections* Quaternary Research Association

Kelly, M., Black, S. and Rowan, J. S. (2000) 'A calcrete-based U/Th chronology for landform evolution in the Sorbas basin, southeast Spain' in *Quaternary Science Reviews* 19 995-1010

Kemp, R. A. (1985) *Soil Micromorphology and The Quaternary* Quaternary Research Association Technical Guide 2, Cambridge.

Khadkikar, A. S., Merh, S. S., Malik, J. N. and Chamyal, L. S. (1998) 'Calcretes in semi-arid alluvial systems: formative pathways and sinks' in *Sedimentary Geology* 116 251 – 260

Khadkikar , A. S., Chamyal, L. S. and Ramesh, R. (2000) 'The character and genesis of calcrete in Late Quaternary alluvial deposits, Gujarat, western India, and its bearing on the interpretation of ancient climates' in *Palaeogeography, Palaeoclimatology and Palaeoecology* 162 239-261

Kirigin, B. (1967) 'Klimatske karakteristike Sjevernog Velebita' in *Zbornik radova X kongresa klimatologa Jugoslavije* Kopaonik: Beograd pp. 189-206

Knox, J. C. (1996) 'Late Quaternary Upper Mississippi River alluvial episodes and their significance to the Lower Mississippi River System' in *Engineering Geology* 45 263-285

Konert, M. and Vandenberghe, J. (1997) 'Comparison of laser grain size analysis with pipette and sieve analysis: a solution for the underestimation of the clay fraction' in *Sedimentology* 44 523-535

Kong, P., Na, C., Fink, D., Zhao, X. and Xiao, W. (2009) 'Moraine dam related to late Quaternary glaciation in the Yulong Mountains, southwest China, and impacts on the Jinsha River' in *Quaternary Science Reviews* 28 3224-3235

Kotarba, A., Hercman, H. and Dramis, F. (2001) 'On the age of Campo Imperatore glaciations, Gran Sasso Massif, Central Italy' in *Geografia Fisica e Dinamica Quaternaria* 24 65-69

Krumbein, W. C. (1941) 'Measurement and geological significance of shape and roundness of sedimentary particles' in *Journal of Sedimentary Petrology* 11 64-72

Ku, T-L. (2000) 'Uranium-Series Methods' in Noller, J. S., Sowers, J. M. and Lettis, W. R. (2000) *Quaternary Geochronology: Methods and Applications* Washington: American Geophysical Union

Kubiëna, W. L. (1970) *Micromorphological Features of Soil Geography* New Brunswick: Rutyers University Press

Kuhlemann, J., Milivojević, M., Krumrei, I and Kubik, P. W. (2009) 'Last glaciation of the Šara Range (Balkan Peninsula): increasing dryness from the LGM to the Holocene' in *Austrian Journal of Earth Sciences* 102 146-158

Kurter, A. (1991) 'Glaciers of the Middle East and Africa: Glaciers of Turkey' in Williams Jr., R. and Ferrigno, J. (Eds.) *Satellite Image Atlas of Glaciers of the World* U.S. Geological Survey Professional Paper, 1386-G, G1– G30

Laabs, B. J. C., Munroe, J. S., Rosenbaum, J. G., Refsnider, K. A., Mickelson, D. M., Singer, B. S. and Caffee, M. W. (2007) 'Chronology of the last glacial maximum in the Upper Bear River Basin, Utah' in *Arctic, Antarctic and Apline Research* 39 4 537-548

Lambeck, K. and Purcell, A. (2005) 'Sea-level change in Mediterranean Sea since the LGM: model predictions for tectonically stable areas' in *Quaternary Science Reviews* 24 1969–1988

Lamplugh, G.W. (1902) 'Calcrete' in *Geological Magazine* 9 575

Langmuir, D. and Herman, J.S. (1980) 'The mobility of Thorium in natural waters at low temperatures' in *Geochimica et Cosmochimica Acta* 44 1753-1766

Lewin, J. and Macklin, M. G. (2003) 'Preservation potential for Late Quaternary alluvium' in *Journal of Quaternary Science* 18(2) 107-120

Lewin, J., Macklin, M. G. and Woodward, J. C. (1991) 'Late Quaternary fluvial sedimentation in the Voidomatis Basin, Epirus, northwest Greece' in *Quaternary Research* 35 103–115

Lewin, J. and Woodward, J. C. (2009) 'Karst Geomorphology and Environmental Change' in Woodward, J. C. (Ed.) *The Physical Geography of the Mediterranean* Oxford: Oxford University Press

Lewis, C. J., McDonald, E. V., Sancho, C., Peña, J. L. and Rhodes, E. J. (2009) 'Climatic implications of correlated Upper Pleistocene glacial and fluvial deposits on the Cinca and Gállego Rivers (NE Spain) based on OSL dating and soil stratigraphy' in *Global and Planetary Change* 67 141-152

Lourens, L. J. and Hilgen, F. J. (1997) 'Long-periodic variations in the Earth's obliquity and their relation to third-order eustatic cycles and Late Neogene glaciations' in *Quaternary International* 40 43–52

Lourens, L. J., Hilgen, F. J., Gudjonsson, L. and Zachariasse, W. J. (1992) 'Late Pliocene to Early Pleistocene astronomically forced sea surface productivity and temperature variations in the Mediterranean' in *Marine Micropaleontology* 19 49–78

Lowe, J. J., Blockley, S., Trincardi, F., Asioli, A., Cattaneo, A., Matthews, I. P., Pollard, M. and Wulf, S. (2007) 'Age modelling of late Quaternary marine sequences in the Adriatic: Towards improved precision and accuracy using volcanic event stratigraphy' in *Continental Shelf Research* 27 560–582

Lowe, J. J., Walker, M. J. C. and Porter, S. C. (2007) 'Understanding Quaternary Climatic Change' in Elias, S. (Ed.) *Encyclopedia of Quaternary Science* London: Elsevier

Machette, M. N. (1985) 'Calcic soils of the southwestern United States' in Weide, D. L (Ed.) *Soils and Quaternary geology of the southwestern United States Geological Society of America, Special Paper* 203 1–21

Macklin, M. G., Fuller, I. C., Lewin, J., Mass, G. S., Passmore D. G., Rose, J., Woodward, J. C., Black, S., Hamlin, R. H. B. and Rowan J. S. (2002) 'Correlation of fluvial sequences in the Mediterranean basin over the last 200 ka and their relationship to climate change' in *Quaternary Science Reviews* 21 1633-1641

Macklin, M. and Woodward, J. C. (2009) 'River Systems and Envoronmental Change' in Woodward, J. C. (Ed.) *The Physical Geography of the Mediterranean* Oxford: Oxford University Press

Macklin, M. G., Lewin, J. and Woodward, J. C. (2012) 'The fluvial record of climate change' in *Philosophical Transactions of the Royal Society A* 370 2143-2172

Maddy, D., Demir, T., Bridgland, D. R., Veldkamp, A., Stemerdink, C., van der Schriek, T. and Westaway, R. (2008) 'The Early Pleistocene development of the Gediz River, Western Turkey: An uplift-driven, climate-controlled system?' in *Quaternary International* 189 115-128

Magaš, D. (2002) 'Natural geographic characteristics of the Boka Kotorska area as the basis of development' in *Geoadria* 7(1) 51-81

Maher, E., Harvey, A. M. and France, D. (2007) 'The impact of a major Quaternary river capture on the alluvial sediments of a beheaded river system, the Rio Alias SE Spain' in *Geomorphology* 84 344 – 356

Mangerud, J., Jakobsson, M., Alexanderson, H., Astakhov, V., Clarke, G. K. C., Henriksen, M., Hjort, C., Krinner, G., Lunkka, J-P., Möller, P., Murray, A., Nikolskaya, O., Saarnisto, M. and Svendsen, J. I. (2004) 'Ice-dammed lakes and rerouting of the drainage of northern Eurasia during the Last Glaciation' in *Quaternary Science Reviews* 23 1313–1332

Manz, L. A. (1998) *Cosmogenic ^{36}Cl chronology for deposits of presumed Pleistocene age on the Eastern Piedmont of Mount Olympus, Pieira, Greece* Unpublished MSc Thesis Ohio University: USA

Marjanac, L. and Marjanac, T. (2004) 'Glacial history of the Croatian Adriatic and Coastal Dinarides' in Ehlers, J. and Gibbard, P. L. (Eds.) *Quaternary Glaciations – Extent and chronology Part 1: Europe* Amsterdam: Elsevier

Marković, S. B., Hambach, U., Catto, N., Jovanović, M., Buggle, B., Machlett, B., Zöller, L., Glaser, B. and Frechen, M. (2009) 'Middle and late Pleistocene loess sequences at Batajnica, Vojvodina, Serbia' in *Quaternary International* 198 255-266

Marren, P. M. (2005) 'Magnitude and frequency in proglacial rivers: a geomorphological and sedimentological perspective' in *Earth-Science Reviews* 70 203-251

Martí Bono, C. and García Ruiz, J. (Eds.) (1994) *El Glaciarismo surpirenaico: nuevas aportaciones* Geoforma Ediciones Logroño

Martín-Algarra, A., Martín-Martín, M., Andreo, B., Julià, R. and González-Gómez, C. (2003) 'Sedimentary patterns in perched spring travertines near Granada (Spain) as indicators of the palaeohydrological and palaeoclimatological evolution of a karst massif' in *Sedimentary Geology* 161 217-228

McCave, I. N., Hall, I. R. and Bianchi, G. G. (2006) 'Laser vs. settling velocity differences in silt grainsize measurements: estimation of palaeocurrent vigour' in *Sedimentology* 53 919–928

McCave, I. N. and Syvitski, J. P. M. (1991) 'Principles and methods of geological particle size analysis' in Syvitski, J. P. M. (Ed.) *Principles, Methods and Application of Particle Size Analysis* Cambridge University Press: Cambridge pp. 3–21

Meigs, A., Krugh, W. C., Davis, K. and Bank, G. (2006) 'Ultra-rapid landscape response and sediment yield following glacier retreat, Icy Bay, southern Alaska' in *Geomorphology* 78 207-221

Menkovic, L., Markovic, M., Cupkovic, T., Pavlovic, R., Trivic, B. and Banjac, N. (2004) 'Glacial morphology of Serbia, with comments on the Pleistocene glaciation of Monte Negro, Macedonia and Albania' in Ehlers, J. and Gibbard, P. L. (Eds.) *Quaternary Glaciations – Extent and chronology Part 1: Europe* Amsterdam: Elsevier

Merritts, D. J. (2007) 'Terrace Sequences' in Elias, S. A. (Ed.) *Encyclopedia of Quaternary Science* London: Elsevier

Messerli, B. (1967) 'Die eiszeitliche und die gegenwärtige Vergletscherung im Mittelmeerraum' in *Geographica Helvetica* 22 105-228

Messerli, B. (1980) 'Mountain glaciers in the Mediterranean area and in Africa' in *World Glacier Inventory International Association of Hydrological Sciences* 126, 197–211

Miall, A. D. (1983) 'Glaciofluvial transport and deposition' in Eyles, N. (Ed.) *Glacial Geology* New York: Pergamon

Miall, A. D. (1985) 'Architectural-element analysis: A new method of facies analysis applied to fluvial deposits' in *Earth Science Reviews* 22 261-308

Miall, A. D. (1996) *The Geology of Fluvial Deposits: Sedimentary facies, basin analysis and petroleum geology* Berlin: Springer

Michoel, A., De Jaeger, N., Sneyers, R., De Wispelaere, W., Geladeé, E., Kern, J., Gorter, W., van Amsterdam, P., Den Tandt, Y., Houtmeyers, E. and Van Cotthem, L. (1994) 'Influence of porosity on the electrical sensing zone and laser diffraction sizing of silicas. A collaborative study' in *Particle and Particle Systems Characterization* 11 391–397

Mileta, M. (2005) 'Fog water collection in Croatia' in *Croatian Meteorological Journal* 41, 624-626

Milivojević, M., Menković, L. and Ćalic, J. (2008) 'Pleistocene glacial relief of the central part of Mt. Prokletije (Albanian Alps)' in *Quaternary International* 190 112-122

Monegato, G., Ravazzi, C., Donegana, M., Pini, R., Calderoni, G. and Wick, L. (2007) 'Evidence of a two-fold glacial advance during the last glacial maximum in the Tagliamento end moraine system (eastern Alps)' in *Quaternary Research* 68 284-302

Moreno, A., Valero-Garcés, B. L., Jiménez-Sánchez, M., Domínguez-Cuesta, M. J., Mata, M. P, Navas, A., González-Sampériz, P., Stoll, H., Farias, P., Morellón, M., Corella, J. P. and Rico, M. (2009) 'The last deglaciation in the Picos de Europa National Park (Cantabrian Mountains, northern Spain)' in *Journal of Quaternary Science* 25 7 1076-1091

Morley, M. W. and Woodward, J. C. (2011) 'The Campanian Ignimbrite (Y5) tephra at Crvena Stijena Rockshelter, Montenegro' in *Quaternary Research* 75(3) 683–696

Munsell (1975) *Soil Color Charts* Baltimore: Kollmorgen Corporation

Muttoni, G., Carcano, C., Garzanti, E., Ghielmi, M., Piccin, A., Pini, R., Rogledi, S. and Sciunnach, D. (2003) 'Onset of major Pleistocene glaciations in the Alps' in *Geology* 31 989-992

Nádor, A., Lantos, M., Tóth-Makk, A. and Thamó-Bozsó, E. (2003) 'Milankovitch sale multi-proxy records from fluvial sediments of the last 2.6Ma, Pannonian Basin, Hungary' in *Quaternary Science Reviews* 22 2157-2175

Nash, D. and Smith, R.F. (1998) 'Multiple calcrete profiles in the Tabernas basin, southeast Spain: their origins and geomorphic implications' in *Earth Surface Processes and Landforms* 23, 1009–1029

Nebout, N. C., Londeix, L., Baudin, F., Turon, J-L., von Grafenstein, R. and Zahn, R. (1999) 'Quaternary marine and continental paleoenvironments in the western Mediterranean (Site 976, Alboran Sea): palynological evidence' in Zahn, R., Comas, M. C., and Klaus, A. (Eds.) *Proceedings of the Ocean Drilling Program, Scientific Results* Vol. 161 457

Nesbitt, H. W. and Young, G. M. (1996) 'Petrogenesis of sediments in the absence of chemical weathering: effects of abrasion and sorting on bulk composition and mineralogy' in *Sedimentology* 43 341-358

Netterberg, F. (1969) 'The interpretation of some basin calcrete types' in *The South African Archaeological Bulletin* 24(95-96) 117 – 122

Nichols, G. (2009) *Sedimentology and Stratigraphy* 2nd Edn. Oxford: Wiley Blackwell

Nicod, J. (2003) 'A little contribution to the karst terminology: special of aberrant cases of poljes?' in *Acta Carsologica* 32(2) 3 29-39

Oluić, M., Cvijanović, D. and Prelogovic, E. (1982) 'Some new data on the tectonic activity in the montenegro coastal region (yugoslavia) based on the landsat imagery' in *Acta Astronautica* 9 (1) 27-33

Ori, G. G. (1982) 'Braided to meandering channel patterns in humid region alluvial fan deposits, River Reno, Po Plain (Northern Italy)' in *Sedimentary Geology* 31 231-248

Østrem, G. (1975) 'Sediment transport in glacial meltwater streams' in Jopling, A. V. and McDonald, B. C. (Eds.) *Glaciofluvial and Glaciolacustrine sedimentation* Society of Economic Palaeontologists and Mineralogists Special Publication No. 23

Owen, L. A., Caffee, M. W., Finkel, R. C. and Bae Seong, Y. (2008) 'Quaternary glaciations of the Himalayn-Tibetan orogen' in *Journal of Quaternary Science* 23(6) 513-531

Owen, L. A., Finkel, R. C., Barnard, P. L., Haizhou, M., Asahi, K., Caffee, M. W. and Derbyshire, E. (2005) 'Climatic and topographic controls on the style and timing of Late Quaternary glaciation throughout Tibet and the Himalaya defined by [10]Be cosmogenic radionuclide surface exposure dating' in *Quaternary Science Reviews* 24 1391-1411

Paiero, G. and Monegato, G. (2003) 'The Pleistocene evolution of Arzino alluvial fan and western part of Tagliamento morainic amphitheatre (Friuli, NE Italy)' in *Il Quaternario: Italian Journal of Quaternary Sciences* 16(1)185-193

Palacios, D., de Marcos, J., and Vázquez-Selem, L. (2010) 'Last Glacial Maximum and deglaciation of Sierra de Gredos, central Iberian Peninsula' in *Quaternary International* 233 (1) 16-26

Pallàs, R., Rodés, Á., Braucher, R., Carcaillet, J., Ortuño, M., Bourdonau, J., Bourlès, D. and Vilaplana, J. M. (2006) 'Late Pleistocene and Holocene glaciation in the Pyrenees: a critical review and new evidence from [10]Be exposure ages, south-central Pyrenees' in *Quaternary Science Reviews* 25 2937–2963

Pallàs, R., Rodés, Á., Braucher, R., Bourlès, D., Delmas, M., Calvet, M. and Gunnell, Y. (2010) 'Small, isolated glacial catchments as priority targets for cosmogenic surface exposure dating of Pleistocene climate fluctuations, southeastern Pyrenees' in *Geology* 38 891-894

Pelfini, M. and Smiraglia, C. (1992) 'Recent fluctuations of glaciers in Valtellina (Italian Alps) and climatic variations' in *Journal of Glaciology* 38 (192) 309-313

Penck, A. (1900) 'Die Eiszeit auf der Balkanhalbinsel' in *Globus* 78 133-178

Penck, A. and Brückner, E. (1909) *Die Alpen im Eiszeitalter* Leipzig: Tauchnitz

Peña, J. L., Sancho, C., Lewis, C., McDonald, E. and Rhodes, E. (2004) 'Datos cronológicos de las morenas terminales del glaciar del Gállego y su relación con las terrazas fluvioglaciares (Pirineo de Huesca)' in Peña, J. L., Longares, L. A. and Sánchez, M. (Eds.) *Geografía Física de Aragón: Aspectos generales y temáticos* Zaragoza: Universidad de Zaragoza e Institución Fernando el Católico

Pentecost, A. (1993) 'British Travertines: a review' in *Proceedings of the Geologists' Association* 104 23-39

Pentecost, A. (2005) *Travertine* Dordrecht, Netherlands: Kluwer Academic Publishers Group

Philips, F. M., Zreda, M. G., Gosse, J. C., Klein, J., Evenson, E. B., Hall, R. D., Chadwick, O. A. and Sharma, P. (1997) 'Cosmogenic ^{36}Cl and ^{10}Be ages of Quaternary glacial and fluvial deposits of the Wind River Range,Wyoming' in *GSA Bulletin* 109(11) 1453-1463

Reading, H. G. (Ed.) (1996) *Sedimentary Environments: Processes, Facies, Stratigraphy* Oxford: Blackwell

Revel, M., Ducassou, E., Grousset, F. E., Bernasconi, S. ., Migeon, S., Revillon, S., Mascle, J., Murat, A., Zaragosi, S. and Bosch, D. (2010) '100,000 years of African monsoon variability recorded in sediments of the Nile margin' in *Quaternary Science* Reviews 29 1342–1362

Reynolds Jr., R. C. and Johnson, N. M. (1972) 'Chemical weathering in the temperate glacial environments of the Northern Cascade Mountains' in *Geochimica et Cosmochimica Acta* 36 537-554

Rinterknecht, V. R., Clark, P. U., Raisbeck, G. M., Yiou, F., Bitinas, A., Brook, E. J., Marks, L., Zelčs, L., Lunkka, J-P., Pavlovskaya, I. E., Piotrowski, J. A. and Raukas, A. (2006) 'The last deglaciation of the southeastern sector of the Scandinavian Ice Sheet' in *Science* 311 1449 – 1452

Rittenour, T. M., Blum, M. D. and Goble, R. J (2007) 'Fluvial evolution of the lower Mississippi River valley during the last 100ky glacial cycle: response to glaciation and sea-level change' in *Geological Society of America Bulletin* 119 586-608

Ritter, D. F. and Ten Brink, N. W. (1986) 'Alluvial Fan Development and the Glacial-Glaciofluvial Cycle, Nenana Valley, Alaska' in *The Journal of Geology* 94(4) 613-625

Rohling, E. J. and Thunell, R. C. (1999) 'Five decades of Mediterranean paleoclimate and sapropel studies' in *Marine Geology* 153 7 – 10

Rohling, E. Abu-Zeid, R., Casford, J., Hayes, A. And Hoogakker, B. (2009) 'The Marine Environment: Past and Present' in Woodward, J. C. (Ed.) *The Physical Geography of the Mediterranean* Oxford: Oxford University Press

Rossignol-Strick, M., (1985) 'Mediterranean Quaternary sapropels, an immediate response of the African Monsoon to variations of insolation' in *Palaeogeography, Palaeoclimatology, Palaeoecology* 49 237– 263

Rossinsky, Jr. V. and Swart, P. K. (1993) 'Influence of climate on the formation and isotopic composition of calcretes' in Swart, P. K., Lohman, K. C., McKenzie, J. and Savin, S. (Eds) *Climate change in continental isotopic records* Geophysical Monograph 78 Washington: American Geophysical Union

Roth von Telegd, K. (1923) 'Das albanisch-montenegrinische Grenzgebiet bei Plav (Mit besonderer Berücksichtigung der Glazialspuren)' in Nowack, E. (Ed.) *Beiträge zur Geologie von Albanien, Neues Jahrbuch für Mineralogie 1* Schweizerbart: Stuttgart 422–494

Rother, H., Jol, H. M. and Shulmeister, J. (2007) 'Stratigraphy and tectonic implications of Late Pleistocene valley fill in the Hope Valley, Canterbury, South Island, New Zealand' in: Baker, G. S., Jol, H. M. (Eds.) *Stratigraphic Analyses using Ground Penetrating Radar (GPR)* Geological Society of America Special Paper 432

Rother, H., Schulmeister, J. and Rieser, U. (2010) 'Stratigraphy, optical dating chronology (IRSL) and depositional model of pre-LGM glacial deposits in the Hope Valley, New Zealand' in *Quaternary Science Reviews* 29 576-592

Salcher, B. C. and Wagreich, M. (2010) 'Climate and tectonic controls on Pleistocene sequence development and river evolution in the Southern Vienna Basin (Austria)' in *Quaternary International* 222 (1-2) 154-167

Sánchez Goñi, M. F., Landais, A., Fletcher, W. J., Naughton, F., Desprat, S. and Duprat, J. (2008) 'Contrasting impacts of Dansgaard–Oeschger events over a western European latitudinal transect modulated by orbital parameters' in *Quaternary Science Reviews* 27(11-12) 1136-1151

Sancho, C., Peña-Monné, J.L., Lewis, C., McDonald, E. and Rhodes, E. (2003) 'Preliminary dating of glacial and fluvial deposits in the Cinca river Valley (NE Spain): chronological evidences for the Glacial Maximum in the Pyrenees' in: Ruiz-Zapata, B., Dorado-Valiño,M., Valdeomillos, A., Gil-García, M.J., Bardají, T., Bustamante,I. and Mendizábal, I. (Eds.) *Quaternary Climatic Changes and Environmental Crises in the Mediterranean Region* Alcalá de Henares, Madrid

Santisteban, J. I. and Schulte, L. (2007) 'Fluvial networks of the Iberian Peninsula: a chronological framework' in *Quaternary Science Reviews* 26 2738–2757

Sarıkaya, M. A., Zreda, M., Çiner, A. and Zweck, C. (2008) 'Cold and wet Last Glacial Maximum on Mount Sandıras, SW Turkey, inferred from cosmogenic dating and glacier modeling' in *Quaternary Science Reviews* 27 769–780

Sarıkaya, M. A., Zreda, M. and Çiner, A. (2009) 'Glaciations and paleoclimate of Mount Erciyes, central Turkey, since the Last Glacial Maximum, inferred from [36]Cl cosmogenic dating and glacier modelling' in *Quaternary Science Reviews* 28 2326–2341

Sawicki, L. von. (1911) 'Die eiszeitliche Vergletscherung des Orjen in Süddalmatien' in *Zeitscrift für Gletscherkunde* 5 339-355

Schildgen, T., Dethier, D. P., Bierman, P. and Caffee, M. (2002) '[26]Al and [10]Be dating of Late Pleistocene and Holocene fill terraces: a record of fluvial deposition and incision, Colorado Front Range' in *Earth Surface Processes and Landforms* 27 773-787

Schulte, L., Julià, R., Burjachs, F. and Hilgers, A. (2008) 'Middle Pleistocene to Holocene geochronology of the River Aguas terrace sequence (Iberian Peninsula): Fluvial response to Mediterranean environmental change' in *Geomorphology* 98 13-33

Schumm, S. A. (1978) *The Fluvial System* New York: John Wiley and Sons

Schwarcz, H. P. (1989) 'Uranium-series dating of Quaternary deposits' in *Quaternary International* 1 7-17

Seret, G., Dricot, E. and Wansard, G. (1990) 'Evidence for an early glacial maximum in the French Vosges during the last glacial cycle' in *Nature* 346 453–456

Serrano-Cañadas, E. (1992) 'Huellas de una glaciación pre-pleniglaciar en la Ribera de Biescas (cuenca del Gállego, Pirineo aragonés)' in *Cuadernos de Sección Historia* 20 213-227

Shackleton, N.J. and Opdyke, N.D (1976) 'Oxygen isotope and palaeomagnetic stratigraphy of equatorial Pacific core V28-239, late Pliocene to latest Pleistocene' in Cline, R. M. and Hays, R. D. (Eds.) *Investigation of Late Quaternary Palaeoceanography and Palaeoclimatology* Memoirs of the Geological Society of America 145 449-464.

Shackleton, N. J., Berger, A. and Peltier, W. R. (1990) 'An alternative astronomical calibration of the lower Pleistocene timescale based on ODP Site 677' in *Transactions of the Royal Society of Edinburgh: Earth Sciences* 81 251-261

Sharp, R. P. (1988) *Living Ice: understanding glaciers and glaciation* Cambridge: Cambridge University Press

Sierro, F. J., Hodell, D. A., Curtis, J. H., Flores, J. A., Reguera, I., Colmenero-Hidalgo, E., Bárcena, M. A., Grimalt, J. O., Caho, I., Frigola, J. and Canals, M. (2005) 'Impact of iceberg melting on Mediterranan thermohaline circulation during heinrich events' in *Paleoceanography* 20 PA2019

Smart, P. L. (1986) 'Origin and development of glaciokarst closed depressions in the Picos de Europa, Spain' in *Zeitschrift für Geomorphologie* 30 423–43.

Smart, P. L. (1991) 'Uranium Series Dating' in Smart, P.L. and Frances, P.D. (Eds.) *Quaternary dating methods - a users guide. Technical Guide No. 4.* Quaternary Research Association 45-83.

Smith, G. W., Nance, D. and Genes, A. N. (1997) 'Quaternary glacial history of Mount Olympus, Greece' in *Geological Society of America Bulletin* 109 809-824

Sperazza, M., Moore, J. N. and Hendrix, M. S. (2004) 'High resolution particle size analysis of naturally occurring very fine grained sediment through laser diffractometry' in *Journal of Sedimentary Research* 74736-743

Soil Survey Staff (1999) *Soil Taxonomy: a basic system of soil classification for making and interpreting soil surveys* 2nd Edn. Washington: United States Department of Agriculture

Spektor, V. B. and Spektor, V. V. (2009) 'Karst Processes and Phenomena in the Perennially Frozen Carbonate Rocks of the Middle Lena River Basin' in *Permafrost and Periglacial Processes* 20 71–78

Stahl, K., Moore, R. D., Shea, J. M., Hutchinson D. and Cannon, A. J. (2008) 'Coupled modelling of glacier and streamflow response to future climate scenarios' in *Water Resources Research* 44 1-13

Starkel, L. (2003) 'Climatically controlled terraces in uplifting mountain areas' in *Quaternary Science Reviews* 22 2189–2198

Stepišnik, U. and Žebre, M. (2011) *Glaciokras Lovčena* E-GeograFF 2. Univerza v Ljubljani, Filozofska fakulteta. Available at:
http://geo.ff.uni-lj.si/sites/default/files/glaciokras_lovcena_0.pdf
Last Accessed (July 27th 2012)

Stepišnik, U., Ferk, M., Kodelja, B., Medenjak, G., Mihevc, A., Natek, K. and Žebre, M. (2009) 'Glaciokarst of western Orjen' in *Cave and Karst Science* 36 21-28

Stokes, M., Mather, A. E., Belfoul, A. and Farik, F. (2008) 'Active and passive tectonic controls for transverse drainage and river gorge development in a collisional mountain belt (Dades Gorges, High Atlas Mountains, Morocco)' in *Geomorphology* 102 2-20

Suggate, R. P. (1965) 'Late Pleistocene geology of the northern part of the South Island, New Zealand' in *New Zealand Geological Survey Bulletin* 77 90

Suggate, R. P. (1990) 'Late Pleistocene and Quaternary glaciations of New Zealand' in *Quaternary Science Reviews* 9 175–197

Surić, M., Juračić, M., Horvatinčić, N. and Krajcar Bronić, I. (2005) 'Late Pleistocene–Holocene sea-level rise and the pattern of coastal karst inundation: records from submerged speleothems along the Eastern Adriatic Coast (Croatia)' in *Marine Geology* 214 (1–3) 163–175

Surić, M., Richards, D. A., Hoffmann, D. L., Tibljaš, D. and Juračić, M. (2009) 'Sea-level change during MIS 5a based on submerged speleothems from the eastern Adriatic Sea (Croatia)' in *Marine Geology* 262 1(1-4) 62–67

Svendsen, J. I., Alexanderson, H., Astakhov, V. I., Demidov, I., Dowdeswell, J. A., Funder, S., Gataullin, V., Henriksen, M., Hjort, C., Houmark-Nielsen, M., Hubberten, H. W., Ingólfsson, Ó., Jakobsson, M., Kjær, K. A., Larsen, E., Lokrantz, H., Lunkka, J. P., Astrid Lyså, A., Mangerud, J., Matiouchkov, A., Murray, A., Möller, P., Niessen, F., Nikolskaya, O., Polyak, L., Saarnisto, M., Siegert, C., Siegert, M. J., Spielhagen, R. F. and Stein, R. (2004) 'Late Quaternary ice sheet history of northern Eurasia' in *Quaternary Science Reviews* 23 1229-1271

Syvitski, J. P. M., Leblanc, K. W. G. and Asprey, K. W. (1991) 'Interlaboratory instrument calibration experiment' in Syvitski, J.P.M. (Ed.) *Principles, Methods and Application of Particle Size Analysis* Cambridge University Press: Cambridge pp. 174–193

Techer, I., Khoury, H. N., Salameh, E., Rassineux, F., Claude, C., Clauer, N., Pagel, M., Lancelot, J., Hamelin, B. and Jacquot, E. (2006) 'Propagation of high-alkaline fluids in an argillaceous formation: Case study of the Khushaym Matruk natural analogue (Central Jordan)' in *Journal of Geochemical Exploration* 90 53–67

Telbisz, T. (2010a) 'Morphology and GIS-analysis of closed depressions in Sinjajevina Mts (Montenegro)' in *Karst Development: Original Papers* 1 (1) 41-47

Telbisz, T. (2010b) 'Glacio-karst features of the Sinjajevina Mts (Montenegro): an overview and DEM-Analysis' in *Karst Development* 1 17-22

Toucanne, S., Zaragosi, S., Bourillet, J. F., Gibbard, P. L., Eynaud, F., Girardeau, J., Turon, J. L., Cremer, M., Cortijo, E., Martinez, P. and Rossignol, L. (2009) 'A 1.2Ma record of glaciation and fluvial discharge from the West European Atlantic margin' in *Quaternary Science Reviews* 28 (25-26) 2974-2981

Tranter, M. (2003) 'Geochemical Weathering in Glacial and Proglacial Environments' in Drever, J. I. (Ed.) *Treatise on Geochemistry* 5 189-205

Tzedakis, P. C. (1994) 'Vegetation Change through Glacial-Interglacial Cycles: A Long Pollen Sequence Perspective' in *Philosophical Transactions: Biological Sciences* 345 (1314) 403-432

Tzedakis, C. (2009) Cenezoic Climate and Vegetation Change' in Woodward, J. C. (Ed.) *The Physical Geography of the Mediterranean* Oxford: Oxford University Press

Tzedakis, P. C., Andrieu, V., de Beaulieu, J-L., Birks, H. J. B., Crowhurst, S., Follieri, M., Hoogheimstra, H., Magri, D., Reille, M., Sadori, L., Shackleton, N. J. and Wijmstra, T. A. (2001) 'Establishing a terrestrial chronological framework as a basis for biostratigraphical comparisons' in *Quaternary Science Reviews* 20 1583-1592

Tzedakis, P. C., Hooghiemstra, H. and Pälike, H. (2006) 'The last 1.35 million years at Tenaghi Philippon: revised chronostratigraphy and long-term vegetation trends' in *Quaternary Science Reviews* 25 3416–3430

Tzedakis, P. C., McManus, P. C., Hooghiemstra, H., Oppo, D. W. and Wijmstra, T. A., (2003) 'Comparison of changes in vegetation in northeast Greece with records of climate variability on orbital and suborbital frequencies over the last 450,000 years' in *Earth and Planetary Science Letters* 212 197–212

van Andel, T. H. (1998) 'Palaeosols, red sediments, and the Old Stone Age in Greece' in *Geoarchaeology: An International Journal* 13 (4) 361-390

Vandenberghe, J. (1995) 'Timescales, climate and river development' in *Quaternary Science Reviews* 14 631-638

Vandenberghe, J. (2008) 'The fluvial cycle at cold-warm-cold transitions in lowland regions: a refinement of theory' in *Geomorphology* 98 275-284

Vezzoli, G. and Garzanti, E. (2009) 'Tracking palaeodrainage in Pleistocene foreland basins' in *The Journal of Geology* 117 445-454

Vidal Romaní, J. R. and Fernández Mosquera, D. (2006) 'Glaciarismo Pleistoceno en el NW de la Península Ibérica (Galicia, España-Norte de Portugal)' in *Enseñanza de las Ciencias de la Tierra* 13.3 270-277

Villemant, B. and Feuillet, N. (2003) 'Dating open systems by the ^{238}U-^{234}U-^{230}Th method: application to Quaternary reef terraces' in *Earth and Planetary Science Letters* 210 105-118

Vita-Finzi, C. (1969) *The Mediterranean Valleys: Geological Changes in Historical Times* Cambridge: Cambridge University Press

Vidic ,N. J. (1998) 'Soil-age relationships and correlations: comparison of chronosequences in the Ljubljana Basin, Slovenia and USA' in *Catena* 34 113-129

von Eynatten, H., Tolosana-Delgado, R. and Karius, V. (2012) 'Sediment generation in modern glacial settings: Grain-size and source-rock control on sediment composition' in *Sedimentary Geology* In Press

von Graftenstein, R., Zahn, R., Tiedmann, R. and Murat, A. (1999) 'Planktonic δ^{18}O records at sites 976 and 977. Alboran Sea: stratigraphy, forcing and palaeoceanographic implications' in Zahn, R., Comas, M. C., and Klaus, A. (Eds.) *Proceedings of the Ocean Drilling Program, Scientific Results* Vol. 161 469

Walker, M. J. C. (2005) *Quaternary Dating Methods* Chichester: John Wiley

Walker, M. and Lowe, J. (2007) 'Quaternary science 2007: a 50 year retrospective' in *Journal of the Geological Society* 164 1073-1092

Watts, W. A., Allen, J. R. M. and Huntley, B. (1996) 'Vegetation history and palaeoclimate of the last glacial period at Lago Grande di Monticchio, southern Italy' in *Quaternary Science Reviews* 15 133–153

Wegmann, K. W. and Pazzaglia, F. J. (2009) , Late Quaternary fluvial terraces of the Romagna and Marche Apennines, Italy: Climatic, lithologic, and tectonic controls on Terrace genesis in an active orogen' in *Quaternary Science Reviews* 28 137-165

Westaway, R., Pringle, M., Yurtmen, S., Demir, T., Bridgland, D., Rowbotham, G. and Maddy, D. (2004) 'Pliocene and Quaternary surface uplift of western Turkey: the Gediz River terrace staircase and the volcanism at Kula' in *Tectonophysics* 391 121–169

Wijmstra, T. A. (1969) 'Palynology of the first 30 metres of a 120 m deep section in Northern Greece' in *Acta Botanica Neerlandica* 18 511-527

Woo, M. and Fitzharris, B. B. (1992) 'Reconstruction of Mass Balance Variations for Franz Josef Glacier, New Zealand, 1913 to 1989' *in Arctic and Alpine Research* 24 281–290

Woodward, J. C. (1990) *Late Quaternary Sedimentary Environments in the Voidomatis Basin, Northwest Greece* Unpublished Ph.D. thesis, University of Cambridge

Woodward, J. C. (2009) 'Editorial Introduction' in Woodward, J. C. (Ed.) *The Physical Geography of the Mediterranean* Oxford: Oxford University Press

Woodward, J.C. and Bailey, G. N. (2000) 'Sediment sources and terminal Pleistocene geomorphological processes recorded in rockshelter sequences in Northwest Greece' in Foster, I. D. L. (Ed.) *Tracers in geomorphology* London: Wiley

Woodward, J. C., Hamlin, R. H. B., Macklin, M. G., Hughes, P. D. and Lewin, J. (2008) 'Glacial activity and catchment dynamics in northwest Greece: Long-term river behaviour and the slackwater sediment record for the last glacial to interglacial transition' in *Geomorphology* 101 44-67

Woodward, J. C., Hamlin, R. H. B., Macklin, M. G., Karkanas, P. and Kotjabopoulou, E. (2001) 'Quantitative Sourcing of Slackwater Deposits at Boila Rockshelter: A Record of Lateglacial Flooding and Paleolithic Settlement in the Pindus Mountains, Northwest Greece' in *Geoarchaeology* 16 (5) 501-536

Woodward, J. C. and Hughes, P. D (2011) 'Glaciation in Greece: A New Record of Cold Stage Environments in the Mediterranean' in Ehlers, J., Gibbard, P. L. and Hughes, P. D. (Eds.) *Quaternary Glaciations - Extent and Chronology: A Closer Look* London: Elsevier

Woodward, J. C., Lewin, J. and Macklin, M.G. (1992) 'Alluvial sediment sources in a glaciated catchment: the Voidomatis basin, northwest Greece' in *Earth Surface Processes and Landforms* 16 205–216

Woodward, J. C., Lewin, J. and Macklin, M. G. (1995) 'Glaciation, river behaviour and the Palaeolithic settlement of upland northwest Greece' in Lewin, J., Macklin, M. G. and Woodward, J. C. (Eds.) *Mediterranean Quaternary River Environments* Balkema: Rotterdam

Woodward, J. C., Porter, P. R., Lowe, A. T., Walling, D. E. and Evans, A. J. (2002) 'Composite suspended sediment particles and flocculation in glacial meltwaters: preliminary evidence from Alpine and Himalayan basins' in *Hydrological Processes* 16 1735-1744

Woodward, J. C., Macklin, M. G. and Smith, G. R. (2004) 'Pleistocene glaciation in the mountains of Greece' in Ehlers, J. and Gibbard, P. L. (Eds.) *Quaternary Glaciations – Extent and chronology Part 1: Europe* Amsterdam: Elsevier

Wright, V. P. (2007) 'Calcrete' in Nash, D. J and McLaren, S. J. (Eds.) *Geochemical sediments and landscapes* RGS-IBG Book Series Oxford: Blackwell

Wright, V. P. and Tucker, M. E. (1991) 'Calcretes: an introduction' in Wright, V. P. and Tucker, M. E. (Eds) *Calcretes* International Association of Sedimentology

Wulf, S., Kraml, M., Brauer, A., Keller, J. and Negendank, J. F. W. (2004) 'Tephrochronology of the 100 ka lacustrine sediment record of Lago Grande di Monticchio (southern Italy)' in *Quaternary International* 122 7–30

Xu, L. and Zhou, S. (2009) 'Quaternary glaciations recorded by glacial and fluvial landforms in the Shaluli Mountains, Southeastern Tibetan Plateau' in *Geomorphology* 103 268-275

Zahno, C., Akçar, N., Yavuz, V., Kubik, P. W. and Schlüchter, C. (2009) 'Surface exposure dating of Late Pleistocene glaciations at the Dedegöl Mountains (Lake Beyşehir, SW Turkey)' in *Journal of Quaternary Science* 24(8) 1016-1028

Zahno, C., Akçar, N., Yavuz, V., Kubik, P. W. and Schlüchter, C. (2010) 'Chronology of Late Pleistocene glacier variations at the Uludağ Mountain, NW Turkey' in *Quaternary Science Reviews* 29 (9-10) 1173-1187

Zolitschka, B. and Negendank, J. F. W. (1996) 'Sedimentology, dating and palaeoclimatic interpretation of a 76.3 ka record from Lago Grande di Monticchio, southern Italy' in *Quaternary Science Reviews* 15 101–112

Zreda, M., Ciner, A., Bayari, S. and Sarikaya, A. (2005) 'Remarkably extensive early Holocene glaciation in Turkey' EGU 2005, 24-29 April 2005 Vienna Geophysical Research Abstracts, volume 7 (06068)

U-SERIES: CHEMICAL PREPARATION AND ANALYSIS

The preparation and analysis procedures for U-series analysis comprise 5 stages. Sample pre-clean and preparation (stage 1) was undertaken by the author at the University of Manchester. All efforts were made to minimise contamination of the samples by maintaining a clean working area and ensuring that laboratory instruments remained clean. All chemical and analytical preparations (stages 2 – 5) were undertaken by the author alongside staff at the Open University Uranium Series Facility (OUUSF) in Milton Keynes following their laboratory protocol.

Stage 1 - Sample pre-clean and preparation
Stage 2 - Sample weighing
Stage 3 - Sample dissolution and spiking
       a. Dissolution
       b. Dissolution of detritally contaminated samples
       c. Sample spiking
       d. Dissolution and spiking of detritus samples
Stage 4 - Separation of U and Th with anion exchange columns
       e. Column preparation and cleaning
       f. Sample addition
Stage 5 – Sample analysis: mass spectrometry

Stage 1 - Sample pre-clean and preparation

1. Samples are cleaned using a handheld drill to remove surface debris.
2. Samples are assessed for overprinted carbonate phases and individual fabrics were identified for further sampling.
3. Each sample is lightly crushed using an agate pestle and mortar and suitable crystals are picked with forceps using a stereo microscope.
4. The crystals are then cleaned in a glass petri dish using 10% HCl vol by vol for several minutes where the surficial $CaCO_3$ reacts with the HCl to remove any remaining detritus.
5. Samples are placed in deionised water to cease the reaction and clean residual HCl.
6. Samples are air dried to prevent the formation of reprecipitation rinds which may occur through drying at high temperatures.

7. For samples comprising smaller calcite crystals (i.e. those not manually separable), the entire sample is placed into HCl and rinsed in deionised water before being air dried.
8. Samples are then crushed to a fine powder using an agate pestle and mortar and retained in a clean, 50 ml centrifuge tube.

9. Two samples are also prepared for detrital correction (detritus samples). These are surficially cleaned with a drill, but not subjected to HCl washing or crystal picking. This ensures that the detrital component of the secondary carbonate remains in the sample and can be used to generate a correction factor for detrital Th.

Stage 2 - Sample weighing

1. Samples are weighed out into clean, dry 60 ml Savillex beakers.
2. Add approximately 0.5 g (or greater) of sample. Accurately weighed to 5d.p.
3. The two detritus samples are prepared in the same way.
4. Two samples of young speleothem (YS), which are used to monitor contamination, are also weighed, as well as two empty beakers as 'total procedural blanks' (TPBs).

Stage 3 - Sample dissolution and spiking

All of the samples are subjected to a series of chemical dissolution phases to remove any detritus from the carbonate (stage 3a). The YS samples and TPBs are also subjected to this procedure. Samples that contain particularly high concentrations of detritus are required to undergo more robust dissolution methods (stage 3b). Samples that have been specifically prepared for detrital correction (detritus samples) undergo a slightly modified version of the dissolution phase (stage 3d).

a) Dissolution

1. The powdered sample is taken into suspension using 2-3 ml milliQ (MQ) H_2O.
2. Dilute nitric acid (TD 7M HNO_3) is added to the sample, drop wise, until the reaction ceases. Concentrated nitric acid (TD 15M HNO_3) may be added, drop-wise, to the solution until there is no further reaction and the calcite is fully dissolved. The addition of TD 15M HNO_3 also ensures that the pH remains low enough to keep the Th in solution.
3. Place the sample on a hot plate at c. 110-120°C for several hours to ensure the reaction is complete. Assuming no detrital material is present within the sample, the solution should be translucent. If the samples remain cloudy, or particles remain in the beaker, then further preparation phases are required (see stage 3b).
4. The YS samples are subjected to this dissolution phase.

b) Dissolution of detritally contaminated samples

This stage separates the detritus from the carbonate so that the detritus can be treated and dissolved separately before it is spiked and reintroduced to the carbonate fraction. The sample can then be analysed as normal.

1. If the samples are cloudy following initial dissolution (stage 3a), the sample solution is transferred from the beaker to a clean 50 ml centrifuge tube using 2-3 ml TD 7M HNO_3.
2. The sample is centrifuged at 4,000 rpm for 5 minutes. The supernatant (i.e. containing the carbonate fraction of the sample) is decanted into a clean 50 ml centrifuge tube and retained.
3. The remaining detritus pellet is agitated into suspension using c. 5 ml of TD 7M HNO_3 and centrifuged again at 4,000 rpm for 5 minutes. The supernatant is decanted and retained.
4. The remaining pellet is transferred back into the 60 ml beaker using TD 7M HNO_3.
5. 1-2 ml hydrofluoric acid (HF) and 1-2 ml TD 15M HNO_3 are added to the sample. The samples are placed on the hot plate at 110°C overnight.
6. The samples are then removed from the hot plate and cooled fully.
7. The beaker lids are then removed and the samples are placed back onto the hot plate and evaporated to dryness. The lids are then replaced and they are left to cool.

8. Further additions of HNO_3 and HCl to the sample will now be used to remove excess fluoride form the sample. c. 1 ml TD 15M HNO_3 is added to the sample. The lid is then replaced and the samples are put back on the hot plate overnight.
9. The lids are removed and the samples are evaporated to dryness. The samples are then removed from the heat and cooled.
10. 1-2 ml TD 6M HCl is added to the sample to take the dry residue back into solution. The lid is replaced and the sample is put on the hot plate. On the addition of HCl the sample may become bright yellow colour as various minerals in the solution are highlighted (e.g. copper and iron).
11. The sample should now be fully dissolved and should be translucent (although possibly still yellow in colour).

c) Sample spiking

1. Once the samples have been fully dissolved they are spiked with a $^{229}Th/^{236}U$ solution. The sample solution is placed on the balance, and zeroed. For most calcites, 5-10 drops of spike are sufficient – the amount depends on the initial quantity of carbonate sample used. The weight of the spike is recorded to 5 d.p.
2. The beakers containing the sample and spike are placed on the hot plate overnight to allow the samples to equilibrate.
3. If extra steps have been taken to dissolve the detritally contaminated samples, the detritus is spiked separately before replacing the pooled carbonate supernatant back into the sample beaker.
4. The sample is agitated into suspension, the lid is removed and the sample is placed on a hot plate at 110°C overnight.
5. Samples are removed from the hot plate to cool, the lids are removed and the sample is returned to the hot plate for 4 hours to evaporate to dryness.
6. The samples are then removed from the hot plate and put back into solution using 2-3 ml TD 7M HNO_3 so that they are prepared for separation in the anion exchange columns.

d) Dissolution and spiking of detritus samples

1. The samples are initially dissolved using TD 7M HNO_3 and TD 15M HNO_3 in the same way as stage 3a, steps 1-4.
2. As with the detritally contaminated samples (stage 3b) the carbonate is separated from the detritus by centrifuging in TD 7M HNO_3 at 4,000 rpm for 5 minutes.
3. The carbonate supernatant is decanted and retained in a separate centrifuge tube.
4. This is repeated and the supernatant pooled.
5. Unlike with the detritally contaminated samples, these detritus samples are specifically analysing the detrital component and the carbonate fraction here can be discarded.
6. The detritus pellet in the base of the centrifuged tube is returned to the sample beaker using 2-3 ml TD 7M HNO_3.
7. The sample is placed on a hot plate at 110°C, with the lid removed, until fully desiccated.
8. The sample, in the beaker, is then reweighed to find the weight of the detritus. This can then be subtracted from the initial weight of the sample.
9. The samples are then subjected to the same HF treatment, HNO_3, and HCl dissolution as the detritally contaminated samples (stage 3b, steps 5-11).
10. The samples are then spiked in the same way as the detritally contaminated samples, but the pooled carbonate supernatant is not returned to the sample beaker to ensure that only the detritus component is analysed.

Stage 4 - Separation of Th and U

The Th and U are purified in an anionic resin column (10 ml Biorad columns). TD 7M HNO_3 is used to load the sample and elute unwanted ions. Th is eluted using TD 6M HCl and collected in clean 7 ml vials. U is eluted using TD 1M HBr and collected in separate vials.

a) Column preparation and cleaning

1. Columns are pre-cleaned in QD 6M HCl, then in MQ H_2O and placed on a hot plate at 110°C for one hour. Samples are then stored in MQ H_2O within large beakers.
2. Columns are removed from their storage beakers and placed into a column rack (with apertures for 6 columns). A clean 50 ml beaker is placed under each beaker to receive waste solutions.
3. The insides of the columns are washed in TD 6M HCl using a squeezable bottle.
4. Columns are then washed with MQ H_2O in the same way. Steps 3 and 4 are repeated.
5. Using a clean, disposable pipette, 2 ml of 1x8 200-400 Biorad anionic resin is added to each column. This should be filled to the first widening of the column. Due to the propensity of the resin to separate within its storage bottle, it may require shaking before use, though care must be taken to avoid the presence of bubbles when the resin is placed in the columns. If too much resin is placed into the columns (i.e. above the first widening), this can be removed by adding a small amount of MQ H_2O, shaking gently to agitate the top layers of resin into suspension, and decanting a drop at a time until the resin reaches the appropriate level.
6. The resin is left for c. 2 hours to settle within the column.
7. 4 ml TD 6M HCl is added to each column and left to pass through the resin into the beakers below until dripping ceases, usually after 20-30 minutes.
8. The resin is cleaned using 4 ml MQ H_2O. This is left to pass through the resin.
9. 4 ml TD 6M HCl is then washed through the resin and left to fully pass through.
10. The columns are filled to the top with a final addition of MQ H_2O and left overnight to settle.
11. The columns are preconditioned with 4 ml TD 7M HNO_3 (i.e. the same acid that is used to take up the samples into solution). This is left to fully pass through the resin.

b) Sample addition and Th/U separation

1. Samples are added to the columns using a Pasteur pipette. c. 2 ml TD 7M HNO_3 is taken up into the pipette and rinsed to ensure that it is clean. This is decanted as waste.
2. The sample is taken up into the pipette, ensuring that none of the sample is left behind in its beaker. It is added, drop-wise into the top of the column. Care is taken to introduce the sample down the side of the column to ensure that the surface of the resin is not disturbed. The resin is seen to change colour as the sample passes through.
3. Once the sample has fully passed through, 6 ml TD 7M HNO_3 is eluted through the column. This is added in three batches of 2 ml. This ensures that the sample is fully washed into the resin. As the resin attracts anions (i.e. Th and U), these are retained within the resin, whilst unwanted components (e.g. Fe or Sr) pass through in solution and can be discarded as waste.
4. Once the 6 ml TD 7M HNO_3 has passed through the resin, 1.5 ml TD 6M HCl is eluted. This is used to wash the Th into the base of the resin. The 1.5 ml TD 6M HCl is collected and discarded as waste.
5. The waste beaker is removed from underneath the column.
6. A clean, dry 7 ml vial is placed underneath the column to collect the Th.

7. 3.5 ml TD 6M HCl is eluted to wash the Th from the resin, collected in the vials and retained.
8. The waste beaker is replaced underneath the columns.
9. 1 ml TD 1M HBr to wash the U into the resin.
10. The waste beaker is removed and replaced with a clean, dry 7 ml vial to collect the U.
11. 4.5 ml TD 1M HBr is eluted, collected in the vial and retained.
12. The vials containing the Th and U fractions are placed on the hotplate at 110°C overnight and evaporated to dryness. Once dry, the sample should now form a small (often barely visible) pellet in the base of the vial.
13. The sample is redissolved in c. 1 ml TD 14M HNO_3 and 2 ml MQ H_2O. The lids are replaced and the sample is ready to analyse.

Stage 5 - Sample analysis: mass spectrometry

Samples are analysed using a Nu Instruments multi-collector inductively coupled plasma-ionisation mass spectrometer (MC-ICPMS). Each sample was run with two bracketing standards and wash cycles. The sample data are normalised to these standards. Standards are run before the samples are analysed to monitor machine performance.

a) Analysing a sample

1. The sample is transferred from its 7 ml vial to a centrifuge tube. TD 3M HNO_3 is used to create a solution of at least 3 ml.
2. Samples are analysed using a standard operating procedure using a Nu Instruments MC-ICPMS.

b) Analysing a standard

Once the sample run is complete, the machine enters a clean-standard-clean cycle.

Each of the two cleaning phases comprises a sequence of 5 reagents, each lasting 2 minutes:
   1. TD 3M HNO_3 (3% HNO_3) and TD 0.2M HF (2% HF)
   2. IPA
   3. TD 1M HCl
   4. MQ H_2O
   5. TD 3M HNO_3 (3% HNO_3) and TD 0.2M HF (2% HF)

All data are analysed and U-series ages calculated by staff at the OUUSF.

The Harden Index is calculated using the following methods (Table B.1) outlined by Harden (1982) and Birkeland (1999). The results of these calculations on the alluvial environment soils of Orjen are presented in Table B.2.

	Part A Quantification of soil properties				Part B Calculation	Part C Current Maximum
Rubification	*10 points/increase in hue redness(dry and moist)* 5Y → 2.5Y →10YR →7.5YR → 5YR →2.5YR →10R→5R *10 points/increase in chroma (dry and moist)* 0 → 1 → 2 → 3 → 4 → 5 → 6 → 7 → 8				$X_r = 10[\text{hue } \Delta X_0 + (\text{chroma } \Delta X_0)]_{dry} + 10[\text{hue } \Delta X_0 + (\text{chroma } \Delta X_0)]_{moist}$	Divide by current maximum (190)
Colour Paling	*10 points/decrease in hue redness* 5Y ← 2.5Y ←10YR ←7.5YR ← 5YR ←2.5YR ←10R ←5R *10 points/decrease in chroma* 0 ← 1 ← 2 ← 3 ← 4 ← 5 ← 6 ← 7 ← 8				$X_{cp} = 10[\text{hue } \Delta X_0 + (\text{chroma } \Delta X_0)]_{dry} + 10[\text{hue } \Delta X_0 + (\text{chroma } \Delta X_0)]_{moist}$	Divide by current maximum (60)
Melanisation	*10 points/decrease in value* 0 ← 1 ← 2 ← 3 ← 4 ← 5 ← 6 ← 7 ← 8 ← 9 ← 10				$X_m = 10(\text{value } \Delta X_0)_{dry} + 10(\text{value } \Delta X_0)_{moist}$	Divide by current maximum (85)
Total Texture	*10 points/line crossing towards clay on texture triangle* *10 points/increase in stickiness* so → ss → s → vs (nonsticky, slightly sticky, sticky, very sticky) *10 points/increase in plasticity* po → ps → p → vp (nonplastic, slightly plastic, plastic, very plastic)				$X_t = 10(\text{textural } \Delta X_0) + (\text{stickiness } \Delta X_0) + (\text{plasticity } \Delta X_0)$	Divide by current maximum (90)
Dry Consistency	*10 points/increase in hardness* lo → so → sh → h → vh → ch (loose, soft, slightly hard, hard, very hard, extremely hard)				$X_{dc} = 10(\text{dry consistence } \Delta X_0)$	Divide by 2 x current maximum (2 x 50 = 100)
Moist Consistency	*10 points/increase in firmness* lo → vfr → fr → fi → vfi → efi (loose, very friable, friable, firm, very firm, extremely firm)				$X_{dc} = 10(\text{moist consistence } \Delta X_0)$	Divide by 2 x current maximum (2 x 50 = 100)

Clay Films	Points	10	20	30	40	$X_{cf} = 10[(\text{abundance} + \text{distinctness} + \text{location of 1° class}) + 1/2(\text{abundance of 2° class})]$	Subtract 20 points from all X_{cf} values >0 and divide by current maximum (130)
	Amount (very few, few, common, many)	v1	1	2	3		
	Distinctness (faint, distinct, prominent)	f	d	p			
	Location (pores, bridges, colloids, ped faces)	po	br				
		co	pf				
	NB: If classes are equal, choose 1° class with greatest abundance						

Structure	Points	5	10	20	30	$X_s = [(\text{grade} + \text{type}) \text{ of } 1°] + 1/2(\text{grade} + \text{type}) \text{ of } 2°]$	Divide by maximum primary possible (60)
	Grade (weak, moderate, strong)		1	2	3		
	Type (platey, granular, prismatic, columnar)	pl	gr	pr	col		

pH	Difference between pH of horizon and pH of parent material					$X_{ph} = \text{pH } \Delta X_0$	Divide by decrease of 3.5 or increase of 1.5

Table B.1 – Calculation stages of the Harden Index (Adapted from Birkeland, 1999).

Table B.2 – Harden Index calculations from soils developed on the alluvial deposits of Orjen

Soil Depth (cm)	Rubification					Colour Paling					Melanization			Structure			Total Texture			Moist Consistency		Dry Consistency		Clay Films					pH		Horizon Index	Depth (cm)	% Profile	Sum Profile
	Munsell Hue (moist)	Munsell Chroma (moist)	Munsell Hue (dry)	Munsell Chroma (dry)	R	Munsell Hue (moist)	Munsell Chroma (moist)	Munsell Hue (dry)	Munsell Chroma (dry)	CP	Munsell Value (moist)	Munsell Value (dry)	Me	Grade	Aggregate	S	Shift to clay	Wet consistency	T	Moist	MC	Dry	DC	Amount	Distinct.	Location		CF	pH Mean	pH				
Current Maximum values (After Birkeland, 1999)	190					60					85			60			90			100		100		130					1.5/3.5					
Grahovo - G1																																		
0-10	10YR	3	10YR	3	0.000	10YR	3	10YR	3	0.667	3	3	0.706	2	Granular	0.500	0	Ps ss	0.111	fr	0.100	so	0.100	1	f	pf		0.385	7.760 1.110	0.317	0.321	10	3.206	
10-20	7.5YR	4	10YR	3	0.053	7.5YR	4	10YR	3	0.667	3	3	0.706	2	Granular	0.500	0	Ps ss	0.111	fr	0.100	so	0.100	2	f	pf		0.462	7.620 1.250	0.357	0.339	10	3.394	
20-30	7.5YR	4	10YR	3	0.053	7.5YR	4	10YR	3	0.667	3	3	0.706	2	Granular	0.500	0	Ps ss	0.111	fr	0.100	so	0.100	2	d	pf	85.000	0.538	8.160 0.710	0.203	0.331	10	3.308	9.909
30-40 PARENT	10YR	6	10YR	4		10YR	6	10YR	4		6	6		1	Granular		0	Po ss		vfr		lo		2	d	oo	0.500		8.870					
Grahovo - G2																																		
0-10	10YR	2	10YR	2	0.000	10YR	2	10YR	2	0.500	3	3	0.706	2	Granular	0.500	0	Ps ss	0.111	fi	0.200	sh	0.200	1	f	pf		0.385	8.107 0.287	0.082	0.298	10	2.982	
20-30	10YR	3	10YR	3	0.000	10YR	3	10YR	3	0.167	5	4	0.353	1	Granular	0.333	0	Ps ss	0.111	fr		so	0.100	1	f	pf	60.000	0.385	8.213 0.180	0.051	0.178	10	1.778	4.760
20-30 PARENT	10YR	4	10YR	3		10YR	4	10YR	3		6	6		1	Granular		0	Po ss		lo		lo		vf	f	pf	0.308		8.393					
Dvrsno - D1																																		
0-10	10YR	2	10YR	2	0.000	10YR	2	10YR	2	0.667	2	2	1.176	2	Granular	0.500	0	Ps ss	0.111	fi	0.200	sh	0.200	vf	f	pf		0.308	8.270 0.913	0.261	0.380	10	3.803	
10-20	10YR	2	10YR	2	0.000	10YR	2	10YR	2	0.667	2	2	1.176	2	Granular	0.500	0	Ps ss	0.111	fr		so	0.100	vf	f	pf		0.308	8.100 1.083	0.310	0.363	10	3.635	
20-30	10YR	3	10YR	2	0.000	10YR	3	10YR	2	0.500	4	3	0.824	2	Granular	0.500	0	Po ss	0.000	vfr		so	0.100	2	f	oo		0.462	8.410 0.773	0.221	0.290	10	2.896	
30-40	10YR	6	10YR	4	0.105	10YR	6	10YR	4	0.000	5	6	0.353	1	Granular	0.333	0	Po ss	0.000	vfr		lo		2	d	oo	75.000	0.462	8.950 0.233	0.067	0.147	10	1.466	11.800
40-50 PARENT	10YR	4	10YR	4		10YR	4	10YR	4		7	7		1	Granular		0	Po ss		vfr		lo		2	d	oo	0.423		9.183					
Dvrsno - D5																																		
0-10	10YR	2	10YR	3	0.053	10YR	2	10YR	3	0.333	2	3	0.941	2	Granular	0.500	0	Ps s	0.222	fr		so	0.100	1	d	pf		0.462	8.537 0.643	0.184	0.333	10	3.327	
20-30	10YR	1	10YR	2	0.000	10YR	1	10YR	2	0.667	2	2	1.059	3	Platey	0.583	0	Ps s	0.222	fi	0.200	sh		1	f	pf	70.000	0.385	8.127 1.053	0.301	0.402	10	4.018	7.346
20-30 PARENT	10YR	4	10YR	3		10YR	4	10YR	3		6	7		1	Platey		0	Po ss		vfr		lo		vf	f	oo	0.385		9.180					
Kruševice - Kr2																																		
0-10	10YR	3	10YR	6	0.000	10YR	3	10YR	6	0.167	3	3	0.941	2	g	0.333	0	ps s	0.333	fi	0.300	sh	0.200	2	d	pf		0.538	6.860 2.530	0.723	0.379	10	3.795	
10-20	7.5YR	3	10YR	6	0.053	7.5YR	3	10YR	6	0.167	2.5	3	1.118	2	g	0.000	0	po ss	0.111	fr		so		1	d	pf		0.462	7.850 1.540	0.440	0.298	10	2.979	
20-30	7.5YR	4	10YR	6	0.053	7.5YR	4	10YR	6	0.000	3	3	0.941	2	g	0.000	0	po ss	0.111	fr	0.200	sh	0.200	1	d	pf		0.462	7.903 1.487	0.425	0.299	10	2.989	
30-40	7.5YR	4	7.5YR	4	0.105	7.5YR	4	7.5YR	4	0.000	3	3	0.941	2	g	0.000	0	po ss	0.111	fr	0.200	sh	0.200	2	d	pf		0.462	8.073 1.317	0.376	0.299	10	2.994	
40-50	10YR	6	10YR	4	0.000	10YR	6	10YR	4	0.000	4	5	0.235	1	g	0.000	0	lo	0.000	lo		lo		1	f	pf	80.000	0.385	8.777 0.613	0.175	0.099	10	0.994	13.751
50-60 PARENT	10YR	4	10YR	4		10YR	4	10YR	4		7	7		1	g		0	po so		lo		lo		2	d	pf	0.462		9.330					
Vrbanje - V4																																		
0-10	7.5YR	3	10YR	3	0.000	7.5YR	3	10YR	3	0.167	3	3	0.353	1	g	0.000	0	po so	0.000	vfr	0.100	lo	0.000	1	f	pf		0.385	8.623 0.510	0.146	0.123	10	1.229	
10-20	10YR	6	10YR	4	0.000	10YR	6	10YR	4	0.000	3	5	2.000	1	g	0.000	0	po so	0.000	vfr	0.100	lo	0.000	1	f	pf		0.385	8.983 0.150	0.043	0.316	10	3.159	
20-30	10YR	6	10YR	4	0.000	10YR	6	10YR	4	0.000	4	6	0.000	1	g	0.000	0	po so	0.000	lo		lo		1	f	pf		0.385	9.103 0.030	0.009	0.049	10	0.491	4.088
30-40 PARENT	10YR	6	10YR	4		10YR	6	10YR	4		5	6		1	g		0	po so		lo		lo		1	f	pf	60.000		9.133					
P. Poljana - P1																																		
0-10	10YR	3	10YR	4	0.053	10YR	3	10YR	4	0.000	3	3	0.941	1	g	0.000	0	po so	0.000	vfr		so	0.000	2	f	oo		0.385	9.000 0.663	0.190	0.208	10	2.085	
10-20	10YR	4	10YR	3	0.105	10YR	4	10YR	3	0.167	3	4	0.824	1	g	0.000	0	po so	0.000	fr		so	0.100	1	f	pf		0.385	9.337 0.327	0.093	0.213	10	2.133	
20-30	10YR	4	10YR	4	0.158	10YR	4	10YR	4	0.000	6	6	0.235	1	g	0.333	0	po so	0.000	lo		lo		1	f	pf	60.000	0.385	9.687 -0.023	-0.016	0.137	10	1.369	5.588
30-40 - PARENT	10YR	3	10YR	3		10YR	3	10YR	3		7	7		1	g		0	po so		lo		lo		1	f	pf	0.308		9.663					
P. Poljana - P2																																		
0-10	7.5YR	3	7.5YR	4	0.105	7.5YR	3	7.5YR	4	0.167	3	4	0.824	2	g	0.000	0	ps ss	0.222	fr	0.200	so	0.100	2	d	pf		0.538	8.803 0.860	0.246	0.267	10	2.669	
10-20	7.5YR	4	10YR	4	0.053	7.5YR	4	10YR	4	0.000	3	4	0.824	1	g	0.000	0	ps ss	0.222	fr	0.200	so	0.100	2	d	oo		0.462	9.380 0.283	0.081	0.216	10	2.157	
20-30	7.5YR	4	7.5YR	4	0.105	7.5YR	4	7.5YR	4	0.000	3	5	0.588	1	g	0.000	0	po so	0.000	vfr	0.100	so	0.100	1	f	pf		0.385	9.500 0.163	0.047	0.147	10	1.472	
30-40	10YR	6	10YR	3	0.105	10YR	6	10YR	3	0.167	4	5	0.588	1	g	0.000	0	po so	0.000	lo	0.100	lo	0.100	2	f	pf		0.462	9.443 0.220	0.063	0.176	10	1.761	
40-50	10YR	6	10YR	4	0.105	10YR	6	10YR	4	0.000	5	6	0.353	1	g	0.000	0	po so	0.000	lo		lo		2	f	pf	85.000	0.462	9.533 0.130	0.037	0.106	10	1.063	9.121
50-60 - PARENT	10YR	4	10YR	4		10YR	4	10YR	4		7	7		1	g		0	po so		lo		lo		2	d	pf	0.500		9.663					

Table B.2 continued — Harden Index calculations from soils developed on the alluvial deposits of Orjen

Soil Depth (cm)	Munsell Hue (moist)	Munsell Chroma (moist)	Munsell Hue (dry)	Munsell Chroma (dry)	R	Munsell Hue (moist)	Munsell Chroma (moist)	Munsell Hue (dry)	Munsell Chroma (dry)	CP	Munsell Value (moist)	Munsell Value (dry)	Me	Grade	Aggregate	S	Shift to clay	Wet consistency		T	Moist	MC	Dry	DC	Amount	Distinct.	Location		CF	pH Mean	pH	Horizon Index	Depth (cm)	% Profile	Sum Profile
Current Maximum values (After Birkeland, 1999)					190					60			85			60				90		100		100					130		1.5/3.5				
Kameno - K2																																			
0-10	7.5YR	2	10YR	2		7.5YR	2	10YR	2		3	3		2	Granular			P	ss		vfi		sh		2	f	pf			8.270		0.379	10	3.792	
	10	0	0	0	0.053	10	20	0	20	0.833	30	30	0.706	20	10	0.500	0	20	10	0.333	20	0.200	10	0.100	30	10	20		0.462	0.790	0.226				
10-20	10YR	3	10YR	3		10YR	3	10YR	3		3	3		2	Granular			P	ss		vfi		so		2	f	pf			8.283		0.306	10	3.062	
	0	0	0	0	0.000	0	10	0	10	0.333	30	30	0.706	20	10	0.500	0	20	10	0.333	20	0.200	0	0.000	30	10	20		0.462	0.777	0.222				
20-30	10YR	3	10YR	3		10YR	3	10YR	3		3	3		2	Granular			P	ss		vfi		so		2	f	pf			8.370		0.303	10	3.035	
	0	0	0	0	0.000	0	10	0	10	0.333	30	30	0.706	20	10	0.500	0	20	10	0.333	20	0.200	0	0.000	30	10	20		0.462	0.690	0.197				
30-40	10YR	4	10YR	4		10YR	4	10YR	4		3	3		1	Granular			P	ss		fr		so		2	d	pf			8.680		0.224	10	2.244	
	0	0	0	0	0.000	0	0	0	0	0.000	30	30	0.706	10	10	0.333	0	20	10	0.333	0	0.000	0	0.000	30	20	20		0.538	0.380	0.109				
40-50	10YR	6	10YR	3		10YR	6	10YR	3		3	5		1	Granular			Ps	ss		fr		so		2	d	pf			8.590		0.219	10	2.190	
	0	20	0	0	0.105	0	0	0	10	0.167	30	10	0.471	10	10	0.333	0	10	10	0.222	0	0.000	0	0.000	30	20	20		0.538	0.470	0.134				
50-60	10YR	6	10YR	4		10YR	6	10YR	4		4	5		1	Granular			Po	ss		fr		so		2	d	pf			8.927		0.164	10	1.644	
	0	20	0	0	0.105	0	0	0	10	0.000	20	10	0.353	10	10	0.333	0	0	10	0.111	0	0.000	0	0.000	30	20	20	85.000	0.538	0.133	0.038				
60-70 PARENT	10YR	4	10YR	4		10YR	4	10YR	4		6	6		1				Po	so		fr		so		2	d	oo	0.500		9.060					15.966
Nudo - ZN1																																			
0-10	10YR	3	10YR	2		10YR	3	10YR	2		5	4		2	Granular			Po	ss		fi		so		2	f	oo			8.567		0.184	10	1.844	
	0	0	0	0	0.000	0	10	0	10	0.333	10	10	0.235	20	10	0.500	0	10	10	0.000	10	0.100	0	0.000	30	10	10	30.000	0.385	0.373	0.107				
10-20 PARENT	10YR	4	10YR	3		10YR	4	10YR	3		6	5		1	Granular			Po	ss		fr		so		1	f	oo	0.231		8.940					1.844
Nudo ZN2																																			
0-10	10YR	2	10YR	2		10YR	2	10YR	2		3	3		2	Granular			Ps	ss		fi		sh		1	f	oo			8.240		0.310	10	3.097	
	0	0	0	0	0.000	0	20	0	10	0.500	30	40	0.824	20	10	0.500	0	10	10	0.000	20	0.200	20	0.200	20	10	10	20.000	0.308	0.897	0.256				
10-20 PARENT	10YR	4	10YR	3		10YR	4	10YR	3		6	7		1	Granular			Po	ss		vfr		lo		1	f	oo	0.154		9.137					3.097
Nudo - VN1																																			
0-10	7.5YR	3	7.5YR	2		7.5YR	3	7.5YR	2		3	3		3	Blocky			P	ss		fi		sh		2	f	oo			8.473		0.253	10	2.528	
	10	0	10	0	0.105	10	10	0	10	0.500	10	10	0.235	30	10	0.667	0	10	0	0.111	10	0.100	10	0.100	30	10	10		0.385	0.253	0.072				
20-30	7.5YR	2	7.5YR	2		7.5YR	2	7.5YR	2		3	3		2	Blocky			P	ss		fi		so		2	f	oo			8.373		0.245	10	2.449	
	10	0	10	0	0.105	10	20	0	10	0.667	10	10	0.235	20	10	0.500	0	10	0	0.111	10	0.100	0	0.000	30	10	10		0.385	0.353	0.101				
30-40	7.5YR	4	10YR	4		7.5YR	4	10YR	4		4	4		2	Blocky			Ps	ss		fr		so		2	f	oo			8.633		0.131	10	1.315	
	10	0	0	10	0.105	10	0	0	10	0.167	0	0	0.000	20	10	0.500	0	0	0	0.000	0	0.000	0	0.000	30	10	10	65.000	0.385	0.093	0.027				
40-50 PARENT	10YR	4	10YR	3		10YR	4	10YR	3		4	4		2	Granular			Ps	ss		fr		so		1	f	oo	0.346		8.727					6.292
Unijerina - U2																																			
0-15	10YR	4	10YR	4		10YR	4	10YR	4		5	5		1	g				po	so		vfr		lo		1	d	oo			8.680		0.141	15	2.115	
	0	10	0	0	0.053	0	0	0	0	0.000	20	20	0.471	10	10	0.000	0	0	0	0.000	10	0.100	0	0.000	20	20	10		0.385	0.420	0.120				
15-25	10YR	4	10YR	4		10YR	4	10YR	4		5	5		1	g				po	so		vfr		lo		2	d	oo			8.757		0.148	10	1.479	
	0	10	0	0	0.053	0	0	0	0	0.000	20	20	0.471	10	10	0.000	0	0	0	0.000	10	0.100	0	0.000	30	20	10		0.462	0.343	0.098				
25-35	10YR	4	10YR	3		10YR	4	10YR	3		6	6		1	g				po	so		lo		lo		1	d	oo			8.737		0.097	10	0.970	
	0	10	0	0	0.053	0	0	0	0	0.000	10	10	0.235	10	10	0.000	0	0	0	0.000	0	0.000	0	0.000	20	20	10		0.385	0.363	0.104				
35-45	10YR	4	10YR	3		10YR	4	10YR	3		6	6		1	g				po	so		lo		lo		1	d	pf			8.865		0.102	10	1.021	
	0	10	0	0	0.053	0	0	0	0	0.167	10	10	0.235	10	10	0.000	0	0	0	0.000	0	0.000	0	0.000	20	20	20		0.462	0.235	0.067				
45-55	10YR	4	10YR	4		10YR	4	10YR	4		7	7		1	g				po	so		lo		lo		1	d	pf			9.100		0.071	10	0.709	
	0	10	0	10	0.105	0	0	0	0	0.000	0	0	0.000	10	10	0.000	0	0	0	0.000	0	0.000	0	0.000	20	20	20	70.000	0.462	0.000	0.000				
55-65 - PARENT	10YR	3	10YR	3		10YR	3	10YR	3		7	7		1	g				po	so		lo		lo		1	d	pf	0.385		9.100					6.293
Unijerina - U3																																			
0-10	10YR	3	10YR	3		10YR	3	10YR	3		3	4		2	Granular				Po	ss		vfr		so		1	d	oo			8.337		0.143	10	1.428	
	0	0	0	0	0.000	0	0	0	0	0.000	10	10	0.235	20	10	0.500	0	0	0	0.000	0	0.000	0	0.000	20	20	10	30.000	0.385	0.343	0.023				
10-20 PARENT	10YR	3	10YR	3		10YR	3	10YR	3		4	5		2	Granular				Po	ss		vfr		so		1	f	oo	0.077		8.680					1.428
Crkvice - C1																																			
0-10	10YR	3	10YR	3		10YR	3	10YR	3		4	4		1	g				ps	ss		vfr		so		1	f	pf			9.237		0.196	10	1.957	
	0	0	10	0	0.053	0	10	0	10	0.333	20	30	0.588	10	10	0.000	0	10	10	0.111	10	0.100	10	0.100	20	10	20		0.385	0.320	0.091				
10-20	10YR	4	10YR	4		10YR	4	10YR	4		6	6		1	g				ps	ss		vfr		so		1	d	pf			9.537		0.105	10	1.054	
	0	0	10	0	0.053	0	0	0	0	0.000	10	10	0.118	10	10	0.000	0	10	10	0.111	10	0.100	10	0.100	30	20	20		0.462	0.020	0.006				
20-30	10YR	4	10YR	4		10YR	4	10YR	4		6	7		1	g				ps	ss		lo		so		2	d	pf			9.517		0.090	10	0.904	
	0	0	10	0	0.053	0	0	0	0	0.000	10	0	0.000	10	10	0.000	0	10	10	0.111	0	0.000	10	0.000	30	20	20	80.000	0.538	0.040	0.011				
30-40 PARENT	10YR	4	10YR	4		10YR	4	10YR	4		6	7		1	g				ps	so		lo		lo		1	f	pf	0.462		9.557					3.915
Crkvice - C2																																			
0-10	10YR	2	10YR	2		10YR	2	10YR	2		5	5		1	g				po	so		lo		lo		1	f	pf			9.130		0.127	10	1.267	
	0	0	0	20	0.000	0	20	0	20	0.333	10	10	0.235	10	10	0.000	0	0	0	0.000	0	0.000	0	0.000	20	10	20		0.385	0.653	0.187				
10-20	10YR	3	10YR	3		10YR	3	10YR	3		5	5		1	g				po	ss		lo		lo		2	f	pf			9.550		0.116	10	1.157	
	0	0	0	0	0.000	0	10	0	10	0.167	20	20	0.235	10	10	0.000	0	0	10	0.111	0	0.000	0	0.000	30	10	20		0.462	0.233	0.067				
20-30	10YR	3	10YR	3		10YR	3	10YR	3		6	6		1	g				po	so		lo		lo		1	d	pf			9.563		0.090	10	0.899	
	0	0	0	0	0.000	0	10	0	10	0.167	10	10	0.118	10	10	0.000	0	0	0	0.000	0	0.000	0	0.000	20	20	20		0.462	0.220	0.063				
30-40	10YR	3	10YR	3		10YR	3	10YR	3		7	7		1	g				po	so		lo		lo		2	d	pf			9.743		0.080	10	0.796	
	0	0	0	0	0.000	0	10	0	10	0.167	0	0	0.000	10	10	0.000	0	0	0	0.000	0	0.000	0	0.000	30	20	20	85.000	0.538	0.040	0.011				
40-50 - PARENT	10YR	4	10YR	4		10YR	4	10YR	4		7	7		1	g				po	so		lo		lo		2	d	oo	0.500		9.783					4.118
Ubli - Ub1																																			
0-10	10YR	2	10YR	2		10YR	2	10YR	2		3	3		2	g				po	so		vfr		lo		2	d	oo			8.627		0.180	10	1.798	
	0	0	0	0	0.000	0	40	0	20	0.333	30	40	0.471	20	10	0.000	0	0	0	0.000	10	0.100	0	0.000	30	20	10		0.462	0.497	0.142				
10-20	10YR	4	10YR	4		10YR	4	10YR	4		5	6		1	g				po	lo		lo		lo		2	d	pf			9.130		0.541	10	5.408	
	0	0	0	0	0.000	0	20	0	0	0.333	10	10	4.000	10	10	0.000	0	0	0	0.000	0	0.000	0	0.000	30	20	20	85.000	0.538	-0.007	-0.004				
20-30 - PARENT	10YR	6	10YR	4		10YR	6	10YR	4		6	7		1	g				po	lo		lo		lo		2	d	oo	0.500		9.123					7.206
Snježnice - S2																																			
0-5	10YR	3	10YR	3		10YR	3	10YR	3		3	4		1	g				po	so		vfr		lo		2	d	oo			8.597		0.139	5	0.696	
	0	0	0	0	0.000	0	30	10	30	0.667	20	20	0.235	10	10	0.000	0	0	0	0.000	10	0.100	0	0.000	30	20	10		0.462	-0.317	-0.211				
5-15	10YR	4	10YR	4		10YR	4	10YR	4		4	4		1	g				po	so		vfr		lo		2	d	pf			8.583		0.130	10	1.302	
	0	0	0	0	0.000	0	20	10	20	0.500	10	20	0.235	10	10	0.000	0	0	0	0.000	10	0.100	0	0.000	30	20	20		0.538	-0.303	-0.202				
15-25	10YR	6	10YR	6		10YR	6	10YR	6		4	5		1	g				po	so		lo		lo		1	f	pf			8.590		0.051	10	0.514	
	0	0	0	0	0.000	0	0	10	0	0.167	10	10	0.118	10	10	0.000	0	0	0	0.000	0	0.000	0	0.000	20	10	20	85.000	0.385	-0.310	-0.207				
25-35 - PARENT	10YR	6	7.5YR	6		10YR	6	7.5YR	6		5	6		1	g				po	so		lo		lo		2	d	pf	0.500		8.280					2.511

Table B.2 continued – Harden Index calculations from soils developed on the alluvial deposits of Orjen

To ensure compatibility between samples analysed using both the standard and nano/micro Malvern Mastersizer methods, a series of calibration measurements have been completed using matrix samples from 10 study sites:

- Grahovo
- Dvrsno
- Unijerina
- Sniježnice
- Kameno

- Kruševice
- Vrbanje
- Pirina Poljana
- Nudo
- Crkvice

Each sample has been analysed using four contrasting particle size analysis methods (Table C.1) that reflect the analysis undertaken during this study. These methods test the viability of comparisons between different measurement techniques, notably the separation of <2 mm and <63 μm size fractions. A particle size distribution curve has been developed for each sample (Figure C.1).

Sample Code	Analysis Method
A	Bulk sample (<2 mm), analysed using standard Malvern sampler
B	<63 μm sample, analysed using standard Malvern sampler
C	<63 μm sample, analysed using Malvern micro-sampler
D	<63 μm insoluble residue sample, analysed using Malvern micro-sampler

Table C.1 – Particle size analysis methods used for the calibration of measurement techniques used within this study.

The particle size curves indicate a strong agreement between all <63 μm samples analysed using both the standard and micro sampling techniques. This verifies that the analytical data from both the <2 mm and <63 μm size fractions within this study are directly compatible. The PSDs of the <63 μm samples analysed using the micro sampler often add greater detail to the fine sediment fraction when compared to the equivalent bulk samples analysed using the <2 mm standard sampler. This suggests that the <63 μm fraction may be obscured within bulk sediment samples. In this study the <63 μm size fraction is isolated and analysed independently of the <2 mm sample to maintain the signal integrity of the fine sediment fraction. The insoluble residue samples yield clear PSA signals, indicating that the fine sediments are effectively recorded using Malvern analytical techniques.
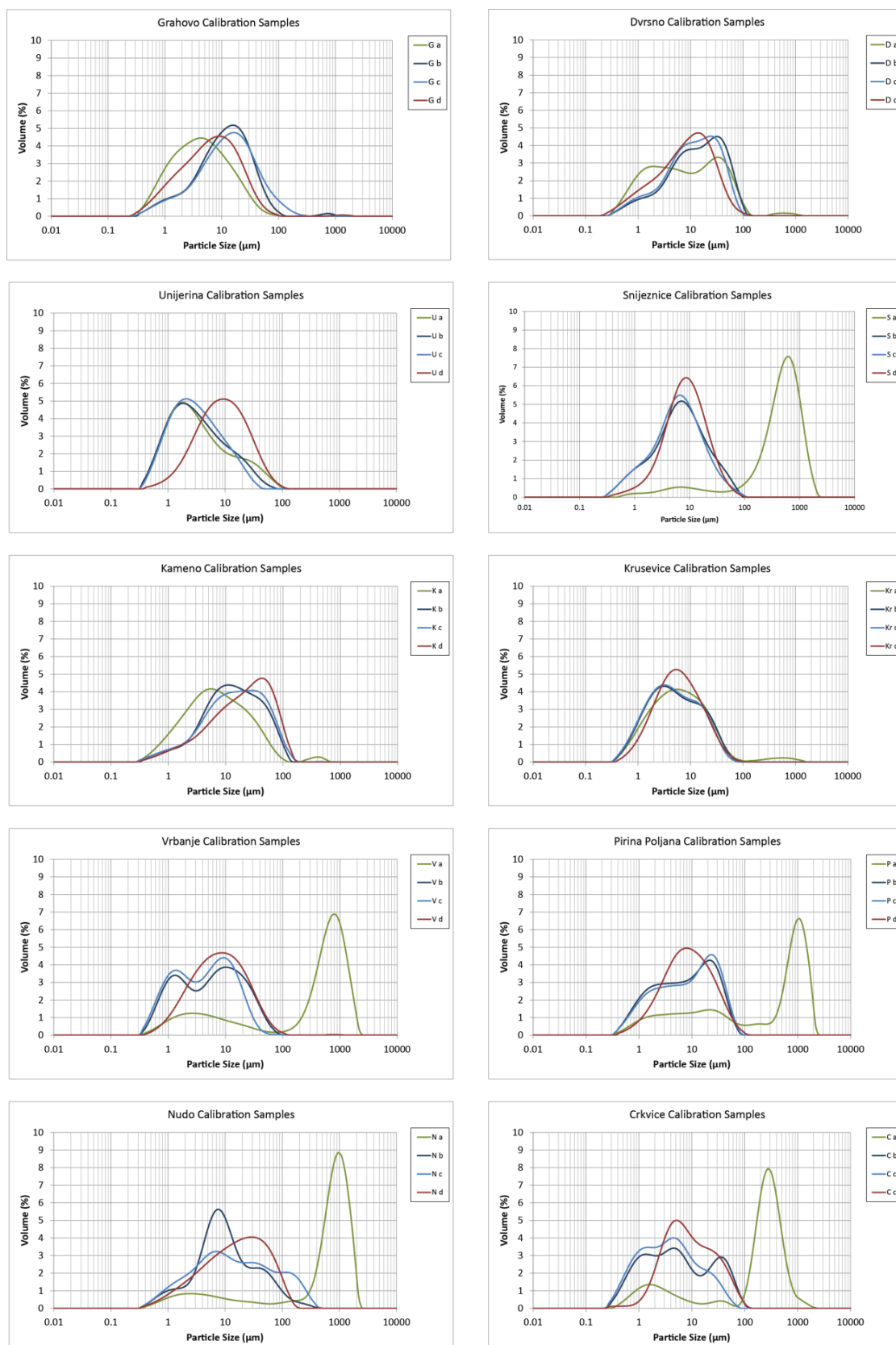
Figure C.1 – Particle size distribution curves for matrix samples from fluvial sediments at 10 sites across Orjen analysed using four methods: A) Green: bulk samples <2 mm, standard sample methods; B) Dark Blue: <63 μm, standard sample methods; C) Light Blue: <63 μm, micro sample methods; D) Red: <63 μm insoluble residue, micro sample methods.